frontiers | Research Topics

Immunologic tumor microenvironment modulators for turning "cold" tumors to "hot" tumors

Edited by
Xin He, Gulderen Yanikkaya Demirel,
Chengwu Zeng and Mazdak Ganjalikhani Hakemi

Published in
Frontiers in Immunology
Frontiers in Oncology

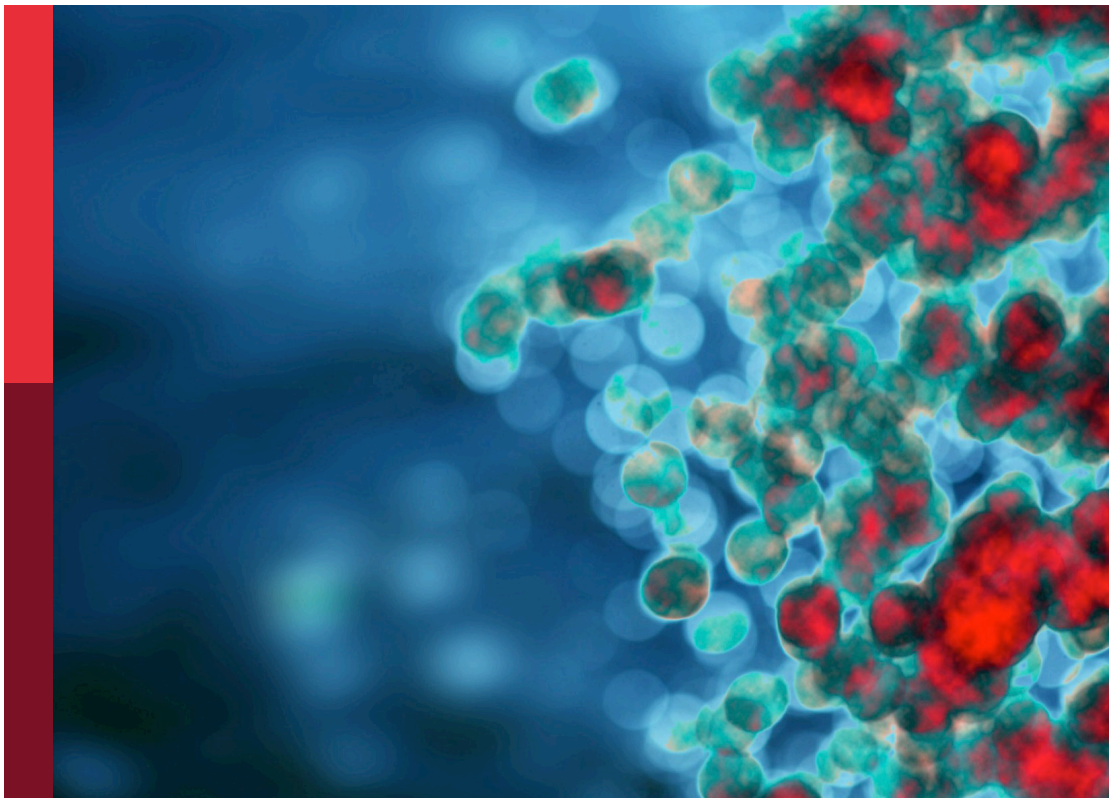

ISSN 1664-8714
ISBN 978-2-8325-4937-7
DOI 10.3389/978-2-8325-4937-7

About Frontiers

Frontiers is more than just an open access publisher of scholarly articles: it is a pioneering approach to the world of academia, radically improving the way scholarly research is managed. The grand vision of Frontiers is a world where all people have an equal opportunity to seek, share and generate knowledge. Frontiers provides immediate and permanent online open access to all its publications, but this alone is not enough to realize our grand goals.

Frontiers journal series

The Frontiers journal series is a multi-tier and interdisciplinary set of open-access, online journals, promising a paradigm shift from the current review, selection and dissemination processes in academic publishing. All Frontiers journals are driven by researchers for researchers; therefore, they constitute a service to the scholarly community. At the same time, the *Frontiers journal series* operates on a revolutionary invention, the tiered publishing system, initially addressing specific communities of scholars, and gradually climbing up to broader public understanding, thus serving the interests of the lay society, too.

Dedication to quality

Each Frontiers article is a landmark of the highest quality, thanks to genuinely collaborative interactions between authors and review editors, who include some of the world's best academicians. Research must be certified by peers before entering a stream of knowledge that may eventually reach the public - and shape society; therefore, Frontiers only applies the most rigorous and unbiased reviews. Frontiers revolutionizes research publishing by freely delivering the most outstanding research, evaluated with no bias from both the academic and social point of view. By applying the most advanced information technologies, Frontiers is catapulting scholarly publishing into a new generation.

What are Frontiers Research Topics?

Frontiers Research Topics are very popular trademarks of the *Frontiers journals series*: they are collections of at least ten articles, all centered on a particular subject. With their unique mix of varied contributions from Original Research to Review Articles, Frontiers Research Topics unify the most influential researchers, the latest key findings and historical advances in a hot research area.

Find out more on how to host your own Frontiers Research Topic or contribute to one as an author by contacting the Frontiers editorial office: frontiersin.org/about/contact

Immunologic tumor microenvironment modulators for turning "cold" tumors to "hot" tumors

Topic editors

Xin He — City of Hope National Medical Center, United States

Gulderen Yanikkaya Demirel — Yeditepe University, Türkiye

Chengwu Zeng — Jinan University, China

Mazdak Ganjalikhani Hakemi — Isfahan University of Medical Sciences, Iran

Citation

He, X., Demirel, G. Y., Zeng, C., Hakemi, M. G., eds. (2024). *Immunologic tumor microenvironment modulators for turning "cold" tumors to "hot" tumors*. Lausanne: Frontiers Media SA. doi: 10.3389/978-2-8325-4937-7

Table of contents

frontiers | Frontiers in Immunology

TYPE Editorial
PUBLISHED 15 May 2024
DOI 10.3389/fimmu.2024.1425136

OPEN ACCESS

EDITED AND REVIEWED BY
Peter Brossart,
University of Bonn, Germany

*CORRESPONDENCE
Mazdak Ganjalıkhani-Hakemi
mghakemi@med.mui.ac.ir;
mazdak.hakemi@medipol.edu.tr

RECEIVED 29 April 2024
ACCEPTED 02 May 2024
PUBLISHED 15 May 2024

CITATION
Ganjalıkhani-Hakemi M, Yanikkaya Demirel G, He X and Zeng C (2024) Editorial: Immunologic tumor microenvironment modulators for turning "cold" tumors to "hot" tumors.
Front. Immunol. 15:1425136.
doi: 10.3389/fimmu.2024.1425136

Editorial: Immunologic tumor microenvironment modulators for turning "cold" tumors to "hot" tumors

Mazdak Ganjalıkhani-Hakemi[1,2]*, Gulderen Yanikkaya Demirel[3], Xin He[4] and Chengwu Zeng[5]

[1]Department of Immunology, Faculty of Medicine, Isfahan University of Medical Sciences, Isfahan, Iran, [2]Regenerative and Restorative Medicine Research Center (REMER), Research Institute for Health Sciences and Technologies (SABITA), Istanbul Medipol University, Istanbul, Türkiye, [3]Department of Immunology, Faculty of Medicine, Yeditepe University, Istanbul, Türkiye, [4]Department of Hematological Malignancies Translational Science, Gehr Family Center for Leukemia Research, Hematologic Malignancies and Stem Cell Transplantation Institute, Beckman Research Institute, City of Hope Medical Center, Duarte, CA, United States, [5]Department of Hematology, The Fifth Affiliated Hospital of Guangzhou Medical University, Guangzhou, China

KEYWORDS

cold tumor, small peptide, small molecule, bioactive peptide, cancer vaccine, immune check-point inhibitor

Editorial on the Research Topic

Immunologic tumor microenvironment modulators for turning "cold" tumors to "hot" tumors

Cancer immunotherapy harnesses the body's immune system to combat tumors while sparing normal cells. Numerous strategies have been explored for this purpose. However, monotherapy using these methods often proves ineffective in clinical trials. Many tumors resist immunotherapy, earning them the designation of "cold" or non-inflammatory tumors. These cold tumors lack sufficient infiltration by CD8+ T cells, hampering immune response. They are characterized by a dearth of cytotoxic T cells, alongside the presence of anti-inflammatory myeloid cells, tumor-associated M2 macrophages, and regulatory T cells. Combining immunotherapy with other cancer treatment modalities, such as chemotherapy or cancer vaccines, holds promise in bolstering efficacy and improving outcomes (1–3).

In their article titled "Overcoming cold tumors: a combination strategy of immune checkpoint inhibitors," Ouyang et al. have explored methods to convert cold tumors into hot ones, including boosting T cell infiltration and adopting therapies like CAR T cells. Despite the groundbreaking impact of Immune Checkpoint Inhibitors (ICIs) on cancer therapy, resistance persists in many cold tumors due to diverse immune evasion mechanisms. The success of immunotherapy hinges on T cells' capacity to recognize and eliminate tumor cells; however, cold tumors lack T cell infiltration, rendering ICI therapy ineffective. Overcoming these challenges, particularly impaired T cell activation and homing, is essential for enhancing ICI therapy efficacy.

In one of the articles within this Research Topic, titled "Optimal combination of MYCN differential gene and cellular senescence gene predicts adverse outcomes in patients with

neuroblastoma," the focus was on predicting neuroblastoma (NB) prognosis. Utilizing a predictive signature based on six optimal candidate genes (TP53, IL-7, PDGFRA, S100B, DLL3, and TP63), the study demonstrates superior prognostic capability compared to an individual gene analysis. The signature also sheds light on the immunosuppressive and aging tumor microenvironment in MYCN-amplified high-risk NB patients.

"Cytotoxic response of tumor-infiltrating lymphocytes of head and neck cancer slice cultures under mitochondrial dysfunction" by Greier et al. is about head and neck squamous cell carcinomas (HNSCC). They have cultivated slice cultures of the HNSCC to test the effect of mitochondrial dysfunction on cytotoxic T cell under different metabolic conditions. They have found that high glucose concentration alone did not have any impact on T cell activity or apoptosis while mitochondrial dysfunction with alone increased the apoptosis in tumor cells.

An article by Cini et al., is about a novel fusion protein SON-1210 (IL-12-FHAB-IL-15) produced with anticipation to amplify the therapeutic impact of interleukins and combination immunotherapies in human tumor microenvironment (TME). SON-1210 is a fused single-chain human IL-12 and native human IL-15 in cis onto a fully human albumin binding (FHAB) domain single-chain antibody fragment (scFv). They have shared the results of their experiments *in vitro* and in animal models on cytotoxicity, pharmacokinetics, potency, functional characteristics, safety, immune response, and efficacy. The authors suggest that linking cytokines to a fully human albumin-binding domain provides an indirect opportunity to target the TME using potent cytokines in cis that can redirect the immune response and control tumor growth.

Same group of researchers have also shared their Phase I trial results with SON-1210 in another article, and declared that SON-1010, a novel presentation for rIL-12, was safe and well tolerated in healthy volunteers up to 300 ng/kg. They emphasize that extended half-life of the drug leads to a prolonged and controlled IFNγ response, which may be important for tumor control in patients.

Despite some successes in immunotherapy for oncological diseases, cold tumors pose a significant therapeutic challenge. It is anticipated that future treatment algorithms will adapt therapeutic strategies to the immune context of tumors, as treatment with checkpoint inhibitors or vaccines alone often falls short. Therefore, combining other therapeutic approaches with existing methods may prove more effective for cold tumors, which either weakly stimulate or resist the immune system (4, 5).

Tong et. al., in their "Making "cold" tumors "hot"-Radiotherapy remodels the tumor immune microenvironment of pancreatic cancer to benefit from Immunotherapy: A case report" titled article, reported a case of advanced metastatic cancer treated with immunotherapy combined with chemotherapy and radiotherapy where they have observed a sharp shift of TIME from T3 to T2. They propose that this combination may have significant therapeutic benefits suggesting a new strategy for the treatment of advanced pancreatic cancers.

Shi et. al., in their review article "Neoadjuvant SBRT combined with immunotherapy in NSCLC: from mechanisms to therapy", have provided updated information on use of Stereotactic Body Radiotherapy (SBRT) inducing direct tumor cell death and stimulation for local and systemic anti-tumor immune responses for early stage resectable non-small-cell lung cancers (NSCLC). They have provided information about the clinical trials combining the immunotherapy and SBRT after surgical resection and also discussed the optimal dosage, therapy schedule and biomarkers to be used in clinical applications.

The article "It's high-time to re-evaluate the value of induced-chemotherapy for reinforcing immunotherapy in colorectal cancer" underscores the importance of induced chemotherapy in enhancing immunotherapy for colorectal cancer (CRC). Certain chemotherapeutic agents exhibit immune-stimulatory properties, such as inducing immunogenic cell death (ICD) and promoting the generation of non-mutated neoantigens (NM-neoAgs). Despite the remaining challenges, clinical trials have shown promise for this combination approach in improving immunotherapy efficacy in CRC.

Wang et al., in their review titled "Utilizing Exosomes as Sparking Clinical Biomarkers and Therapeutic Response in acute myeloid leukemia," comprehensively outline advancements in understanding the involvement of exosomes in AML pathogenesis. This synthesis is pivotal for advancing the utilization of exosomes in both diagnosis and treatment strategies for AML.

In another work titled "Targeting LSD1 in Tumor Immunotherapy: Rationale, Challenges, and Prospects," Bao et al. succinctly encapsulated recent progress in the intersection of LSD1 and tumor immunity, proposing a potential therapeutic avenue by integrating LSD1 inhibition with immunotherapy protocols.

While CAR T cell therapy shows promise in hematological cancers, its efficacy in solid tumors like pancreatic cancer is limited by the immunosuppressive tumor microenvironment (TME). Akbari et al. consider the role of Prostaglandin E2 (PGE2) in their article entitled "PGE2-EP2/EP4 signaling elicits mesoCAR T cell immunosuppression in pancreatic cancer." Their investigations reveal a negative correlation between PGE2 expression and memory T cell gene signatures in pancreatic cancer tissue. They conclude that blocking PGE2-EP2/EP4 signaling may enhance CAR T cell activity in this challenging TME.

Additionally, Meymandi et al., in their work entitled "PX-478, an HIF-1a inhibitor, impairs mesoCAR T cell antitumor function in cervical cancer," consider hypoxia's impact on HIF-1a expression and CAR T cell therapy's low success rate in solid tumors like cervical cancer. Their experiments demonstrate that PX-478 inhibits T cell proliferation, impairs cytotoxicity, and induces exhaustion, highlighting the relevance of HIF-1a in T and CAR T cell function.

To combat immunosuppressive TMEs, targeted treatments utilizing small molecules, peptides, or other materials capable of disrupting the TME can be employed as adjuvant therapies. Ghadiri et al. reviewed bioactive peptides from plant and animal sources in their article "Bioactive peptides: an alternative therapeutic approach for cancer management." These peptides have shown promise in inhibiting cancer cell proliferation, inducing apoptosis, and suppressing tumor growth and metastasis.

This Research Topic covers advances in immunology, medical chemistry, biochemistry, pharmacology, food engineering, and molecular biology relevant to cancer treatment. Out of 26 articles received, 14 were accepted for publication, including 8 reviews, 5 original articles, 1 clinical trial, and 1 case report. These contributions paved the way toward new research directions related to immunologic tumor microenvironment modulators, aiming to convert cold tumors into hot ones. It is hoped that these efforts and the articles presented in this Research Topic will be interesting, informative, and inspiring to readers, encouraging further exploration of this important subject.

Author contributions

MG-H: Writing – review & editing, Writing – original draft, Supervision, Conceptualization. GYD: Writing – review & editing, Writing – original draft. XH: Writing – review & editing, Writing – original draft. CZ: Writing – review & editing, Writing – original draft.

Acknowledgments

The authors express gratitude to all contributors and reviewers for their dedicated efforts in advancing knowledge on this subject.

Conflict of interest

The authors declare that the research was conducted in the absence of any commercial or financial relationships that could be construed as a potential conflict of interest.

Publisher's note

References

1. Binnewies M, Roberts EW, Kersten K, Chan V, Fearon DF, Merad M, et al. Understanding the tumor immune microenvironment (TIME) for effective therapy. *Nat Med*. (2018) 24:541–50. doi: 10.1038/s41591-018-0014-x

2. Zongyi Y, Xiaowu L. Immunotherapy for hepatocellular carcinoma. *Cancer Lett*. (2020) 470:8–17. doi: 10.1016/j.canlet.2019.12.002

3. Rezaei M, Danilova ND, Soltani M, Savvateeva LV, Tarasov VV, Ganjalikhani-Hakemi M, et al. Cancer vaccine in cold tumors: clinical landscape, challenges, and opportunities. *Curr Cancer Drug Targets*. (2022) 22:437–53. doi: 10.2174/1568009622666220214103533

4. Mehta A, Kim YJ, Robert L, Tsoi J, Comin-Anduix B, Berent-Maoz B, et al. Immunotherapy resistance by inflammation-induced dedifferentiation. *Cancer Discovery*. (2018) 8:935–43. doi: 10.1158/2159-8290.CD-17-1178

5. Adamaki M, Zoumpourlis V. Immunotherapy as a precision medicine tool for the treatment of prostate cancer. *Cancers*. (2021) 13:173. doi: 10.3390/cancers13020173

frontiers | Frontiers in Immunology

TYPE Original Research
PUBLISHED 30 June 2023
DOI 10.3389/fimmu.2023.1209572

OPEN ACCESS

EDITED BY
Mazdak Ganjalikhani Hakemi,
Isfahan University of Medical Sciences, Iran

REVIEWED BY
Mohammad Hossein Kazemi,
University of Southern California,
United States
Mahzad Akbarpour,
University of Chicago Medicine,
United States

*CORRESPONDENCE
Hamid Reza Mirzaei
h-mirzaei@tums.ac.ir
Christine E. Brown
cbrown@coh.org

RECEIVED 20 April 2023
ACCEPTED 13 June 2023
PUBLISHED 30 June 2023

CITATION
Akbari B, Soltantoyeh T, Shahosseini Z, Jadidi-Niaragh F, Hadjati J, Brown CE and Mirzaei HR (2023) PGE2-EP2/EP4 signaling elicits mesoCAR T cell immunosuppression in pancreatic cancer.
Front. Immunol. 14:1209572.
doi: 10.3389/fimmu.2023.1209572

PGE2-EP2/EP4 signaling elicits mesoCAR T cell immunosuppression in pancreatic cancer

Behnia Akbari[1], Tahereh Soltantoyeh[1], Zahra Shahosseini[2,3], Farhad Jadidi-Niaragh[4], Jamshid Hadjati[1], Christine E. Brown[5,6]* and Hamid Reza Mirzaei[1,7,8]*

[1]Department of Medical Immunology, School of Medicine, Tehran University of Medical Sciences, Tehran, Iran, [2]Department of Medical Biotechnology, School of Allied Medical Sciences, Iran University of Medical Sciences, Tehran, Iran, [3]Virology Department, Pasteur Institute of Iran, Tehran, Iran, [4]Department of Immunology, Faculty of Medicine, Tabriz University of Medical Sciences, Tabriz, Iran, [5]Department of Hematology & Hematopoietic Cell Transplantation, City of Hope Medical Center, Duarte, CA, United States, [6]Department of Immuno-Oncology, City of Hope Beckman Research Institute, Duarte, CA, United States, [7]Department of Genetics, University of Pennsylvania Perelman School of Medicine, Philadelphia, PA, United States, [8]Institute for Immunology and Immune Health, University of Pennsylvania Perelman School of Medicine, Philadelphia, PA, United States

Introduction: For many years, surgery, adjuvant and combination chemotherapy have been the cornerstone of pancreatic cancer treatment. Although these approaches have improved patient survival, relapse remains a common occurrence, necessitating the exploration of novel therapeutic strategies. CAR T cell therapies are now showing tremendous success in hematological cancers. However, the clinical efficacy of CAR T cells in solid tumors remained low, notably due to presence of an immunosuppressive tumor microenvironment (TME). Prostaglandin E2, a bioactive lipid metabolite found within the TME, plays a significant role in promoting cancer progression by increasing tumor proliferation, improving angiogenesis, and impairing immune cell's function. Despite the well-established impact of PGE2 signaling on cancer, its specific effects on CAR T cell therapy remain under investigation.

Methods: To address this gap in knowledge the role of PGE2-related genes in cancer tissue and T cells of pancreatic cancer patients were evaluated *in-silico*. Through our *in vitro* study, we manufactured fully human functional mesoCAR T cells specific for pancreatic cancer and investigated the influence of PGE2-EP2/EP4 signaling on proliferation, cytotoxicity, and cytokine production of mesoCAR T cells against pancreatic cancer cells.

Results: *In-silico* investigations uncovered a significant negative correlation between PGE2 expression and gene signature of memory T cells. Furthermore, *in vitro* experiments demonstrated that the activation of PGE2 signaling through EP2 and EP4 receptors suppressed the proliferation and major antitumor functions of mesoCAR T cells. Interestingly, the dual blockade of EP2 and EP4 receptors effectively reversed PGE2-mediated suppression of mesoCAR T cells, while individual receptor antagonists failed to mitigate the PGE2-induced suppression.

Discussion: In summary, our findings suggest that mitigating PGE2-EP2/EP4 signaling may be a viable strategy for enhancing CAR T cell activity within the challenging TME, thereby improving the efficacy of CAR T cell therapy in clinical settings.

KEYWORDS

mesoCAR T cell, pancreatic cancer, pharmacological targeting, prostaglandin E2, EP2, EP4

Introduction

Pancreatic ductal adenocarcinoma (PDAC), the most prevalent form of pancreatic cancer, is associated with a highly unfavorable prognosis and poor overall survival rates (1, 2). Recent data indicate an increasing prevalence of PDAC, with over 60% of patients presenting with advanced metastatic disease and a median overall survival ranging from 8 to 11 months under current chemotherapeutic regimens (3, 4). Despite localized tumor presentation, the majority of patients eventually progress to metastatic disease. Thus, the development of effective systemic therapies is crucial for improving clinical outcomes in pancreatic cancer patients.

Immunotherapeutic approaches have emerged as a unique treatment option in various solid and hematologic cancers. A promising immunotherapeutic approach involves T cells engineered to express chimeric antigen receptors (CARs), which have shown remarkable clinical utility in treating hematological malignancies (5). Notably, several clinical trials utilizing CAR T cells in solid tumors, including pancreatic cancer, have reported promising therapeutic outcomes (6, 7). Among the different types of CAR T cells developed for solid tumors, mesoCAR T cells have demonstrated specific killing ability against pancreatic tumor cells in both *in vitro* and *in vivo* settings (8). These mesoCAR T cells are designed to target mesothelin (MSLN), a tumor-associated antigen with minimal or negligible expression in healthy cells, making it an ideal target for CAR T cell therapy in pancreatic cancer (8, 9). However, despite the development of mesoCAR T cells, their clinical success in treating pancreatic cancer has been modest, largely due to the highly immunosuppressive tumor microenvironment (TME) (10). The TME contains various metabolic immunosuppressive molecules produced by stromal cells, tumor cells, and infiltrating immune cells, which contribute to immune suppression (11, 12).

Prostaglandins (PGs), bioactive lipid metabolites generated from arachidonic acid by key enzymes such as cyclooxygenases (COXs) and PGE synthases, play a significant role in suppressing the antitumor immune response (11, 13). In fact, PG synthesis inhibitors, such as nonsteroidal anti-inflammatory drugs (NSAIDs), have demonstrated prophylactic and therapeutic advantages in cancer patients (14). Among the PGs, prostaglandin E2 (PGE2) is the most abundant in several tumors, particularly in pancreatic cancer (15–17). PGE2 exerts its functions through four G protein-coupled receptors: EP1, EP2, EP3, and EP4 (18). PGE2 has been shown to promote tumor cell proliferation, invasiveness, and tumor-associated angiogenesis, while also reprogramming myeloid cells into tumor-associated macrophages (TAMs) with an M2 phenotype. Furthermore, PGE2 suppresses the production of interferon-gamma (IFN-γ) by Natural Killer cells (NK cells) and T cells (19–21). Among the four cognate receptors of PGE2, EP2 and EP4 receptors, which increase intracellular cyclic AMP (cAMP) and protein kinase A (PKA) phosphorylation upon PGE2 ligation, have been implicated in cancer development and the suppression of antitumor immune responses (22, 23). While previous studies have provided insights into the potential actions of PGE2 in the TME and its effects on T cells, they have neither revealed the association between PG-related genes expression and PDAC development and patients' survival nor addressed the role of PGE2 signaling on antitumor function of mesoCAR T cells in context of pancreatic cancer.

To address these questions, we investigated the effects of PGE2 on patient survival and identified correlations between PGE2-related gene expression and different T cell phenotypes. Additionally, to simulate PGE2-mediated immunosuppression within the TME, we cultured T cells and mesoCAR T cells in presence of PGE2 and evaluated the immunosuppressive effects of PGE2 on these cells. Lastly, we assessed the impact of pharmacologically targeting PGE2-mediated immunosuppression using specific PGE2 receptor antagonists on the function of mesoCAR T cells *in vitro*.

Material and methods

Bioinformatics analyses

Differentially expressed genes (DEGs) were extracted from the Cancer Genome Atlas (TCGA) dataset using the GEPIA2 database (http://gepia2.cancer-pku.cn) (24). The DEGs in pancreatic ductal adenocarcinoma were obtained by applying the "Differential Genes" module of GEPIA2, with the dataset set to PAAD and the

Abbreviations: cAMP, Cyclic AMP; CAR T cells, Chimeric antigen receptors; IFN-γ, Interferon-gamma; mesoCAR T, Fully human anti-mesothelin CAR T cells; NK cell, Natural Killer cells; PGE2, Prostaglandin E2; PKA, Protein Kinase A; TME, Tumor microenvironment.

differential method set to ANOVA. VolcaNoseR was used to visualize the extracted DEGs (25). GEPIA2 was also utilized to determine Overall Survival and Disease-Free Survival of PAAD patients. The "Survival Analysis" module was employed with Group Cutoff set to the median. Hazard ratios (HRs) with 95% confidence intervals (CIs) and log-rank P-values were calculated. The "Correlation Analysis" module of GEPIA2 was employed to identify the correlation between the gene signature of different phenotypes of T cells and PGE-related genes, using tumor and normal TCGA datasets for PDAC patients. The HPA (Human Protein Atlas "proteinatlas.org") database was used to obtain the single-cell expression of PGE receptors (EP2/EP4) in different cells under physiological conditions (26).

Cell lines

HEK293T, Jurkat, AsPC-1, and PANC-1 cells were obtained from the Iranian Biological Resource Center (IBRC). HEK293T and PANC-1 cells were cultured in D10 media, composed of DMEM (Gibco, Life Technologies), 10% fetal bovine serum (FBS), and 1% penicillin/streptomycin (Gibco, Life Technologies). AsPC-1 and Jurkat cells were cultured in R10 media, consisting of RPMI-1640 (Gibco, Life Technologies) supplemented with 10% FBS, 25 mM HEPES (Sigma Aldrich), 2 mM glutamine (Gibco), and 1% penicillin/streptomycin. Prior to experiments, mesothelin expression was authenticated by flow cytometry on the relevant cell lines. All cell lines were regularly tested for mycoplasma contamination.

Lentiviral vector production

Lentiviral vectors were produced as previously described (27). Briefly, HEK293T cells were transfected with lentiviral CAR and packaging plasmids using the calcium phosphate method. Lentiviral supernatants were collected at 48- and 72-hours post-transfection and concentrated through high-speed centrifugation. The resulting concentrated lentivirus batches were then resuspended in cold RPMI-1640 media and stored at -80°C. Lentiviral vectors were titrated using Jurkat cells.

T cell isolation and CAR T cell manufacturing

Healthy donor white blood cells were obtained from the Iranian Blood Transfusion Organization (IBTO). Peripheral blood mononuclear cells (PBMCs) were isolated using standard methods with Histopaque®-1077 (Sigma Aldrich). T cells were negatively selected using immunomagnetic beads (Pan T Cell Isolation Kit, Miltenyi Biotec) and stored at -80°C. For mesoCAR T cell production, 1×10^6 T cells were seeded in each well of 12-well Costar tissue culture plates and activated using Dynabeads™ Human T-Expander CD3/CD28 (Gibco, Life Technologies, 11161D) at a 1:1 ratio in TM10 media, which consisted of TexMACS™ Medium (Miltenyi Biotec) supplemented with 10% AB serum and 100 IU/mL premium-grade rhIL-2 (Miltenyi Biotec). Twenty-four hours post-activation, lentiviral vectors supplemented with 8 µg/mL Polybrene (Santacruz) were added to the early activated T cells at a multiplicity of infection (MOI) of five. Centrifugation at 850g for 1 hour at 32°C was performed to enhance transduction efficacy. Two hours after centrifugation, 2 mL/well of TM10 media were added to the transduced T cells. At day 4 post-transduction, Dynabeads™ were removed from the transduced T cells using a DynaMag™ magnet, and GFP expression, as a representative of mesoCAR expression, was assessed using flow cytometry.

PGE2, PF-04418948, and E7046 dose-response

To determine the most effective concentration of PGE2 (MedChemExpress), PF-04418948 (MedChemExpress), and E7046 (Cayman Chemical), 1×10^5 CFSE-labeled T cells were seeded in 96-well Costar tissue culture plates and cultured with various doses of PGE2, PF-04418948, and E7046. The cells were activated with Dynabeads™ Human T-Expander CD3/CD28 (Gibco, Life Technologies, 11161D) at a 1:1 ratio in TM10 media. After three days, T cells were harvested, and their proliferation was determined using flow cytometry.

In vitro cytotoxicity assay

mesoCAR T cells and untransduced T cells were co-incubated at 1:1, 5:1, 10:1, and 30:1 ratios with 1×10^4 CFSE stained target cells for 4 hours in TM10 media in 96-well U-bottomed plates, with a final volume of 200 µl/well. To distinguish between effector and target cells, the cell suspension was harvested and stained with anti-human CD3 conjugated with APC (Clone: UCHT1, BioLegend). To stain for dead cells, 7-AAD (Miltenyi Biotec) was added 30 minutes before flow cytometry. Flow cytometry analysis was performed using CFSE, CD3 and 7-AAD staining to distinguish T cells from dead tumor cells. The frequency of lysed target cells (CFSE+/CD3-/7-AAD+ cells) was calculated by subtracting the percentage of spontaneous lysis of target cells from the percentage of target cells in coculture with mesoCAR T cells. Specific lysis was reported by normalizing target cell lysis based on the expression of mesothelin on target cells.

In vitro proliferation and cytokine production assays

Target cells were treated with 50 µg/ml of mitomycin C (Sigma Aldrich) for 30 minutes at 37°C and extensively washed (28). To track cell proliferation using CFSE dye (Life Technologies), mesoCAR T cells and untransduced T cells (1.2×10^7/ml) were stained with 5 µM CFSE at room temperature for 8 minutes. The reaction was terminated by adding an equal amount of FBS. After

washing three times with complete RPMI 1640 medium, CFSE-labeled cells (0.2×10^6/well) were cocultured at a 1:1 ratio with either target cells or cultured in media (without target cells) in the absence of exogenous IL-2 in 48-well plates, with a final volume of 800 µl/well. The supernatant was harvested 24 hours after plating and stored at −20°C until subsequent cytokine analysis by enzyme-linked immunosorbent assay (ELISA) to quantify IFN-γ and IL-2. After 72 hours, cells were stained with anti-CD3-APC (Clone: UCHT1, BioLegend), and CFSE dilution of CD3+ cells, as a measure of proliferation, was determined by flow cytometry, as previously described (29).

Flow cytometric analysis

To check the purity of isolated T cells using magnetic beads, isolated T cells were stained with APC-conjugated anti-human CD3 (Clone: UCHT1, BioLegend). Mesothelin expression was detected using PE-conjugated anti-human mesothelin (Clone: #420411, R&D Systems). All samples were acquired with a BD FACSCalibur (BD Biosciences) and analyzed using FlowJo software (v10.6). All assays were performed in duplicate and repeated two to three times.

Statistical analysis

Normality tests, one-way and two-way analysis of variance (ANOVA), were used to identify possible differences among different treatment groups using GraphPad Prism software (v9). p-values less than 0.05 were considered statistically significant.

Results

Prostaglandin E2 and its receptors may modulate T cell responses in pancreatic cancer patients

To investigate the significance of PG-related genes in PDAC, we utilized Gepia2 and VolcaNoseR to extract and visualize differentially expressed genes (DEGs). Our data indicate that prostaglandin E synthase and prostaglandin-endoperoxide synthase genes, including PTGES, PTGES2, PTGES3, PTGS1, and PTGS2, are highly enriched in PDAC patients (Figure 1A). However, among the prostaglandin receptors, only the PTGER2 (EP2) gene showed upregulation, while PTGER1, PTGER3, and PTGER4 exhibited no significant change in expression in PDAC patients. Next, to determine the prognostic value of PG-related genes, we conducted Kaplan-Meier survival analyses using Gepia2. Our findings suggest that elevated expression of prostaglandin synthesis enzymes is an unfavorable prognostic marker for PDAC patients. Specifically, high expression of PTGES and PTGES3 significantly decreases overall survival of patients (Figures 1B, C). Moreover, high PTGES expression significantly decreases disease-free survival of patients (Figure 1D). Although not statistically significant, patients with higher expression of PTGS1 and PTGS2 genes, as well as genes corresponding to prostaglandin receptors, showed decreased overall survival and disease-free survival (Figures S1A–S1L).

To further understand the role of prostaglandin E signaling in immune cells, we utilized single-cell RNA-seq data from the Human Protein Atlas. According to these data, EP1 and EP3 receptors have no to low expression in T cells (Data not shown). However, EP2 and EP4 are highly expressed in immune cells, especially T cells (Figures 1E, F), with EP4 being part of a cluster related to T cell immune response and showing the highest correlation (0.8687) with the PD1 gene (Figure 1G). Based on single-cell RNA-seq data, ICOS, IL7R, CCR7, CTLA4, CCR8, and FAS are also immunologically important genes in the neighborhood of the EP4 receptor (Figure 1G). Previous studies have indicated that PGE2 ligation with EP2 and EP4 receptors can promote immunosuppression in T cells by inhibiting IL-2 production, reducing CD25 expression, and, most importantly, impairing IFN-γ secretion and T cell effector function (11, 23). Therefore, we conducted several correlation analyses to elucidate the role of prostaglandin E2 receptor signaling in promoting T cell immunosuppression. Our results demonstrate that PGE2 expression is negatively correlated with the gene signature of central memory (Figure 1H) and effector memory (Figure 1I) T cells. This negative correlation was also observed in the gene signature related to effector T cells (Figure 1J). Interestingly, a significant positive correlation was observed between the gene signatures of central memory, effector memory, and exhausted T cells with EP2 and EP4 receptors (Figure S2). These data collectively indicate that PGE2 and its immunoinhibitory receptors (EP2 and EP4) can possibly modulate T cell responses in PDAC patients.

PGE2 suppresses T cell proliferation through EP2/EP4 signaling

T cell expansion and proliferation are key determinants of successful cellular therapy in clinical settings (30). Previous reports have demonstrated that low concentrations of PGE2 are essential for T cell activation and differentiation (31), whereas higher concentrations of PGE2 (>1 µM), commonly found at the tumor site, induce subversion of CD8 differentiation, suppression of T cell proliferation, and inhibition of CD4 T cell helper functions (23). Therefore, to understand the function of PGE2 on T cell proliferation through EP2 and EP4 receptor signaling and determine suitable doses for our study, we exposed T cells activated with anti-CD3/CD28 coated beads to different concentrations of PGE2 and orally available EP2 and EP4 antagonists, PF-04418948 and E7046, respectively. Our findings suggest that PGE2 can decrease antigen-nonspecific T cell proliferation in a dose-dependent manner, with 10 µM of PGE2 demonstrating maximal efficacy in inhibiting T cell proliferation (Figures 2A, B).

Next, to determine if pharmacological blockade of EP2 and EP4 receptors can diminish the inhibitory effects of PGE2, we used different concentrations (ranging from 0.01 µM to 10 µM) of PF-04418948 or E7046 in cultures of T cells treated with 10 µM of

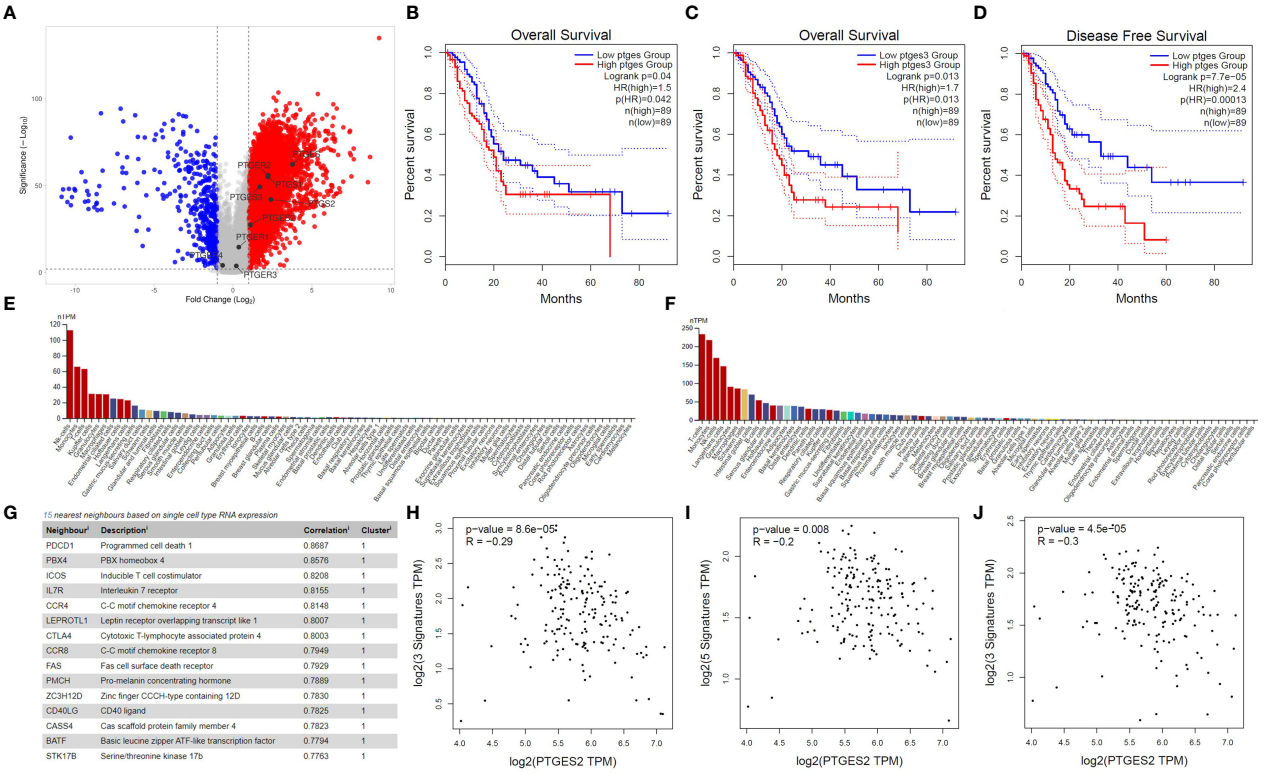

Neighbour	Description	Correlation	Cluster
PDCD1	Programmed cell death 1	0.8687	1
PBX4	PBX homeobox 4	0.8576	1
ICOS	Inducible T cell costimulator	0.8208	1
IL7R	Interleukin 7 receptor	0.8155	1
CCR4	C-C motif chemokine receptor 4	0.8148	1
LEPROTL1	Leptin receptor overlapping transcript like 1	0.8007	1
CTLA4	Cytotoxic T-lymphocyte associated protein 4	0.8003	1
CCR8	C-C motif chemokine receptor 8	0.7949	1
FAS	Fas cell surface death receptor	0.7929	1
PMCH	Pro-melanin concentrating hormone	0.7889	1
ZC3H12D	Zinc finger CCCH-type containing 12D	0.7830	1
CD40LG	CD40 ligand	0.7825	1
CASS4	Cas scaffold protein family member 4	0.7823	1
BATF	Basic leucine zipper ATF-like transcription factor	0.7794	1
STK17B	Serine/threonine kinase 17b	0.7763	1

FIGURE 1
Bioinformatics investigation of PGE2 genes in pancreatic cancer. **(A)** Volcano plot illustrating the differential expression of genes in pancreatic cancer patients compared to healthy samples, with a focus on PGE2-related genes. **(B, C)** Kaplan-Meier survival curves showing the overall survival time of patients with high expression of PTGES and PTGES3 compared to patients with low expression. **(D)** Kaplan-Meier survival curve demonstrating the disease-free survival time in patients with high expression of PTGES compared to patients with low expression. Dotted lines represent the 95% confidence interval in the Kaplan-Meier plots. **(E, F)** Immunohistochemistry data from the Human Protein Atlas (HPA) showing high expression of EP2 and EP4 receptors on T cells. **(G)** List of genes showing a significant correlation with EP4 receptor expression in T cells. **(H–J)** Scatter plots depicting the negative correlation between PTGES2 expression and gene signatures of central memory **(H)**, effector memory **(I)**, and effector T cells **(J)** in pancreatic cancer patients.

PGE2 and activated by anti-CD3/CD28 coated beads. Interestingly, pharmacological blockade of these receptors enhances T cell proliferation in a dose-dependent manner. Based on dose-response analyses, a 0.1 μM dose of PF-04418948 (Figures 2C, D) and a 1 μM dose of E7047 (Figures 2E, F) show maximal efficacy in enhancing T cell proliferation. However, single pharmacological blockade of these receptors fails to fully eliminate the inhibitory function of PGE2 on antigen-nonspecific T cell proliferation.

Manufacturing and functional characterization of fully human MesoCAR T cells against pancreatic cancer cell lines

Primary human CD3+ T cells were efficiently infected with replication-defective lentiviral particles encoding the second-generation mesoCAR transgene at an MOI of 5, with reproducible transduction efficacy of approximately 30% (Figure 3A). To further characterize and measure the *in vitro* antitumor capacity of the produced mesoCAR T cells, we utilized PANC-1 and AsPC-1 cells as mesothelin-negative and positive pancreatic cancer cells in our experiments (Figures 3B, C).

The cytolytic abilities of T cells expressing the mesoCAR transgene were evaluated using a 4-hour CD3/7AAD-based cytotoxicity assay. Genetically modified mesoCAR T cells specifically lysed mesothelin+ AsPC-1 cells. We observed antigen-specific lysis of AsPC-1 cells even at an E:T ratio as low as 1:1 (Figure 3D). Lysis of PANC-1 cells by mesoCAR T cells and lysis of AsPC-1 cells by untransduced T cells were not detected, demonstrating the antigen specificity of the cytolysis and the lack of natural activity of the generated mesoCAR T cells (Figure 3D). T cell proliferation and cytokine production are two other key components in the generation of a robust and sustained antitumor immune response. To assess whether the designed mesoCAR T cells can proliferate and produce cytokines against pancreatic cancer cells, we investigated the proliferation capacity of mesoCAR T cells and their production of IL-2 and IFN-γ compared to untransduced T cells upon antigen-specific stimulation *in vitro*. Following CAR T cell restimulation with AsPC-1 and PANC-1 cells, T cells expressing the mesoCAR exhibited a significantly high mesothelin-specific proliferation rate comparable to untransduced T cells stimulated *via* the endogenous TCR (Figures 3E, F). Cytokine measurements using ELISA following mesoCAR activation with AsPC-1 cells revealed that CAR T cells produce large quantities of IFN-γ and IL-

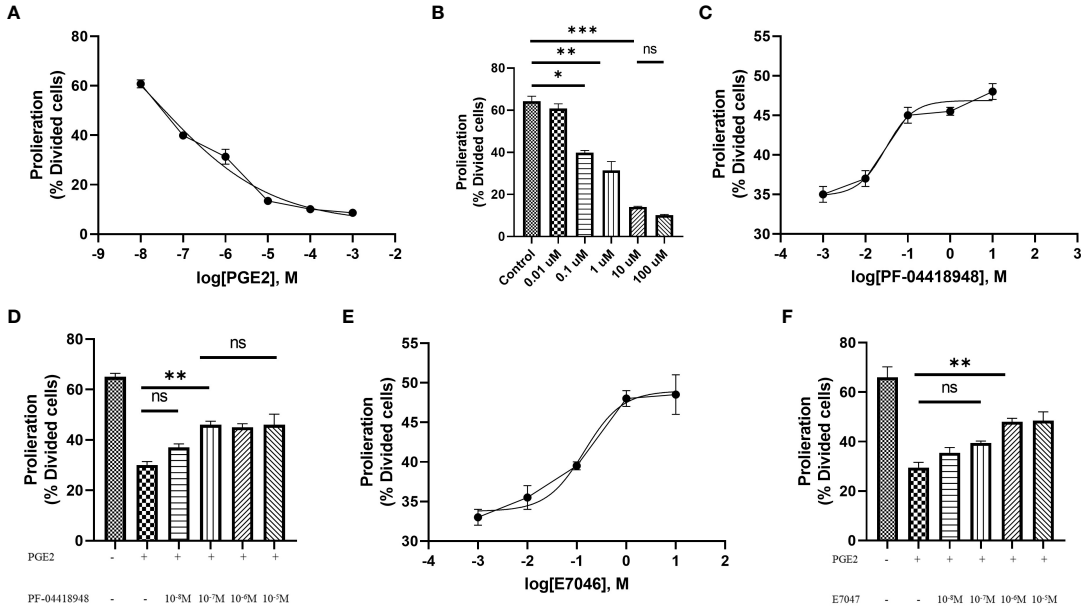

FIGURE 2
Antigen-independent proliferation of T cells in culture with PGE2 and EP2/4 antagonists. **(A)** Dose-response analysis of T cell proliferation mediated by CD3/28 stimulation in the presence of various concentrations of PGE2. **(B)** Significant inhibition of T cell proliferation by PGE2 at concentrations of 0.1, 1, and 10 μM. **(C)** Dose-response analysis of T cell proliferation in the presence of 10 μM PGE2 and different concentrations of PF-04418948, an EP2/4 antagonist. **(D)** Significant reversal of PGE2-mediated suppression of T cell proliferation by PF-04418948 at a concentration of 0.1 μM. **(E)** Dose-response analysis of antigen-independent proliferation of T cells in the presence of 10 μM PGE2 and various concentrations of E7046, an EP4 antagonist. **(F)** Significant enhancement of T cell proliferation by 1 μM E7046 in the presence of 10 μM PGE2. Statistical analysis was performed using ordinary one-way ANOVA and Tukey multiple comparison test. *P < 0.05; **P < 0.01; ***P < 0.001. Data are presented as mean ± SD.

2, comparable to untransduced T cells (Figures 3G,H). No IL-2 and IFN-γ secretion was detected in cultures of T cells or tumor cells alone or irrelevant target cells (PANC-1). This shows that T cell activation through the mesoCAR could lead to the induction of mesothelin-specific IL-2 and IFN-γ production. The cytokine production pattern aligns with the Th1-like phenotype of T cells generated by anti-CD3 and CD28-coated beads and, thereby, supports an effective antitumor cellular immune response (32).

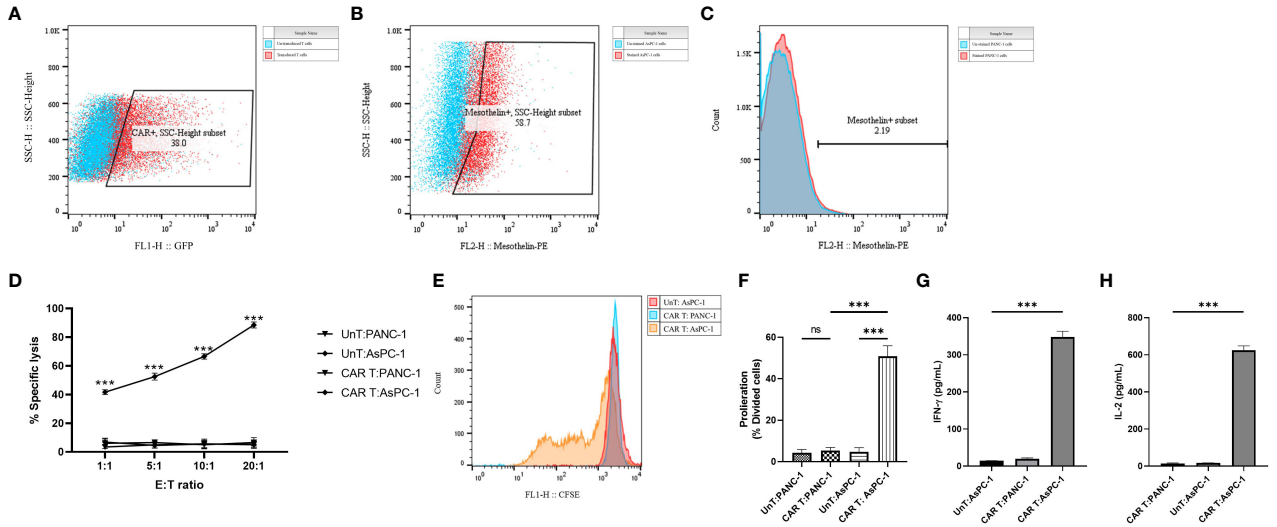

FIGURE 3
Antigen specificity of mesoCAR T cells against pancreatic cancer cells. **(A)** Flow cytometry dot plot demonstrating the expression of the chimeric antigen receptor (CAR) on mesoCAR T cells after manufacturing. **(B, C)** Representative dot and histogram plots showing the mesothelin expression on AsPC-1 and PANC-1 cells, respectively. **(D)** Specific lysis of target cells by mesoCAR T cells at different effector-to-target ratios. **(E, F)** Proliferation of mesoCAR T cells in response to target cells. **(G, H)** Production of IFN-γ and IL-2 by mesoCAR T cells in coculture with target cells. Statistical analysis was performed using ordinary one-way ANOVA **(E–H)** and two-way ANOVA **(D)** followed by Tukey multiple comparison test. ***P < 0.001. Data are presented as mean ± SD.

PGE2 signaling through EP2/EP4 receptors diminishes MesoCAR T cell antitumor function

To investigate the role of PGE2 in antigen-specific immunosuppression, we aimed to measure the proliferation capacity, cytotoxic function, and cytokine production of mesoCAR T cells in coculture with AsPC-1 cells using different concentrations of PGE2, PF-04418948, and E7046. Our findings suggest that PGE2 at a dose of 10 μM significantly decreases the proliferation of mesoCAR T cells. Interestingly, the addition of EP2 has no significant impact on mesoCAR T cell proliferation. Although EP4 blockade alone significantly enhances mesoCAR T cell proliferation, it fails to fully restore mesoCAR T cell proliferation (Figure 4A). In contrast, the double pharmacological blockade of these receptors successfully removes the inhibitory effects of PGE2 on mesoCAR T cell proliferation (Figure 4A).

Furthermore, PGE2 was found to inhibit the cytotoxic function of mesoCAR T cells against pancreatic cancer cells, even at low ratios such as 1:1 (Figure 4B). The blockade of the EP2 receptor in the presence of PGE2 was shown to slightly enhance mesoCAR T cell cytotoxicity at 10:1 and 20:1 ratios (Figure 4C). Interestingly, EP4 blockade was shown to improve mesoCAR T cell cytotoxicity even at low ratios (5:1), indicating that EP4 signaling is more important for mesoCAR T cell cytotoxic function against pancreatic cancer cells (Figure 4D). Additionally, the double blockade of EP2 and EP4 receptors was shown to completely restore the cytotoxic function of mesoCAR T cells in the presence of PGE2 (Figure 4E).

Lastly, it was observed that PGE2 is able to suppress both IFN-γ and IL-2 production from mesoCAR T cells (Figures 4F, G). Although EP2 blockade alone fails to enhance IL-2 production from mesoCAR T cells in the presence of PGE2, EP4 blockade and the double blockade of these receptors improve the production of IL-2 against tumor cells in the presence of PGE2 (Figure 4F). In terms of IFN-γ, EP4 targeting showed the greatest impact on IFN-γ production (Figure 4G). Overall, simultaneous pharmacological blockade of EP2 and EP4 receptors boosted IFN-γ and IL-2 production from mesoCAR T cells in the presence of PGE2.

Discussion

The hostile and complex TME surrounding PDAC tumors poses a significant challenge to the effectiveness of adoptive cellular therapy. This TME is characterized by a dense desmoplastic stroma and the presence of immunosuppressive metabolites, along with extensive infiltration of immunosuppressive cells such as tumor-associated macrophages (TAMs), myeloid-derived suppressor cells (MDSCs), and regulatory T cells (33). In this study, our aim was to investigate the role of a bioactive metabolite, prostaglandin E2 (PGE2), in the context of PDAC.

Our *in-silico* analyses revealed a significant upregulation of PG-related genes in PDAC tumors, and we observed a negative correlation between the expression of Prostaglandin E Synthase (PTGES) and the survival rate of PDAC patients. Additionally, we identified a strong negative correlation between PTGE2 expression

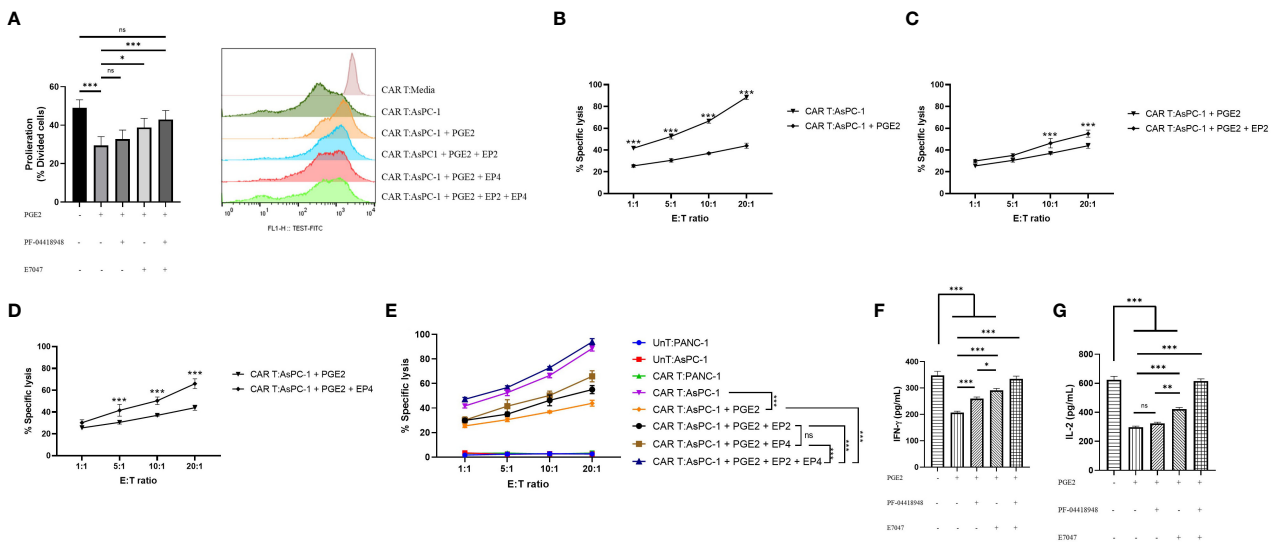

FIGURE 4
The effects of PGE2-EP2/EP4 signaling on the antitumor function of mesoCAR T cells. **(A)** Antigen-specific proliferative capacity of mesoCAR T cells over a three-day period in the presence of PGE2 alone or in combination with EP2 and/or EP4 antagonists. **(B)** Specific lysis of AsPC-1 cells by mesoCAR T cells in the presence of 10 μM PGE2. **(C, D)** Cytotoxic function of mesoCAR T cells against AsPC-1 cells after blockade of EP2 **(C)** and EP4 **(D)** receptors. **(E)** Overlaid plot demonstrating mesoCAR T cell cytotoxicity against AsPC-1 cells in the presence of PGE2 alone or in combination with EP2 and/or EP4 antagonists. **(F, G)** Production of IFN-γ and IL-2 by mesoCAR T cells in coculture with AsPC-1 cells in the presence of PGE2 alone or in combination with EP2 and/or EP4 antagonists. Statistical analysis was performed using ordinary one-way ANOVA **(A, F, G)**, two-way ANOVA **(B–E)**, and Tukey multiple comparison test. *P < 0.05; **P < 0.01; ***P < 0.001. Data are presented as mean ± SD.

and effector and memory T cells in PDAC. We also found a strong positive correlation between the expression of the EP4 receptor and PD-1 in T cells, suggesting a potential combination therapy involving PD-1 blockade and inhibition of PGE2 signaling. Consistent with our findings, previous studies have demonstrated that high expression of PGE2 and activation of EP2/EP4 signaling not only increase PD-1 expression in T cells (34) but also promote PD-L1 expression in TAMs and MDSCs, which are highly abundant suppressive cells in PDAC (35). Further investigations revealed that PGE2 promotes the expression and secretion of ARG1 and iNOS in MDSCs, while pharmacological blockade of EP4 inhibits the secretion of these proteins, thereby inhibiting the function of MDSCs (36).. Recent studies have shown that combining EP4 blockade with anti-PD-1 immunotherapy synergistically enhances the antitumor response of tumor-specific cytotoxic T lymphocytes (CTLs) (35, 37).

Subsequently, through our sets of *in vitro* studies on mesoCAR T cells we demonstrate that PGE2 signaling through EP2 and EP4 receptors is responsible for limited antitumor function of these cells in PGE2-rich tumors. From a mechanistical point of view, EP2/EP4 downstream signaling in T cells were previously shown to initiate and activate PKA and PI3K signaling pathways, leading to cAMP accumulation and dysregulation of the AKT/mTOR pathway within T cells, respectively (11, 23). It has been previously shown that accumulation of cAMP in T cells impairs their normal function, resulting in T cell dysfunction in chronic infections and tumors (38). Moreover, reducing cAMP accumulation through targeting upstream molecules, such as the A2a receptor, has shown promising results in CAR T cells by empowering CAR T cells antitumor properties (39–41). Additionally, blocking the PKA pathway, for example through AKT inhibition, in CAR T cells has led to improved CAR T cell persistence, proliferation, and effector function both *in vitro* and *in vivo* (42–45). These results altogether suggests that mesoCAR T cell therapy in combination with EP2/EP4 antagonists can achieve improved preclinical and clinical responses in PDAC.

The presence of tumor-infiltrating T cells and CAR T cells is indicative of tumor immunosurveillance and holds significant therapeutic and prognostic relevance (46). However, the dense desmoplastic stroma, which constitutes nearly 50% of the total tumor mass in PDAC, acts as a barrier to the infiltration of antitumor immune cells such as CAR T cells (47). Notably, previous studies have demonstrated that pharmacological blockade of EP4 improves the infiltration of tumor-specific T cells into the tumor site and promotes tumor rejection in a colorectal cancer syngeneic mouse model (35). Clinical data from patients with advanced tumors showing high MDSC infiltration who received daily doses of the EP4 antagonist E7046 as monotherapy demonstrated stable disease for more than 18 weeks, increased serum levels of CXCL10 (a T cell recruiting chemokine), and improved infiltration of CD3+ cells into the tumor site (48). Single-cell data from prostate cancer patients revealed EP4 as a universal marker of T cell exhaustion, and targeting the EP4 receptor was able to restore T cell infiltration into the TME and promote the proliferation of tumor-specific T cells (36). Most recently, a dual EP2/EP4 antagonist called TPST-1495 is currently being evaluated as a single agent and in combination with pembrolizumab in a clinical trial (NCT04344795). According to preliminary and unpublished data, TPST-1495 has shown the ability to block PGE2-mediated suppression of T cells, significantly enhance IFN-γ production in response to cognate peptide antigen, reduce tumor outgrowth in mouse models of solid tumors, and increase the infiltration of cytotoxic NK cells and tumor-specific and non-specific T cells at the tumor site (49). Collectively, pharmacological blockade of these two receptors holds great promise in combination with CAR T cell therapy, particularly in immunologically cold tumors such as pancreatic cancer.

Limitations of our study include the focus on PGE2 and its interaction with specific receptors (EP2 and EP4) without considering other immunosuppressive factors and signaling pathways within the tumor microenvironment. Furthermore, through our study we primarily relied on *in vitro* experiments using cell lines and isolated T cells, which may not fully capture the complexity and dynamics of the immune system in the human body. *In vivo* validation of the findings is lacking, and the clinical relevance of the observed effects and therapeutic implications requires further investigation through preclinical and clinical studies. Finally, future studies should extensively explore potential confounding factors such as other soluble mediators, genetic variations, or the heterogeneity of T cell populations, which could influence the observed effects in our study.

Conclusions

In conclusion, our study elucidates the roles of PGE2 and its receptors EP2 and EP4 in the immunosuppressive TME of PDAC. The findings highlight the potential of targeting PGE2 signaling pathways as a strategy to enhance the antitumor function of CAR T cells and improve therapeutic responses in PDAC. Further research is warranted to validate these findings in *in vivo* models and clinical settings, and to explore the combination of EP2/EP4 antagonists with immunotherapies such as PD-1 blockade for enhanced efficacy.

Data availability statement

The original contributions presented in the study are included in the article/Supplementary Material. Further inquiries can be directed to the corresponding authors.

Ethics statement

The studies involving human participants were reviewed and approved by the Research Ethics Committees of the School of Medicine, Tehran University of Medical Sciences [IR.TUMS.MEDICINE.REC.1399.876]. The patients/participants provided their written informed consent to participate in this study.

Author contributions

Conception and design of studies: BA, CB, and HM. Acquisition, analysis and interpretation: BA, TS, ZS, and FJ-N. Drafting article: BA. Critical review and discussion: BA, CB, JH, and HM. All authors contributed to the article and approved the submitted version.

Funding

Research reported in this publication was supported by Tehran University of Medical Sciences (grants nos. 50756 and 50760, awarded to HM).

Conflict of interest

The authors declare that the research was conducted in the absence of any commercial or financial relationships that could be construed as a potential conflict of interest.

Publisher's note

Supplementary material

The Supplementary Material for this article can be found online at: https://www.frontiersin.org/articles/10.3389/fimmu.2023.1209572/full#supplementary-material

SUPPLEMENTARY FIGURE 1
Survival plots of PDAC patients. **(A-F).** Kaplan-Meier survival curves showing the overall survival time of patients with high expression of PTGS1 **(A)**, PTGS2 **(B)**, PTGER1 **(C)**, PTGER2 **(D)**, PTGER3 **(E)**, and PTGER4 **(F)** compared to patients with low expression. **(G-L).** Kaplan-Meier survival curve demonstrating the disease-free survival time in patients with high expression of PTGS1 **(G)**, PTGS2 **(H)**, PTGER1 **(I)**, PTGER2 **(J)**, PTGER3 **(K)**, and PTGER4 **(L)** compared to patients with low expression.

SUPPLEMENTARY FIGURE 2
Correlation between PGTER2 and PTGER4 gene expression with immune-phenotype of T cells. **(A-C).** Scatter plots depicting the correlation between PTGER2 expression and gene signatures of central memory **(A)**, effector memory **(B)**, and exhausted T cells **(C)** in pancreatic cancer patients. **(D-F).** Scatter plots depicting the correlation between PTGER4 expression and gene signatures of central memory **(D)**, effector memory **(E)**, and exhausted T cells **(F)** in pancreatic cancer patients.

References

1. Hidalgo M. Pancreatic cancer. *N Engl J Med* (2010) 362(17):1605–17. doi: 10.1056/NEJMra0901557

2. Rahib L, Smith BD, Aizenberg R, Rosenzweig AB, Fleshman JM, Matrisian LM. Projecting cancer incidence and deaths to 2030: the unexpected burden of thyroid, liver, and pancreas cancers in the united states. *Cancer Res* (2014) 74(11):2913–21. doi: 10.1158/0008-5472.CAN-14-0155

3. Von Hoff DD, Ervin T, Arena FP, Chiorean EG, Infante J, Moore M, et al. Increased survival in pancreatic cancer with nab-paclitaxel plus gemcitabine. *N Engl J Med* (2013) 369(18):1691–703. doi: 10.1056/NEJMoa1304369

4. Conroy T, Desseigne F, Ychou M, Bouché O, Guimbaud R, Bécouarn Y, et al. FOLFIRINOX versus gemcitabine for metastatic pancreatic cancer. *N Engl J Med* (2011) 364(19):1817–25. doi: 10.1056/NEJMoa1011923

5. Lu J, Jiang G. The journey of CAR-T therapy in hematological malignancies. *Mol Cancer* (2022) 21(1):194. doi: 10.1186/s12943-022-01663-0

6. Wagner J, Wickman E, DeRenzo C, Gottschalk S. CAR T cell therapy for solid tumors: bright future or dark reality? *Mol Ther* (2020) 28(11):2320–39. doi: 10.1016/j.ymthe.2020.09.015

7. Newick K, O'Brien S, Moon E, Albelda SM. CAR T cell therapy for solid tumors. *Annu Rev Med* (2017) 68(1):139–52. doi: 10.1146/annurev-med-062315-120245

8. Argani P, Iacobuzio-Donahue C, Ryu B, Rosty C, Goggins M, Wilentz RE, et al. Mesothelin is overexpressed in the vast majority of ductal adenocarcinomas of the pancreas: identification of a new pancreatic cancer marker by serial analysis of gene expression (SAGE). *Clin Cancer Res* (2001) 7(12):3862–8.

9. Hassan R, Ho M. Mesothelin targeted cancer immunotherapy. *Eur J Cancer* (2008) 44(1):46–53. doi: 10.1016/j.ejca.2007.08.028

10. Akce M, Zaidi MY, Waller EK, El-Rayes BF, Lesinski GB. The potential of CAR T cell therapy in pancreatic cancer. *Front Immunol* (2018) 9. doi: 10.3389/fimmu.2018.02166

11. Wang D, DuBois RN. Eicosanoids and cancer. *Nat Rev Cancer* (2010) 10 (3):181–93. doi: 10.1038/nrc2809

12. Johnson AM, Kleczko EK, Nemenoff RA. Eicosanoids in cancer: new roles in immunoregulation. *Front Pharmacol* (2020) 11. doi: 10.3389/fphar.2020.595498

13. Ricciotti E, FitzGerald GA. Prostaglandins and inflammation. *Arterioscler Thromb Vasc Biol* (2011) 31(5):986–1000. doi: 10.1161/ATVBAHA.110.207449

14. Greten FR, Grivennikov SI. Inflammation and cancer: triggers, mechanisms, and consequences. *Immunity* (2019) 51(1):27–41. doi: 10.1016/j.immuni.2019.06.025

15. Eberhart CE, Coffey RJ, Radhika A, Giardiello FM, Ferrenbach S, DuBois RN. Up-regulation of cyclooxygenase 2 gene expression in human colorectal adenomas and adenocarcinomas. *Gastroenterology* (1994) 107(4):1183–8. doi: 10.1016/0016-5085(94)90246-1

16. Matsubayashi H, Infante JR, Winter J, Klein AP, Schulick R, Hruban R, et al. Tumor COX-2 expression and prognosis of patients with resectable pancreatic cancer. *Cancer Biol Ther* (2007) 6(10):1569–75. doi: 10.4161/cbt.6.10.4711

17. Khuri FR, Wu H, Lee JJ, Kemp BL, Lotan R, Lippman SM, et al. Cyclooxygenase-2 overexpression is a marker of poor prognosis in stage I non-small cell lung cancer. *Clin Cancer Res* (2001) 7(4):861–7.

18. Sugimoto Y, Narumiya S. Prostaglandin e receptors*. *J Biol Chem* (2007) 282 (16):11613–7. doi: 10.1074/jbc.R600038200

19. Greenhough A, Smartt HJ, Moore AE, Roberts HR, Williams AC, Paraskeva C, et al. The COX-2/PGE2 pathway: key roles in the hallmarks of cancer and adaptation to the tumour microenvironment. *Carcinogenesis* (2009) 30(3):377–86. doi: 10.1093/carcin/bgp014

20. Bonavita E, Bromley CP, Jonsson G, Pelly VS, Sahoo S, Walwyn-Brown K, et al. Antagonistic inflammatory phenotypes dictate tumor fate and response to immune checkpoint blockade. *Immunity* (2020) 53(6):1215–1229.e8. doi: 10.1016/j.immuni.2020.10.020

21. Sinha P, Clements VK, Fulton AM, Ostrand-Rosenberg S. Prostaglandin E2 promotes tumor progression by inducing myeloid-derived suppressor cells. *Cancer Res* (2007) 67(9):4507–13. doi: 10.1158/0008-5472.CAN-06-4174

22. Okuyama T, Ishihara S, Sato H, Rumi MA, Kawashima K, Miyaoka Y, et al. Activation of prostaglandin E2-receptor EP2 and EP4 pathways induces growth inhibition in human gastric carcinoma cell lines. *J Lab Clin Med* (2002) 140(2):92–102. doi: 10.1016/S0022-2143(02)00023-9

23. Sreeramkumar V, Fresno M, Cuesta N. Prostaglandin E2 and T cells: friends or foes? *Immunol Cell Biol* (2012) 90(6):579–86. doi: 10.1038/icb.2011.75

24. Tang Z, Kang B, Li C, Chen T, Zhang Z. GEPIA2: an enhanced web server for large-scale expression profiling and interactive analysis. *Nucleic Acids Res* (2019) 47 (W1):W556–w560. doi: 10.1093/nar/gkz430

25. Goedhart J, Luijsterburg MS. VolcaNoseR is a web app for creating, exploring, labeling and sharing volcano plots. *Sci Rep* (2020) 10(1):20560. doi: 10.1038/s41598-020-76603-3

26. Thul PJ, Åkesson L, Wiking M, Mahdessian D, Geladaki A, Ait Blal H, et al. A subcellular map of the human proteome. *Science* (2017) 356(6340). doi: 10.1126/science.aal3321

27. Akbari B, Soltantoyeh T, Shahosseini Z, Yarandi F, Hadjati J, Mirzaei HR. The inhibitory receptors PD1, Tim3, and A2aR are highly expressed during mesoCAR T cell manufacturing in advanced human epithelial ovarian cancer. *Cancer Cell Int* (2023) 23(1):104. doi: 10.1186/s12935-023-02948-0

28. Vincent C, Fournel S, Wijdenes J, Revillard JP. Specific hyporesponsiveness of alloreactive peripheral T cells induced by CD4 antibodies. *Eur J Immunol* (1995) 25 (3):816–22. doi: 10.1002/eji.1830250328

29. Rufener GA, Press OW, Olsen P, Lee SY, Jensen MC, Gopal AK, et al. Preserved activity of CD20-specific chimeric antigen receptor-expressing T cells in the presence of rituximab. *Cancer Immunol Res* (2016) 4(6):509–19. doi: 10.1158/2326-6066.CIR-15-0276

30. Soltantoye T, Akbari B, Mirzaei HR, Hadjati J. Soluble and immobilized anti-CD3/28 distinctively expand and differentiate primary human T cells: an implication for adoptive T cell therapy. *Iran J Allergy Asthma Immunol* (2022) 21(6):630–7. doi: 10.18502/ijaai.v21i6.11521

31. Yao C, Sakata D, Esaki Y, Li Y, Matsuoka T, Kuroiwa K, et al. Prostaglandin E2-EP4 signaling promotes immune inflammation through Th1 cell differentiation and Th17 cell expansion. *Nat Med* (2009) 15(6):633–40. doi: 10.1038/nm.1968

32. Levine BL, Bernstein WB, Connors M, Craighead N, Lindsten T, Thompson CB, et al. Effects of CD28 costimulation on long-term proliferation of CD4+ T cells in the absence of exogenous feeder cells. *J Immunol* (1997) 159(12):5921–30. doi: 10.4049/jimmunol.159.12.5921

33. Goulart MR, StasinosK , Fincham REA, Delvecchio FR, Kocher HM. T Cells in pancreatic cancer stroma. *World J Gastroenterol* (2021) 27(46):7956–68. doi: 10.3748/wjg.v27.i46.7956

34. Wang J, Zhang L, Kang D, Yang D, Tang Y. Activation of PGE2/EP2 and PGE2/EP4 signaling pathways positively regulate the level of PD-1 in infiltrating CD8(+) T cells in patients with lung cancer. *Oncol Lett* (2018) 15(1):552–8. doi: 10.3892/ol.2017.7279

35. Wang Y, Cui L, Georgiev P, Singh L, Zheng Y, Yu Y, et al. Combination of EP(4) antagonist MF-766 and anti-PD-1 promotes anti-tumor efficacy by modulating both lymphocytes and myeloid cells. *Oncoimmunology* (2021) 10(1):1896643. doi: 10.1080/2162402X.2021.1896643

36. Peng S, Hu P, Xiao YT, Lu W, Guo D, Hu S, et al. Single-cell analysis reveals EP4 as a target for restoring T-cell infiltration and sensitizing prostate cancer to immunotherapy. *Clin Cancer Res* (2022) 28(3):552–67. doi: 10.1158/1078-0432.CCR-21-0299

37. Miao J, Lu X, Hu Y, Piao C, Wu X, Liu X, et al. Prostaglandin E(2) and PD-1 mediated inhibition of antitumor CTL responses in the human tumor microenvironment. *Oncotarget* (2017) 8(52):89802–10. doi: 10.18632/oncotarget.21155

38. Huang S, Apasov S, Koshiba M, Sitkovsky M. Role of A2a extracellular adenosine receptor-mediated signaling in adenosine-mediated inhibition of T-cell activation and expansion. *Blood* (1997) 90(4):1600–10. doi: 10.1182/blood.V90.4.1600

39. Giuffrida L, Sek K, Henderson MA, Lai J, Chen AXY, Meyran D, et al. CRISPR/Cas9 mediated deletion of the adenosine A2A receptor enhances CAR T cell efficacy. *Nat Commun* (2021) 12(1):3236. doi: 10.1038/s41467-021-23331-5

40. Masoumi E, Jafarzadeh L, Mirzaei HR, Alishah K, Fallah-Mehrjardi K, Rostamian H, et al. Genetic and pharmacological targeting of A2a receptor improves function of anti-mesothelin CAR T cells. *J Exp Clin Cancer Res* (2020) 39(1):49. doi: 10.1186/s13046-020-01546-6

41. Beavis PA, Henderson MA, Giuffrida L, Mills JK, Sek K, Cross RS, et al. Targeting the adenosine 2A receptor enhances chimeric antigen receptor T cell efficacy. *J Clin Invest* (2017) 127(3):929–41. doi: 10.1172/JCI89455

42. Newick K, O'Brien S, Sun J, Kapoor V, Maceyko S, Lo A, et al. Augmentation of CAR T-cell trafficking and antitumor efficacy by blocking protein kinase a localization. *Cancer Immunol Res* (2016) 4(6):541–51. doi: 10.1158/2326-6066.CIR-15-0263

43. Urak R, Walter M, Lim L, Wong CW, Budde LE, Thomas S, et al. *Ex vivo* akt inhibition promotes the generation of potent CD19CAR T cells for adoptive immunotherapy. *J Immunother Cancer* (2017) 5:26. doi: 10.1186/s40425-017-0227-4

44. Klebanoff CA, Crompton JG, Leonardi AJ, Yamamoto TN, Chandran SS, Eil RL, et al. Inhibition of AKT signaling uncouples T cell differentiation from expansion for receptor-engineered adoptive immunotherapy. *JCI Insight* (2017) 2(23). doi: 10.1172/jci.insight.95103

45. Zhang Q, Ding J, Sun S, Liu H, Lu M, Wei X, et al. Akt inhibition at the initial stage of CAR-T preparation enhances the CAR-positive expression rate, memory phenotype and in vivo efficacy. *Am J Cancer Res* (2019) 9(11):2379–96.

46. Zhang J, Endres S, Kobold S. Enhancing tumor T cell infiltration to enable cancer immunotherapy. *Immunotherapy* (2019) 11(3):201–13. doi: 10.2217/imt-2018-0111

47. Balachandran VP, Beatty GL, Dougan SK. Broadening the impact of immunotherapy to pancreatic cancer: challenges and opportunities. *Gastroenterology* (2019) 156(7):2056–72. doi: 10.1053/j.gastro.2018.12.038

48. Hong DS, Parikh A, Shapiro GI, Varga A, Naing A, Meric-Bernstam F, et al. First-in-human phase I study of immunomodulatory E7046, an antagonist of PGE(2)-receptor e-type 4 (EP4), in patients with advanced cancers. *J Immunother Cancer* (2020) 8(1). doi: 10.1136/jitc-2019-000222

49. Francica B, Lopez J, Holtz A, Freund D, Wang D, Enstrom A, et al. Abstract 1333: dual blockade of the EP2 and EP4 PGE2 receptors with TPST-1495 is an optimal approach for drugging the prostaglandin pathway. *Cancer Res* (2022) 82 (12_Supplement):1333–3. doi: 10.1158/1538-7445.AM2022-1333

frontiers | Frontiers in Immunology

TYPE Review
PUBLISHED 07 July 2023
DOI 10.3389/fimmu.2023.1214675

OPEN ACCESS

EDITED BY
Xin He,
City of Hope National Medical Center,
United States

REVIEWED BY
Patrick M. Woster,
Medical University of South Carolina,
United States
Antonello Mai,
Sapienza University of Rome, Italy

*CORRESPONDENCE
Ye Qin
ycqinye@163.com
Yinhong Song
syh728@ctgu.edu.cn

†These authors have contributed equally to this work

RECEIVED 30 April 2023
ACCEPTED 23 June 2023
PUBLISHED 07 July 2023

CITATION
Bao L, Zhu P, Mou Y, Song Y and Qin Y (2023) Targeting LSD1 in tumor immunotherapy: rationale, challenges and potential.
Front. Immunol. 14:1214675.
doi: 10.3389/fimmu.2023.1214675

Targeting LSD1 in tumor immunotherapy: rationale, challenges and potential

Lei Bao[1,2†], Ping Zhu[3,4†], Yuan Mou[1,2], Yinhong Song[1,2,4*] and Ye Qin[1,2*]

[1]Hubei Key Laboratory of Tumor Microenvironment and Immunotherapy, China Three Gorges University, Yichang, China, [2]College of Basic Medical Science, China Three Gorges University, Yichang, China, [3]Department of Nephrology, The First College of Clinical Medical Science, China Three Gorges University, Yichang, China, [4]Institute of Infection and Inflammation, China Three Gorges University, Yichang, China

Lysine-specific demethylase 1 (LSD1) is an enzyme that removes lysine methylation marks from nucleosome histone tails and plays an important role in cancer initiation, progression, metastasis, and recurrence. Recent research shows that LSD1 regulates tumor cells and immune cells through multiple upstream and downstream pathways, enabling tumor cells to adapt to the tumor microenvironment (TME). As a potential anti-tumor treatment strategy, immunotherapy has developed rapidly in the past few years. However, most patients have a low response rate to available immune checkpoint inhibitors (ICIs), including anti-PD-(L)1 therapy and CAR-T cell therapy, due to a broad array of immunosuppressive mechanisms. Notably, inhibition of LSD1 turns "cold tumors" into "hot tumors" and subsequently enhances tumor cell sensitivity to ICIs. This review focuses on recent advances in LSD1 and tumor immunity and discusses a potential therapeutic strategy for combining LSD1 inhibition with immunotherapy.

KEYWORDS

LSD1, immunotherapy, PD-(L)1, tumor microenvironment, combination therapy

1 Introduction

Based on the interactions between the tumor and the immune system, cancer immunotherapy that targets the immune system has revolutionized cancer treatment (1, 2). At present, immunotherapy has developed two mainstream branches: one is immune checkpoint inhibitors represented by PD-(L)1/CTLA4 inhibitors, and the other is adoptive cell therapies represented by chimeric antigen receptor (CAR) T cell therapy, including CAR-NKs (3–6). However, the current reality is that most patients have low response rates to available checkpoint therapies due to a broad array of immunosuppressant mechanisms such as hostile metabolic states, nutritional deprivation, T cell apoptosis triggered, secretion of suppressive cytokines and lack of antigen presentation (1, 3). As a result, the more successful combination medicines are discovered, the more patients will get benefit (3).

Epigenetics is a regulatory process that changes mediating heritable patterns of gene expression without altering the DNA sequence (7). Epigenetic modifications influence immune cells activation, differentiation, and functional fate, and they play critical roles in tumor development, progression, and metastasis (8–10). Histone lysine demethylases (KDMs) are a series of epigenetic enzymes that regulate gene transcription by demethylation of lysine during development and malignant transformation (11). As the first identified KDMs family member, Lysine-specific demethylase 1 (LSD1, also known as KDM1A) also plays an important role in epigenetic regulation (12).

LSD1 was firstly identified by Dr. Shi in 2004, and this discovery also demonstrated that histone methylation is reversible (13). Then LSD1 has gradually become a research hotspot, as it is involved in a variety of physiological and pathological processes, including cancer development, progression, metastases as well as recurrence (14). Of note, although LSD1 is overexpressed in a variety of tumors and has been reported to correlate with overall survival in patients (15–19), it does not seem to be a potent oncogene (20). However, LSD1 regulates gene expression in cancer cells and immune cells, allowing tumor cells to adapt to the tumor microenvironment (TME) (20). Therefore, an in-depth understanding of the role of LSD1 in tumor immunity is critical for developing more effective combination immunotherapeutic targets.

Here, we summarize the regulatory roles and mechanisms of LSD1 on antitumor immunity, including effects on tumor immunogenicity, various immune cells, and cancer-associated fibroblasts (CAFs). Further, we discuss potential innovative therapeutic strategies combining LSD1 inhibitors and multiple immunotherapies to improve the efficacy of mainstream cancer immunotherapies.

2 LSD1 and tumor immunity

2.1 LSD1 inhibition promotes the tumor immunogenicity

Recent studies have shown that loss of LSD1 improved tumor immunogenicity, provoking the immune system to fight against tumors (21). Tumor immunogenicity is associated with the expression of tumor-associated antigens (TAA) and tumor-specific antigens (TSA) as well as the ability of tumor antigen presentation (22). However, low or non-immunogenic tumor cells avoid being recognized and killed by immune cells due to weaker antigen expression and presentation capabilities (23), which often associates with poor prognosis (24). Therefore, enhancing the immunogenicity of tumors is a potential immunotherapy strategy. A growing body of evidence suggested that inhibition of LSD1 improves tumor immunogenicity in low or non-immunogenic tumors (Figure 1A) (25, 26).

Sheng et al. reported that knocking down LSD1 in tumor cells downregulates RNA-induced silencing complex (RISC) components expression and induces the expression of repetitive elements, including endogenous retroviral elements (ERVs), leading to double-stranded RNA (dsRNA) stress (26). Melanoma differentiation-associated gene 5 (MDA5) senses the accumulation of dsRNA, which is similar to a viral infection (viral mimicry), this leads to activation of innate antiviral pathways, resulting in the production of type I and type III interferon (IFN) as well as the processing and presentation of antigens (23, 26, 27). Meanwhile, knockout of LSD1 promoted MHC-1 expression on the surface of tumor cells (26). Likewise, Zhou et al. also proved that inhibition of LSD1 could activate the expression of genes associated with antigen processing and presentation through the ERV-dsRNA-IFN pathway (28).

Cancer testis antigens (CTAs) promote immune system recognition and killing of tumor cells by increasing tumor immunogenicity (25). The reactivation of CTAs in tumors is considered an ideal immunotherapy target because they are not expressed in most antigen-presenting cells from normal tissues (29). It is worth noting that inhibition of LSD1 could upregulate the expression of a range of representative CTAs, which enhanced tumor immunogenicity (25).

Collectively, these studies suggested that blockading LSD1 promotes tumor immunogenicity in multiple tumor models and provides a new therapeutic strategy for immunotherapy of low-immunogenic or non-immunogenic tumors (25, 26).

2.2 LSD1 regulates $CD8^+$ T cell

2.2.1 LSD1 inhibition promotes $CD8^+$ T cell infiltration

Lymphocytes that infiltrate the tumor are called tumor-infiltrating lymphocytes (TILs) (30). According to TILs abundance, tumors have been divided into “cold tumors” versus “hot tumors” (31, 32). Currently, a pathway that can turn “cold tumors” into “hot tumors” is urgently needed, due to the poor clinical response by “cold tumors” (23, 33). “Cold tumors” are characterized by a lack of T lymphocyte infiltration, whereas “hot tumors” are typified by the infiltration of $CD8^+$ cytotoxic T cells (31, 34). In particular, infiltration of $CD8^+$ T cells is known to be associated with favorable prognosis (35). Hence, it is critical to explore ways to activate $CD8^+$ T cells infiltration into the TME. A growing number of studies had shown that LSD1 blockade increases $CD8^+$ T cell infiltration in the tumor tissue and promotes anti-tumor immunity (Figure 1A) (26, 36–40).

A recent study demonstrated that LSD1 ablation does not increase the expression of Granzyme-B (a cytotoxic factor) and Ki-67 (a proliferation marker), but significantly promotes the infiltration of T effector cells into the melanoma cells and then restrains tumor growth (26). Besides, Ji et al. observed the increasing proportion of $CD8^+$ T cells and the ratio of $CD8^+$ T cells to Tregs (CD8/Treg) in TME of triple-negative breast cancer (TNBC) when treating with an innovative hydrogel-loaded LSD1 inhibitor GSK-LSD1 (36). Likewise, LSD1 inhibitor SP-2509 promoted $CD8^+$ T cell infiltration in head and neck squamous cell (HNSCC) and oral squamous cell carcinoma (OSCC) cells (37, 38). Interestingly, suppression of LSD1 simultaneously promoted the infiltration of $CD8^+$, $CD4^+$, $CD4^+CD8^+$ double positive T cells and $CD56^+$ NKT cell infiltration in small cell carcinoma of the ovary hypercalcemic type (SCCOHT) (39).

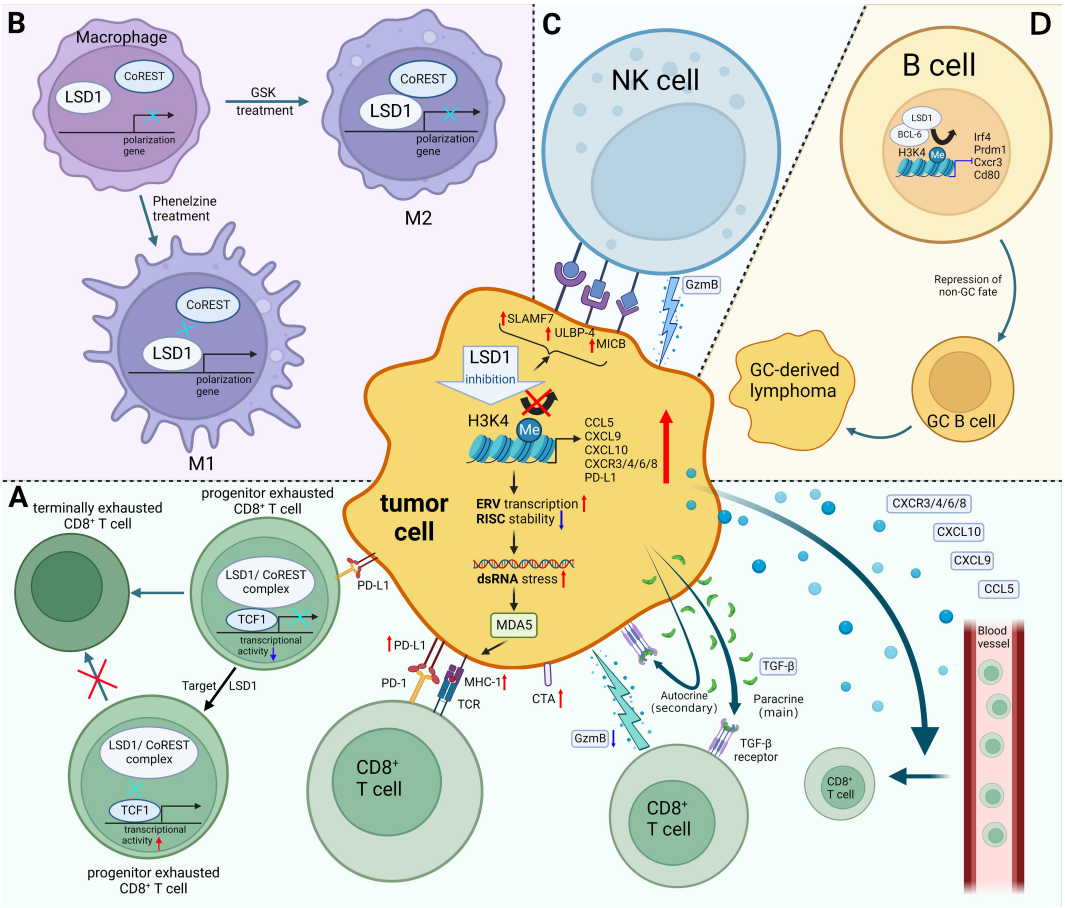

FIGURE 1
Mechanisms of LSD1 regulating tumor immunity. **(A)** LSD1 inhibition enhances the tumor immunogenicity, promotes $CD8^+$ T cell infiltration, and induces TGF-β as well as PD-L1 expression of tumor cells, which provides a potential strategy for enhancing tumor response rates to PD-L1 blockade therapy. There have been few examples in which LSD1 inhibition downregulates PD-L1, e.g. in cervical cancer. Moreover, inhibition of T cell-intrinsic LSD1 sustains T cell invigoration. **(B)** LSD1 inhibition favors M1 macrophage polarization by disrupting the LSD1-CoREST complex. **(C)** LSD1 inhibition confers tumor cells sensitivity to NK cell lysis *via* inducing the expression of ligands on the surface of tumor cells. **(D)** LSD1 induces the progression of GC-derived lymphomas by promoting the differentiation of GC B cells. Red upward arrows indicate upregulation, blue downward arrows indicate downregulation, black arrows indicate transition. Figure created using BioRender.

Mechanistically, LSD1 blockade increases the enrichment of H3K4me2 at proximal elements or core regions of the transcription start site of $CD8^+$ T cell-attracting chemokine promoters, which induces the expression of $CD8^+$ T cell-attracting chemokines (CCL5, CXCL9, CXCL10), thereby promoting the infiltration of $CD8^+$ T cell into tumor tissues and exerting tumor-killing effects (40). Similarly, LSD1 expression is inversely proportional to T cell chemokine gene expressions, such as CXCR3, CXCR4, CXCR6, CXCR8, CCL5, CXCL9, and CXCL10 in HNSCC (37). Notably, other chemokines such as CCL2, CCL3 or CCL4 are recognized to have tumor promoting effects (41). Those chemokines' expression is insignificantly regulated by LSD1 expression (40).

Taken together, LSD1 inhibition increases $CD8^+$T cell infiltration by inducing tumor cells to secrete $CD8^+$ T cell-attracting chemokine. This may turn "cold tumors" (immunotherapy-insensitive) into "hot tumors" (immunotherapy-sensitive).

2.2.2 LSD1 inhibition sustains T cell invigoration

Programmed death-ligand 1 (PD-L1) expressed in tumors interacts with programmed death receptor 1 (PD-1), resulting in prolonged stimulation of T cell receptor (TCR) by cognate antigens, inducing $CD8^+$ T cells to differentiate into exhausted $CD8^+$ T cells (Tex cells) (42). Under persistent antigen stimulation, progenitor Tex cells differentiate into terminally exhausted T cells (43). Current evidence suggested that the progenitor Tex cells had better cytokine-producing and proliferation capacity, and could maintain self-renewal while continuously producing more cytotoxic differentiated cells (44). T-cell factor 1 (TCF-1) was identified as a key transcription factor during progenitor Tex cells differentiation (45).

Mechanistically, LSD1/nuclear REST corepressor 1 (CoREST) complex interacts with the long isoform of TCF-1 in progenitor Tex cells and inhibits the transcriptional activity of TCF-1, thereby

promoting terminal differentiation of progenitor Tex cells (46). It could be reversed by suppression of T cell-intrinsic LSD1, which increases the persistence of progenitor Tex cells and provides a continuous source of proliferative conversion into numerically greater terminally Tex cells with tumoricidal cytotoxicity (Figure 1A) (46).

2.2.3 LSD1 suppression induces TGF-β expression of tumor cells

TGF-β plays a crucial role in immune homeostasis and tolerance, which is secreted by cancer cells and several other cells present in the TME (47). It was upregulated in LSD1-knockout tumor cells and antagonized the antitumor effects of LSD1 inhibition-induced $CD8^+$ T cell infiltration (48). Currently, TGF-β has three well-known mechanisms accounting for tumor immune escape, including repressing the cytotoxicity of $CD8^+$ T cells (49), promoting the conversion of $CD4^+CD25^-$ T cells to T(reg) cells (50), and blocking T cells infiltration (51, 52). Nevertheless, the latter two mechanisms did not appear to be decisive for antagonizing the antitumor effects induced by LSD1 inhibition. For example, fluctuations of TGF-β levels did not lead to significant alternation in Treg cell frequency in B16 (48) and EMT6 (51) tumors. In addition, $CD8^+$ T cell infiltration was not further increased in tumor cells knocked out of both LSD1 and TGF-β comparing to tumor cells knocked out of LSD1 alone, which suggested that TGF-β increased by LSD1 blockade did not significantly block $CD8^+$ T cell infiltration (48). This is somewhat expected since IFN pathway activation is more important than TGF-β pathway activation for $CD8^+$ T cell infiltration induced by LSD1 inhibition (26, 48).

In particular, TGF-β has two opposing effects in tumors according to its different targets' cells (48). Primarily, paracrine TGF-β attenuates the cytotoxicity and the tumor-killing ability of $CD8^+$ T cells through its action on αβ T cells, thereby reducing the percentage of $GzmB^+$ $CD8^+$ TILs. Secondarily, autocrine TGF-β inhibits tumor growth by acting directly on tumor cells to partially inhibit cell cycle progression and promote tumor cell apoptosis. Overall, the tumor-promoting effect of paracrine TGF-β is stronger than the tumor-inhibitory effect of autocrine, that TGF-β induced by LSD1 inhibition helps tumors escape from host immune responses by repressing the anti-tumor activity of $CD8^+$ cytotoxic T cells (Figure 1A) (48). Hence, inhibiting or blocking the paracrine effect of TGF-β is one of the potential strategies to enhance the tumor-killing effect of LSD1 inhibitors (48).

2.3 LSD1 inhibition favors M1 macrophage polarization

Macrophages have different phenotypes and functions in different microenvironments, and they are divided into two categories according to their function: M1 macrophages (classically activated macrophages) and M2 macrophages (alternatively activated macrophages) (53, 54). Currently, increasing studies had demonstrated that LSD1 could regulate macrophages polarization (55–60).

In non-tumor tissues, activation of the LPS/TLR4/NFκB/PARP1-LSD1/SOD2 signaling pathway regulates the resistance of M1 macrophages to hydrogen peroxide (55). The mechanism mentioned was that LSD1 represses SOD2 transcription by enriching in the SOD2 gene promoter region and increasing H3K4 demethylation. Thus, LSD1 inhibition can prevent hydrogen peroxide-induced oxidative stress damage to M1 macrophages by promoting SOD2 transcription (55). Notably, Sobczak et al. observed that LSD1 suppression promoted catalase expression during M1 polarization, which in turn inhibited the expression of pro-inflammatory cytokines and M1-related surface markers (such as CD14, TNF-α, COX2, IL1-β, IFNAR, and TLR2), which suggested that LSD1 inhibition can limit the macrophage M1 specialization in the non-tumor tissues (56).

In the TME, M1 macrophages exert anti-tumor effects, while M2 macrophages promote tumor proliferation, metastasis, and angiogenesis (61). Therefore, inducing the polarization of M1 macrophages in the TME provides a potential therapeutic strategy for treatment of tumors (62). Of note, Boulding et al. reported that LSD1 blockade promotes the M1 macrophage polarization and infiltration (57). They observed the increased expression of CCR7 and CD38 (M1 markers) and the decreased expression of CD206 and EGR2 (M2 markers) in the MDA-MB-231 tumor tissues following treatment with LSD1 inhibitor phenelzine (57). Moreover, significantly higher infiltration of M1 macrophages after the combination therapy of phenelzine and nab-paclitaxel was observed, which implied that LSD1 blockade could serve as a potential epigenetic adjuvant therapy strategy (57). Interestingly, Phenelzine, an LSD1 inhibitor targeting the flavin adenine dinucleotide (FAD) and CoREST binding domains, increased the transcription and expression of M1-associated genes by disrupting the LSD1-CoREST complex. In contrast, GSK2879552, an LSD1 inhibitor targeting the FAD domain, failed to polarize macrophages to the M1 phenotype (Figure 1) (58). These evidences emphasized the importance of targeting the LSD1-CoREST complex to reprogram macrophages toward M1 phenotype for therapeutic benefit.

Current studies showed that inhibition of LSD1 not only inhibits the proliferation and migration of mixed lineage leukemia (MLL) rearranged leukemia cells, but also increases the proportion of macrophages in peripheral blood and spleen (59, 60). The cells expressing high levels of CD11b and CD14, surface-specific markers of differentiated macrophages/monocytes, were significantly increased after LSD1 inhibition (59). Similarly, the percentages expressing CD11b or CD14 were also significantly upregulated following treatment with a structurally new LSD1 inhibitor (spirooxindole-based FY-56) in MLL-rearranged leukemia cells (60). These results might be attributed to differentiation of stem-like leukemia cells into more mature macrophage-like cells caused by LSD1inhibition (59, 60).

2.4 LSD1 inhibition confers tumor cells sensitivity to NK cell

Natural killer (NK) cells, as an important member of the immune tumor microenvironment, limit the growth and spread of cancer cells (63). It is well known that NK cells are activated upon detection of abnormal signals of malignant transformation. Once activated, NK cells secrete pro-inflammatory cytokines and lyse target cells *via* the perforin/granzyme pathway (63).

Current research had shown that catalytic LSD1 inhibitors could induce the expression of ligands on the surface of tumor cells that could activate NK cells (Figure 1C) (64, 65). Bailey et al. reported that irreversible catalytic LSD1 inhibitors (RN-1, tranylcypromine and GSK-LSD1) could induce NK cells to kill tumor cells (65). Mechanistically, LSD1 inhibition could increase the expression of innate immune receptors (SLAMF7, MICB, and ULBP-4) on the surface of tumor cells in diffuse pontine glioma (DIPG). These receptors act as self-ligating or as ligands for natural killer group 2 member D (NKG2D) to activates NK cells, sensitizing tumor to NK cell lysis (65). Similarly, Liu et al. reported that LSD1 inhibition upregulated the expression of innate immune receptors in acute myeloid leukemia (AML) cells with low expression of CCAAT/enhancer-binding protein α (C/EBPα) (64). They further demonstrated that the expression of C/EBPα was upregulated after treatment with LSD1 inhibitor tranylcypromine which was enriched at the enhancer region of the *ULBP2/5/6* genes, and subsequently induced the ULBP2/5/6 which were ligands for NK cell receptors and activate NK cells by binding to NKG2D. In this way, catalytic LSD1 inhibitors confer sensitivity of tumor cells to NK-mediated lysis (64).

Notably, the two classes of inhibitors targeting different domains of LSD1 have different biological effects on NK cells (20). In contrast to catalytic inhibitors, the reversible scaffolding LSD1 inhibitors (SP-2577 and SP-2509) inhibits NK cells metabolism and lysis capacity (66). Mechanistically, scaffold LSD1 inhibitors downregulates NK cell ligand expression and attenuates NK cell toxicity, whereas glutathione supplementation abolishes these effects and rescues NK cell lysis capacity (66). Thus, glutathione supplementation might relieve the inhibition of NK cell activity when treated with LSD inhibitors.

2.5 LSD1 regulates B cells involved in tumor progression

There is a close relationship between tumor-infiltrating B cells and tumors. An analysis of 69 available studies found that B cell infiltration is associated with a positive patient prognosis in 19 tumors, while less than 10% of the studies indicated the opposite phenomenon (67). And it was also reported that LSD1 is required for B cell proliferation and differentiation (68, 69).

In recent years, studies have shown that different infiltration patterns or different directions of B cells induced by TME, therefore, B cells play two opposite roles of anti-tumor and tumor-promoting (67, 70). Interestingly, LSD1 acts as a tumor promoter or suppressor in some different tumors, due to the regulation of B cell differentiation by LSD1 (71–73). On the one hand, LSD1, a germline predisposition gene for multiple myeloma, inhibits multiple myeloma development by regulating abnormal plasma cells (PC) (72). On the other hand, LSD1 induces the progression of germinal center (GC)-derived lymphomas by promoting the differentiation of GC B cells (Figure 1D) (73). Mechanistically, LSD1 and the transcriptional repressor BCL6 forms a complex that subsequently represses the expression of genes involved in GC exit, terminal differentiation as well as proliferation, thereby inducing GC B-cell differentiation and promoting the progression of GC-derived lymphomas (73). Notably, conditional deletion of LSD1 inhibited GC proliferation, while catalytic LSD1 inhibitors have little effect on GC proliferation and lymphoma progression (73). Therefore, the development of novel inhibitors that target non-catalytic LSD1–protein interactions might become an attractive therapeutic intervention for GC-derived lymphomas (71).

2.6 The connection between LSD1 and CAFs

CAFs are abundant in the TME and closely related to cancer progression. CAFs affects tumor cells and other stromal cells through cell-to-cell contacts, release a variety of regulatory factors, synthesize and remodel the extracellular matrix, thereby impacting the cancer progression (74). Current research suggests that there is a connection between LSD1 and CAFs (57, 75).

CAFs induced LSD1 deacetylation and maintain LSD1 stability by activating Notch3 signaling, resulting in the promotion of cancer stem-like cell (CSC) self-renewal and tumor growth (75). Another study identified that CAFs increased in the TME following mono-chemotherapy with nab-paclitaxel, whereas CAFs decreased following LSD1 inhibitor administration alone or in combination with chemotherapy in the MDA-MB-231 mouse xenografts (57). This research demonstrated that suppression of LSD1 could effectively reduce the CAFs burden (57). However, the specific subtypes of CAFs that affected by LSD1 remain to be further investigated.

3 LSD1 in immunotherapy

3.1 LSD1 inhibitor combined with PD-1/PD-L1 blockade

PD-L1 is commonly found on the surface of tumor cells, which inhibits $CD8^+$ T cell cytotoxicity and leads to $CD8^+$ T cell exhaustion by binding to PD-1 on the surface of T cells, thereby mediating immune escape of tumor cells (44, 76). Therefore, PD-1/PD-L1 blockade promotes anti-tumor immunity and kill tumor cells (77). Some cancer patients who initially responded to anti-PD-(L)1 therapy eventually develop drug resistance and tumor progression after long-term treatment, though PD-1/PD-L1 therapy elicits more potent antitumor activity in some patients (78, 79). It should be noted that in most cancer patients, the PD-1/

PD-L1 pathway is not the only speed-limiting factor of anti-tumor immunity, so blocking the PD-1/PD-L1 pathway alone is not sufficient to elicit effective antitumor immune response (79). On the one hand, negative factors such as other immune checkpoints, immunosuppressive immune cells or cytokines, cancer-associated adipocytes, abnormal angiogenesis, hyperactive CAFs contribute to tumor immune tolerance (80–85). Removing these negative factors might overcome drug resistance. On the other hand, positive factors such as immune supporting cytokines, immunogenic cancer cell death, and professional antigen-presenting cells promote immune clearance (86). Strengthening these positive factors might reshape "cold tumors" into "hot tumors", thereby increasing the response rate to PD-1/PD-L1 blockade therapy (86).

It has been validated that epigenetic modulators might be an appropriate partner with PD-1/PD-L1 blockade to achieve superior antitumor efficacies and long-term cancer control (79). LSD1 blockade, as a novel strategy for epigenetic regulation, enhances antitumor effects through multiple sides as discussed previously. On the tumor cell intrinsic side, LSD1 suppression promotes antigen processing and presentation and induces ligand expression. In immune cells, LSD1 suppression regulates the development, differentiation, cytotoxicity, and cytokine production of T cell, and involves in the regulation of macrophages, NK cells, and CAFs in TME, thereby turning "cold tumors" into "hot tumors".

Existing studies had shown that LSD1 was involved in the regulation of immune checkpoints on the surface of tumor cells. For example, knockdown of LSD1 directly downregulated the expression of PD-L1 and CD47 in cervical cancer through increasing the enrichment of H3K4me2 at promoters of PD-L1 and CD47 (87). Besides, the LSD1/wild-type p53/miR-34a signaling axis indirectly regulated the expression of CD47/PD-L1 by targeting the 3' untranslated region (3' UTR) of CD47/PD-L1. Further studies reported that combination therapy with PD-(L)1/CD47 blockade and LSD1 inhibition significantly inhibited tumor growth compared with the single-agent treatment group (87). However, LSD1 blockade upregulated PD-L1 expression in most tumors, including melanoma (26), SWI/SNF-deficient ovarian cancer (39), HNSCC (37) and OSCC (38). Likewise, the expression of PD-L1 was proved to be increased by LSD1 inhibitor HCI-2509 in a dose-dependent manner in MDA-MB-231 cells and mouse TNBC cell line models 4T1 and EMT6 (40). H3K4me2 occupancy at a distant region upstream of the TSS site of PD-L1 promoters was enhanced after LSD1 inhibition. Meanwhile, the enrichment of H3K4me2 at proximal elements or core regions of transcription start site at promoters of PD-L1 was increased (Figure 1A) (40). This explains why inhibition of LSD1 induces PD-L1 in a variety of tumors.

Given the dramatic effect of LSD1 inhibition in enhancing tumor immunogenicity and promoting T cell infiltration, combination with LSD1 suppression and PD-(L)1 blockade may have potential therapeutic value (26). Several observations support this hypothesis. For example, LSD1-knockout B16 mice showed a slow increase in tumor volume and significantly prolonged survival after PD-1 blockade (26). Another study points out that tumor grew significantly more slowly in BALB/c mice bearing orthotopic EMT6 tumors following combination therapy with HCI-2509 and PD-1 blockade. Likewise, combination treatment inhibited tumor growth and lung metastasis in 4T1 tumor-bearing BALB/c mice, compared with single-agent treatment (40). These had also been demonstrated in HNSCC (37) and OSCC (38). These studies suggest that the combination of LSD1 inhibition and PD-(L)1 blockade is a potential strategy for anti-tumor immunotherapy.

In addition to regulating the expression of PD-L1 on the surface of the cell membrane as discussed previously, LSD1 deletion had been shown to reduce the expression of exosomal PD-L1 (88). PD-L1 is released from tumor cells and exists in extracellular forms, including soluble PD-L1 and exosomal PD-L1 (89). Existing studies suggest that exosomal PD-L1 played an important role in tumor immune escape, promoting tumor development by inhibiting cytokine production and promoting T cell apoptosis (90, 91). Correspondingly, reducing the content of exosomal PD-L1 might enhance the sensitivity of tumor patients to anti-PD-L1/PD-1 therapy (89). Shen et al. reported that LSD1 deletion could reduce PD-L1 accumulation in exosomes and inhibit PD-L1 transport to other cancer cells *via* exosomes, thereby enhancing the activity of T cells and restoring the ability of T cells to kill tumor cells in TME, thus overcoming immunosuppression (88).

Nevertheless, the limitations of combination therapies of LSD1 inhibition and PD-(L)1 blockade remain to be resolved. For example, LSD1 suppression-induced TGF-β acted on αβ T cells and reduces the toxicity of $CD8^+$ T cells. This limited the anti-tumor immune response of the dual-combination therapy to some extent (48). Therefore, the triple-combination of PD-1/TGF-β blockade and LSD1 inhibition had been shown to effectively inhibit tumor cell growth through increasing the cytotoxicity and infiltration of $CD8^+$ T cells. Triple therapy overcomes the limitations of dual therapy and provides a new treatment strategy for low-immunogenicity tumors (48).

It is worth noting that tumor cells are not the only target of LSD1 inhibition therapy. The progenitor Tex cells is reported as the key determinant of effective responses to anti-PD1 therapy (92, 93). Inhibition of T cell-intrinsic LSD1 disrupted the interaction of the LSD1/CoREST complex with TCF-1 in Tex progenitor cells, which in turn induced TCF-1 transcriptional activity, thereby inhibiting the terminal differentiation of Tex progenitor cells (46). This expanded the pool size of progenitor Tex cells, leading to durable and effective responses to anti-PD1 therapy (46).Taken together, blockade of T cell-intrinsic LSD1 provides another promising target for epigenetic modulation in cancer immunotherapy.

Collectively, combination therapy with PD-(L)1 blockade and LSD1 inhibition reduce tumor growth more effectively. These results suggest that inhibition of LSD1 may be an effective adjunct to immunotherapy, broadening potential therapeutic strategies for low-immunogenic or non-immunogenic tumors. Such a phase I and phase II clinical trial combination with LSD1 inhibitor and anti-PD-1 is currently recruiting lung small cell carcinoma patients (NCT05191797). In addition, based on the combination therapy of inhibiting LSD1 and blocking PD-(L)1, further inhibition of tumor growth-promoting cytokines (e.g.TGF-β) induced by LSD1 inhibition could potentially improve the effectiveness of combination therapy for poorly immunogenic tumors.

3.2 LSD1 inhibitor combined with CAR-T therapy

In recent years, research on CAR-T cell therapy has grown exponentially due to its tremendous clinical success in lymphoma and leukemia patients (94). CAR-T cell therapy enables T cells to bind tumor cell surface antigens through antigen-binding domains (usually a single chain variable fragments (scFv)), mediating MHC-unrestricted tumor cell killing (95). CAR-T cell mainly kills tumor cells through the granzyme perforin pathway, but the Fas/FasL pathway has been shown to be closely related to the killing ability of CAR-T cell on tumor cells (96). However, overcoming drug resistance of treating solid tumors and further improving the efficacy of treating leukemia and lymphoma are still the most challenging issues in CAR-T cell therapy (97, 98). Hence, the discovery of promising new targets and the innovative design of CAR-T cells are crucial (94).

Recent studies have shown that inhibition or knockout of LSD1 can indirectly or directly enhance the ability of CAR-T cells to kill tumor cells (99, 100). Sulejmani et al. showed that inhibiting LSD1 in tumor cells promoted TP53-mediated transcriptional activation of genes, which leads to increased expression of Fas on the tumor cell surface, allowing FasL on CAR T cells to bind to Fas on the surface of tumor cells lacking antigen expression, thereby lysing and killing tumor cells (99). It should be noted that the above results are based on *in vitro* experiments, and it is necessary to further study the toxicity and effectiveness of this strategy *in vivo* through animal experiments (99). Unlike Sulejmani O et al. who targeted LSD1 in tumor cells, Zhang J et al. suggested that targeted knockdown of LSD1 in anti-CD19 CAR-T cells have stronger anti-tumor effect (100). *In vitro* experiments showed that the knockdown of LSD1 promoted anti-CD19 CAR-T cells to secrete IFN-γ, TNF-α, and IL-2 and enhanced their cytotoxic and cytolytic activities. *In vivo* experiments showed that LSD1-knockdown anti-CD19 CAR-T cells exhibited stronger IFN-γ secretion capacity and better expansion rate. This suggested that LSD1 downregulation may contribute to the long-term antitumor activity of anti-CD19 CAR-T cells (100).

These studies suggested that LSD1 may become a promising adjuvant strategy for CAR-T cell therapy and provide new ideas for the innovative design of CAR-T cells.

4 Conclusions

As a histone lysine demethylase, LSD1 regulates chromatin domains that are activated or repressed by histone demethylation, which modulates the expression of immune cell-related genes, thereby affecting the tumor immune response in the TME. LSD1 blockade, as a novel strategy for epigenetic regulation, enhances antitumor effects through multiple sides. On the tumor cell intrinsic side, LSD1 suppression promotes antigen processing and presentation. Some important ligands expression also can be induced by LSD1 suppression. In immune cells, LSD1 suppression regulates the development, differentiation, cytotoxicity, and cytokine production of T cells, and is involved in the regulation of macrophages, NK cells, and CAFs in TME, thereby turning "cold tumors" into "hot tumors". In brief, inhibition of LSD1 can inhibit tumor immune escape and effectively kill tumor cells through multiple mechanisms. Furthermore, inhibition of LSD1 suppresses the progression of GC-derived lymphomas by inhibiting the differentiation of GC B cells. However, whether LSD1 inhibition can suppress tumorigenesis and tumor development by inducing immune cells to differentiate into subtypes remains to be studied. Overall, the extensive effects of inhibiting LSD1 on tumor immunity need to be fully explored.

Although anti-PD-(L)1 antibody therapy and CAR-T therapy are currently the most popular immunotherapy strategies, it is undeniable that immunotherapy is less than ideal for a variety of cancers. Current researches focus on the efficacy of LSD1 inhibition combined with anti-PD-(L)1 antibody therapy and CAR-T therapy. More evidences are needed to determine whether LSD1 blockade is suitable as a potential combination strategy for more immunotherapies such as CTLA-4 inhibitors or CAR-NK therapy. Altogether, targeting LSD1 may offer an exciting avenue to improve the efficacy of immunotherapy.

Author contributions

YQ and YS contributed to conception and design of the study. LB and PZ completed the review of literature and wrote the first draft of the manuscript. YM contributed to the graphic visualization. All authors contributed to the article and approved the submitted version.

Funding

This work was supported by The National Natural Science Foundation of China (No. 81671397), Hubei Provincial Department of Education Natural Science Research Project Fund (B2017024) and Yichang Medical and Health Research Project Fund (A20-2-002).

Conflict of interest

The authors declare that the research was conducted in the absence of any commercial or financial relationships that could be construed as a potential conflict of interest.

Publisher's note

References

1. Hegde PS, Chen DS. Top 10 challenges in cancer immunotherapy. *Immunity* (2020) 52:17–35. doi: 10.1016/j.immuni.2019.12.011

2. Hiam-Galvez KJ, Allen BM, Spitzer MH. Systemic immunity in cancer. *Nat Rev Cancer* (2021) 21:345–59. doi: 10.1038/s41568-021-00347-z

3. Yap TA, Parkes EE, Peng W, Moyers JT, Curran MA, Tawbi HA. Development of immunotherapy combination strategies in cancer. *Cancer Discovery* (2021) 11:1368–97. doi: 10.1158/2159-8290.CD-20-1209

4. Maskalenko NA, Zhigarev D, Campbell KS. Harnessing natural killer cells for cancer immunotherapy: dispatching the first responders. *Nat Rev Drug Discovery* (2022) 21:559–77. doi: 10.1038/s41573-022-00413-7

5. Hodgins JJ, Khan ST, Park MM, Auer RC, Ardolino M. Killers 2.0: NK cell therapies at the forefront of cancer control. *J Clin Invest* (2019) 129:3499–510. doi: 10.1172/JCI129338

6. Demaria O, Cornen S, Daëron M, Morel Y, Medzhitov R, Vivier E. Harnessing innate immunity in cancer therapy. *Nature* (2019) 574:45–56. doi: 10.1038/s41586-019-1593-5

7. Topper MJ, Vaz M, Marrone KA, Brahmer JR, Baylin SB. The emerging role of epigenetic therapeutics in immuno-oncology. *Nat Rev Clin Oncol* (2020) 17:75–90. doi: 10.1038/s41571-019-0266-5

8. Dai E, Zhu Z, Wahed S, Qu Z, Storkus WJ, Guo ZS. Epigenetic modulation of antitumor immunity for improved cancer immunotherapy. *Mol Cancer* (2021) 20. doi: 10.1186/s12943-021-01464-x

9. Yu M, Hazelton WD, Luebeck GE, Grady WM. Epigenetic aging: more than just a clock when it comes to cancer. *Cancer Res* (2020) 80:367–74. doi: 10.1158/0008-5472.CAN-19-0924

10. Jones PA, Baylin SB. The epigenomics of cancer. *Cell* (2007) 128:683–92. doi: 10.1016/j.cell.2007.01.029

11. Sterling J, Menezes SV, Abbassi RH, Munoz L. Histone lysine demethylases and their functions in cancer. *Int J Cancer* (2021) 148:2375–88. doi: 10.1002/ijc.33375

12. Højfeldt JW, Agger K, Helin K. Histone lysine demethylases as targets for anticancer therapy. *Nat Rev Drug Discovery* (2013) 12:917–30. doi: 10.1038/nrd4154

13. Shi Y, Lan F, Matson C, Mulligan P, Whetstine JR, Cole PA, et al. Histone demethylation mediated by the nuclear amine oxidase homolog LSD1. *Cell* (2004) 119:941–53. doi: 10.1016/j.cell.2004.12.012

14. Fang Y, Liao G, Yu B. LSD1/KDM1A inhibitors in clinical trials: advances and prospects. *J Hematol Oncol* (2019) 12:129. doi: 10.1186/s13045-019-0811-9

15. Nagasawa S, Sedukhina AS, Nakagawa Y, Maeda I, Kubota M, Ohnuma S, et al. LSD1 overexpression is associated with poor prognosis in basal-like breast cancer, and sensitivity to PARP inhibition. *PloS One* (2015) 10:e118002. doi: 10.1371/journal.pone.0118002

16. Wu J, Hu L, Du Y, Kong F, Pan Y. Prognostic role of LSD1 in various cancers: evidence from a meta-analysis. *Onco Targets Ther* (2015) 8:2565–70. doi: 10.2147/OTT.S89597

17. Theisen ER, Gajiwala S, Bearss J, Sorna V, Sharma S, Janat-Amsbury M. Reversible inhibition of lysine specific demethylase 1 is a novel anti-tumor strategy for poorly differentiated endometrial carcinoma. *BMC Cancer* (2014) 14:752. doi: 10.1186/1471-2407-14-752

18. Hayami S, Kelly JD, Cho HS, Yoshimatsu M, Unoki M, Tsunoda T, et al. Overexpression of LSD1 contributes to human carcinogenesis through chromatin regulation in various cancers. *Int J Cancer* (2011) 128:574–86. doi: 10.1002/ijc.25349

19. Schulte JH, Lim S, Schramm A, Friedrichs N, Koster J, Versteeg R, et al. Lysine-specific demethylase 1 is strongly expressed in poorly differentiated neuroblastoma: implications for therapy. *Cancer Res* (2009) 69:2065–71. doi: 10.1158/0008-5472.CAN-08-1735

20. Kim D, Kim KI, Baek SH. Roles of lysine-specific demethylase 1 (LSD1) in homeostasis and diseases. *J BioMed Sci* (2021) 28. doi: 10.1186/s12929-021-00737-3

21. Zappasodi R, Merghoub T, Wolchok JD. Emerging concepts for immune checkpoint blockade-based combination therapies. *Cancer Cell* (2018) 33:581–98. doi: 10.1016/j.ccell.2018.03.005.

22. Richters MM, Xia H, Campbell KM, Gillanders WE, Griffith OL, Griffith M. Best practices for bioinformatic characterization of neoantigens for clinical utility. *Genome Med* (2019) 11. doi: 10.1186/s13073-019-0666-2

23. Loo Yau H, Ettayebi I, De Carvalho DD. The cancer epigenome: exploiting its vulnerabilities for immunotherapy. *Trends Cell Biol* (2019) 29:31–43. doi: 10.1016/j.tcb.2018.07.006

24. O'Donnell JS, Teng M, Smyth MJ. Cancer immunoediting and resistance to T cell-based immunotherapy. *Nat Rev Clin Oncol* (2019) 16:151–67. doi: 10.1038/s41571-018-0142-8

25. Cheng W, Li H, Xi S, Zhang X, Zhu Y, Xing L, et al. Growth differentiation factor 1-induced tumour plasticity provides a therapeutic window for immunotherapy in hepatocellular carcinoma. *Nat Commun* (2021) 12:7142. doi: 10.1038/s41467-021-27525-9

26. Sheng W, LaFleur MW, Nguyen TH, Chen S, Chakravarthy A, Conway JR, et al. LSD1 ablation stimulates anti-tumor immunity and enables checkpoint blockade. *Cell* (2018) 174:549–63. doi: 10.1016/j.cell.2018.05.052

27. Mendez FM, Núñez FJ, Garcia-Fabiani MB, Haase S, Carney S, Gauss JC, et al. Epigenetic reprogramming and chromatin accessibility in pediatric diffuse intrinsic pontine gliomas: a neural developmental disease. *Neuro Oncol* (2020) 22:195–206. doi: 10.1093/neuonc/noz218

28. Zhou X, Singh M, Sanz Santos G, Guerlavais V, Carvajal LA, Aivado M, et al. Pharmacologic activation of p53 triggers viral mimicry response thereby abolishing tumor immune evasion and promoting antitumor immunity. *Cancer Discovery* (2021) 11:3090–105. doi: 10.1158/2159-8290.CD-20-1741

29. Simpson AJG, Caballero OL, Jungbluth A, Chen Y, Old LJ. Cancer/testis antigens, gametogenesis and cancer. *Nat Rev Cancer* (2005) 5:615–25. doi: 10.1038/nrc1669

30. Spranger S. Mechanisms of tumor escape in the context of the T-cell-inflamed and the non-t-cell-inflamed tumor microenvironment. *Int Immunol* (2016) 28:383–91. doi: 10.1093/intimm/dxw014

31. Sharma P, Hu-Lieskovan S, Wargo JA, Ribas A. Primary, adaptive, and acquired resistance to cancer immunotherapy. *Cell* (2017) 168:707–23. doi: 10.1016/j.cell.2017.01.017

32. van der Woude LL, Gorris MAJ, Halilovic A, Figdor CG, de Vries IJM. Migrating into the tumor: a roadmap for T cells. *Trends Cancer* (2017) 3:797–808. doi: 10.1016/j.trecan.2017.09.006

33. Marra A, Viale G, Curigliano G. Recent advances in triple negative breast cancer: the immunotherapy era. *BMC Med* (2019) 17. doi: 10.1186/s12916-019-1326-5

34. Bonaventura P, Shekarian T, Alcazer V, Valladeau-Guilemond J, Valsesia-Wittmann S, Amigorena S, et al. Cold tumors: a therapeutic challenge for immunotherapy. *Front Immunol* (2019) 10:168. doi: 10.3389/fimmu.2019.00168

35. Disis ML, Taylor MH, Kelly K, Beck JT, Gordon M, Moore KM, et al. Efficacy and safety of avelumab for patients with recurrent or refractory ovarian cancer. *JAMA Oncol* (2019) 5:393. doi: 10.1001/jamaoncol.2018.6258

36. Ji X, Guo D, Ma J, Yin M, Yu Y, Liu C, et al. Epigenetic remodeling hydrogel patches for multidrug-resistant triple-negative breast cancer. *Adv Mater* (2021) 33:2100949. doi: 10.1002/adma.202100949

37. Han Y, Xu S, Ye W, Wang Y, Zhang X, Deng J, et al. Targeting LSD1 suppresses stem cell-like properties and sensitizes head and neck squamous cell carcinoma to PD-1 blockade. *Cell Death Dis* (2021) 12:993. doi: 10.1038/s41419-021-04297-0

38. Alhousami T, Diny M, Ali F, Shin J, Kumar G, Kumar V, et al. Inhibition of LSD1 attenuates oral cancer development and promotes therapeutic efficacy of immune checkpoint blockade and Yap/Taz inhibition. *Mol Cancer Res* (2022), 20:712–21. doi: 10.1158/1541-7786.MCR-21-0310

39. Soldi R, Ghosh Halder T, Weston A, Thode T, Drenner K, Lewis R, et al. The novel reversible LSD1 inhibitor SP-2577 promotes anti-tumor immunity in SWItch/Sucrose-NonFermentable (SWI/SNF) complex mutated ovarian cancer. *PloS One* (2020) 15:e235705. doi: 10.1371/journal.pone.0235705

40. Qin Y, Vasilatos SN, Chen L, Wu H, Cao Z, Fu Y, et al. Inhibition of histone lysine-specific demethylase 1 elicits breast tumor immunity and enhances antitumor efficacy of immune checkpoint blockade. *Oncogene* (2019) 38:390–405. doi: 10.1038/s41388-018-0451-5

41. Nagarsheth N, Wicha MS, Zou W. Chemokines in the cancer microenvironment and their relevance in cancer immunotherapy. *Nat Rev Immunol* (2017) 17:559–72. doi: 10.1038/nri.2017.49

42. Wherry EJ, Kurachi M. Molecular and cellular insights into T cell exhaustion. *Nat Rev Immunol* (2015) 15:486–99. doi: 10.1038/nri3862

43. Sharpe AH, Pauken KE. The diverse functions of the PD1 inhibitory pathway. *Nat Rev Immunol* (2018) 18:153–67. doi: 10.1038/nri.2017.108

44. McLane LM, Abdel-Hakeem MS, Wherry EJ. CD8 T cell exhaustion during chronic viral infection and cancer. *Annu Rev Immunol* (2019) 37:457–95. doi: 10.1146/annurev-immunol-041015-055318

45. Chen Z, Ji Z, Ngiow SF, Manne S, Cai Z, Huang AC, et al. TCF-1-Centered transcriptional network drives an effector versus exhausted CD8 T cell-fate decision. *Immunity* (2019) 51:840–55. doi: 10.1016/j.immuni.2019.09.013

46. Liu Y, Debo B, Li M, Shi Z, Sheng W, Shi Y. LSD1 inhibition sustains T cell invigoration with a durable response to PD-1 blockade. *Nat Commun* (2021) 12:6831. doi: 10.1038/s41467-021-27179-7

47. Batlle E, Massagué J. Transforming growth factor-b signaling in immunity and cancer. *Immunity* (2019) 50:924–40. doi: 10.1016/j.immuni.2019.03.024

48. Sheng W, Liu Y, Chakraborty D, Debo B, Shi Y. Simultaneous inhibition of LSD1 and TGFbeta enables eradication of poorly immunogenic tumors with anti-PD-1 treatment. *Cancer Discovery* (2021) 11:1970–81. doi: 10.1158/2159-8290.CD-20-0017

49. Thomas DA, Massagué J. TGF-β directly targets cytotoxic T cell functions during tumor evasion of immune surveillance. *Cancer Cell* (2005) 8:369–80. doi: 10.1016/j.ccr.2005.10.012

50. Liu VC, Wong L, Shah AH, Park I, Yang X. Tumor evasion of the immune system by converting CD4+CD25- T cells into CD4+CD25+ T regulatory cells: role of tumor-derived TGF-beta. *J Immunol* (2007) 178:2883–92. doi: 10.4049/jimmunol.178.5.2883

51. Mariathasan S, Turley SJ, Nickles D, Castiglioni A, Yuen K, Wang Y, et al. TGFβ attenuates tumour response to PD-L1 blockade by contributing to exclusion of T cells. *Nature* (2018) 554:544–48. doi: 10.1038/nature25501

52. Tauriello DVF, Palomo-Ponce S, Stork D, Berenguer-Llergo A, Badia-Ramentol J, Iglesias M, et al. TGFβ drives immune evasion in genetically reconstituted colon cancer metastasis. *Nature* (2018) 554:538–43. doi: 10.1038/nature25492

53. Gordon S. Alternative activation of macrophages. *Nat Rev Immunol* (2003) 3:23–35. doi: 10.1038/nri978

54. Murray PJ. Macrophage polarization. *Annu Rev Physiol* (2017) 79:541–66. doi: 10.1146/annurev-physiol-022516-034339

55. Tokarz P, Ploszaj T, Regdon Z, Virag L, Robaszkiewicz A. PARP1-LSD1 functional interplay controls transcription of SOD2 that protects human pro-inflammatory macrophages from death under an oxidative condition. *Free Radic Biol Med* (2019) 131:218–24. doi: 10.1016/j.freeradbiomed.2018.12.004

56. Sobczak M, Strachowska M, Gronkowska K, Karwaciak I, Pulaski L, Robaszkiewicz A. LSD1 facilitates pro-inflammatory polarization of macrophages by repressing catalase. *Cells* (2021) 10. doi: 10.3390/cells10092465

57. Boulding T, McCuaig RD, Tan A, Hardy K, Wu F, Dunn J, et al. LSD1 activation promotes inducible EMT programs and modulates the tumour microenvironment in breast cancer. *Sci Rep* (2018) 8. doi: 10.1038/s41598-017-17913-x

58. Tan AHY, Tu W, McCuaig R, Hardy K, Donovan T, Tsimbalyuk S, et al. Lysine-specific histone demethylase 1A regulates macrophage polarization and checkpoint molecules in the tumor microenvironment of triple-negative breast cancer. *Front Immunol* (2019) 10:1351. doi: 10.3389/fimmu.2019.01351

59. Feng Z, Yao Y, Zhou C, Chen F, Wu F, Wei L, et al. Pharmacological inhibition of LSD1 for the treatment of MLL-rearranged leukemia. *J Hematol Oncol* (2016) 9:13–24. doi: 10.1186/s13045-016-0252-7

60. Yang C, Fang Y, Luo X, Teng D, Liu Z, Zhou Y, et al. Discovery of natural product-like spirooxindole derivatives as highly potent and selective LSD1/KDM1A inhibitors for AML treatment. *Bioorg Chem* (2022) 120:105596. doi: 10.1016/j.bioorg.2022.105596

61. Sun P, Zhang SJ, Maksim S, Yao YF, Liu HM, Du J. Epigenetic modification in macrophages: a promising target for tumor and inflammation-associated disease therapy. *Curr Top Med Chem* (2019) 19:1350–62. doi: 10.2174/1568026619666190619143706

62. Dey P. Epigenetics meets the tumor microenvironment. *Med Epigenet* (2013) 1:31–6. doi: 10.1159/000354283

63. Myers JA, Miller JS. Exploring the NK cell platform for cancer immunotherapy. *Nat Rev Clin Oncol* (2021) 18:85–100. doi: 10.1038/s41571-020-0426-7

64. Liu M, Du M, Yu J, Qian Z, Gao Y, Pan W, et al. CEBPA mutants down-regulate AML cell susceptibility to NK-mediated lysis by disruption of the expression of NKG2D ligands, which can be restored by LSD1 inhibition. *Oncoimmunology* (2022) 11:2016158. doi: 10.1080/2162402X.2021.2016158

65. Bailey CP, Figueroa M, Gangadharan A, Yang Y, Romero MM, Kennis BA, et al. Pharmacologic inhibition of lysine-specific demethylase 1 as a therapeutic and immune-sensitization strategy in pediatric high-grade glioma. *Neuro Oncol* (2020) 22:1302–14. doi: 10.1093/neuonc/noaa058

66. Bailey CP, Figueroa M, Gangadharan A, Lee DA, Chandra J. Scaffolding LSD1 inhibitors impair NK cell metabolism and cytotoxic function through depletion of glutathione. *Front Immunol* (2020) 11:2196. doi: 10.3389/fimmu.2020.02196

67. Wouters MCA, Nelson BH. Prognostic significance of tumor-infiltrating b cells and plasma cells in human cancer. *Clin Cancer Res* (2018) 24:6125–35. doi: 10.1158/1078-0432.CCR-18-1481

68. Haines RR, Barwick BG, Scharer CD, Majumder P, Randall TD, Boss JM. The histone demethylase LSD1 regulates b cell proliferation and plasmablast differentiation. *J Immunol* (2018) 201:2799–811. doi: 10.4049/jimmunol.1800952

69. Su S, Ying H, Chiu Y, Lin F, Chen M, Lin K. Involvement of histone demethylase LSD1 in blimp-1-Mediated gene repression during plasma cell differentiation. *Mol Cell Biol* (2009) 29:1421–31. doi: 10.1128/MCB.01158-08

70. Sharonov GV, Serebrovskaya EO, Yuzhakova DV, Britanova OV, Chudakov DM. B cells, plasma cells and antibody repertoires in the tumour microenvironment. *Nat Rev Immunol* (2020) 20:294–307. doi: 10.1038/s41577-019-0257-x

71. Good-Jacobson KL. B cells turn on, tune in with LSD1. *Nat Immunol* (2019) 20:3–05. doi: 10.1038/s41590-018-0281-1

72. Wei X, Calvo-Vidal MN, Chen S, Wu G, Revuelta MV, Sun J, et al. Germline lysine-specific demethylase 1 (LSD1/KDM1A) mutations confer susceptibility to multiple myeloma. *Cancer Res* (2018) 78:2747–59. doi: 10.1158/0008-5472.CAN-17-1900

73. Hatzi K, Geng H, Doane AS, Meydan C, LaRiviere R, Cardenas M, et al. Histone demethylase LSD1 is required for germinal center formation and BCL6-driven lymphomagenesis. *Nat Immunol* (2019) 20:86–96. doi: 10.1038/s41590-018-0273-1

74. Chen X, Song E. Turning foes to friends: targeting cancer-associated fibroblasts. *Nat Rev Drug Discovery* (2019) 18:99–115. doi: 10.1038/s41573-018-0004-1

75. Liu C, Liu L, Chen X, Cheng J, Zhang H, Zhang C, et al. LSD1 stimulates cancer-associated fibroblasts to drive Notch3-dependent self-renewal of liver cancer stem–like cells. *Cancer Res* (2018) 78:938–49. doi: 10.1158/0008-5472.CAN-17-1236

76. Juneja VR, McGuire KA, Manguso RT, LaFleur MW, Collins N, Haining WN, et al. PD-L1 on tumor cells is sufficient for immune evasion in immunogenic tumors and inhibits CD8 T cell cytotoxicity. *J Exp Med* (2017) 214:895–904. doi: 10.1084/jem.20160801

77. Doroshow DB, Bhalla S, Beasley MB, Sholl LM, Kerr KM, Gnjatic S, et al. PD-L1 as a biomarker of response to immune-checkpoint inhibitors. *Nat Rev Clin Oncol* (2021) 18:345–62. doi: 10.1038/s41571-021-00473-5

78. Sun C, Mezzadra R, Schumacher TN. Regulation and function of the PD-L1 checkpoint. *Immun (Cambridge Mass.)* (2018) 48:434–52. doi: 10.1016/j.immuni.2018.03.014

79. Yi M, Zheng X, Niu M, Zhu S, Ge H, Wu K. Combination strategies with PD-1/PD-L1 blockade: current advances and future directions. *Mol Cancer* (2022) 21. doi: 10.1186/s12943-021-01489-2

80. Bai X, Yi M, Jiao Y, Chu Q, Wu K. Blocking TGF-beta signaling to enhance the efficacy of immune checkpoint inhibitor. *Onco Targets Ther* (2019) 12:9527–38. doi: 10.2147/OTT.S224013

81. Wu Q, Li B, Li J, Sun S, Yuan J, Sun S. Cancer-associated adipocytes as immunomodulators in cancer. *biomark Res* (2021) 9. doi: 10.1186/s40364-020-00257-6

82. Liu T, Han C, Wang S, Fang P, Ma Z, Xu L, et al. Cancer-associated fibroblasts: an emerging target of anti-cancer immunotherapy. *J Hematol Oncol* (2019) 12:86. doi: 10.1186/s13045-019-0770-1

83. Qin S, Xu L, Yi M, Yu S, Wu K, Luo S. Novel immune checkpoint targets: moving beyond PD-1 and CTLA-4. *Mol Cancer* (2019) 18:155. doi: 10.1186/s12943-019-1091-2

84. Yi M, Jiao D, Qin S, Chu Q, Wu K, Li A. Synergistic effect of immune checkpoint blockade and anti-angiogenesis in cancer treatment. *Mol Cancer* (2019) 18:60. doi: 10.1186/s12943-019-0974-6

85. Yi M, Xu L, Jiao Y, Luo S, Li A, Wu K. The role of cancer-derived microRNAs in cancer immune escape. *J Hematol Oncol* (2020) 13:25. doi: 10.1186/s13045-020-00848-8

86. Smyth MJ, Ngiow SF, Ribas A, Teng MW. Combination cancer immunotherapies tailored to the tumour microenvironment. *Nat Rev Clin Oncol* (2016) 13:143–58. doi: 10.1038/nrclinonc.2015.209

87. Xu S, Wang X, Yang Y, Li Y, Wu S. LSD1 silencing contributes to enhanced efficacy of anti-CD47/PD-L1 immunotherapy in cervical cancer. *Cell Death Dis* (2021) 12. doi: 10.1038/s41419-021-03556-4

88. Shen D, Pang J, Bi Y, Zhao L, Li Y, Zhao L, et al. LSD1 deletion decreases exosomal PD-L1 and restores T-cell response in gastric cancer. *Mol Cancer* (2022) 21. doi: 10.1186/s12943-022-01557-1

89. Shao B, Dang Q, Chen Z, Chen C, Zhou Q, Qiao B, et al. Effects of tumor-derived exosome programmed death ligand 1 on tumor immunity and clinical applications. *Front Cell Dev Biol* (2021) 9:760211. doi: 10.3389/fcell.2021.760211

90. Poggio M, Hu T, Pai C, Chu B, Belair CD, Chang A, et al. Suppression of exosomal PD-L1 induces systemic anti-tumor immunity and memory. *Cell* (2019) 177:414–27. doi: 10.1016/j.cell.2019.02.016

91. Chen G, Huang AC, Zhang W, Zhang G, Wu M, Xu W, et al. Exosomal PD-L1 contributes to immunosuppression and is associated with anti-PD-1 response. *Nature* (2018) 560:382–86. doi: 10.1038/s41586-018-0392-8

92. Kim KH, Kim HK, Kim HD, Kim CG, Lee H, Han JW, et al. PD-1 blockade-unresponsive human tumor-infiltrating CD8(+) T cells are marked by loss of CD28 expression and rescued by IL-15. *Cell Mol Immunol* (2021) 18:385–97. doi: 10.1038/s41423-020-0427-6

93. Miller BC, Sen DR, Al Abosy R, Bi K, Virkud YV, LaFleur MW, et al. Subsets of exhausted CD8+ T cells differentially mediate tumor control and respond to checkpoint blockade. *Nat Immunol* (2019) 20:326–36. doi: 10.1038/s41590-019-0312-6

94. Larson RC, Maus MV. Recent advances and discoveries in the mechanisms and functions of CAR T cells. *Nat Rev Cancer* (2021) 21:145–61. doi: 10.1038/s41568-020-00323-z

95. Long AH, Haso WM, Shern JF, Wanhainen KM, Murgai M, Ingaramo M, et al. 4-1BB costimulation ameliorates T cell exhaustion induced by tonic signaling of chimeric antigen receptors. *Nat Med* (2015) 21:581–90. doi: 10.1038/nm.3838

96. Benmebarek M, Karches CH, Cadilha BL, Lesch S, Endres S, Kobold S. Killing mechanisms of chimeric antigen receptor (CAR) T cells. *Int J Mol Sci* (2019) 20:1283. doi: 10.3390/ijms20061283

97. Martinez M, Moon EK. CAR T cells for solid tumors: new strategies for finding, infiltrating, and surviving in the tumor microenvironment. *Front Immunol* (2019) 10:128. doi: 10.3389/fimmu.2019.00128

98. Xu X, Sun Q, Liang X, Chen Z, Zhang X, Zhou X, et al. Mechanisms of relapse after CD19 CAR T-cell therapy for acute lymphoblastic leukemia and its prevention and treatment strategies. *Front Immunol* (2019) 10:2664. doi: 10.3389/fimmu.2019.02664

99. Sulejmani O, Grunewald L, Andersch L, Schwiebert S, Klaus A, Winkler A, et al. Inhibiting lysine demethylase 1A improves L1CAM-specific CAR T cell therapy by unleashing antigen-independent killing *via* the FAS-FASL axis. *Cancers (Basel)* (2021) 13:5489. doi: 10.3390/cancers13215489

100. Zhang J, Zhu J, Zheng G, Wang Q, Li X, Feng Y, et al. Co-Expression of miR155 or LSD1 shRNA increases the anti-tumor functions of CD19 CAR-T cells. *Front Immunol* (2022) 12:811364. doi: 10.3389/fimmu.2021.811364

frontiers | Frontiers in Immunology

TYPE Review
PUBLISHED 03 August 2023
DOI 10.3389/fimmu.2023.1213222

OPEN ACCESS

EDITED BY
Gulderen Yanikkaya Demirel,
Yeditepe University, Türkiye

REVIEWED BY
Fiori Alite,
Geisinger Commonwealth School of Medicine, United States
Charles B. Simone,
Memorial Sloan Kettering Cancer Center, United States

*CORRESPONDENCE
Tianyun Qiao
15667097813@163.com
Bingwei Dong
rxrfdbw@126.com

†These authors have contributed equally to this work

RECEIVED 27 April 2023
ACCEPTED 24 July 2023
PUBLISHED 03 August 2023

CITATION
Shi Y, Ma X, He D, Dong B and Qiao T (2023) Neoadjuvant SBRT combined with immunotherapy in NSCLC: from mechanisms to therapy.
Front. Immunol. 14:1213222.
doi: 10.3389/fimmu.2023.1213222

Neoadjuvant SBRT combined with immunotherapy in NSCLC: from mechanisms to therapy

Yanhong Shi[1†], Xiaoyan Ma[2†], Dan He[3], Bingwei Dong[1*] and Tianyun Qiao[4*]

[1]Department of Pathology, Xianyang Central Hospital, Xianyang, China, [2]Department of Pathology, Division of Experimental Diagnostic, KingMed Medical Laboratory (Xi'an) Co., Ltd., Xi'an, China, [3]Department of Pathology, Xi'an Central Hospital, Xi'an, China, [4]Department of Thoracic Surgery, Tangdu Hospital, Fourth Military Medical University, Xi'an, China

The utilisation of neoadjuvant immunotherapy has demonstrated promising preliminary clinical outcomes for early-stage resectable non-small-cell lung cancer (NSCLC). Nevertheless, it is imperative to develop novel neoadjuvant combination therapy regimens incorporating immunotherapy to further enhance the proportion of patients who derive benefit. Recent studies have revealed that stereotactic body radiotherapy (SBRT) not only induces direct tumour cell death but also stimulates local and systemic antitumour immune responses. Numerous clinical trials have incorporated SBRT into immunotherapy for advanced NSCLC, revealing that this combination therapy effectively inhibits local tumour growth while simultaneously activating systemic antitumour immune responses. Consequently, the integration of SBRT with neoadjuvant immunotherapy has emerged as a promising strategy for treating resectable NSCLC, as it can enhance the systemic immune response to eradicate micrometastases and recurrent foci post-resection. This review aims to elucidate the potential mechanism of combination of SBRT and immunotherapy followed by surgery and identify optimal clinical treatment strategies. Initially, we delineate the interplay between SBRT and the local tumour immune microenvironment, as well as the systemic antitumour immune response. We subsequently introduce the preclinical foundation and preliminary clinical trials of neoadjuvant SBRT combined with immunotherapy for treating resectable NSCLC. Finally, we discussed the optimal dosage, schedule, and biomarkers for neoadjuvant combination therapy in its clinical application. In conclusion, the elucidation of potential mechanism of neoadjuvant SBRT combined immunotherapy not only offers a theoretical basis for ongoing clinical trials but also contributes to determining the most efficacious therapy scheme for future clinical application.

KEYWORDS

non-small cell cancer (NSCLC), stereotactic body radiation therapy (SBRT), neoadjuvant therapy, immunotherapy, biomarker

1 Introduction

Stereotactic body radiation therapy (SBRT) has demonstrated promising outcomes in various solid tumours, particularly in early-stage non-small-cell lung cancer (NSCLC) (1–4). Compared to traditional radiotherapy, SBRT can significantly improve patient prognosis while posing a low risk of toxicity by precisely targeting local tumours and delivering high-dose, hypofractionated therapy (5–8). It is noteworthy that SBRT has a significant advantage over conventional radiotherapy due to its potent immune-activating effect (9). Conventional radiotherapy was previously believed to have immunosuppressive effects, as evidenced by bone marrow myelosuppression and reduced peripheral blood count during treatment (10). This notion was further supported by the use of whole-body irradiation as a myeloablative conditioning before haematopoietic stem cell transplantation (11). However, unlike conventional radiotherapy, the advent of SBRT enables patients to receive higher doses of precise radiotherapy in fewer fractions. The advantage enables SBRT to minimise the potential persistent immunosuppressive effects on the host when compared to conventional radiotherapy (12). In fact, researchers are increasingly recognizing the potent immunomodulatory effects of SBRT, which can convert refractory "cold" tumours into immunotherapy-responsive "hot" tumours (13). For instance, the incorporation of SBRT with immunotherapy in advanced NSCLC patients not only prolonged survival but also significantly increased cytotoxic T cell infiltration within the tumour microenvironment (TME) (14). Given the promising results of combing SBRT and immunotherapy, it is worthwhile to explore whether this approach can be applied to early-stage NSCLC for improved local tumour control and prevention of postoperative recurrence and metastasis.

Clinically, neoadjuvant immunotherapy has demonstrated promising potential in the treatment of early operable NSCLC (15, 16). Unlike traditional neoadjuvant chemotherapy, neoadjuvant immunotherapy not only promotes local tumour control but also activates the systemic antitumour immune response, which is considered a crucial factor in preventing postoperative recurrence and metastasis (17). Numerous clinical trials have confirmed that combining neoadjuvant immunotherapy with chemotherapy can significantly improve the pathological remission rate in patients (16, 18). For example, the CheckMate-816 trial demonstrated that neoadjuvant nivolumab combined with chemotherapy not only significantly increased both pathological complete response (pCR) (24% vs. 2.2%) and event-free survival (EFS) (31.6 months vs. 20.8 months), without increasing the risk of adverse events, compared to neoadjuvant chemotherapy alone (19). Based in these promising clinical trials, neoadjuvant immunotherapy combined with chemotherapy has been approved as the first-line treatment for early operable NSCLC (19). Given this success, it is worthwhile to investigate whether SBRT can also be combined with immunotherapy as neoadjuvant therapy for early operable NSCLC. Indeed, there are ongoing preclinical and clinical trials exploring the potential synergies between SBRT and immunotherapy in the neoadjuvant setting (20–22). However, before conducting further clinical trials and applications, it is important to fully understand the mechanism of interaction between SBRT and antitumour immune response, as well as determine the optimal dosage and scheduling for combination therapy.

Herein, we present an overview of the current status and potential mechanism of neoadjuvant SBRT in combination with immunotherapy, followed by surgery, for the treatment of NSCLC. We also discuss the optimal therapy schedule and predictive biomarkers for clinical application. Furthermore, we highlight future research directions and challenges that require further investigation.

2 The interplay between SBRT and antitumour immune response

Several studies have suggested that SBRT can promote the antitumour immune response through various pathways beyond its direct DNA damage to tumour cells (23–25). Previous studies have demonstrated that SBRT can induce the presentation of antigens by promoting the release of major histocompatibility complex 1 (MHC-1) and immunogenic cell death (ICD) of tumour cells. Additionally, it can directly stimulate dendritic cell (DC) maturation and $CD8^+$ cytotoxic T lymphocyte infiltration in the TME (12, 26, 27). Notably, conventional radiotherapy has been demonstrated to mobilise several immunosuppressive cells, including regulatory T cells (Tregs), M2 macrophages, and bone marrow-derived suppressor cells (28). However, studies on SBRT-related immunosuppressive modification are scarce. A recent study compared the effects of SBRT (40 Gy/3 fractions) with conventional radiotherapy (62 Gy/20 fractions or 66-69 Gy/30 fractions) on the tumour immune microenvironment. The results showed that conventional radiotherapy has a negative impact on systemic immunity, resulting in an increase in neutrophils/lymphocytes and a decrease in total lymphocyte count. In contrast, SBRT increased B cell, central memory T cell, and effector $CD8^+$ T cell infiltration in the TME, as well as increased CD8/Treg ratio (29). In summary, SBRT could activate the immune system through multiple pathways and create an ideal TME for subsequent immunotherapy (Figure 1).

When tumour cells are exposed to lethal stimuli such as radiation or chemotherapy, a cascade of signaling molecules known as damage-associated molecular patterns (DAMPs) is released (30). These DAMPs include calreticulin, which is exposed to the cell surface, high mobility group box 1 (HMGB1), which is secreted by tumour cells as well as ATP molecules and heat shock proteins (HSP70 and HSP90) (31). Studies have shown that DAMPs induced by ICD could promote cytotoxic T lymphocyte infiltration by facilitating dendritic cell maturation and antigen presentation (32). Moreover, SBRT can stimulate the release of various chemokines such as C-X-C motif chemokine ligand-9/10/16 and interferons (IFNs), which play a crucial role in recruiting activated T cells to infiltrate the TME (33, 34). It has also been reported that SBRT can trigger the exposure and release of numerous tumour-associated antigens, which can be taken up by DCs, transported to lymph nodes, and presented as antigens (35, 36). Overall, these SBRT-induced factors are critical for the activation of local and systemic antitumour immune responses.

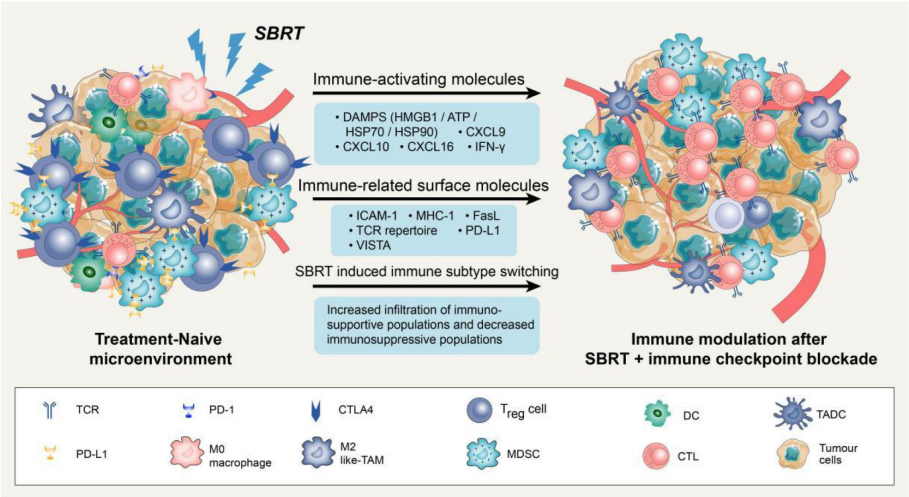

FIGURE 1
Potential mechanisms of synergy with SBRT and immune checkpoint blockade. Stereotactic body radiation therapy (SBRT) can transfer treatment-naive tumour microenvironment (TME) into "hot" tumour by producing immune-activating molecules and immune-related surface molecules, as well as by directly regulating immune cells composition. Compared with treatment-naive TME, the synergy with SBRT and immune checkpoint blockade could promote the infiltration of immune cells *via* up-regulation of adhesion molecules (ICAM-1) or chemokine (CXCL9/10/16). Notably, SBRT can contribute to adaptive immune resistance *via* IFN-γ mediated up-regulation of PD-L1 and VISTA expression on tumour cells. Blockade of these checkpoints by inhibitors permits the activation of T cells in tumour-associated draining lymph node and TME.

SBRT can also enhance the immunogenicity and antigenicity of tumour cells by regulating the expression of cell surface molecules and receptors. For instance, in a dose-dependent manner, SBRT can up-regulate cell surface markers such as intercellular adhesion molecule 1 (ICAM-1), MHC-1, and death receptor Fas (27, 37). It is widely recognized that MHC-1 is an essential co-stimulatory molecule for activating $CD8^+$ T cells (38). ICAM-1 is the key adhesion molecule that facilitates immune cell adhesion and migration into the TME (39). The up-regulation of these surface molecules could enhance T cell-mediated antitumour immune response and increase the sensitivity of cytotoxic T lymphocytes to recognize and eliminate tumour cells (40). Notably, SBRT could also increase immune checkpoint expression on the surface of tumour cells. For example, the analysis of paired lung cancer samples following SBRT revealed an increase in the diversity of the T cell receptor repertoire and programmed cell death ligand 1 (PD-L1) expression, while no significant increase of $CD8^+$ T cell and IFN expression was observed within tumour tissues (33). In addition to PD-L1, SBRT can also significantly up-regulate V-domain immunoglobulin suppressor of T cell activation (VISTA) expression in $CD8^+$ T cells (29). It is worth noting that not all immune checkpoints are elevated following SBRT. Studies have reported that SBRT can significantly increase the frequency of $Ki67^+$ programmed cell death protein 1 $(PD\text{-}1)^+$ T cells and natural killer cells in advanced tumours without a significant increase in immune checkpoints such as T cell immunoglobulin and mucin domain-containing protein 3 (TIM-3) and Lymphocyte activation gene-3 (LAG-3) (41). In conclusion, SBRT-induced up-regulation of certain immune checkpoints might render patients more sensitive to subsequent immune checkpoint inhibitors, resulting in higher response rates and prolonging overall survival (OS).

Previous studies have demonstrated that SBRT can also transfer immunosuppressive microenvironments into "hot" tumors by directly regulating the immune cell composition (42). Reprogramming of the TME after SBRT is primarily induced by the production of chemokines and cytokines to recruit specific immune cell subsets. In mouse tumours, a single high-dose radiotherapy increased the influx of $CD8^+$ T cells and simultaneously decreased Treg cell invasion (43). This change may attributed to the release of chemokine and vascular morphological (44). The enhanced homing of immune cells creates an ideal microenvironment for subsequent immunotherapy to effectively elicit antitumour response. A phase 2 clinical trial was conducted to evaluate the efficacy of combing pembrolizumab (a PD-1 inhibitor) with SBRT in NSCLC patients and further studied the reprogramming of TME. Results demonstrated a significant increase in the overall response rate (4.87-fold vs. 2.56-fold) and $CD103^+$cytotoxic T cell infiltration after 6 weeks of SBRT plus pembrolizumab therapy, as compared to pembrolizumab monotherapy (14).

In addition to its direct tumour-killing effect, SBRT can induce tumour shrinkage in non-irradiated and distant metastatic tumours through the abscopal effect (45). The current understanding is that local immune activation triggered by SBRT can initiated a systemic immune response that produces cytokines and circulating $CD8^+$ T cells. These molecules can then act on distant non-irradiated sites and effectively inhibit metastatic tumour progression (46). While this phenomenon is rare in SBRT monotherapy, combining it with immunotherapy is expected to increase its incidence.

3 The preclinical foundation of neoadjuvant SBRT combined with immunotherapy

It is widely acknowledged that neoadjuvant immunotherapy has the potential to not only control local tumours but also inhibit

postoperative recurrence and metastasis through systemic immunity (47). While the effects of SBRT on the local TME have been studied, the impact of combining it with immunotherapy on systemic immunity remains unclear. The activation of systemic antitumour immune response is believed to be the mechanism underlying the radiotherapy-induced abscopal effect (48, 49). In a study with mice bearing breast cancer, combining radiotherapy with immunotherapy resulted in significant tumour shrinkage at both irradiated and non-irradiated sites. Notably, the abscopal effect was abolished in T cell-deficient mice (nude mice), indicating that T cells are essential for radiotherapy-induced distal tumour suppression (50).

Tumour-draining lymph nodes (TDLNs) are acknowledged as the primary sites for initiating antitumour immune responses, where immune cells differentiate into progenitor cells upon binding to antigens presented by DCs. These progenitor cells then differentiate and migrate into the TME, contributing to systemic immunity (51). Recently, Huang et al. proposed a novel concept suggesting that the antitumour effects of immune checkpoint inhibitors primarily occur in TDLNs rather than TME. The research found that injecting PD-L1 inhibitors into TDLNs significantly inhibited tumour growth, whereas injecting PD-L1 inhibitors directly into tumours had no effect. Furthermore, surgical removal of TDLNs abrogated the antitumour effects of PD-L1 inhibitors. Further mechanistic studies demonstrated that immune checkpoint inhibitor therapy initially promotes the amplification of T cell factor 1 (TCF-1)$^{+}$ thymocyte selection-associated HMGB (TOX)$^{-}$ CD8^{+} T cells), which are tumour-specific memory cells in TDLNs, These cells subsequently migrated to the TME and peripheral immunity where they differentiate into effector T cells (52). This novel concept highlights the importance of TDLNs and systemic immunity in the antitumour response to immunotherapy (Figure 2).

According to research, SBRT has demonstrated a greater potential than conventional radiotherapy in activating immune cells in TDLNs, leading to a more robust systemic immune response capable of eliminating potential metastases. Lee et al. were among the first to report that high-dose radiotherapy (15-25 Gy×1) could enhance the activation of immune cells in TDLNs of advanced tumours, resulting in activated CD8^{+} T cells that not only targeted primary tumours but also eliminated distant metastases in some cases. Moreover, the incorporation of immunotherapy into high-dose radiotherapy resulted in enhanced tumour eradication and systemic antitumour immune response (53). Additionally, Walker et al. demonstrated that the combination of high-dose radiotherapy with bempegaldesleukin (a CD122-preferential interleukin-2 pathway agonist) not only impedes the growth of irradiated tumours but also activated tumour-specific CD8^{+} T cells in systemic immunity, leading to the elimination of non-irradiated metastases (54). Additionally, in a preclinical model featuring disseminated metastasis (4T1 and mouse oral carcinoma 2), researchers discovered that the addition immune checkpoint inhibitors to radiotherapy plus bempegaldesin significantly prolonged the survival of mice by preventing distant metastasis. The effect was achieved by generating immune memory cells in TDLNs (55). Collectively, these preclinical studies suggest that combining SBRT with immunotherapy may enhance the incidence of the abscopal effect by promoting immune cell activation in TDLNs, generating a systemic immune response.

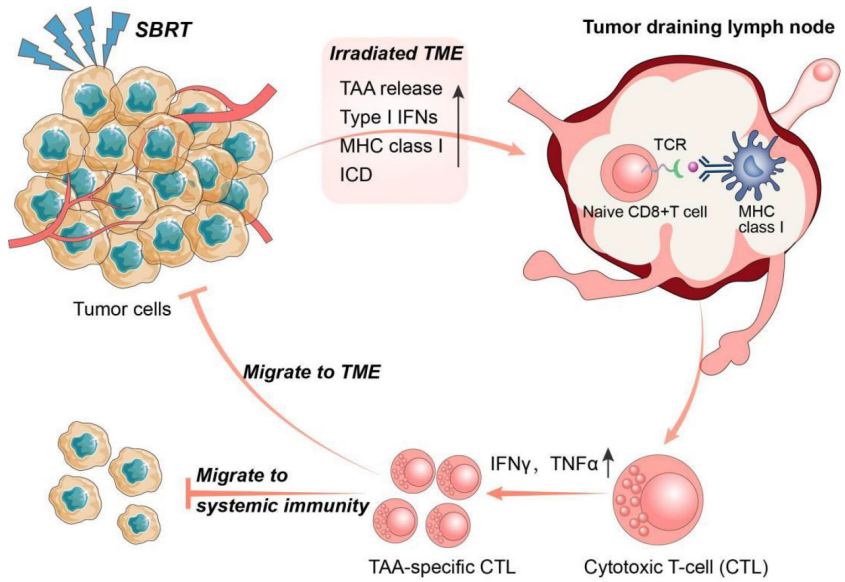

FIGURE 2
The interplay between SBRT and antitumour immune response. Stereotactic body radiation therapy (SBRT) could promote the activation of anti-tumour immune system through multiple pathways. In turn, activated anti-tumour immune responses also play a key role in the radio-induced abscopal effect. Specifically, SBRT can initiate antigen presentation by promoting the release of tumor-associated antigens (TAA) and major histocompatibility complex I (MHC I), and induce immunogenic cell death (ICD) in tumour cells. Tumour draining lymph nodes (TDLNs) are the main sites of anti-tumour immunity initiation where immune cells develop into progenitor cells after binding to antigens presented by dendritic cells (DCs). The progenitor cells subsequently differentiate into TAA-specific cytotoxic T lymphocytes (CTLs) and migrate into the tumour microenvironment (TME) and systemic immunity.

The dose and fraction of SBRT have also been demonstrated to impact the activation of TDLN-mediated systemic immune response. However, there are conflicting data and divergent opinions on the superiority of low-dose SBRT and single high-dose SBRT. Lee et al. discovered that low-dose SBRT (5 Gy×4 over 2 weeks) was significantly less effective in inducing a systemic antitumour immune response than a single dose of SBRT (20 Gy), possibly due to the gradual elimination of effector T cells and subsequent early relapse (53). In contrast, other reports have demonstrated that low-dose SBRT can elicit more favourable local and systemic immune responses and synergize with immunotherapy. For instance, Dewan et al. found that in a bilateral preclinical model of breast cancer, low-dose radiotherapy (8 Gy×3 or 6 Gy×5) combined with immunotherapy was more effective than administering a single high dose of 20 Gy. This combination not only slowed down tumour growth at the irradiation site but also significantly inhibiting lung metastasis and prolonging the survival of mice (56). Furthermore, Schaue et al. demonstrated in a mouse model loaded with B16-OVA melanoma cells that low-dose SBRT (7.5 Gy×2 and 5 Gy×3) was generally superior to a single dose of radiotherapy (15 Gy) in inducing peripheral tumour-specific immune responses (57).

A noteworthy finding from Savage et al. in a preclinical model of lung cancer was the efficacy of a new radiotherapy regimen (22 Gy followed by 0.5 Gy × 4 days) in increasing the infiltration of Granzyme B^+CD8^+ T cells within TME, while simultaneously reducing immune suppression caused by Tregs and M2 macrophages when compared to standard SBRT. Further immunoassay of secondary lymphoid organs indicated a significant increase in Granzyme B^+CD8^+ T cells and IFN-γ^+CD8^+ T cells in TDLNs of mice treated with the new radiotherapy regimen. These promising preclinical results offer a potential new radiotherapy regimen for clinical application to enhance its immunogenic potential (58). Overall, the above preclinical studies provide a foundation for the use of neoadjuvant SBRT combined with immunotherapy in early NSCLC to prevent distant metastasis.

4 Advances in neoadjuvant SBRT combined with immunotherapy for NSCLC

The combination of SBRT and immunotherapy has exhibited substantial potential in triggering a systematic antitumour immune response, as evidenced by preclinical studies. Clinically, Shaverdian et al. conducted a prospective analysis and demonstrated that advanced NSCLC patients who received radiotherapy prior to pembrolizumab treatment had significantly longer progression-free survival and overall survival compared to those without previous radiotherapy (59). As for neoadjuvant therapy, preliminarily clinical trials have shown that neoadjuvant SBRT combined with immunotherapy can prolong the survival of patients in several tumours by inducing a systemic antitumour immune response. For instance, in a study of 30 patients with locally advanced oral cavity squamous cell carcinoma, the addition of SBRT to neoadjuvant nivolumab therapy resulted in significant rates of major pathological response (MPR)(60.0%) and pCR (33.3%) in the neoadjuvant therapy group. Additionally, the group receiving combined treatment had an improved 24-month disease-free survival rate (70.4%) and OS rates (76.4%) (60). In another prospective study of locally advanced head and neck squamous cell carcinoma, the combination of neoadjuvant nivolumab and SBRT (40 Gy×5 or 24 Gy×3) significantly improved pathological responses in patients, with 86% achieving MPR and 67% achieving pCR (60).

Several phase II clinical trials have been initiated in resectable early NSCLC to investigate the feasibility, toxicity, and optimal schedule of neoadjuvant SBRT combined with immunotherapy based on increasing preclinical and clinical evidence (Table 1). For instance, a multicentre phase II trial (NCT04245514) evaluated the safety and efficacy of adding immunotherapy to neoadjuvant radiotherapy in patients with resectable stage III NSCLC. Durvalumab was administered in combination with SBRT (5 Gy×5 and 8 Gy×3) or conventional radiotherapy (2 Gy×20) to observe 12-month EFS after surgery, with recurrence-free survival and OS as secondary outcomes. Notably, the timing of SBRT initiation in neoadjuvant therapy remains inconsistent across current clinical trials. For instance, in one clinical trial (NCT05319574) for operable stage IB to III NSCLC, SBRT (8 Gy×3) was initiated 1-7 days before the first cycle of immunochemotherapy, whereas another trial (NCT05500092) started SBRT (8 Gy×3) therapy at the end of the first immunotherapy cycle (three cycles of neoadjuvant nivolumab plus chemotherapy). Additionally, in the clinical trial (NCT03110978) conducted by chang et al., nivolumab was administered either 36 hours before or after the initial fraction of SBRT. Significantly, the recent report on this trial demonstrated that combination therapy effectively enhances the 4-year EFS rate to 77%, compared to only 53% (95% CI 42–67%) achieved with SBRT monotherapy (61). The variation in therapy schedules among these clinical trials facilitates the exploration of optimal combination therapy strategies and underscores the need for a thorough understanding of the underlying mechanisms of neoadjuvant combination therapy.

5 Future challenges and directions for neoadjuvant combination therapy

Further research is needed to determine the optimal dosage, fraction, and schedule of radiotherapy in neoadjuvant combination therapy to enhance the systemic antitumour immune response, which remains a challenging task (62).

Limited research has been conducted on the impact of varying doses and fractions of radiotherapy on local and systemic immune responses in NSCLC patients. A recent clinical trial investigated the safety and efficacy of pembrolizumab combined with SBRT (50 Gy in four fractions) or conventional radiotherapy (45 Gy in 15 fractions) for treating lung and liver metastases in metastatic NSCLC. The results revealed that the group receiving pembrolizumab plus SBRT had an objective response rate of 38%,

TABLE 1 Clinical trials of neoadjuvant SBRT combined with immunotherapy in NSCLC.

NCT number	Patient tumour stage	Radiotherapy planning	Immunotherapy planning	Primary outcome	Secondary Outcome	Phase
NCT04245514	Resectable Stage III (N2)	Cohort A: 2Gy × 20 weekdaily Cohort B: 5Gy × 5 weekdaily Cohort C: 8Gy × 3 q2d	1 cycle of durvalumab	Event-free survival (EFS) at 12 months	Event-free survival (EFS) Recurrence-free survival (RFS) Overall survival (OS)	2
NCT05319574	Operable stage IB to III	8Gy in 3 daily fractions	2 cycles of tislelizumab (200mg) with platinum-based doublet chemotherapy administered pre-surgery	Major Pathological Response (MPR)	Pathologic Complete response (PCR) Resected rate Disease-free survival	2
NCT05500092	Resectable stage IIA to IIIB	8Gy in 3 daily fractions	3 cycles of neoadjuvant nivolumab and platinum-based doublet chemotherapy	Complete pathological response rate (CPR)	Major Pathological Response (MPR) Event Free Survival (EFS)	2
NCT04933903	Operable stage IB - III	7Gy × 1; 4Gy × 2	Ipilimumab + nivolumab	Number of Patients with a Pathologic Response	Incidence of Treatment-Emergent Adverse Events	2
NCT03217071	Resectable stage I-IIIA	Single 12 Gy	2 cycles of pembrolizumab every 3 weeks	Change in number of infiltrating CD3+ T cells/μm^2 Proportion of achieving a two-fold increase	Treatment-Related Adverse Events (AEs) Grade 3 immune-related AEs Overall Survival	2
NCT04271384	Stage I	18 Gy × 3 or 10 Gy × 5 or 7.5 Gy × 8	3 cycles of nivolumab every 3 weeks	Pathologic complete response (pCR)	Major pathological response (MPR) Treatment-related adverse events Objective response rate (ORR)	2
NCT03110978	Stage I-IIA or Recurrent	SBRT over 1-2 weeks	3 cycles of nivolumab every 4 weeks	Event-free survival (EFS)	Overall survival (OS) Incidence of treatment-related adverse events	2

while only 10% was observed in the group receiving pembrolizumab plus conventional radiotherapy (63). This clinical trial demonstrated the superiority of SBRT over conventional radiotherapy in antitumour metastasis, no differences were observed between different SBRT regimens. Therefore, a convincing preclinical study is required to address this issue. However, the challenge with current preclinical research is the disparity between its findings and applicability in clinical practice (64). The inconsistency maybe attributed to the absence of preclinical models that can accurately replicate the immune microenvironment of patients. Current preclinical models primarily employ murine-derived cell lines in normal mice, and their use of murine-derived immune system and immune checkpoint inhibitors further undermines the reliability of preclinical research outcomes (56). Therefore, the development of a humanised mouse model, in which human immune cells are transplanted into mice with severe combined immunodeficiency, is anticipated to offer a solution to this challenge (65).

In addition to investigating the effects of radiotherapy dosage and fraction on the immune system, determining the optimal schedule is also critical in neoadjuvant therapy. To this end, Dewan et al. conducted a preclinical study using a bilateral breast cancer model to investigate the effect of combination therapy when altering the timing of immunotherapy relative to radiotherapy. The study aimed to investigate the impact of initiating immunotherapy 2 days before, on that same day as, or 2 days after SBRT (8 Gy×3) completion on tumour growth. Results showed that initiating immunotherapy 2 days before or on the same day as radiotherapy ended inhibited tumour growth at both irradiated and non-irradiated sites. However, delaying immunotherapy until 2 days after the completion of radiotherapy reduced therapeutic efficacy, resulting in complete regression of only one of the six primary tumours and reduced growth inhibition in the non-irradiated sites. This indicates that the timing of immunotherapy vs. radiotherapy might influence the efficacy of the combination therapy (56). Similarly, Dovedi et al. investigated the optimal schedule for combining immunotherapy with SBRT (10 Gy×5) by varying the timing of treatment. The results showed that adding immunotherapy at the beginning or end of SBRT did not significantly affect the OS in mice. However, initiating immunotherapy one week after the end of SBRT was entirely ineffective in improving OS, similar to radiotherapy alone. Furthermore, they analysed the dynamics of $CD4^+$ T cells and $CD8^+$ T cells in the TME to explore the underlying mechanisms of the optimal combination schedule. Results indicated a significant increase in PD-1^+CD4^+ and PD-1^+CD8^+ T cell proportions within the tumour one day after SBRT completion, but a significant decrease in PD-1^+CD8^+ T cells seven days post-radiotherapy (66). Collectively, these preclinical studies suggest that SBRT leads to an acute increase in tumour-specific $CD8^+$ T cells. Adding

immunotherapy after the completion of the radiotherapy cycle might result in a significant decrease in the treatment's efficacy due to the anergy of these cells.

Identification of predictive biomarkers for neoadjuvant combination therapy is crucial in determining the population that will benefit and dynamically evaluating therapy efficacy (67). Nevertheless, the biomarkers of neoadjuvant SBRT in combination with immunotherapy remain unknown as classical immunotherapy biomarkers such as PD-L1 and tumour mutation burden fail to dynamically reflect the changes in the TME and systemic antitumour immune response (68). Recent studies have focused on the kinetics of specific immune cell subsets in systemic immunity and their correlation with efficacy (69). For example, Huang et al. reported that TCF-1^{+}TOX^{-}CD8^{+} T cells in TDLNs are bona fide memory T cells that can migrate and differentiate into systemic immunity after immune checkpoint inhibitor therapy (52). Therefore, the kinetics of CD8^{+} T cell subsets in peripheral immunity after neoadjuvant immunotherapy might be closely associated with efficacy. In addition, Kamphorst et al. reported that increased Ki67^{+}PD-1^{+}CD8^{+} T cells could be detected in the peripheral blood of approximately 70% of patients with lung cancer 4 weeks after receiving immunotherapy. These cells are considered to be tumour-specific T cells, and their kinetics are correlated with positive clinical outcomes (70). In summary, specific immune subpopulations in systemic immunity might serve as potential biomarkers for dynamically monitoring immune responses in patients with NSCLC undergoing neoadjuvant combination therapy.

6 Discussion

Preliminary preclinical findings demonstrate the significant potential of SBRT in combination with immunotherapy in neoadjuvant setting for resectable NSCLC. Furthermore, several ongoing clinical trials are investigating the feasibility and toxicity of this novel neoadjuvant combination therapy; however, it will take some time for data to confirm its clinical efficacy. In addition, the determination of optimal dosage and fractions, identification of predictive biomarkers, and establishment of an optimal schedule for combination therapy are all crucial factors that impact the efficacy of neoadjuvant therapy. Therefore, further preclinical and clinical studies are imperative to address these challenges prior to widespread implementation it in clinical practice.

Author contributions

YS, XM and DH contribute to the literature research, figures and drafted the manuscript. BD and TQ provided supervision and editing the final manuscript. All authors have agreed to the published version of the manuscript.

Conflict of interest

XM was employed by KingMed Medical Laboratory Xi'an Co., Ltd.

The remaining authors declare that the research was conducted in the absence of any commercial or financial relationships that could be construed as a potential conflict of interest.

Publisher's note

References

1. Bezjak A, Paulus R, Gaspar L, Timmerman R, Straube W, Ryan W, et al. Safety and efficacy of a five-fraction stereotactic body radiotherapy schedule for centrally located non-small-cell lung cancer: NRG oncology/RTOG 0813 trial. *J Clin Oncol: Off J Am Soc Clin Oncol* (2019) 37(15):1316–25. doi: 10.1200/JCO.18.00622

2. Collen C, Christian N, Schallier D, Meysman M, Duchateau M, Storme G, et al. Phase II study of stereotactic body radiotherapy to primary tumour and metastatic locations in oligometastatic nonsmall-cell lung cancer patients. *Ann Oncol: Off J Eur Soc Med Oncol* (2014) 25(10):1954–9. doi: 10.1093/annonc/mdu370

3. Iyengar P, Westover K, Timmerman RD. Stereotactic ablative radiotherapy (SABR) for non-small cell lung cancer. *Semin Respir Crit Care Med* (2013) 34:845–54. doi: 10.1055/s-0033-1358554

4. Videtic G, Donington J, Giuliani M, Heinzerling J, Karas T, Kelsey C, et al. Stereotactic body radiation therapy for early-stage non-small cell lung cancer: executive summary of an ASTRO evidence-based guideline. *Pract Radiat Oncol* (2017) 7(5):295–301. doi: 10.1016/j.prro.2017.04.014

5. Nyman J, Hallqvist A, Lund J, Brustugun O, Bergman B, Bergström P, et al. SPACE - A randomized study of SBRT vs conventional fractionated radiotherapy in medically inoperable stage I NSCLC. *Radiother Oncol: J Eur Soc Ther Radiol Oncol* (2016) 121(1):1–8. doi: 10.1016/j.radonc.2016.08.015

6. Jeppesen S, Schytte T, Jensen H, Brink C, Hansen O. Stereotactic body radiation therapy versus conventional radiation therapy in patients with early stage non-small cell lung cancer: an updated retrospective study on local failure and survival rates. *Acta Oncol (Stockholm Sweden).* (2013) 52(7):1552–8. doi: 10.3109/0284186X.2013.813635

7. Li C, Wang L, Wu Q, Zhao J, Yi F, Xu J, et al. A meta-analysis comparing stereotactic body radiotherapy vs conventional radiotherapy in inoperable stage I non-small cell lung cancer. *Medicine* (2020) 99(34):e21715. doi: 10.1097/MD.0000000000021715

8. von Reibnitz D, Shaikh F, Wu A, Treharne G, Dick-Godfrey R, Foster A, et al. Stereotactic body radiation therapy (SBRT) improves local control and overall survival compared to conventionally fractionated radiation for stage I non-small cell lung cancer (NSCLC). *Acta Oncol (Stockholm Sweden)* (2018) 57(11):1567–73. doi: 10.1080/0284186X.2018.1481292

9. Timmerman R, Herman J, Cho L. Emergence of stereotactic body radiation therapy and its impact on current and future clinical practice. *J Clin Oncol: Off J Am Soc Clin Oncol* (2014) 32(26):2847–54. doi: 10.1200/JCO.2014.55.4675

10. Mac Manus M, Lamborn K, Khan W, Varghese A, Graef L, Knox S. Radiotherapy-associated neutropenia and thrombocytopenia: analysis of risk factors and development of a predictive model. *Blood* (1997) 89(7):2303–10. doi: 10.1182/blood.V89.7.2303

11. Tse E, Kwong Y. The diagnosis and management of NK/T-cell lymphomas. *J Hematol Oncol* (2017) 10(1):85. doi: 10.1186/s13045-017-0452-9

12. Mills B, Qiu H, Drage M, Chen C, Mathew J, Garrett-Larsen J, et al. Modulation of the human pancreatic ductal adenocarcinoma immune microenvironment by stereotactic body radiotherapy. *Clin Cancer Res: an Off J Am Assoc Cancer Res* (2022) 28(1):150–62. doi: 10.1158/1078-0432.CCR-21-2495

13. Swamy K. Vascular normalisation and immunotherapy: spawning a virtuous cycle. *Front Oncol* (2022) 12:1002957. doi: 10.3389/fonc.2022.1002957

14. van der Woude L, Gorris M, Wortel I, Creemers J, Verrijp K, Monkhorst K, et al. Tumour microenvironment shows an immunological abscopal effect in patients with NSCLC treated with pembrolizumab-radiotherapy combination. *J Immunother Cancer* (2022) 10(10):e005248. doi: 10.1136/jitc-2022-005248

15. Cascone T, Leung C, Weissferdt A, Pataer A, Carter B, Godoy M, et al. Neoadjuvant chemotherapy plus nivolumab with or without ipilimumab in operable non-small cell lung cancer: the phase 2 platform NEOSTAR trial. *Nat Med* (2023) 29 (3):593–604. doi: 10.1038/s41591-022-02189-0

16. Forde P, Chaft J, Smith K, Anagnostou V, Cottrell T, Hellmann M, et al. Neoadjuvant PD-1 blockade in resectable lung cancer. *N Engl J Med* (2018) 378 (21):1976–86. doi: 10.1056/NEJMoa1716078

17. Hwang M, Canzoniero J, Rosner S, Zhang G, White J, Belcaid Z, et al. Peripheral blood immune cell dynamics reflect antitumour immune responses and predict clinical response to immunotherapy. *J Immunother Cancer* (2022) 10(6):e004688. doi: 10.1136/jitc-2022-004688

18. Rothschild S, Zippelius A, Eboulet E, Savic Prince S, Betticher D, Bettini A, et al. SAKK 16/14: durvalumab in addition to neoadjuvant chemotherapy in patients with stage IIIA(N2) non-small-cell lung cancer-A multicenter single-arm phase II trial. *J Clin Oncol: Off J Am Soc Clin Oncol* (2021) 39(26):2872–80. doi: 10.1200/JCO.21.00276

19. Forde P, Spicer J, Lu S, Provencio M, Mitsudomi T, Awad M, et al. Neoadjuvant nivolumab plus chemotherapy in resectable lung cancer. *N Engl J Med* (2022) 386 (21):1973–85. doi: 10.1056/NEJMoa2202170

20. Leidner R, Crittenden M, Young K, Xiao H, Wu Y, Couey M, et al. Neoadjuvant immunoradiotherapy results in high rate of complete pathological response and clinical to pathological downstaging in locally advanced head and neck squamous cell carcinoma. *J Immunother Cancer* (2021) 9(5):e002485. doi: 10.1136/jitc-2021-002485

21. Daro-Faye M, Kassouf W, Souhami L, Marcq G, Cury F, Niazi T, et al. Combined radiotherapy and immunotherapy in urothelial bladder cancer: harnessing the full potential of the anti-tumour immune response. *World J Urol* (2021) 39(5):1331–43. doi: 10.1007/s00345-020-03440-4

22. Wang Z, Qiang Y, Shen Q, Zhu X, Song Y. Neoadjuvant programmed cell death protein 1 blockade combined with stereotactic body radiation therapy for stage III(N2) non-small cell lung cancer: a case series. *Front Oncol* (2022) 12:779251. doi: 10.3389/fonc.2022.779251

23. Rodríguez Plá M, Dualde Beltrán D, Ferrer Albiach E. Immune checkpoints inhibitors and SRS/SBRT synergy in metastatic non-small-cell lung cancer and melanoma: a systematic review. *Int J Mol Sci* (2021) 22(21):11621. doi: 10.3390/ijms222111621

24. Azghadi S, Daly M. Radiation and immunotherapy combinations in non-small cell lung cancer. *Cancer Treat Res Commun* (2021) 26:100298. doi: 10.1016/j.ctarc.2020.100298

25. Simone C, Burri S, Heinzerling J. Novel radiotherapy approaches for lung cancer: combining radiation therapy with targeted and immunotherapies. *Trans Lung Cancer Res* (2015) 4(5):545–52. doi: 10.3978/j.issn.2218-6751.2015.10.05

26. Tubin S, Yan W, Mourad W, Fossati P, Khan M. The future of radiation-induced abscopal response: beyond conventional radiotherapy approaches. *Future Oncol (London England)* (2020) 16(16):1137–51. doi: 10.2217/fon-2020-0063

27. Muraro E, Furlan C, Avanzo M, Martorelli D, Comaro E, Rizzo A, et al. Local high-dose radiotherapy induces systemic immunomodulating effects of potential therapeutic relevance in oligometastatic breast cancer. *Front Immunol* (2017) 8:1476. doi: 10.3389/fimmu.2017.01476

28. Vaupel P, Multhoff G. Adenosine can thwart antitumor immune responses elicited by radiotherapy: Therapeutic strategies alleviating protumor ADO activities. *Strahlenther Onkol* (2016) 192(5):279–87. doi: 10.1007/s00066-016-0948-1

29. Palermo B, Bottero M, Panetta M, Faiella A, Sperduti I, Masi S, et al. Stereotactic ablative radiation therapy in 3 fractions induces a favorable systemic immune cell profiling in prostate cancer patients. *Oncoimmunology* (2023) 12(1):2174721. doi: 10.1080/2162402X.2023.2174721

30. Zhu M, Yang M, Zhang J, Yin Y, Fan X, Zhang Y, et al. Immunogenic cell death induction by ionizing radiation. *Front Immunol* (2021) 12:705361. doi: 10.3389/fimmu.2021.705361

31. Ahmed A, Tait S. Targeting immunogenic cell death in cancer. *Mol Oncol* (2020) 14(12):2994–3006. doi: 10.1002/1878-0261.12851

32. Li Z, Lai X, Fu S, Ren L, Cai H, Zhang H, et al. Immunogenic cell death activates the tumour immune microenvironment to boost the immunotherapy efficiency. *Adv Sci (Weinheim Baden-Wurttemberg Germany)* (2022) 9(22):e2201734. doi: 10.1002/advs.202201734

33. Zhou P, Chen D, Zhu B, Chen W, Xie Q, Wang Y, et al. Stereotactic body radiotherapy is effective in modifying the tumour genome and tumour immune microenvironment in non-small cell lung cancer or lung metastatic carcinoma. *Front Immunol* (2020) 11:594212. doi: 10.3389/fimmu.2020.594212

34. Rao A, Liu Y, von Eyben R, Hsu C, Hu C, Rosati L, et al. Multiplex proximity ligation assay to identify potential prognostic biomarkers for improved survival in locally advanced pancreatic cancer patients treated with stereotactic body radiation therapy. *Int J Radiat Oncol Biol Phys* (2018) 100(2):486–9. doi: 10.1016/j.ijrobp.2017.10.001

35. Choi C, Jeong M, Park Y, Son C, Lee H, Koh E. Combination treatment of stereotactic body radiation therapy and immature dendritic cell vaccination for augmentation of local and systemic effects. *Cancer Res Treat* (2019) 51(2):464–73. doi: 10.4143/crt.2018.186

36. Singh A, Winslow T, Kermany M, Goritz V, Heit L, Miller A, et al. A pilot study of stereotactic body radiation therapy combined with cytoreductive nephrectomy for metastatic renal cell carcinoma. *Clin Cancer Res* (2017) 23(17):5055–65. doi: 10.1158/1078-0432.CCR-16-2946

37. Guo L, Ding G, Xu W, Lu Y, Ge H, Jiang Y, et al. Prognostic biological factors of radiation pneumonitis after stereotactic body radiation therapy combined with pulmonary perfusion imaging. *Exp Ther Med* (2019) 17(1):244–50. doi: 10.3892/etm.2018.6936

38. Friedrich M, Neri P, Kehl N, Michel J, Steiger S, Kilian M, et al. The pre-existing T cell landscape determines the response to bispecific T cell engagers in multiple myeloma patients. *Cancer Cell* (2023) 41(4):711–25.e6. doi: 10.1016/j.ccell.2023.02.008

39. Lee H, Guo Y, Ross J, Schoen S, Degertekin F, Arvanitis C. Spatially targeted brain cancer immunotherapy with closed-loop controlled focused ultrasound and immune checkpoint blockade. *Sci Adv* (2022) 8(46):eadd2288. doi: 10.1126/sciadv.add2288

40. Garnett C, Palena C, Chakraborty M, Tsang K, Schlom J, Hodge J. Sublethal irradiation of human tumour cells modulates phenotype resulting in enhanced killing by cytotoxic T lymphocytes. *Cancer Res* (2004) 64(21):7985–94. doi: 10.1158/0008-5472.CAN-04-1525

41. Guo Y, Shen R, Wang F, Wang Y, Xia P, Wu R, et al. Carbon ion irradiation induces DNA damage in melanoma and optimizes the tumour microenvironment based on the cGAS-STING pathway. *J Cancer Res Clin Oncol* (2023) 149(9):6315–28. doi: 10.1007/s00432-023-04577-6

42. Mireştean C, Iancu R, Iancu D. Immunotherapy and radiotherapy as an antitumoral long-range weapon-A partnership with unsolved challenges: dose, fractionation, volumes, therapeutic sequence. *Curr Oncol (Toronto Ont)* (2022) 29 (10):7388–95. doi: 10.3390/curroncol29100580

43. Ji D, Song C, Li Y, Xia J, Wu Y, Jia J, et al. Combination of radiotherapy and suppression of Tregs enhances abscopal antitumour effect and inhibits metastasis in rectal cancer. *J Immunother Cancer* (2020) 8(2):e000826. doi: 10.1136/jitc-2020-000826

44. Frey B, Rückert M, Deloch L, Rühle P, Derer A, Fietkau R, et al. Immunomodulation by ionizing radiation-impact for design of radio-immunotherapies and for treatment of inflammatory diseases. *Immunol Rev* (2017) 280(1):231–48. doi: 10.1111/imr.12572

45. Ashrafizadeh M, Farhood B, Eleojo Musa A, Taeb S, Rezaeyan A, Najafi M. Abscopal effect in radioimmunotherapy. *Int Immunopharmacol* (2020) 85:106663. doi: 10.1016/j.intimp.2020.106663

46. Kimura T, Fujiwara T, Kameoka T, Adachi Y, Kariya S. The current role of stereotactic body radiation therapy (SBRT) in hepatocellular carcinoma (HCC). *Cancers* (2022) 14(18):4383. doi: 10.3390/cancers14184383

47. Cloughesy T, Mochizuki A, Orpilla J, Hugo W, Lee A, Davidson T, et al. Neoadjuvant anti-PD-1 immunotherapy promotes a survival benefit with intratumoral and systemic immune responses in recurrent glioblastoma. *Nat Med* (2019) 25(3):477–86. doi: 10.1038/s41591-018-0337-7

48. Liu Y, Dong Y, Kong L, Shi F, Zhu H, Yu J. Abscopal effect of radiotherapy combined with immune checkpoint inhibitors. *J Hematol Oncol* (2018) 11(1):104. doi: 10.1186/s13045-018-0647-8

49. Ngwa W, Irabor O, Schoenfeld J, Hesser J, Demaria S, Formenti S. Using immunotherapy to boost the abscopal effect. *Nat Rev Cancer* (2018) 18(5):313–22. doi: 10.1038/nrc.2018.6

50. Demaria S, Ng B, Devitt M, Babb J, Kawashima N, Liebes L, et al. Ionizing radiation inhibition of distant untreated tumors (abscopal effect) is immune mediated. *Int J Radiat Oncol Biol Phys* (2004) 58(3):862–70. doi: 10.1016/j.ijrobp.2003.09.012

51. Dammeijer F, van Gulijk M, Mulder E, Lukkes M, Klaase L, van den Bosch T, et al. The PD-1/PD-L1-checkpoint restrains T cell immunity in tumor-draining lymph nodes. *Cancer Cell* (2020) 38(5):685–700.e8. doi: 10.1016/j.ccell.2020.09.001

52. Huang Q, Wu X, Wang Z, Chen X, Wang L, Lu Y, et al. The primordial differentiation of tumor-specific memory CD8 T cells as bona fide responders to PD-1/PD-L1 blockade in draining lymph nodes. *Cell* (2022) 185(22):4049–66.e25. doi: 10.1016/j.cell.2022.09.020

53. Lee Y, Auh S, Wang Y, Burnette B, Wang Y, Meng Y, et al. Therapeutic effects of ablative radiation on local tumour require CD8+ T cells: changing strategies for cancer treatment. *Blood* (2009) 114(3):589–95. doi: 10.1182/blood-2009-02-206870

54. Walker J, Rolig A, Charych D, Hoch U, Kasiewicz M, Rose D, et al. NKTR-214 immunotherapy synergizes with radiotherapy to stimulate systemic CD8 T cell responses capable of curing multi-focal cancer. *J Immunother Cancer* (2020) 8(1):e000464. doi: 10.1136/jitc-2019-000464

55. Pieper A, Rakhmilevich A, Spiegelman D, Patel R, Birstler J, Jin W, et al. Combination of radiation therapy, bempegaldesleukin, and checkpoint blockade eradicates advanced solid tumors and metastases in mice. *J Immunother Cancer* (2021) 9(6):e002715. doi: 10.1136/jitc-2021-002715

56. Dewan M, Galloway A, Kawashima N, Dewyngaert J, Babb J, Formenti S, et al. Fractionated but not single-dose radiotherapy induces an immune-mediated abscopal effect when combined with anti-CTLA-4 antibody. *Clin Cancer Res: an Off J Am Assoc Cancer Res* (2009) 15(17):5379–88. doi: 10.1158/1078-0432.CCR-09-0265

57. Schaue D, Ratikan J, Iwamoto K, McBride W. Maximizing tumour immunity with fractionated radiation. *Int J Radiat Oncol Biol Phys* (2012) 83(4):1306–10. doi: 10.1016/j.ijrobp.2011.09.049

58. Savage T, Pandey S, Guha C. Postablation modulation after single high-dose radiation therapy improves tumour control *via* enhanced immunomodulation. *Clin Cancer Res: an Off J Am Assoc Cancer Res* (2020) 26(4):910–21. doi: 10.1158/1078-0432.CCR-18-3518

59. Shaverdian N, Lisberg A, Bornazyan K, Veruttipong D, Goldman J, Formenti S, et al. Previous radiotherapy and the clinical activity and toxicity of pembrolizumab in the treatment of non-small-cell lung cancer: a secondary analysis of the KEYNOTE-001 phase 1 trial. *Lancet Oncol* (2017) 18(7):895–903. doi: 10.1016/S1470-2045(17)30380-7

60. Shen P, Qiao B, Jin N, Wang S. Neoadjuvant immunoradiotherapy in patients with locally advanced oral cavity squamous cell carcinoma: a retrospective study. *Investigational New Drugs* (2022) 40(6):1282–9. doi: 10.1007/s10637-022-01293-9

61. Chang J, Lin S, Dong W, Liao Z, Gandhi S, Gay C, et al. Stereotactic ablative radiotherapy with or without immunotherapy for early-stage or isolated lung parenchymal recurrent node-negative non-small-cell lung cancer: an open-label, randomised, phase 2 trial. *Lancet (London England)* (2023) S0140-6736(23)01406-X. doi: 10.1016/S0140-6736(23)01384-3

62. Moran A, Azghadi S, Maverakis E, Christensen S, Dyer B. Combined immune checkpoint blockade and stereotactic ablative radiotherapy can stimulate response to immunotherapy in metastatic melanoma: a case report. *Cureus* (2019) 11(2):e4038. doi: 10.7759/cureus.4038

63. Welsh J, Menon H, Chen D, Verma V, Tang C, Altan M, et al. Pembrolizumab with or without radiation therapy for metastatic non-small cell lung cancer: a randomized phase I/II trial. *J Immunother Cancer* (2020) 8(2):e001001. doi: 10.1136/jitc-2020-001001

64. McBride S, Sherman E, Tsai C, Baxi S, Aghalar J, Eng J, et al. Randomized phase II trial of nivolumab with stereotactic body radiotherapy versus nivolumab alone in metastatic head and neck squamous cell carcinoma. *J Clin Oncol: Off J Am Soc Clin Oncol* (2021) 39(1):30–7. doi: 10.1200/JCO.20.00290

65. Guo W, Zhang C, Qiao T, Zhao J, Shi C. Strategies for the construction of mouse models with humanized immune system and evaluation of tumour immune checkpoint inhibitor therapy. *Front Oncol* (2021) 11:673199. doi: 10.3389/fonc.2021.673199

66. Dovedi S, Adlard A, Lipowska-Bhalla G, McKenna C, Jones S, Cheadle E, et al. Acquired resistance to fractionated radiotherapy can be overcome by concurrent PD-L1 blockade. *Cancer Res* (2014) 74(19):5458–68. doi: 10.1158/0008-5472.CAN-14-1258

67. Yamauchi T, Hoki T, Oba T, Jain V, Chen H, Attwood K, et al. T-cell CX3CR1 expression as a dynamic blood-based biomarker of response to immune checkpoint inhibitors. *Nat Commun* (2021) 12(1):1402. doi: 10.1038/s41467-021-21619-0

68. Deng H, Zhao Y, Cai X, Chen H, Cheng B, Zhong R, et al. PD-L1 expression and tumour mutation burden as pathological response biomarkers of neoadjuvant immunotherapy for early-stage non-small cell lung cancer: A systematic review and meta-analysis. *Crit Rev Oncol/Hematol* (2022) 170:103582. doi: 10.1016/j.critrevonc.2022.103582

69. Hiam-Galvez K, Allen B, Spitzer M. Systemic immunity in cancer. *Nat Rev Cancer* (2021) 21(6):345–59. doi: 10.1038/s41568-021-00347-z

70. Kamphorst A, Pillai R, Yang S, Nasti T, Akondy R, Wieland A, et al. Proliferation of PD-1+ CD8 T cells in peripheral blood after PD-1-targeted therapy in lung cancer patients. *Proc Natl Acad Sci USA* (2017) 114(19):4993–8. doi: 10.1073/pnas.1705327114

frontiers | Frontiers in Immunology

TYPE Review
PUBLISHED 18 October 2023
DOI 10.3389/fimmu.2023.1241208

OPEN ACCESS

EDITED BY
Chengwu Zeng,
Jinan University, China

REVIEWED BY
Maha Mohamed Saber-Ayad,
University of Sharjah, United Arab Emirates
Francis Yew Fu Tieng,
National University of Malaysia, Malaysia

*CORRESPONDENCE
Ketao Jin
jinketao2001@zju.edu.cn
Huanrong Lan
lanhr2018@163.com

†These authors have contributed equally to this work

RECEIVED 16 June 2023
ACCEPTED 09 October 2023
PUBLISHED 18 October 2023

CITATION
Yao S, Han Y, Yang M, Jin K and Lan H (2023) It's high-time to re-evaluate the value of induced-chemotherapy for reinforcing immunotherapy in colorectal cancer.
Front. Immunol. 14:1241208.
doi: 10.3389/fimmu.2023.1241208

It's high-time to re-evaluate the value of induced-chemotherapy for reinforcing immunotherapy in colorectal cancer

Shiya Yao[1†], Yuejun Han[1†], Mengxiang Yang[1†], Ketao Jin[1*] and Huanrong Lan[2*]

[1]Department of Colorectal Surgery, Affiliated Jinhua Hospital, Zhejiang University School of Medicine, Jinhua, Zhejiang, China, [2]Department of Surgical Oncology, Hangzhou Cancer Hospital, Hangzhou, Zhejiang, China

Immunotherapy has made significant advances in the treatment of colorectal cancer (CRC), revolutionizing the therapeutic landscape and highlighting the indispensable role of the tumor immune microenvironment. However, some CRCs have shown poor response to immunotherapy, prompting investigation into the underlying reasons. It has been discovered that certain chemotherapeutic agents possess immune-stimulatory properties, including the induction of immunogenic cell death (ICD), the generation and processing of non-mutated neoantigens (NM-neoAgs), and the B cell follicle-driven T cell response. Based on these findings, the concept of inducing chemotherapy has been introduced, and the combination of inducing chemotherapy and immunotherapy has become a standard treatment option for certain cancers. Clinical trials have confirmed the feasibility and safety of this approach in CRC, offering a promising method for improving the efficacy of immunotherapy. Nevertheless, there are still many challenges and difficulties ahead, and further research is required to optimize its use.

KEYWORDS

colorectal cancer, immunotherapy, inducing chemotherapy, immunogenic cell death, combination therapy, clinical trial, tumor microenvironment

1 Introduction

Colorectal cancer (CRC) is the third most common malignancy globally, after lung cancer, and is the second leading cause of cancer-related deaths in both men and women (1, 2). Despite improved screening for early detection, the global burden of disease and mortality has not significantly decreased (1). Approximately 20% of patients present with metastatic disease at diagnosis, and an additional 25% of patients who present with localized disease will

subsequently develop metastases (3). Most patients with metastatic CRC (mCRC) cannot be cured and are managed with palliative systemic therapy, resulting in poor prognosis with a median overall survival (mOS) of approximately 30 months (3). In the past five years, immunotherapy has made a significant impact on the treatment of CRC, with immune checkpoint inhibitors (ICIs) being particularly prominent. The tumor immune microenvironment (TIME) is intimately linked with tumor immunotherapy and represents a key obstacle to successful antitumor immune therapy, potentially limiting its clinical benefit. Numerous studies have demonstrated the efficacy of ICIs in the treatment of microsatellite instability (MSI-H)/mismatch repair-deficient (dMMR) mCRC. However, 95% of mCRC patients are microsatellite stable (MSS)/proficient mismatch repair (pMMR) subtype and are insensitive to immune therapy (4, 5). We will discuss the reasons for poor response to ICIs in this patient population, including defects in antigen presentation and peptide transport, immune evasion, abnormalities in the TIME, low tumor mutation burden, and targeting of apoptotic pathways, among others. Efforts are currently underway to overcome these barriers and improve the sensitivity of immune therapy in this patient population.

It was previously believed that chemotherapy was solely an immunosuppressive agent. However, recent data indicate that chemotherapy drugs can promote immune activation through various pathways, notably via the induction of immunogenic cell death (ICD) mechanisms (6–9). Certain chemotherapy drugs, such as doxorubicin (DOX), paclitaxel (PTX), and oxaliplatin (OXA), can kill tumor cells via ICD, thereby activating innate and adaptive antitumor immune responses. ICD is characterized by the release of danger-associated molecular patterns (DAMPs) and the generation and processing of non-mutated neoantigens (NM-neoAgs) tumor-associated antigens to enhance antigen presentation by promoting dendritic cell (DC) maturation and cytotoxic T lymphocyte (CTL) infiltration (10). This process can reverse the tumor immune suppressive microenvironment and increase the sensitivity of immunotherapy. A series of clinical studies supporting the combination of chemotherapy and ICIs in mCRC is currently ongoing. Based on this, the concept of inducing chemotherapy has been introduced, which involves administering chemotherapy prior to immunotherapy to convert the tumor microenvironment (TME) from "cold" to "hot," thereby enhancing the response to immunotherapy. Inducing chemotherapy combined with immunotherapy has become part of the standard treatment for certain cancers, with clinical trials confirming its feasibility in CRC. However, many challenges remain in the treatment of mCRC. The fusion of immunotherapy and Single-cell RNA sequencing (scRNA-seq) holds promise for providing truly personalized treatment for an increasing number of mCRC patients, enabling us to achieve personalized treatment strategies (11). Additionally, significant research is needed to optimize this combined treatment approach, including how to optimize dosage regimens, such as dose, timing, and sequence, and biomarker prediction studies. We look forward to further breakthroughs in the future to provide more effective and safer treatment options for cancer patients.

2 Exploring the progress and challenges of immunotherapy in CRC

Immune checkpoint inhibitors (ICIs) have brought new opportunities in cancer treatment (12–15). The programmed cell death protein 1/programmed death-ligand 1 (PD-1/PD-L1) signaling pathway in tumors is a crucial mechanism for evading immune surveillance. The FDA first approved the use of immunotherapy drugs for treating mCRC in 2017 (16–19). Pembrolizumab (an anti-PD-1 monoclonal antibody) has been established as the new standard for first-line treatment in MSI-H/dMMR mCRC (20).

Despite the tremendous potential of immunotherapy in CRC treatment, there are also challenges and limitations. CRC is a common malignancy, with the majority being MSS/pMMR type. Compared to MSI-H/dMMR tumors, MSS/pMMR tumors have poorer response to immunotherapy, primarily due to immune suppression or immune desertification (21–23), characterized by low levels or defects in T-cell infiltration and reduced checkpoint protein expression (5). They generally do not benefit from immune therapies such as PD-1/PD-L1 inhibitors (24, 25), indicating obstacles to the effectiveness of immunotherapy (26). The mechanisms of resistance to immunotherapy in MSS/pMMR CRC are highly complex (Figure 1) (27).

Mutations in antigen presentation-related genes in tumor cells lead to loss of antigens within tumor cells, which makes it difficult for T cells to recognize and attack tumor cells, thereby reducing the sensitivity of tumor cells to immunotherapy. For example, the BRAF ^{V600E} mutation has been shown to reduce T cells infiltration into the TME and eliminate neoantigen presentation on cancer cells (28, 29). Inhibiting BRAF signaling has been demonstrated to reduce myeloid-derived suppressor cells, increase the recruitment of tumor-infiltrating lymphocytes, enhance neoantigen presentation on antigen-presenting cells, and collectively enhance anti-tumor immune responses (28, 30–32).

MSS/pMMR CRC tumor cells have a lower tumor mutation burden, which means that the effectiveness of immunotherapy is relatively poor. These types of tumors exhibit a relative deficiency in CD8+ T cell infiltration (33, 34), as well as lower tumor mutation burdens (35–38) and multiple immune antigen defects, leading to tumor immune evasion (39, 40). Immune escape refers to the ability of tumor cells to evade attacks from the immune system through various mechanisms (41). Immune escape mechanisms in MSS/pMMR CRC include the lack of immune stimulatory molecules, overexpression of immune inhibitory molecules, deficiency in major histocompatibility complex class I (MHC I) molecules, and lack of T cell infiltration (42–44). The activating mutations of KRAS, as an upstream regulator of BRAF and a potent activator of MAPK, may play a role in immune escape by impairing interferon-mediated antigen presentation and recruitment of effector T cells to the TME (45, 46). Another preclinical study showed that RAS oncogenes induce immune escape by stabilizing PD-1 RNA and leading to sustained expression of PD-1 (47).

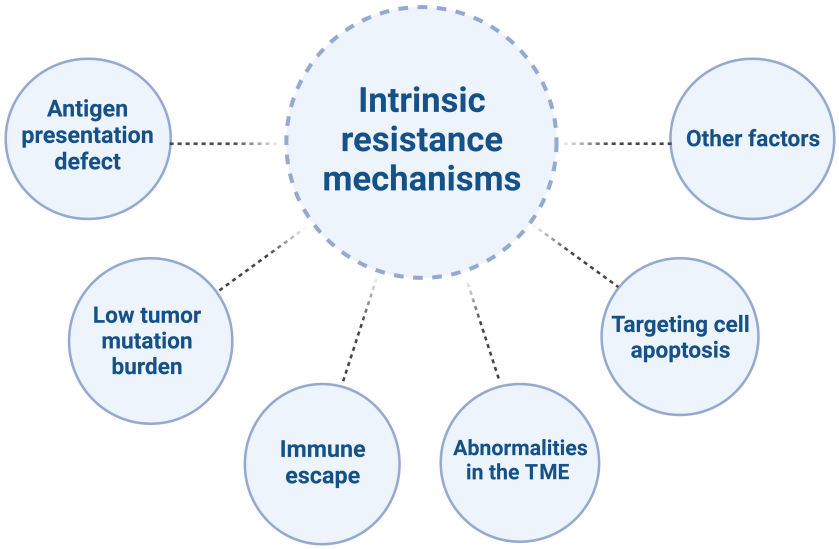

FIGURE 1
The intrinsic resistance mechanisms of MSS/pMMR mCRC to ICIs.

Increasing evidence suggests that the MAPK pathway may also be involved in immune exclusion, serving as another biological barrier to the success of immune therapy.

MSS/pMMR CRC is typically characterized by a "cold" or "excluded" TME, meaning that immune cells are unable to infiltrate the tumor or, even if they do, they are unable to exert their cytotoxic effects. Studies have shown that there is a reduced infiltration and activation of T cells in MSS/pMMR CRC, while the levels of immune suppressive cells (such as Tregs and myeloid-derived suppressor cells (MDSCs)) and immune inhibitory molecules (such as IDO1 and transforming growth factor-beta (TGF-β)) are elevated (48–50). This may weaken the anti-tumor response of T cells. For example, the increase in TGF-β is associated with an increase in Tregs, leading to downregulation of anti-tumor immunity. These data also support the role of the TGF-β pathway in downregulating NK cell activity, as NK cells play a role in innate immunity by recognizing cancer cells (51). It is worth noting that TGF-β activation has been observed in CRC liver metastasis, resulting in downregulation of CD4+ and CD8+ T cells (52). Activated B cells were found to be significantly depleted in liver metastases of CRC through scRNA-seq. The inhibitory effect on cancer cells was mediated by the suppression of the Wnt and TGF-β pathways through the SDF-1-CXCR4 axis, which promoted the migration of activated B cells (53).

In MSS/pMMR CRC, inhibition of the tumor cell apoptosis pathway renders the tumor cells insensitive to attacks from the immune system. Aberrant activation of the WNT/β-catenin signaling pathway is frequently observed in MSS CRC but is rare in MSI-H CRC (54, 55). Abnormal activation of the Wnt signaling pathway is associated with T cell exclusion and insufficient infiltration, which may lead to the inhibition of tumor cell apoptosis pathways and consequently result in treatment resistance (25, 54, 56–58). By inhibiting β-catenin pharmacologically, it is possible to increase the number of dendritic cells (DCs), upregulate CCL4, and promote the infiltration of CD8+ T cells in various tumor models, including CRC, thereby reactivating anti-tumor immune responses (59–61). Additionally, the overexpression of members of the Bcl-2 family and the presence of an immune suppressive microenvironment may also lead to the inhibition of tumor cell apoptosis pathways and consequently result in treatment resistance (62, 63). Other factors that may contribute to immunotherapy resistance in CRC include changes in the gut microbiome, which can impact the efficacy of immune therapy and lead to treatment resistance (64).

In summary, immunotherapy has had a profound impact on the traditional treatment of CRC, but it also poses challenges and limitations. Future research needs to further explore the combination of immunotherapy with conventional chemotherapy, overcome immune resistance mechanisms, and understand the influence of the TIME on the efficacy of immune therapy in order to enhance the effectiveness of immunotherapy and advance the treatment of CRC.

3 Mechanism of chemotherapy in promoting immune activation

Recent research in the field of immunotherapy has demonstrated that chemotherapy drugs not only enhance the immunogenicity of cancer cells but also induce immune stimulation by activating effector T cells and inhibiting immune suppressive cells. These exciting findings suggest that the combination of chemotherapy and ICIs may have synergistic anti-cancer effects, providing a promising treatment option for tumor patients who have a poor response to monotherapy with ICIs.

Studies have shown that chemotherapy drugs may exert their effects through immune stimulation mechanisms (65). For example,

anthracycline drugs can induce immunogenic cell death (ICD) and directly block immune inhibitory pathways in the TIME, leading to the release of neoantigens (NM-neoAgs) from cancer cells (6, 66–72). ICD is characterized by the presentation of dying cancer cells to antigen-presenting cells (APCs) in the form of danger-associated molecular patterns (DAMPs), which act as lymphoma adjuvant-like signals (73). Specifically, during the early stages of apoptosis, ICD induces the exposure of calreticulin (CRT) on the cell surface and releases extracellular ATP by upregulating autophagy during the detachment phase of apoptosis. It also promotes the release of high mobility group box 1 (HMGB1) during the secondary necrosis phase of cell death (71, 72, 74–82). CRT, ATP, and HMGB1 bind to their respective receptors (CD91 receptor, purinergic P2Y2 or P2X7 receptors, and TLR4) expressed on DCs, triggering their entry into the tumor tissue and upregulating antigen uptake processes. The resulting mature DCs (mDCs) present antigens and trigger a series of further immune responses. New antigens and danger signal molecules are released, forming a "cancer immune cycle" (83) (Figure 2). Overall, the ability of DCs to capture and present antigens is enhanced, and their ability to process NM-neoAgs and recruit CD4+ T cells/CD8+ T cells for an enhanced adaptive immune response in the tumor is more effective, thereby enhancing the immune system's ability to clear cancer cells (66). Additionally, pro-inflammatory cytokines such as TNF, IL-6, and IL-1β, which are detected during and after ICD induction, can increase MHC I expression on APCs, promote T cell differentiation, and activate NK cells (85). Activated DCs (such as IL-12) and other innate immune cells (such as cytokines produced by IFN-α/β) enhance NK cell function, leading to the secretion of IFN-γ and TNF (86).

The TIME is a key barrier to anti-tumor immunity and may limit the clinical efficacy of immunotherapy (87, 88). Immune cells not only act as "gatekeepers" of the tumor but can also have positive or negative effects on tumor growth and metastasis (89, 90). For example, Tregs and MDSCs can suppress the immune response of T cells and natural killer cells (NK cells), providing favorable conditions for cancer invasion, inhibiting anti-tumor immune responses, and promoting metastasis (91, 92). TAMs can exhibit anti-tumor properties (93). When activated, TAMs can promote the proliferation and activation of anti-tumor T cells, thereby inhibiting tumor growth and metastasis (93).Although the number and function of NK cells may be suppressed, recent research has shown that certain drugs can enhance the function of NK cells and play a significant role in tumor treatment (94). Studies have shown that chemotherapy can eliminate specific cells, such as Tregs and MDSCs (95, 96), which have immunosuppressive characteristics. This can transform non-inflammatory tumors (referred to as "cold tumors") into tumors rich in cytotoxic cells (referred to as "hot tumors") (97), especially when used at doses below the maximum tolerated dose. Recent research indicates that anti-PD-1 therapy can reshape the tumor immune microenvironment based on chemotherapy-induced changes, providing new insights for improving the effectiveness of combination immunotherapy and chemotherapy (98).

Furthermore, some studies suggest that chemotherapy-induced DNA damage fragments in the cell nucleus may actively translocate

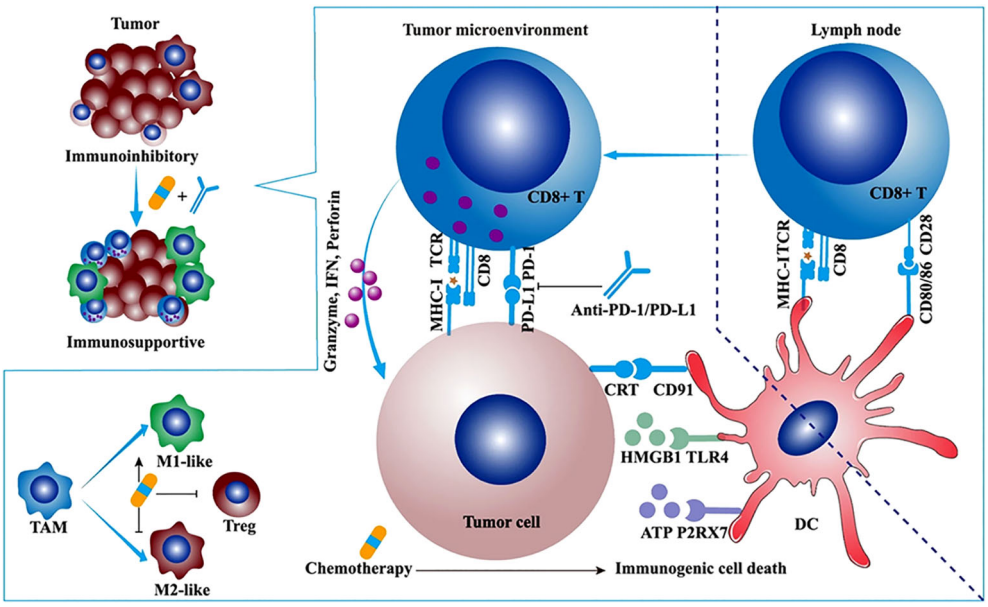

FIGURE 2
The synergistic antitumor efficacies and mechanisms of α-PD-1/PD-L1 in combination with chemotherapy, radiotherapy, or angiogenesis inhibitor. Chemotherapy synergizes with α-PD-1/PD-L1. Some cytotoxic chemotherapeutic drugs could induce immunogenic cell death and stimulate antitumor immune response. Immunogenic cell death (ICD) is featured with some upregulated damage-associated molecular patterns (DAMPs) such as calreticulin (CRT), ATP, and high-mobility group box 1 (HMGB1). The ATP-P2RX7, CRT-CD91, and HMGB1-TLR4 pathways facilitate the antigen capture and presentation of DC, ultimately motivating adaptive antitumor immune response. Apart from ICD, low-dose chemotherapy depletes regulatory T cells (Tregs) and promotes the repolarization of tumor-associated macrophage (TAM) from M2-like to M1-like phenotype (84).

to the cytoplasm to prevent their erroneous insertion into the genomic DNA. This process activates the innate immune cGAS-STING (cyclic GMP-AMP synthase/stimulator of interferon genes) pathway, leading to an immune-rich microenvironment and triggering innate immune responses (Figure 3A) (99–102).

Recent research has revealed new mechanisms of chemotherapy-induced immune modulation. Effective chemotherapy can induce B-cell-centered effector T-cell responses, suggesting that chemotherapy holds promising potential as a combination therapy with ICIs. This can be achieved by upregulating MHC I expression to directly modulate tumor immunogenicity and by enhancing the efficacy and quantity of CD8+ T cells through the enhanced interaction between endogenous-like B cells (ILBs) and effector helper T cells (T_H cells) (Figure 3B). ILBs enhance T_{FH} and T_H1 cells via the ICOSL-ICOS axis. The inducible T-cell co-stimulatory (ICOS) pathway is another important pathway in tumor immunotherapy. ICOS is a co-stimulatory receptor expressed on activated T cells and is crucial for their survival and function. The ICOS pathway plays a critical role in balancing effector T cells and Tregs, and its dysregulation has been associated with the development and progression of various types of cancer (103). Lu et al. (104) also found that chemotherapy induces complement signaling pathways, enhancing the anti-tumor properties of B cells. Overall, these data suggest that in addition to therapeutic interventions targeting the restoration of conventional DC function, chemotherapy interventions can reshape the plasticity of B cells and establish an anti-tumor environment. Similar findings and breakthroughs are hoped to be achieved in CRC.

In conclusion, the mechanisms of immune modulation activated by chemotherapy provide new insights for the clinical treatment of combination immunotherapy. Further research is needed to explore the combined strategies of chemotherapy and immunotherapy in order to achieve better treatment outcomes and wider clinical applications.

4 Cytotoxic chemotherapy drugs that promote anti-tumor immunity

Chemotherapy drugs were initially designed to directly inhibit or kill malignant cells to achieve their therapeutic effect. Recently, some frontline drugs have been found to further promote anti-tumor immunity by increasing tumor immunogenicity, improving T cells infiltration, or depleting immune-suppressive populations (Figure 4). There is increasing evidence that chemotherapy triggers complex immune events (105–109), which is due to the ability of drugs to induce ICD in tumor cells and to directly modulate immune cells. Some chemotherapy drugs have been shown to exert immune-stimulatory effects by inhibiting immune-suppressive cells and/or activating effector cells, or by increasing immunogenicity and T cells infiltration (110–112). Chemotherapy drugs that promote anti-tumor immunity can be classified into several categories based on their mechanisms (Table 1).

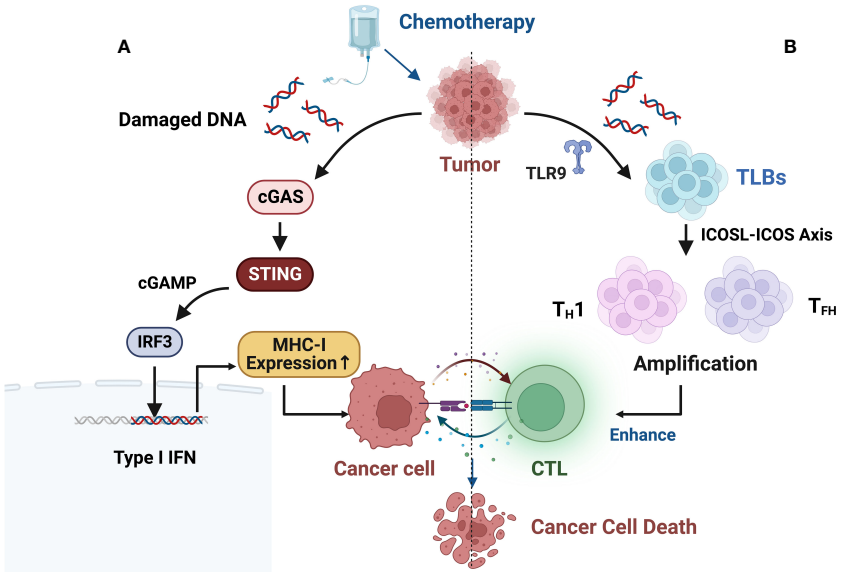

FIGURE 3
(A) Chemotherapy-induced DNA damage fragments in the nucleus may be actively exported to the cytoplasm to prevent their erroneous insertion into genomic DNA, thereby activating the innate immune cGAS-STING (cyclic GMP-AMP synthase/stimulator of interferon genes) pathway, resulting in an immune-rich microenvironment and triggering innate immune responses. **(B)** B cell-centered anti-tumor immune network. B-cell-centered anti-tumor immune network. Gemcitabine plus cisplatin (GP) chemotherapy activates an anti-tumor immune response dominated by a type of innate immune B cell (ILB). GP-mediated release of tumor cell DNA fragments can induce an ILB subset located in the third lymphoid structure induced by chemotherapy via Toll-like receptor 9 (TLR9) signaling. Subsequently, ILB promotes the expansion of type 1 helper T cells (T_H1) and follicular helper T cells (T_FH) via the ICOSL-ICOS signaling axis, thereby facilitating the cytotoxicity of CD8+ T lymphocytes (CTLs). Meanwhile, ILB can also activate the STING-IFN-I pathway of tumor cells, upregulating the expression of MHC I on tumor cells, forming a positive feedback loop.

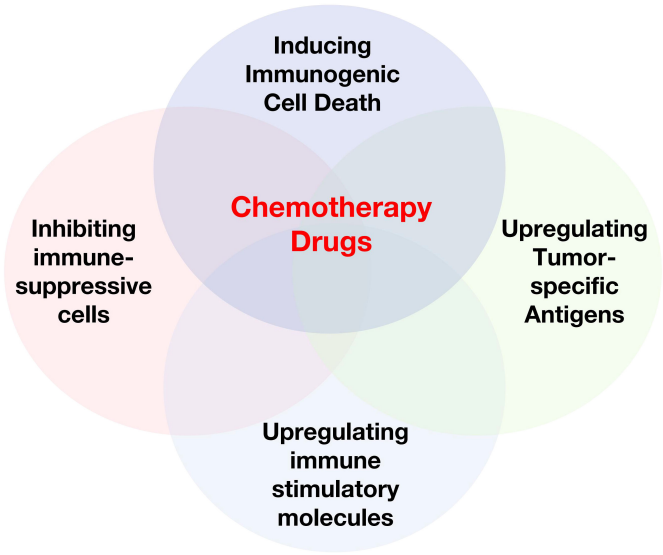

FIGURE 4
Cytotoxic Chemotherapy Drugs that Promote Anti-tumor Immunity. Some chemotherapy drugs have been shown to exert immune-stimulating effects by inducing immunogenic cell death, inhibiting immune suppressor cells, and/or activating effector cells, or upregulating tumor-specific antigens.

4.1 Inducing ICD

ICD is a form of apoptosis that can induce an effective anti-tumor immune response. Drugs that induce ICD include anthracycline chemotherapy drugs, OXA, and PTX (146–149). As mentioned earlier, these drugs induce an anti-tumor immune response by activating DCs and subsequent specific T cells responses.

Specifically, anthracycline chemotherapy drugs can induce ICD, which is a form of apoptosis that induces an effective anti-tumor immune response by activating DCs and subsequent specific T cells responses (150). Recent studies have found that drugs that induce ICD can also regulate anti-tumor CTL immunity through tumor-infiltrating NK and B cells. In human ovarian cancer, platinum-based and taxane-based chemotherapy significantly increased NK cells infiltration and local T cells oligoclonal expansion (116). In human breast cancer, a neoadjuvant regimen of DOX, cyclophosphamide(CTX), and PTX converted infiltrating tumor B cells to a new ICOSL+ phenotype. These newly appearing B cells participated in the formation of TLS and significantly increased the number and cytotoxicity of tumor-specific CD8+ T cells (104).Another topoisomerase II inhibitor, teniposide, can induce ICD, but its mechanism of action is different from that of anthracyclines. Topoisomerase II inhibitors induce proliferation arrest or death of tumor cells by increasing DNA double-strand breaks (130). As mentioned earlier, teniposide activates the endogenous type I interferon (IFN) response in tumor cells and upregulates features of ICD (Figure 3A). In murine colon cancer, teniposide induced potent anti-tumor CD8+ T cells immunity and significant tumor suppression. Administration of teniposide reversed the resistance of KRAS-mutant CT26 colon cancer to PD-1 blockade (151). Although it has positive immunomodulatory effects in mouse tumors, it remains unclear whether teniposide acts as an ICD inducer in human cancers. Considering its ability to activate anti-tumor CTL responses, chemotherapy drugs that induce ICD are thought to be able to enhance the therapeutic effect of ICIs. The combination of DOX and PD-1 or PD-L1 antibodies shows significant anti-tumor effects in various mouse cancers, such as melanoma and breast cancer (152, 153). In human metastatic triple-negative breast cancer (TNBC), short-term treatment with DOX induces sensitivity to PD-1 blockade (154). Similarly, OXA has been shown to enhance the anti-tumor effect of anti-PD-L1 therapy in mouse lung cancer, melanoma, and CRC (155). The combination of PTX and ICIs produce superior tumor suppression in non-immunogenic squamous non-small cell lung cancer (NSCLC) (156).

4.2 Upregulating tumor-specific antigens

Certain chemotherapy drugs can induce tumor cells to express antigens, thereby enhancing T cells recognition and killing of tumor cells.

For example, Irinotecan and Topotecan are derivatives of camptothecin, which can enhance T cells recognition of tumor cells and upregulate tumor-specific antigens (157). An *in vitro* experiment revealed the upregulation of DAMPs, HMGB1, and heat shock protein 70 (HSP70) after treatment with Irinotecan (131). In melanoma, they can upregulate tumor-specific antigens. Surviving tumor cells upregulate MHC I and Fas expression after treatment with Topotecan (85, 133), making them more susceptible to immune cells killing. PTX can stimulate DC maturation and antigen presentation through various mechanisms, such as the NF-κB and MAPK signaling pathways, TLR4/MyD88 pathways, etc.

10.3389/fimmu.2023.1241208

TABLE 1 Immunological effects of conventional antitumor agents.

Agent	Effect	Notes	Reference
Anthracyclines	Inducing ICD	Activation of DCs and subsequent specific T cell responses	(113)
	Facilitating antigen presentation by DCs	Promoting the proliferation of CD8 +T cells of specific antigens in TDLNs and the infiltration of tumors by CD8+ T cells produced by IFN-γ	(114, 115)
Cisplatin	Inducing ICD	Increasing the infiltration of NK cells and local T cells oligoclonal dilation	(116)
	Inhibiting immune-suppressive cells	Consuming MDSCs and Tregs	(117)
	Upregulating the expression of immune stimulatory molecules	Recruitment of effector cells by upregulating MHC I expression of antigen-presenting cells	(118–120)
	Upregulating tumor-specific antigens	Immunosuppressive effect by upregulation of PD-L1	(121)
		Reducing IFN-γ production in T cells	(122)
PTX	Inducing ICD	Increasing the infiltration of NK cells and local T cells oligoclonal dilation	(116)
		B cells regulate antitumor CTL immunity	(104)
	Upregulating tumor-specific antigens	Promoting the proliferation of CD8+ T cells and T+H1 cells	(123–126)
	Inhibiting immune-suppressive cells	Consuming MDSCs and Tregs	(127, 128)
	Upregulating the expression of immune stimulatory molecules	Upregulating the expression of TAA and MHC I in tumor cells	(129)
Etoposide	Inducing ICD	Activating the IFN response of tumor cells	(130)
Irinotecan	Upregulating tumor-specific antigens	Upregulation of DAMPs and HMGB1 and HSP70	(131)
	Inhibiting immune-suppressive cells	Inhibiting Tregs proliferation and function	(132)
Topotecan	Upregulating tumor-specific antigens	Upregulation of MHC I and Fas expression	(85, 133)
OXA	Inducing ICD	Upregulation of DAMPs and HMGB1 and ATP	(76)
	Upregulating tumor-specific antigens	Inducing DCs to upregulate PD-L1 expression	(134)
	Upregulating the expression of immune stimulatory molecules	Increasing immune cells infiltration	(135)
Gemcitabine	Upregulating tumor-specific antigens	Inducing HLA1 expression	(136)
	Inhibiting immune-suppressive cells	Consuming MDSCs and Tregs	(137–139)
5-FU	Inducing ICD	Upregulation of DAMPs and HSP70 and ATP	(96, 140)
	Upregulating tumor-specific antigens	Promoting the maturation and functional enhancement of DCs	(141)
	Inhibiting immune-suppressive cells	Consuming MDSCs and Tregs	(96)
Teniposide	Upregulating tumor-specific antigens	Enhancing T cells recognition	(101)
Dacarbazine	Upregulating tumor-specific antigens	Leading to NK cells activation and release of IFN-γ	(142)
CTX	Inhibiting immune-suppressive cells	Inhibiting Tregs proliferation and function	(143, 144)
	Upregulating tumor-specific antigens	MHC I expression	(136)
MTX	Upregulating the expression of immune stimulatory molecules	Upregulating CD40, CD80 and CD83 to promote the maturation of DCs	(145)
Docetaxel	Inhibiting immune-suppressive cells	Consuming MDSCs and Tregs.	(67)

ICD, immunogenic cell death; TDLNs, tumor draining lymph nodes; MHC I, major histocompatibility complex class I;CTL, cytotoxic T lymphocyte; TAA, tumor-associated antigen; DAMPs, damage-associated molecular patterns; HLA1, human leukocyte antigen 1; HSP70, heat shock protein 70; ATP, adenosine triphosphate; MTX, methotrexate; CTX, cyclophosphamide; 5-FU, 5-fluorouracil; OXA, oxaliplatin; PTX, paclitaxel.

(158). In addition, PTX can promote an immune response of tumor-specific T cells (123–126) and promote the proliferation of CD8+T cells and T+H1 cells, thereby playing a role in the treatment of tumors. Platinum-based drugs and gemcitabine increase antigen specificity by inducing HLA1 expression (136). OXA can induce upregulation of PD-L1 expression on DCs, while carboplatin upregulates PD-1 mRNA expression. Studies have shown that in patients with head and neck squamous cells carcinoma receiving standard cisplatin treatment, cisplatin can have an immune suppressive effect through upregulation of PD-L1 (121). The expression of PD-L1 may also impede the response of anti-cancer T cells. *In vitro*, high-dose cisplatin significantly reduced IFN-γ

production by T cells (122) and decreased the cytotoxicity of NK cells in ovarian cancer patients (159). Standard doses of 5-FU may produce an immune-stimulatory effect, for example, by promoting antigen uptake by DCs (141). DOX promotes antigen presentation by DCs, promotes the proliferation of CD8+ T cells specific for certain antigens in tumor-draining lymph nodes, and increases IFN-γ production by CD8+ T cells infiltrating the tumor (114, 115). Temozolomide enhances the tumor cells antigen presentation mechanism and enhances T cells recognition (101). Dacarbazine is currently only used in melanoma patients who are not eligible for new therapies or have failed other treatments. Dacarbazine can upregulate NK cells activation and IFN-γ release. Increased levels of IFN-γ lead to upregulation of MHC I expression in tumor cells, which is necessary for T cells recognition (142).

4.3 Inhibiting immune-suppressive cells

Certain chemotherapy drugs can inhibit the activity of immune-suppressive cells, thereby enhancing anti-tumor immune response. For example, platinum-based drugs, CTX, 5-FU, docetaxel, and other chemotherapy drugs can reduce the inhibitory effect of Tregs on the anti-tumor immune response. These chemotherapy drugs can also promote the polarization of tumor-associated macrophages, thereby enhancing their anti-tumor activity. Moreover, the combination of certain ICIs and chemotherapy drugs can further enhance the anti-tumor immune response.

Specifically, Platinum-based drugs reduce the immune-suppressive microenvironment by depleting MDSCs and Tregs (117). PTX can selectively inhibit the number and function of Tregs (114, 123, 124, 160–166). One study found that patients with advanced disease had a significant decrease in the anti-inflammatory cytokine IL-10 levels after receiving PTX treatment (167). PTX can also repolarize TAM2. It has recently been identified as an agonist for TLR4 on TAMs and directly polarizes this anti-inflammatory population towards a pro-inflammatory phenotype (168, 169). Breast cancer patients treated with PTX exhibit peripheral pro-inflammatory features (170). After PTX treatment, ovarian cancer patients have gene enrichment associated with the inflammatory macrophage phenotype (168). Studies have shown that the combination of atezolizumab and nab-PTX prolongs progression-free survival (PFS) in patients with metastatic TNBC (171, 172). Low-dose CTX not only reduces the number of Tregs in tumors but also inhibits Tregs function (143). A recent study found that CTX preferentially targets CCR2+ Tregs in a highly active and proliferative state, namely effector Tregs (173). A clinical trial also showed that repeated low-dose CTX induction of Tregs depletion and enhanced anti-tumor immunity in patients with end-stage metastatic CRC ultimately contributes to prolonged progressive survival (174). CTX can also deplete tumor-infiltrating Tregs and improve the survival rate of mice with neuroblastoma when used in combination with anti-PD-1 therapy (144). Similar to CTX, topoisomerase I inhibitor camptothecin can also inhibit the production and function of Tregs. By removing the suppression of Tregs, irinotecan promotes the initiation and proliferation of CD8+ T cells in draining lymph nodes and inhibits the growth of lung cancer and CRC in a CD8+ T cell-dependent manner (175). Similarly, it has been reported that the FOLFIRI chemotherapy regimen containing irinotecan can reduce the inhibitory activity of peripheral Tregs in CRC patients (132). 5-FU selectively kills MDSCs *in vivo* while preserving other lymphocyte subtypes (96). Gemcitabine can deplete circulating or tumor-infiltrating MDSCs in various cancers, which benefits the restoration of CTL infiltration and cytotoxic activity (67). The use of standard doses can reduce the number of MDSCs while enhancing the cross-presentation of malignant antigens (136). In pancreatic cancer patients, standard-dose gemcitabine leads to the depletion of Tregs (139). Interestingly, there is no significant decrease in other lymphocyte subtypes after treatment.

4.4 Upregulating immune stimulatory molecules

Certain chemotherapy drugs can upregulate the expression of immune stimulatory molecules, thereby enhancing anti-tumor immune response. For example, PTX and its analogs can upregulate the expression of TAA and MHC I on tumor cells (129).

High-dose methotrexate can cause bone marrow suppression (176), but low-dose methotrexate exhibits immune stimulatory properties (145). In an *in vitro* experiment, non-cytotoxic low-dose methotrexate concentrations promoted DC maturation by upregulating CD40, CD80, and CD83 (145). In turn, DCs stimulated T cells proliferation, which may lead to a stronger anti-tumor response. This suggests that low-dose methotrexate can be used as an immune stimulant. CTX can induce MHC I expression (136) and deplete Tregs cells (114). Cisplatin also exhibits immune stimulatory properties by upregulating MHC I expression on antigen-presenting cells (118, 119), recruiting effector cells to the tumor site, and stimulating their proliferation (120). A single dose of OXA increased immune cell infiltration in a CRC mouse model (135). In ovarian cancer, a single dose of gemcitabine increased CD8+ T cell tumor infiltration and PD-L1 expression both *in vivo* and *in vitro* (139, 177).

5 Clinical application of the combination of chemotherapy and immunotherapy in CRC

As previously discussed, chemotherapy can activate immune regulation through various mechanisms, thereby enhancing patients' response to immunotherapy. Combination immunotherapy has become an effective strategy for treating certain tumors. Therefore, combining chemotherapy and immunotherapy may be a new treatment strategy. In fact, some studies have already demonstrated the clinical efficacy of this combination strategy. For example, in first-line treatment for NSCLC, Pembrolizumab in combination with chemotherapy has been approved for first-line treatment of advanced non-squamous NSCLC regardless of PD-L1 levels (178). Other promising combinations include Atezolizumab, carboplatin, and etoposide

for small cell lung cancer (SCLC), and nab-PTX or PTX in combination with Atezolizumab for advanced/metastatic breast cancer (179). Combination chemotherapy and immunotherapy have been shown to significantly improve patient survival. However, due to tumor heterogeneity and immune escape, a subset of patients with CRC lack response to immunotherapy. Currently, a series of clinical trials are being conducted for the combination of chemotherapy and immunotherapy in MSS/pMMR mCRC, with the aim of finding a breakthrough in treatment for these patients.

FOLFOX plus bevacizumab is the first-line standard of care (SOC) for MSS mCRC. The Checkmate 9X8 study (180) challenged first-line treatment of mCRC with the combination of nivolumab plus mFOLFOX6 and bevacizumab versus mFOLFOX6 and bevacizumab, with 95% of the patients being MSS/pMMR. The phase II results showed that, compared to the control group (current standard treatment regimen), the experimental group had a higher PFS rate starting at 12 months, with significantly improved 15-month PFS rate (45% *vs.* 21.5%) and 18-month PFS rate (28% *vs.* 9%), and ORR increased from 46% to 60%.

The BACCI phase II trial (181) (NCT0287319) evaluated the efficacy of adding Atezolizumab to Capecitabine and Bevacizumab in refractory mCRC. The addition of Atezolizumab to Capecitabine and Bevacizumab significantly extended progression-free survival (PFS), demonstrating a positive research advancement. This is the first positive study targeting the PD-1/PD-L1 pathway, chemotherapy, and the VEGF pathway, highlighting the need for further analysis and research.

The domestic BBCAPX study (182) is a study of the first-line treatment of MSS/RAS mutation mCRC with sintilimab + CapeOX + bevacizumab. The phase II single-arm trial results showed an ORR of up to 84%, a DCR of 100%, and unexpected conversion to R0 resection in 3 cases (12%). The study results demonstrated that the combination of sintilimab with CapeOX and bevacizumab for the treatment of RAS gene mutations and MSS-type mCRC showed good clinical benefits, with a high objective response rate and unexpected conversion rate, as well as low toxicity and tolerable safety. Based on the results of this phase II study, the ongoing BBCAPX phase III study holds great promise.

The objective of the single-arm phase II MEDITREME trial was to (183) evaluate the efficacy of the combination treatment with pembrolizumab, tremelimumab, and mFOLFOX6 in patients with MSS mCRC. The study results showed that the combination treatment resulted in a 3-month PFS rate of 90.7%, an overall response rate (ORR) of 64.5%, a median PFS (mPFS) of 8.2 months, and overall survival (OS) has not been reached yet.

NIVACOR (NCT04072198) (184) is a single-arm, open-label, multicenter phase II study with a safety assessment phase. Eligible patients with KRAS/BRAF-mutated metastatic CRC can participate and receive first-line treatment. Patients will receive FOLFOXIRI/Bevacizumab in combination with Nivolumab as induction therapy every two weeks, followed by maintenance therapy. Preliminary safety results indicate that this combination regimen is generally well-tolerated with acceptable toxicities. There is a high expectation for positive outcomes.

A study (185) evaluated the efficacy of PD-1/PD-L1 inhibitors in combination with the OXA-fluorouracil-leucovorin (mFOLFOX6) regimen in 30 patients with unresectable mCRC. The results showed a disease stabilization rate of 100% at 8 weeks and an overall response rate of 53% at 24 weeks. OXA and 5-FU led to increased ICD and antigen presentation. The study emphasized the potential benefits of combining chemotherapy with ICIs, as the combination of mFOLFOX6 and anti-PD-1 therapy was within an acceptable toxicity profile. The results showed that ICIs should be given concurrently or early after FOLFOX treatment and demonstrated clinical efficacy in pMMR CRC patients, showing promising results in patients with unresectable CRC.

Chemoradiotherapy also plays an important role in enhancing tumor response to immunotherapy. Current research indicates that radiation therapy can increase the expression of antigens on tumor cells, enhance tumor cell immunogenicity, and promote immune cell infiltration (186, 187). Therefore, combining immunotherapy with radiotherapy may lead to better therapeutic outcomes. For example, Lin et al. (188) used short-course therapy combining radiotherapy, sequential immunotherapy, and chemotherapy to treat CRC patients, which showed a pCR rate of up to 48%. In addition, the ongoing TORCH trial (189) is using toripalimab in combination with chemoradiotherapy or CapeOX in MSS CRC patients, with a proportion of 81.3% achieving cCR or pCR. These results suggest that combining immunotherapy with chemoradiotherapy may be an effective option for the treatment of CRC patients.

Most immunogenic chemotherapy agents have been shown to evoke immune stimulation not only by increasing the immunogenicity of cancer cells, but also by activating effector T cells and suppressing immune suppressor cells. These results suggest that the combination of chemotherapy and ICIs can have a synergistic anticancer effect and indicate that chemotherapy in combination with immunotherapy may be suitable for tumors that respond poorly to ICIs monotherapy. There are also ongoing prospective studies whose safety has been proven feasible, and the results of which are highly anticipated.

6 Preclinical and clinical studies of inducing chemotherapy combined with immunotherapy

Considering the immune-activating effects of chemotherapy drugs, the combination of chemotherapy and ICIs is an appropriate partner to achieve rapid and long-term cancer control. Based on these findings, we propose the concept of inducing chemotherapy, which involves using immunogenic chemotherapy drugs to change the timing before immunotherapy, converting "cold" tumors into "hot" metastases to initiate or restore anti-tumor immune responses, thereby enhancing the efficacy of ICIs (190). Some preclinical studies are being conducted in targeted preclinical models of CRC.

Song et al. (155) investigated the efficacy of OXA and anti-PD-L1 drugs in a microsyngeneic transplantation mouse model based

on the CT26 cell line and found that the combination therapy of OXA and anti-PD-L1 drugs significantly slowed tumor growth compared to the use of OXA alone (191).

Dosset et al. conducted an interesting preclinical study using a microsyngeneic mouse model of two MSI-H CRCs (CT26 and MC38) and observed that adding adjuvant ICIs after FOLFOX could induce complete and durable tumor responses, whereas FOLFOX or ICIs alone were ineffective (192). Therefore, adding ICIs enables CD8+ T cells recruited by FOLFOX to induce effective anti-tumor immune responses (140). This is the first description of the PD-1/PD-L1 pathway as part of FOLFOX chemotherapy-induced adaptive immune resistance, indicating that chemotherapy can enhance the efficacy of ICIs (192). This correlation can attract a population of effective T cells which creating a favorable environment for immunotherapy to work. It has been shown to be associated with improved patient survival, especially after the emergence of immunotherapy (193).

The successful outcomes achieved in these preclinical trials provide strong evidence for the future implementation of clinical trials involving inducing chemotherapy (Table 2). Studies have shown that inducing chemotherapy has become one of the standard treatment options for certain tumors. For example, the combination of pembrolizumab with platinum and 5-FU was recently approved for metastatic and recurrent head and neck cancer based on its OS benefit (197).

Ma et al. (198) presented the results of a phase III multicenter randomized controlled clinical trial on sequential treatment of locally advanced nasopharyngeal carcinoma with PD-1 inhibitor sintilimab and concurrent chemoradiotherapy after inducing chemotherapy at the 2023 American Society of Clinical Oncology (ASCO) Annual Meeting. Patients were randomly assigned to two groups, one receiving standard GP inducing chemotherapy and concurrent chemoradiotherapy, and the other adding sintilimab to the standard treatment. The primary endpoint was event-free survival (EFS). From December 2018 to March 2020, a total of 425 patients were recruited, and after a median follow-up of 42 months, sintilimab increased the 3-year EFS rate from 76% to 86%, a 10% improvement, and reduced the risk of relapse, metastasis, and death by 41%. The risks of local-regional recurrence and distant metastasis were reduced by 48% and 43%, respectively. This trial is the first to achieve a positive EFS result in all locally advanced head and neck cancers, demonstrating the feasibility of inducing chemotherapy as a promising strategy to optimize anti-tumor treatment. In addition, concurrent chemoradiotherapy after inducing chemotherapy is the standard treatment for locally advanced nasopharyngeal carcinoma. Zhang et al. (199) conducted a multicenter randomized trial, assigning patients to receive concurrent chemoradiotherapy or GP inducing chemotherapy followed by concurrent chemoradiotherapy. The median follow-up time was 69.8 months, and the 5-year OS rate in the inducing chemotherapy group was significantly higher than that in the concurrent chemoradiotherapy group (87.9% *vs*. 78.8%), with equivalent risks of late toxicities (≥grade 3) (11.3% *vs*. 11.4%). This study suggests that inducing chemotherapy before concurrent chemoradiotherapy can significantly improve the OS of patients with locally advanced nasopharyngeal carcinoma without increasing the risk of late toxicities.

Based on the effective results obtained from preclinical trials, a series of clinical trials combining chemotherapy induction with immunotherapy have also been conducted in CRC, and significant progress has been achieved.

According to studies, TAM depletion induced by trifluridine/tipiracil (FTD/TPI), OXA, or combination therapy, especially TAM2, results in changes in the TAM1/TAM2 ratio, as well as enhanced infiltration and activation of cytotoxic CD8+ T cells, enhanced production of granzyme B, IFNγ, and TNFα in CD8+ T cells within the tumor, and upregulation of PD-L1 and PD-1 expression (Figure 5) (194). The combination use of FTD/TPI and OXA also induces ICD *in vivo*, providing a basis for using these drugs to eliminate immune-suppressive cells and improve checkpoint efficacy in patients with metastatic MSS CRC. The combination of FTP/TPI and OXA has been shown to be safe and effective in a phase I human clinical trial (200).

A phase II clinical trial (195) is currently ongoing to evaluate the safety, tolerability, and initial efficacy of pembrolizumab in combination with capecitabine and bevacizumab for the treatment of MSS mCRC patients. Bevacizumab, capecitabine, and pembrolizumab are used for treatment in the trial. The study results showed that the ORR among 40 evaluable patients was 5%, with a mPFS of 4.3 months and a mOS of 9.6 months. It is worth noting that MSS mCRC is rarely responsive to monotherapy with pembrolizumab, but capecitabine and bevacizumab may promote immune stimulation. These results suggest that the combination of pembrolizumab with capecitabine and bevacizumab may have some efficacy for MSS mCRC patients. However, it is important to note that the size of this trial is smaller, and further research and large-scale Phase III trials are needed to confirm the effectiveness and safety of this treatment regimen.

The MAYA II phase clinical trial (NCT03832621) (196) studied the combination of Nivolumab, Ipilimumab, and Temozolomide (TMZ) for the treatment of MSS, MGMT silenced unresectable mCRC patients who have not progressed, regardless of RAS mutational status. In the pre-selected 716 patients, 33 patients (24%) achieved disease control, which represents the final study population. The mPFS was 7.0 months, the mOS was 18.4 months, and the ORR was 45%. A series of temozolomide initiation followed by low-dose ipilimumab and nivolumab combination may induce durable clinical benefits in MSS and MGMT silenced mCRC. The initiation of treatment with tremelimumab provides the basic principle for immune sensitization induced by hypermutation in pMMR/MSS (MGMT-silenced) mCRC.

A randomized phase II trial (201) evaluated the safety of immunotherapy in combination with SOC in untreated MSS mCRC patients. Patients were randomized to receive SOC alone or SOC plus immunotherapy, which included mFOLFOX6 + Bevacizumab with or without AdCEA vaccine and Avelumab. In this small, randomized trial, the addition of immunotherapy did not significantly improve mPFS or overall response rate (ORR) compared to SOC alone. However, the SOC + immunotherapy regimen yielded biological activity in the form of substantial

increases in multifunctional CD4+ and CD8+ T cells specific for the cascade antigens MUC1 and brachyury. Among them, the MUC1 and Brachyury pathways play important roles in cancer development and immune evasion and have become potential targets for tumor immunotherapy (202, 203).

A study (204) aimed to evaluate the safety, activity, and biomarker patterns of FOLFOX treatment with atezolizumab (anti-PD-L1) and bevacizumab (anti-VEGF-A) in patients with MSS mCRC. As of September 1, 2015, 52% of patients showed RECIST responses, with a mPFS time of 14.1 months and a median

TABLE 2 Summary of clinical trials and preclinical studies of chemotherapy combined with immunotherapy.

Summary of Clinical Trial Results of ICIs Combined with Chemotherapy in CRC								
Study	Patient characteristics	Treatment	Expected outcome				NCT Identifier	Reference
			median PFS (mo)		OS (12 mo)	ORR (%)	DCR (%)	
BACCI	pMMR/MSS	Cap, 850 or 1000 mg/m^2 D1-14, Bev, 7.5 mg/kg D1, Atezo, 1200 mg D1 in 21 D cycles.	ArmA	4.4	43%	4.35	N/A	NCT02873195	(181)
	Arm A, 46 pts				52%	8.54			
	Arm B, 82 pts		ArmB	3.3	N/A	8.54			
CheckMate 9X8	180 untreated pts with mCRC	Nivo, 240 mg every 2w + mFOLFOX/ Bev every 2w	1.9		N/A	60	91	NCT03414983	(180)
		mFOLFOX/Bev every 2w				46	84		
BBCAPX	25 unresectable, RAS-mutated, MSS mCRC	Sintilimab (200mg, D1) +Cap (1 g/m^2, bid, D1-14) OXA (135 mg/m^2, D1) + Bev (7.5 mg/kg, D1), in 21 D cycles.	N/A		N/A	84	100	NCT05171660	(182)
MEDITREME	57 cases of unresectable RAS mutant mCRC	Dur (750 mg, once every 2w) + Tre (75 mg, once every 4w) + mFOLFOX6. Pts with SD or PD: Dur (750mg, once every 2w) for maintenance	8.2		N/A	64.5	N/A	NCT03202758	(183)
NIVACOR	73 untreated pts with advanced RAS/ BRAF-mutated mCRC	Nivo 240 mg, Bev 5 mg/kg + FOLFOXIRI administered every 2w for a total of 8 cycles.	10.1		N/A	76.7	N/A	NCT04072198	(184)

Summary of Clinical Trial Results of ICIs Combined with Radiotherapy in LARC Studies						
Study	Patient char-acteristics	Treatment	Expected outcome		NCT Identifier	Reference
			MSS			
TORCH	130 LARC	Arm A: SCRT (25 Gy/5Fx) + 6 cycles ToriCAPOX. Arm B: 2 cycles ToriCAPOX+ SCRT+ 4 cycles ToriCAPOX.	**pCR**	**cCR**	NCT04518280	(189)
			72.73%	81.25%		

Preclinical Studies of Inducing Chemotherapy Combined with Immunotherapy in CRC			
Experimental subjects	Experimental drugs	Outcome	Reference
CT26 micro-allotransplanted mice	OXA+ engineered PD-L1 trap	Combination therapy slowed tumor growth.	(155)
CT26 and MC38 mouse models	FOLFOX+ anti-PD1 blocking antibody	FOLFOX activated tumor-specific PD-1 CD8 + T cells in TME.	(192)

Clinical trials combining chemotherapy induction with immunotherapy in CRC				
Patient characteristics	Treatment	Outcome	NCT Number	Reference
Cohort A:37 mCRC Cohort B: 17 MSS mCRC	Cohort A: FTD/TPI 35 mg/m^2 (bid, D1-5) + OXA 85 mg/m^2 and Bev 5 mg/kg (D1). Cohort B: Nivo 3 mg/kg.	Increase of enzyme granules B, IFNγ and TNFα, upregulation of PD-L1 and PD-1 expression	NCT02848443	(194)
MSS mCRC with SD or PD on prior fluoropyrimidine-based therapy	Cap 1000 mg/m^2 po bid D1-14 Q21 D (confirmed RP2D) + Pem 200 mg IV D1 Q21D + Bev 7.5 mg/kg IV D1 Q21 D	ORR: 5% mPFS: 4.3 m, mOS: 9.6 m	NCT03396926	(195)

(Continued)

TABLE 2 Continued

Clinical trials combining chemotherapy induction with immunotherapy in CRC				
Patient characteristics	Treatment	Outcome	NCT Number	Reference
MSS, MGMT silent unresectable mCRC	Phase I: Tem 150 mg/sqm po, D1-5, q4w for two cycles; Phase II: Tem 150 mg/sqm po, D1-5, q4w, + Nivo 480 mg q4w + ipi 1 mg/kg q8w.	mPFS: 7.0m, mOS: 18.4m, ORR:45%	NCT03832621	(196)

Atezo, atezolizumab; Bev, bevacizumab; Cap, capecitabine; Pem, pembrolizumab; Dur, Durvalumab; Tem, Temozolomide; Tre, Tremelimumab; Ipi, ipilimumab; CRC, colorectal cancer; DCR, disease control rate; MSI-H, microsatellite instability-high; pMMR, proficient DNA mismatch repair; MSS, microsatellite stable; Nivo, nivolumab; N/A, not available; NCT, National Clinical Trial; ORR, overall response rate; OS, overall survival; PFS, progression-free survival; 5-fluorouracil, 5-FU; OXA, oxaliplatin; mo, month; pts, patients; D, day; w, week; LARC, Locally advanced rectal cancer; pCR, pathological complete response; cCR clinical, complete response; ToriCAPOX, Toripalimab plus capecitabine and oxaliplatin; SCRT, short-course radiotherapy; SD, stable disease; PD, progressive disease; RP2D, recommended phase II dose; mDOR, median Duration of Response; TME, tumor microenvironment; FTD/TPI trifluridine/tipiracil; IV, intravenous; ivgtt, intravenously guttae; FOLFOX: OXA: 100 mg/m^2 D1; Tetrahydrofolate: 200 mg/m^2 ivgtt D1-5; 5-Fu: 500 mg/m^2 ivgtt D1-5.
mFOLFOX6: Leucovorin, 400 mg/m^2 D1; OXA, 85 mg/m^2 D1, and 5-FU (400 mg/m^2 bolus and then 2, 400 mg/m^2 over 46 hours).

response duration of 11.4 months. No unexpected toxicities were observed. Wallin et al. found an increase in the expression of CD8+ T cells and PD-L1 in tumors after FOLFOX treatment alone and after combined FOLFOX, atezolizumab, and bevacizumab treatment. In some patients' tumors, there was also an increase in cytotoxic T-cell markers (such as IFN-γ, GZMB, EOMES). Patients with increased tumor-infiltrating CD8+ T cells, which were consistent with increases in cytotoxic T-cell markers and PD-L1 expression, showed sustained responses or long-term disease control. These data further confirm that the combination of FOLFOX, atezolizumab, and bevacizumab may promote immune-related activities in CRC, thereby enhancing efficacy.

Although inducing chemotherapy combined with immunotherapy has achieved significant results, studies have shown that some chemotherapy drugs exhibit different immunogenic effects depending on their regimen, timing, dose, or administration sequence, even when used in combination with ICIs. One study investigated the impact of drug administration sequence and found that CTX given one day before anti-CTLA-4 therapy resulted in immune-mediated anti-tumor responses. However, when the sequence was reversed, CD8+ T cells underwent massive apoptosis, and the anti-tumor effect of anti-CTLA-4 was weakened (205). Another study tested three different regimens in NSCLC patients: a phase II study evaluating chemotherapy given before ipilimumab, a concurrent regimen, and a control group receiving placebo and chemotherapy (206). The primary endpoint of improved PFS was only achieved in the sequential regimen. A study investigated the effect of various types of chemotherapy on the treatment of metastatic triple-negative breast cancer (TNBC) and found that 2 weeks of low-dose chemotherapy during the induction period was more effective than nivolumab monotherapy (207). In addition, compared to the no-induction period, the number and clonality of T cells in the tumor were higher after chemotherapy-induced treatment (208).

Excitingly, inducing chemotherapy has become one of the standard treatment options for certain tumors, and a series of clinical trials on inducing chemotherapy have been conducted in CRC, achieving promising results. We propose the exploration of

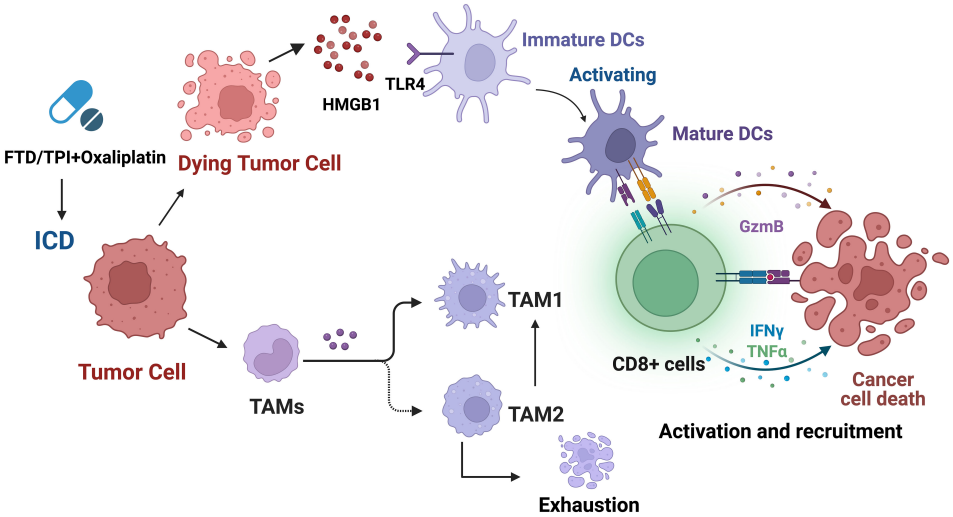

FIGURE 5
Trifluridine/tipiracil (FTD/TPI), oxaliplatin, or their combination not only induces ICD but also leads to enhanced infiltration and activation of cytotoxic CD8+ T cells, and increases the production of granzyme B, IFNγ, and TNFα in CD8+ T cells within the tumor. In addition, it leads to TAM depletion, especially TAM2, resulting in changes in the TAM1/TAM2 ratio, and upregulation of PD-L1 and PD-1 expression.

personalized treatment plans, gradually reducing the chemotherapy regimen and combining it with immunotherapy after inducing chemotherapy, until only oral chemotherapy is maintained, and eventually achieving maintenance therapy with a single immunotherapy. We look forward to further confirmation and application in the future.

7 Challenges and future

In the field of CRC treatment, the combination of inducing chemotherapy and immunotherapy has emerged as a promising therapeutic strategy. However, there are still challenges and directions that need to be addressed in the future.

The TIME in CRC typically exhibits immunosuppressive features that limit the activity of immune cells. Future research can further explore the underlying mechanisms by which chemotherapy-induced immunotherapy overcomes this immune suppression, such as enhancing the activity of immune cells, modulating the polarization state of tumor-associated macrophages, disrupting tumor vasculature, and so on (87). To improve the success rate of chemotherapy-induced immunotherapy, it is crucial to explore innovative treatment targets/strategies and identify patients who respond better to specific treatment regimens.

scRNA-seq technology provides us with an opportunity to gain in-depth understanding of tumor and immune cell heterogeneity (209, 210). This technology can be used to reveal the roles of different cell subpopulations in chemotherapy-induced immunotherapy, thereby helping optimize treatment strategies and select the most suitable patients (211, 212). Combination therapies of chemotherapy and immunotherapy may yield better treatment outcomes compared to monotherapies. However, determining the optimal combination strategies and dosages remains challenging. Future research should focus on identifying the optimal drug combinations, timing of administration, dosages, and the best concentration-time curves in representative preclinical models (112, 213). Single-cell data can be utilized in future studies to achieve more precise treatment optimization. Other therapies such as photodynamic therapy, photothermal therapy, radiation therapy, and magnetic fluid hyperthermia can further induce ICD in tumor cells, enhance the efficacy of anti-tumor immunotherapy, expand their potential applications, and maximize clinical benefits (214).

Due to the limited predictive ability of current biomarkers such as PD-L1 expression and tumor mutation burden in cancer precision medicine, alternative biomarkers are still being explored (215, 216). A recent study has shown that advanced NSCLC patients with high PD-L1 expression and high immune infiltration can actually respond to PD-1 therapy plus chemotherapy in the first-line setting. For patients lacking PD-L1 expression or immune infiltration, chemotherapy may be a better treatment choice (217). This suggests that in the future, it is also significant to further explore alternative biomarkers in CRC, for guiding precision medicine in the clinical practice of CRC treatment.

Furthermore, due to significant biological differences among CRC patients, personalized immunotherapy approaches become crucial. scRNA-seq may reveal potential mechanisms regulating immune cell exhaustion and identify advanced biomarkers, thereby facilitating the design of novel personalized immunotherapy strategies (11, 218–220). By utilizing scRNA-seq to better understand individual variations, we can design optimal individualized chemotherapy-induced immunotherapy regimens for specific patients. These efforts are expected to provide more effective treatment choices and personalized treatment plans for CRC patients.

8 Conclusion

Immunotherapy has made significant progress in CRC, revolutionizing treatment outcomes. The TIME is closely related to tumor immunotherapy, which is a key obstacle to anti-tumor immunity and may limit the clinical benefits of immunotherapy. Recent studies have shown that some chemotherapy drugs can promote immune activation and enhance the efficacy of immunotherapy. By inducing ICD and exposing new antigens, it can activate CD8+ T cells and enhance the immune response to cancer. A large body of research has shown that most chemotherapy drugs exert immunostimulatory effects by inhibiting immune-suppressive cells or activating effector cells, or by increasing immunogenicity and T cells infiltration. inducing chemotherapy combined with immunotherapy has become a standard part of treatment in some tumors, and clinical trials have demonstrated its feasibility and safety in CRC. These combination therapies typically transform “cold” tumors that are insensitive to immune response into “hot” tumors. We propose a personalized exploration of inducing chemotherapy, gradually reducing chemotherapy regimens after systemic chemotherapy induction, combining with immunotherapy until only oral chemotherapy is maintained, and eventually transitioning to immune monotherapy maintenance treatment. In summary, chemotherapy-induced immunotherapy has enormous potential in the field of CRC. Future research will focus on overcoming the immune-suppressive microenvironment, applying scRNA-seq technology, achieving personalized treatment, researching predictive biomarkers, and optimizing combination therapy, among other challenges, to benefit more cancer patients in the near future.

Author contributions

KJ and HL contributed to the conception and design of the study. SY drafted the initial manuscript and prepared the figures. YH and MY wrote sections of the manuscript. All authors participated in revising the manuscript, read, and approved the final version for submission.

Funding

This work was supported by National Natural Science Foundation of China [grant no. 82104445 to HL], Zhejiang Provincial Science and Technology Projects (grant no.

LGF22H160046 to HL), Jinhua Municipal Science and Technology Projects (grants no. 2021-3-040 to KJ, and 2021-3-046 to HL).

Conflict of interest

The authors declare that the research was conducted in the absence of any commercial or financial relationships that could be construed as a potential conflict of interest.

Publisher's note

References

1. Siegel RL, Miller KD, Wagle NS, Jemal A. Cancer statistics, 2023. *CA Cancer J Clin* (2023) 73:17–48. doi: 10.3322/caac.21763

2. Sung H, Ferlay J, Siegel RL, Laversanne M, Soerjomataram I, Jemal A, et al. Global cancer statistics 2020: GLOBOCAN estimates of incidence and mortality worldwide for 36 cancers in 185 countries. *CA: A Cancer J Clin* (2021) 71:209–49. doi: 10.3322/caac.21660

3. Biller LH, Schrag D. Diagnosis and treatment of metastatic colorectal cancer: A review. *Jama* (2021) 325:669–85. doi: 10.1001/jama.2021.0106

4. Kalyan A, Kircher S, Shah H, Mulcahy M, Benson A. Updates on immunotherapy for colorectal cancer. *J Gastrointest Oncol* (2018) 9:160–9. doi: 10.21037/jgo.2018.01.17

5. Ganesh K, Stadler ZK, Cercek A, Mendelsohn RB, Shia J, Segal NH, et al. Immunotherapy in colorectal cancer: rationale, challenges and potential. *Nat Rev Gastroenterol Hepatol* (2019) 16:361–75. doi: 10.1038/s41575-019-0126-x

6. Kroemer G, Galluzzi L, Kepp O, Zitvogel L. Immunogenic cell death in cancer therapy. *Annu Rev Immunol* (2013) 31:51–72. doi: 10.1146/annurev-immunol-032712-100008

7. Apetoh L, Ghiringhelli F, Tesniere A, Obeid M, Ortiz C, Criollo A, et al. Toll-like receptor 4-dependent contribution of the immune system to anticancer chemotherapy and radiotherapy. *Nat Med* (2007) 13:1050–9. doi: 10.1038/nm1622

8. Kepp O, Senovilla L, Vitale I, Vacchelli E, Adjemian S, Agostinis P, et al. Consensus guidelines for the detection of immunogenic cell death. *Oncoimmunology* (2014) 3:e955691. doi: 10.4161/21624011.2014.955691

9. Li Y, Liu X, Zhang X, Pan W, Li N, Tang B. Immune cycle-based strategies for cancer immunotherapy. *Adv Funct Mater* (2021) 31:2107540. doi: 10.1002/adfm.202107540

10. Grimaldi A, Cammarata I, Martire C, Focaccetti C, Piconese S, Buccilli M, et al. Combination of chemotherapy and PD-1 blockade induces T cell responses to tumor non-mutated neoantigens. *Commun Biol* (2020) 3:85. doi: 10.1038/s42003-020-0811-x

11. Tieng FYF, Lee LH, Ab Mutalib NS. Deciphering colorectal cancer immune microenvironment transcriptional landscape on single cell resolution - A role for immunotherapy. *Front Immunol* (2022) 13:959705. doi: 10.3389/fimmu.2022.959705

12. Pardoll DM. The blockade of immune checkpoints in cancer immunotherapy. *Nat Rev Cancer* (2012) 12:252–64. doi: 10.1038/nrc3239

13. Hodi FS, Chiarion-Sileni V, Gonzalez R, Grob JJ, Rutkowski P, Cowey CL, et al. Nivolumab plus ipilimumab or nivolumab alone versus ipilimumab alone in advanced melanoma (CheckMate 067): 4-year outcomes of a multicentre, randomised, phase 3 trial. *Lancet Oncol* (2018) 19:1480–92. doi: 10.1016/s1470-2045(18)30700-9

14. Reck M, Rodríguez-Abreu D, Robinson AG, Hui R, Csőszi T, Fülöp A, et al. Updated analysis of KEYNOTE-024: pembrolizumab versus platinum-based chemotherapy for advanced non-small-cell lung cancer with PD-L1 tumor proportion score of 50% or greater. *J Clin Oncol* (2019) 37:537–46. doi: 10.1200/jco.18.00149

15. Motzer RJ, Rini BI, McDermott DF, Arén Frontera O, Hammers HJ, Carducci MA, et al. Nivolumab plus ipilimumab versus sunitinib in first-line treatment for advanced renal cell carcinoma: extended follow-up of efficacy and safety results from a randomised, controlled, phase 3 trial. *Lancet Oncol* (2019) 20:1370–85. doi: 10.1016/s1470-2045(19)30413-9

16. Le DT, Uram JN, Wang H, Bartlett BR, Kemberling H, Eyring AD, et al. PD-1 blockade in tumors with mismatch-repair deficiency. *N Engl J Med* (2015) 372:2509–20. doi: 10.1056/NEJMoa1500596

17. Overman MJ, Lonardi S, Wong KYM, Lenz HJ, Gelsomino F, Aglietta M, et al. Durable clinical benefit with nivolumab plus ipilimumab in DNA mismatch repair-deficient/microsatellite instability-high metastatic colorectal cancer. *J Clin Oncol* (2018) 36:773–9. doi: 10.1200/jco.2017.76.9901

18. Overman MJ, McDermott R, Leach JL, Lonardi S, Lenz HJ, Morse MA, et al. Nivolumab in patients with metastatic DNA mismatch repair-deficient or microsatellite instability-high colorectal cancer (CheckMate 142): an open-label, multicentre, phase 2 study. *Lancet Oncol* (2017) 18:1182–91. doi: 10.1016/s1470-2045(17)30422-9

19. Marcus L, Lemery SJ, Keegan P, Pazdur R. FDA approval summary: pembrolizumab for the treatment of microsatellite instability-high solid tumors. *Clin Cancer Res* (2019) 25:3753–8. doi: 10.1158/1078-0432.Ccr-18-4070

20. André T, Shiu K-K, Kim TW, Jensen BV, Jensen LH, Punt C, et al. Pembrolizumab in microsatellite-instability–high advanced colorectal cancer. *N Engl J Med* (2020) 383:2207–18. doi: 10.1056/NEJMoa2017699

21. Ji RR, Chasalow SD, Wang L, Hamid O, Schmidt H, Cogswell J, et al. An immune-active tumor microenvironment favors clinical response to ipilimumab. *Cancer Immunol Immunother* (2012) 61:1019–31. doi: 10.1007/s00262-011-1172-6

22. Hegde PS, Karanikas V, Evers S. The where, the whenand the how of immune monitoring for cancer immunotherapies in the era of checkpoint inhibition. *Clin Cancer Res* (2016) 22:1865–74. doi: 10.1158/1078-0432.Ccr-15-1507

23. Higgs B, Robbins PB, Blake-Haskins JA, Morehouse C, Brohawn PZ, Rebelatto M, et al. 15LBA High tumoral IFNγ mRNA, PD-L1 proteinand combined IFNγ mRNA/PD-L1 protein expression associates with response to durvalumab (anti-PD-L1) monotherapy in NSCLC patients. *Eur J Cancer* (2015) 51:S717. doi: 10.1016/S0959-8049(16)31937-2

24. Le DT, Hubbard-Lucey VM, Morse MA, Heery CR, Dwyer A, Marsilje TH, et al. A blueprint to advance colorectal cancer immunotherapies. *Cancer Immunol Res* (2017) 5:942–9. doi: 10.1158/2326-6066.Cir-17-0375

25. Ghiringhelli F, Fumet JD. Is there a place for immunotherapy for metastatic microsatellite stable colorectal cancer? *Front Immunol* (2019) 10:1816. doi: 10.3389/fimmu.2019.01816

26. Kim CW, Chon HJ, Kim C. Combination immunotherapies to overcome intrinsic resistance to checkpoint blockade in microsatellite stable colorectal cancer. *Cancers (Basel)* (2021) 13. doi: 10.3390/cancers13194906

27. Sahin IH, Ciombor KK, Diaz LA, Yu J, Kim R. Immunotherapy for microsatellite stable colorectal cancers: challenges and novel therapeutic avenues. In: *American Society of Clinical Oncology Educational Book* (2022) 242–53. doi: 10.1200/edbk_349811

28. Wilmott JS, Long GV, Howle JR, Haydu LE, Sharma RN, Thompson JF, et al. Selective BRAF inhibitors induce marked T-cell infiltration into human metastatic melanoma. *Clin Cancer Res* (2012) 18:1386–94. doi: 10.1158/1078-0432.Ccr-11-2479

29. Bradley SD, Chen Z, Melendez B, Talukder A, Khalili JS, Rodriguez-Cruz T, et al. BRAFV600E co-opts a conserved MHC class I internalization pathway to diminish antigen presentation and CD8+ T-cell recognition of melanoma. *Cancer Immunol Res* (2015) 3:602–9. doi: 10.1158/2326-6066.Cir-15-0030

30. Liu C, Peng W, Xu C, Lou Y, Zhang M, Wargo JA, et al. BRAF inhibition increases tumor infiltration by T cells and enhances the antitumor activity of adoptive immunotherapy in mice. *Clin Cancer Res* (2013) 19:393–403. doi: 10.1158/1078-0432.Ccr-12-1626

31. Hu-Lieskovan S, Mok S, Homet Moreno B, Tsoi J, Robert L, Goedert L, et al. Improved antitumor activity of immunotherapy with BRAF and MEK inhibitors in BRAF(V600E) melanoma. *Sci Transl Med* (2015) 7:279ra41. doi: 10.1126/scitranslmed.aaa4691

32. Frederick DT, Piris A, Cogdill AP, Cooper ZA, Lezcano C, Ferrone CR, et al. BRAF inhibition is associated with enhanced melanoma antigen expression and a more favorable tumor microenvironment in patients with metastatic melanoma. *Clin Cancer Res* (2013) 19:1225–31. doi: 10.1158/1078-0432.Ccr-12-1630

33. Spranger S, Spaapen RM, Zha Y, Williams J, Meng Y, Ha TT, et al. Up-regulation of PD-L1, IDOand T(regs) in the melanoma tumor microenvironment is driven by CD8(+) T cells. *Sci Transl Med* (2013) 5:200ra116. doi: 10.1126/scitranslmed.3006504

34. Llosa NJ, Cruise M, Tam A, Wicks EC, Hechenbleikner EM, Taube JM, et al. The vigorous immune microenvironment of microsatellite instable colon cancer is balanced by multiple counter-inhibitory checkpoints. *Cancer Discov* (2015) 5:43–51. doi: 10.1158/2159-8290.Cd-14-0863

35. Li X, Song W, Shao C, Shi Y, Han W. Emerging predictors of the response to the blockade of immune checkpoints in cancer therapy. *Cell Mol Immunol* (2019) 16:28–39. doi: 10.1038/s41423-018-0086-z

36. Cristescu R, Mogg R, Ayers M, Albright A, Murphy E, Yearley J, et al. Pan-tumor genomic biomarkers for PD-1 checkpoint blockade-based immunotherapy. *Science* (2018) 362. doi: 10.1126/science.aar3593

37. Xiong Y, Wang Y, Tiruthani K. Tumor immune microenvironment and nano-immunotherapeutics in colorectal cancer. *Nanomedicine* (2019) 21:102034. doi: 10.1016/j.nano.2019.102034

38. Chalmers ZR, Connelly CF, Fabrizio D, Gay L, Ali SM, Ennis R, et al. Analysis of 100,000 human cancer genomes reveals the landscape of tumor mutational burden. *Genome Med* (2017) 9:34. doi: 10.1186/s13073-017-0424-2

39. Tauriello DVF, Palomo-Ponce S, Stork D, Berenguer-Llergo A, Badia-Ramentol J, Iglesias M, et al. TGFβ drives immune evasion in genetically reconstituted colon cancer metastasis. *Nature* (2018) 554:538–43. doi: 10.1038/nature25492

40. Gutting T, Burgermeister E, Härtel N, Ebert MP. Checkpoints and beyond - Immunotherapy in colorectal cancer. *Semin Cancer Biol* (2019) 55:78–89. doi: 10.1016/j.semcancer.2018.04.003

41. Makaremi S, Asadzadeh Z, Hemmat N, Baghbanzadeh A, Sgambato A, Ghorbaninezhad F, et al. Immune checkpoint inhibitors in colorectal cancer: challenges and future prospects. *Biomedicines* (2021) 9. doi: 10.3390/biomedicines9091075

42. Ravi R, Noonan KA, Pham V, Bedi R, Zhavoronkov A, Ozerov IV, et al. Bifunctional immune checkpoint-targeted antibody-ligand traps that simultaneously disable TGFβ enhance the efficacy of cancer immunotherapy. *Nat Commun* (2018) 9:741. doi: 10.1038/s41467-017-02696-6

43. Lin RL, Zhao LJ. Mechanistic basis and clinical relevance of the role of transforming growth factor-β in cancer. *Cancer Biol Med* (2015) 12:385–93. doi: 10.7497/j.issn.2095-3941.2015.0015

44. Guo L, Zhang Y, Zhang L, Huang F, Li J, Wang S. MicroRNAs, TGF-β signalingand the inflammatory microenvironment in cancer. *Tumour Biol* (2016) 37:115–25. doi: 10.1007/s13277-015-4374-2

45. Ischenko I, D'Amico S, Rao M, Li J, Hayman MJ, Powers S, et al. KRAS drives immune evasion in a genetic model of pancreatic cancer. *Nat Commun* (2021) 12:1482. doi: 10.1038/s41467-021-21736-w

46. Klampfer L, Huang J, Corner G, Mariadason J, Arango D, Sasazuki T, et al. Oncogenic Ki-ras inhibits the expression of interferon-responsive genes through inhibition of STAT1 and STAT2 expression. *J Biol Chem* (2003) 278:46278–87. doi: 10.1074/jbc.M304721200

47. Glodde N, Hölzel M. RAS and PD-L1: A masters' Liaison in cancer immune evasion. *Immunity* (2017) 47:1007–9. doi: 10.1016/j.immuni.2017.12.001

48. Guinney J, Dienstmann R, Wang X, de Reyniès A, Schlicker A, Soneson C, et al. The consensus molecular subtypes of colorectal cancer. *Nat Med* (2015) 21:1350–6. doi: 10.1038/nm.3967

49. Owyang SY, Zhang M, Walkup GA, Chen GE, Grasberger H, El-Zaatari M, et al. The effect of CT26 tumor-derived TGF-β on the balance of tumor growth and immunity. *Immunol Lett* (2017) 191:47–54. doi: 10.1016/j.imlet.2017.08.024

50. Calon A, Lonardo E, Berenguer-Llergo A, Espinet E, Hernando-Momblona X, Iglesias M, et al. Stromal gene expression defines poor-prognosis subtypes in colorectal cancer. *Nat Genet* (2015) 47:320–9. doi: 10.1038/ng.3225

51. Otegbeye F, Ojo E, Moreton S, Mackowski N, Lee DA, de Lima M, et al. Inhibiting TGF-beta signaling preserves the function of highly activated, in *vitro* expanded natural killer cells in AML and colon cancer models. *PloS One* (2018) 13:e0191358. doi: 10.1371/journal.pone.0191358

52. Huang XM, Zhang NR, Lin XT, Zhu CY, Zou YF, Wu XJ, et al. Antitumor immunity of low-dose cyclophosphamide: changes in T cells and cytokines TGF-beta and IL-10 in mice with colon-cancer liver metastasis. *Gastroenterol Rep (Oxf)* (2020) 8:56–65. doi: 10.1093/gastro/goz060

53. Xu Y, Wei Z, Feng M, Zhu D, Mei S, Wu Z, et al. Tumor-infiltrated activated B cells suppress liver metastasis of colorectal cancers. *Cell Rep* (2022) 40:111295. doi: 10.1016/j.celrep.2022.111295

54. Luke JJ, Bao R, Sweis RF, Spranger S, Gajewski TF. WNT/β-catenin pathway activation correlates with immune exclusion across human cancers. *Clin Cancer Res* (2019) 25:3074–83. doi: 10.1158/1078-0432.Ccr-18-1942

55. Panarelli NC, Vaughn CP, Samowitz WS, Yantiss RK. Sporadic microsatellite instability-high colon cancers rarely display immunohistochemical evidence of Wnt signaling activation. *Am J Surg Pathol* (2015) 39:313–7. doi: 10.1097/pas.0000000000000380

56. Sun X, Liu S, Wang D, Zhang Y, Li W, Guo Y, et al. Colorectal cancer cells suppress CD4+ T cells immunity through canonical Wnt signaling. *Oncotarget* (2017) 8:15168–81. doi: 10.18632/oncotarget.14834

57. Grasso CS, Giannakis M, Wells DK, Hamada T, Mu XJ, Quist M, et al. Genetic mechanisms of immune evasion in colorectal cancer. *Cancer Discov* (2018) 8:730–49. doi: 10.1158/2159-8290.Cd-17-1327

58. Pai SG, Carneiro BA, Mota JM, Costa R, Leite CA, Barroso-Sousa R, et al. Wnt/beta-catenin pathway: modulating anticancer immune response. *J Hematol Oncol* (2017) 10:101. doi: 10.1186/s13045-017-0471-6

59. Xue J, Yu X, Xue L, Ge X, Zhao W, Peng W. Intrinsic β-catenin signaling suppresses CD8(+) T-cell infiltration in colorectal cancer. *BioMed Pharmacother* (2019) 115:108921. doi: 10.1016/j.biopha.2019.108921

60. Feng M, Jin JQ, Xia L, Xiao T, Mei S, Wang X, et al. Pharmacological inhibition of β-catenin/BCL9 interaction overcomes resistance to immune checkpoint blockades by modulating T(reg) cells. *Sci Adv* (2019) 5:eaau5240. doi: 10.1126/sciadv.aau5240

61. Ganesh S, Shui X, Craig KP, Park J, Wang W, Brown BD, et al. RNAi-mediated β-catenin inhibition promotes T cell infiltration and antitumor activity in combination with immune checkpoint blockade. *Mol Ther* (2018) 26:2567–79. doi: 10.1016/j.ymthe.2018.09.005

62. Hafezi S, Rahmani M. Targeting BCL-2 in cancer: advances, challengesand perspectives. *Cancers (Basel)* (2021) 13. doi: 10.3390/cancers13061292

63. Bortolomeazzi M, Keddar MR, Montorsi L, Acha-Sagredo A, Benedetti L, Temelkovski D, et al. Immunogenomics of colorectal cancer response to checkpoint blockade: analysis of the KEYNOTE 177 trial and validation cohorts. *Gastroenterology* (2021) 161:1179–93. doi: 10.1053/j.gastro.2021.06.064

64. Gopalakrishnan V, Helmink BA, Spencer CN, Reuben A, Wargo JA. The influence of the gut microbiome on cancer, immunityand cancer immunotherapy. *Cancer Cell* (2018) 33:570–80. doi: 10.1016/j.ccell.2018.03.015

65. Shaked Y. The pro-tumorigenic host response to cancer therapies. *Nat Rev Cancer* (2019) 19:667–85. doi: 10.1038/s41568-019-0209-6

66. Galluzzi L, Vitale I, Aaronson SA, Abrams JM, Adam D, Agostinis P, et al. Molecular mechanisms of cell death: recommendations of the Nomenclature Committee on Cell Death 2018. *Cell Death Differ* (2018) 25:486–541. doi: 10.1038/s41418-017-0012-4

67. Galluzzi L, Buqué A, Kepp O, Zitvogel L, Kroemer G. Immunological effects of conventional chemotherapy and targeted anticancer agents. *Cancer Cell* (2015) 28:690–714. doi: 10.1016/j.ccell.2015.10.012

68. Casciola-Rosen LA, Anhalt G, Rosen A. Autoantigens targeted in systemic lupus erythematosus are clustered in two populations of surface structures on apoptotic keratinocytes. *J Exp Med* (1994) 179:1317–30. doi: 10.1084/jem.179.4.1317

69. Rawson PM, Molette C, Videtta M, Altieri L, Franceschini D, Donato T, et al. Cross-presentation of caspase-cleaved apoptotic self antigens in HIV infection. *Nat Med* (2007) 13:1431–9. doi: 10.1038/nm1679

70. Garg AD, More S, Rufo N, Mece O, Sassano ML, Agostinis P, et al. Trial watch: Immunogenic cell death induction by anticancer chemotherapeutics. *Oncoimmunology* (2017) 6:e1386829. doi: 10.1080/2162402x.2017.1386829

71. Casares N, Pequignot MO, Tesniere A, Ghiringhelli F, Roux S, Chaput N, et al. Caspase-dependent immunogenicity of doxorubicin-induced tumor cell death. *J Exp Med* (2005) 202:1691–701. doi: 10.1084/jem.20050915

72. Paroli M, Bellati F, Videtta M, Focaccetti C, Mancone C, Donato T, et al. Discovery of chemotherapy-associated ovarian cancer antigens by interrogating memory T cells. *Int J Cancer* (2014) 134:1823–34. doi: 10.1002/ijc.28515

73. Garg AD, Agostinis P. Cell death and immunity in cancer: From danger signals to mimicry of pathogen defense responses. *Immunol Rev* (2017) 280:126–48. doi: 10.1111/imr.12574

74. Wang HT, Lee HI, Guo JH, Chen SH, Liao ZK, Huang KW, et al. Calreticulin promotes tumor lymphocyte infiltration and enhances the antitumor effects of immunotherapy by up-regulating the endothelial expression of adhesion molecules. *Int J Cancer* (2012) 130:2892–902. doi: 10.1002/ijc.26339

75. Saenz R, Futalan D, Leutenez L, Eekhout F, Fecteau JF, Sundelius S, et al. TLR4-dependent activation of dendritic cells by an HMGB1-derived peptide adjuvant. *J Transl Med* (2014) 12:211. doi: 10.1186/1479-5876-12-211

76. Tesniere A, Schlemmer F, Boige V, Kepp O, Martins I, Ghiringhelli F, et al. Immunogenic death of colon cancer cells treated with oxaliplatin. *Oncogene* (2010) 29:482–91. doi: 10.1038/onc.2009.356

77. Tel J, Hato SV, Torensma R, Buschow SI, Figdor CG, Lesterhuis WJ, et al. The chemotherapeutic drug oxaliplatin differentially affects blood DC function dependent on environmental cues. *Cancer Immunol Immunother* (2012) 61:1101–11. doi: 10.1007/s00262-011-1189-x

78. Galluzzi L, Buqué A, Kepp O, Zitvogel L, Kroemer G. Immunogenic cell death in cancer and infectious disease. *Nat Rev Immunol* (2017) 17:97–111. doi: 10.1038/nri.2016.107

79. Chang CL, Hsu YT, Wu CC, Lai YZ, Wang C, Yang YC, et al. Dose-dense chemotherapy improves mechanisms of antitumor immune response. *Cancer Res* (2013) 73:119–27. doi: 10.1158/0008-5472.Can-12-2225

80. Lesterhuis WJ, Punt CJ, Hato SV, Eleveld-Trancikova D, Jansen BJ, Nierkens S, et al. Platinum-based drugs disrupt STAT6-mediated suppression of immune responses against cancer in humans and mice. *J Clin Invest* (2011) 121:3100–8. doi: 10.1172/jci43656

81. Palombo F, Focaccetti C, Barnaba V. Therapeutic implications of immunogenic cell death in human cancer. *Front Immunol* (2014) 4:503. doi: 10.3389/fimmu.2013.00503

82. Martins I, Tesniere A, Kepp O, Michaud M, Schlemmer F, Senovilla L, et al. Chemotherapy induces ATP release from tumor cells. *Cell Cycle* (2009) 8:3723–8. doi: 10.4161/cc.8.22.10026

83. Kwon M, Jung H, Nam GH, Kim IS. The right Timing, right combination, right sequenceand right delivery for Cancer immunotherapy. *J Control Release* (2021) 331:321–34. doi: 10.1016/j.jconrel.2021.01.009

84. Yi M, Zheng X, Niu M, Zhu S, Ge H, Wu K. Combination strategies with PD-1/PD-L1 blockade: current advances and future directions. *Mol Cancer* (2022) 21:28. doi: 10.1186/s12943-021-01489-2

85. Wan S, Pestka S, Jubin RG, Lyu YL, Tsai YC, Liu LF. Chemotherapeutics and radiation stimulate MHC class I expression through elevated interferon-beta signaling in breast cancer cells. *PloS One* (2012) 7:e32542. doi: 10.1371/journal.pone.0032542

86. Ross ME, Caligiuri MA. Cytokine-induced apoptosis of human natural killer cells identifies a novel mechanism to regulate the innate immune response. *Blood* (1997) 89:910–8. doi: 10.1182/blood.V89.3.910

87. Binnewies M, Roberts EW, Kersten K, Chan V, Fearon DF, Merad M, et al. Understanding the tumor immune microenvironment (TIME) for effective therapy. *Nat Med* (2018) 24:541–50. doi: 10.1038/s41591-018-0014-x

88. Gotwals P, Cameron S, Cipolletta D, Cremasco V, Crystal A, Hewes B, et al. Prospects for combining targeted and conventional cancer therapy with immunotherapy. *Nat Rev Cancer* (2017) 17:286–301. doi: 10.1038/nrc.2017.17

89. Balkwill FR, Capasso M, Hagemann T. The tumor microenvironment at a glance. *J Cell Sci* (2012) 125:5591–6. doi: 10.1242/jcs.116392

90. Barcellos-Hoff MH, Lyden D, Wang TC. The evolution of the cancer niche during multistage carcinogenesis. *Nat Rev Cancer* (2013) 13:511–8. doi: 10.1038/nrc3536

91. Quail DF, Joyce JA. Microenvironmental regulation of tumor progression and metastasis. *Nat Med* (2013) 19:1423–37. doi: 10.1038/nm.3394

92. Mascaux C, Angelova M, Vasaturo A, Beane J, Hijazi K, Anthoine G, et al. Immune evasion before tumour invasion in early lung squamous carcinogenesis. *Nature* (2019) 571:570–5. doi: 10.1038/s41586-019-1330-0

93. Mantovani A, Marchesi F, Malesci A, Laghi L, Allavena P. Tumour-associated macrophages as treatment targets in oncology. *Nat Rev Clin Oncol* (2017) 14:399–416. doi: 10.1038/nrclinonc.2016.217

94. Mellman I, Coukos G, Dranoff G. Cancer immunotherapy comes of age. *Nature* (2011) 480:480–9. doi: 10.1038/nature10673

95. Limagne E, Euvrard R, Thibaudin M, Rébé C, Derangère V, Chevriaux A, et al. Accumulation of MDSC and th17 cells in patients with metastatic colorectal cancer predicts the efficacy of a FOLFOX-bevacizumab drug treatment regimen. *Cancer Res* (2016) 76:5241–52. doi: 10.1158/0008-5472.Can-15-3164

96. Vincent J, Mignot G, Chalmin F, Ladoire S, Bruchard M, Chevriaux A, et al. 5-Fluorouracil selectively kills tumor-associated myeloid-derived suppressor cells resulting in enhanced T cell-dependent antitumor immunity. *Cancer Res* (2010) 70:3052–61. doi: 10.1158/0008-5472.Can-09-3690

97. Duan Q, Zhang H, Zheng J, Zhang L. Turning Cold into Hot: Firing up the Tumor Microenvironment. *Trends Cancer* (2020) 6:605–18. doi: 10.1016/j.trecan.2020.02.022

98. Hui Z, Ren Y, Zhang D, Chen Y, Yu W, Cao J, et al. PD-1 blockade potentiates neoadjuvant chemotherapy in NSCLC via increasing CD127(+) and KLRG1(+) CD8 T cells. *NPJ Precis Oncol* (2023) 7:48. doi: 10.1038/s41698-023-00384-x

99. Corrales L, McWhirter SM, Dubensky TW Jr., Gajewski TF. The host STING pathway at the interface of cancer and immunity. *J Clin Invest* (2016) 126:2404–11. doi: 10.1172/jci86892

100. Barber GN. STING-dependent cytosolic DNA sensing pathways. *Trends Immunol* (2014) 35:88–93. doi: 10.1016/j.it.2013.10.010

101. Parkes EE, Walker SM, Taggart LE, McCabe N, Knight LA, Wilkinson R, et al. Activation of STING-dependent innate immune signaling by S-phase-specific DNA damage in breast cancer. *J Natl Cancer Inst* (2017) 109. doi: 10.1093/jnci/djw199

102. Kciuk M, Kołat D, Kałuzińska-Kołat Ż, Gawrysiak M, Drozda R, Celik I, et al. PD-1/PD-L1 and DNA damage response in cancer. *Cells* (2023) 12. doi: 10.3390/cells12040530

103. Garaude J, Blander JM. ICOStomizing immunotherapies with T(H)17. *Sci Transl Med* (2010) 2:55ps52. doi: 10.1126/scitranslmed.3001722

104. Lu Y, Zhao Q, Liao JY, Song E, Xia Q, Pan J, et al. Complement signals determine opposite effects of B cells in chemotherapy-induced immunity. *Cell* (2020) 180:1081–1097.e24. doi: 10.1016/j.cell.2020.02.015

105. Medler TR, Cotechini T, Coussens LM. Immune response to cancer therapy: mounting an effective antitumor response and mechanisms of resistance. *Trends Cancer* (2015) 1:66–75. doi: 10.1016/j.trecan.2015.07.008

106. Bracci L, Schiavoni G, Sistigu A, Belardelli F. Immune-based mechanisms of cytotoxic chemotherapy: implications for the design of novel and rationale-based combined treatments against cancer. *Cell Death Differ* (2014) 21:15–25. doi: 10.1038/cdd.2013.67

107. Machiels J-PH, Reilly RT, Emens LA, Ercolini AM, Lei RY, Weintraub D, et al. Cyclophosphamide, doxorubicinand paclitaxel enhance the antitumor immune response of granulocyte/macrophage-colony stimulating factor-secreting whole-cell vaccines in HER-2/neu tolerized mice1. *Cancer Res* (2001) 61:3689–97.

108. Foukakis T, Lövrot J, Matikas A, Zerdes I, Lorent J, Tobin N, et al. Immune gene expression and response to chemotherapy in advanced breast cancer. *Br J Cancer* (2018) 118:480–8. doi: 10.1038/bjc.2017.446

109. Hodge JW, Garnett CT, Farsaci B, Palena C, Tsang K-Y, Ferrone S, et al. Chemotherapy-induced immunogenic modulation of tumor cells enhances killing by cytotoxic T lymphocytes and is distinct from immunogenic cell death. *Int J Cancer* (2013) 133:624–36. doi: 10.1002/ijc.28070

110. Galluzzi L, Senovilla L, Zitvogel L, Kroemer G. The secret ally: immunostimulation by anticancer drugs. *Nat Rev Drug Discov* (2012) 11:215–33. doi: 10.1038/nrd3626

111. Tanaka H, Matsushima H, Mizumoto N, Takashima A. Classification of chemotherapeutic agents based on their differential *in vitro* effects on dendritic cells. *Cancer Res* (2009) 69:6978–86. doi: 10.1158/0008-5472.Can-09-1101

112. Heinhuis KM, Ros W, Kok M, Steeghs N, Beijnen JH, Schellens JHM. Enhancing antitumor response by combining immune checkpoint inhibitors with chemotherapy in solid tumors. *Ann Oncol* (2019) 30:219–35. doi: 10.1093/annonc/mdy551

113. Sistigu A, Yamazaki T, Vacchelli E, Chaba K, Enot DP, Adam J, et al. Cancer cell-autonomous contribution of type I interferon signaling to the efficacy of chemotherapy. *Nat Med* (2014) 20:1301–9. doi: 10.1038/nm.3708

114. Ghiringhelli F, Menard C, Puig PE, Ladoire S, Roux S, Martin F, et al. Metronomic cyclophosphamide regimen selectively depletes CD4+CD25+ regulatory T cells and restores T and NK effector functions in end stage cancer patients. *Cancer Immunol Immunother* (2007) 56:641–8. doi: 10.1007/s00262-006-0225-8

115. Mattarollo SR, Loi S, Duret H, Ma Y, Zitvogel L, Smyth MJ. Pivotal role of innate and adaptive immunity in anthracycline chemotherapy of established tumors. *Cancer Res* (2011) 71:4809–20. doi: 10.1158/0008-5472.Can-11-0753

116. Jiménez-Sánchez A, Cybulska P, Mager KL, Koplev S, Cast O, Couturier DL, et al. Unraveling tumor-immune heterogeneity in advanced ovarian cancer uncovers immunogenic effect of chemotherapy. *Nat Genet* (2020) 52:582–93. doi: 10.1038/s41588-020-0630-5

117. Huang X, Cui S, Shu Y. Cisplatin selectively downregulated the frequency and immunoinhibitory function of myeloid-derived suppressor cells in a murine B16 melanoma model. *Immunol Res* (2016) 64:160–70. doi: 10.1007/s12026-015-8734-1

118. Jackaman C, Majewski D, Fox SA, Nowak AK, Nelson DJ. Chemotherapy broadens the range of tumor antigens seen by cytotoxic CD8(+) T cells in vivo. *Cancer Immunol Immunother* (2012) 61:2343–56. doi: 10.1007/s00262-012-1307-4

119. Nio Y, Hirahara N, Minari Y, Iguchi C, Yamasawa K, Toga T, et al. Induction of tumor-specific antitumor immunity after chemotherapy with cisplatin in mice bearing MOPC-104E plasmacytoma by modulation of MHC expression on tumor surface. *Anticancer Res* (2000) 20:3293–9.

120. Hu J, Kinn J, Zirakzadeh AA, Sherif A, Norstedt G, Wikström AC, et al. The effects of chemotherapeutic drugs on human monocyte-derived dendritic cell differentiation and antigen presentation. *Clin Exp Immunol* (2013) 172:490–9. doi: 10.1111/cei.12060

121. Ock CY, Kim S, Keam B, Kim S, Ahn YO, Chung EJ, et al. Changes in programmed death-ligand 1 expression during cisplatin treatment in patients with head and neck squamous cell carcinoma. *Oncotarget* (2017) 8:97920–7. doi: 10.18632/oncotarget.18542

122. Tran L, Allen CT, Xiao R, Moore E, Davis R, Park SJ, et al. Cisplatin alters antitumor immunity and synergizes with PD-1/PD-L1 inhibition in head and neck squamous cell carcinoma. *Cancer Immunol Res* (2017) 5:1141–51. doi: 10.1158/2326-6066.Cir-17-0235

123. Thomas SN, Vokali E, Lund AW, Hubbell JA, Swartz MA. Targeting the tumor-draining lymph node with adjuvanted nanoparticles reshapes the anti-tumor immune response. *Biomaterials* (2014) 35:814–24. doi: 10.1016/j.biomaterials.2013.10.003

124. Sevko A, Kremer V, Falk C, Umansky L, Shurin MR, Shurin GV, et al. Application of paclitaxel in low non-cytotoxic doses supports vaccination with melanoma antigens in normal mice. *J Immunotoxicol* (2012) 9:275–81. doi: 10.3109/1547691X.2012.655343

125. Pfannenstiel LW, Lam SSK, Emens LA, Jaffee EM, Armstrong TD. Paclitaxel enhances early dendritic cell maturation and function through TLR4 signaling in mice. *Cell Immunol* (2010) 263:79–87. doi: 10.1016/j.cellimm.2010.03.001

126. Yuan L, Wu L, Chen J, Wu Q, Hu S. Paclitaxel acts as an adjuvant to promote both Th1 and Th2 immune responses induced by ovalbumin in mice. *Vaccine* (2010) 28:4402–10. doi: 10.1016/j.vaccine.2010.04.046

127. Ma Y, Adjemian S, Mattarollo SR, Yamazaki T, Aymeric L, Yang H, et al. Anticancer chemotherapy-induced intratumoral recruitment and differentiation of antigen-presenting cells. *Immunity* (2013) 38:729–41. doi: 10.1016/j.immuni.2013.03.003

128. Kodumudi KN, Weber A, Sarnaik AA, Pilon-Thomas S. Blockade of myeloid-derived suppressor cells after induction of lymphopenia improves adoptive T cell therapy in a murine model of melanoma. *J Immunol* (2012) 189:5147–54. doi: 10.4049/jimmunol.1200274

129. Bezu L, Gomes-de-Silva LC, Dewitte H, Breckpot K, Fucikova J, Spisek R, et al. Combinatorial strategies for the induction of immunogenic cell death. *Front Immunol* (2015) 6:187. doi: 10.3389/fimmu.2015.00187

130. Bansal S, Bajaj P, Pandey S, Tandon V. Topoisomerases: resistance versus sensitivity, how far we can go? *Med Res Rev* (2017) 37:404–38. doi: 10.1002/med.21417

131. Frey B, Stache C, Rubner Y, Werthmöller N, Schulz K, Sieber R, et al. Combined treatment of human colorectal tumor cell lines with chemotherapeutic agents and

ionizing irradiation can in *vitro* induce tumor cell death forms with immunogenic potential. *J Immunotoxicol* (2012) 9:301–13. doi: 10.3109/1547691x.2012.693547

132. Roselli M, Formica V, Cereda V, Jochems C, Richards J, Grenga I, et al. The association of clinical outcome and peripheral T-cell subsets in metastatic colorectal cancer patients receiving first-line FOLFIRI plus bevacizumab therapy. *Oncoimmunology* (2016) 5:e1188243. doi: 10.1080/2162402x.2016.1188243

133. Alagkiozidis I, Facciabene A, Tsiatas M, Carpenito C, Benencia F, Adams S, et al. Time-dependent cytotoxic drugs selectively cooperate with IL-18 for cancer chemo-immunotherapy. *J Transl Med* (2011) 9:77. doi: 10.1186/1479-5876-9-77

134. Lin N, Song X, Chen B, Ye H, Wang Y, Cheng X, et al. Leptin is upregulated in epididymitis and promotes apoptosis and IL-1β production in epididymal epithelial cells by activating the NLRP3 inflammasome. *Int Immunopharmacol* (2020) 88:106901. doi: 10.1016/j.intimp.2020.106901

135. Wang W, Wu L, Zhang J, Wu H, Han E, Guo Q. Chemoimmunotherapy by combining oxaliplatin with immune checkpoint blockades reduced tumor burden in colorectal cancer animal model. *Biochem Biophys Res Commun* (2017) 487:1–7. doi: 10.1016/j.bbrc.2016.12.180

136. Liu WM, Fowler DW, Smith P, Dalgleish AG. Pre-treatment with chemotherapy can enhance the antigenicity and immunogenicity of tumours by promoting adaptive immune responses. *Br J Cancer* (2010) 102:115–23. doi: 10.1038/sj.bjc.6605465

137. Nowak AK, Robinson BW, Lake RA. Gemcitabine exerts a selective effect on the humoral immune response: implications for combination chemo-immunotherapy. *Cancer Res* (2002) 62:2353–8.

138. Mundy-Bosse BL, Lesinski GB, Jaime-Ramirez AC, Benninger K, Khan M, Kuppusamy P, et al. Myeloid-derived suppressor cell inhibition of the IFN response in tumor-bearing mice. *Cancer Res* (2011) 71:5101–10. doi: 10.1158/0008-5472.Can-10-2670

139. Homma Y, Taniguchi K, Nakazawa M, Matsuyama R, Mori R, Takeda K, et al. Changes in the immune cell population and cell proliferation in peripheral blood after gemcitabine-based chemotherapy for pancreatic cancer. *Clin Transl Oncol* (2014) 16:330–5. doi: 10.1007/s12094-013-1079-0

140. Bruchard M, Mignot G, Derangère V, Chalmin F, Chevriaux A, Végran F, et al. Chemotherapy-triggered cathepsin B release in myeloid-derived suppressor cells activates the Nlrp3 inflammasome and promotes tumor growth. *Nat Med* (2013) 19:57–64. doi: 10.1038/nm.2999

141. Galetto A, Buttiglieri S, Forno S, Moro F, Mussa A, Matera L. Drug- and cell-mediated antitumor cytotoxicities modulate cross-presentation of tumor antigens by myeloid dendritic cells. *Anticancer Drugs* (2003) 14:833–43. doi: 10.1097/00001813-200311000-00010

142. Ugurel S, Paschen A, Becker JC. Dacarbazine in melanoma: from a chemotherapeutic drug to an immunomodulating agent. *J Invest Dermatol* (2013) 133:289–92. doi: 10.1038/jid.2012.341

143. Ghiringhelli F, Larmonier N, Schmitt E, Parcellier A, Cathelin D, Garrido C, et al. CD4+CD25+ regulatory T cells suppress tumor immunity but are sensitive to cyclophosphamide which allows immunotherapy of established tumors to be curative. *Eur J Immunol* (2004) 34:336–44. doi: 10.1002/eji.200324181

144. Webb ER, Moreno-Vincente J, Easton A, Lanati S, Taylor M, James S, et al. Cyclophosphamide depletes tumor infiltrating T regulatory cells and combined with anti-PD-1 therapy improves survival in murine neuroblastoma. *iScience* (2022) 25:104995. doi: 10.1016/j.isci.2022.104995

145. Kaneno R, Shurin GV, Tourkova IL, Shurin MR. Chemomodulation of human dendritic cell function by antineoplastic agents in low noncytotoxic concentrations. *J Transl Med* (2009) 7:58. doi: 10.1186/1479-5876-7-58

146. Terenzi A, Pirker C, Keppler BK, Berger W. Anticancer metal drugs and immunogenic cell death. *J Inorg Biochem* (2016) 165:71–9. doi: 10.1016/j.jinorgbio.2016.06.021

147. Pol J, Vacchelli E, Aranda F, Castoldi F, Eggermont A, Cremer I, et al. Trial Watch: Immunogenic cell death inducers for anticancer chemotherapy. *Oncoimmunology* (2015) 4:e1008866. doi: 10.1080/2162402x.2015.1008866

148. Rufo N, Garg AD, Agostinis P. The unfolded protein response in immunogenic cell death and cancer immunotherapy. *Trends Cancer* (2017) 3:643–58. doi: 10.1016/j.trecan.2017.07.002

149. Krysko DV, Garg AD, Kaczmarek A, Krysko O, Agostinis P, Vandenabeele P. Immunogenic cell death and DAMPs in cancer therapy. *Nat Rev Cancer* (2012) 12:860–75. doi: 10.1038/nrc3380

150. Fucikova J, Kralikova P, Fialova A, Brtnicky T, Rob L, Bartunkova J, et al. Human tumor cells killed by anthracyclines induce a tumor-specific immune response. *Cancer Res* (2011) 71:4821–33. doi: 10.1158/0008-5472.Can-11-0950

151. Wang Z, Chen J, Hu J, Zhang H, Xu F, He W, et al. cGAS/STING axis mediates a topoisomerase II inhibitor-induced tumor immunogenicity. *J Clin Invest* (2019) 129:4850–62. doi: 10.1172/jci127471

152. Lu J, Liu X, Liao YP, Wang X, Ahmed A, Jiang W, et al. Breast cancer chemo-immunotherapy through liposomal delivery of an immunogenic cell death stimulus plus interference in the IDO-1 pathway. *ACS Nano* (2018) 12:11041–61. doi: 10.1021/acsnano.8b05189

153. Mei L, Liu Y, Rao J, Tang X, Li M, Zhang Z, et al. Enhanced tumor retention effect by click chemistry for improved cancer immunochemotherapy. *ACS Appl Mater Interfaces* (2018) 10:17582–93. doi: 10.1021/acsami.8b02954

154. Voorwerk L, Slagter M, Horlings HM, Sikorska K, van de Vijver KK, de Maaker M, et al. Immune induction strategies in metastatic triple-negative breast cancer to enhance the sensitivity to PD-1 blockade: the TONIC trial. *Nat Med* (2019) 25:920–8. doi: 10.1038/s41591-019-0432-4

155. Song W, Shen L, Wang Y, Liu Q, Goodwin TJ, Li J, et al. Synergistic and low adverse effect cancer immunotherapy by immunogenic chemotherapy and locally expressed PD-L1 trap. *Nat Commun* (2018) 9:2237. doi: 10.1038/s41467-018-04605-x

156. Paz-Ares L, Luft A, Vicente D, Tafreshi A, Gümüş M, Mazières J, et al. Pembrolizumab plus chemotherapy for squamous non-small-cell lung cancer. *N Engl J Med* (2018) 379:2040–51. doi: 10.1056/NEJMoa1810865

157. Maker AV, Ito H, Mo Q, Weisenberg E, Qin LX, Turcotte S, et al. Genetic evidence that intratumoral T-cell proliferation and activation are associated with recurrence and survival in patients with resected colorectal liver metastases. *Cancer Immunol Res* (2015) 3:380–8. doi: 10.1158/2326-6066.Cir-14-0212

158. Michels T, Shurin GV, Naiditch H, Sevko A, Umansky V, Shurin MR. Paclitaxel promotes differentiation of myeloid-derived suppressor cells into dendritic cells in *vitro* in a TLR4-independent manner. *J Immunotoxicol* (2012) 9:292–300. doi: 10.3109/1547691x.2011.642418

159. Garzetti GG, Ciavattini A, Muzzioli M, Romanini C. Cisplatin-based polychemotherapy reduces the natural cytotoxicity of peripheral blood mononuclear cells in patients with advanced ovarian carcinoma and their in *vitro* responsiveness to interleukin-12 incubation. *Cancer* (1999) 85:2226–31. doi: 10.1002/(sici)1097-0142(19990515)85:10<2226::aid-cncr18>3.0.co;2-x

160. Liu N, Zheng Y, Zhu Y, Xiong S, Chu Y. Selective Impairment of CD4+CD25+Foxp3+Regulatory T cells by paclitaxel is explained by Bcl-2/Bax mediated apoptosis. *Int Immunopharmacol* (2011) 11:212–9. doi: 10.1016/j.intimp.2010.11.021

161. Zhang L, Dermawan K, Jin M, Liu R, Zheng H, Xu L, et al. Differential impairment of regulatory T cells rather than effector T cells by paclitaxel-based chemotherapy. *Clin Immunol* (2008) 129:219–29. doi: 10.1016/j.clim.2008.07.013

162. Vicari AP, Luu R, Zhang N, Patel S, Makinen SR, Hanson DC, et al. Paclitaxel reduces regulatory T cell numbers and inhibitory function and enhances the anti-tumor effects of the TLR9 agonist PF-3512676 in the mouse. *Cancer Immunol Immunother* (2009) 58:615–28. doi: 10.1007/s00262-008-0586-2

163. Zhu Y, Liu N, Xiong SD, Zheng YJ, Chu YW. CD4+Foxp3+ Regulatory T-cell impairment by paclitaxel is independent of toll-like receptor 4. *Scandinavian J Immunol* (2011) 73:301–8. doi: 10.1111/j.1365-3083.2011.02514.x

164. Kodumudi KN, Woan K, Gilvary DL, Sahakian E, Wei S, Djeu JY. A novel chemoimmunomodulating property of docetaxel: suppression of myeloid-derived suppressor cells in tumor bearers. *Clin Cancer Res* (2010) 16:4583–94. doi: 10.1158/1078-0432.Ccr-10-0733

165. Li JY, Duan XF, Wang LP, Xu YJ, Huang L, Zhang TF, et al. Selective depletion of regulatory T cell subsets by docetaxel treatment in patients with nonsmall cell lung cancer. *J Immunol Res* (2014) 2014:286170. doi: 10.1155/2014/286170

166. Roselli M, Cereda V, di Bari MG, Formica V, Spila A, Jochems C, et al. Effects of conventional therapeutic interventions on the number and function of regulatory T cells. *Oncoimmunology* (2013) 2:e27025. doi: 10.4161/onci.27025

167. Tong AW, Seamour B, Lawson JM, Ordonez G, Vukelja S, Hyman W, et al. Cellular immune profile of patients with advanced cancer before and after taxane treatment. *Am J Clin Oncol* (2000) 23:463–72. doi: 10.1097/00000421-200010000-00007

168. Wanderley CW, Colón DF, Luiz JPM, Oliveira FF, Viacava PR, Leite CA, et al. Paclitaxel reduces tumor growth by reprogramming tumor-associated macrophages to an M1 profile in a TLR4-dependent manner. *Cancer Res* (2018) 78:5891–900. doi: 10.1158/0008-5472.Can-17-3480

169. Cullis J, Siolas D, Avanzi A, Barui S, Maitra A, Bar-Sagi D. Macropinocytosis of nab-paclitaxel drives macrophage activation in pancreatic cancer. *Cancer Immunol Res* (2017) 5:182–90. doi: 10.1158/2326-6066.Cir-16-0125

170. Pusztai L, Mendoza TR, Reuben JM, Martinez MM, Willey JS, Lara J, et al. Changes in plasma levels of inflammatory cytokines in response to paclitaxel chemotherapy. *Cytokine* (2004) 25:94–102. doi: 10.1016/j.cyto.2003.10.004

171. Kim IS, Gao Y, Welte T, Wang H, Liu J, Janghorban M, et al. Immuno-subtyping of breast cancer reveals distinct myeloid cell profiles and immunotherapy resistance mechanisms. *Nat Cell Biol* (2019) 21:1113–26. doi: 10.1038/s41556-019-0373-7

172. Schmid P, Adams S, Rugo HS, Schneeweiss A, Barrios CH, Iwata H, et al. Atezolizumab and nab-paclitaxel in advanced triple-negative breast cancer. *N Engl J Med* (2018) 379:2108–21. doi: 10.1056/NEJMoa1809615

173. Loyher PL, Rochefort J, Baudesson de Chanville C, Hamon P, Lescaille G, Bertolus C, et al. CCR2 influences T regulatory cell migration to tumors and serves as a biomarker of cyclophosphamide sensitivity. *Cancer Res* (2016) 76:6483–94. doi: 10.1158/0008-5472.Can-16-0984

174. Scurr M, Pembroke T, Bloom A, Roberts D, Thomson A, Smart K, et al. Low-dose cyclophosphamide induces antitumor T-cell responses, which associate with survival in metastatic colorectal cancer. *Clin Cancer Res* (2017) 23:6771–80. doi: 10.1158/1078-0432.Ccr-17-0895

175. Hibino S, Chikuma S, Kondo T, Ito M, Nakatsukasa H, Omata-Mise S, et al. Inhibition of nr4a receptors enhances antitumor immunity by breaking treg-mediated immune tolerance. *Cancer Res* (2018) 78:3027–40. doi: 10.1158/0008-5472.Can-17-3102

176. Grosflam J, Weinblatt ME. Methotrexate: mechanism of action, pharmacokinetics, clinical indicationsand toxicity. *Curr Opin Rheumatol* (1991) 3:363–8. doi: 10.1097/00002281-199106000-00006

177. Peng J, Hamanishi J, Matsumura N, Abiko K, Murat K, Baba T, et al. Chemotherapy induces programmed cell death-ligand 1 overexpression via the nuclear factor-κB to foster an immunosuppressive tumor microenvironment in ovarian cancer. *Cancer Res* (2015) 75:5034–45. doi: 10.1158/0008-5472.Can-14-3098

178. Horn L, Mansfield AS, Szczęsna A, Havel L, Krzakowski M, Hochmair MJ, et al. First-line atezolizumab plus chemotherapy in extensive-stage small-cell lung cancer. *N Engl J Med* (2018) 379:2220–9. doi: 10.1056/NEJMoa1809064

179. Kang C, Syed YY. Atezolizumab (in combination with nab-paclitaxel): A review in advanced triple-negative breast cancer. *Drugs* (2020) 80:601–7. doi: 10.1007/s40265-020-01295-y

180. Tabernero J, Yoshino T, Cohn AL, Kochenderfer MD, Holdridge RC, Couture F, et al. Open-label phase II/III study of nivolumab plus standard of care versus standard of care for first-line treatment of metastatic colorectal cancer: Checkmate-9X8. *J Clin Oncol* (2019) 37:TPS718–8. doi: 10.1200/JCO.2019.37.4_suppl.TPS718

181. Mettu NB, Twohy E, Ou FS, Halfdanarson TR, Lenz HJ, Breakstone R, et al. 533PD - BACCI: A phase II randomized, double-blind, multicenter, placebo-controlled study of capecitabine (C) bevacizumab (B) plus atezolizumab (A) or placebo (P) in refractory metastatic colorectal cancer (mCRC): An ACCRU network study. *Ann Oncol* (2019) 30:v203. doi: 10.1093/annonc/mdz246.011

182. Fang X, Zhong C, Zhu N, Weng S, Hu H, Wang J, et al. A phase 2 trial of sintilimab (IBI 308) in combination with CAPEOX and bevacizumab (BBCAPX) as first-line treatment in patients with RAS-mutant, microsatellite stable, unresectable metastatic colorectal cancer. *J Clin Oncol* (2022) 40:3563–3. doi: 10.1200/JCO.2022.40.16_suppl.3563

183. Fumet JD, Chibaudel B, Bennouna J, Borg C, Martin-Babau J, Cohen R, et al. 433P Durvalumab and tremelimumab in combination with FOLFOX in patients with previously untreated RAS-mutated metastatic colorectal cancer: First results of efficacy at one year for phase II MEDITREME trial. *Ann Oncol* (2021) 32:S551. doi: 10.1016/j.annonc.2021.08.954

184. Damato A, Iachetta F, Normanno N, Bergamo F, Maiello E, Zaniboni A, et al. NIVACOR: Phase II study of nivolumab in combination with FOLFOXIRI/bevacizumab in first-line chemotherapy for advanced colorectal cancer RASm/BRAFm patients. *J Clin Oncol* (2020) 38:TPS4118–TPS4118. doi: 10.1200/JCO.2020.38.15_suppl.TPS4118

185. Shahda S, Noonan AM, Bekaii-Saab TS, O'Neil BH, Sehdev A, Shaib WL, et al. A phase II study of pembrolizumab in combination with mFOLFOX6 for patients with advanced colorectal cancer. *J Clin Oncol* (2017) 35:3541–1. doi: 10.1200/JCO.2017.35.15_suppl.3541

186. Formenti SC, Demaria S. Combining radiotherapy and cancer immunotherapy: a paradigm shift. *J Natl Cancer Inst* (2013) 105:256–65. doi: 10.1093/jnci/djs629

187. Sharabi AB, Lim M, DeWeese TL, Drake CG. Radiation and checkpoint blockade immunotherapy: radiosensitisation and potential mechanisms of synergy. *Lancet Oncol* (2015) 16:e498–509. doi: 10.1016/s1470-2045(15)00007-8

188. Lin Z, Cai M, Zhang P, Li X, Cai K, Nie X, et al. Short-course radiotherapy and subsequent CAPOX plus camrelizumab followed by delayed surgery for locally advanced rectal cancer:Short-term results of a phase II trial. *J Clin Oncol* (2021) 39:63–3. doi: 10.1200/JCO.2021.39.3_suppl.63

189. Wang Y, Xia F, Shen L, Wan J, Zhang H, Wu R, et al. Short-course radiotherapy based total neoadjuvant therapy combined with toripalimab for locally advanced rectal cancer: preliminary findings from a randomized, prospective, multicenter, double-arm, phase II trial (TORCH). *Int J Radiat Oncol Biol Phys* (2022) 114:e152. doi: 10.1016/j.ijrobp.2022.07.1009

190. Leduc C, Adam J, Louvet E, Sourisseau T, Dorvault N, Bernard M, et al. TPF induction chemotherapy increases PD-L1 expression in tumour cells and immune cells in head and neck squamous cell carcinoma. *ESMO Open* (2018) 3:e000257. doi: 10.1136/esmoopen-2017-000257

191. Castle JC, Loewer M, Boegel S, de Graaf J, Bender C, Tadmor AD, et al. Immunomic, genomic and transcriptomic characterization of CT26 colorectal carcinoma. *BMC Genomics* (2014) 15:190. doi: 10.1186/1471-2164-15-190

192. Dosset M, Vargas TR, Lagrange A, Boidot R, Végran F, Roussey A, et al. PD-1/PD-L1 pathway: an adaptive immune resistance mechanism to immunogenic chemotherapy in colorectal cancer. *Oncoimmunology* (2018) 7:e1433981. doi: 10.1080/2162402x.2018.1433981

193. Galon J, Costes A, Sanchez-Cabo F, Kirilovsky A, Mlecnik B, Lagorce-Pagès C, et al. Type, densityand location of immune cells within human colorectal tumors predict clinical outcome. *Science* (2006) 313:1960–4. doi: 10.1126/science.1129139

194. Limagne E, Thibaudin M, Nuttin L, Spill A, Derangère V, Fumet J-D, et al. Trifluridine/tipiracil plus oxaliplatin improves PD-1 blockade in colorectal cancer by inducing immunogenic cell death and depleting macrophages. *Cancer Immunol Res* (2019) 7:1958–69. doi: 10.1158/2326-6066.Cir-19-0228

195. Bocobo AG, Wang R, Behr S, Carnevale JC, Cinar P, Collisson EA, et al. Phase II study of pembrolizumab plus capecitabine and bevacizumab in microsatellite stable (MSS) metastatic colorectal cancer (mCRC): Interim analysis. *J Clin Oncol* (2021) 39:77–7. doi: 10.1200/JCO.2021.39.3_suppl.77

196. Morano F, Raimondi A, Pagani F, Lonardi S, Salvatore L, Cremolini C, et al. Temozolomide followed by combination with low-dose ipilimumab and nivolumab in patients with microsatellite-stable, O(6)-methylguanine-DNA methyltransferase-silenced metastatic colorectal cancer: the MAYA trial. *J Clin Oncol* (2022) 40:1562–73. doi: 10.1200/jco.21.02583

197. Luo H, Lu J, Bai Y, Mao T, Wang J, Fan Q, et al. Effect of camrelizumab vs placebo added to chemotherapy on survival and progression-free survival in patients with advanced or metastatic esophageal squamous cell carcinoma: the ESCORT-1st randomized clinical trial. *Jama* (2021) 326:916–25. doi: 10.1001/jama.2021.12836

198. Sun Y, Liu X, Yang K-Y, Zhang N, Jin F, Zou G, et al. PD-1 blockade with sintilimab plus induction chemotherapy and concurrent chemoradiotherapy (IC-CCRT) versus IC-CCRT in locoregionally-advanced nasopharyngeal carcinoma (LANPC): A multicenter, phase 3, randomized controlled trial (CONTINUUM). *J Clin Oncol* (2023) 41:LBA6002–LBA6002. doi: 10.1200/JCO.2023.41.17_suppl.LBA6002

199. Zhang Y, Chen L, Hu GQ, Zhang N, Zhu XD, Yang KY, et al. Final overall survival analysis of gemcitabine and cisplatin induction chemotherapy in nasopharyngeal carcinoma: A multicenter, randomized phase III trial. *J Clin Oncol* (2022) 40:2420–5. doi: 10.1200/jco.22.00327

200. Hollebecque A, Calvo A, Andre T, Argiles G, Cervantes A, Leger C, et al. Phase I multicenter, open-label study to establish the maximum tolerated dose (MTD) of trifluridine/tipiracil (TAS-102) and oxaliplatin combination in patients (pts) with metastatic colorectal cancer (mCRC). *J Clin Oncol* (2018) 36:816–6. doi: 10.1200/JCO.2018.36.4_suppl.816

201. Redman JM, Tsai YT, Weinberg BA, Donahue RN, Gandhy S, Gatti-Mays ME, et al. A randomized phase II trial of mFOLFOX6 + Bevacizumab alone or with adCEA vaccine + Avelumab immunotherapy for untreated metastatic colorectal cancer. *Oncologist* (2022) 27:198–209. doi: 10.1093/oncolo/oyab046

202. Xu J, Chen M, Wu Y, Zhang H, Zhou J, Wang D, et al. The role of transcriptional factor brachyury on cell cycle regulation in non-small cell lung cancer. *Front Oncol* (2020) 10:1078. doi: 10.3389/fonc.2020.01078

203. Nath S, Mukherjee P. MUC1: a multifaceted oncoprotein with a key role in cancer progression. *Trends Mol Med* (2014) 20:332–42. doi: 10.1016/j.molmed.2014.02.007

204. Wallin J, Pishvaian M, Hernandez G, Yadav M, Jhunjhunwala S, Delamarre L, et al. Abstract 2651: Clinical activity and immune correlates from a phase Ib study evaluating atezolizumab (anti-PDL1) in combination with FOLFOX and bevacizumab (anti-VEGF) in metastatic colorectal carcinoma. *Cancer Res* (2016) 76:2651–1. doi: 10.1158/1538-7445.AM2016-2651

205. Iida Y, Harashima N, Motoshima T, Komohara Y, Eto M, Harada M. Contrasting effects of cyclophosphamide on anti-CTL-associated protein 4 blockade therapy in two mouse tumor models. *Cancer Sci* (2017) 108:1974–84. doi: 10.1111/cas.13337

206. Lynch TJ, Bondarenko I, Luft A, Serwatowski P, Barlesi F, Chacko R, et al. Ipilimumab in combination with paclitaxel and carboplatin as first-line treatment in stage IIIB/IV non-small-cell lung cancer: results from a randomized, double-blind, multicenter phase II study. *J Clin Oncol* (2012) 30:2046–54. doi: 10.1200/jco.2011.38.4032

207. Kok M, Voorwerk L, Horlings H, Sikorska K, Vijver K, Slagter M, et al. Adaptive phase II randomized trial of nivolumab after induction treatment in triple negative breast cancer (TONIC trial): Final response data stage I and first translational data. *J Clin Oncol* (2018) 36:1012–2. doi: 10.1200/JCO.2018.36.15_suppl.1012

208. Gray A, de la Luz Garcia-Hernandez M, van West M, Kanodia S, Hubby B, Kast WM. Prostate cancer immunotherapy yields superior long-term survival in TRAMP mice when administered at an early stage of carcinogenesis prior to the establishment of tumor-associated immunosuppression at later stages. *Vaccine* (2009) 27 Suppl 6:G52–9. doi: 10.1016/j.vaccine.2009.09.106

209. Wu AR, Neff NF, Kalisky T, Dalerba P, Treutlein B, Rothenberg ME, et al. Quantitative assessment of single-cell RNA-sequencing methods. *Nat Methods* (2014) 11:41–6. doi: 10.1038/nmeth.2694

210. Papalexi E, Satija R. Single-cell RNA sequencing to explore immune cell heterogeneity. *Nat Rev Immunol* (2018) 18:35–45. doi: 10.1038/nri.2017.76

211. Jiang P, Gu S, Pan D, Fu J, Sahu A, Hu X, et al. Signatures of T cell dysfunction and exclusion predict cancer immunotherapy response. *Nat Med* (2018) 24:1550–8. doi: 10.1038/s41591-018-0136-1

212. Zhang L, Li Z, Skrzypczynska KM, Fang Q, Zhang W, O'Brien SA, et al. Single-cell analyses inform mechanisms of myeloid-targeted therapies in colon cancer. *Cell* (2020) 181:442–459.e29. doi: 10.1016/j.cell.2020.03.048

213. Emens LA, Middleton G. The interplay of immunotherapy and chemotherapy: harnessing potential synergies. *Cancer Immunol Res* (2015) 3:436–43. doi: 10.1158/2326-6066.Cir-15-0064

214. Galon J, Bruni D. Approaches to treat immune hot, altered and cold tumours with combination immunotherapies. *Nat Rev Drug Discov* (2019) 18:197–218. doi: 10.1038/s41573-018-0007-y

215. Socinski MA, Jotte RM, Cappuzzo F, Orlandi F, Stroyakovskiy D, Nogami N, et al. Atezolizumab for first-line treatment of metastatic nonsquamous NSCLC. *N Engl J Med* (2018) 378:2288–301. doi: 10.1056/NEJMoa1716948

216. Garassino M, Rodriguez-Abreu D, Gadgeel S, Esteban E, Felip E, Speranza G, et al. OA04.06 evaluation of TMB in KEYNOTE-189: pembrolizumab plus chemotherapy vs placebo plus chemotherapy for nonsquamous NSCLC. *J Thorac Oncol* (2019) 14:S216–7. doi: 10.1016/j.jtho.2019.08.427

217. Sun D, Liu J, Zhou H, Shi M, Sun J, Zhao S, et al. Classification of tumor immune microenvironment according to programmed death-ligand 1 expression and immune infiltration predicts response to immunotherapy plus chemotherapy in advanced patients with NSCLC. *J Thorac Oncol* (2023) 18:869–81. doi: 10.1016/j.jtho.2023.03.012

218. McGranahan N, Swanton C. Clonal heterogeneity and tumor evolution: past, presentand the future. *Cell* (2017) 168:613–28. doi: 10.1016/j.cell.2017.01.018

219. Galon J, Bruni D. Tumor immunology and tumor evolution: intertwined histories. *Immunity* (2020) 52:55–81. doi: 10.1016/j.immuni.2019.12.018

220. Wu Y, Biswas D, Swanton C. Impact of cancer evolution on immune surveillance and checkpoint inhibitor response. *Semin Cancer Biol* (2022) 84:89–102. doi: 10.1016/j.semcancer.2021.02.013

10.3389/fimmu.2023.1241208

Glossary

ICD	immunogenic cell death
NM-neoAgs	non-mutated neoantigens
CRC	colorectal cancer
mCRC	metastatic CRC
mOS	median overall survival
ICIs	immune checkpoint inhibitors
TME	tumor microenvironment
TIME	tumor immune microenvironment
MSI-H	microsatellite instability
dMMR	mismatch repair-deficient
MSS	microsatellite stable
pMMR	proficient mismatch repair
DOX	doxorubicin
PTX	paclitaxel
OXA	oxaliplatin
DAMPs	danger-associated molecular patterns
NM-neoAgs	non-mutated neoantigens
CTL	cytotoxic T lymphocyte
scRNA-seq	single-cell RNA sequencing
PD-1/PD-L1	programmed death receptor 1/programmed death-ligand 1
FDA	Food and Drug Administration
Tregs	regulatory T cells
MDSCs	myeloid-derived suppressor cells
TAMs	tumor-associated macrophages
NK cells	natural killer cells
MHC I	major histocompatibility complex class I
TGF-β	transforming growth factor β
DCs	dendritic cells
5-fluorouracil	5-FU
EGFR	epidermal growth factor receptor
DAMPs	danger-associated molecular patterns
CRT	calreticulin
HMGB1	high mobility group box 1
mDCs	mature DCs
APCs	antigen-presenting cells
NSCLC	non-small cell lung cancer
GP	gemcitabine plus cisplatin
TAM1	tumor-associated macrophages type 1
TAM2	tumor-associated macrophages type 2
cGAS-STING	cyclic GMP-AMP synthase/stimulator of interferon genes
ICOS	inducible T cell co-stimulator
ILBs	innate-like B cells
T_H cells	helper T cells
IFN	interferon
TNBC	triple-negative breast cancer
HSP70	heat shock protein 70
PFS	progression-free survival
CTX	cyclophosphamide
MTX	methotrexate
SCLC	small cell lung cancer
SOC	standard of care
FTD/TPI	trifluridine/tipiracil
OS	overall survival
ASCO	American Society of Clinical Oncology
EFS	event-free survival
mPFS	median progression-free survival
ORR	overall response rate
ILB	innate immune B cell
T_FH	follicular helper T cells
T_H1	type 1 helper T cells
TAA	tumor-associated antigen
LARC	Locally advanced rectal cancer

(Continued)

Continued

frontiers | Frontiers in Immunology

TYPE Original Research
PUBLISHED 16 November 2023
DOI 10.3389/fimmu.2023.1309138

OPEN ACCESS

EDITED BY
Chengwu Zeng,
Jinan University, China

REVIEWED BY

Zhongyan Hua,
China Medical University, China
Xiuli Wu,
Jinan University, China
Pengliang Wang,
Sun Yat-sen University, China

*CORRESPONDENCE
Qiang Zhao
zhaoqiang@tjmuch.com
Baocheng Gong
bcgong@cmu.edu.cn
Yuren Xia
xiayuren8910@tmu.edu.cn

†These authors have contributed equally to this work and share first authorship

RECEIVED 07 October 2023
ACCEPTED 31 October 2023
PUBLISHED 16 November 2023

CITATION
Tan J, Wang C, Jin Y, Xia Y, Gong B and Zhao Q (2023) Optimal combination of MYCN differential gene and cellular senescence gene predicts adverse outcomes in patients with neuroblastoma. *Front. Immunol.* 14:1309138. doi: 10.3389/fimmu.2023.1309138

Optimal combination of MYCN differential gene and cellular senescence gene predicts adverse outcomes in patients with neuroblastoma

Jiaxiong Tan[1,2,3†], Chaoyu Wang[1,2,3†], Yan Jin[1,2,3,4†], Yuren Xia[1,2,3*], Baocheng Gong[1,2,3*] and Qiang Zhao[1,2,3,4*]

[1]Tianjin Medical University Cancer Institute and Hospital, National Clinical Research Center for Cancer, Tianjin, China, [2]Tianjin's Clinical Research Center for Cancer, Tianjin, China, [3]Key Laboratory of Cancer Prevention and Therapy, Tianjin, China, [4]Department of Pediatric Oncology, Tianjin Medical University Cancer Institute and Hospital, National Clinical Research Center for Cancer, Tianjin, China

Introduction: Neuroblastoma (NB) is a common extracranial tumor in children and is highly heterogeneous. The factors influencing the prognosis of NB are not simple.

Methods: To investigate the effect of cell senescence on the prognosis of NB and tumor immune microenvironment, 498 samples of NB patients and 307 cellular senescence-related genes were used to construct a prediction signature.

Results: A signature based on six optimal candidate genes (TP53, IL-7, PDGFRA, S100B, DLL3, and TP63) was successfully constructed and proved to have good prognostic ability. Through verification, the signature had more advantages than the gene expression level alone in evaluating prognosis was found. Further T cell phenotype analysis displayed that exhausted phenotype PD-1 and senescence-related phenotype CD244 were highly expressed in CD8+ T cell in MYCN-amplified group with higher risk-score.

Conclusion: A signature constructed the six MYCN-amplified differential genes and aging-related genes can be used to predict the prognosis of NB better than using each high-risk gene individually and to evaluate immunosuppressed and aging tumor microenvironment.

KEYWORDS

neuroblastoma, cellular senescence, tumor microenvironment, COLD TUMOR, prognosis

Abbreviations: DLL3, delta-like 3; DEGs, differentially expressed genes; EFS, event-free survival; GEO, Gene Expression Omnibus; ICIs, immune checkpoint inhibitors; NB, neuroblastoma; mAbs, monoclonal antibodies; MHC-I, major histocompatibility complex I; OS, overall survival; SMs, senescence molecules; SASP, senescence-related secretory phenotype; TME, tumor microenvironment.

Introduction

Neuroblastoma (NB) is the most common pediatric solid tumor, but it poses a challenge in terms of treatment. Approximately half of the patients are diagnosed with high-risk NB and undergo intensive multimodal therapy, yet the 5-year overall survival (OS) rate remains below 20% (1). The occurrence and development of most tumors are closely related to the MYC gene family, and one of the well-known MYC genes is involved in proliferation, apoptosis, and differentiation are also associated with PD-L1 expression (2). MYCN, another member of the MYC gene family, is mainly involved in nervous system development and tumor formation (3). Prognosis in NB is known to be influenced by factors such as age, tumor cell differentiation, and MYCN amplification, but the MYCN gene itself is not easily targeted therapeutically (4). While tumor-specific monoclonal antibodies (mAbs) targeting GD2 have become a standard component of therapy for high-risk NB patients, the risk of relapse remains high. This highlights the potential for immunotherapeutic approaches to reduce the risk of recurrence (5).

Immune checkpoint inhibitors (ICIs) therapy, which enhances certain aspects of the immune system to recognize and eliminate tumor cells, has shown efficacy in several solid tumors but has limited curative effect in NB (6). In 2009, Camus et al. first classified tumors into "cold" and "hot" based on the distribution of immune cells, particularly T lymphocytes, and their differential responses to immunotherapy (7). NB is considered a good experimental model for studying immunotherapy resistance, as it is a cold tumor and presents an opportunity to investigate strategies to transform it into a hot tumor to improve the efficacy of immunotherapy (8). In our preliminary study, we observed that Anlotinib, an orally administered small-molecule multitarget tyrosine kinase inhibitor, induced a T cell inflamed tumor microenvironment (TME) by facilitating vessel normalization, thereby enhancing the efficacy of PD-1 checkpoint blockade in NB (9). Additionally, NB tumor cells have a low mutation load and lack major histocompatibility complex I (MHC-I) expression, which contributes to their low immunogenicity and prevents T cells from recognizing them (10). The bromodomain and extra-terminal domain (BET) protein family mediates T cell exhaustion and hinders proliferation and differentiation of NB cells (11, 12). However, the above description does not fully explain the immune escape mechanism of NB or provide a comprehensive understanding of the differential expression of multiple immunosuppressive receptors. Senescence was first described by Hayflick and Moorhead in 1961 based on observations of *in vitro* cultured human fibroblasts. It refers to the loss of proliferative potential in cells after a defined number of passages (13). Under normal circumstances, senescent cells undergo a permanent cell-cycle arrest but remain metabolically active in the G0 phase, with physiological implications for cellular metabolism. However, recent observations have shown that senescent cells can reprogram into a stem cell state and re-enter the cell cycle in tumor mice (14). When chemotherapy-induced senescence therapy is discontinued, tumor cells can exit the senescent state and even resume enhanced growth (15). Cellular senescence is a complex adaptive process that involves the expression of senescence-related secretory phenotype (SASP) and the release of cytokines and growth factors, contributing to tumor immune escape and progression (16). One crucial aspect of tumor immune escape and targeted cell cycle drug killing is that tumor cells enter the G0 phase by expressing a senescent phenotype to evade recognition and clearance by the immune system and chemotherapy drugs (17). Importantly, senescence-related genes are significantly associated with adverse clinical outcomes in various cancers, providing valuable insights for risk stratification and understanding the immunosuppressive tumor microenvironment (18, 19).

In this study, we investigated the effects of senescence gene combinations on outcomes and the immune microenvironment in NB by screening differential genes between MYCN-amplified and non-MYCN-amplified NB samples. Ultimately, we successfully constructed a prognosis prediction signature of NB based on six genes. Validation experiments revealed that the score calculated by this signature closely predicted prognosis compared to the relative expression of a single high-risk gene. Our findings were further validated using NB cell line and *in vitro* co-culture experiments. The results demonstrated that different tumor antigens influenced the distribution of T cell subsets, with the depletion phenotype PD-1 and cell senescence phenotype CD244 overexpressed in CD8+T cell subsets.

Methods

Data source

The gene expression profiles and clinical information from 498 primary NBs were obtained from the Gene Expression Omnibus (GEO) database, specifically the GSE49710 dataset, using RNA-Seq and microarrays. The GEO database can be accessed at https://www.ncbi.nlm.nih.gov/geo/. To investigate cellular senescence in NB, we utilized a list of 307 cellular senescence-related genes downloaded from the Cell-Age database. This database can be found at https://genomics.senescence.info/cells/. For external validation of our signature, we utilized the E-MTAB-8248 dataset from the ArrayExpress database. This dataset consists of 223 samples and can be accessed at https://www.ebi.ac.uk/biostudies/arrayexpress.

Building and verification of the signature

The 498 samples from the GSE49710 dataset were used for signature development, and samples from E-MTAB-8248 were used for model validation. Firstly, we identified 476 differentially expressed genes (DEGs) using the R package "limma". Then, we performed univariate Cox analysis to identify the intersection of differential genes and cellular senescence-related genes. Next, we analyzed the relationship between the selected overlapping genes and the prognosis of NB patients using Kaplan-Meier (K-M) survival statistics. To further screen the DEGs, we employed random forest analysis and least absolute shrinkage and selection operator (LASSO) regression analysis. Using mean decrease

accuracy and mean decrease gini coefficients, we identified the top six genes (TP53, IL-7, PDGFRA, S100B, DLL3, and TP63) with the highest coefficients. LASSO assigned regression coefficients to each gene and combined them into an algorithmic model. The predictive performance of the model was assessed using Kaplan-Meier analysis and the area under the curve (AUC) of the receiver operating characteristic (ROC) curve. The above processes were shown in Figure 1.

Analysis of immune microenvironment and tumor cell stemness

To assess the level of immune infiltration, we employed four algorithms: "Estimation of Stromal and Immune cells in Malignant Tumors using Expression data (ESTIMATE)" (20), "Cell-type Identification By Estimating Relative Subsets Of RNA Transcripts (CIBERSORT) (21) ", "Microenvironment Cell Populations-counter (MCP-Counter) (22)", and "xCell" (23). Then the correlation between the risk score and tumor cell stemness was analyzed. All the data analyzed in this study were obtained from the GSE49710 dataset.

Cell culture system *in vitro*

Peripheral blood mononuclear cells (PBMCs) were isolated using lymphocyte separation solution. First, the peripheral blood of volunteers was diluted 1:1 with PBS, and then the diluted blood was spread on 4ml lymphocyte separation solution and centrifuged for 15 minutes at 1500rpm. Then, the cells in the suspended particle layer were absorbed by a glue head dropper and transferred to a centrifuge tube equipped with PBS, mixed and cleaned, and centrifuged at 1000rpm for 10 minutes. The PBMCs were then plated in a petri dish at a concentration of 1x10^6 cells. The culture medium consisted of a mixture of 1640 and 10% fetal bovine serum at a ratio of 9:1. To activate the T cells, IL-2 (at a concentration of 1000u/mL) and CD3/CD28 antibodies were added to the cell culture as per the instructions provided. SK-N-BE (2) (MYCN-amplified) and SH-SY5Y (non-MYCN amplified) cell lines as different tumor antigens were selected. DMEM/F12 was used as a culture medium for cell lines, and 10% fetal bovine serum (FBS) and 1% Penicillin/Streptomycin were added, pre-heated to 37°C, and sterilized by filtration under sterile conditions. The cell suspensions are transferred to sterile cell culture vials, with enough medium added to each vial to make the cell density appropriate (usually 70-80% bottle surface coverage). The cell culture vial is placed in a cell incubator at 37°C to provide the appropriate temperature and CO2 concentration (5%) and the medium is changed every two to three days to maintain healthy cell growth. These cell lines were chosen to ensure that T cells could be fully exposed to the tumor antigens and evaluate the impact of the tumor microenvironment (TME) on T cell responses.

Real-time quantitative PCR

The sequence of primers associated with each gene for qPCR is provided in Supplemental Table 1 (submitted). SK-N-BE (2) cell lines and SH-SY5Y NB cell lines were amplified using conventional cell culture methods. Briefly, mRNA was extracted using a commercial kit (Total RNA Purification Kit, NORGEN) and quantified using the spectrophotometer (Thermo Fisher Scientific). The mRNA was reverse transcribed in cDNA using

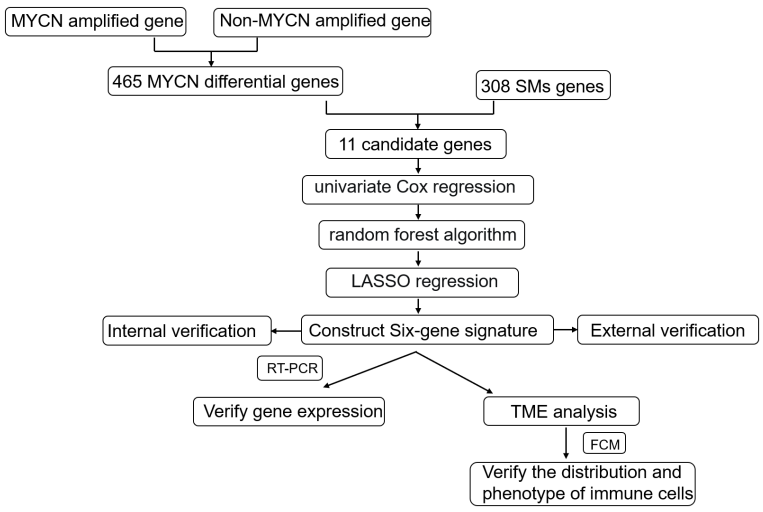

FIGURE 1
Schematic diagram of the study design. Gene expression and clinical information from 498 primary NBs were obtained from the GSE49710 dataset and internal verification through the same database;308 cellular senescence-related genes were obtained from the Cell-Age database; 223 sample data from the E-MTAB-8248 dataset were used for external validation. The internal verification included the relationship between 11 candidate genes and NB prognosis, the relationship between the constructed signature and NB prognosis, and the relationship between age, INSS stratification, clinical risk, and MYCN status; External validation focused on the relationship between signature and NB prognosis and the fit degree of prognosis prediction.

the High-Capacity RNA-to-cDNA™ Kit (Applied Biosystems™), and qPCR was carried out using SYBR green PCR master mix (Applied Biosystems™) in Bio-Rad CFX Manager.

Flow cytometry

To detect the proportional and phenotypic changes in T cell subsets, cell surface staining analysis was conducted using multi-colored fluorescent flow cytometry. The following antibodies were used: CD3-FITC (clone HTT3a), CD8-Cy5.5 (clone SK1), CD244 (2B4)-PE (clone C1.7), CD4-APC-H7 (clone RPA-T4), PD-1-PE-CY7 (clone A17188B), PE-CY7-isotype control (clone MPO-11). These antibodies were ordered from BD Biosciences (San Jose, USA) and Biolegend. First, PBMC after exposure to tumor antigen were centrifuged for standby staining. Then, fluorescent monoclonal antibodies were added to the cells and incubated in the dark at room temperature for 15-20 minutes. The samples were washed twice with 1x PBS to remove excess fluorescent antibodies and broken cell fragments. Fully viable cells were acquired for analysis using a BD FACS-CantoIIflow cytometer (BD Biosciences, San Jose, USA), and subsequent analysis was performed using Flowjo software (Flowjo LLC, USA). Prior to obtaining the target cells, dead and sticky cells were subsequently excluded using FSC-A/FSC-H.

Statistical methods

Statistical analysis and graphing were performed using the R software (version 4.2.1) and GraphPad Prism 8. To compare differences between two groups, we employed two-tailed unpaired Student's t-test and Wilcoxon test. The Fisher's exact test was used to compare differences in qualitative variables between the two groups. Statistical significance was defined as $P < 0.05$.

Results

Screened target associated with NB prognosis from MYCN amplified differential genes and senescence molecules (SMs) gene

MYCN amplification in NB patients has been identified as a poor prognostic factor (4). Therefore, it is crucial to first screen for MYCN-related differential genes. After downloading the GSE49710 dataset, we preprocessed the expression profile data and identified differentially expressed genes (DEGs). The volcano plot for the DEGs is presented separately in Figure 2A. 465 differential genes met the criteria for further analysis ($|\log2$ fold change (FC)$| > 1.5$ and adjusted p-value < 0.05). To identify the intersection between MYCN-amplified differential genes and 307 SMs genes, we identified eleven genes, as shown in Figure 2B. Subsequently, we included these eleven identified genes in the univariate Cox regression model to analyze their relationship with prognosis. The results demonstrated that all genes were significantly associated with poor OS in NB patients in the GSE49710 dataset, as depicted in Figure 2C (p-value < 0.001).

Construction of the six-gene signature

To further assess the significance of the 11 genes, we incorporated them into the random forest algorithm. As depicted in Figure 2D, we identified the top six genes (TP53, IL-7, PDGFRA, S100B, DLL3, and TP63) to proceed with the subsequent step of the LASSO regression model. The outcomes of the LASSO regression model, including the inclusion of the 6 genes, are presented in Figures 2E, F, with the corresponding coefficients assigned to each gene displayed in Figure 2E. The expression patterns and levels of these six genes are illustrated in Figures 3A, E. Based on the "lambda.min" coefficient shown in Figure 2F, all coefficients associated with the six genes are suitable for further analysis. The risk score was calculated using the following formula:

risk score = (0.506 * expression of PDGFRA) + (0.472 * expression of DLL3) + (0.390 * expression of TP53) - (0.598 * expression of S100B) - (0.363 * expression of IL7) - (0.360 * expression of TP63).

Internal verification of the signature

The predictive performance of the signature was assessed using Kaplan-Meier survival analysis and the AUC of the ROC curve. The results of the survival analysis demonstrated a close relationship between the six genes included in the model and the prognosis of NB patients, as shown in Figures 4A-C, E-G. This finding is consistent with the coefficient trend of the constructed model. Further analysis revealed that patients with low scores had significantly better prognosis in terms of OS or event-free survival (EFS), as depicted in Figures 4D, H. The results of the remaining five genes that were not included in the signature are displayed in Supplementary Figures 1A-E, respectively. The ROC curve exhibited a high AUC value (AUC=0.968), indicating that the signature possesses excellent predictive ability for OS and EFS (Figures 3B, C). During the internal validation process using the GSE49710 dataset, an interesting result emerged: regardless of the 3-year or 5-year EFS or OS, the signature we constructed appeared to have a better fit for predicting the prognosis of NB patients compared to evaluating the prognosis based on MYCN amplification (AUC values of 3 years and 5 years EFS: 0.718 vs. 0.620; 0.709 vs. 0.603, AUC values of 3 years and 5 years OS: 0.824 vs.0.769; 0.793 vs.0.692, respectively), as shown in Figures 3B, C, F, G). Another differential analysis revealed that among the 498 NB samples, the group with MYCN amplification had a higher risk score, as illustrated in Figure 3K ($P<0.0001$). This finding is consistent with the differential expression of each gene in the MYCN amplification and non-amplification groups included in the signature, as shown in Figure 2G ($P<0.0001$).

Next, we assessed the relationship between risk scores and age, INSS stages, tumor aggression, and clinical risk stratification. The

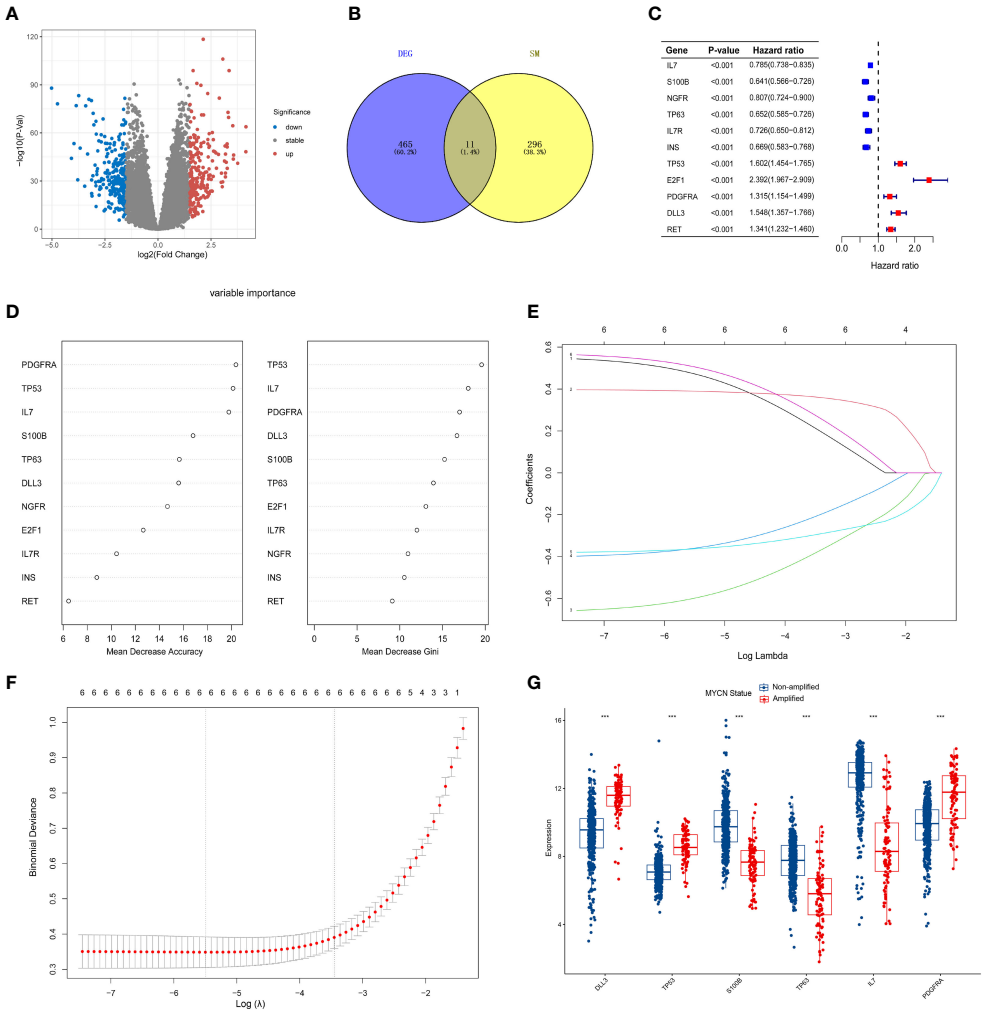

FIGURE 2
Screening of candidate genes and construction of signature **(A)** The volcano plot for differentially expressed genes (DEGs) (|log2FC| > 1.5 and adjusted $p < 0.05$), and the red, gray and blue circles indicate up- regulated, stable expressed and down-regulated of MYCN genes, respectively. **(B)** The blue regions represent 465 MYCN-amplified differential genes, while the yellow regions represent 308 SMs genes. **(C)** Forest diagram displaying the univariate Cox proportional hazard regression model for eleven genes and all candidate genes were associated with poor OS in GSE49710 datasets. **(D)** random forest algorithm results of 11 genes. **(E, F)** Results of LASSO regression analysis of the top six genes. **(G)** Differences between the MYCN amplified and non-amplified groups of six candidate genes and the risk-score signature constructed based on the candidate genes. ***p < 0.01.

results indicated that older NB patients had higher genetic ratings for aging ($p < 0.001$), as depicted in Figure 3D. The INSS classification, a commonly used prognostic assessment tool, revealed a higher aging gene score in INSS stage 4 groups compared to others ($p < 0.001$), as shown in Figure 3J. Detailed risk score comparison results are presented in Figure 3I. Additionally, clinical high risk and high aggression can be clearly distinguished based on the risk score ($p < 0.001$), as illustrated in Figures 3H, L.

External validation of the signature

To validate the signature, we utilized the E-MTAB-8248 dataset, which included 223 NB patients. Consistent with the findings from the GSE49710 dataset, the low score group in the E-MTAB-8248 dataset exhibited a significantly better prognosis in terms of OS and EFS compared to the high score group ($p < 0.001$), as shown in Figures 5A, B). Furthermore, our signature demonstrated superior predictive ability for the prognosis of NB patients compared to evaluating prognosis based on MYCN amplification alone, as evidenced by higher AUC values for 3-year and 5-year EFS (0.710 vs. 0.581; 0.698 vs. 0.576) and OS (0.813 vs. 0.581; 0.855 vs. 0.576), as shown in Figures 5C-F).

Positive correlation between risk score, tumor immune microenvironment, and stemness in NB

Gene set enrichment analysis using ESTIMATE effectively captured the presence of stroma in tumor tissue and analyzed

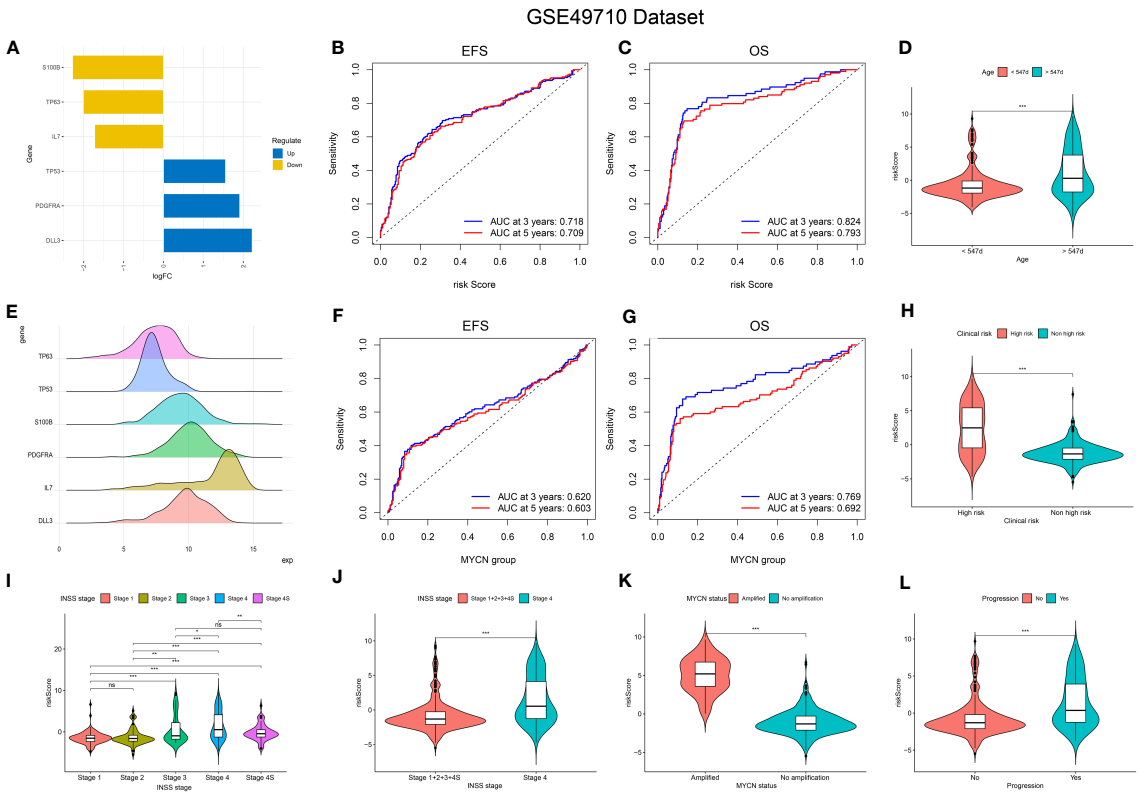

FIGURE 3
Relationship of signature with age, MYCN-status, clinical prognosis, and INSS grading. **(A, E)**, Expression trends and amounts of six genes included in the model; **(B, C, F, G)**: the ROC curve of the signature and MYCN status regarding EFS and OS; **(D, H, I-L)**, The relationship between risk-score and age, clinical prognosis stratification, INSS grading, MYCN status and disease aggressiveness were analyzed respectively. *p < 0.1; **p < 0.05; ***p < 0.01, respectively.

immune cell infiltration. Through advanced machine learning techniques, we observed that lower aging gene scores were associated with higher matrix proportion in tumor tissue (p < 0.001), increased immune cell infiltration (p < 0.001), and consequently, lower tumor cell purity (p < 0.001), as shown in Figure 6A). We further employed MCP (Microenvironment Cell Populations)-counter to conduct a detailed analysis of immune cell subpopulations in NB tissues. As depicted in Figure 6B), NB

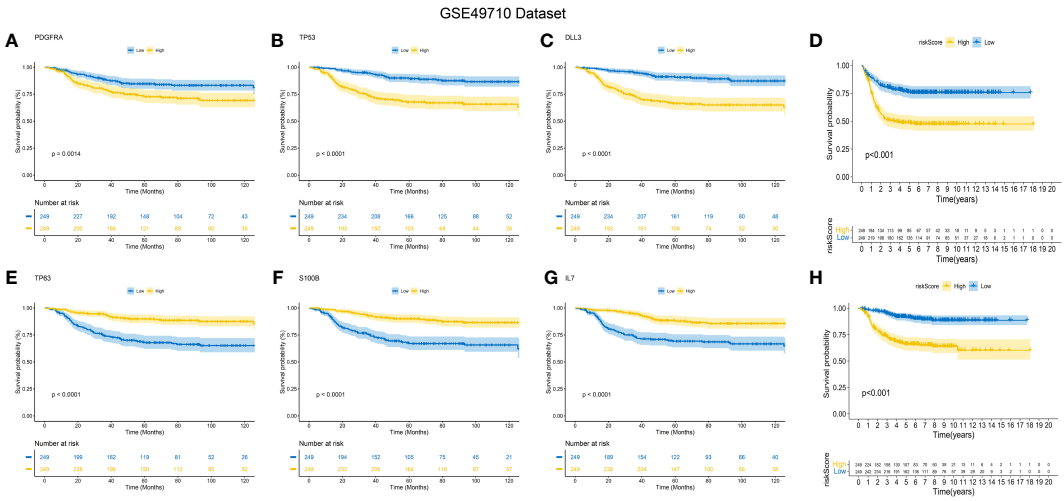

FIGURE 4
K-M Curve for Prognostic Prediction in NB. **(A-C, E-G)** Survival curves of the relationship between TP53, IL-7, PDGFRA, S100B, DLL3 and TP63 genes and the prognosis of NB patients, respectively. The blue curve indicates low gene expression, while the yellow curve indicates high gene expression. **(D, H)** are the survival curves of EFS and OS of NB patients in the dataset. Blue is the low-risk score, and red is the high-risk score.

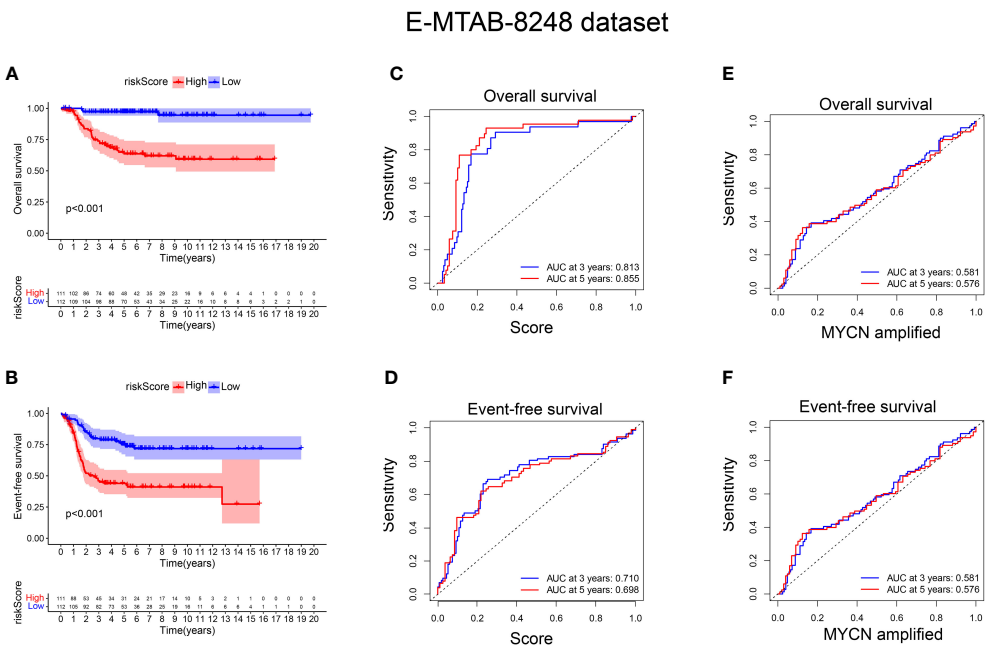

FIGURE 5
External verification of the relationship between risk score and prognosis of NB patients. **(A, B)** The OS and EFS curves of 223 NB patients were respectively presented, with the blue curve representing patients with low-risk score and the red curve representing patients with high-risk score; **(C, D)** ROC curve shows the value of risk score in evaluating OS and EFS; **(E, F)** ROC curve shows the value of MYCN status in evaluating OS and EFS.

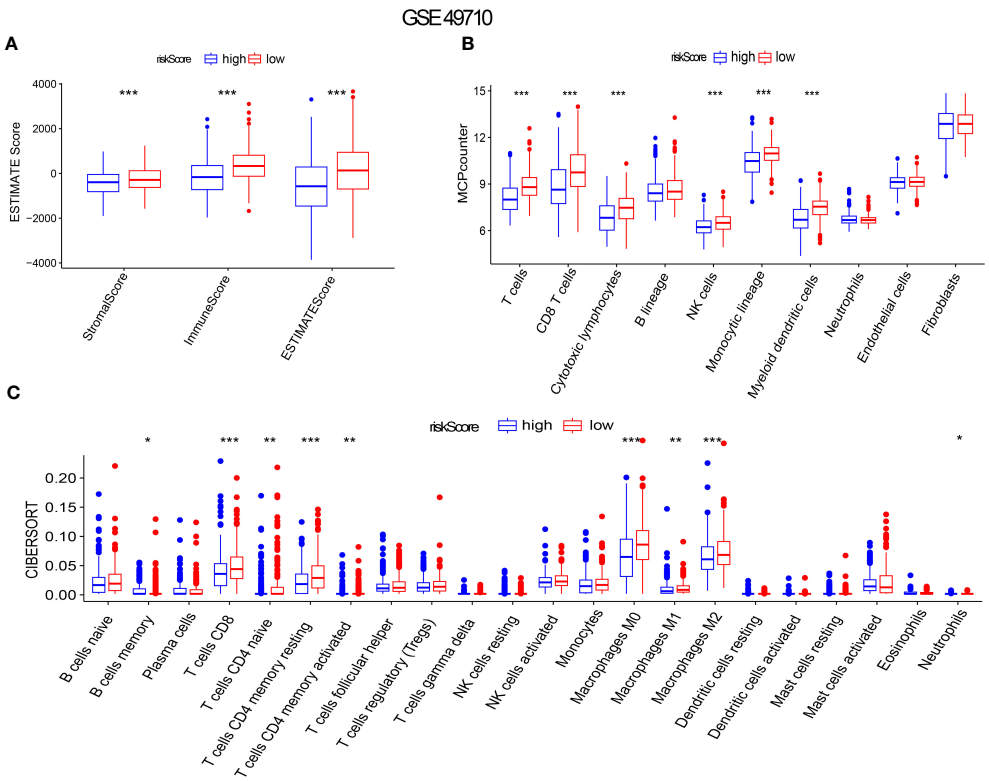

FIGURE 6
Aging gene score to evaluate immune infiltration in NB tumor microenvironment. **(A-C)** ESTIMATE Score, MICP-counter and CIBERSPORT were used to evaluate immune cell infiltration. The red box represents low-risk score group, while the blue box represents high-risk score group. *p < 0.1; **p < 0.05; ***p < 0.01, respectively.

patients with lower aging gene scores exhibited higher infiltration of T cells, NK cells, myeloid dendritic cells, and monocytes in tumor tissues, with T cells primarily consisting of CD8+ T cells (cytotoxic lymphocytes) ($p < 0.001$). Additionally, the CIBERSORT algorithm identified four highly infiltrated immune cell subpopulations, namely CD4 naïve T cells, CD4 memory resting T cells, CD4 memory activated T cells, and macrophages, in patients with low scores ($p < 0.01$, $p < 0.001$, $p < 0.01$, $p < 0.001$, respectively) (Figure 6C). Supplementary Figure 1G provides a more detailed analysis of immune cell subsets. Tumor cell stemness is closely associated with disease occurrence, drug resistance, recurrence, and metastasis. Correlation analysis revealed a significant positive correlation between aging gene score and tumor cell stemness ($R = 0.51$, $p < 0.001$) (Supplementary Figure 1F).

High aging-related prognostic scores are associated with T cell exhaustion and phenotypic changes related to aging

In order to initially validate the impact of our aging-related prognostic scoring system on major T cell subsets, we measured the relative expression levels of six target genes in two NB cell lines with different MYCN amplification, as depicted in Figures 7A–F. By applying normalization processing to our constructed model, we calculated the aging prognosis score. The results demonstrated that the SK-N-BE (2) group had a higher aging prognosis score compared to the SH-SY5Y group (risk score: -5.12 vs. -57.45). Next, we employed flow cytometry to assess changes in major T cell subpopulations and phenotypic alterations in PBMCs following contact with NB cells. The findings revealed that the proportion of CD4:CD8 T cells in PBMCs exposed to SK-N-BE (2) was higher than that in the SH-SY5Y group (1.29 vs. 0.85) (Figure 8). Further phenotypic analysis indicated that CD8+ T cells exposed to SK-N-BE (2) displayed a higher expression of the exhaustion phenotype marker PD-1, while CD4+ T cells exhibited a higher proportion of the aging phenotype marker CD244 (3.09% vs. 0.65%, 24.2% vs. 16.7%, respectively) (Figures 9A–D). Additionally, PBMCs exposed to SK-N-BE (2) showed a higher proportion of the CD244+PD-1 +CD8+ T cell subset (3.36% vs. 1.67%) (Figures 8A–H).

Discussion

NB is the most common extracranial tumor in children, and there is currently no standardized prognostic evaluation system, which due to NB is a highly heterogeneous tumor (5, 10). Despite the utilization of genetic testing techniques in clinical practice, only a

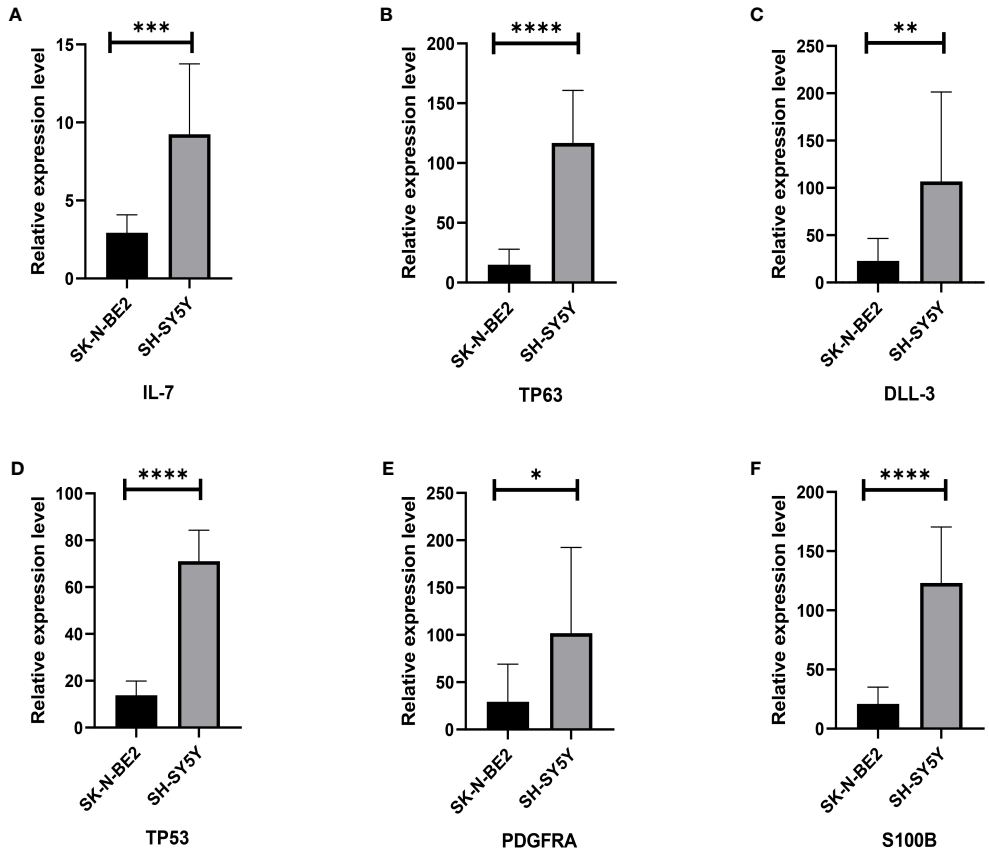

FIGURE 7
Relative gene expression of 6 included genes A: The **(A–F)** shows qRT-PCR results of IL-7, TP63, DLL3, TP53, PDGFRA and S100B genes in two neuroblastoma cell lines, SH-SY5Y and SK-N-BE (2), respectively. The black column represents the relative expression of gene in SH-SY5Y, and the gray column represents the relative expression of gene in SK-N-BE (2). *p < 0.1; **p < 0.05; ***p < 0.01; ****p < 0.001, respectively.

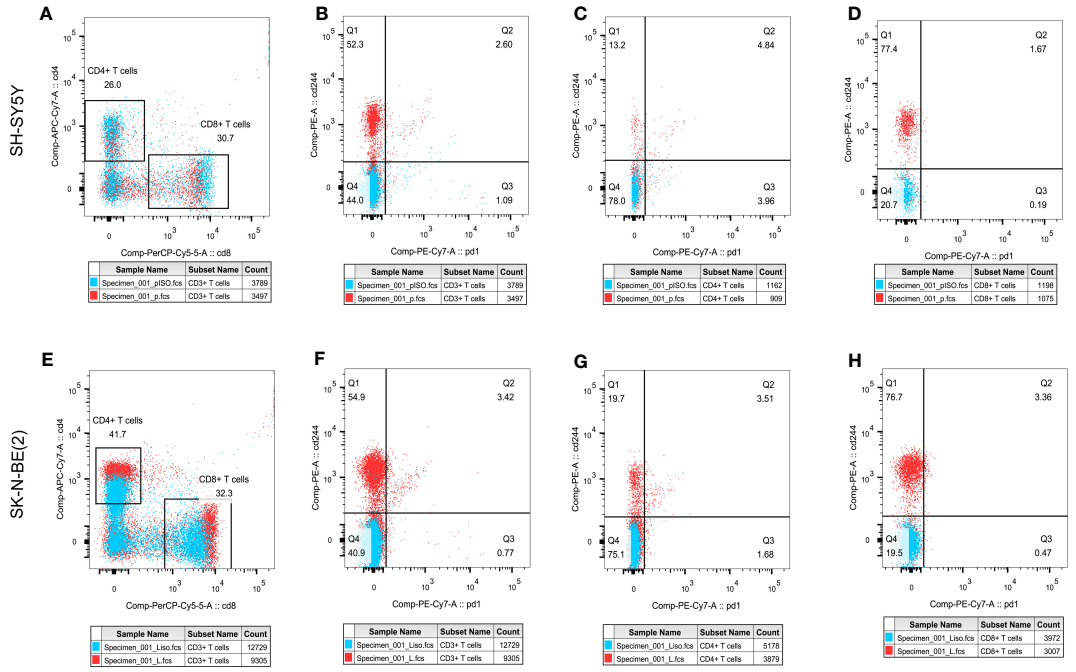

FIGURE 8
T cell subpopulation distribution and phenotypic changesThe effect of different antigen stimulation on the distribution of T cell subsets and the co-expression of PD-1 and CD244 in different T cell subsets were shown. **(A, E)** show the proportion of CD4+T cell distribution and CD8+T cell distribution after stimulation by SH-SY5Y and SK-N-BE(2), respectively. **(B–D)** reflects the co-expression of CD244 and PD-1 in CD3+, CD4+ and CD8+T cell subsets after SH-SY5Y stimulation. **(F–H)** reflects the co-expression of CD244 and PD-1 in CD3+, CD4+ and CD8+T cell subsets after SK-N-BE(2) stimulation, respectively.

limited number of genes have established prognostic value in NB (24, 25). It is still unclear why some patients experience poor clinical outcomes despite the absence of commonly detected high-risk genes, while others exhibit positive clinical outcomes despite the presence of individual high-risk gene expression. This discrepancy suggests that there are additional factors beyond the currently recognized high-risk genes that influence the prognosis of NB (25, 26). Redefining the prognostic model of NB based on the expression levels of high-risk genes combined with other mechanisms that may impact prognosis holds significant value. This will ultimately enhance clinical decision-making and optimize patient outcomes.

On the other hand, Prognostic evaluation needs to consider the increasing use of immunotherapy over the past decade, which has been altering the tumor's prognosis (1, 4). In this study, we constructed six gene composition evaluation models, specifically targeting TP53, PDGFRA, S100B and TP63. These genes are widely recognized as important prognostic indicators in clinical testing and offer the advantages of universality and easy accessibility compared to other pathway models (27–30).

Since the initial description of senescence by Hayflick and Moorhead, our understanding of senescence has continuously evolved (31). The traditional classical theory defines senescence as a state where cells enter permanent cycle arrest while remaining metabolically active in the G0 phase. However, recent studies have challenged this notion and demonstrated that senescence is not necessarily an irreversible state (31). Cells that enter quiescence can still re-enter the replication cycle under certain growth conditions (32, 33). A mouse model study on lymphoma has suggested that senescent cells can be reprogrammed to possess stem cell properties and may re-enter the cell cycle when specific conditions are restored (14). This concept aligns with the definition of tumor cell stemness, which is strongly associated with tumor recurrence and metastasis (14). Our study also found a positive correlation between high senescence scores and tumor cell stemness. Additionally, senescent cells secrete various bioactive cytokines known as SASP (34). SASP may contribute to shaping the immunosuppressive TME, by inducing immune cells to express high senescence phenotype, such as CD244, and exhausted phenotype like PD-1, TIM-3, et al, aiding tumor cell immune escape (11, 35–38). It is important to highlight that senescent tumor cells, upon entering the G0 stage, have the ability to evade the cytotoxic effects of traditional chemotherapy drugs that primarily target actively dividing cells (14). This allows the senescent cells to maintain their survival and potentially contribute to disease progression (14). Considering these findings, it becomes crucial to explore the link between cellular senescence and the inefficacy of immunotherapy in NB.

In a study, cell senescence as an important feature was found in NB samples with MYCN amplification, which is associated with poor prognosis (39). This part of the results aligns with our findings, which indicate a significant difference in the aging score between samples with different MYCN status. Furthermore, we observed a strong correlation between the aging score and prognosis. These findings support the notion that the aging process plays a crucial role in NB progression and can serve as a prognostic indicator (14, 17). The association between MYCN status and aging score suggests that MYCN amplification may contribute to accelerated aging processes

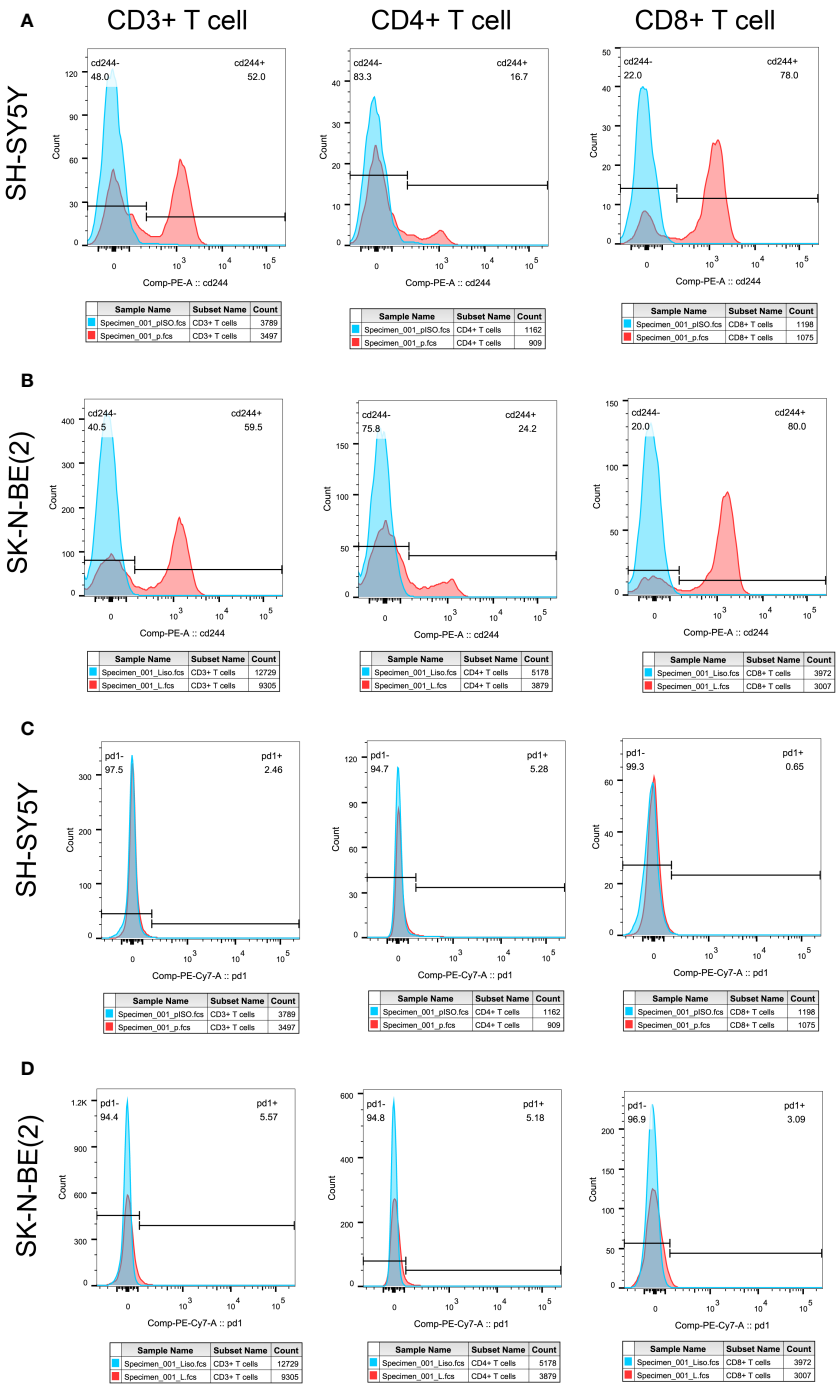

FIGURE 9
Tumor antigens on T cell exhausted molecules and aging phenotypesT cell exhaustion was shown by the expression ratio of PD-1 molecule, while CD244 was used as the phenotype of T cell senescence. Differential expression of PD-1 and CD244 in CD3+, CD4+ and CD8+T cells were shown. **(A, C)** showed the separate expression of CD244 and PD-1 in CD3+, CD4+, and CD8+T cell subsets after SH-SY5Y stimulation, respectively. **(B, D)** showed the separate expression of CD244 and PD-1 in CD3+, CD4+, and CD8+T cell subsets after SK-N-BE(2) stimulation, respectively. The blue crest comes from the Isotype control, the red crest comes from the fully dyed sample, and all the gates are set according to the Isotype control.

in NB cells (40). This could potentially explain the aggressive behavior and poor prognosis associated with MYCN-amplified tumors. Further investigations are warranted to elucidate the underlying mechanisms linking MYCN amplification, aging, and prognosis in NB.

In our subsequent analysis, we focused on examining the correlation between the model constructed based on the six aging-related genes and the prognosis of NB patients. We conducted a comparison of the relative expression levels of six genes in two groups of cell lines with and without MYCN amplification (41). Interestingly, we observed that the relative expression levels of these six high-risk genes were lower in SK-N-BE(2) cells, which are derived from patients with bone marrow metastasis and accompanied by MYCN

amplification (41), compared to SH-SY5Y cell lines. This finding is consistent with the clinical observation of lower high-risk gene expression but poor prognosis. On the contrary, using the predictive mode, the SK-N-BE (2) score is indeed much higher than the SH-SY5Y score. This also reflects the fact that our model seems to predict prognosis more accurately and closely to clinical development than analyzing the relative expression of each gene alone. However, further validation with additional clinical data is necessary to confirm these results. It is worth noting that the higher the clinical prognostic stratification of high-risk NB, as indicated by INSS grading, the higher the calculated senescence score in the subgroup with MYCN amplification, shown in Figure 3.

Studies on the TME have demonstrated that the formation of an immunosuppressive TME contributes to the poor prognosis of NB patients and the limited effectiveness of immunotherapy (42, 43). In a previous study conducted by our group, we successfully reconstructed normal blood vessels in a mouse model of NB using a multi-target tyrosine kinase inhibitor (TKI) called Anlotinib (9). This approach maximized the efficacy of immunotherapy when combined with a PD-1 inhibitor, highlighting the crucial role of the TME in immunotherapy (9). NB has been recognized as an excellent model for studying cold tumors, making the analysis of immune cell infiltration within NB tumor tissues vital for understanding the TME (44). By analyzing the composition of tumor tissues in different senescence score subgroups, we observed that high-scoring NB tumor tissues exhibited lower immune scores and stromal scores, indicating a lower percentage of immune cells. Further subpopulation analysis revealed significantly reduced infiltration of CD8+ T cells, NK cells, myeloid dendritic cells, monocytes, and macrophages in high-scoring NB tissues. These findings are consistent with studies that decreased immune cell infiltration in the TME of NB patients with poor prognosis and ineffective immunotherapy (45, 46). CD244 (2B4) binding to the ligand CD48 has been found to be a signaling pathway for co-stimulation or negative regulation of multiple immune cells in tumor, that currently considered to be an important marker of immune cell senescence (47, 48). CD244+ CD8+ aging T cells exhibited features of exhaustion, including lower levels of cytokine, impaired proliferation, and intrinsic transcriptional regulation (49). Phenotype analysis showed that the proportion of CD8+ T cells did not increase after PBMC exposure to SK-N-BE (2) tumor antigen as it did after exposure to SH-SY5Y tumor antigen. What's even more interesting is that CD8+ T cells exposed to SK-N-BE (2) displayed a higher expression of the exhaustion phenotype marker PD-1, while CD4+ T cells exhibited a higher proportion of the aging phenotype marker CD244 were found. Additionally, PBMCs exposed to SK-N-BE (2) showed a higher proportion of the CD244+PD-1+CD8+ T cell subset. The increase in the proportion of CD244+PD-1+ T cells was found in acute myeloid leukemia and non-Hodgkin's lymphoma significantly, that may be related to the occurrence and development of tumor (50–52). This indicate that CD8+ T cells exposed to SK-N-BE (2) antigen may enter a state of functional exhaustion and cellular senescence.

However, it is important to acknowledge the limitations of our study. Firstly, considering the addition of cytokines and cell-activating antibodies in our experiments, we did not specifically measure cytokine levels. To address this limitation, we plan to use plasma samples from NB patients in future experiments to investigate the SASP. Additionally, the operability and prognostic value of this model should be verified through extensive clinical practice. By addressing these limitations and conducting additional research, we aim to strengthen the validity and applicability of our findings. Ultimately, our goal is to contribute to the advancement of NB prognosis prediction and guide personalized treatment strategies for improved patient outcomes.

Conclusion

In summary, this study focused on identifying MYCN-related differential genes and senescence molecules in NB patients. The researchers constructed a six-gene signature and validated its predictive ability for the prognosis of NB patients. The signature was also found to be associated with the tumor immune microenvironment and stemness in NB.

Data availability statement

The datasets presented in this study can be found in online repositories. The names of the repository/repositories and accession number(s) can be found in the article/Supplementary Material.

Ethics statement

Ethical approval was not required for the studies on animals in accordance with the local legislation and institutional requirements because only commercially available established cell lines were used.

Author contributions

JT: Data curation, Formal Analysis, Methodology, Validation, Writing – original draft, Writing – review & editing. CW: Data curation, Software, Writing – review & editing. YJ: Conceptualization, Formal Analysis, Writing – review & editing. YX: Funding acquisition, Writing – review & editing. BG: Investigation, Software, Writing – review & editing. QZ: Formal Analysis, Funding acquisition, Supervision, Writing – review & editing.

Funding

The author(s) declare financial support was received for the research, authorship, and/or publication of this article. This study was supported by Tianjin Health Science and Technology Project

(No.TJWJ2022QN105), National Key R&D Program of China (No. 2018YFC1313000) and Tianjin Key Medical Discipline (Specialty) Construction Project (TJYXZDXK-009A).

Conflict of interest

The authors declare that the research was conducted in the absence of any commercial or financial relationships that could be construed as a potential conflict of interest.

Publisher's note

All claims expressed in this article are solely those of the authors and do not necessarily represent those of their affiliated organizations, or those of the publisher, the editors and the reviewers. Any product that may be evaluated in this article, or claim that may be made by its manufacturer, is not guaranteed or endorsed by the publisher.

Supplementary material

The Supplementary Material for this article can be found online at: https://www.frontiersin.org/articles/10.3389/fimmu.2023.1309138/full#supplementary-material

SUPPLEMENTARY FIGURE 1

The relationship between aging genes and prognosis, tumor cell stemness and immune invasion. **(A-E)** The remaining five genes that were not included in the signature was associated with poor OS in GSE49710 datasets. **(F)** Correlation analysis between risk score and the stemness of NB tumor cell. **(G)** xCell method was used to analyze the relationship between risk score and immune cell infiltration in NB tumor tissue. *p < 0.1; **p < 0.05; ***p < 0.01; ****p < 0.001, respectively.

References

1. Anderson J, Majzner RG, Sondel PM. Immunotherapy of neuroblastoma: facts and hopes. *Clin Cancer Res* (2022) 28(15):3196–206. doi: 10.1158/1078-0432.CCR-21-1356

2. Liu Z, Yu X, Xu L, Li Y, Zeng C. Current insight into the regulation of PD-L1 in cancer. *Exp Hematol Oncol* (2022) 11(1):44. doi: 10.1186/s40164-022-00297-8

3. Alborzinia H, Florez AF, Kreth S, Bruckner LM, Yildiz U, Gartlgruber M, et al. MYCN mediates cysteine addiction and sensitizes neuroblastoma to ferroptosis. *Nat Cancer* (2022) 3(4):471–85. doi: 10.1038/s43018-022-00355-4

4. Zafar A, Wang W, Liu G, Wang X, Xian W, McKeon F, et al. Molecular targeting therapies for neuroblastoma: Progress and challenges. *Medicinal Res Rev* (2021) 41 (2):961–1021. doi: 10.1002/med.21750

5. Croteau N, Nuchtern J, LaQuaglia MP. Management of neuroblastoma in pediatric patients. *Surg Oncol Clinics North America* (2021) 30(2):291–304. doi: 10.1016/j.soc.2020.11.010

6. Wagner LM, Adams VR. Targeting the PD-1 pathway in pediatric solid tumors and brain tumors. *OncoTargets Ther* (2017) 10:2097–106. doi: 10.2147/OTT.S124008

7. Camus M, Tosolini M, Mlecnik B, Pages F, Kirilovsky A, Berger A, et al. Coordination of intratumoral immune reaction and human colorectal cancer recurrence. *Cancer Res* (2009) 69(6):2685–93. doi: 10.1158/0008-5472.CAN-08-2654

8. El-Hajjar M, Gerhardt L, Hong MMY, Krishnamoorthy M, Figueredo R, Zheng X, et al. Inducing mismatch repair deficiency sensitizes immune-cold neuroblastoma to anti-CTLA4 and generates broad anti-tumor immune memory. *Mol Ther J Am Soc Gene Ther* (2023) 31(2):535–51. doi: 10.1016/j.ymthe.2022.08.025

9. Su Y, Luo B, Lu Y, Wang D, Yan J, Zheng J, et al. Anlotinib induces a T cell-inflamed tumor microenvironment by facilitating vessel normalization and enhances the efficacy of PD-1 checkpoint blockade in neuroblastoma. *Clin Cancer Res* (2022) 28 (4):793–809. doi: 10.1158/1078-0432.CCR-21-2241

10. Wienke J, Dierselhuis MP, Tytgat GAM, Kunkele A, Nierkens S, Molenaar JJ. The immune landscape of neuroblastoma: Challenges and opportunities for novel therapeutic strategies in pediatric oncology. *Eur J Cancer* (2021) 144:123–50. doi: 10.1016/j.ejca.2020.11.014

11. Zhong M, Gao R, Zhao R, Huang Y, Chen C, Li K, et al. BET bromodomain inhibition rescues PD-1-mediated T-cell exhaustion in acute myeloid leukemia. *Cell Death Dis* (2022) 13(8):671. doi: 10.1038/s41419-022-05123-x

12. Alleboina S, Aljouda N, Miller M, Freeman KW. Therapeutically targeting oncogenic CRCs facilitates induced differentiation of NB by RA and the BET bromodomain inhibitor. *Mol Ther oncolytics* (2021) 23:181–91. doi: 10.1016/j.omto.2021.09.004

13. Hayflick L, Moorhead PS. The serial cultivation of human diploid cell strains. *Exp Cell Res* (1961) 25:585–621. doi: 10.1016/0014-4827(61)90192-6

14. Milanovic M, Fan DNY, Belenki D, Dabritz JHM, Zhao Z, Yu Y, et al. Senescence-associated reprogramming promotes cancer stemness. *Nature* (2018) 553 (7686):96–100. doi: 10.1038/nature25167

15. Saleh T, Tyutyunyk-Massey L, Murray GF, Alotaibi MR, Kawale AS, Elsayed Z, et al. Tumor cell escape from therapy-induced senescence. *Biochem Pharmacol* (2019) 162:202–12. doi: 10.1016/j.bcp.2018.12.013

16. Wiley CD, Velarde MC, Lecot P, Liu S, Sarnoski EA, Freund A, et al. Mitochondrial dysfunction induces senescence with a distinct secretory phenotype. *Cell Metab* (2016) 23(2):303–14. doi: 10.1016/j.cmet.2015.11.011

17. Sager R. Senescence as a mode of tumor suppression. *Environ Health Perspect* (1991) 93:59–62. doi: 10.1289/ehp.919359

18. Lin W, Wang X, Wang Z, Shao F, Yang Y, Cao Z, et al. Comprehensive analysis uncovers prognostic and immunogenic characteristics of cellular senescence for lung adenocarcinoma. *Front Cell Dev Biol* (2021) 9:780461. doi: 10.3389/fcell.2021.780461

19. Tubita A, Lombardi Z, Tusa I, Lazzeretti A, Sgrignani G, Papini D, et al. Inhibition of ERK5 Elicits Cellular Senescence in Melanoma via the Cyclin-Dependent Kinase Inhibitor p21. *Cancer Res* (2022) 82(3):447–57. doi: 10.1158/0008-5472.CAN-21-0993

20. Yoshihara K, Shahmoradgoli M, Martinez E, Vegesna R, Kim H, Torres-Garcia W, et al. Inferring tumour purity and stromal and immune cell admixture from expression data. *Nat Commun* (2013) 4:2612. doi: 10.1038/ncomms3612

21. Newman AM, Liu CL, Green MR, Gentles AJ, Feng W, Xu Y, et al. Robust enumeration of cell subsets from tissue expression profiles. *Nat Methods* (2015) 12 (5):453–7. doi: 10.1038/nmeth.3337

22. Becht E, Giraldo NA, Lacroix L, Buttard B, Elarouci N, Petitprez F, et al. Estimating the population abundance of tissue-infiltrating immune and stromal cell populations using gene expression. *Genome Biol* (2016) 17(1):218. doi: 10.1186/s13059-016-1070-5

23. Aran D, Hu Z, Butte AJ. xCell: digitally portraying the tissue cellular heterogeneity landscape. *Genome Biol* (2017) 18(1):220. doi: 10.1186/s13059-017-1349-1

24. Tian XM, Xiang B, Yu YH, Li Q, Zhang ZX, Zhanghuang C, et al. A novel cuproptosis-related subtypes and gene signature associates with immunophenotype and predicts prognosis accurately in neuroblastoma. *Front Immunol* (2022) 13:999849. doi: 10.3389/fimmu.2022.999849

25. Fetahu IS, Taschner-Mandl S. Neuroblastoma and the epigenome. *Cancer metastasis Rev* (2021) 40(1):173–89. doi: 10.1007/s10555-020-09946-y

26. Chen G, Luo D, Zhong N, Li D, Zheng J, Liao H, et al. GPC2 is a potential diagnostic, immunological, and prognostic biomarker in pan-cancer. *Front Immunol* (2022) 13:857308. doi: 10.3389/fimmu.2022.857308

27. Wang H, Wang X, Xu L, Zhang J. TP53 and TP53-associated genes are correlated with the prognosis of paediatric neuroblastoma. *BMC genomic Data* (2022) 23(1):41. doi: 10.1186/s12863-022-01059-5

28. Mei Y, Wang Z, Zhang L, Zhang Y, Li X, Liu H, et al. Regulation of neuroblastoma differentiation by forkhead transcription factors FOXO1/3/4 through the receptor tyrosine kinase PDGFRA. *Proc Natl Acad Sci USA* (2012) 109(13):4898–903. doi: 10.1073/pnas.1119535109

29. Bernardini C, Lattanzi W, Businaro R, Leone S, Corvino V, Sorci G, et al. Transcritpional effects of S100B on neuroblastoma cells: perturbation of cholesterol homeostasis and interference on the cell cycle. *Gene Expression* (2010) 14(6):345–59. doi: 10.3727/105221610X12718619643013

30. Levrero M, De Laurenzi V, Costanzo A, Gong J, Wang JY, Melino G. The p53/p63/p73 family of transcription factors: overlapping and distinct functions. *J Cell Sci* (2000) 113(Pt 10):1661–70. doi: 10.1242/jcs.113.10.1661

31. de Magalhaes JP, Passos JF. Stress, cell senescence and organismal ageing. *Mech Ageing Dev* (2018) 170:2–9. doi: 10.1016/j.mad.2017.07.001

32. Foster DA, Yellen P, Xu L, Saqcena M. Regulation of G1 cell cycle progression: distinguishing the restriction point from a nutrient-sensing cell growth checkpoint(s). *Genes Cancer* (2010) 1(11):1124–31. doi: 10.1177/1947601910392989

33. Liu J, Wang L, Wang Z, Liu JP. Roles of telomere biology in cell senescence, replicative and chronological ageing. *Cells* (2019) 8(1):54. doi: 10.3390/cells8010054

34. Birch J, Gil J. Senescence and the SASP: many therapeutic avenues. *Genes Dev* (2020) 34(23-24):1565–76. doi: 10.1101/gad.343129.120

35. Giroud J, Bouriez I, Paulus H, Pourtier A, Debacq-Chainiaux F, Pluquet O. Exploring the communication of the SASP: dynamic, interactive, and adaptive effects on the microenvironment. *Int J Mol Sci* (2023) 24(13):10788. doi: 10.3390/ijms241310788

36. Mabrouk N, Ghione S, Laurens V, Plenchette S, Bettaieb A, Paul C. Senescence and cancer: role of nitric oxide (NO) in SASP. *Cancers* (2020) 12(5):1145. doi: 10.3390/cancers12051145

37. Takasugi M, Yoshida Y, Ohtani N. Cellular senescence and the tumour microenvironment. *Mol Oncol* (2022) 16(18):3333–51. doi: 10.1002/1878-0261.13268

38. Agresta L, Hoebe KHN, Janssen EM. The emerging role of CD244 signaling in immune cells of the tumor microenvironment. *Front Immunol* (2018) 9:2809. doi: 10.3389/fimmu.2018.02809

39. Ackermann S, Cartolano M, Hero B, Welte A, Kahlert Y, Roderwieser A, et al. A mechanistic classification of clinical phenotypes in neuroblastoma. *Science* (2018) 362 (6419):1165–70. doi: 10.1126/science.aat6768

40. Matthay KK, Maris JM, Schleiermacher G, Nakagawara A, Mackall CL, Diller L, et al. Neuroblastoma. *Nat Rev Dis Primers* (2016) 2:16078. doi: 10.1038/nrdp.2016.78

41. Hossain MM, Banik NL, Ray SK. Survivin knockdown increased anti-cancer effects of (-)-epigallocatechin-3-gallate in human Malignant neuroblastoma SK-N-BE2 and SH-SY5Y cells. *Exp Cell Res* (2012) 318(13):1597–610. doi: 10.1016/j.yexcr.2012.03.033

42. Sha YL, Liu Y, Yang JX, Wang YY, Gong BC, Jin Y, et al. B3GALT4 remodels the tumor microenvironment through GD2-mediated lipid raft formation and the c-met/AKT/mTOR/IRF-1 axis in neuroblastoma. *J Exp Clin Cancer Res CR* (2022) 41(1):314. doi: 10.1186/s13046-022-02523-x

43. Rivera Z, Escutia C, Madonna MB, Gupta KH. Biological insight and recent advancement in the treatment of neuroblastoma. *Int J Mol Sci* (2023) 24(10):8470. doi: 10.3390/ijms24108470

44. Voeller J, Erbe AK, Slowinski J, Rasmussen K, Carlson PM, Hoefges A, et al. Combined innate and adaptive immunotherapy overcomes resistance of immunologically cold syngeneic murine neuroblastoma to checkpoint inhibition. *J immunotherapy Cancer* (2019) 7(1):344. doi: 10.1186/s40425-019-0823-6

45. Sherif S, Roelands J, Mifsud W, Ahmed EI, Raynaud CM, Rinchai D, et al. The immune landscape of solid pediatric tumors. *J Exp Clin Cancer Res CR* (2022) 41 (1):199. doi: 10.1186/s13046-022-02397-z

46. Vanichapol T, Chutipongtanate S, Anurathapan U, Hongeng S. Immune escape mechanisms and future prospects for immunotherapy in neuroblastoma. *BioMed Res Int* (2018) 2018:1812535. doi: 10.1155/2018/1812535

47. Sun L, Gang X, Li Z, Zhao X, Zhou T, Zhang S, et al. Advances in understanding the roles of CD244 (SLAMF4) in immune regulation and associated diseases. *Front Immunol* (2021) 12:648182. doi: 10.3389/fimmu.2021.648182

48. Pita-Lopez ML, Gayoso I, DelaRosa O, Casado JG, Alonso C, Munoz-Gomariz E, et al. Effect of ageing on CMV-specific CD8 T cells from CMV seropositive healthy donors. *Immun Ageing I A* (2009) 6:11. doi: 10.1186/1742-4933-6-11

49. Wang X, Wang D, Du J, Wei Y, Song R, Wang B, et al. High levels of CD244 rather than CD160 associate with CD8(+) T-cell aging. *Front Immunol* (2022) 13:853522. doi: 10.3389/fimmu.2022.853522

50. Tan J, Yu Z, Huang J, Chen Y, Huang S, Yao D, et al. Increased PD-1+Tim-3+ exhausted T cells in bone marrow may influence the clinical outcome of patients with AML. *biomark Res* (2020) 8:6. doi: 10.1186/s40364-020-0185-8

51. Huang S, Liang C, Zhao Y, Deng T, Tan J, Zha X, et al. Increased TOX expression concurrent with PD-1, Tim-3, and CD244 expression in T cells from patients with acute myeloid leukemia. *Cytometry Part B Clin cytometry* (2022) 102(2):143–52. doi: 10.1002/cyto.b.22049

52. Huang S, Liang C, Zhao Y, Deng T, Tan J, Lu Y, et al. Increased TOX expression concurrent with PD-1, Tim-3, and CD244 in T cells from patients with non-Hodgkin lymphoma. *Asia-Pacific J Clin Oncol* (2022) 18(1):143–9. doi: 10.1111/ajco.13545

frontiers | Frontiers in Immunology

TYPE Original Research
PUBLISHED 20 December 2023
DOI 10.3389/fimmu.2023.1326927

OPEN ACCESS

EDITED BY
Gulderen Yanikkaya Demirel,
Yeditepe University, Türkiye

REVIEWED BY
Dafne Müller,
University of Stuttgart, Germany
Karine Rachel Prudent Breckpot,
Vrije University Brussels, Belgium

*CORRESPONDENCE
John K. Cini
johncini@sonnetbio.com

RECEIVED 24 October 2023
ACCEPTED 05 December 2023
PUBLISHED 20 December 2023

CITATION
Cini JK, Dexter S, Rezac DJ, McAndrew SJ, Hedou G, Brody R, Eraslan R-N, Kenney RT and Mohan P (2023) SON-1210 - a novel bifunctional IL-12 / IL-15 fusion protein that improves cytokine half-life, targets tumors, and enhances therapeutic efficacy. *Front. Immunol.* 14:1326927. doi: 10.3389/fimmu.2023.1326927

SON-1210 - a novel bifunctional IL-12 / IL-15 fusion protein that improves cytokine half-life, targets tumors, and enhances therapeutic efficacy

John K. Cini[1]*, Susan Dexter[1], Darrel J. Rezac[2], Stephen J. McAndrew[1], Gael Hedou[3], Rich Brody[4], Rukiye-Nazan Eraslan[5], Richard T. Kenney[1] and Pankaj Mohan[1]

[1]Sonnet BioTherapeutics, Inc., Princeton, NJ, United States, [2]Latham Biopharm Group, Inc., Elkridge, MD, United States, [3]Sonnet BioTherapeutics, CH S.A., Geneva, GE, Switzerland, [4]InfinixBio, Inc., Athens, OH, United States, [5]Invivotek, LLC., Hamilton, NJ, United States

Background: The potential synergy between interleukin-12 (IL-12) and IL-15 holds promise for more effective solid tumor immunotherapy. Nevertheless, previous clinical trials involving therapeutic cytokines have encountered obstacles such as short pharmacokinetics, limited tumor microenvironment (TME) targeting, and substantial systemic toxicity.

Methods: To address these challenges, we fused single-chain human IL-12 and native human IL-15 in *cis* onto a fully human albumin binding (F_HAB) domain single-chain antibody fragment (scFv). This novel fusion protein, IL12-F_HAB-IL15 (SON-1210), is anticipated to amplify the therapeutic impact of interleukins and combination immunotherapies in human TME. The molecule was studied *in vitro* and in animal models to assess its pharmacokinetics, potency, functional characteristics, safety, immune response, and efficacy.

Results: SON-1210 demonstrated robust binding affinity to albumin and exhibited the anticipated *in vitro* activity and tumor model efficacy that might be expected based on decades of research on native IL-12 and IL-15. Notably, in the B16F10 melanoma model (a non-immunogenic, relatively "cold" tumor), the murine counterpart of the construct, which had mouse (m) and human (h) cytokine sequences for the respective payloads (mIL12-F_HAB-hIL15), outperformed equimolar doses of the co-administered native cytokines in a dose-dependent manner. A single dose caused a marked reduction in tumor growth that was concomitant with increased IFNγ levels; increased Th1, CTL, and activated NK cells; a shift in macrophages from the M2 to M1 phenotype; and a reduction in Treg cells. In addition, a repeat-dose non-human primate (NHP) toxicology study displayed excellent tolerability up to 62.5 μg/kg of SON-1210 administered three times, which was accompanied by the anticipated increases in IFNγ levels. Toxicokinetic analyses showed sustained serum levels of SON-1210, using a sandwich ELISA with anti-IL-15 for capture and biotinylated anti-IL-12 for detection,

along with sustained IFNγ levels, indicating prolonged kinetics and biological activity.

Conclusion: Collectively, these findings support the suitability of SON-1210 for patient trials in terms of activity, efficacy, and safety, offering a promising opportunity for solid tumor immunotherapy. Linking cytokine payloads to a fully human albumin binding domain provides an indirect opportunity to target the TME using potent cytokines in *cis* that can redirect the immune response and control tumor growth.

KEYWORDS

interleukin-12, interleukin-15, cancer, tumor microenvironment, immunomodulation, Fully human albumin binding (FHAB) domain, interferon gamma, immunotherapy

1 Introduction

Interleukin-12 (IL-12) is a multifunctional cytokine that regulates cell-mediated innate and adaptive immune responses and orchestrates potent anticancer effects, either alone or synergistically with other cytokines (1). IL-12 primes natural killer (NK) cells and T-helper type 1 (Th1) cells to secrete IFNγ, reactivate and enhance the survival of memory $CD4^+$ T cells, help differentiate $CD8^+$ T cells, and upregulate IL-15, IL-18, and IL-2-receptor expression while decreasing the levels of Treg cells and their impact on immunosuppression (2). IL-12 can also inhibit neovascularization due to induction of IFNγ (3) via upregulation of angiostatin (4) or suppression of the vascular endothelial growth factor receptor 3 (VEGFR3) (5). IL-15 shares many biological properties with IL-12, including upregulation of IL-12 beta receptor expression and maturation, as well as NK and memory $CD8^+$ T-cell proliferation and activation. The prolonged survival of $CD8^+$ memory T cells enhances the duration of tumor immune surveillance for months and potentially even years.

The combination of IL-15 with other cytokines in *cis* can enhance antitumor activity compared to either cytokine alone, which correlates with the synergistic upregulation of each cytokine's receptors, resulting in a marked induction of IFNγ (6). The capacity of dendritic cells (DCs) to secrete IL-12 and present IL-15 is crucial. Both IL-12 and IL-15 mediate NK-cell activation by DCs in human lymphoid organs (7). Cultured DCs from either blood or spleen primarily stimulate $CD56^{bright}CD16^-$ NK cells, which are enriched in secondary lymphoid tissue. Blocking of IL-12 abolished the DC-induced IFNγ secretion by NK cells *in vitro*, whereas membrane-bound IL-15 on DCs is essential for NK cell proliferation and survival. DCs colocalize with NK cells *in vivo* in the T-cell areas of lymph nodes. CD40 ligation promotes the highest IL-15 surface presentation during maturation of the DCs and leads to the strongest NK cell proliferation. This causes increased IFNγ production, which increases MHC on DCs, making antigen presentation more efficient. Combining IL-15 with IL-12 drives the generation of more NK maturation, creating highly functional NK cells *in vitro*, resulting in >70% positivity for CD16 and/or KIR within 2 weeks after infusion into mice (6). There is a clear potential for further SON-1210 combination *in vivo* with checkpoint inhibitors or cell-based therapy. The interplay between activation of NK cells, $CD4^+$ T cells, and $CD8^+$ T cells and local delivery of cytokines and αPD-L1 therapeutics to immune cell-containing *in vitro* melanoma tumors was recently modeled (8). Both NK cells and $CD8^+$ T cells were shown to be necessary for tumor cell killing and $CD4^+$ T-cell activation was reduced without NK cells. Delivery of IL-15/IL-15Rα to tumor cells effectively mediated anti-tumor activity and sensitized the tumor microenvironment (TME) for therapy with αPD-L1 therapeutics, mainly by impacting NK cells.

The effectiveness of cancer immunomodulators depends on the interplay between the physical properties of the drug and the TME, including permeability, resident immune cell activation or suppression of inhibition, retention time within the tumor, and serum pharmacokinetic (PK) properties (9–11). Smaller proteins (< 100 kDa) favor improved penetration into solid tumors, whereas longer protein half-lives (up to 21 days vs. minutes to hours) can extend the duration of tumor exposure (12). We devised a strategy to prolong cytokine PK half-life ($t_{1/2}$) and target the TME by proposing the use of an albumin single-chain antibody fragment (scFv), which is a fully human albumin-binding (F_HAB) domain (13, 14). The F_HAB domain exploits the physiological recycling of albumin by binding to the neonatal Fc receptor (FcRn) in a manner similar to FcRn recycling of IgG (15), leading to increased half-life. Notably, a more important consideration is that albumin facilitates targeted delivery of the F_HAB to the TME due to its marked accumulation in tumors by enhanced penetration and retention (16).

To find an appropriate binding moiety, a fully human single chain antibody fragment phage library (XOMA, Emeryville, CA) with $> 1 \times 10^{11}$ variable heavy and variable kappa/lambda light

chain diversities was screened using a number of criteria to isolate an anti-albumin scFv. The desired characteristics used to identify the best F_HAB include (i) high-affinity binding to human, mouse, and cynomolgus serum albumin; (ii) low double-digit nanomolar binding at physiological pH 7.2 and binding at a lower pH 5.8, which is characteristic of the acidic TME; (iii) selection of an anti-albumin epitope that preserves the binding site for FcRn, thus preventing renal clearance while retaining the benefit of FcRn-mediated recycling of albumin for extended PK; and (iv) preservation of the binding sites on albumin for albondin (GP60) and the "secreted protein acidic and rich in cysteine" (SPARC) tumor antigens, to enable extended TME accumulation and retention (17). SON-1210 is a novel drug candidate based on the F_HAB platform (Figure 1) that includes single-chain IL-12 and native IL-15 attached via flexible linkers to the amino and carboxy termini of the F_HAB domain, respectively, to create IL12-F_HAB-IL15. Linkers were designed to minimize potential steric hindrance of the attached protein(s). This design enables the extended half-life and activity of both cytokines, while bridging certain synergies of innate and adaptive tumor immunity.

Mechanistic proof of concept was originally demonstrated using a 4T1 mouse mammary tumor model positive for high expression of TGFβ (13). Both the isolated F_HAB and anti-TGFβ linked to the F_HAB efficiently targeted the implanted tumor and were present from 0.5 to 24 h after injection (Supplementary Material, Figure 1.2). However, the anti-TGFβ scFv, which strongly binds to TGFβ with a K_d of 10 nM, targeted the tumor alone, but was only present in lysates for up to 4 h, suggesting that it had diffused out of the tumor at later time points. Murine IL-12 was similarly linked to F_HAB to target murine B16F10 tumors and enhance its efficacy compared with native IL-12. This approach provided at least a 30-fold improvement in the therapeutic index (18). The monofunctional human IL12-F_HAB (SON-1010) is currently being tested clinically (19, 20).

IL-12 and IL-15 are strong inducers of antitumor activity and have been evaluated in numerous clinical studies (21–23). Combinatorial approaches using stimulatory cytokines, checkpoint inhibitors, chemotherapy, and/or radiation therapy are known to improve overall survival of patients with cancer (24, 25). However, recombinant interleukins have had limited clinical success owing to their short circulating half-life, inefficient TME targeting, and requirement for frequent dosing, leading to substantial systemic toxicities (26). To address these challenges, the F_HAB platform provides immunomodulators in a mono- or bifunctional format by employing the scFv to bind albumin, which improves their PK profiles and enhances TME targeting. Albumin binds efficiently to proteins such as FcRn, GP60, and SPARC, which are overexpressed in many solid tumors, to provide concentration

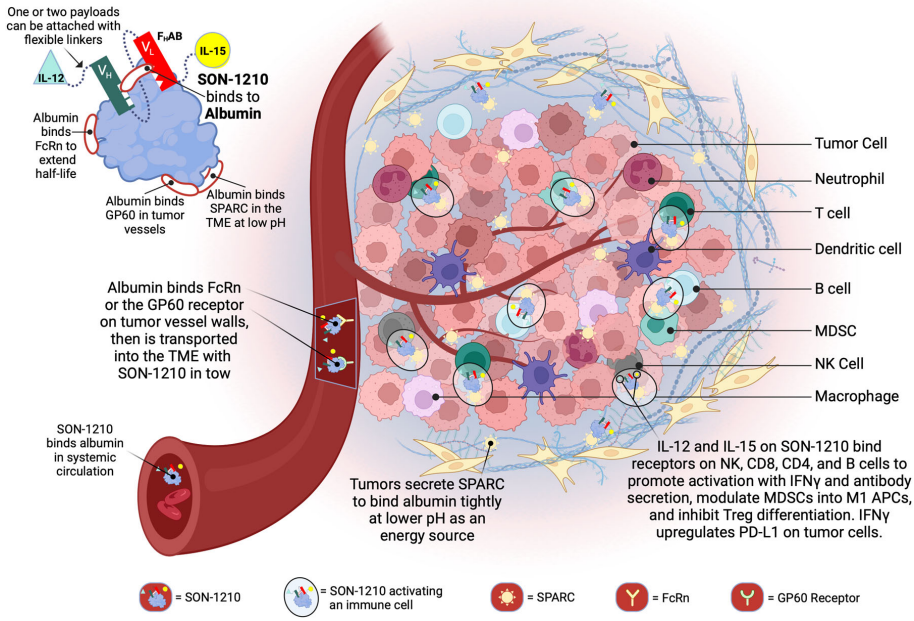

FIGURE 1
Schematic Representation of SON-1210 and its Mechanism of Action. The F_HAB molecule on the top left consists of a scFv heavy chain (V_H in green) linked using ($[GGGGS]_3$) to a light (V_L in red) chain that comprises an albumin-binding domain. Therapeutic payloads can be fused to each side of the central construct using flexible linkers ($[GGGGS]_5$), as indicated by the light green triangle and yellow circle (14). The conformation shown here represents SON-1210 (comprising single-chain hIL-12 and native hIL-15 sequence linked to the F_HAB for monkey or human use) or mIL12-F_HAB-hIL15, consisting of the mouse cognate of IL-12 and the human version of IL-15 for rodent studies. The F_HAB construct can interact with albumin from all 3 species, which binds systemically to FcRn, to share albumin's extended PK. The entire complex can be carried into the tumor tissue through the bloodstream, where the FcRn and GP60 receptors are upregulated, to be transported across the endothelium into the acidic TME. Once there, the albumin binds tightly in dynamic equilibrium via interaction with SPARC, which is overexpressed in the TME. The IL-12 and IL-15 cytokine domains can activate resident immune cells and recruit more cells, upregulating expression of IFNγ from NK, $CD4^+$, and $CD8^+$ T cells, which then upregulates PD-L1 on tumor cells and antibody production from B cells. Created with BioRender.com.

and retention of a drug molecule that is bound to an albumin molecule in the TME. IL-12 also transforms pro-tumor M2 myeloid-derived suppressor cells (MDSCs) into inflammatory M1 antigen presenting cells (APCs) leading to recovery of their macrophage function, thus turning "cold" tumors into "hot" tumors (27). The consequence of binding to albumin and being transported to the tumor tissue has the potential to be more effective than native IL-12 at lower doses, which further decreases the risk of toxicity and results in a broader therapeutic index. The significant cancer therapy potential of the combination of IL-12 and IL-15 promises to take advantage of IL-12's ability to prime innate/adaptive immune responses, while IL-15 can boost and maintain an antitumor response (28, 29). In this way, the synergies associated with each of the biological functions of these cytokines can be leveraged, namely, the ability of IL-12 to rapidly activate innate and adaptive immune responses and that of IL-15 to potently stimulate the proliferation of $CD4^+$ T cells and maintain memory $CD8^+$ T cells (6, 26, 30).

2 Material and methods

2.1 Protein production and reagents

The murine version of SON-1210, which has mouse (m) and human (h) cytokine sequences in the respective payload positions (mIL12-F_HAB-hIL15), was produced in CHO cells using shake flasks. The monofunctional mIL12-F_HAB, hIL12-F_HAB, and hIL15-F_HAB molecules, as well as mIL-12, hIL-12, hIL-15, and their His-tagged versions were produced in the same way (31). The SON-1210 clinical manufacturing process was performed using continuous perfusion during a 15-day manufacturing process. Purification was accomplished using multiple chromatography steps, resulting in a Good Manufacturing Process (GMP) product quality that is suitable for human use. All molecules were formulated in histidine-based buffer containing trehalose, DTPA, and polysorbate 20 at pH 7.3. The diluent used as the negative control was identical to the formulation buffer. Some recombinant human IL-12 (hIL-12), murine IL-12 (mIL-12), and human IL-15 (hIL-15) reference material and reagents used in these studies were purchased from Peprotech (Cat# 200-12, Cat# 200-15, respectively), and R&D Systems (Cat# 419-ML-010/CF).

2.2 Characterization of the F_HAB platform

To develop IL12-F_HAB-IL15 (SON-1210) as a human therapeutic, the compound must be tested for safety and efficacy in at least one relevant animal species. The first requirement of establishing an animal model is demonstrating that the F_HAB domain binds to that animal's serum albumin. This binding event was investigated by Surface Plasmon Resonance (SPR) to show relative affinity, comparing human and monkey serum albumin *in vitro*. The mIL12-F_HAB and hIL15-F_HAB constructs also demonstrated that mice can be used to show the effects of the extended PK due to binding of albumin *in vivo*. The second requirement for assessing the relevance of an animal species is that the cytokine portions of the target compound, single-chain hIL-12 and native hIL-15, bind to and activate the IL-12 and IL-15 receptors on the relevant animal's PBMCs. This requirement was tested by treating PBMCs from the selected animal species with hIL12-F_HAB-hIL15 in at least one potency assay for each cytokine component. Human and cynomolgus monkey PBMCs were purchased from IQ Biosciences (Cat# IQB-PBMC103 and IQB-MnPB102, respectively).

2.2.1 Surface plasmon resonance assay of F_HAB binding

Selection of an appropriate species for testing of hIL12-F_HAB-hIL15 was done using SPR to evaluate its binding to albumin at physiologic pH 7.4 and at an acidic pH of 5.8, to approximate conditions in the TME. Species studied included rat (Sigma Cat# A6414), Syrian hamster (Bio-world Cat# 22070085-1, further purified by InfinixBio), canine (Abcam Cat# ab119814), or macaque (Athens Research Cat# 16-16-011202-CM) serum albumin, compared to the degree of binding to human serum albumin (Abcam Cat# ab205808) (RSA, HamSA, CSA, MSA, and HSA, respectively). Assay details are included in the Supplementary Materials Section 1.1.

2.2.2 hIL12-F_HAB-hIL15 (SON-1210) binding to Albumin

The solution dissociation constant (K_d) of SON-1210 was determined for binding to various concentrations of albumin (Supplementary Materials Sections 1.2) (32). Briefly, to determine the solution K_d for binding to albumin, ELISA plates were coated with the appropriate species albumin. Test samples that contained 2 nM SON-1210 were incubated with different concentrations of either HSA or MSA in buffer, or no albumin as control. Aliquots were transferred to the ELISA plate, incubated for 1h, then for another hour after adding an anti-human IL-12p70 biotinylated detection antibody (ThermoFisher Cat#CUST77216). After washing, samples were incubated with Streptavidin-HRP (ThermoFisher 21130), washed four times, and visualized with TMB (Sera Care Cat#5120-0083) for 10 minutes before quenching with 0.05 mL 1 M HCl and reading the plate at 450 nm. The K_d value was determined at each concentration of added albumin.

2.2.3 SPARC binding to HSA or HSA : IL12-F_HAB

To determine the solution K_d of HSA binding to SPARC, ELISA plates were coated with HSA. At the same time samples containing Biotinylated (B)-SPARC were incubated for 1h in polypropylene microtiter plates with different concentrations of HSA (3000 nM – >3 nm; 2 fold dilutions) in in pH 6.0 PBS + 0.05% Tween 20. Aliquots of the samples containing B-SPARC and HSA were then transferred to the coated plates and incubated for 1h at room temperature. After washing, the plates were incubated for 1h with 0.25 µg/mL Streptavidin-HRP (ThermoFisher). The plates were then visualized with TMB (Sera Care) for 20 minutes before quenching with 0.05 mL 1 M HCl and reading the plate at 450 nm. (further detail in Supplementary Material Section 1.3).

To show that SPARC binds to the HSA : IL12-F_HAB complex in pH 6.0 PBS + 0.05% Tween 20, ELISA plates were coated with HSA and then incubated with mixtures of B-SPARC (0.15 nM) + IL12-F_HAB (1500 nM, 750 nM, or 0 nM). The concentrations of IL12-F_HAB used in this experiment were shown to saturate the HSA on the plate in a prior study. After washing three times, the binding of B-SPARC to IL12-F_HAB on the plate was visualized by incubation with 0.25 μg/mL Streptavidin-HRP as described above.

2.2.4 Naïve mouse pharmacokinetics

To evaluate PK, three C57BL/6 mice for each time point were administered a single intravenous (IV) dose of 5 μg mIL12-F_HAB-His, hIL15-F_HAB-His, mIL-12-His, or hIL-15-His. Quantitation of each compound in serum was performed with an ELISA, based on consistent detection of a histidine (His) tag to avoid potential interference from the native cytokines. Plates were coated overnight with 6x-His Epitope Tag Antibody (Pierce Cat#His.H8) at 2-8°C, then washed, and sample dilutions added for 1 h incubation at room temperature. Rabbit anti-6-His biotinylated secondary antibody (Bethyl Cat# A190-114B) was then added to the wells for 1 h at room temperature, followed by streptavidin poly-HRP (ThermoScientific Cat# 21140) for 30 minutes at 37°C. The reaction was stopped with H_2SO_4 and the plates were read at 450nm.

2.2.5 Lymphoblast proliferation assay for IL-12 activity

The lymphoblast proliferation assay is a functional assessment of the ability of IL-12 to stimulate the proliferation of PHA-activated T lymphoblasts ("PHA blasts"). Lymphoblast formation is triggered by the treatment of healthy human donor PBMCs (Precision for Medicine) with phytohemagglutinin P (PHA-P) for 4 days, with the addition of IL-2 during the final 24 hrs, before the proliferation assay is done. Once the PHA blasts are formed, their proliferation can be stimulated by the presence of functional recombinant hIL-12 (R&D Cat# 219-IL-005) or mIL12-F_HAB-hIL15 over a period of 48 hours using the CellTiter Aqueous One Solution Cell Proliferation kit (Promega Cat# G3580), which includes media supplemented with 5% FBS. Cell proliferation is quantitated by the addition of CellTiter-Glo® Luminescent Reagent (Promega Cat# G7571) using a microplate reader with luminometer attached. A 4-parameter logistic curve is generated to assess cell proliferation and to determine EC_{50} values.

2.2.6 IFNγ secretion by PHA blasts

IL-12 or IL-15 functional activity can be assessed by their ability to induce the secretion of IFNγ from PHA blasts. Lymphoblasts were prepared and stimulated as described above. After incubation with hIL12-F_HAB (SON-1010), hIL12-F_HAB-hIL15, or recombinant hIL-12, the culture medium was then processed for the detection of IFNγ with a human IFNγ ELISA. Increased IFNγ secretion by hIL12-F_HAB-hIL15, as compared to that induced by a hIL-12 control standard, indicates that an IL-12 functional product was present in the culture.

2.2.7 CTLL-2 proliferation assay for IL-15 activity

This functional assay is based on the ability of hIL-15 to stimulate the proliferation of the murine cytotoxic T-cell line CTLL-2 (ATCC Cat#TIB-214). CTLL-2 cells are able to proliferate in response to either human or mouse IL-15. This proliferative response can be measured under controlled tissue culture conditions for IL-15 products over a 48 hour period. Cell proliferation was quantitated by the addition of CellTiter 96® Aqueous One Solution Cell Proliferation Assay Reagent (MTS) and a microplate reader with luminometer attached. A 4-parameter logistic curve is generated to assess cell proliferation and to determine EC_{50} values.

2.2.8 Tumor accumulation of radiolabeled mIL12-F_HAB

The B16F10 model (Section 2.4) was used to assess biodistribution of mIL12-F_HAB-His compared to mIL-12-His in a preliminary study (Charles River Laboratories, Mattawan, MI). Both the recombinant molecules used in this study were expressed in CHO cells and purified to > 95% by SDS-PAGE and SE-HPLC (Abzena, Cambridge, UK). The final products demonstrated activity by the HEK-Blue assay, which confirms STAT4 phosphorylation as discussed below (Section 2.3.2). We showed that the mIL12-F_HAB-His binds HSA and mouse serum albumin using SPR with a K_d ranging from 30-50 nM.

Both mIL12-F_HAB-His and mIL-12-His products were then radiolabeled with technitium-99m (^{99m}Tc), and were then purified using standard methods (33) to make [^{99m}Tc]-mIL-12-His and [^{99m}Tc]-mIL12-F_HAB-His. Groups of mice with or without tumors were injected with 1 μg/g of each product containing ≤ 200μCi per animal IV, once the tumors had reached about 200 mm^3, and were then imaged with a Mediso nanoSPECT/CT scanner over the next 96 h. Image processing and analysis was performed using VivoQuant™ Software.

2.3 Characterization of SON-1210

2.3.1 Physical characteristics of SON-1210

Samples from two GMP batches were run using a 4-20% Bis-Tris gel by sodium dodecyl sulfate-polyacrylamide gel electrophoresis (SDS-PAGE) compared to molecular weight (MW) markers at Enzene Biosciences, Ltd. (Pune, India). Purity was assessed by size exclusion-high pressure liquid chromatography (SE-HPLC). Charge heterogeneity was evaluated by imaged capillary isoelectric focusing (iCIEF) using standard techniques (34).

2.3.2 Potency measurement of the IL-12 and IL-15 moieties in SON-1210

Activation of IL-12 and IL-15 receptors by their natural ligands induces phosphorylation of STAT4 and STAT5, respectively. HEK-Blue is a reporter gene assay that can be used to measure the potency of IL-12 and IL-15 as independent entities in the bifunctional molecule, SON-1210 (Supplementary Material

Section 1.5). HEK-Blue IL-12 cells express a STAT4-inducible secreted embryonic alkaline phosphatase (SEAP) reporter gene triggered by the binding of IL-12 to its receptor (35). The cytokines hIL-2 and hIL-15 are closely related and share the heterodimeric CD122 (IL-2Rβ)/CD132 (IL-2Rγ) receptor to deliver signals to the target cells. Therefore, to determine the relative bioactivity of hIL-15, SON-1210 was tested using HEK-Blue IL-2 reporter cells that express STAT5-inducible SEAP upon binding of IL-15 to the IL-2 receptor (36). Both assays were done in growth medium containing 10% heat-inactivated FBS.

2.3.3 Comparative stimulation of IFNγ production

The functionality of the IL-12 and IL-15 moieties of SON-1210 was evaluated by measuring IFNγ production from both human and monkey PBMCs *in vitro* after prior stimulation of the cells with PHA-L for 72 hours, then IL-2 for 24 h. Washed cell aliquots were incubated with the SON-1210, IL-12 (Peprotech, Cat# 200-12), or media alone for 48h, and the level of IFNγ was determined by ELISA (Human IFNγ High Sensitivity ELISA Kit [Abcam, Cat# ab46048]; Monkey IFNγ ELISA PRO Kit [Mabtech, Cat# 3421M-1HP-1]) (Supplementary Material Section 1.6).

2.3.4 T-cell proliferation

The ability of SON-1210 to promote T- and NK-cell proliferation was studied in monocyte-depleted human PBMCs to avoid intrinsic IL-12 interference. Cells were stimulated with PHA-L for three days, then IL-2 was added for another 24 h. The cells were washed and incubated with the media containing SON-1210 or IL-15 (with or without anti-IL-15 antibody [R&D Systems, Cat# MAB247]) for 48 h and cell proliferation was determined using a luminescence assay. As SON-1210 and IL12-F_HAB share the same IL-12 domain, the proliferation effect was compared using equimolar concentrations of the two stimulators or was neutralized with an anti-IL-12 antibody (R&D Systems, Cat# MAB219) (Supplementary Material Section 1.7). Based on these results, 25 μg/mL of anti-IL-12 antibody was found to be sufficient to block the function of hIL12-F_HAB at 50 pM or lower.

2.4 Safety and efficacy in B16F10 tumor-bearing mice

The antitumor efficacy of mIL12-F_HAB-hIL15 was assessed in a subcutaneous (SC) B16F10 syngeneic mouse melanoma model using C57BL/6 mice by measuring the evolution of tumor volume and survival over time. Animals were randomly grouped (Table 1) with sample size based on prior experience. Treatments were initiated when the mean tumor volume reached approximately 100 mm^3, seven days after inoculation of 0.2×10^6 B16F10 melanoma cells (Supplementary Material Section 2). The effect of IV administration of a single dose of mIL12-F_HAB-hIL15 at several dose levels or three doses at 5 μg/dose was compared with that of the vehicle, as well as equimolar administration of recombinant mIL-12, hIL-15, their combination, or mIL12-F_HAB. The Tumor-Bearing Placebo group received the melanoma cells and placebo administration, while the Non-Tumor Bearing (naïve) group received no treatment and was used for hematology and clinical chemistries on day 0. Treatments were administered by IV injection in 200 μL of 0.02% Tween 20 in PBS on the day of dosing (day 0).

Body weight was used as an early indicator of toxicity, along with hematological and clinical chemical analyses. The levels of IFNγ, IL-10, IL-12p70, IL-1β, IL-2, IL-4, IL-5, IL-6, KC/gro (IL-8-

TABLE 1 Design of the B16F10 mouse efficacy study.

Treatment	Single Dose	Dose 3x (Day 0, 2, 4)	Terminal Bleeds (n=)			FACS (n=)	Efficacy (n=)	Total Mice (N=173)
			Day 0	Day 3	Day 8			
Tumor-Bearing Placebo	–	–	4	4	4	4	8	24
mIL12-F_HAB-hIL15	1 μg	-	-	5	5	-	8	18
mIL12-F_HAB-hIL15	5 μg	-	-	5	5	5	8	23
mIL12-F_HAB-hIL15	10 μg	-	-	5	5	-	8	18
mIL12 reference (based on 5ug dose)	3 ug	-	-	4	4	-	-	8
hIL15 reference (based on 5ug dose)	0.8 ug	-	-	5	5	-	-	10
mIL12 + hIL-15 references	3 μg + 0.8 μg	-	-	4	4	5	8	21
mIL12-F_HAB-hIL15	-	5 μg	-	5	5	5	8	23
mIL12-F_HAB	5 μg	-	-	5	5	5	8	23
Non-Tumor Bearing Placebo (Naïve Mice)			5	–	–	–	–	5

C57BL/6 females were randomly assigned to treatment groups as described. Control groups are shown in white, purple, and blue. The number of mice per group and analysis conducted are shown on each of the columns. Acclimation was 2 weeks; age at initiation was 10-11 weeks. Animals were excluded if their tumors were < 100 mm^3 or > 150 mm^3 on the day of dosing. None of the animals entered onto the study were excluded from the analysis. Tumors for FACS were harvested on Day 3. Efficacy was assessed with measurements of tumor volume on even days until sacrifice. Animals were euthanized if the tumors exceeded 1800 mm^3 or body weight loss was >20% as indicated in the IACUC approval.

related protein in rodents), and TNFα were determined in sera using an electrochemiluminescence panel (Meso Scale Discovery, Cat# K15048D).

Tumor samples were collected for FACS analysis when the average tumor size was approximately 250 mm^3 on day three (Supplementary Material Figure 2). Single cell suspensions from freshly collected spleens and tumors were prepared by transferring individual tissues into gentleMACS C Tubes containing 5 ml of RPMI, which were placed onto a gentleMACS tissue dissociator (Miltenyi Biotec). The single cell suspensions were filtered through Falcon 100 µm nylon filters and centrifuged. The staining panel included markers for live/dead, CD45, TCR-beta, CD8, CD4, CD25, FoxP3, IFNγ, CD49b, F4/80, CD206, CD11b, CD11c and MCHII.

2.5 Toxicokinetic evaluation of repeated SON-1210 dosing in non-human primates

Hamster, rat, dog, and macaque cells were screened to determine the best species to use for toxicology studies with an *in vitro* assessment of binding and biopotency. Macaque cells were the only ones that responded similarly to the human control cells. A preliminary dose-ranging study was done with SON-1210 in non-human primates (NHPs). A total of 28 male and female Mauritian cynomolgus macaques received SON-1210 given subcutaneously (SC) at 15.6 to 125.0 µg/kg, either one time on day 0 or twice, on days 0 and 15. This study was intended to establish the maximum tolerated dose (MTD).

In the subsequent Good Laboratory Practice (GLP) study, the safety, toxicology, and toxicokinetic (TK) attributes of SON-1210 were evaluated in 32 male and female cynomolgus macaque NHPs (Table 2 and Supplementary Material Section 3). The dose range of 15.625, 31.25, and 62.5 µg/kg was targeted to assess the maximum pharmacological effect, using 3 dose levels plus a control group, with sample size based on prior experience. Three males and 3 females were enrolled as the main group (studied for 6 weeks), with 2 additional animals of each sex at the highest dose and controls, added as a recovery group (studied for 11 weeks). The protocol and procedures involving the care and use of animals in the study were reviewed and approved by Charles River Institutional Animal Care and Use Committee (IACUC) before conduct. This study was aligned with the ICH and FDA guidelines for preclinical assessment of biopharmaceutical products.

Following three SC administrations on days 1, 15, and 29, animals were followed closely for clinical observations, body weight, and food consumption. Animals were routinely monitored ophthalmologically and by electrocardiography, along with comprehensive hematological and clinical chemistry assessments. Necropsy included gross dissection, organ weights, and histopathology. Bioanalytical samples were taken at various points during the study for cytokines, immunophenotyping, anti-drug antibody (ADA), and toxicokinetics (TK) analysis. The cytokines assessed included IFNγ, TNFα, IL-6, IL-8, IL-10, and IL-1β. ADA (IgG or IgM) was quantified in sera in two stages, starting with a screening assay followed by a confirmatory assay.

SON-1210 was quantified for TK analysis using a validated IL-12/IL-15 combination assay and was made specific by first capturing the molecule with an IL-15 domain-specific antibody (ThermoFisher, Cat# 88-7620-88), and then detecting the quantity of captured material with a biotinylated IL-12 domain-specific antibody (Thermofisher, Cat# CUST77216). Background levels of monkey IL-12 and IL-15 were negligible, so were not considered to interfere with the assay. The upper and lower limits of quantitation (ULOQ and LLOQ) for the assay were determined to be 400 pg/mL and 12 pg/mL, respectively. LLOQ results were estimated at 6 pg/mL for graphing, while the NCA analysis treated these results as zero before dosing and as missing after dosing. Samples were diluted into the quantifiable range if the initial result was above the ULOQ. TK parameters were estimated using non-compartmental analysis (Pheonix WinNonlin). Further details are included in the Supplementary Material Section 3.

2.6 Statistical analysis

All data are presented as mean ± SEM. A two-way analysis of variance (ANOVA) was performed with a between-subject variable of treatment and a repeated measurement factor of time. Tumor growth curves were evaluated using the ANOVA and Dunnett's multiple comparison test. The Gehan-Breslow-Wilcoxon test was

TABLE 2 Design of the GLP toxicology study in NHPs.

Group No.	Test Article	Dose Level Days 1, 15, & 29 (µg/kg/dose)	Dose Volume[a] (mL/kg)	Main Study	Recovery Study	Total NHPs (N=32)
				No. of Animals	No. of Animals	
1	Vehicle	0	2	3 M and 3 F	2 M/2F	10
2	SON-1210	15.6	2	3 M and 3 F	–	6
3	SON-1210	31.2	2	3 M and 3 F	–	6
4	SON-1210	62.5	2	3 M and 3 F	2 M/2F	10

Male and female NHPs were assigned to groups upon animal transfer based on established pairs but were randomized separately. Animals in poor health or at extremes of body weight range were not assigned to groups. A minimum acclimation period of 10 days was allowed between animal transfer and the start of treatment to accustom the animals to the laboratory environment. Before the initiation of dosing, one animal was rejected from the study due to hematology findings and was replaced by a spare animal. Vehicle control was the histidine formulation buffer for SON-1210. Dosing occurred once every 14 days on Days 1, 15, and 29.

[a]Based on the most recent body weight measurement. No., number; -, not applicable.

applied to survival curves. One-way ANOVA was applied to each cytokine response and safety laboratory test. All calculations were performed using R (R Foundation for Statistical Computing) and the GraphPad (Prism Software).

3 Results

3.1 Development and characterization of the F_HAB platform

A schematic representation of SON-1210 is shown in the Figure 1 inset, along with the relevant binding sites on albumin. The mechanism of delivery of the IL12-F_HAB-IL15:albumin complex to the tumor, along with its retention and activation of immune cells in the TME, is described in the rest of Figure 1. The studies described below required production of both the human and murine versions of the bifunctional molecule that is shown, as well as the monofunctional molecules (hIL12-F_HAB [aka SON-1010], mIL12-F_HAB, and hIL15-F_HAB).

Binding of the F_HAB domain to albumin was evaluated using species-specific responses in several types of assays. We first showed that the species most closely resembling human binding of hIL12-F_HAB-hIL15 was cynomolgus macaque by SPR both at physiologic conditions (pH 7.4), and more importantly at conditions that mimic the extravascular space in the TME (pH 5.8) (Figure 2A and Supplementary Material Figure S1). Rat serum albumin binding of hIL12-F_HAB-hIL15 at both conditions was much weaker, while Syrian hamster and canine serum albumin samples showed no binding. Thus, the macaque was selected as the best model for further comparisons with potential human use of hIL12-F_HAB-hIL15.

The affinity of two molecules can also be studied by measuring the binding and unbinding reactions of receptor (R) and ligand (L) molecules in solution. This is expressed as an association constant (K_a) or more typically as its inverse, the dissociation constant (K_d). The solution K_d for the binding of hIL12-F_HAB-hIL15 to HSA and MSA was studied at pH 7.4 and pH 6.2 (the method is described in Supplementary Material Section 1.2). Binding to HSA revealed K_d values of 60 ± 30 nM and 80 ± 10 nM, respectively. Binding to MSA showed K_d of 400 ± 200 nM and 600 ± 300 nM at pH 7.4 and 6.2, respectively. Thus, the binding of hIL12-F_HAB-hIL15 to HSA was approximately seven times stronger than its binding to MSA at both pH 7.4 and 6.2.

In contrast, binding of HSA to SPARC in conditions resembling the TME was even tighter, with a K_d of 10 nM at pH 6.0 (the method is described in Supplementary Material Section 1.3), whereas minimal binding was detected at pH 7.2 by ELISA. The solution binding constant of B-SPARC to HSA:hIL12-F_HAB could not be measured, but the binding of B-SPARC to immobilized HSA and immobilized HSA:hIL12-ABD was similar. This suggests that once the complex is delivered to the TME by FcRn- or GP60-based shuttling of receptor-bound albumin across the tumor endothelium, the F_HAB : HSA complex is retained in that space by binding to SPARC in a dynamic equilibrium with slow release (17).

The *in vivo* half-lives of monofunctional mIL12-F_HAB (Figure 2B, left panel) and hIL15-F_HAB (Figure 2B, right panel) were higher compared to their native counterparts, mIL-12 and hIL-15. The half-lives of mIL-12 and hIL-15 in mouse serum improved by 3.8- and 11.6-fold, respectively, when the cytokine was linked to F_HAB. These preclinical studies were felt to reflect the platform adequately, so a PK study of the bifunctional hIL12-F_HAB-hIL15 molecule will wait for the first clinical study.

The next step was to confirm that human IL-12 and human IL-15 bind to and activate the IL-12 and IL-15 receptors on the relevant animal's PBMCs. Activation of the IL-12 receptor was studied using PHA lymphoblasts made from human PBMCs. Cell proliferation following exposure to hIL12-F_HAB-hIL15 closely resembled stimulation by recombinant hIL-12 (Figure 2C, left panel). Activation of the IL-15 receptor was studied using the murine cytotoxic T-cell line CTLL-2. Proliferation assessed with multiple concentrations of hIL12-F_HAB-hIL15 was nearly as effective as hIL-15 (Figure 2C, right panel). Finally, the physiologic impact was assessed by IFNγ production using PHA blasts. While the effect of hIL12-F_HAB was nearly the same as recombinant hIL-12, hIL12-F_HAB-hIL15 stimulated the production of IFNγ more efficiently at concentrations above 6 pM (Figure 2C, center panel).

In addition, while biodistribution studies have not yet been conducted with the IL12-F_HAB-IL15 molecule, a study has been completed using the monofunctional IL12-F_HAB in mice. Tumor accumulation of the mIL12-F_HAB platform molecule and mIL-12 was measured by radiolabeling both His-tagged molecules with ^{99m}Tc. After IV administration of each labeled molecule into a cohort of B16F10 tumor-bearing or control C57BL/6 mice, the [^{99m}Tc]-mIL12-F_HAB molecule accumulated 1.7- to 3.1-fold higher over a 0.5- to 24-hour period in the tumor, compared to the [^{99m}Tc]-mIL12 control (Figure 2D, left panel). The radiolabel analysis was terminated at 24 hours due to the rapid decay of the label (the $t_{1/2}$ of ^{99m}Tc is 6 hours). Tumors were followed with measurements until sacrifice showing prolonged suppression of growth by the mIL12-F_HAB molecule (Figure 2D, right panel).

3.2 Characterization of SON-1210

3.2.1 Physical characteristics of SON-1210

Samples from two GMP drug substance (DS) batches of hIL12-F_HAB-hIL15 (SON-1210) were evaluated by non-reduced SDS-PAGE. While the theoretical MW is 99 kDa, the observed MW was about 115 kDa due to glycosylation (Figure 3A, left panel). The purity of the products was next studied by SE-HPLC. The main peak resolved at about 14.3 m and each was > 97% pure, with minor high MW (HMWs) and low MW (LMWs) peaks flanking the main peak (Figure 3A, center panel). Charge heterogeneity was assessed by iCIEF. Charge variations of biomolecules are common and can generally include those caused deamidation, formation of N-terminal pyroglutamate, aggregation, isomerization, sialylated glycans, antibody fragmentation, and glycosylation (34). A representative graph from the

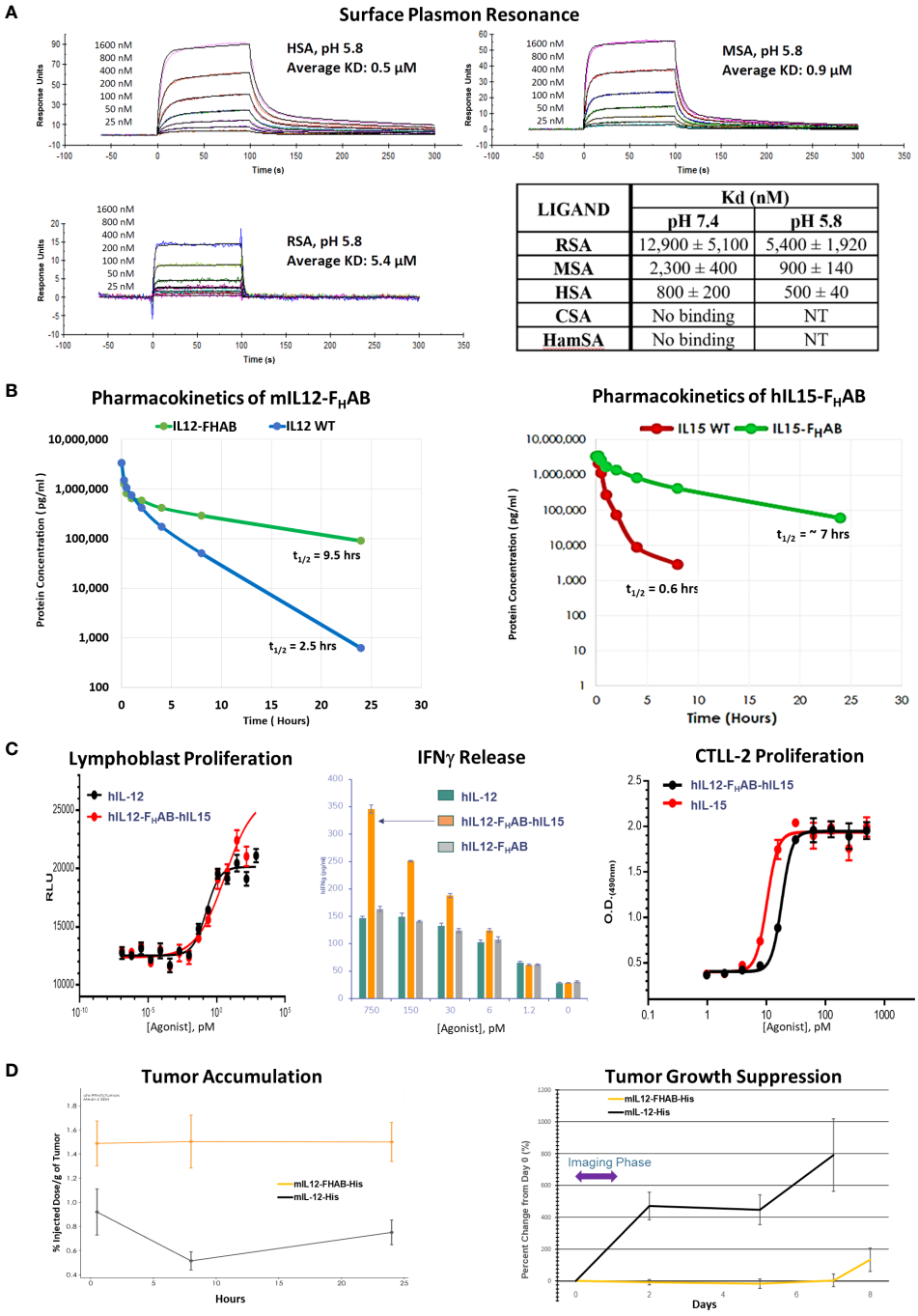

LIGAND	Kd (nM)	
	pH 7.4	pH 5.8
RSA	12,900 ± 5,100	5,400 ± 1,920
MSA	2,300 ± 400	900 ± 140
HSA	800 ± 200	500 ± 40
CSA	No binding	NT
HamSA	No binding	NT

FIGURE 2
Characterization of the FHAB Platform. **(A)** Surface plasmon resonance curves at pH 5.8 of species-specific serum albumin binding to hIL12-F_HAB-hIL15 (SON-1210). The K_d is the dissociation constant; a lower K_d indicates stronger binding affinity. Abbreviations: RSA = rat serum albumin, MSA = monkey serum albumin, HSA = human serum albumin, CSA = canine serum albumin, HamSA = hamster serum albumin. **(B)** Pharmacokinetic assessment of the mIL12-F_HAB concentration by ELISA in the serum of naïve mice (left panel) after a single IV injection compared with injection of mIL-12. The same approach using hIL15-F_HAB compared with hIL-15 (right panel). **(C)** A lymphoblast assay of human PBMCs was used to assess relative proliferation (left panel), comparing hIL-12 with hIL12-F_HAB-hIL15 *in vitro*. Supernatant IFNγ released from PHA blasts following stimulation with varying concentrations of hIL-12, hIL12-F_HAB (SON-1010), or hIL12-F_HAB-hIL15 (center panel). IL-15 bioactivity was studied using proliferation of the murine cytotoxic T-cell line CTLL-2 (right panel) after exposure to various concentrations of hIL-15 or hIL12-F_HAB-hIL15. **(D)** A biodistribution study designed to show tumor accumulation was done in B16F10 tumor-bearing or control mice after injection of [^{99m}Tc]-mIL12-F_HAB or [^{99m}Tc]-mIL12, once the tumors had reached ~200 mm^3. The mice were imaged by SPECT/CT over 24 hours. Tumor growth was measured over the next 8 days.

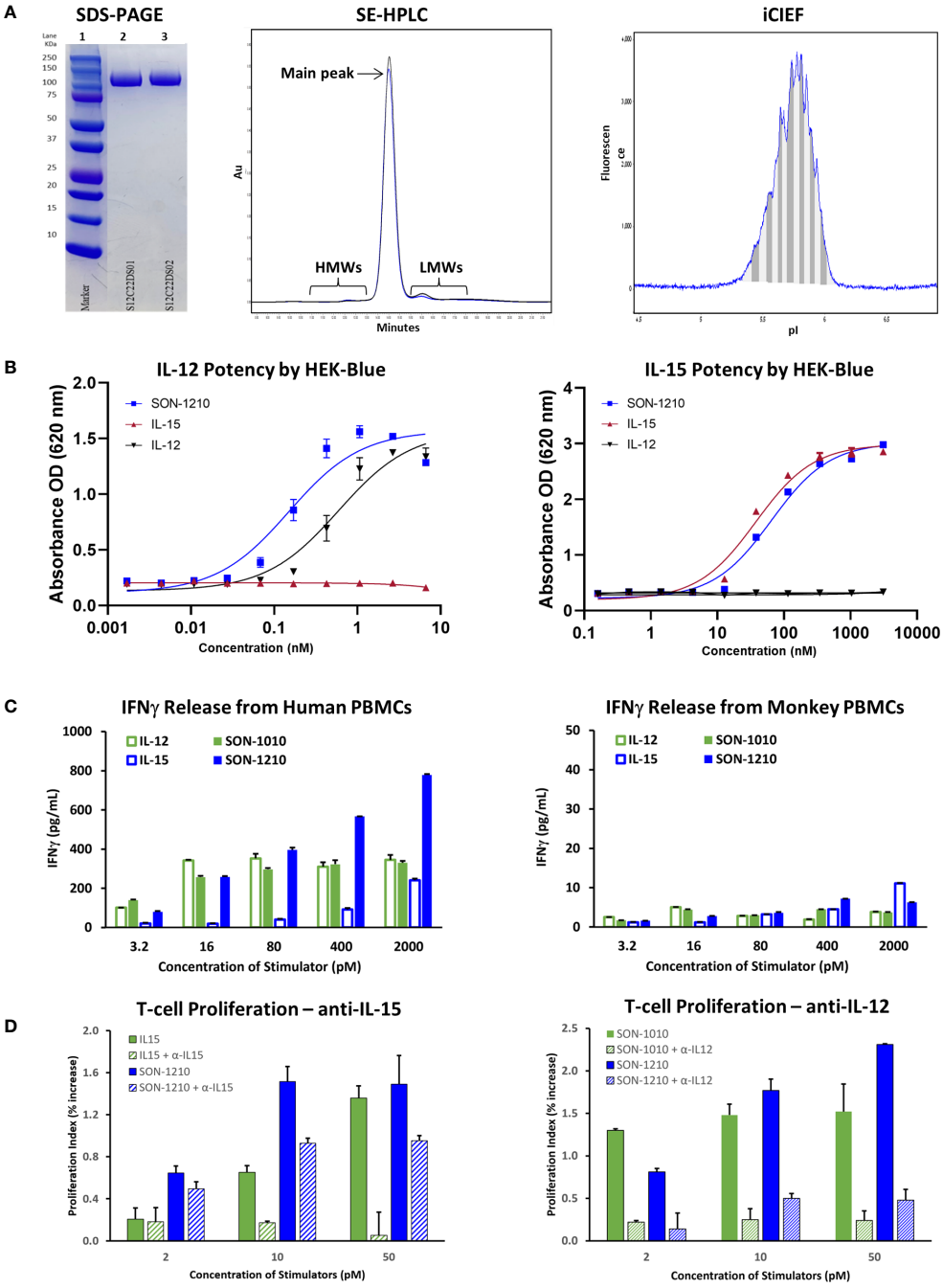

FIGURE 3
Characterization of SON-1210. **(A)** Non-reducing SDS-PAGE of SON-1210 (left panel). Samples from two GMP drug substance batches (lanes 2 and 3) were run on a 4-20% Bis-Tris gel with MW markers (lane 1). The purity of two GMP batches of SON-1210 was evaluated by size exclusion HPLC (center panel), which shows > 97% monomeric product in each. Minor high MW (HMWs) and low MW (LMWs) peaks flank the main peak at about 14.3 m. Charge heterogeneity of SON-1210 was assessed by imaged capillary isoelectric focusing (iCIEF) (right panel); a representative sample is shown. **(B)** The potency of the IL-12 (left panel) and IL-15 (right panel) moieties of SON-1210 was assessed using HEK-Blue 12 or HEK-Blue 2 cells. **(C)** Production of IFNγ by SON-1210 or hIL12-F_HAB (SON-1010) in the supernatant of cultured PBMCs from both humans (left panel) and monkeys (right panel). **(D)** Assessment of the individual moieties of SON-1210 to stimulate the proliferation of PHA-L and IL-2 stimulated, monocyte-depleted human PBMCs (to preactivate the T-cells) in the presence or absence of anti-IL15 or anti-IL12 antibodies. hIL-15 is used as the control for SON-1210 (left panel) and SON-1010 is the control in the right panel.

analysis of one of the DS batches shows minor heterogeneity with an isoelectric point (pI) of 5.3 to 6.0 (Figure 3A, right panel), compared to the theoretical pI of 5.3 to 5.4. These results were all within their prespecified acceptance criteria ranges, allowing further processing to make SON-1210 drug product (DP).

3.2.2 Potency by HEK-Blue assay

HEK-Blue cells expressed a STAT4-inducible SEAP reporter that was triggered by the binding of IL-12 to the IL-12 receptor (Figure 3B, left panel). SON-1210 exhibited approximately three-

fold higher potency (EC_{50} = 0.16 nM) than native hIL-12 (EC_{50} = 0.48 nM).

The activity of the IL-15 portion of SON-1210 was measured using a HEK-Blue IL-2 reporter assay (Figure 3B, right panel). This revealed IL-15 activity of SON-1210 of approximately 60% of the IL-15 positive control with EC_{50} values of 57.4 pM versus 33.1 pM, respectively.

3.2.3 IFNγ production by PBMCs

In human PBMCs, SON-1210 induced clear dose-dependent stimulation of IFNγ release. The induction of IFNγ by SON-1210 was higher than that elicited by the native IL-12 control at doses higher than 16 pM and higher than that of native IL-15 at all doses (Figure 3C, left panel). This result is consistent with our previous findings in tumor B16F10 mouse models, showing that mIL12-F_HAB stimulates more IFNγ than mIL-12 at higher dose levels (18). SON-1210 also generated higher IFNγ levels than hIL12-F_HAB (SON-1010), presumably because of the addition of IL-15 in *cis* to the former molecule.

In monkey PBMCs, SON-1210 induced higher levels of IFNγ than hIL-12 controls (except at the lowest doses) and hIL-15 controls (except at the highest dose tested) (Figure 3C, right panel). While they are the only type of animal PBMCs that responded measurably to human constructs, monkey cells are expected to respond to human cytokines less efficiently, owing to species sequence differences of the cytokines and receptors (37).

3.2.4 T-cell proliferation assay for the contribution of IL-12 and IL-15

SON-1210, IL-12, and IL-15 should all trigger a dose-dependent proliferative effect in human PBMCs. The ability of SON-1210 to stimulate T- and NK-cell proliferation was compared to that of hIL12-F_HAB (SON-1010) and hIL15-F_HAB in human PBMCs using specific HEK-Blue assays to qualitatively establish the activity of each moiety individually. Both IL-12 and IL-15 have been shown to induce PHA-L-stimulated T- and NK-cell proliferation (38). In the presence of anti-IL-15 antibody at 50 μg/mL, the function of hIL-15 was blocked; SON-1210 induced stronger proliferation of human PBMCs than hIL-12, with or without anti-IL-15. This indicates that the IL-12 portion of SON-1210 remained active in this assay (Figure 3D, left panel). SON-1210 also stimulated T-cell proliferation despite blocking the function of the IL-12 portion of SON-1210 with a 25 μg/mL anti-IL-12 antibody, indicating that the IL-15 portion of SON-1210 was also active in this assay (Figure 3D, right panel). The effective stimulation range for the IL-12 portion of SON-1210 was found to be 2-10 pM, and the effective stimulation range for the IL-15 portion of SON-1210 was 2-50 pM.

3.3 Safety and efficacy in tumor-bearing mice

The B16F10 syngeneic SC mouse melanoma non-immunogenic "cold" tumor model (39) was used to evaluate the antitumor efficacy of mIL12-F_HAB-hIL15. No clinical signs or deaths were reported during the study. Body weight of the mice (n=8/group) was measured three times per week until a tumor volume of 1800 mm^3 was achieved (Figure 4A, left panel). A two-way ANOVA with multiple comparisons showed that treatment with a single dose of mIL12-F_HAB-hIL15 resulted in moderate weight loss on day 4 (placebo vs. 10 μg mIL12-F_HAB-hIL15, $p < 0.05$) that began to rebound by day 6. Despite a significant reduction in body weight after the highest single dose treatment, animals recovered on day 8 and did not differ substantially from the tumor-bearing placebo group. Three doses of mIL12-F_HAB-hIL15 resulted in a more dramatic weight loss on days 4-10 (placebo vs. 5 μg × 3 qod of mIL12-F_HAB-hIL15, $p < 0.0001$) that fully recovered by Day 12. This degree of toxicity did not require sacrifice of any mice but may be a limiting factor in doing repeat-dose studies in this model.

Compared to placebo-treated mice, mIL12-F_HAB-hIL15 mice (n=8/group) showed slower tumor growth in a dose-dependent manner (Figure 4A, center panel). A single dose of 5 μg was fully effective, whereas a single dose of 10 μg did not further slow the tumor volume increase. The 3x group showed an even more effective response, with tumor growth delayed until day 14. All groups treated with mono- or bifunctional cytokine(s) linked to F_HAB showed significant growth inhibition, starting on day 4. Bonferroni's post test revealed significant differences ($p < 0.001$) in tumor volume between the tumor-bearing placebo group and all cytokine groups starting on day 6.

Finally, a time-to-event efficacy approach in the mice (n=8/group) revealed an increase in survival following mIL12-F_HAB-hIL15 treatment (Figure 4A, right panel), with 1 μg inducing 12-day median survival, whereas 10 μg induced 19-day median survival, compared to 10 days in the tumor-bearing placebo mice. Thus, there was a clear dose-dependent effect of mIL12-F_HAB-hIL15 treatment on survival (log-rank test for the trend: $p < 0.01$). The median survival with a single mIL12-F_HAB-hIL15 dose of 5 μg was 18.5 days, which was prolonged to 21 days after 3 doses.

Analysis of the pharmacodynamic (PD) cytokine response 3 days after dosing (Figure 4B) showed that mIL12-F_HAB-hIL15 increased IFNγ, IL-10, IL-12, IL-6, and TNFα levels in a dose-dependent manner compared to the tumor-bearing placebo group, with no evidence of cytokine release syndrome. There was a substantial increase in IFNγ levels with a single dose of mIL12-F_HAB-hIL15 to over 2000 pg/mL at 3 days, whereas mild increases were observed in other cytokines. Two doses of 5 μg increased the peak response to almost 9000 pg/mL. By day 8, the cytokine response pattern was sustained but generally dampened, with maximal IFNγ levels returning to 500 pg/mL after a single dose or 2100 pg/mL after three doses of mIL12-F_HAB-hIL15 at 5 μg. However, TNFα levels remained elevated.

Hematological and chemistry examination 3 days after IV dosing showed that mIL12-F_HAB-hIL15 treatment led to a dose-dependent reduction in neutrophils and lymphocytes on day 3 (Figure 4C, left panels) compared to the corresponding levels in placebo-treated tumor-bearing mice. RBCs were stable on day 3 in all groups but fell significantly in the high-dose and 3x groups by day 8 (Supplementary Material, Figure S3). Platelet counts also fell to half the pretreatment levels at all doses on day 3 and then rebounded by day 8 in all but the 3x group. Blood chemistry showed

10.3389/fimmu.2023.1326927

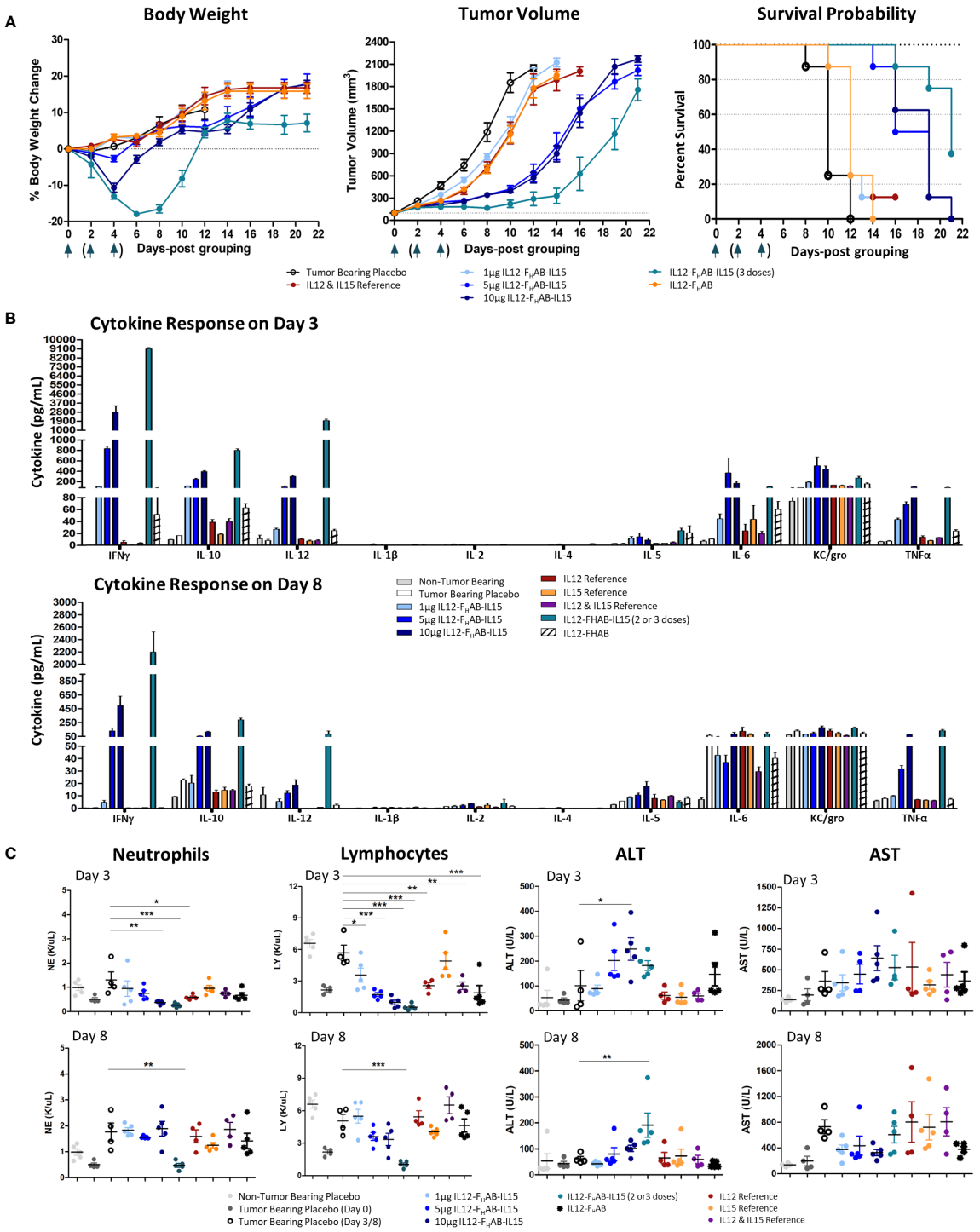

FIGURE 4
Safety and Efficacy of mIL12-FHAB-hIL15 in the Mouse. **(A)** Mice were implanted with B16F10 murine melanoma cells via SC inoculation and the tumors were allowed to grow to approximately 100 mm^3 before the start of the study. Groups of mice were dosed once on day 0 as shown in the legend or three times on days 0, 2, and 4 (arrows). Body weight gain was expressed as a percentage change compared with the initial weight of each animal (left panel). The tumor volume was measured using a caliper on alternate days until euthanasia. All groups were significantly different from the tumor-bearing placebo control by day 6 (Bonferroni's post-test: $p < 0.001$) (center panel). The survival probability is displayed over time as a function of treatment (log-rank test for the trend: $p < 0.01$) (right panel). **(B)** Blood cytokine levels measured on days 3 and 8 after a single dose of each compound on day 0, or after 2 doses (measured on day 3, top panel) or 3 doses (measured on day 8, bottom panel) of mIL12-F_HAB-hIL15. **(C)** Hematological analyses evaluating neutrophil (1st panel) and lymphocyte (2nd panel) counts on days 3 and 8. Clinical chemistry analysis for alanine (ALT, 3rd panel) and aspartate aminotransferase (AST, 4th panel) levels measured on days 3 (top panels) and 8 (bottom panels). Dunnett's multiple comparison test: * ($p < 0.5$), ** ($p < 0.01$), *** ($p < 0.001$).

a mild, dose-dependent, transient increase in alanine aminotransferase (ALT) levels by day 3 with mIL12-F_HAB-hIL15 that were significant at the 10 μg dose (but not after 2 doses of 5 μg), with no significant increases in aspartate aminotransferase (AST) at either day 3 or day 8 (Figure 4C, right panels).

FACS analysis was performed on tumors cells harvested on day 3 to compare the pattern of cellular responses after treatment with one dose of 1, 5, or 10 μg (or two doses of 5 μg) mIL12-F_HAB-hIL15 versus a single dose of equimolar amounts of the co-administered cytokines as a control (Figure 5). A 3-fold increase in NK cells over placebo was observed, with a 2-fold increase compared to cytokine controls. Activated IFNγ$^+$ NK cells increased 5-fold compared to cytokine controls. Activated (CD8$^+$ IFNγ$^+$) cytotoxic T cells (CTLs) were detected in the tumor upon treatment with mIL12-F_HAB-hIL15 at a 2.5-fold increase compared with the control. As expected (40), activated CD4 Th1 cells increased and Treg cells decreased, but there was no significant change. The number of myeloid cells and total macrophages was reduced in the mIL12-F_HAB-hIL15 dose group, along with a significant increase in M1 macrophages, whereas M2 macrophages were slightly decreased. A second dose of mIL12-F_HAB-hIL15 showed the same pattern as a single dose for activated NK cells. In all cases of treatment or doses, no significant effect was observed on dendritic cells (See Supplementary Material Section 2 for T-cell gating strategy [Table S1], along with tumor [Figure S5] and spleen [Figure S6] sample results).

3.4 Toxicokinetic evaluation of SON-1210 in NHPs

In the preliminary non-GLP study that was designed to establish the MTD, SON-1210 was well tolerated up to 62.5 μg/kg in single and repeat subcutaneous doses in both males and female NHPs. Mild decreases were seen in the white blood cell count (WBC) and lymphocytes at day 3 with recovery to predose levels by days 7 to 10 for all groups. There was a mild increase in total

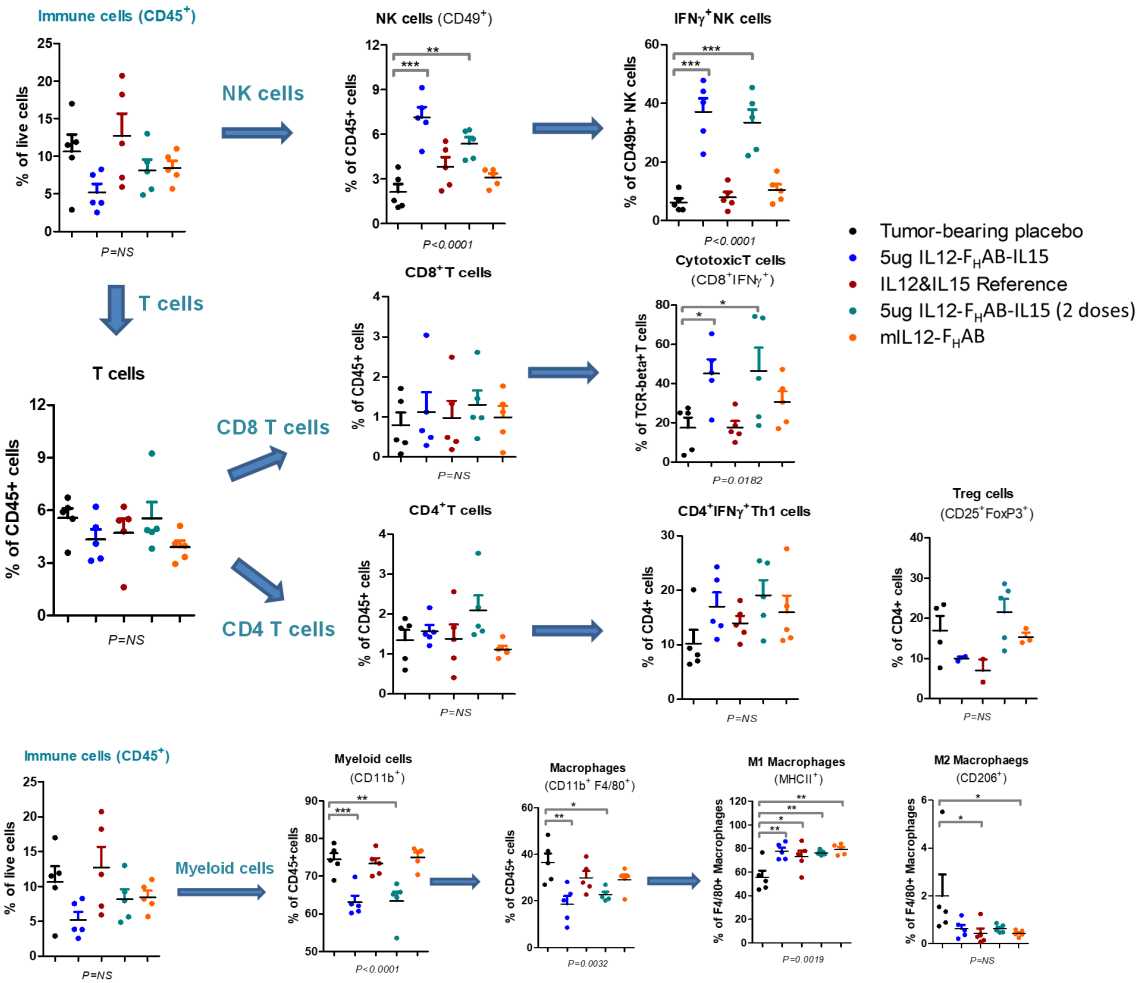

FIGURE 5
Cell Subsets in B16F10 Tumors by FACS Analysis. Flow cytometry was used to analyze the cellular distribution of tumors harvested on day 3 after one or two doses of mIL12-F_HAB-hIL15. NK cells were gated on CD45$^+$TCR$^-$CD49b$^+$, CD4 T cells on CD45$^+$TCR$^+$CD49b$^-$CD4$^+$, CD8 T cells on CD45$^+$TCR$^+$CD49b$^-$CD8$^+$, Tregs on CD45$^+$TCR$^+$CD49b$^-$CD4$^+$CD25$^+$FoxP3$^+$, and M1 vs. M2 macrophages on CD45$^+$TCR$^-$CD11b$^+$F4/80$^+$MHCII$^+$CD206$^-$ vs. CD45$^+$TCR$^-$CD11b$^+$F4/80$^+$MHCII$^-$CD206$^+$. P-values are shown as * ($p < 0.5$), ** ($p < 0.01$), *** ($p < 0.001$). The FACS gating strategy and more results are presented in Supplementary Material Section 2. The FACS analysis was done with FlowJo software (BD Biosciences).

bilirubin at day 3 with resolution by day 7, along with a mild increase in aspartate transaminase (AST) at day 7 with resolution to predose levels by day 14 or sooner for all groups. IFNγ was increased at 48 to 96 h in all groups; no responses or abnormal increases were seen in the other cytokines measured (IL-1β, IL-6, IL-8, IL-10, or TNFα). B, T, and NK cells were all decreased at day 3 by FACS analysis with general recovery by day 7 to 10 in all groups. Severe clinical abnormalities were seen in the non-GLP study after a dose of 125 μg/kg in both females at days 8 and 10, warranting euthanasia of those two NHPs. Thus, the 62.5 μg/kg dose was considered as the MTD. SON-1210 at that dose was associated with a maximum serum concentration (C_{max}) of 25 ng/mL, an area under the concentration-time curve (AUC_{∞}) of 975 h*ng/mL and a terminal half-life ($t_{½}$) of 18h.

The GLP toxicology study in cynomolgus monkeys formally evaluated the safety and tolerability of SON-1210 (Table 2). Repeated (days 1, 15, and 29) SC administration of SON-1210 at 15.6, 31.2, or 62.5 μg/kg/dose was well tolerated. Mild symptoms, consistent with rhIL-12 clinical effects in humans, occurred that were transient without off-target effects. The 'no observed adverse effect level' (NOAEL) was determined to be at least 62.50 μg/kg/dose of SON-1210, based on the overall results.

Clinical observations included transient effects, such as reduced appetite, hunched posture, and tremors, were transient and considered to be mildly adverse; no mortality related to SON-1210 was observed. SON-1210 had no effect on body weight, electrocardiographic, coagulation, or urinalysis parameters. Ophthalmic or macroscopic pathological findings were not observed. Hematology and clinical chemistry during the dosing period were indicative of affected hematopoiesis (bone marrow effect), increased red blood cell turnover, an inflammatory response, and mild dehydration. All observed findings returned to baseline during the recovery period by day 43. Following a 6-week recovery period, no SON-1210-related effects were noted, confirming the transient nature of the clinical effects of SON-1210.

Samples were collected for ADA analysis at various time points; only one of the monkeys had pre-existing IgG antibodies that recognized SON-1210. Following SON-1210 treatment, IgG ADA was detected in 14 of the 18 NHPs in the main group on day 15 and in all 18 by day 35 (Table 3) Sporadic IgM ADA was detected on days 15 and 35. Experience with administration of recombinant human cytokines to NHPs has led to the conclusion that the majority of these drugs, although inducing similar (if not identical) biologic effects, are highly immunogenic and can become neutralizing in these models (37).

The serum levels of SON-1210 (Figure 6A) were used to estimate multiple TK parameters using WinNonlin pharmacokinetic software following the first and third doses (on days 1 and 29, respectively) at specific time points 0-, 4-, 8-, 24-, 48-, 96-, and 120-h post dosing. As expected, a clear dose-dependent increase in both C_{max} and AUC_{∞} was evident overall (Table 4). The $t_{½}$ values also increased as the dose increased, yielding nonlinear toxicokinetics that may be suggestive of target mediated drug disposition (TMDD) for SON-1210. The nonlinearity of the normalized values of C_{max}/D and AUC_{∞}/D also suggest TMDD. The variability in the data combined with the relatively small group sizes (two animals per sex per dose level) precluded the observation of any trends with respect to gender differences in the toxicokinetic data from the escalating dose studies. Three animals displayed similar concentration versus time profiles for the initial and third doses. However, the ADA titers for these animals were not significantly lower than the ADA titers of other subjects.

SON-1210-related increases in IFNγ levels were observed at all doses within 24 to 48 h of SC administration (Figure 6B). However, IgG ADA appeared to suppress IFNγ responses following dosing on day 29. After the third dose on day 29 and by day 43, all cytokine levels, including plasma levels of IFNγ, IL-1β, IL-8, IL-6, IL-10, and TNFα, returned to baseline and did not suggest cytokine release syndrome. SON-1210 did not affect the absolute counts of total T lymphocytes, T helper cells, CTLs, B lymphocytes, or NK cell populations as assessed by FACS.

SON-1210 toxicity was compared to the reported toxicity of each recombinant human molecule. With SON-1210's molecular weight of 105 kDa, the percentage contributions of IL-12 (60 kDa) and IL-15 (16 kDa) to the measured TK parameters of SON-1210 were 57% and 16%, respectively. The NOAEL in this study was 35.6

TABLE 3 Anti-drug antibody (ADA) response in the NHP toxicology study.

		Pretest		Day 15		Day 35	
Dose group	Gender	IgG	IgM	IgG	IgM	IgG	IgM
0 μg/kg	**M**	–	–	–	–	–	–
	F	–	–	–	–	–	–
15.62 μg/kg	**M**	–	–	++	–	+++	–
	F	–	–	++	+	+++	–
31.25 μg/kg	**M**	–	–	++	–	+++	–
	F	+	–	++	+	+++	+
62.50 μg/kg	**M**	–	–	++	–	+++	–
	F	–	–	++	–	+++	–

NHPs were dosed with SON-1210 or placebo under GLP conditions on days 0, 15, and 29. Anti-drug antibodies (ADA) were assessed prestudy, at 15 days, and at sacrifice. ADA were analyzed as described and the highest response is shown.
-, absent; +, slight positive response; ++, definite positive response; +++, high positive response.

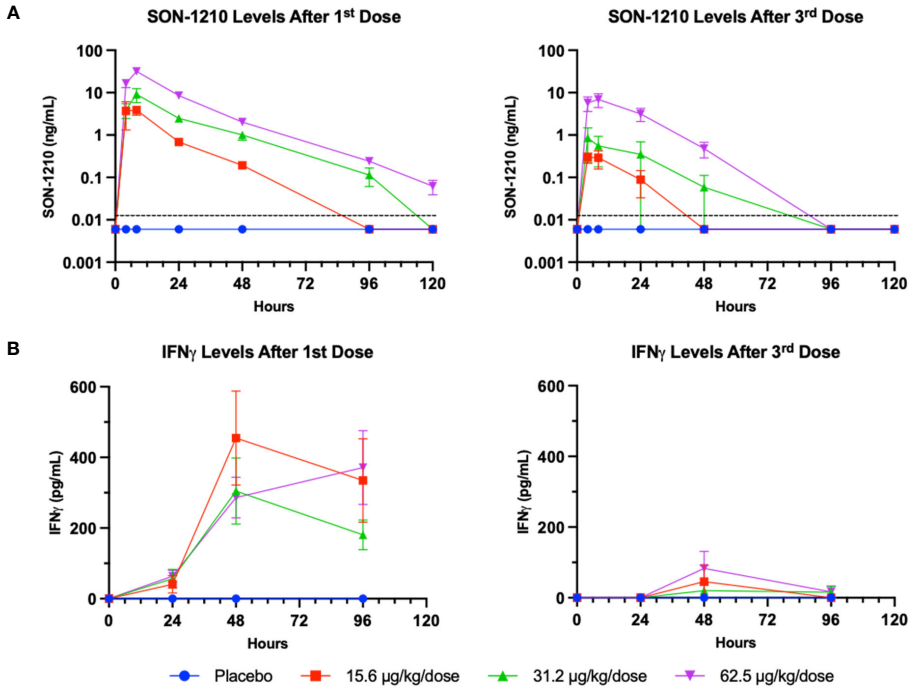

FIGURE 6
SON-1210 and IFNγ in NHP. Results from SON-1210 dosing after day 1 (left panels) and after day 29 (right panels). **(A)** A validated IL-12/IL-15 quantitative combination ELISA was used to ensure specificity. Drug levels are shown as the mean ± SEM for the SON-1210 dose response in NHP sera. The dotted black line represents the LLOQ; results below the level of quantitation are graphed as half the LLOQ by convention. **(B)** IFNγ levels were augmented after the 1st dose at all dose levels and remained elevated for at least 96 h, although a significant dose-dependent response was not observed. After the 3rd dose on day 29, a modest increase was still observed, despite the development of ADA impacting the effect of SON-1210 after the first dose.

TABLE 4 Toxicokinetic data obtained from the NHP toxicology study.

Dose (µg)	Sex	Dose Day	Group	C_{max} (ng/ml)	C_{max}/D (kg*ng/ml/µg)	T_{max} (h)	T_{last} (h)	$t_{1/2}$ (h)	AUC_{∞} (h*ng/ml)	AUC_{∞}/D (h*kg*ng/ml/µg)
17.1	*M	1	2	3.9	0.229	8	48	10.0	64.8	3.8
15.6	F	1	2	6.1	0.392	4	48	8.5	79.6	5.1
34.2	M	1	3	12.5	0.364	8	96	18.4	267.1	7.8
31.3	*F	1	3	5.8	0.185	8	48	14.0	127.0	4.1
68.4	M	1	4	34.8	0.509	8	120	18.9	715.9	10.5
62.5	F	1	4	28.6	0.457	8	120	16.6	566.0	9.1
15.6	M	29	2	0.6	0.041	8	24	ND	ND	ND
15.6	F	29	2	0.4	0.023	4	8	ND	ND	ND
31.3	M	29	3	0.5	0.017	4	8	ND	ND	ND
31.3	*F	29	3	2.1	0.066	24	48	18.0	72.7	2.3
62.5	*M	29	4	6.2	0.099	8	48	13.4	143.4	2.3
62.5	F	29	4	8.0	0.128	4	48	12.1	215.7	3.4

Pharmacokinetic parameters calculated by noncompartmental analysis (NCA) of the mean concentration versus time profiles for subjects grouped by dose and sex for the initial dose (day 1) and third repeated dose (day 29). Intended dose levels were 15.625 µg/kg (Group 2), 31.25 µg/kg (Group 3), and 62.5 µg/kg (Group 4). Note that the initial dose on day 1 for all male subjects was 1.1x higher than the doses on day 15 and day 29 due to a calculation error. All parameters are estimates, as data was limited.
* Test subjects wherein the C_{max} value had to be incorporated as one of the three points in fitting the clearance phase to calculate the $t_{1/2}$, AUC_{∞}, and AUC_{∞}/D, which is not standard practice, so the resultant values may be unreliable for these groups. ND, Not Determined; as there were less than three points in the clearance phase, even if the C_{max} was included.

μg/kg for IL-12 and 10 μg/kg for IL-15. IL-12 concentration reached a maximum at 19.5 ng/mL and 4.6 ng/mL while the maximal IL-15 concentration was 4.6 and 1.3 ng/mL after the first and second administration, respectively. These levels were well-tolerated in monkeys, representing approximately 50 times the expected dose for safety and efficacy in human clinical trials.

4 Discussion

4.1 SON-1210 Mechanism of Action

The therapeutic-enhancing properties of the F_HAB domain are rooted in its ability to bind albumin, the most abundant macromolecule in the blood (Figure 1). The F_HAB platform demonstrated high affinity for both human and monkey albumin at the serum physiological pH of 7.2 and even more so at an acidic pH, which is often present in the TME. Single-chain IL-12 and native IL-15 were successfully linked in *cis* (6) to each side of the F_HAB domain using $(GGGGS)_5$ linkers (41), creating a novel bifunctional therapeutic drug candidate called SON-1210. The G4S linker construct is water soluble, non-immunogenic, flexible, and resistant to most proteases. The number of repeats used in the construct was optimized to avoid steric hindrance of the side arms. F_HAB binds to albumin in the serum, which can target FcRn and GP60 receptors that are often upregulated in tumor endothelium to transport albumin into the TME. Tumors tend to utilize extracellular proteins as a source of amino acids to drive cellular growth (17), and the complex can bind tightly to SPARC in the acidic TME, enhancing retention and activation of local immune cells in solid tumors.

Given the complementary mechanisms of action of IL-12 and IL-15 and their cross-upregulation of receptors (2), various attempts have been made to evaluate their combined therapeutic effects in controlling the growth of tumors. For instance, SC injection of B78-H1 cells that were genetically modified to express IL-12 delayed melanoma growth in mice (42), an effect that was enhanced by IL-15 administration (43). IL-15 plays a role in preventing apoptosis of $CD8^+$ memory cells and enhancing long-term memory surveillance. On the other hand, the use of albumin combined with therapeutic molecules has been shown to enhance transport to target sites, extend residence time in the TME, and improve efficacy while reducing toxicity (44–47). Various strategies, including fusing the therapeutic agent with HSA itself, native or recombinant, or with an albumin-binding domain, have improved the characteristics of pharmacological agents that target different mechanisms of action (48, 49). Given the potential of interleukins to be powerful therapeutic agents, along with their challenging pharmacokinetic and safety profiles, resolving some of these issues by interacting with native HSA is particularly important.

We recently began to study the properties of HSA to enhance the potential therapeutic benefits of IL-12 in ongoing clinical trials of the monofunctional IL12-F_HAB molecule (SON-1010) (19, 20), which is distinct from other approaches being used to reduce its potential for toxicity (50). Alternative strategies have been employed to extend the pK of IL-12, such as linking it to an antibody (51), or to ensure a tumor effect by expressing IL-12 in oncolytic adenovirus for direct tumor injection (52, 53). Instead, we leveraged the properties of native HSA to target tumor tissue using the F_HAB platform to extend the PK of IL-12 in humans, resulting in prolonged but controlled induction of IFNγ and decreased toxicity (19).

4.2 Characterization of the F_HAB and SON-1210

To begin to characterize SON-1210, we sought to establish the best species to use as a model for further study and found that monkey albumin was closest to human albumin in its affinity to the F_HAB domain using SPR, compared to rat, hamster, and canine albumin (Figure 2). The initial PK analysis of the F_HAB platform was done in mice, comparing mIL12-F_HAB or hIL15-F_HAB to mIL-12 or hIL-15, respectively. The His-tagged versions of these molecules were produced to ensure that the native cytokines would not interfere with quantitation of each recombinant product. Extended PK of the SON-1210 molecule was subsequently confirmed in monkeys; further demonstration of the PK of the bifunctional molecule is planned for the first clinical study. SON-1210 promoted lymphocyte proliferation about the same as hIL-12 or hIL-15 *in vitro*. However, even though hIL12-F_HAB (SON-1010) induced a similar amount of IFNγ release compared to hIL-12 *in vitro*, when both cytokines were present on the F_HAB backbone substantially more IFNγ was produced by SON-1210, presumably due to the added IL-15 moiety that amplified the release. Finally, a biodistribution study of His-tagged mIL12-F_HAB was done in mice that showed up to 3.1-fold increase in tumor accumulation compared to mIL-12 with prolonged tumor suppression.

SON-1210 was then studied using material manufactured for clinical use (Figure 3). Drug substance was produced using continuous perfusion after process development and qualification. The observed MW of 115 kDa by SDS-PAGE is consistent with appropriate glycosylation. Purity of > 97% was established by SE-HPLC. Charge heterogeneity is expected in biological products manufactured in CHO cells and can be demonstrated by iCIEF; SON-1210 showed mild variability, presumably due to glycosylation, and the results were within established specifications to proceed to further processing. Potency required evaluation of STAT4 activation by the IL-12 moiety, as well as STAT5 activation by the IL-15 moiety; HEK-Blue assays were used with specific cell lines to show SEAP induction in each case. Functional activity was established by detection of IFNγ release from human PBMCs. While macaque PBMCs were also able to release IFNγ, the quantity was expected to be less due to species differences in the native cytokines and receptors (37). Finally, the ability to stimulate T-cell proliferation was compared to the individual cytokines in the presence of antibody that blocked the complementing cytokine; SON-1210 outperformed both hIL-15 and hIL12-F_HAB (SON-1010) used as controls.

Compared to the individual hIL-12 and hIL-15 interleukins, hIL12-F_HAB-hIL15 showed similar proliferative activity *in vitro* (Figure 2). The ability to induce proliferation by each cytokine was also shown in isolation by blocking the complementary cytokine (Figure 3). When the cytokines were presented in *cis* and linked on the F_HAB and studied using mIL12-F_HAB-hIL15 *in vivo*, they

showed greater tumor growth suppression and survival efficacy compared to the individual cytokines, even when those were used together (Figure 4). While three doses of the F_HAB construct administered two days apart resulted in an even stronger suppression of tumor growth, this dosing strategy resulted in increased toxicity. As ADA could not have impacted the dose response in this timeframe, the closely spaced doses in the mice resulted in a marked induction of IFNγ, IL-10, and IL-12. This scenario is reminiscent of the severe toxicity observed in the first Phase 2 clinical study that started with repeated daily dosing of recombinant hIL-12, even though the original Phase 1 dose escalation study had been so successful when a 'test dose' had been given two weeks before daily dosing (54, 55). The difference between the safety results in the two rhIL-12 clinical studies can be ascribed to tachyphylaxis caused by induction of the suppressors of cytokine signaling (SOCS) (56), a class of cellular proteins that participate in negative feedback regulation of cytokine signaling. SOCS proteins appear to have allowed the toxic effects of IFNγ to be restrained in the Phase 1 study of rhIL-12. The lack of feedback and severe toxicity associated with immediate daily dosing in the Phase 2 study may have been similar to the aggravated toxicity in our B16F10 mouse tumor model, which we found when three doses of mIL12-F_HAB-hIL15 were given every other day. If enough time is allowed before a second dose, the SOCS proteins can be induced to limit IFNγ toxicity.

Pharmacodynamic responses in the mice (Figure 4) and NHPs (Figure 6) showed moderate and prolonged increases in IFNγ levels with mild increases in other inflammatory cytokines, rapidly reversible cytopenia, and mild (except with 3x dosing in the mice) ALT elevation. FACS analysis in mice (Figure 5) showed a significant induction of activated T- and NK-cell responses, along with the conversion of M2 MDSCs to M1 APCs. Our *in vitro* data suggest that SON-1210 should stimulate the expected mechanisms associated with the therapeutic efficacy of the molecule, particularly T- and NK-cell stimulation and IFNγ production, which is important for local tumor surveillance (57). Such an effect has been previously reported using IL-15 attached to an albumin construct alone or in combination with a PD-L1 inhibitor (58, 59). Based on our FACS data, we conclude that treatment with mIL12-F_HAB-hIL15 transformed the "cold" B16F10 tumor into a "hot" tumor. Interestingly, administration of equimolar doses of IL-12 and IL-15 failed to fully reproduce these effects in our model. These improved PD effects, compared to native interleukins, may be attributed to the F_HAB platform's tumor targeting by binding to albumin (17) and *cis* presentation of IL-12 and IL-15 (6), resulting in extended *in vivo* $t_{½}$ and tumor retention for prolonged cytokine presentation to immune cells in the TME with limited toxicity.

4.3 Impact of Extended PK and Tumor Targeting by F_HAB

The F_HAB platform exhibits three pivotal characteristics *in vivo*: i) an enhanced $t_{½}$ owing to the binding of albumin, ii) targeting of tumor tissue by binding to FcRn and GP60 receptors that are overexpressed in many solid tumors, and iii) retention in the acidic TME upon binding or rebinding to SPARC. Although we are currently focused on solid tumor indications, these findings suggest that the F_HAB platform offers significant flexibility, allowing one or two therapeutic payloads for various modalities to benefit from $t_{½}$ extension and/or HSA-based targeting of tumors and lymph nodes. While the current clinical product candidates have cytokines on either side, the F_HAB platform can host various payloads, such as antibody motifs or other small molecules, as single- or bi-functional constructs, leveraging the F_HAB's on-off mechanism to gently interact with host tissues. The F_HAB platform can bind, dissociate, and re-bind to albumin, setting up a dynamic equilibrium and slow elimination, allowing lower doses to be delivered and retained in the TME with greater effect in that space to enhance the therapeutic index. This is in contrast to drugs that use static covalent attachment to HSA or specific tumor targets, which typically do not re-bind, leaving the drug in its first location (45).

Our results suggest that by directing therapeutic cytokines to the TME using SON-1210, the anticipated therapeutic efficacy based on their biological activity can be achieved. In addition, our approach addresses the paramount safety and tolerability factors, which have traditionally hindered the use of therapeutic cytokines in the treatment of solid tumors, by improving the therapeutic index. The candidate drug activates the immune response in the TME, which upregulates IFNγ and increases PD-L1 expression, potentially making checkpoint inhibitors more active (25). It can also be combined with cell-based therapy to extend the half-life and activity of CAR-T cells (60). This novel approach could help to redefine the cancer battle and the results presented here position SON-1210 for its initial human cancer trials.

Data availability statement

The raw data supporting the conclusions of this article will be made available by the authors, without undue reservation.

Ethics statement

Ethical approval was not required for the studies on humans in accordance with the local legislation and institutional requirements because only commercially available established cell lines were used. The animal studies were approved by Institutional Animal Care and Use Committee (IACUC) of Invivotek and the IACUC of Charles River Laboratories. The studies were conducted in accordance with the local legislation and institutional requirements.

Author contributions

JC: Conceptualization, Data curation, Formal Analysis, Methodology, Project administration, Supervision, Writing – original draft, Writing – review & editing, Software. SD: Writing – original draft, Writing – review & editing, Conceptualization, Data curation, Project administration, Supervision. DR: Conceptualization, Data curation, Formal Analysis, Writing – original draft, Writing – review & editing. SM: Conceptualization,

Formal Analysis, Project administration, Supervision, Writing – original draft, Writing – review & editing. GH: Data curation, Formal Analysis, Visualization, Writing – original draft, Writing – review & editing. RB: Conceptualization, Data curation, Formal Analysis, Investigation, Methodology, Supervision, Writing – review & editing. RE: Data curation, Formal Analysis, Investigation, Methodology, Software, Supervision, Validation, Visualization, Writing – review & editing. RK: Conceptualization, Data curation, Formal Analysis, Visualization, Writing – original draft, Writing – review & editing, Software, Validation. PM: Conceptualization, Funding acquisition, Project administration, Supervision, Writing – original draft, Writing – review & editing.

Funding

The author(s) declare financial support was received for the research, authorship, and/or publication of this article. This study was supported by Sonnet BioTherapeutics.

Acknowledgments

The authors wish to thank Miglena Prabagar for her excellent work on *in vivo* experiments at Invivotek LLC. Portions of this work were reported at the AACR Annual Meeting, New Orleans, 2022.

Conflict of interest

JC, SD, SM, GH, RK, and PM were employed and have stock in Sonnet BioTherapeutics. DR was employed by the Latham Biopharm Group, a consultant for Sonnet BioTherapeutics. RB was employed by, and has stock in, InfinixBio, a contract research laboratory. R-NE was employed by Invivotek, a contracted research laboratory.

Publisher's note

Supplementary material

The Supplementary Material for this article can be found online at: https://www.frontiersin.org/articles/10.3389/fimmu.2023.1326927/full#supplementary-material

References

1. Del Vecchio M, Bajetta E, Canova S, Lotze MT, Wesa A, Parmiani G, et al. Interleukin-12: biological properties and clinical application. *Clin Cancer Res Off J Am Assoc Cancer Res* (2007) 13(16):4677–85. doi: 10.1158/1078-0432.CCR-07-0776

2. Propper DJ, Balkwill FR. Harnessing cytokines and chemokines for cancer therapy. *Nat Rev Clin Oncol* (2022) 19(4):237–53. doi: 10.1038/s41571-021-00588-9

3. Voest EE, Kenyon BM, O'Reilly MS, Truitt G, D'Amato RJ, Folkman J. Inhibition of angiogenesis in *vivo* by interleukin 12. *J Natl Cancer Inst* (1995) 87(8):581–6. doi: 10.1093/jnci/87.8.581

4. Albini A, Brigati C, Ventura A, Lorusso G, Pinter M, Morini M, et al. Angiostatin anti-angiogenesis requires IL-12: the innate immune system as a key target. *J Trans Med* (2009) 7:5. doi: 10.1186/1479-5876-7-5

5. Sorensen EW, Gerber SA, Frelinger JG, Lord EM. IL-12 suppresses vascular endothelial growth factor receptor 3 expression on tumor vessels by two distinct IFN-gamma-dependent mechanisms. *J Immunol* (2010) 184(4):1858–66. doi: 10.4049/jimmunol.0903210

6. Cany J, van der Waart AB, Spanholtz J, Tordoir M, Jansen JH, van der Voort R, et al. Combined IL-15 and IL-12 drives the generation of CD34(+)-derived natural killer cells with superior maturation and alloreactivity potential following adoptive transfer. *Oncoimmunology* (2015) 4(7):e1017701. doi: 10.1080/2162402X.2015.1017701

7. Ferlazzo G, Pack M, Thomas D, Paludan C, Schmid D, Strowig T, et al. Distinct roles of IL-12 and IL-15 in human natural killer cell activation by dendritic cells from secondary lymphoid organs. *Proc Natl Acad Sci United States America* (2004) 101 (47):16606–11. doi: 10.1073/pnas.0407522101

8. Awad RM, De Vlaeminck Y, Meeus F, Ertveldt T, Zeven K, Ceuppens H, et al. *In vitro* modelling of local gene therapy with IL-15/IL-15Ralpha and a PD-L1 antagonist in melanoma reveals an interplay between NK cells and CD4(+) T cells. *Sci Rep* (2023) 13(1):18995. doi: 10.1038/s41598-023-45948-w

9. LV B, Wang Y, Ma D, Cheng W, Liu J, Yong T, et al. Immunotherapy: reshape the tumor immune microenvironment. *Front Immunol* (2022) 13:844142. doi: 10.3389/fimmu.2022.844142

10. Pitt JM, Marabelle A, Eggermont A, Soria JC, Kroemer G, Zitvogel L. Targeting the tumor microenvironment: removing obstruction to anticancer immune responses and immunotherapy. *Ann Oncol Off J Eur Soc Med Oncol ESMO* (2016) 27(8):1482–92. doi: 10.1093/annonc/mdw168

11. Gao S, Hsu TW, Li MO. Immunity beyond cancer cells: perspective from tumor tissue. *Trends Cancer* (2021) 7(11):1010–9. doi: 10.1016/j.trecan.2021.06.007

12. Yang M, Li J, Gu P, Fan X. The application of nanoparticles in cancer immunotherapy: Targeting tumor microenvironment. *Bioact Mater* (2021) 6 (7):1973–87. doi: 10.1016/j.bioactmat.2020.12.010

13. Huang H, Haenssen K, Bhate A, Sanglikar S, Baradei J, Liu S, et al. Enhanced efficacy of immune modulators with albumin binding domains (ABD). *Mol Cancer Ther* (2018) 17(1_Supplement):B004. doi: 10.1158/1535-7163.TARG-17-B004

14. Cini JK, Huang H. inventors. Albumin-binding domain fusion proteins. (2019) 16:2017. Available at: https://patentimages.storage.googleapis.com/dc/ab/41/134f48deb1d391/US20190016793A1.pdf

15. Sand KM, Bern M, Nilsen J, Noordzij HT, Sandlie I, Andersen JT. Unraveling the interaction between fcRn and albumin: opportunities for design of albumin-based therapeutics. *Front Immunol* (2014) 5:682. doi: 10.3389/fimmu.2014.00682

16. Hassanin I, Elzoghby A. Albumin-based nanoparticles: a promising strategy to overcome cancer drug resistance. *Cancer Drug Resist* (2020) 3(4):930–46. doi: 10.20517/cdr.2020.68

17. Hoogenboezem EN, Duvall CL. Harnessing albumin as a carrier for cancer therapies. *Advanced Drug Delivery Rev* (2018) 130:73–89. doi: 10.1016/j.addr.2018.07.011

18. Cini J, McAndrew S, Evans N, Eraslan RN, Prabagar MG, Dexter S, et al. An innovative human platform for targeted delivery of bispecific interleukins to tumors. *Cancer Res* (2022) 82(12_Supplement):4229. doi: 10.1158/1538-7445.AM2022-4229

19. Chawla SP, Chua V, Gordon E, Cini J, Dexter S, DaFonseca M, et al. Clinical development of a novel form of interleukin-12 with extended pharmacokinetics. *Cancer Res* (2023) 83(8_Supplement):CT245. doi: 10.1158/1538-7445.AM2023-CT245

20. NLM. Combination of SON-1010 (IL12-FHAB) and atezolizumab in patients with platinum-resistant ovarian cancer (NCT05756907). (2023). Available at: https://clinicaltrials.gov/study/NCT05756907

21. Weiss JM, Subleski JJ, Wigginton JM, Wiltrout RH. Immunotherapy of cancer by IL-12-based cytokine combinations. *Expert Opin Biol Ther* (2007) 7(11):1705–21. doi: 10.1517/14712598.7.11.1705

22. Waldmann TA. Cytokines in cancer immunotherapy. *Cold Spring Harb Perspect Biol* (2018) 10(12):1–23. doi: 10.1101/cshperspect.a028472

23. Uppendahl LD, Dahl CM, Miller JS, Felices M, Geller MA. Natural killer cell-based immunotherapy in gynecologic Malignancy: A review. *Front Immunol* (2017) 8:1825. doi: 10.3389/fimmu.2017.01825

24. Garris CS, Arlauckas SP, Kohler RH, Trefny MP, Garren S, Piot C, et al. Successful anti-PD-1 cancer immunotherapy requires T cell-dendritic cell crosstalk involving the cytokines IFN-gamma and IL-12. *Immunity* (2018) 49(6):1148–61 e7. doi: 10.1016/j.immuni.2018.09.024

25. Rahimi Kalateh Shah Mohammad G, Ghahremanloo A, Soltani A, Fathi E, Hashemy SI. Cytokines as potential combination agents with PD-1/PD-L1 blockade for cancer treatment. *J Cell Physiol* (2020) 235(7-8):5449–60. doi: 10.1002/jcp.29491

26. Sneller MC, Kopp WC, Engelke KJ, Yovandich JL, Creekmore SP, Waldmann TA, et al. IL-15 administered by continuous infusion to rhesus macaques induces massive expansion of CD8+ T effector memory population in peripheral blood. *Blood* (2011) 118(26):6845–8. doi: 10.1182/blood-2011-09-377804

27. Choi JN, Sun EG, Cho SH. IL-12 enhances immune response by modulation of myeloid derived suppressor cells in tumor microenvironment. *Chonnam Med J* (2019) 55(1):31–9. doi: 10.4068/cmj.2019.55.1.31

28. Robinson TO, Schluns KS. The potential and promise of IL-15 in immuno-oncogenic therapies. *Immunol Lett* (2017) 190:159–68. doi: 10.1016/j.imlet.2017.08.010

29. Isvoranu G, Surcel M, Munteanu AN, Bratu OG, Ionita-Radu F, Neagu MT, et al. Therapeutic potential of interleukin-15 in cancer (Review). *Exp Ther Med* (2021) 22 (1):675. doi: 10.3892/etm.2021.10107

30. Orengo AM, Di Carlo E, Comes A, Fabbi M, Piazza T, Cilli M, et al. Tumor cells engineered with IL-12 and IL-15 genes induce protective antibody responses in nude mice. *J Immunol* (2003) 171(2):569–75. doi: 10.4049/jimmunol.171.2.569

31. Huang H, Luo Y, Baradei H, Liu S, Haenssen KK, Sanglikar S, et al. A novel strategy to produce high level and high purity of bioactive IL15 fusion proteins from mammalian cells. *Protein Expr Purif* (2018) 148:30–9. doi: 10.1016/j.pep.2018.03.010

32. Friguet B, Chaffotte AF, Djavadi-Ohaniance L, Goldberg ME. Measurements of the true affinity constant in solution of antigen-antibody complexes by enzyme-linked immunosorbent assay. *J Immunol Methods* (1985) 77(2):305–19. doi: 10.1016/0022-1759(85)90044-4

33. Vallabhajosula S, Nikolopoulou A, Babich JW, Osborne JR, Tagawa ST, Lipai I, et al. 99mTc-labeled small-molecule inhibitors of prostate-specific membrane antigen: pharmacokinetics and biodistribution studies in healthy subjects and patients with metastatic prostate cancer. *J Nucl Med Off Publication Soc Nucl Med* (2014) 55 (11):1791–8. doi: 10.2967/jnumed.114.140426

34. Sosic Z, Houde D, Blum A, Carlage T, Lyubarskaya Y. Application of imaging capillary IEF for characterization and quantitative analysis of recombinant protein charge heterogeneity. *Electrophoresis* (2008) 29(21):4368–76. doi: 10.1002/elps.200800157

35. Xue D, Moon B, Liao J, Guo J, Zou Z, Han Y, et al. A tumor-specific pro-IL-12 activates preexisting cytotoxic T cells to control established tumors. *Sci Immunol* (2022) 7(67):eabi6899. doi: 10.1126/sciimmunol.abi6899

36. McArdel SL, Dugast AS, Hoover ME, Bollampalli A, Hong E, Castano Z, et al. Anti-tumor effects of RTX-240: an engineered red blood cell expressing 4-1BB ligand and interleukin-15. *Cancer Immunol Immunother* (2021) 70(9):2701–19. doi: 10.1007/s00262-021-03001-7

37. Villinger F, Brar SS, Mayne A, Chikkala N, Ansari AA. Comparative sequence analysis of cytokine genes from human and nonhuman primates. *J Immunol* (1995) 155 (8):3946–54. doi: 10.4049/jimmunol.155.8.3946

38. Tortorella C, Pisconti A, Piazzolla G, Antonaci S. APC-dependent impairment of T cell proliferation in aging: role of CD28- and IL-12/IL-15-mediated signaling. *Mech Ageing Dev* (2002) 123(10):1389–402. doi: 10.1016/S0047-6374(02)00079-9

39. Overwijk WW, Restifo NP. B16 as a mouse model for human melanoma. *Curr Protoc Immunol* (2001) 39:20.1.1–20.1.29. doi: 10.1002/0471142735.im2001s39

40. Zhao J, Zhao J, Perlman S. Differential effects of IL-12 on Tregs and non-Treg T cells: roles of IFN-gamma, IL-2 and IL-2R. *PloS One* (2012) 7(9):e46241. doi: 10.1371/journal.pone.0046241

41. Chen X, Zaro JL, Shen WC. Fusion protein linkers: property, design and functionality. *Advanced Drug Delivery Rev* (2013) 65(10):1357–69. doi: 10.1016/j.addr.2012.09.039

42. Lasek W, Basak G, Switaj T, Jakubowska AB, Wysocki PJ, Mackiewicz A, et al. Complete tumour regressions induced by vaccination with IL-12 gene-transduced tumour cells in combination with IL-15 in a melanoma model in mice. *Cancer Immunol Immunother* (2004) 53(4):363–72. doi: 10.1007/s00262-014-1523-1

43. Kimura K, Nishimura H, Matsuzaki T, Yokokura T, Nimura Y, Yoshikai Y. Synergistic effect of interleukin-15 and interleukin-12 on antitumor activity in a murine Malignant pleurisy model. *Cancer Immunol Immunother* (2000) 49(2):71–7. doi: 10.1007/s002620050604

44. Mester S, Evers M, Meyer S, Nilsen J, Greiff V, Sandlie I, et al. Extended plasma half-life of albumin-binding domain fused human IgA upon pH-dependent albumin engagement of human FcRn in *vitro* and in vivo. *MAbs* (2021) 13(1):1893888. doi: 10.1080/19420862.2021.1893888

45. Pilati D, Howard KA. Albumin-based drug designs for pharmacokinetic modulation. *Expert Opin Drug Metab Toxicol* (2020) 16(9):783–95. doi: 10.1080/17425255.2020.1801633

46. Tao C, Chuah YJ, Xu C, Wang DA. Albumin conjugates and assemblies as versatile bio-functional additives and carriers for biomedical applications. *J Mater Chem B* (2019) 7(3):357–67. doi: 10.1039/C8TB02477D

47. Tao HY, Wang RQ, Sheng WJ, Zhen YS. The development of human serum albumin-based drugs and relevant fusion proteins for cancer therapy. *Int J Biol Macromol* (2021) 187:24–34. doi: 10.1016/j.ijbiomac.2021.07.080

48. Zhang Y, Sun T, Jiang C. Biomacromolecules as carriers in drug delivery and tissue engineering. *Acta Pharm Sin B* (2018) 8(1):34–50. doi: 10.1016/j.apsb.2017.11.005

49. Kratz F, Elsadek B. Clinical impact of serum proteins on drug delivery. *J Control Release* (2012) 161(2):429–45. doi: 10.1016/j.jconrel.2011.11.028

50. Jia Z, Ragoonanan D, Mahadeo KM, Gill J, Gorlick R, Shpal E, et al. IL12 immune therapy clinical trial review: Novel strategies for avoiding CRS-associated cytokines. *Front Immunol* (2022) 13:952231. doi: 10.3389/fimmu.2022.952231

51. Strauss J, Heery CR, Kim JW, Jochems C, Donahue RN, Montgomery AS, et al. First-in-human phase I trial of a tumor-targeted cytokine (NHS-IL12) in subjects with metastatic solid tumors. *Clin Cancer Res Off J Am Assoc Cancer Res* (2019) 25(1):99–109. doi: 10.1158/1078-0432.CCR-18-1512

52. Choi IK, Lee JS, Zhang SN, Park J, Sonn CH, Lee KM, et al. Oncolytic adenovirus co-expressing IL-12 and IL-18 improves tumor-specific immunity via differentiation of T cells expressing IL-12Rbeta2 or IL-18Ralpha. *Gene Ther* (2011) 18(9):898–909. doi: 10.1038/gt.2011.37

53. Barton KN, Siddiqui F, Pompa R, Freytag SO, Khan G, Dobrosotskaya I, et al. Phase I trial of oncolytic adenovirus-mediated cytotoxic and interleukin-12 gene therapy for the treatment of metastatic pancreatic cancer. *Mol Ther Oncolytics* (2021) 20:94–104. doi: 10.1016/j.omto.2020.11.006

54. Atkins MB, Robertson MJ, Gordon M, Lotze MT, DeCoste M, DuBois JS, et al. Phase I evaluation of intravenous recombinant human interleukin 12 in patients with advanced Malignancies. *Clin Cancer Res Off J Am Assoc Cancer Res* (1997) 3(3):409–17. Available at: https://www.ncbi.nlm.nih.gov/pubmed/9815699

55. Leonard JP, Sherman ML, Fisher GL, Buchanan LJ, Larsen G, Atkins MB, et al. Effects of single-dose interleukin-12 exposure on interleukin-12-associated toxicity and interferon-gamma production. *Blood* (1997) 90(7):2541–8. Available at: https://www.ncbi.nlm.nih.gov/pubmed/9326219

56. Sobah ML, Liongue C, Ward AC. SOCS proteins in immunity, inflammatory diseases, and immune-related cancer. *Front Med (Lausanne)* (2021) 8:727987. doi: 10.3389/fmed.2021.727987

57. Riemensberger J, Bohle A, Brandau S. IFN-gamma and IL-12 but not IL-10 are required for local tumour surveillance in a syngeneic model of orthotopic bladder cancer. *Clin Exp Immunol* (2002) 127(1):20–6. doi: 10.1046/j.1365-2249.2002.01734.x

58. Hsu FT, Liu YC, Tsai CL, Yueh PF, Chang CH, Lan KL. Preclinical evaluation of recombinant human IL15 protein fused with albumin binding domain on anti-PD-L1 immunotherapy efficiency and anti-tumor immunity in colon cancer and melanoma. *Cancers* (2021) 13(8):1–25. doi: 10.3390/cancers13081789

59. Hsu FT, Tsai CL, Chiang IT, Lan KH, Yueh PF, Liang WY, et al. Synergistic effect of Abraxane that combines human IL15 fused with an albumin-binding domain on murine models of pancreatic ductal adenocarcinoma. *J Cell Mol Med* (2022) 26 (7):1955–68. doi: 10.1111/jcmm.17220

60. Silveira CRF, Corveloni AC, Caruso SR, Macedo NA, Brussolo NM, Haddad F, et al. Cytokines as an important player in the context of CAR-T cell therapy for cancer: Their role in tumor immunomodulation, manufacture, and clinical implications. *Front Immunol* (2022) 13:947648. doi: 10.3389/fimmu.2022.947648

frontiers | Frontiers in Immunology

TYPE Case Report
PUBLISHED 20 December 2023
DOI 10.3389/fimmu.2023.1277810

OPEN ACCESS

EDITED BY
Gulderen Yanikkaya Demirel,
Yeditepe University, Türkiye

REVIEWED BY
Yanxun Han,
First Affiliated Hospital of Anhui Medical University, China
Bin Li,
Shanghai Jiao Tong University, China

*CORRESPONDENCE
Juan Du
dujuanglyy@163.com
Weiwei Kong
kongvv@126.com
Baorui Liu
baoruiliu@nju.edu.cn

†These authors have contributed equally to this work

RECEIVED 15 August 2023
ACCEPTED 07 December 2023
PUBLISHED 20 December 2023

CITATION
Tong F, Sun Y, Zhu Y, Sha H, Ni J, Qi L, Gu Q, Zhu C, Xi W, Liu B, Kong W and Du J (2023) Making "cold" tumors "hot"-radiotherapy remodels the tumor immune microenvironment of pancreatic cancer to benefit from immunotherapy: a case report. *Front. Immunol.* 14:1277810. doi: 10.3389/fimmu.2023.1277810

Making "cold" tumors "hot"-radiotherapy remodels the tumor immune microenvironment of pancreatic cancer to benefit from immunotherapy: a case report

Fan Tong[1,2†], Yi Sun[1†], Yahui Zhu[1], Huizi Sha[1], Jiayao Ni[1,2], Liang Qi[1], Qing Gu[3], Chan Zhu[4], Wenjing Xi[4], Baorui Liu[1*], Weiwei Kong[1*] and Juan Du[1,2*]

[1]Department of oncology, Nanjing Drum Tower Hospital, Affiliated Hospital of Medical School, Nanjing University, Nanjing, China, [2]The Comprehensive Cancer Center of Drum Tower Hospital, Clinical College of Traditional Chinese and Western Medicine, Nanjing University of Chinese Medicine, Nanjing, China, [3]National Institute of Healthcare Data Science, Nanjing University, Nanjing, China, [4]State Key Laboratory of Neurology and Oncology Drug Development Jiangsu Simcere Diagnostics Co, Ltd, Nanjing, China

Immune checkpoint inhibitors have limited efficacy in metastatic pancreatic cancer due to the complex tumor immune microenvironment (TIME). Studies have shown that radiotherapy can cause cell lesions to release tumor antigens and then take part in the remodeling of the tumor environment and the induction of ectopic effects *via* regional and systemic immunoregulation. Here, we reported a case of advanced metastatic pancreatic cancer treated with immunotherapy combined with chemotherapy and radiotherapy and a sharp shift of the TIME from T3 to T2 was also observed. One hepatic metastasis within the planning target volume (PTV) was evaluated complete response (CR), the other one was evaluated partial response (PR) and 2 hepatic metastases outside the PTV were surprisingly considered PR. In the study, we found that immunotherapy combined with chemotherapy and radiotherapy achieved significant therapeutic benefits, which may provide a new strategy for the treatment of advanced pancreatic cancer.

KEYWORDS

immune checkpoint inhibitors, tumor immune microenvironment, radiotherapy, metastatic pancreatic cancer, second-line treatment

1 Introduction

Pancreatic cancer has very poor prognosis with a 5-year survival rate of only 8% (1). About 50% of patients with pancreatic cancer are diagnosed at an advanced stage (2) and there is no clear consensus on the second-line treatment when first-line treatment based on gemcitabine fails.

In recent years, immune checkpoint inhibitors (ICIs) have achieved decisive breakthroughs in many solid tumors (3–5), but the efficacy of ICIs in pancreatic cancer is still confronted with challenges. The complex TIME of pancreatic cancer limits the effectiveness of ICIs (6), but more and more clinical studies and experiments have proved that radiotherapy combined with immunotherapy can regulate the TIME, so as to strengthen the control of tumor (7, 8).

Here, we presented an advanced pancreatic cancer case with robust survival benefit from immunotherapy combined with chemotherapy and radiotherapy, while obvious TIME remodeling and an ectopic effect were also observed. Briefly, this comprehensive treatment mode remodulated pancreatic cancer from "cold" tumors to "hot" tumors in our case.

2 Case presentation

We presented a case of a 59-year-old male who was hospitalized with intermittent upper abdominal pain in October 2021. Contrast-enhanced computed tomography (CT) scan showed a 2.2cm x 2cm mass at the neck of the pancreas with distal pancreatic duct dilatation (Figure 1A). The mass was closely related to the splenic vein. But after discussion, the Multiple Disciplinary Team (MDT) believed that the patient was also accompanied by superior mesenteric artery (SMA) invasion less than 180° (Figure 1B). But no distant metastasis was detected at that time. In addition, the baseline value of carbohydrate antigen 19-9 (CA19-9) was 12.99 U/ml. Endoscopic ultrasound-guided fine-needle aspiration (EUS-FNA) was performed and subsequently cancer cells were verified pathologically (Figure 1C). The patient was definitely diagnosed with borderline resectable pancreatic cancer based on pathology and imaging. But the patient refused to consider the possibility of follow-up operation firmly at the very start.

From November 2021 to March 2022, the patient received 5 cycles (21 days for one complete cycle) of gemcitabine 1000 mg/m2 and nab-paclitaxel 125 mg/m2 on day 1 and day 8 and the patient stayed a stable disease. After 5 cycles of the treatment, CA19-9 increased to 76.7U/ml. In addition, CT scan revealed that the size of pancreatic primary tumor had increased remarkably and four new hepatic masses appeared (Figure 1G-T1). Pathology for Ultrasound guided biopsy of the hepatic mass was concordant with liver metastasis of pancreatic ductal adenocarcinoma (Figure 1D). The patient was assessed progressive disease (PD).

Subsequently, S-1 plus oxaliplatin combined with immunotherapy and radiotherapy were used in second-line treatment. In detail, the patient received 3 cycles of S-1 80mg/day on day1-14 plus oxaliplatin 130mg/m2 on day 1 and Sintilimab 200mg on day 1 (21 days for a complete cycle) while 8Gy*3 fractions radiotherapy of liver metastases within PTV was conducted before Cycle2 started (Figure 2A).

After finishing 3 cycles of this treatment, the patient developed toxic epidermal necrolysis (TEN) and after the Multiple Disciplinary Team (MDT) discussion, the experts unanimously assessed TEN as immune-related adverse event (irAE). After methylprednisolone, anti-infection, fluid infusion treatment, his symptoms quickly relieved (Figure 2B) and tumor marker CA19-9 decreased to 19.2 U/ml by the TIME. CT scan revealed that the primary pancreatic tumor and hepatic metastases had both shrunk remarkably (Figure 1G-T2). Surprisingly, a hepatic metastasis within the scope of radiotherapy had disappeared in CT scan. Obvious inflammatory cell infiltration was confirmed by pathology and no cancer cells was found in the biopsy tissues (Figure 1E). One hepatic metastasis within the scope of radiotherapy was assessed CR, the other one was evaluated PR, and other two hepatic metastases outside the scope of radiotherapy were also considered PR according to the Response Evaluation Criteria in Solid Tumors (RECIST1.1) criteria.

We conducted the SOX regimen for another 3 cycles when symptoms related to TEN were greatly relieved. At the time, CA19-9 decreased to 6.94U/ml and all tumors continued to shrink as CT indicated (Figure 1G-T3). Tumor diameter changes were demonstrated in Figure 1F. The concomitant changes of CA199 and timeline of events were demonstrated in Figure 3 in details.

To comprehensively assess the alteration of TIME before and after treatment, we performed multiplexed immunofluorescence histochemical (mIHC) analysis at the protein level and gene expression analysis at the RNA level on M2 hepatic metastasis prior and post treatment, respectively. The spatial immune microenvironments of tumor tissues prior (Figure 4A) and post treatment (Figure 4B) were shown by mIHC assay. The relative values of CD8+, CD68+, CD163+, Foxp3+, and PD-L1+ were 7.74, 3.9, 1.91, 2.84, and 0.69 respectively, showing a high infiltration of immune cells and low expression of PD-L1 (subtype TIME-3, immune escape type). After 3 cycles of immunotherapy combined chemoradiotherapy, the relative values of CD8+, CD68+, CD163+, Foxp3+, and PD-L1+ were 19.02, 6.06, 30.44, 8.11, and 21.76 respectively, showing a high infiltration of immune cells and high expression of PD-L1 (subtype TIME-2, immune response type). The RNA-level expression assay of TIME was detected by 289 immune-related genes (NanoString Technologies, Seattle, USA) at Jiangsu Simcere Diagnostics Co., Ltd, and the selection of immune-related genes is shown in Supplementary Materials. The abundance of immune cells related with the tumor microenvironment was shown in Figure 4C, and the abundances of all immune cells were elevated to different degrees, and other immune signatures in Figure 4D.

Abbreviations: TIME, tumor immune microenvironment; CR, complete response; PR, partial response; ICIs, immune checkpoint inhibitors; CT, contrast-enhanced computed tomography; EUS-FNA, endoscopic ultrasound-guided fine-needle aspiration biopsy; PD, progressive disease; TEN, toxic epidermal necrolysis; MDT, multiple Disciplinary Team; irAE, immune-related adverse event; RECIST, Response Evaluation Criteria in Solid Tumors; mIHC, multiplexed immunofluorescence histochemical.

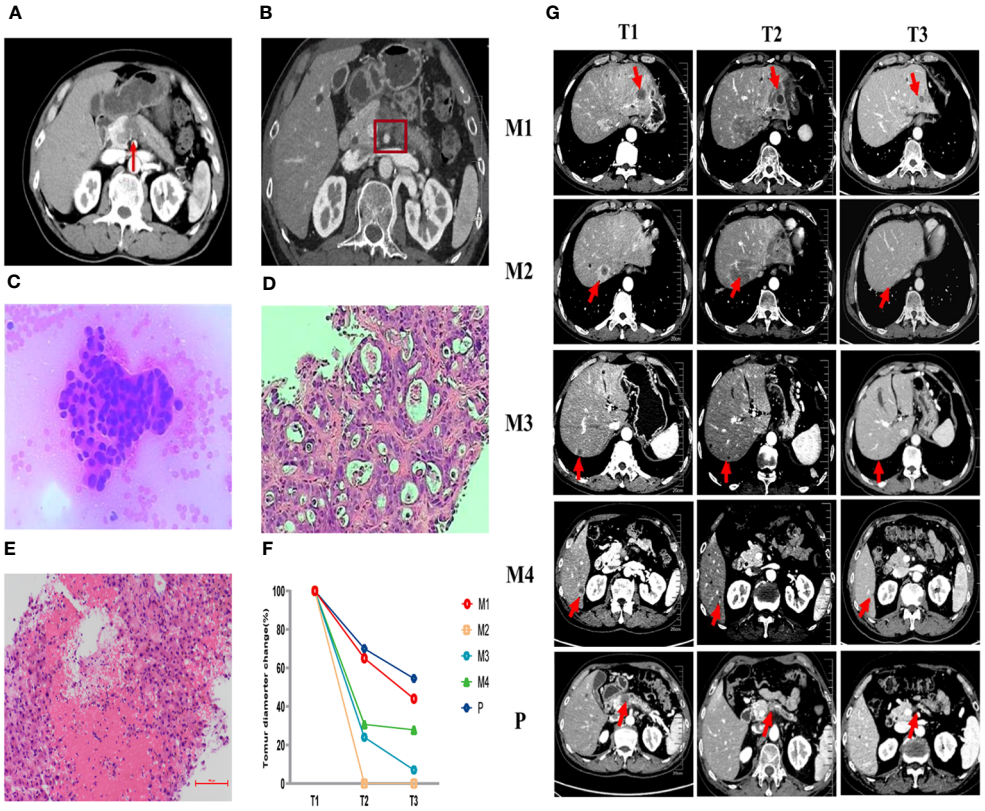

FIGURE 1
Pathological and imaging evaluations during the first-line (AG) and second-line (SOXPR) treatment. **(A, B)** A 2.2cm × 2cm mass at the neck of the pancreas was detected with superior mesenteric artery (SMA) invasion less than 180° on abdominal CT at baseline. **(C)** Cancer cells were observed in pancreas biopsy (×200) at T0. **(D)** Ultrasound guided biopsy of the hepatic mass (M2) was concordant with liver metastasis of pancreatic ductal adenocarcinoma (×200) at T1. **(E)** Pathology of M2 showed inflammatory cells and no residual tumor cells (×200) at T2. **(F, G)** Abdominal CT during second-line (SOXPR) treatment and the tumor diameter variation. T0, The baseline prior to first-line therapy; T1, The baseline prior to second-line therapy; T2, Obvious relief of TEN symptoms; T3,: Three additional cycles of SOX to end; M1-M4, 4 hepatic metastases; P, primary pancreatic cancer locus.

For example, the CD8+ T cell score increased from 4.13 to 7.48, and the Macrophage gene score improved from 6.05 to 8.07, and the Treg gene score improved from 3.32 to 5.36. In addition, the mIHC results also revealed an increase in Treg cells and M2 macrophages, consistent with previous study that the effect of radiotherapy on the tumor microenvironment may be dual, inducing both an immunostimulatory effect (recruitment of T cells) and an immunosuppressive effect (expansion of Treg cells) (9). Therefore, we hypothesized that this coexistence of immunostimulatory and immunosuppressive effect in radiotherapy leads to stabilization of the patient's disease and may provide opportunities for immunomodulation (10). Scores of other signatures or markers also increased, such as the scores of IFNγ from 5.29 to 8.51, cytotoxic T lymphocyte from 4.43 to 7.64. Interestingly, the change in the scores for B7-H3 showed a decreasing trend in contrast to the other scores, and previous studies have also shown a negative correlation between its high expression and treatment response. Additional immune scores were shown in Supplementary Table 1. Both mIHC, as well as TIME assays at the RNA level, reveal that immunotherapy combined with chemoradiotherapy enhances immune cell infiltration, which may be responsible for promoting the immune response and benefiting patient's clinical response.

FIGURE 2
Occurrence of TEN after SOXPR. **(A)** Planning target volume of hepatic metastases radiotherapy. **(B)** Skin changes during treatment of TEN.

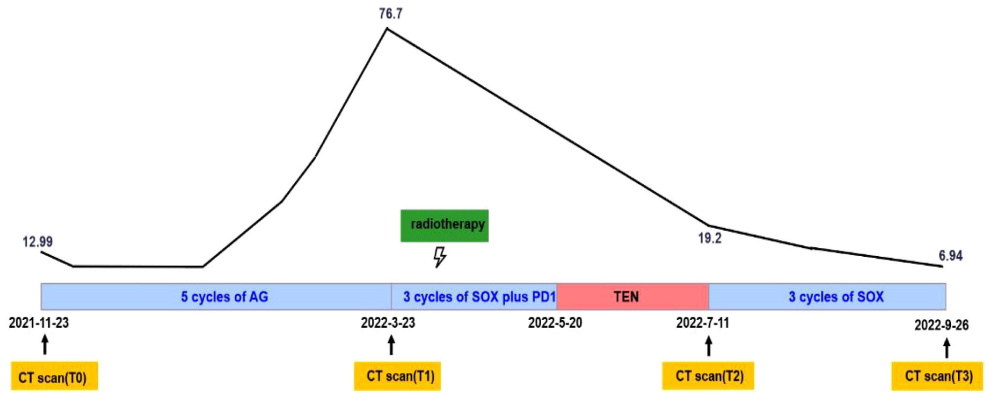

FIGURE 3
Systemic illustrations of clinical therapy flow chart. Broken Line indicates CA19-9 levels of this patient during the treatment.

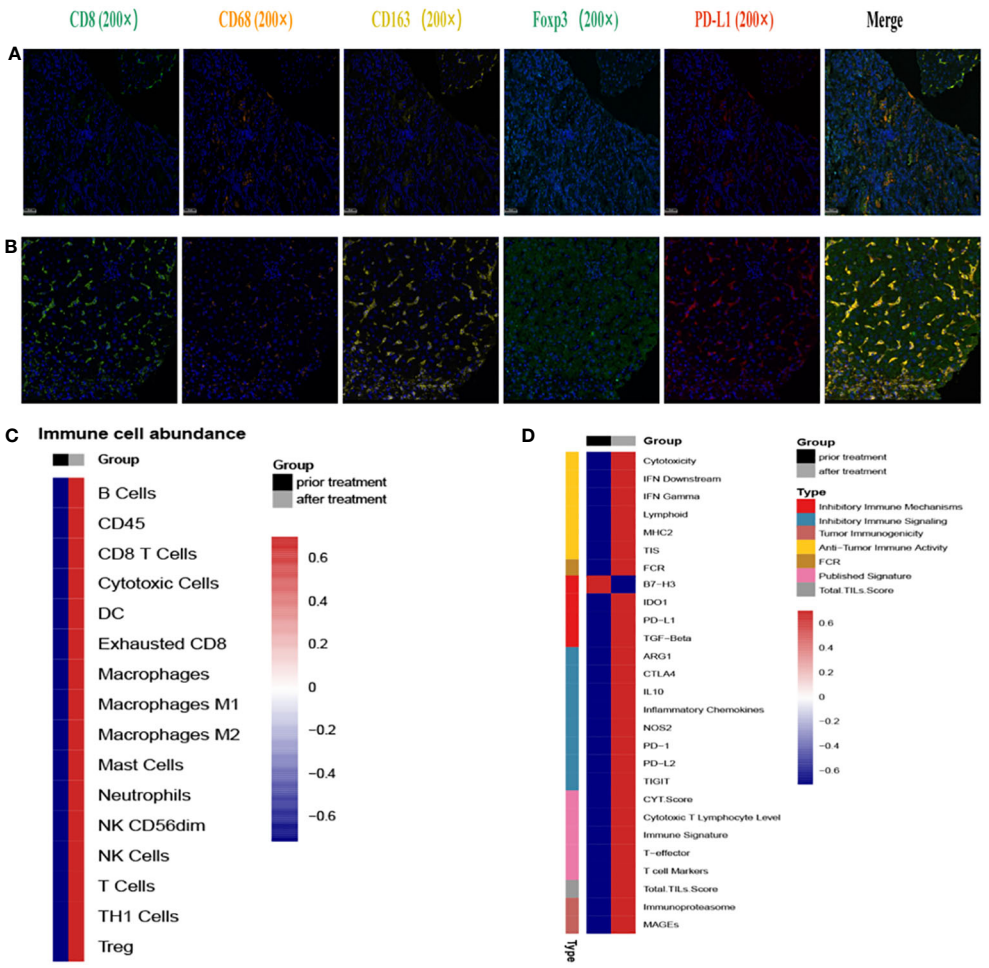

FIGURE 4
Immunofluorescence and RNA immune-related panel sequencing prior and post second-line treatment. **(A)** The representative immunofluorescent images of CD8, CD68, CD163, FoxP3 and PD-L1 of tumor tissues prior second-line treatment. **(B)** The representative immunofluorescent images of CD8, CD68, CD163, FoxP3 and PD-L1 of tumor tissues post second-line treatment. **(C)** Immune cell-related gene expression prior and after second-line treatment. Black indicates pre-treatment, gray indicates post-treatment; blue indicates decreased expression, red indicates increased expression. **(D)** Immune signature-related gene expression prior and after second-line treatment. Black indicates pre-treatment, gray indicates post-treatment; blue indicates decreased expression, red indicates increased expression.

3 Discussion

At present, chemotherapy is still the main treatment for advanced pancreatic cancer. With the deepening understanding of the pathogenesis of pancreatic cancer, immunotherapy based on remodeling TIME has become a hot topic of pancreatic cancer treatment (11). However, the specific and complex TIME of pancreatic cancer limits the effectiveness of immune checkpoint inhibitors therapy (12–15). Studies have shown that nearly 50% of the stroma cellular component of pancreatic cancer tissue is immune-related cells, but only a few are anti-tumor-related effector cells (16). Single-agent immunotherapy rarely works in second-line therapy in advanced pancreatic cancer, but we made breakthroughs and achieved unexpected clinical efficacy by a cocktail therapy consisted of immunotherapy combined with chemotherapy and radiotherapy in our case.

To better predict the response of immunotherapy in solid tumors, researchers divided the TIME into 4 subtypes based on PDL1 expression and the presence of tumor-infiltrating lymphocytes (TILs): T1 (PDL1−, TIL−), T2 (PDL1+, TIL+), T3 (PDL1−, TIL+), and T4 (PDL1+, TIL−) (17). T2 are considered to be the type to better predict the immune response. Radiation upregulated the expression of PD-L1 (8, 18, 19)and increased the infiltration of CD8+ T cells (20, 21), which changed the TIME from type 3 to type 2 in our case. Hot tumors were remodeled in this way to achieve enhanced clinical efficacy.

On one hand, radiation accelerates tumor cell lesions and death to promote the exposure and presentation of tumor associated antigens. On the other hand, high infiltration of CD8+ T cell is influenced by chemokines such as CXCL9 and CXCL10 (22, 23). Radiotherapy induces the production of these chemokines, and promote the recruitment of T cells to tumor tissues (24–26).T cells infiltration and antigens exposure activate T cell response to release IFN- γ and IFN- γ stimulates the upregulation of PD-L1 (27, 28). Besides, radiotherapy can also up-regulate PDL1 by activating cGAS-STING (cyclic guanosine monophosphate-adenosine monophosphate synthase-stimulator of interferon gene) pathway to lay basis for use of ICIs (29, 30). In addition, radiotherapy has been reported to induce normalization of blood vessels to achieve T cell infiltration, but the exact mechanism has not been fully elucidated (31).

In addition, the mIHC results showed an increase in Foxp3+ regulatory T cells (Foxp3+ Treg), which was consistent with previous studies. In bladder and liver cancer, increased accumulation of Treg cells was observed in tumor tissues after radiotherapy, which was shown to be related to radiation-induced Akt pathway activation (32, 33); In prostate cancer, radiotherapy provides a growth and survival advantage for Tregs by inducing TGF-β (34). However, our study hasn't explored the mechanism by which radiation therapy increases Foxp3+ Treg cells yet, which need to be explained deeply.

In previous studies, some researchers have paid attention to the ectopic effect of radiotherapy, and the specific mechanism of ectopic effect of radiotherapy is attributed to immune effect (35–37). Radiotherapy can induce immune cells to infiltrate into tumor tissue, produce a large number of reactive oxygen species, activate cytotoxic T lymphocytes (CTLs), and lead to apoptosis of tumor cells (38), this was also confirmed by our results of multiple immunofluorescence histochemistry and tumor microenvironment detection. Therefore, we conclude that the synergistic effect of ectopic radiotherapy and immunotherapy enhances the immune response and provides a new therapeutic strategy for advanced pancreatic cancer.

However, not all patients can benefit from radiotherapy combined with immunotherapy. It is well-known that the timing of radiotherapy and the dose of radiotherapy will affect the effect of immunotherapy. There is no consensus of the best time for radiotherapy, but existing studies have found that simultaneous administration of radiotherapy and immunotherapy or timely immunotherapy after radiotherapy is beneficial to the clinical outcome (39, 40). Taking two factors into consideration, we chose to introduce radiotherapy in the middle course of ICIs usage. One point, immunotherapy enhances the tumor's sensitivity to radiotherapy by cellular pathways. The other point, radiotherapy upregulated PD-L1 to better response to subsequent ICIs. Up to the optimal dose for radiotherapy, studies have shown that both low-dose and high-dose radiotherapy can affect the efficacy of immunotherapy by inflaming tumors, but the reason is not clear (39, 41). Whether it is related to the type of cancer needs to be further explored. Therefore, our patient benefited from synchronous radiotherapy and chemotherapy combined with immunotherapy, and benefited from high-dose radiotherapy ((8Gy*3f). Our patient also benefited from the sensitizing effect of radiotherapy on chemotherapeutic drugs. Clinical studies have shown that S-1 and oxaliplatin can be used as radiosensitizers in the treatment of solid tumors (42–44). S-1 can inhibit the repair of radiation-induced DNA damage and oxaliplatin can inhibit DNA replication and transcription.

More and more studies have shown that immune-related adverse events(irAEs) are related to better therapeutic effects (45, 46). Researchers believe that severity of irAEs are bystander effect from activated T cells (47). Thus, patients who experience more severe irAEs may acquire better clinical outcomes, but this conclusion needs to be supported by more clinical data. Our patient developed TEN after treatment with PD1, and CT scan showed a good tumor regression after remission of symptoms.

In conclusion, we provide a potential treatment strategy for the use of immunotherapy combined with chemotherapy and radiotherapy in patients with advanced pancreatic cancer. We consider that this is a typical case that comprehensive treatment mode can convert pancreatic cancer from "cold" tumors to "hot" tumors. More randomized clinical trials are needed to verify the safety and efficacy.

Data availability statement

The original contributions presented in the study are included in the article/Supplementary Material. Further inquiries can be directed to the corresponding authors.

Ethics statement

The studies involving humans were approved by the Medical Ethics Committee of Drum Tower Hospital Affiliated to Nanjing University Medical School. The studies were conducted in accordance with the local legislation and institutional requirements. The participants provided their written informed consent to participate in this study. Written informed consent was obtained from the individual(s) for the publication of any potentially identifiable images or data included in this article.

Author contributions

FT: Writing – original draft. YS: Writing – original draft. YZ: Formal analysis, Writing – review & editing. HS: Formal analysis, Writing – review & editing. JN: Writing – review & editing, Data curation. LQ: Data curation, Writing – review & editing. QG: Writing – review & editing, Methodology. CZ: Writing – review & editing, Methodology. WX: Writing – review & editing, Formal analysis. BL: Writing – review & editing, Conceptualization, Methodology. WK: Conceptualization, Writing – review & editing. JD: Conceptualization, Writing – review & editing, Methodology.

Funding

The author(s) declare financial support was received for the research, authorship, and/or publication of this article. This work was supported by the following grants: National Natural Science Foundation of China (82072926); National Key Research and Development Program of China (2020YFA0713804); Special Fund of Health Science and Technology Development of Nanjing (YKK20080). Fundings for Clinical Trials from the Affiliated Drum Tower Hospital, Medical School of Nanjing University (2023-LCYJ-PY-29). the National Natural Science Foundation of China (Nos. 82373280 and 82072926).

Conflict of interest

Authors CZ and WX were employed by Oncology Drug Development Jiangsu Simcere Diagnostics Co,Ltd.

The remaining authors declare that the research was conducted in the absence of any commercial or financial relationships that could be construed as a potential conflict of interest.

Publisher's note

Supplementary material

The Supplementary Material for this article can be found online at: https://www.frontiersin.org/articles/10.3389/fimmu.2023.1277810/full#supplementary-material

References

1. Siegel RL, Miller KD, Jemal A. Cancer statistics, 2018. *CA: Cancer J Clin* (2018) 68 (1):7–30. doi: 10.3322/caac.21442

2. Siegel RL, Miller KD, Jemal A. Cancer statistics, 2019. *CA: Cancer J Clin* (2019) 69 (1):7–34. doi: 10.3322/caac.21551

3. Heery CR, O'Sullivan-Coyne G, Madan RA, Cordes L, Rajan A, Rauckhorst M, et al. Avelumab for metastatic or locally advanced previously treated solid tumours (JAVELIN Solid Tumor): a phase 1a, multicohort, dose-escalation trial. *Lancet Oncol* (2017) 18(5):587–98. doi: 10.1016/S1470-2045(17)30239-5

4. Herzberg B, Campo MJ, Gainor JF. Immune checkpoint inhibitors in non-small cell lung cancer. *Oncologist* (2017) 22(1):81–8. doi: 10.1634/theoncologist.2016-0189

5. Muro K, Chung HC, Shankaran V, Geva R, Catenacci D, Gupta S, et al. Pembrolizumab for patients with PD-L1-positive advanced gastric cancer (KEYNOTE-012): a multicentre, open-label, phase 1b trial. *Lancet Oncol* (2016) 17 (6):717–26. doi: 10.1016/S1470-2045(16)00175-3

6. Ullman NA, Burchard PR, Dunne RF, Linehan DC. Immunologic strategies in pancreatic cancer: making cold tumors hot. *J Clin Oncol* (2022) 40(24):2789–805. doi: 10.1200/JCO.21.02616

7. Antonia SJ, Villegas A, Daniel D, Vicente D, Murakami S, Hui R, et al. Durvalumab after chemoradiotherapy in stage III non-small-cell lung cancer. *New Engl J Med* (2017) 377(20):1919–29. doi: 10.1056/NEJMoa1709937

8. Tang Z, Wang Y, Liu D, Wang X, Xu C, Yu Y, et al. The Neo-PLANET phase II trial of neoadjuvant camrelizumab plus concurrent chemoradiotherapy in locally advanced adenocarcinoma of stomach or gastroesophageal junction. *Nat Commun* (2022) 13(1):6807. doi: 10.1038/s41467-022-34403-5

9. Zhai D, An D, Wan C, Yang K. Radiotherapy: Brightness and darkness in the era of immunotherapy. *Transl Oncol* (2022) 19:101366. doi: 10.1016/j.tranon.2022.101366

10. Weichselbaum RR, Liang H, Deng L, Fu Y-X. PMID: 28094262. *Nat Rev Clin Oncol* (2017) 14(6):365–79. doi: 10.1038/nrclinonc.2016.211

11. Huber M, Brehm CU, Gress TM, Buchholz M, Alashkar Alhamwe B, von Strandmann EP, et al. The immune microenvironment in pancreatic cancer. *Int J Mol Sci* (2020) 21(19):7307. doi: 10.3390/ijms21197307

12. Groot VP, Rezaee N, Wu W, Cameron JL, Fishman EK, Hruban RH, et al. Patterns, timing, and predictors of recurrence following pancreatectomy for pancreatic ductal adenocarcinoma. *Ann Surg* (2018) 267(5):936–45. doi: 10.1097/SLA.0000000000002234

13. Mizrahi JD, Surana R, Valle JW, Shroff RT. Pancreatic cancer. *Lancet* (2020) 395 (10242):2008–20. doi: 10.1016/S0140-6736(20)30974-0

14. Rahib L, Smith BD, Aizenberg R, Rosenzweig AB, Fleshman JM, Matrisian LM. Projecting cancer incidence and deaths to 2030: the unexpected burden of thyroid, liver, and pancreas cancers in the United States. *Cancer Res* (2014) 74(11):2913–21. doi: 10.1158/0008-5472.CAN-14-0155

15. Topalian SL, Drake CG, Pardoll DM. Immune checkpoint blockade: a common denominator approach to cancer therapy. *Cancer Cell* (2015) 27(4):450–61. doi: 10.1016/j.ccell.2015.03.001

16. Clark CE, Hingorani SR, Mick R, Combs C, Tuveson DA, Vonderheide RH. Dynamics of the immune reaction to pancreatic cancer from inception to invasion. *Cancer Res* (2007) 67(19):9518–27. doi: 10.1158/0008-5472.CAN-07-0175

17. Zhang Y, Chen L. Classification of advanced human cancers based on tumor immunity in the microEnvironment (TIME) for cancer immunotherapy. *JAMA Oncol* (2016) 2(11):1403–4. doi: 10.1001/jamaoncol.2016.2450

18. Deng L, Liang H, Burnette B, Beckett M, Darga T, Weichselbaum RR, et al. Irradiation and anti-PD-L1 treatment synergistically promote antitumor immunity in mice. *J Clin Invest.* (2014) 124(2):687–95. doi: 10.1172/JCI67313

19. Yoshino H, Sato Y, Nakano M. KPNB1 inhibitor importazole reduces ionizing radiation-increased cell surface PD-L1 expression by modulating expression and nuclear import of IRF1. *Curr Issues Mol Biol* (2021) 43(1):153–62. doi: 10.3390/cimb43010013

20. Chen HY, Xu L, Li LF, Liu XX, Gao JX, Bai YR. Inhibiting the CD8(+) T cell infiltration in the tumor microenvironment after radiotherapy is an important mechanism of radioresistance. *Sci Rep* (2018) 8(1):11934. doi: 10.1038/s41598-018-30417-6

21. Miyauchi S, Sanders PD, Guram K, Kim SS, Paolini F, Venuti A, et al. HPV16 E5 mediates resistance to PD-L1 blockade and can be targeted with rimantadine in head and neck cancer. *Cancer Res* (2020) 80(4):732–46. doi: 10.1158/0008-5472.CAN-19-1771

22. Dangaj D, Bruand M, Grimm AJ, Ronet C, Barras D, Duttagupta PA, et al. Cooperation between constitutive and inducible chemokines enables T cell engraftment and immune attack in solid tumors. *Cancer Cell* (2019) 35(6):885–900. doi: 10.1016/j.ccell.2019.05.004

23. Harlin H, Meng Y, Peterson AC, Zha Y, Tretiakova M, Slingluff C, et al. Chemokine expression in melanoma metastases associated with CD8+ T-cell recruitment. *Cancer Res* (2009) 69(7):3077–85. doi: 10.1158/0008-5472.CAN-08-2281

24. Matsumura S, Wang B, Kawashima N, Braunstein S, Badura M, Cameron TO, et al. Radiation-induced CXCL16 release by breast cancer cells attracts effector T cells. *J Immunol* (2008) 181(5):3099–107. doi: 10.4049/jimmunol.181.5.3099

25. Meng Y, Mauceri HJ, Khodarev NN, Darga TE, Pitroda SP, Beckett MA, et al. Ad.Egr-TNF and local ionizing radiation suppress metastases by interferon-beta-dependent activation of antigen-specific CD8+ T cells. *Mol Ther* (2010) 18(5):912–20. doi: 10.1038/mt.2010.18

26. Wang C-L, Ho A-S, Chang C-C, Sie Z-L, Peng C-L, Chang J, et al. Radiotherapy enhances CXCR3highCD8+ T cell activation through inducing IFNγ-mediated CXCL10 and ICAM-1 expression in lung cancer cells. *Cancer Immunol Immunother* (2023) 72(6):1865–80. doi: 10.1007/s00262-023-03379-6

27. Dong H, Strome SE, Salomao DR, Tamura H, Hirano F, Flies DB, et al. Tumor-associated B7-H1 promotes T-cell apoptosis: a potential mechanism of immune evasion. *Nat Med* (2002) 8(8):793–800. doi: 10.1038/nm730

28. Taube JM, Anders RA, Young GD, Xu H, Sharma R, McMiller TL, et al. Colocalization of inflammatory response with B7-h1 expression in human melanocytic lesions supports an adaptive resistance mechanism of immune escape. *Sci Transl Med* (2012) 4(127):127ra37. doi: 10.1126/scitranslmed.3003689

29. Du S-S, Chen G-W, Yang P, Chen Y-X, Hu Y, Zhao Q-Q, et al. Radiation Therapy Promotes Hepatocellular Carcinoma Immune Cloaking *via* PD-L1 Upregulation Induced by cGAS-STING Activation. *Int J Radiat Oncol Biol Phys* (2022) 112(5):1243–55. doi: 10.1016/j.ijrobp.2021.12.162

30. Jiang M, Jia K, Wang L, Li W, Chen B, Liu Y, et al. Alterations of DNA damage response pathway: Biomarker and therapeutic strategy for cancer immunotherapy. *Acta Pharm Sin B* (2021) 11(10):2983–94. doi: 10.1016/j.apsb.2021.01.003

31. Hauth F, Ho AY, Ferrone S, Duda DG. Radiotherapy to enhance chimeric antigen receptor T-cell therapeutic efficacy in solid tumors: A narrative review. *JAMA Oncol* (2021) 7(7):1051–9. doi: 10.1001/jamaoncol.2021.0168

32. Wang M, Gou X, Wang L. Protein kinase B promotes radiation-induced regulatory T cell survival in bladder carcinoma. *Scand J Immunol* (2012) 76(1):70–4. doi: 10.1111/j.1365-3083.2012.02707.x

33. Li C-G, He M-R, Wu F-L, Li Y-J, Sun A-M. Akt promotes irradiation-induced regulatory T-cell survival in hepatocellular carcinoma. *Am J Med Sci* (2013) 346 (2):123–7. doi: 10.1097/MAJ.0b013e31826ceed0

34. Wu C-T, Hsieh C-C, Yen T-C, Chen W-C, Chen M-F. TGF-β1 mediates the radiation response of prostate cancer. *J Mol Med (Berl).* (2015) 93(1):73–82. doi: 10.1007/s00109-014-1206-6

35. Golden EB, Demaria S, Schiff PB, Chachoua A, Formenti SC. An abscopal response to radiation and ipilimumab in a patient with metastatic non-small cell lung cancer. *Cancer Immunol Res* (2013) 1(6):365–72. doi: 10.1158/2326-6066.CIR-13-0115

36. Reynders K, Illidge T, Siva S, Chang JY, De Ruysscher D. The abscopal effect of local radiotherapy: using immunotherapy to make a rare event clinically relevant. *Cancer Treat Rev* (2015) 41(6):503–10. doi: 10.1016/j.ctrv.2015.03.011

37. Twyman-Saint Victor C, Rech AJ, Maity A, Rengan R, Pauken KE, Stelekati E, et al. Radiation and dual checkpoint blockade activate non-redundant immune mechanisms in cancer. *Nature* (2015) 520(7547):373–7. doi: 10.1038/nature14292

38. Bernstein MB, Krishnan S, Hodge JW, Chang JY. Immunotherapy and stereotactic ablative radiotherapy (ISABR): a curative approach? *Nat Rev Clin Oncol* (2016) 13(8):516–24. doi: 10.1038/nrclinonc.2016.30

39. Theelen WSME, Peulen HMU, Lalezari F, van der Noort V, de Vries JF, Aerts JGJV, et al. Effect of pembrolizumab after stereotactic body radiotherapy vs pembrolizumab alone on tumor response in patients with advanced non-small cell lung cancer: results of the PEMBRO-RT phase 2 randomized clinical trial. *JAMA Oncol* (2019) 5(9):1276–82. doi: 10.1001/jamaoncol.2019.1478

40. Woody S, Hegde A, Arastu H, Peach MS, Sharma N, Walker P, et al. Survival is worse in patients completing immunotherapy prior to SBRT/SRS compared to those receiving it concurrently or after. *Front Oncol* (2022) 12:785350. doi: 10.3389/fonc.2022.785350

41. Herrera FG, Ronet C, Ochoa de Olza M, Barras D, Crespo I, Andreatta M, et al. Low-dose radiotherapy reverses tumor immune desertification and resistance to immunotherapy. *Cancer Discov* (2022) 12(1):108–33. doi: 10.1158/2159-8290.CD-21-0003

42. Xu J, Li X, Lv X. Effect of oxaliplatin combined with 5-fluorouracil on treatment efficacy of radiotherapy in the treatment of elderly patients with rectal cancer. *Exp Ther Med* (2019) 17(3):1517–22. doi: 10.3892/etm.2018.7119

43. Lee EM, Hong YS, Kim K-P, Lee J-L, Kim SY, Park YS, et al. Phase II study of preoperative chemoradiation with S-1 plus oxaliplatin in patients with locally advanced rectal cancer. *Cancer Sci* (2013) 104(1):111–5. doi: 10.1111/cas.12041

44. Tang M, Lu X, Zhang C, Du C, Cao L, Hou T, et al. Downregulation of SIRT7 by 5-fluorouracil induces radiosensitivity in human colorectal cancer. *Theranostics* (2017) 7(5):1346–59. doi: 10.7150/thno.18804

45. Dupont R, Bérard E, Puisset F, Comont T, Delord JP, Guimbaud R, et al. The prognostic impact of immune-related adverse events during anti-PD1 treatment in melanoma and non-small-cell lung cancer: a real-life retrospective study. *Oncoimmunology* (2020) 9(1):1682383. doi: 10.1080/2162402X.2019.1682383

46. Schweizer C, Schubert P, Rutzner S, Eckstein M, Haderlein M, Lettmaier S, et al. Prospective evaluation of the prognostic value of immune-related adverse events in patients with non-melanoma solid tumour treated with PD-1/PD-L1 inhibitors alone and in combination with radiotherapy. *Eur J Cancer* (2020) 140:55–62. doi: 10.1016/j.ejca.2020.09.001

47. Das S, Johnson DB. Immune-related adverse events and anti-tumor efficacy of immune checkpoint inhibitors. *J Immunother Cancer* (2019) 7(1):306. doi: 10.1186/s40425-019-0805-8

frontiers | Frontiers in Immunology

TYPE Review
PUBLISHED 16 January 2024
DOI 10.3389/fimmu.2023.1315453

OPEN ACCESS

EDITED BY
Xin He,
City of Hope National Medical Center, United States

REVIEWED BY
Kuo Chen,
First Affiliated Hospital of Zhengzhou University, China
Concha Herrera,
Hospital Reina Sofía de Córdoba, Spain

*CORRESPONDENCE
Xiuli Wu
siulier@163.com
Ling Xu
lingxu114@163.com
Zhenyi Jin
jinzhenyijnu@163.com

†These authors have contributed equally to this work and share first authorship

RECEIVED 10 October 2023
ACCEPTED 29 December 2023
PUBLISHED 16 January 2024

CITATION
Wang W, Wu X, Zheng J, Yin R, Li Y, Wu X, Xu L and Jin Z (2024) Utilizing exosomes as sparking clinical biomarkers and therapeutic response in acute myeloid leukemia. *Front. Immunol.* 14:1315453. doi: 10.3389/fimmu.2023.1315453

Utilizing exosomes as sparking clinical biomarkers and therapeutic response in acute myeloid leukemia

Wandi Wang[1†], Xiaofang Wu[1†], Jiamian Zheng[1†], Ran Yin[1], Yangqiu Li[1], Xiuli Wu[1,2*], Ling Xu[1,2*] and Zhenyi Jin[3,4*]

[1]Institute of Hematology, School of Medicine, Jinan University, Guangzhou, China, [2]Key Laboratory for Regenerative Medicine of Ministry of Education, Jinan University, Guangzhou, China, [3]Department of Pathology, School of Medicine, Jinan University, Guangzhou, China, [4]Key Laboratory of Viral Pathogenesis and Infection Prevention and Control, Jinan University, Guangzhou, China

Acute myeloid leukemia (AML) is a malignant clonal tumor originating from immature myeloid hematopoietic cells in the bone marrow with rapid progression and poor prognosis. Therefore, an in-depth exploration of the pathogenesis of AML can provide new ideas for the treatment of AML. In recent years, it has been found that exosomes play an important role in the pathogenesis of AML. Exosomes are membrane-bound extracellular vesicles (EVs) that transfer signaling molecules and have attracted a large amount of attention, which are key mediators of intercellular communication. Extracellular vesicles not only affect AML cells and normal hematopoietic cells but also have an impact on the bone marrow microenvironment and immune escape, thereby promoting the progression of AML and leading to refractory relapse. It is worth noting that exosomes and the various molecules they contain are expected to become the new markers for disease monitoring and prognosis of AML, and may also function as drug carriers and vaccines to enhance the treatment of leukemia. In this review, we mainly summarize to reveal the role of exosomes in AML pathogenesis, which helps us elucidate the application of exosomes in AML diagnosis and treatment.

KEYWORDS

acute myeloid leukemia, exosomes, prognosis, biomarker, immune evasion

Introduction

Acute myeloid leukemia (AML) is an aggressive hematological malignancy that affects adults. It is characterized by the abnormal proliferation and differentiation of immature myeloblasts, which accumulate in the bone marrow (BM) and peripheral blood and impair normal hematopoiesis. Although 50% of patients with AML can achieve complete remission after induction chemotherapy and post-remission treatment, more than 20%

of patients with AML remain unresponsive and refractory (1). The precise treatment of AML is impeded by the disease's aggressive and heterogeneous nature, which is characterized by genetic abnormalities, extensive epigenetic changes, and abnormal tumor microenvironment (TME) (2, 3). Therefore, understanding of the pathogenesis of AML must be improved, and novel biomarkers for diagnosis for its diagnosis and prognosis must be developed.

Exosomes, also known as intraluminal vesicles, are 30-100nm extracellular vesicles (EVs) secreted by various cells, including tumor cells, into the body fluids, blood, urine, semen, saliva, breast milk, amniotic fluid, ascitic fluid, cerebrospinal fluid, and bile (4). The circulatory system serves as the primary medium for exosomes to perform their long-distance communication function (5, 6). Tumor-derived exosomes (TEXs) induce vascular leakage, inflammation, and BM progenitor recruitment during pre-metastatic niche formation and metastasis (7), and finally induce tumor growth and metastasis, affecting tumor progression and prognosis (8).

TEXs in TME transport a substantial amount of genetic material from maternal tumor cells (9). By regulating the physiology of recipient cells, including signaling to tumor and stromal cells, exosomes secreted into the extracellular environment can reshape the TME and promote tumor growth. Exosomes are crucial components in tumorigenesis and tumor proliferation, angiogenesis, invasion, and metastasis (10). This intercellular communication influences cells of various lineages remotely or in situ. Exosomal communication involving immune cells can induce intricate cellular modifications and considerably influence the course of cancer progression by eliciting an immune response. Recent evidence suggests that exosomes greatly influence cell-to-cell and cell-to-environment communication in AML (11). Exosomes are essential for the progression of leukemia and facilitate the survival and chemoresistance of leukemic cells by transferring their molecular cargo (12, 13). Therefore, TEXs are essential to the evaluation of the effects of AML disease activity, severity, and treatment response. In this review, we briefly describe the production of exosomes and how vesicles mediate cellular communication, and then explore the potential use of exosomes in AML diagnosis and treatment.

Origin and mechanisms of exosomes

Approximately 50 years ago, scientists observed that cells in culture fluid "shed" small vesicles of unknown function -called exosomes. Previously, "waste" produced by cellular physiological metabolism. Owing to the development of high-throughput proteomics and genomics, exosomes have been demonstrated to be involved in intercellular communication in living organisms.

Exosome biogenesis

Exosome biogenesis is a multistep process involving several pathways. First, multivesicular bodies (MVBs) are generated through two stages of inward membrane budding. The invagination of the cell membrane generates early endosomes, from which exosomes bud inward and late endosomes or MVBs are formed (14). Then, MVBs fuse with the plasma membrane through exocytosis and release exosomes from the cells in tubular vesicles (15). The mechanisms underlying MVB formation including endosomal sorting complex required for transport (ESCRT) pathway, and tetraspanin-dependent pathway (16, 17). ESCRT consists of four subunits (ESCRT-0, ESCRT-I, ESCRT-II, and ESCRT-III) and related molecules (VPS4, VTA1, and ALIX). ESCRT-0 complex initiates the ESCRT pathway through its subunit hepatocyte growth factor-regulated tyrosine kinase substrate, which not only recognizes ubiquitinated proteins and binds to phosphoinositide in the endosomal membrane but also recruits ESCRT-I by binding its TSG101 subunit (18–22). Then, ESCRT-I, and -II promote membrane endosome invagination, ESCRT-III and VPS4 drive the abscission of vesicles from the membrane, and exosomes are generated (23–29). However, the ESCRT system is not the sole pathway for regulating exosome formation. Several tetraspanins, such as CD63, CD81, and CD9, can sequester multiple proteins and form tetraspanin-enriched exosomes (30, 31). Apart from these pathways, other regulators have been identified, including syntenin, ceramide activation via neutral sphingomyelinase, and lipid-raft formation (32–34).

Secretion of exosome

The mechanism by which MVBs are delivered to the plasma membrane is still not fully understood. Nevertheless, research has demonstrated that the process is controlled by small GTPase molecules that interact with cytoskeletal proteins, and cortactin and ALIX play roles in the intracellular distribution of MVBs (35–37). MVBs fuse with the plasma membrane through a series of proteins, including the soluble N-ethylmaleimide-sensitive factor attachment protein receptor (SNARE). Vesicle-associated membrane proteins bind to the plasma membrane proteins syntaxin and SNAP and then *trans*-SNARE complexes are formed, which provide the necessary force for the movement of MVBs toward the plasma membrane (38). Finally, other SNARE proteins promote the fusion of MVBs and exosome (38–40).

Exosome uptake

After secretion, exosomes with cargoes are released into the extracellular environment. The membranes of exosomes can protect biomacromolecules that exist stably in the body fluid. Therefore, peripheral blood is the main environment in which exosomes perform long-distance communication functions (5, 6). *In vivo*, exosomes can be assimilated by target cells through the direct fusion of membranes, ligand-receptor interactions, or endocytosis. First, exosomes can directly activate receptors on the surfaces of target cells through protein molecules on the surfaces or lipid ligands, generating signaling complexes and activating intracellular signaling pathways (41). Second, in the extracellular matrix, exosomes release intracellular substances that act as ligands to bind to receptors on the cell membrane, thereby activating intracellular signaling pathways (42). Third, exosomes encode

essential integrin molecules and fuse with the plasma membranes of target cells or are endocytosed directly into the cells and release nonspecific proteins, noncoding RNA, and nucleic acids (43). Biomolecules transferred by exosomes can alter the phenotypes and functions of recipient cells by altering gene expression and are involved in many physiological and pathological processes in recipient and donor cells (44, 45). Figure 1 shows the relevant mechanism.

Content of exosome

Recent data obtained from the Exosome Database reveal that exosomes comprise 1116 lipids, 9769 proteins, 3408 mRNAs, and 2838 microRNAs (miRNAs). The lipid content of exosomes consists of cholesterol, sphingomyelin, ceramide, phosphatidylserine, lysophosphatidic acid, and prostaglandins, which are important for the mechanistic and biophysical aspects of bilayer formation, curvature, and fluidity and affect membrane fusion (46). Proteins in exosomes include tetraspanins, which are membrane transport and fusion proteins on the surfaces of exosomes and act as specific markers. They include specific proteins that are excellent markers for exosome recognition, heat shock proteins (HSP-60, HSP-70, and HSP-90), chaperone proteins, adhesion proteins, MHC (e.g., MHC I and MHC II, which are evolved in antigen presentation), cytoskeletal proteins, multivesicular body synthesis proteins, and lipid-associated proteins (47). In addition, AML-derived exosomes contain the tumor antigens CD33, CD34, and CD117 (48). Exosomes express the adhesion molecules ICAM-1 and integrins, which mediate the interaction and binding of exosomal membranes to receptor cells

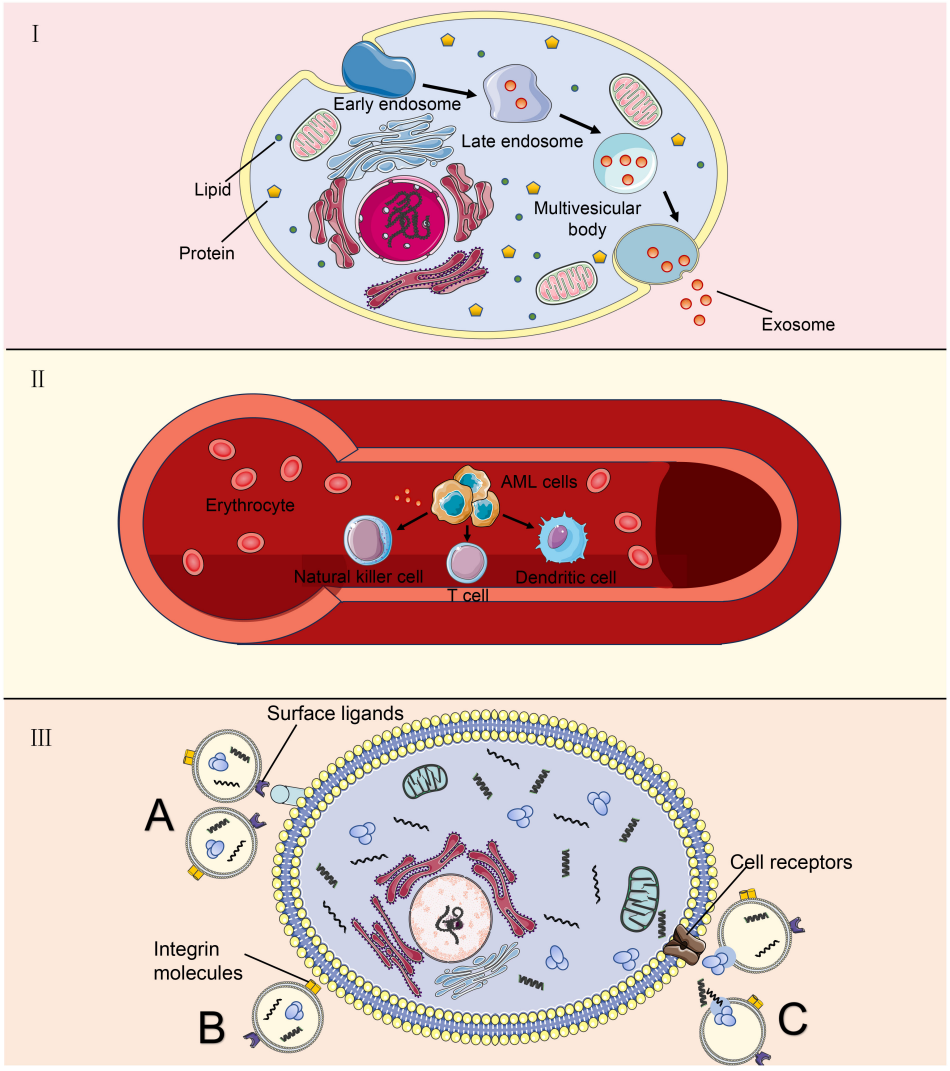

FIGURE 1
Exosomes derived from AML cells are used as target cells. **(A)** AML cells undergo a process from tubular vesicles (early intracellular bodies) to late intracellular bodies to multivesicular bodies, and finally, they release exosomes into the extracellular space through fusion with the plasma membrane. **(B)** AML-derived exosomes play a long-distance communication role mainly through peripheral blood, which can affect some immune cells; **(C)** Exosomes communicate with target cells. Exosomes can directly activate receptors on the surface of target cells through surface ligands. Integrin molecules on the membrane of exosomal cells directly fuse with the plasma membrane of target cells or endocytosis enters the cell. Outside the cell, exosomes release intracellular substances that bind to receptors on the cell membrane.

for cargo delivery (49). Nucleic acids, including DNA, mRNA, and noncoding RNA, are associated with the detection of cancer-associated mutations in serum exosomes (50). Thus, exosome-specific nucleic acids and proteins are crucial for identifying biomarkers of serum exosomes associated with tumor gene mutations and predicting tumor development and prognosis (51).

AML-derived exosomes cause the dysfunction of immune cells

Exosomes originating from AML induce T-cell differentiation towards a pro-tumor phenotype

The efficacy of tumor immunotherapy is restricted by tumor cells evading host immune system surveillance and downregulating the function of immune cells, especially antitumor effector cells, including $CD8^+$ T and $CD4^+$ T cells, natural killer cells (NK), and dendritic cells (DCs) (52, 53). Immune cell dysfunction is a common feature of AML. AML-derived exosomes are key mediators in the TME and function as immunosuppressants, enabling AML cells to evade immune surveillance (12). Exosomes isolated from the plasma of AML patients are loaded with leukemia-associated antigens and inhibitory molecules, which can disrupt the functions of immune cells used in adoptive cell therapy, thereby limiting the expected therapeutic effect of adoptive cell therapy and resulting in immune dysfunction (54). Human TEXs induce apoptosis in activated $CD8^+$ T cells, promote the expansion and function of regulatory T (Treg) cells, and thus promote tumor evasion. The proliferation of activated $CD8^+$ T cells is inhibited by co-cultivation with TEX, but TEXs increase the proportion of activated $CD4^+$ T cells. Additionally, TEXs promote Treg cell expansion and transport transforming growth factor β (TGFβ) and IL-10, which promote the conversion of T cells into Treg cells (55). Treg cells constitute a subpopulation of T cells, mainly $CD4^+CD25^+$ cells, and are classified according to their origin. Elevated levels of Treg cells in peripheral blood are associated with poor outcomes in patients with AML (56). Pando et al. investigated the effects of AML-derived EVs on T cell subsets by an *in vitro* approach to study the effects of EVs derived from the human AML cell line MOLM-14 cells on $CD4^+$, $CD4^+CD39^+$, and $CD8^+$ T cell subsets from healthy individuals; the results showed that tumor-derived EVs modulate T cell responses by upregulating immune processes, such as immunosuppression and oncogenic gene expression (57).

AML-derived exosomes downregulate the natural killer receptor of NK cells

NK cells are major innate immune cells in the bloodstream and target tumor cells. In AML, the ability of NK cells to eliminate leukemic cells is dependent on the predominance of activation signals. Weak activation signals among NK cells lead to their inability to exert their cytotoxicity and render them unresponsive to leukemic cells (58). The low expression of the activation receptor natural killer group 2D (NKG2D) of NK cells in patients with AML results in a decline in NK cell activity and the inhibition of its killing function (59). Szczepanski et al. examined serum exosomes from 19 patients with AML and 14 healthy controls and found that serum exosomes from patients with AML disrupted NK cell activation by downregulating the expression of NKG2D; this effect reduced the toxicity of NK cells to tumor cells, but interleukin 15 counteracted this inhibitory effect (60). AML-derived exosomes reduced the cytolytic activity of normal NK cells by downregulating NKG2D receptor expression and inducing Smad phosphorylation in NK cells (61). Hong et al. isolated exosomes from the plasma of the AML human-derived tissue xenograft model they developed; they observed that the expression levels of surface markers in the exosomes were similar to those in the exosomes from patients with AML. The AML-derived exosomes that carried immunosuppressive ligands activated on human NK cell or $CD8^+$ T cell receptors, leading to their dysfunction (62).

AML-derived exosomes inhibit the direct and indirect anti-tumor effects of DCs

DCs are major antigen-presenting cells and play an important role in innate immunity. However, DCs generated in the presence of TEX under express costimulatory molecules and produce suppressive cytokines, thus inducing the dose-dependent suppression of T cell proliferation and antitumor cytotoxicity (63). In the context of AML, type I interferons produced by plasmacytoid DCs can clear AML cells. This finding suggests that DCs eliminate AML cells. Benites et al. used exosomes or lysates derived from the leukemia K562 cell line as antigen sources of DC pulses, which initiated the maturation of DCs into a cytotoxic phenotype and markedly enhanced the cleavage of target cells; conversely, when the serum exosomes of patients with AML were used as the pulse sources, opposite effects were observed, which may have induced the immune tolerance of DCs. Considering these contrasting effects can contribute to the mitigation of *in vivo* immune tumor evasion mechanisms (64). In summary, AML-derived exosomes transport substances that induce dysfunction in immune cells and exert a suppressive effect on the immune system (Figure 2).

AML-derived exosomes related to AML progress

Exosomes participate in BM microenvironment reconstitution

The leukemic microenvironment is a complex and heterogeneous ecological niche composed of various cells, including leukemic, immune, mesenchymal stem, and endothelial

10.3389/fimmu.2023.1315453

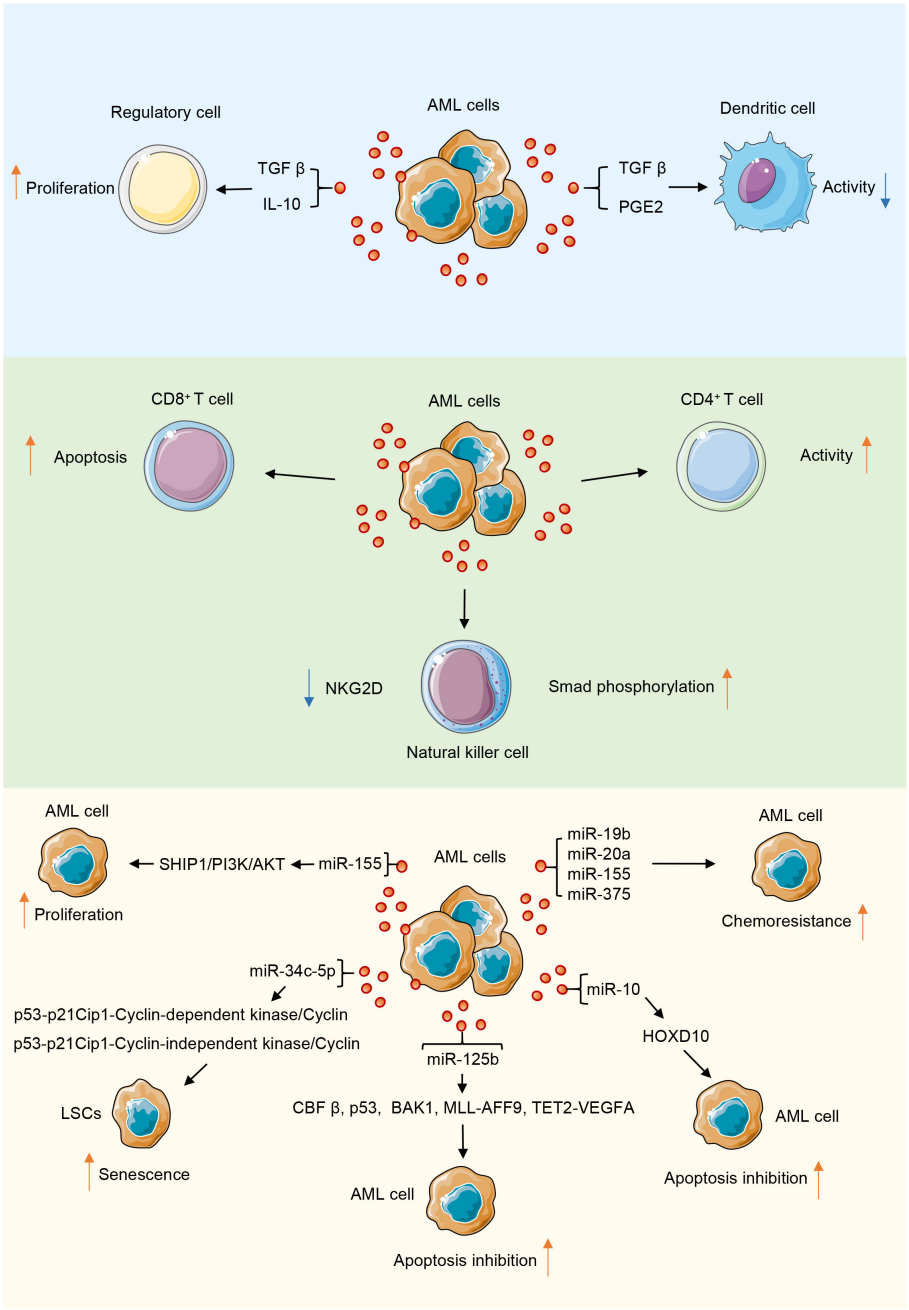

FIGURE 2
AML-derived exosomes play a role in promoting or inhibiting tumor progression through their contents in the tumor microenvironment. During the interaction of AML-derived exosomes with immune cells, their contents mainly inhibit the function of immune cells.

cells. The interaction of tumor cells with the microenvironment and tumor stem cells in the BM promotes the relapse of leukemia and metastasis to lymphoid tissues (65). Exosomes are important for the induction of immune responses in a pro-tumor microenvironment and for tumor progression and survival. They promote tumor survival by remodeling the extracellular matrix and inducing angiogenesis and tumor cell proliferation (66). AML can reconstitute the BM microenvironment to one that promotes the growth of leukemic cells but inhibits normal hematopoietic function by secreting exosomes. Exosomes released by AML cells upregulate DKK1 in BM mesenchymal stromal cells and thereby inhibit normal hematopoiesis through the WNT signaling pathway, and AML-derived exosomes stimulate vascular endothelial growth factor (VEGF) signaling in human umbilical vein endothelial cells (HUVECs) by transferring angiogenic factors or proteins and miRNAs, which form vascular tubular structures that promote tumor growth (4, 67). Some studies have confirmed that exosomal miRNAs secreted by AML cells contribute to the progression of AML by altering the expression of downstream genes (68). Point mutation inactivation and reduced SHIP1 gene

activity have been observed in patients with AML, and the miR-155-mediated suppression of SHIP1 expression is involved in the pathogenesis of AML. The miR-155/SHIP1/PI3K/AKT signaling pathway potentially has a tumor-suppressive function in the pathogenesis of AML (69). miR-155 is upregulated in FLT3-ITD-associated AML and targets the myeloid transcription factor PU.1. The knockdown of miR-155 inhibits proliferation of FLT3-ITD-associated leukemic cells and induces their apoptosis (70). miR-34c-5p is a core miRNA in pathways regulating aging. It is expressed through the p53-p21Cip1-cyclin-dependent kinase (CDK)/cyclin or the p53-independent CDK/cyclin pathway (p53-p21Cip1-CDK/cyclin or p53-independent CDK/cyclin pathway (p53-p21Cip1-CDK/cyclin or p53-independent CDK/cyclin pathways) and promotes leukemia stem cells senescence. However, miR-34c-5p is downregulated in AML (excluding APL) stem cells; poor prognosis and poor therapeutic effect are clinical manifestations of this outcome (71).

The role of exosomes in the apoptosis of AML

Apoptosis is one of the key mechanisms affecting the survival of AML cells, and the dysregulation of apoptosis may lead to the chemoresistance of AML cells and disease relapse (72). Exosomes carry many complex cargoes, which can serve as the key mediators of intercellular communication and regulate cell proliferation (73). Exosomal miRNAs enter body fluids through autocrine secretion and create a microenvironment in malignant regulatory pathways that facilitate the growth of AML cells by cross talk with other cells, thereby promoting leukemic cell survival, proliferation, and migratory infiltration (74). AML cells highly resistant to apoptosis can affect the expression of apoptosis-related proteins in chemo-sensitive cells. Jiang et al. showed that exosomes secreted by AML cells are enriched in miR-125b (75). The mechanisms by which miR-125b affects apoptosis in AML cells are as follows: First, miR-125b partly targets core binding factor β (CBFβ) and blocks apoptosis by downregulating multiple genes involved in the p53 pathway (76). Second, it inhibits apoptosis and promotes cell proliferation by affecting brassinosteroid-insensitive 1-associated receptor kinase 1 (BAK1) expression (77). Third, miR-125b facilitates the progression of leukemia by promoting the expression of oncogenic MLL-AFF9 *in vivo*, and it upregulates VEGFA, providing conditions conducive to the expansion of leukemic cells. This process involves carcinogenic miRNAs mediating noncellular endogenous leukemia and promoting the miR-125b-TET2-VEGFA pathway. Fourth, caudal-related homeobox transcription factor 2 (CDX2) binds to the promoter region of the miR-125b gene and activates the expression of miR-125b in malignant myeloid cells, and the generated miR-125b inhibits the translation of CBFβ, thereby inhibiting the differentiation of myeloid cells in granulocyte lineaments and promoting the occurrence of leukemia (78). Exosomes in the sera of patients with AML are enriched in miR-10, and miR-10b can inhibit apoptosis and homeobox D10 expression in AML cells by directly targeting homeobox D10 (79).

Exosomes are involved in the development of drug resistance in AML

Co-culturing of exosomes with multi-drug-resistant AML cell line with chemo-sensitive HL-60 may cause chemo-resistance because of the transfer of miR-19b and miR-20a to the exosomes; thus, exosomes can make chemo-sensitive cells resistant to chemotherapy (80). Chen et al. demonstrated that exosomes secreted by the AML cell KG1α can drive BM stromal cells to produce IL-8, which can inhibit the chemotherapy-induced apoptosis of AML cells (81). Moreover, an exosome-mediated communication mechanism may impede drug therapy. Hekmatirad et al. found that U937 cells (an AML cell line) increase their resistance to the cytotoxic effects of doxorubicin (PLD) in pegylated liposomes through exosome-mediated drug expulsion (82). Another study that investigated the chemoresistance of AML-BMSC exosomes showed that miR-155 and miR-375 in exosomes derived from AML cells are responsible for chemoresistance to chemotherapeutic drugs cytarabine and AC220; the possible mechanism is the miRNA-induced downregulation of the promoters of apoptosis or cell differentiation under the guidance; free leukemic cells become independent of the kinase pathway through this mechanism (83).

Application of exosomes in the diagnosis and prognosis of AML

Exosomes as biomarkers of tumors have attracted considerable interest (84). They are present in various body fluids and easy to isolate and can be extracted from a small amount of serum (85). Moreover, they have a unique molecular profile (61). AML-secreted exosomal miRNAs are involved in the progression of AML and can be used as entry points for AML treatment (86, 87).

AML might reflect unique miRNA profiles. Compared with the sera of healthy individuals, the sera of patients with tumors contain a large number of exosomes and specific pathogenic information molecules of parental cell origin, which represent the biological behavior of parental cells (88). For example, miRNAs, are important cargoes carried by exosomes because they act in tumor tissues through targeted molecules. miRNAs are important biomarkers of tumor development and prognosis and are protected by exosomal surface membranes with highly conserved sequences. These membranes are stable under extreme conditions and can prevent miRNAs from being released into the circulation (89). miRNAs have potential use in the diagnosis of multiple diseases (90). Exosomal miRNA can be collected from 20 μL of serum and can be used as an ideal molecular marker for the targeted diagnosis and prognosis of leukemia (91). Serum exosomal miR-10b is an independent prognostic factor for overall survival in AML patients. miR-10b expression levels are elevated in the sera of patients with AML, and its expression levels are strongly correlated with poor prognosis, and miR-10b level considerably increases in patients with AML (92–94). Therefore, serum exosomal miR-10b is a potential diagnostic and prognostic marker for AML.

The expression levels of miR-146a/b, miR-181a/b/d, miR-130a, miR-663, and miR-135b were high in M1, whereas those of miR-21, miR-193a, and miR-370 were high in M5 (95). In addition, miR-155 is downregulated in peripheral blood mononuclear cells from patients with multi-drug-resistant AML and adriamycin-resistant AML cell lines and showed a positive correlation in these patients. miR-155 can be used as a monitoring indicator for drug resistance and micro-residual focus with high sensitivity (96).

As mentioned above, numerous biomarkers can demonstrate powerful uniqueness in the diagnostic prediction of AML (Table 1). AML-derived exosomes are rich in CD33, CD34, and CD117, and their overall protein content is significantly higher than that of healthy controls; the content of some proteins, such as TGF-β1, decreases at the initial diagnosis and effective treatment of AML and can thus be used for detecting leukemia relapse and drug resistance status (97). Plasma exosomal lncRNAs are potential cell-free indicators for the diagnosis and therapeutic monitoring of AML and offer novel and cutting-edge concepts for the liquid biopsy of hematologic cancers (98). Bernardi et al. first used the commercially available CE-IVD-based kits for exosome-enrichment methods to investigate leukemic sources and exosomal dsDNA target resequencing for adult AML marker detection; they performed next-generation sequencing analysis of exosome-derived dsDNA isolated from 14 adult patients with AML and identified the optimal amount of exosomal dsDNA as a potential AML biomarker for liquid biopsies; they found exosomal dsDNA can be developed as a tool that can facilitate the monitoring of AML progression and the early diagnosis of relapse after allogeneic hematopoietic stem cell transplantation (99). In summary, exosomes may offer a novel perspective on AML diagnosis and treatment response (Table 2).

Use of exosomes in the treatment of AML

Currently, patients with refractory/recurrent AML experience an aggressive clinical course and have poor prognoses. Therefore, complementary alternative therapies are urgently needed to improve conventional treatments and increase survival rate (103). Blocking exosome-induced production, secretion, and reprogramming has emerged as a novel approach to treating AML and other types of leukemia. This exosome-targeted therapy may be financially beneficial for elderly patients with AML or patients with AML who cannot tolerate strongly induced chemotherapy (101, 104). Therefore, exosome-based immunotherapy has attracted considerable interest. In T-cell lymphoma mice, it effectively eliminated minimal residual disease and prolonged disease-free survival (100). TEX-carrying tumor-associated antigens are potential cell-free tumor treatments for the specific eradication of minimal residual leukemic cells (105). Huang et al. found that

TABLE 1 Currently AML biomarkers carried by exosomes.

Substance		Expression	Sample	Reference
Micro-RNA	miR-10b	Upregulated	Bone marrow	(15)
	miR-125b	Upregulated	Plasma	(12)
	miR-155	Upregulated	Plasma	(12)
	miR-21	Upregulated	Bone marrow	(87)
	miR-523	Upregulated	Bone marrow	(88)
	miR-10a-5p	Upregulated	serum	
	miR-93-5p	Upregulated	serum	
	miR-129-5p	Upregulated	serum	
	miR-155-5p	Upregulated	serum	
	miR-181b-5p	Upregulated	serum	
	miR-320d	Upregulated	serum	
Protein	CD33	Upregulated	Plasma	(61)
	CD117	Upregulated	Plasma	
	CD34	Upregulated	Plasma	(47)
	TGF-β1	Upregulated	Plasma	(4)
lncRNA	LINC00265	Downregulated	Plasma	(59)
	LINC00467	Downregulated	Plasma	
	UCA1	Downregulated	Plasma	
	SNHG1	Upregulated	Plasma	

TABLE 2 Promising therapy directions of exosomes in AML.

		Introduction	Reference
Tumor vaccines	TEX-based vaccines	Using exosomes from $LEX_{TGF-\beta1si}$ as a prophylactic and therapeutic cancer vaccine in a mouse model showed a higher induction-specific antitumor effect, exhibiting more pronounced tumor Growth inhibition and prolongation of survival.	(100)
	T cells-based vaccines	*In vitro* analysis showed that tumor-specific $CD4^+$ and $CD8^+$ IFN-γ-secreting cells could be efficiently expanded from immunized mice, suggesting that the T helper 1 response is involved in tumor rejection and can kill tumor cells	(82)
	DC-based vaccines	Exosomes are extracted from the serum of AML patients to pulse DC, so that DC recognizes and absorbs the specific antigen contained in it, and DC further activates tumor-specific cytotoxic T cells to generate an immune response and kill AML cells.	(64)
Therapeutic target		Reduce the level of exosome secretion by interfering with the synthesis, release and uptake of exosomes and interfere with their signaling pathways mediated in target cells	(101)
		miR-34c-5p promotes AML cell eradication by selectively targeting RAB27B to inhibit exosome shedding and induce cellular senescence.	(49)
		Transfer of miR-222-3p into THP-1 cells promotes proliferation inhibition and apoptosis of AML cells by targeting the IRF2/INPP4B signaling pathway.	(100)
		miR-29 targets protein kinase b (Akt2) and cyclin D2 proteins, as well as the negative feedback loop of MYC proto-oncogene (c-Myc) -Akt2 on miR-29.	(87)
		miR-451 is involved in the late maturation of erythroid cells, but the introduction of miR-451 into AML cell lines decreased the cell proliferation rate and increased the apoptotic activity.	
Remission of drug resistance		Exosomes can transfer drug resistance between cells through contents, and inhibiting the secretion of these contents helps to alleviate drug resistance	(102)

lentiviral shRNA– silenced TGF-β1 expression in parental cells of mouse acute lymphoblastic leukemia cell lines and exosomes from TGF-β1-silenced leukemia cells ($LEX_{TGF-\beta1si}$) had a higher induction-specific antitumor effect than unmodified leukemia cell–derived exosomes. In mouse models, $LEX_{TGF-\beta1si}$ inhibited tumor growth and prolonged survival as a prophylactic and therapeutic cancer drug (102). This finding suggests that exosomal immune vaccines hold promise for the treatment of leukemia through immunotherapy.

As actionable drug-resistant mediators, exosomes may play a key role in current and future AML treatment. Hekmatirad et al. found that tumor cells can excrete drugs through exosomes and result in resistance and that inhibiting exosome release with GW4869 increases the sensitivity of U937 cells to PLD Therefore, the use of exosome inhibitors is a potential strategy for increasing the sensitivity of cancer cells to treatment. Inhibitors that pharmacologically inhibit exosome release (such as neticonazole, ketotifen, cannabidiol, and GW4869) are effective. Mortality and morbidity in AML are associated with frequent cytopenia, and exosomes may be involved in the suppression of normal hematopoiesis in leukemia (82). Namburi et al. found that exosomes isolated from the plasma of AML patients carry abundant dipeptidyl peptidase 4 (DPP4) and inhibit the differentiation of normal hematopoietic progenitor cells *in vitro*; pharmacologically inhibiting DPP4 reverses exosome-mediated colony formation; therefore, reversing the negative effects of DPP4 exosomes, improving platelet and neutrophil counts, and restoring BM function in patients are promising treatment approaches for AML; however, many regulatory proteins in exosomes contain DPP4 truncation sites and may have different induction, enhancement, or inhibition effects on hematopoiesis (106).

The systematic design of drug delivery vehicles can address many issues, such as low water solubility, poor biocompatibility, rapid metabolism *in vivo*, easy accumulation in nonpathological tissues, and poor ability to penetrate the membranes of some drugs (107). Exosomes as drug delivery vehicles are mainly dependent on their unique natural physicochemical properties, including phospholipid membrane structure that protects them from destruction by nucleases and proteases, high stability in blood, and long blood half-life (108). Nanoscale and lipid bilayer membranes prevents their removal by mononuclear phagocytes and reduce immunogenicity (especially of autologous cell origin), resulting in low cytotoxicity. The specific lipid and protein composition makes them highly stable in body fluids and enables them to readily fuse with target cells, rendering them chemotactic for specific target cells. Exosomes possess distinctive membrane structures that enables them to easily cross the biofilm barrier and act as carriers through specific delivery modes and modifications (109). These advantageous features of exosomes as drug carriers render them highly attractive for precision medicine. Bellavia et al. used HEK293T cells to express Lamp2b, an exosomal protein fused to an IL-3 fragment, and showed that IL3-Lamp2b exosomes loaded with imatinib targeted chronic myelogenous leukemic cells and inhibited cancer cell growth *in vitro* and *in vivo* (110). Kim et al. used exosomes to deliver paclitaxel or doxorubicin to mitigate multidrug resistance in lung cancer (111).

However, exosomes as drug carriers for AML treatment are currently underdeveloped.

Conclusion

During the progression of AML, exosomes secreted by AML cells can promote the development of AML by affecting the

proliferation and apoptosis of AML cells, regulating the BM microenvironment, affecting angiogenesis, and inhibiting hematopoiesis. Therefore, according to the characteristics of AML cell-derived exosomes, exosomes can also be used as biomarkers of AML prognosis, preparing vaccines and drug carriers.

Author contributions

WDW: Writing – original draft. XFW: Writing – original draft. RY: Visualization, Writing – review & editing. JMZ: Validation, Writing – review & editing. YQL: Writing – review & editing. XLW: Writing – review & editing. LX: Writing – review & editing. ZYJ: Writing – review & editing.

Funding

The author(s) declare financial support was received for the research, authorship, and/or publication of this article. This study was supported by grants from the Science and Technology Program of Guangzhou City (202201010164), the National Natural Science Foundation of China (81800143, 81770150, 81200388, and 82170220), the Natural Science Foundation of Guangdong Province (2020A1515010817, 2022A1515010313, and 2023A1515030271), the National Innovation and Entrepreneurship Training Program for Undergraduates (202310559054), Guangdong's Innovation and Entrepreneurship Training Program for Undergraduates (202010559081 and 202210559083), and Guangdong College Students' Scientific and Technological Innovation (CX23304).

Conflict of interest

The authors declare that the research was conducted in the absence of any commercial or financial relationships that could be construed as a potential conflict of interest.

Publisher's note

References

1. Burnett A, Wetzler M, Lowenberg B. Therapeutic advances in acute myeloid leukemia. *J Clin Oncol* (2011) 29(5):487–94. doi: 10.1200/JCO.2010.30.1820

2. Cheng Y, Wang X, Qi P, Liu C, Wang S, Wan Q, et al. Tumor microenvironmental competitive endogenous RNA network and immune cells act as robust prognostic predictor of acute myeloid leukemia. *Front Oncol* (2021) 11:584884. doi: 10.3389/fonc.2021.584884

3. Tang BJ, Sun B, Chen L, Xiao J, Huang ST, Xu P. The landscape of exosome-derived non-coding RNA in leukemia. *Front Pharmacol* (2022) 13:912303. doi: 10.3389/fphar.2022.912303

4. Mirfakhraie R, Noorazar L, Mohammadian M, Hajifathali A, Gholizadeh M, Salimi M, et al. Treatment failure in acute myeloid leukemia: focus on the role of extracellular vesicles. *Leukemia Res* (2022) 112:106751. doi: 10.1016/j.leukres.2021.106751

5. Keller S, Ridinger J, Rupp A-K, Janssen JWG, Altevogt P. Body fluid derived exosomes as a novel template for clinical diagnostics. *J Trans Med* (2011) 9:86. doi: 10.1186/1479-5876-9-86

6. Huang F, Wan J, Hu W, Hao S. Enhancement of anti-leukemia immunity by leukemia–derived exosomes *via* downregulation of TGF-β1 expression. *Cell Physiol Biochem* (2017) 44(1):240–54. doi: 10.1159/000484677

7. Hoshino A, Costa-Silva B, Shen TL, Rodrigues G, Hashimoto A, Mark MT, et al. Tumour exosome integrins determine organotropic metastasis. *Nat* (2015) 527 (7578):329–35. doi: 10.1038/nature15756

8. Azmi AS, Bao B, Sarkar FH. Exosomes in cancer development, metastasis, and drug resistance: a comprehensive review. *Cancer Metastasis Rev* (2013) 32(3-4):623–42. doi: 10.1007/s10555-013-9441-9

9. Meng W, Hao Y, He C, Li L, Zhu G. Exosome-orchestrated hypoxic tumor microenvironment. *Mol Cancer* (2019) 18(1):57. doi: 10.1186/s12943-019-0982-6

10. Rajagopal C, Harikumar KB. The origin and functions of exosomes in cancer. *Front Oncol* (2018) 8:66. doi: 10.3389/fonc.2018.00066

11. Wolf-Dennen K, Kleinerman ES. Exosomes: dynamic mediators of extracellular communication in the tumor microenvironment. *Adv Exp Med Biol* (2020) 1258:189–97. doi: 10.1007/978-3-030-43085-6_13

12. Amin AH, Al Sharifi LM, Kakhharov AJ, Opulencia MJC, Alsaikhan F, Bokov DO, et al. Role of Acute Myeloid Leukemia (AML)-Derived exosomes in tumor progression and survival. *Biomed Pharmacother* (2022) 150:113009. doi: 10.1016/j.biopha.2022.113009

13. Kumar B, Garcia M, Murakami JL, Chen C-C. Exosome-mediated microenvironment dysregulation in leukemia. *Biochim Et Biophys Acta-Molecular Cell Res* (2016) 1863(3):464–70. doi: 10.1016/j.bbamcr.2015.09.017

14. Zuo Z, Hong CS, Muller L, Boyiadzis M, Whiteside TL. Isolation and characterization of CD34+ Blast-derived exosomes in acute myeloid leukemia. *PloS One* (2014) 9(8):e103310. doi: 10.1371/journal.pone.0103310

15. Stahl PD, Raposo G. Extracellular vesicles: exosomes and microvesicles, integrators of homeostasis. *Physiol* (2019) 34(3):169–77. doi: 10.1152/physiol.00045.2018

16. Hurley JH. ESCRT complexes and the biogenesis of multivesicular bodies. *Curr Opin Cell Biol* (2008) 20(1):4–11. doi: 10.1016/j.ceb.2007.12.002

17. Rädler J, Gupta D, Zickler A, Andaloussi SE. Exploiting the biogenesis of extracellular vesicles for bioengineering and therapeutic cargo loading. *Mol Ther J Am Soc Gene Ther* (2023) 31(5):1231–50. doi: 10.1016/j.ymthe.2023.02.013

18. Bilodeau PS, Urbanowski JL, Winistorfer SC, Piper RC. The Vps27p Hse1p complex binds ubiquitin and mediates endosomal protein sorting. *Nat Cell Biol* (2002) 4(7):534–9. doi: 10.1038/ncb815

19. Raiborg C, Bache KG, Gillooly DJ, Madshus IH, Stang E, Stenmark H. Hrs sorts ubiquitinated proteins into clathrin-coated microdomains of early endosomes. *Nat Cell Biol* (2002) 4(5):394–8. doi: 10.1038/ncb791

20. Wegner CS, Schink KO, Stenmark H, Brech A. Monitoring phosphatidylinositol 3-phosphate in multivesicular endosome biogenesis. *Methods enzymol* (2014) 534:3–23. doi: 10.1016/B978-0-12-397926-1.00001-9

21. Bache KG, Brech A, Mehlum A, Stenmark H. Hrs regulates multivesicular body formation *via* ESCRT recruitment to endosomes. *J Cell Biol* (2003) 162(3):435–42. doi: 10.1083/jcb.200302131

22. Lu Q, Hope LW, Brasch M, Reinhard C, Cohen SN. TSG101 interaction with HRS mediates endosomal trafficking and receptor down-regulation. *Proc Natl Acad Sci United States America* (2003) 100(13):7626–31. doi: 10.1073/pnas.0932599100

23. Teo H, Gill DJ, Sun J, Perisic O, Veprintsev DB, Vallis Y, et al. ESCRT-I core and ESCRT-II GLUE domain structures reveal role for GLUE in linking to ESCRT-I and membranes. *Cell* (2006) 125(1):99–111. doi: 10.1016/j.cell.2006.01.047

24. Gill DJ, Teo H, Sun J, Perisic O, Veprintsev DB, Emr SD, et al. Structural insight into the ESCRT-I/-II link and its role in MVB trafficking. *EMBO J* (2007) 26(2):600–12. doi: 10.1038/sj.emboj.7601501

25. Teis D, Saksena S, Emr SD. Ordered assembly of the ESCRT-III complex on endosomes is required to sequester cargo during MVB formation. *Dev Cell* (2008) 15 (4):578–89. doi: 10.1016/j.devcel.2008.08.013

26. Wollert T, Wunder C, Lippincott-Schwartz J, Hurley JH. Membrane scission by the ESCRT-III complex. *Nat* (2009) 458(7235):172–7. doi: 10.1038/nature07836

27. Lata S, Schoehn G, Jain A, Pires R, Piehler J, Gottlinger HG, et al. Helical structures of ESCRT-III are disassembled by VPS4. *Sci (New York NY)* (2008) 321 (5894):1354–7. doi: 10.1126/science.1161070

28. Saksena S, Wahlman J, Teis D, Johnson AE, Emr SD. Functional reconstitution of ESCRT-III assembly and disassembly. *Cell* (2009) 136(1):97–109. doi: 10.1016/j.cell.2008.11.013

29. Jackson CE, Scruggs BS, Schaffer JE, Hanson PI. Effects of inhibiting VPS4 support a general role for ESCRTs in extracellular vesicle biogenesis. *Biophys J* (2017) 113(6):1342–52. doi: 10.1016/j.bpj.2017.05.032

30. Perez-Hernandez D, Gutiérrez-Vázquez C, Jorge I, López-Martín S, Ursa A, Sánchez-Madrid F, et al. The intracellular interactome of tetraspanin-enriched microdomains reveals their function as sorting machineries toward exosomes. *J Biol Chem* (2013) 288(17):11649–61. doi: 10.1074/jbc.M112.445304

31. Jankovičová J, Sečová P, Michalková K, Antalíková J. Tetraspanins, more than markers of extracellular vesicles in reproduction. *Int J Mol Sci* (2020) 21(20):7568. doi: 10.3390/ijms21207568

32. Wei D, Zhan W, Gao Y, Huang L, Gong R, Wang W, et al. RAB31 marks and controls an ESCRT-independent exosome pathway. *Cell Res* (2021) 31(2):157–77. doi: 10.1038/s41422-020-00409-1

33. Chairoungdua A, Smith DL, Pochard P, Hull M, Caplan MJ. Exosome release of β-catenin: a novel mechanism that antagonizes Wnt signaling. *J Cell Biol* (2010) 190 (6):1079–91. doi: 10.1083/jcb.201002049

34. Arya SB, Chen S, Jordan-Javed F, Parent CA. Ceramide-rich microdomains facilitate nuclear envelope budding for non-conventional exosome formation. *Nat Cell Biol* (2022) 24(7):1019–28. doi: 10.1038/s41556-022-00934-8

35. Mittelbrunn M, Gutiérrez-Vázquez C, Villarroya-Beltri C, González S, Sánchez-Cabo F, González M, et al. Unidirectional transfer of microRNA-loaded exosomes from T cells to antigen-presenting cells. *Nat Commun* (2011) 2:282. doi: 10.1038/ncomms1285

36. Sinha S, Hoshino D, Hong NH, Kirkbride KC, Grega-Larson NE, Seiki M, et al. Cortactin promotes exosome secretion by controlling branched actin dynamics. *J Cell Biol* (2016) 214(2):197–213. doi: 10.1083/jcb.201601025

37. Cabezas A, Bache KG, Brech A, Stenmark H. Alix regulates cortical actin and the spatial distribution of endosomes. *J Cell science* (2005) 118(Pt 12):2625–35. doi: 10.1242/jcs.02382

38. Han J, Pluhackova K, Böckmann RA. The multifaceted role of SNARE proteins in membrane fusion. *Front Physiol* (2017) 8:5. doi: 10.3389/fphys.2017.00005

39. Gross JC, Chaudhary V, Bartscherer K, Boutros M. Active Wnt proteins are secreted on exosomes. *Nat Cell Biol* (2012) 14(10):1036–45. doi: 10.1038/ncb2574

40. Wei Y, Wang D, Jin F, Bian Z, Li L, Liang H, et al. Pyruvate kinase type M2 promotes tumour cell exosome release *via* phosphorylating synaptosome-associated protein 23. *Nat Commun* (2017) 8:14041. doi: 10.1038/ncomms14041

41. Fitzner D, Schnaars M, van Rossum D, Krishnamoorthy G, Dibaj P, Bakhti M, et al. Selective transfer of exosomes from oligodendrocytes to microglia by macropinocytosis. *J Cell Science* (2011) 124(3):447–58. doi: 10.1242/jcs.074088

42. Feng D, Zhao W-L, Ye Y-Y, Bai X-C, Liu R-Q, Chang L-F, et al. Cellular internalization of exosomes occurs through phagocytosis. *Traffic* (2010) 11(5):675–87. doi: 10.1111/j.1600-0854.2010.01041.x

43. Morelli AE, Larregina AT, Shufesky WJ, Sullivan MLG, Stolz DB, Papworth GD, et al. Endocytosis, intracellular sorting, and processing of exosomes by dendritic cells. *Blood* (2004) 104(10):3257–66. doi: 10.1182/blood-2004-03-0824

44. Kourembanas S. Exosomes: vehicles of intercellular signaling, biomarkers, and vectors of cell therapy. *Annu Rev Physiol* (2015) 77(1):13–27. doi: 10.1146/annurev-physiol-021014-071641

45. Yáñez-Mó M, Siljander PRM, Andreu Z, Bedina Zavec A, Borràs FE, Buzas EI, et al. Biological properties of extracellular vesicles and their physiological functions. *J Extracellular Vesicles* (2015) 4(1):27066. doi: 10.3402/jev.v4.27066

46. Merchant ML, Rood IM, Deegens JKJ, Klein JB. Isolation and characterization of urinary extracellular vesicles: implications for biomarker discovery. *Nat Rev Nephrol* (2017) 13(12):731–49. doi: 10.1038/nrneph.2017.148

47. Singh N, Huang L, Wang DB, Shao N, Zhang XE. Simultaneous detection of a cluster of differentiation markers on leukemia-derived exosomes by multiplex immuno-polymerase chain reaction *via* capillary electrophoresis analysis. *Analytical Chem* (2020) 92(15):10569–77. doi: 10.1021/acs.analchem.0c01464

48. Kalra H, Drummen G, Mathivanan S. Focus on extracellular vesicles: introducing the next small big thing. *Int J Mol Sci* (2016) 17(2):170. doi: 10.3390/ijms17020170

49. Chaput N, Taieb J, Schartz NEC, Andre F, Angevin E, Zitvogel L. Exosome-based immunotherapy. *Cancer Immunol Immunother* (2004) 53(3):234–9. doi: 10.1007/s00262-003-0472-x

50. Salehi M, Sharifi M. Exosomal miRNAs as novel cancer biomarkers: Challenges and opportunities. *J Cell Physiol* (2018) 233(9):6370–80. doi: 10.1002/jcp.26481

51. Zhu L, Sun HT, Wang S, Huang SL, Zheng Y, Wang CQ, et al. Isolation and characterization of exosomes for cancer research. *J Hematol Oncol* (2020) 13(1):152. doi: 10.1186/s13045-020-00987-y

52. Whiteside T. Immune suppression in cancer: Effects on immune cells, mechanisms and future therapeutic intervention. *Semin Cancer Biol* (2006) 16(1):3–15. doi: 10.1016/j.semcancer.2005.07.008

53. Wieckowski EU, Visus C, Szajnik M, Szczepanski MJ, Storkus WJ, Whiteside TL. Tumor-derived microvesicles promote regulatory T cell expansion and induce apoptosis in tumor-reactive activated CD8+ T lymphocytes. *J Immunol* (2009) 183 (6):3720–30. doi: 10.4049/jimmunol.0900970

54. Hong C-S, Sharma P, Yerneni SS, Simms P, Jackson EK, Whiteside TL, et al. Circulating exosomes carrying an immunosuppressive cargo interfere with cellular immunotherapy in acute myeloid leukemia. *Sci Rep* (2017) 7(1):14684. doi: 10.1038/s41598-017-14661-w

55. Szajnik M, Czystowska M, Szczepanski MJ, Mandapathil M, Whiteside TL. Tumor-derived microvesicles induce, expand and up-regulate biological activities of human regulatory T cells (Treg). *PloS One* (2010) 5(7):e11469. doi: 10.1371/journal.pone.0011469

56. Zhang SH, Han YX, Wu JB, Yu K, Bi LX, Zhuang Y, et al. Elevated frequencies of CD4(+)CD25(+)CD127(lo) regulatory T cells is associated to poor prognosis in patients with acute myeloid leukemia. *Int J Cancer* (2011) 129(6):1373–81. doi: 10.1002/ijc.25791

57. Pando A, Schorl C, Fast LD, Reagan JL. Tumor derived extracellular vesicles modulate gene expression in T cells. *Gene* (2023) 850:146920. doi: 10.1016/j.gene.2022.146920

58. Lion E, Willemen Y, Berneman ZN, Van Tendeloo VFI, Smits ELJ. Natural killer cell immune escape in acute myeloid leukemia. *Leukemia* (2012) 26(9):2019–26. doi: 10.1038/leu.2012.87

59. Venton G, Labiad Y, Colle J, Fino A, Afridi S, Torres M, et al. Natural killer cells in acute myeloid leukemia patients: from phenotype to transcriptomic analysis. *Immunologic Res* (2016) 64(5-6):1225–36. doi: 10.1007/s12026-016-8848-0

60. Hong C-S, Muller L, Whiteside TL, Boyiadzis M. Plasma exosomes as markers of therapeutic response in patients with acute myeloid leukemia. *Front Immunol* (2014) 5:160. doi: 10.3389/fimmu.2014.00160

61. Szczepanski MJ, Szajnik M, Welsh A, Whiteside TL, Boyiadzis M. Blast-derived microvesicles in sera from patients with acute myeloid leukemia suppress natural killer cell function *via* membrane-associated transforming growth factor- 1. *Haematologica* (2011) 96(9):1302–9. doi: 10.3324/haematol.2010.039743

62. Hong C-S, Danet-Desnoyers G, Shan X, Sharma P, Whiteside TL, Boyiadzis M. Human acute myeloid leukemia blast-derived exosomes in patient-derived xenograft mice mediate immune suppression. *Exp Hematol* (2019) 76:60–6. doi: 10.1016/j.exphem.2019.07.005

63. Valenti R, Huber V, Filipazzi P, Pilla L, Sovena G, Villa A, et al. Human tumor-released microvesicles promote the differentiation of myeloid cells with transforming growth factor-beta-mediated suppressive activity on T lymphocytes. *Cancer Res* (2006) 66(18):9290–8. doi: 10.1158/0008-5472.CAN-06-1819

64. Benites BD, Duarte ADS, Longhini ALF, Santos I, Alvarez MC, Ribeiro LND, et al. Exosomes in the serum of Acute Myeloid Leukemia patients induce dendritic cell tolerance: Implications for immunotherapy. *Vaccine* (2019) 37(11):1377–83. doi: 10.1016/j.vaccine.2019.01.079

65. Deng W, Wang L, Pan M, Zheng J. The regulatory role of exosomes in leukemia and their clinical significance. *J Int Med Res* (2020) 48(8):300060520950135. doi: 10.1177/0300060520950135

66. Kumar B, Garcia M, Weng L, Jung X, Murakami JL, Hu X, et al. Acute myeloid leukemia transforms the bone marrow niche into a leukemia-permissive microenvironment through exosome secretion. *Leukemia* (2017) 32(3):575–87. doi: 10.1038/leu.2017.259

67. Miyamoto KN, Bonatto D. Circulating cells and exosomes in acute myelogenous leukemia and their role in disease progression and survival. *Clin Immunol* (2020) 217:108489. doi: 10.1016/j.clim.2020.108489

68. Pei Y, Zhang H, Lu K, Tang X, Li J, Zhang E, et al. Circular RNA circRNA_0067934 promotes glioma development by modulating the microRNA miR-7/ Wnt/β-catenin axis. *Bioengineered* (2022) 13(3):5792–802. doi: 10.1080/21655979.2022.2033382

69. Xue H, Hua LM, Guo M, Luo JM. SHIP1 is targeted by miR-155 in acute myeloid leukemia. *Oncol Rep* (2014) 32(5):2253–9. doi: 10.3892/or.2014.3435

70. Gerloff D, Grundler R, Wurm AA, Bräuer-Hartmann D, Katzerke C, Hartmann JU, et al. NF-κB/STAT5/miR-155 network targets PU.1 in FLT3-ITD-driven acute myeloid leukemia. *Leukemia* (2014) 29(3):535–47. doi: 10.1038/leu.2014.231

71. Peng DY, Wang HF, Li L, Ma X, Chen Y, Zhou H, et al. miR-34c-5p promotes eradication of acute myeloid leukemia stem cells by inducing senescence through selective RAB27B targeting to inhibit exosome shedding. *Leukemia* (2018) 32(5):1180–8. doi: 10.1038/s41375-018-0015-2

72. Sharawat SK, Bakhshi R, Vishnubhatla S, Gupta R, Bakhshi S. BAX/BCL2RMFI ratio predicts better induction response in pediatric patients with acute myeloid leukemia. *Pediatr Blood Cancer* (2013) 60(8):E63–E6. doi: 10.1002/pbc.24518

73. Li Z, Lu J, Sun M, Mi S, Zhang H, Luo RT, et al. Distinct microRNA expression profiles in acute myeloid leukemia with common translocations. *Proc Natl Acad Sci United States America* (2008) 105(40):15535–40. doi: 10.1073/pnas.0808266105

74. Iorio MV, Croce CM. MicroRNAs in cancer: small molecules with a huge impact. *J Clin Oncol* (2009) 27(34):5848–56. doi: 10.1200/JCO.2009.24.0317

75. Jiang LJ, Deng TR, Wang D, Xiao Y. Elevated serum exosomal miR-125b level as a potential marker for poor prognosis in intermediate-risk acute myeloid leukemia. *Acta Haematologica* (2018) 140(3):183–92. doi: 10.1159/000491584

76. Bousquet M, Nguyen D, Chen C, Shields L, Lodish HF. MicroRNA-125b transforms myeloid cell lines by repressing multiple mRNA. *Haematologica* (2012) 97(11):1713–21. doi: 10.3324/haematol.2011.061515

77. Liu J, Guo B, Chen Z, Wang N, Iacovino M, Cheng J, et al. miR-125b promotes MLL-AF9–driven murine acute myeloid leukemia involving a VEGFA-mediated non–cell-intrinsic mechanism. *Blood* (2017) 129(11):1491–502. doi: 10.1182/blood-2016-06-721027

78. Lin K-Y, Zhang X-J, Feng D-D, Zhang H, Zeng C-W, Han B-W, et al. miR-125b, a target of CDX2, regulates cell differentiation through repression of the core binding factor in hematopoietic Malignancies. *J Biol Chem* (2011) 286(44):38253–63. doi: 10.1074/jbc.M111.269670

79. Wang CJ, Zou H, Feng GF. MiR-10b regulates the proliferation and apoptosis of pediatric acute myeloid leukemia through targeting HOXD10. *Eur Rev Med Pharmacol Sci* (2018) 22(21):7371–8. doi: 10.26355/eurrev_201811_16275

80. Bouvy C, Wannez A, Laloy J, Chatelain C, Dogné J-M. Transfer of multidrug resistance among acute myeloid leukemia cells *via* extracellular vesicles and their microRNA cargo. *Leukemia Res* (2017) 62:70–6. doi: 10.1016/j.leukres.2017.09.014

81. Chen T, Zhang G, Kong L, Xu S, Wang Y, Dong M. Leukemia-derived exosomes induced IL-8 production in bone marrow stromal cells to protect the leukemia cells against chemotherapy. *Life Sci* (2019) 221:187–95. doi: 10.1016/j.lfs.2019.02.003

82. Hekmatirad S, Moloudizargari M, Moghadamnia AA, Kazemi S, Mohammadnia-Afrouzi M, Baeeri M, et al. Inhibition of exosome release sensitizes U937 cells to PEGylated liposomal doxorubicin. *Front Immunol* (2021) 12:692654. doi: 10.3389/fimmu.2021.692654

83. Viola S, Traer E, Huan J, Hornick NI, Tyner JW, Agarwal A, et al. Alterations in acute myeloid leukaemia bone marrow stromal cell exosome content coincide with gains in tyrosine kinase inhibitor resistance. *Br J Haematol* (2016) 172(6):983–6. doi: 10.1111/bjh.13551

84. Makler A, Asghar W. Exosomal biomarkers for cancer diagnosis and patient monitoring. *Expert Rev Mol Diagnostics* (2020) 20(4):387–400. doi: 10.1080/14737159.2020.1731308

85. Hornick NI, Huan J, Doron B, Goloviznina NA, Lapidus J, Chang BH, et al. Serum exosome microRNA as a minimally-invasive early biomarker of AML. *Sci Rep* (2015) 5:11295. doi: 10.1038/srep11295

86. Fletcher D, Brown E, Javadala J, Uysal-Onganer P, Guinn B. microRNA expression in acute myeloid leukaemia: New targets for therapy? *eJHaem* (2022) 3 (3):596–608. doi: 10.1002/jha2.441

87. Buhagiar A, Borg J, Ayers D. Overview of current microRNA biomarker signatures as potential diagnostic tools for leukaemic conditions. *Non-Coding RNA Res* (2020) 5(1):22–6. doi: 10.1016/j.ncrna.2020.02.001

88. Tickner JA, Richard DJ, O'Byrne KJEV. Microvesicles/microRNAs and stem cells in cancer. *Adv Exp Med Biol* (2018) 1056:123–35. doi: 10.1007/978-3-319-74470-4_8

89. He Y, Lin J, Kong D, Huang M, Xu C, Kim T-K, et al. Current state of circulating microRNAs as cancer biomarkers. *Clin Chem* (2015) 61(9):1138–55. doi: 10.1373/clinchem.2015.241190

90. Ni L, Tang C, Wang Y, Wan J, Charles MG, Zhang Z, et al. Construction of a miRNA-based nomogram model to predict the prognosis of endometrial cancer. *J personalized Med* (2022) 12(7):1154. doi: 10.3390/jpm12071154

91. Abdelhamed S, Butler JT, Jung S, Chen D-W, Jenkins G, Gao L, et al. Rational biomarker development for the early and minimally invasive monitoring of AML. *Blood Advances* (2021) 5(21):4515–20. doi: 10.1182/bloodadvances.2021004621

92. Fang ZG, Wang XZ, Wu JY, Xiao RZ, Liu JJ. High serum extracellular vesicle miR-10b expression predicts poor prognosis in patients with acute myeloid leukemia. *Cancer Biomarkers* (2020) 27(1):1–9. doi: 10.3233/CBM-190211

93. Zou Q, Tan S, Yang ZL, Wang J, Xian JR, Zhang SS, et al. The human nucleophosmin 1 mutation A inhibits myeloid differentiation of leukemia cells by modulating miR-10b. *Oncotarget* (2016) 7(44):71477–90. doi: 10.18632/oncotarget.12216

94. Bi L, Sun L, Jin Z, Zhang S, Shen Z. MicroRNA-10a/b are regulators of myeloid differentiation and acute myeloid leukemia. *Oncol letters* (2018) 15(4):5611–9. doi: 10.3892/ol.2018.8050

95. Lutherborrow M, Bryant A, Jayaswal V, Agapiou D, Palma C, Yang YH, et al. Expression profiling of cytogenetically normal acute myeloid leukemia identifies microRNAs that target genes involved in monocytic differentiation. *Am J Hematol* (2011) 86(1):2–11. doi: 10.1002/ajh.21864

96. Yu YN, Kou DQ, Liu B, Huang YR, Li SD, Qi Y, et al. LncRNA MEG3 contributes to drug resistance in acute myeloid leukemia by positively regulating ALG9 through sponging miR-155. *Int J Lab Hematol* (2020) 42(4):464–72. doi: 10.1111/ijlh.13225

97. Boyiadzis M, Whiteside TL. Plasma-derived exosomes in acute myeloid leukemia for detection of minimal residual disease: are we ready? *Expert Rev Mol Diagnostics* (2016) 16(6):623–9. doi: 10.1080/14737159.2016.1174578

98. Xiao QL, Lin C, Peng MX, Ren J, Jing YP, Lei L, et al. Circulating plasma exosomal long non-coding RNAs LINC00265, LINC00467, UCA1, and SNHG1 as biomarkers for diagnosis and treatment monitoring of acute myeloid leukemia. *Front Oncol* (2022) 12:1033143. doi: 10.3389/fonc.2022.1033143

99. Bernardi S, Farina M, Bosio K, Di Lucanardo A, Leoni A, Re F, et al. Feasibility of leukemia-derived exosome enrichment and co-isolated dsDNA sequencing in acute myeloid leukemia patients: A proof of concept for new leukemia biomarkers detection. *Cancers* (2022) 14(18):4504. doi: 10.3390/cancers14184504

100. Menay F, Herschlik L, De Toro J, Cocozza F, Tsacalian R, Jose Gravisaco M, et al. Exosomes isolated from ascites of T-cell lymphoma-bearing mice expressing surface CD24 and HSP-90 induce a tumor-specific immune response. *Front Immunol* (2017) 8:286. doi: 10.3389/fimmu.2017.00286

101. Zhang F, Lu Y, Wang M, Zhu J, Li J, Zhang P, et al. Exosomes derived from human bone marrow mesenchymal stem cells transfer miR-222-3p to suppress acute myeloid leukemia cell proliferation by targeting IRF2/INPP4B. *Mol Cell probes* (2020) 51:101513. doi: 10.1016/j.mcp.2020.101513

102. Hessvik NP, Llorente A. Current knowledge on exosome biogenesis and release. *Cell Mol Life Sci* (2018) 75(2):193–208. doi: 10.1007/s00018-017-2595-9

103. Zeichner SB, Gleason S, Antun AG, Langston A, Heffner LT Jr., Kota VK, et al. Survival of patients diagnosed with primary refractory and relapsed acute myeloid leukemia from 2008-2012: A single institution experience. *Blood* (2015) 126(23):4955. doi: 10.1182/blood.V126.23.4955.4955

104. Rashed MH, Bayraktar E, Helal GK, Abd-Ellah MF, Amero P, Chavez-Reyes A, et al. Exosomes: from garbage bins to promising therapeutic targets. *Int J Mol Sci* (2017) 18(3):538. doi: 10.3390/ijms18030538

105. Whiteside Theresa L. Immune modulation of T-cell and NK (natural killer) cell activities by TEXs (tumour-derived exosomes). *Biochem Soc Trans* (2013) 41(1):245–51. doi: 10.1042/BST20120265

106. Namburi S, Broxmeyer HE, Hong CS, Whiteside TL, Boyiadzis M. DPP4(+) exosomes in AML patients' plasma suppress proliferation of hematopoietic progenitor cells. *Leukemia* (2021) 35(7):1925–32. doi: 10.1038/s41375-020-01047-7

107. Peng H, Ji WH, Zhao RC, Yang J, Lu ZG, Li Y, et al. Exosome: a significant nano-scale drug delivery carrier. *J Materials Chem B* (2020) 8(34):7591–608. doi: 10.1039/D0TB01499K

108. Yong TY, Zhang XQ, Bie NN, Zhang HB, Zhang XT, Li FY, et al. Tumor exosome-based nanoparticles are efficient drug carriers for chemotherapy. *Nat Commun* (2019) 10(1):3838. doi: 10.1038/s41467-019-11718-4

109. Bunggulawa EJ, Wang W, Yin TY, Wang N, Durkan C, Wang YZ, et al. Recent advancements in the use of exosomes as drug delivery systems. *J Nanobiotechnol* (2018) 16(1):81. doi: 10.1186/s12951-018-0403-9

110. Bellavia D, Raimondo S, Calabrese G, Forte S, Cristaldi M, Patinella A, et al. Interleukin 3- receptor targeted exosomes inhibit in *vitro* and in *vivo* Chronic Myelogenous Leukemia cell growth. *Theranostics* (2017) 7(5):1333–45. doi: 10.7150/thno.17092

111. Kim MS, Haney MJ, Zhao Y, Mahajan V, Deygen I, Klyachko NL, et al. Development of exosome-encapsulated paclitaxel to overcome MDR in cancer cells. *Nanomed-Nanotechnol Biol Med* (2016) 12(3):655–64. doi: 10.1016/j.nano.2015.10.012

frontiers | Frontiers in Immunology

TYPE Review
PUBLISHED 24 January 2024
DOI 10.3389/fimmu.2024.1310443

OPEN ACCESS

EDITED BY
Sansana Sawasdikosol,
Icahn School of Medicine at Mount Sinai, United States

REVIEWED BY
Ricardo Alexandre Azevedo,
University of Texas MD Anderson Cancer Center, United States
Donatien Kamdem Toukam,
University of Cincinnati, United States

*CORRESPONDENCE
Ziwei Liao
lzw122623@aliyun.com
Mazdak Ganjalıkhani-Hakemi
mazdak.hakemi@medipol.edu.tr

RECEIVED 09 October 2023
ACCEPTED 08 January 2024
PUBLISHED 24 January 2024

CITATION
Ghadiri N, Javidan M, Sheikhi S, Taştan Ö, Parodi A, Liao Z, Tayybi Azar M and Ganjalıkhani-Hakemi M (2024) Bioactive peptides: an alternative therapeutic approach for cancer management. *Front. Immunol.* 15:1310443. doi: 10.3389/fimmu.2024.1310443

Bioactive peptides: an alternative therapeutic approach for cancer management

Nooshin Ghadiri[1], Moslem Javidan[1], Shima Sheikhi[2], Özge Taştan[3], Alessandro Parodi[4], Ziwei Liao[5]*, Mehdi Tayybi Azar[6] and Mazdak Ganjalıkhani-Hakemi[2,7]*

[1]Department of Immunology, Faculty of Medicine, Ahvaz Jundishapour University of Medical Sciences, Ahvaz, Iran, [2]Department of Immunology, Faculty of Medicine, Isfahan University of Medical Sciences, Isfahan, Iran, [3]Department of Food Engineering, Faculty of Engineering, Yeditepe University, Istanbul, Türkiye, [4]Scientific Center for Translation Medicine, Sirius University of Science and Technology, Sochi, Russia, [5]Department of Hematology, Guangzhou Women and Children's Medical Center, Guangzhou Medical University, Guangzhou, China, [6]Department of Biophysics, Faculty of Medicine, Yeditepe University, Istanbul, Türkiye, [7]Regenerative and Restorative Medicine Research Center (REMER), Research Institute for Health Sciences and Technologies (SABITA), Istanbul Medipol University, Istanbul, Türkiye

Cancer is still considered a lethal disease worldwide and the patients' quality of life is affected by major side effects of the treatments including post-surgery complications, chemo-, and radiation therapy. Recently, new therapeutic approaches were considered globally for increasing conventional cancer therapy efficacy and decreasing the adverse effects. Bioactive peptides obtained from plant and animal sources have drawn increased attention because of their potential as complementary therapy. This review presents a contemporary examination of bioactive peptides derived from natural origins with demonstrated anticancer, ant invasion, and immunomodulation properties. For example, peptides derived from common beans, chickpeas, wheat germ, and mung beans exhibited antiproliferative and toxic effects on cancer cells, favoring cell cycle arrest and apoptosis. On the other hand, peptides from marine sources showed the potential for inhibiting tumor growth and metastasis. In this review we will discuss these data highlighting the potential befits of these approaches and the need of further investigations to fully characterize their potential in clinics.

KEYWORDS

anticancer, bioactive peptide, cancer therapy, immunomodulation, cancer immunotherapy

1 Introduction

Cancer treatments vary depending on tumor type and stage, with chemotherapy, radiation therapy, and surgery being the primary approaches for reducing related mortality. Cancer poses a huge global public health challenge that necessitates substantial attention and allocation of resources (1, 2). Based on a recent cross-continental study conducted in 21 countries, it has been found that cancer is the leading cause of death in many countries (3). One of the primary obstacles in treating this disease is the development of multidrug resistance, wherein cancer cells become resistant to numerous drugs. Despite the significant improvements in the field, there is still a pressing need for the development of more effective and tailored treatments (4). A crucial component of cancer treatment is the precise delivery of chemotherapeutics to cancerous cells, to enhance the treatment efficacy while avoiding adverse effects on healthy tissue (5, 6). "Bioactive peptide" (BP) are organic substances linked by amino acids with peptide covalent bonds. Most BPs are inactive in the main protein and are released after enzymatic processes. Some BPs are also prepared by chemical synthesis. BPs play an important role in human health by influencing different body organs and are considered as a new generation of biologically active regulators (7). The potential anticancer effects of bioactive peptides have garnered significant attention. Peptide-based methodologies present numerous benefits in the realm of cancer therapy, such as heightened selectivity, diminished toxicity towards healthy tissues, and adaptability in the targeting of diverse molecular pathways implicated in the progression of cancer (8–11). A broad variety of engineered and natural peptides have been intensively investigated, encompassing several therapeutic domains. Therapeutic peptides can function for several purposes, including growth factors, hormones, neural transmitters, ion channel compounds, and anti-infective drugs. Cell membrane receptors possess a remarkable level of both affinity and specificity, allowing them to efficiently attach to ligands and subsequently trigger specific intracellular reactions. Therapeutic peptides demonstrate similarities in their mechanism of action to biological ligands and antigens, such as antibodies and therapeutic proteins, hence providing focused and precise therapeutic strategies. In comparison with antibodies for example, despite some limitations including reduced half-life due to rapid excretion and susceptibility to enzyme degradation, they showed clear advantages including cost-effectiveness, extensive tissue penetration, effective cellular internalization, decreased immunogenicity, reduced toxicity to the bone marrow and the liver, and their amenability to chemical modification (12, 13). In the scenario of their use in cancer treatment, bioactive peptides were extensively texted for their ability to induce apoptosis, representing a common strategy to decrease cancer cell proliferation (14). Bioactive peptides in the context of immune modulation, can enhance or suppress immune responses, making them valuable tools for immune modulation (15). They can induce proliferation or activation of immune cells and cytokines, promoting a robust immune defense against pathogens or cancer cells. Additionally, bioactive peptides can inhibit cell migration by influencing cell adhesion, chemotaxis, and tissue remodeling processes (16). This property is particularly important in preventing the migration of cells associated with diseases like cancer, where metastasis is a significant concern (Figure 1) (17). Overall, bioactive peptides offer a promising avenue for therapeutic interventions, harnessing the body's immune system and preventing unwanted cell migration for improved health outcomes (18, 19). This review scope encompasses the most recent research on the anticancer and immunomodulatory properties of bioactive peptides derived from natural sources.

2 Peptides with anticancer function

Bioactive peptides have demonstrated several anti-cancer effects on well-established cancer cell lines, including the inhibition of cell migration, suppression of angiogenesis, antioxidant properties,

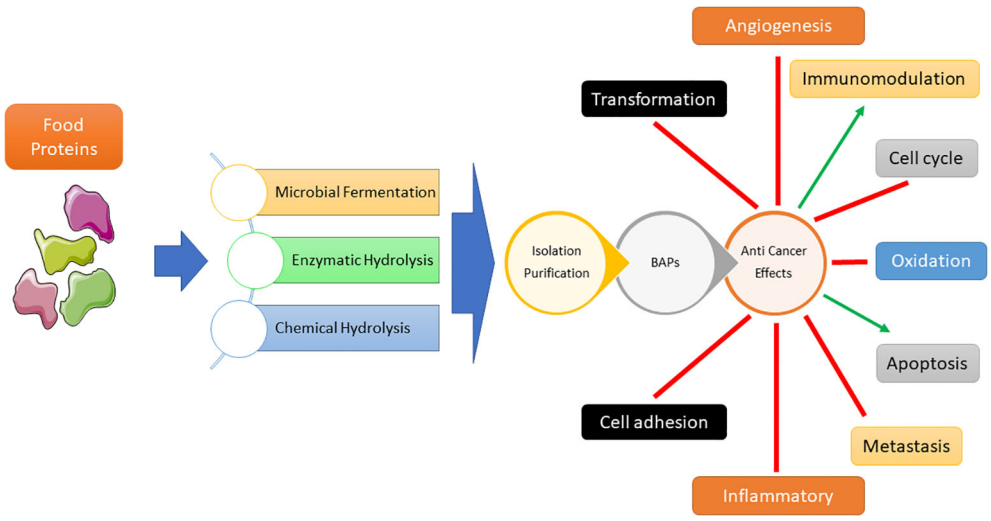

FIGURE 1
Bioactive peptides (BAPs) production processes and their impacts on various cellular events leading to anti-cancer effect.

inhibition of cell proliferation, induction of apoptosis, and cytotoxicity (13). The consolidated information can be found in Table 1. Altered peptides augment the efficacy of cancer treatment, resulting in enhanced activity of antigen-presenting cells (APCs) for pharmaceuticals and immunizations and the primary objective of the development of modified anticancer peptides (ACPs) is for clinical against cancer. The use of natural biomaterials such as protein hydrolysates or peptides is considered an option in cancer treatment, mainly due to their cost-effectiveness and safety for human health. Peptide-based drugs and vaccines represent a valuable class of therapeutics due to their high permeability, high selectivity, and easy modification (33). They also play an important role in preventing cancer by regulating various genetic pathways. The potential of food protein hydrolysates and peptides as drugs of anti-inflammatory origin has been fully evaluated by *in vitro* and *in vivo* experiments at various levels. Additionally, many anti-inflammatory peptides have been tested as drugs and vaccines in phase I/II clinical trials (33). For example, dTCAPF, a novel hormonal peptide that enters cells through the toll/interleukin-1 receptor, has been shown to be safe and effective in treating patients with prostate cancer, liver cancer/metastatic cancer. Its anticancer activity appears to be associated with the inhibition of angiogenic factors, induction of anticancer cells activity and proliferation, and endoplasmic reticulum stress (34). The relationship between antigenic peptides and correlation structure showed that most antigenic peptides have short segments of 3 to 25 amino acids. Shorter peptides allow greater molecular mobility and expansion and can interact with cancer cells more effectively. Moreover, the antimicrobial activity of peptides is also affected by their amino acid composition, segment, length, total charge, and hydrophobicity (35). Hydrophobic amino acids including Ala, Leu, Pro, Gly and the presence of some specific amino acids such as one or more residues of Arg, Lys, Tyr, Thr, Glu, and Ser are believed to be involved in the selective attack to cancer cells and potent cytotoxic activity (20, 35) because they increase interactions between the peptide and the outer leaflet of cancer cells' membrane bilayer containing high phospholipid contents (20). It has also been reported that the amount of heterocyclic amino acids greatly enhances the immunity of food peptides (35). However, the exact molecular mechanism of the anti-cancer effect is not clear so far, but many studies have shown that the anti-inflammatory effect of food protein hydrolysates or peptides is associated with the induction of apoptosis of cancer cells. Cell cycle arrest, permeabilization/cell membrane damage, inhibition of cell adhesion, inhibition of topoisomerase, immune system, and intracellular signaling in cancer cells are other possible mechanisms (20, 35).

TABLE 1 Bioactive peptides with anticancer effects.

Product	Bioactive Components	Function	Reference
Raja porosa (skate)	FIMGPY (726.9 Da)	Antiproliferative activity by induction of apoptosis on HeLa cell line	(20)
Phaseolus vulgaris	GLTSK (505.48 Da), LSGNK (518.29 Da), GEGSGA (521.22 Da), MPACGSS (656.01 Da) and MTEEY (671.98 Da)	Inhibition of cell growth and modification of expression of cell cycle regulatory proteins p53, p21, cyclin B1, BAD on HCT-116, RKO and KM12L4 (human colon cancer cell lines)	(21)
Seaweed (Eucheuma serra)	Lectins	Anticancer effect by cytotoxicity, apoptosis, and inhibition of tumor growth	(22, 23)
Soybean	Peptied fractions: < 5 kDa, 3–5 kDa, 1–3 kDa, >1 kDa	Antimicrobial, antioxidant, and antitumor functions	(24, 25)
Amaranth	VW, GQ/PYY, RWY, WY, RW PWW, PWR, PW, PWY WYS/VGECVRGRCPSGMCCSQF GYCGKGPKYCG	Anticancer, antioxidant and antimicrobial functions	(26, 27)
(28)	GLTSK, LSGNK, GEGSGA, MPACGSS, MTEEY	Anticancer	(29)
Whey protein hydrolysate	Lactoferricin	Anticancer and antimicrobial activity	(30)
Crocodylus siamensis (fresh water crocodile)	NGVQPKYKWWKWWKKWW (2.433 kDa) and NGVQPKYRWWRWWRRWW (2.545 kDa	Induction of cell death by apoptosis on HeLa and CaSki (cervix) cancer cell lines	(28)
Capra aegagrus hircus (goat)	8 kDa	Cell grows inhibition on HCT-116 (human colon cancer cell line)	(31)
Telligarca granosa (Blood clam)	WPP (398.44 Da)	Cytotoxicity and change of PC-3 cells morphology on PC-3, DU-145, H-1299 and HeLa cell lines	(32)

2.1 Anticancer peptides from plant proteins

Anticancer peptides can be generated by rice and soy protein hydrolysis, specifically through the process of alcalase digestion of rice bran proteins. This discovery established a fundamental basis for the potential utilization of these protein hydrolysates in cancer prevention strategies (36). A study has reported the identification of five peptides (GLTSK, LSGNK, GEGSGA, MPACGSS and MTEEY) obtained from a common bean that exhibited antiproliferative properties on human colon cancer cell lines (HCT-116, RKO, and KM12L4). The peptides were found to affect the activity of enzymes regulating cell proliferation, consequently inducing cell cycle arrest and further apoptosis (21). An ACP with a molecular weight of 1.155 kD, derived from chickpeas, hydrolysis by Flavorzyme has been demonstrated to possess anti-proliferative properties in breast cancer cell lines, specifically MDA-MB231 and MCF-7. This effect is achieved by upregulating the expression of the P53 protein (37), usually activated by different cellular stresses (i.e., DNA damage), and regulating cell cycle progression and death pathways. The peptide sequences SSDEEVREEKELDLSSNE and KELPPSDADW, which were investigated in a study conducted by Karami et al. and obtained from wheat germ protein, had cytotoxic effects on A549 lung cancer cells. The IC50 values for these peptides were measured to be 2.34 µM and 7.25 µM, respectively (38). M. Li et al., reported the dose- and time-dependent cytotoxic activity of papain-hydrolyzed mung bean protein against hepatocellular carcinoma (HepG2) cells with an IC value of 2.99 mg/mL. The authors confirmed that peptides isolated from mung bean protein (Val-Glu-Gly, Pro-Gln-Gly, Leu-Ala-Phe, and Glu-Gly-Ala) could induce apoptosis in hepatocellular carcinoma (HepG2) cells. While high doses may stop cell cycle at the G0/G1 phase and inhibit its progress to the S phase, low concentrations suppress the cell growth during S phase (39). Similarly, glutamic acid from pepsin/trypsin-digested germinated soybeans also showed dose-dependent *in vitro* antiproliferative effects on Caco-2, HT-29, and HCT 116 human cancer cells (40). Peptides extracted from black soybean, mung bean, and adzuki bean have demonstrated the ability to inhibit cancer cells within a concentration range of 200-600 µg/ml (41). Zheng et al. in their study documented the utilization of alcalase and trypsin for the enzymatic hydrolysis of D. catenatum to extract nine distinct peptide fractions. Among these fractions, it was noted that fraction A3 exhibited the highest level of antiproliferative activity against liver (HepG-2), gastric (SGC-7901), and breast (MCF-7) cancer cell lines and the development inhibition rate of cytotoxicity reached a peak of 70%. Notably, the A3 fraction contained three peptides that were abundant: RHPFDGPLLPPGD (1.416 kDa), RCGVNAFLPKSYLVHFGWKLLFHFD (2.994 kDa), and KPEEVGGAGDRWTC (1.504 kDa), and displayed significant pro-apoptotic effects (42). Bioactive peptides derived from Phaseolus vulgaris, soybean meal, amaranth, and seaweed have demonstrated anti-cancer, antioxidant, and cytotoxic properties (22, 24–27, 29), showing potential for complementary utilization in conjunction with conventional cancer therapies. Lunasin is a bioactive peptide derived from soybean or wheat, has been the focus of extensive studies exploring its potential anti-cancer properties (30). Other soy protein peptides exhibit anticancer properties, although their potency is comparatively lower than that of Lunasin (43). The anticancer properties of Lunasin are contingent upon its unique amino acid sequence, which encompasses Arg-Gly-Asp for cellular adhesion and the bending of the polyaspartate acid chain consisting of nine aspartic acid residues. Research findings indicate that Lunasin exhibits promising potential as an adjuvant therapy for cancer and may serve as an effective agent against inflammation, tumor growth, and metastasis in various cancer types (44, 45). Lunasin may potentially serve as a chemo preventive agent in mitigating the incidence of colorectal cancer, breast cancer, and other related malignancies. This function can be executed via various modes and has the capability to impede the interaction between adipocytes and neoplastic cells. Adipocytes, or fat cells, are essential for energy storage, hormone regulation, and overall metabolic health. They play a role in obesity-related health issues and are central to understanding conditions like diabetes and cardiovascular disease. Neoplastic cells, on the other hand, are cancer cells and are crucial in cancer research and treatment. Studying neoplastic cells informs early detection methods, advances in personalized cancer therapies, and strategies for cancer prevention. Both adipocytes and neoplastic cells have far-reaching implications for public health and medical progress, with adipocytes impacting metabolic health, and neoplastic cells being pivotal in the fight against cancer (46, 47). The incorporation of Lunasin into the rice genome yields Lunasin-rich rice, which is anticipated to serve as a functional food for cancer patients (48). The potential integration of Lunasin into the rice genome has been acknowledged as a promising strategy for developing useful food options targeted at individuals affected by cancer.

2.2 Anticancer peptides from animal proteins

In a recent study, two short peptides Trp-pro-pro and Gln-Pro have been isolated from the protein hydrolysate of blood clam (Tegillarca granosa) muscle through a combination of ultrafiltration and successive chromatographic techniques. The authors demonstrate that Trp-Pro-Pro might be employed to counteract the surplus generation of reactive oxygen species (ROS) during oxidative stress situations and mitigate the risk of cancers resulting from the accumulation of excessive free radicals within cells. The peptides demonstrated noteworthy cytotoxic properties against diverse cancer cell lines, namely PC-3 (human prostate), DU-145 (human prostate), H-1299 (lung), and HeLa (cervical), in a dose-dependent fashion. Additionally, the treatment with the peptides resulted in notable morphological changes in PC-3 cells (32). Theansungnoen et al. conducted an experiment on cervix cancer cell lines, specifically HeLa and CaSki. They examined the effectiveness of two peptides KT2 (NGVQPKYKWWKW) and RT2 (NGVQPKYRWWRWWR RWW), obtained from freshwater crocodile, and found that they can cause the death of HeLa cells (28). Su et al. in their research involving the utilization of 8 kDa anticancer peptides derived from goat spleen, have shown a notable

suppression in the proliferation of HCT116 cells (a type of human colon cancer cells) following a treatment duration of 4-6 days. Furthermore, it was observed that these particular anticancer peptides increased cancer cell apoptosis after a 6–12-hour treatment. This apoptosis induction happened by upregulating the expression of poly (ADP-ribose) polymerase (PARP) and p53 and downregulating the expression of Mcl-1 (31). Chalamaiah et al. discovered that protein hydrolysates (PH) derived from rohu eggs had antiproliferative properties. The study conducted hydrolysis using pepsin on a colon cancer cell line called Caco-2. The findings indicated that the pH had an inhibitory effect on Caco-2 cells, with the strength of the effect increasing with the dosage (23). Chi et al. extracted two peptides from the muscle of the blood clam. One of the peptides was identified and its sequence was determined. WPP (398.44 Da) exhibited potent cytotoxic effects on PC-3 (human prostate), DU-145 (human prostate), H-1299 (lung), and HeLa (cervical) cancer cell lines in a dose-dependent manner. Furthermore, WPP induced significant morphological changes in PC-3 cells also WPP demonstrated the ability to eliminate excessive reactive oxygen species (ROS), thereby preventing the formation of cancers caused by an abundance of free radicals (32). Milk proteins have also been documented as exceptional reservoirs of anticancer peptides. An analysis of Himalayan cheese fermented with probiotic strains of Lactobacillus plantarum NCDC 012, *Lactobacillus casei* NCDC 297, and Lactobacillus brevis NCDC021 has revealed significant *in-vitro* anticancer activity on various cancer cell lines, including human breast cancer (MCF-7), colon cancer cells (HCT-116), transformed human embryonic kidney cells (HEK-T), and neuroblastoma (IMR-32). This activity is primarily attributed to the production of bioactive peptides during fermentation with the added probiotics (49). Ayyash et al. (2018) examined the anti-proliferative effects of camel and bovine milk that had been fermented by probiotic strains of *L. acidophilus* DSM9126 and *Lactococcus Lactis* KX881782. The research group discovered that camel milk, when fermented with Lc. Lactis KX881782, had stronger anti-proliferative effects against cervical cells (HeLa), colon cancer cells (Caco-2), and MCF-7 cancer cells compared to bovine milk. The reduction of proliferation exhibited a robust positive association with the proteolytic activity and DPPH scavenging ability of camel milk that was fermented with *L. acidophilus*, which is accountable for its anti-cancer properties (50). In a study conducted by Yang et al. researchers found that when roe protein from Epinephelus lanceolatus was broken down using protease N, the resulting hydrolysates showed antiproliferative effects on two human oral cancer cell lines (Ca9-22 and CAL 27). These effects were achieved by inducing apoptosis and halting cell cycle progression at the sub-G1 phase (51). Dolastatin 10 is a short peptide comprising five residues that incorporate non proteogenic amino acids (52). This peptide derived from a marine mollusk demonstrated antimitotic characteristics by inhibiting the polymerization of tubulin, suggesting its potential as an agent for anticancer treatment. Dolastatin 10 is classified among a diverse array of marine-derived bioactive compounds that exhibit antineoplastic properties through the inhibition of microtubule growth (53–55). Much like Hemiasterlins, a class of linear peptide derivatives obtained from a marine sponge, Dolastatin 10 also exhibits these characteristics. Research suggests that Dolastatin 10 and Hemiasterlins share similar functions and display encouraging attributes. Su's team identified an anticancer bioactive peptide-3 (ACPB-3) (56, 57) derived from the spleens or livers of goats. It demonstrates anti-cancer properties against human gastric cancer cell lines (BGC-823) and gastric cancer stem cells (GCSCs), both in laboratory settings and in living organisms. This includes the ability to limit the proliferation of BGC-823 cells and $CD44^+$ cells in a manner that is dose dependent, as well as boosting the tolerance to chemotherapy in mice. ACBP-3 also inhibits tumor growth in living organisms (57, 58). Guha and his colleagues discovered TFD-100, a 100 KDa Thomsen-Friedenreich (TF) glycopeptide containing a TF disaccharide (TFD) which can bind to galactin-3, a lectin that specifically binds to β-galactosides. Furthermore, TFD-100 has been shown to prevent the adhesion of androgen-independent prostate cancer cells (PC3), as well as angiogenesis and galactin-3-induced T-cell death (59). Bioactive peptides obtained from diverse origins possess promising potential as agents for combating cancer. However, additional investigation is necessary to comprehensively elucidate their underlying mechanisms of action and ascertain their prospective clinical utility.

2.3 Anticancer peptides from animal venoms

Venoms are enriched reservoirs of bioactive peptides that can be utilized for the creation of novel pharmaceutical compounds. However, due to their toxicity, many venoms necessitate chemical alterations before they can be safely employed, and the intricate procedure requires substantial cost and time. Peptides found in venom can interact with certain biological components. This offers potential for the development of new medications that can target prevalent diseases like cancer and neurological disorders (60). The intricated and expensive endeavor of manufacturing novel medications from toxins necessitates substantial financial commitment, especially throughout the clinical stages of II and III, with no assurance of success (60).

Several biologically active peptides found in scorpion venoms exhibit potential anti-cancer properties both in *in vitro* and *in vivo*. One of these peptides has successfully completed phase I and phase II clinical trials (61, 62). The venoms of snakes, scorpions, spiders, honeybees, and cone snails contain bioactive peptides that show potential as abundant reservoirs of chemotherapeutic agents for various human diseases, including chronic inflammation, autoimmune disorders, and cancer (63–66).

2.3.1 Scorpion venom

Scorpions, the most ancient arthropods on Earth, have a venom apparatus attached to their telson, which they employ to inject venom. Scorpions can be classified into 18 separate groups based on their evolutionary relationships. There are around 1,500 species (67) of families, including scorpions. For centuries, venom has been utilized in traditional medicine (68). However, a comprehensive

analysis has been conducted on only <1% of all venoms derived from identified sources among different species of scorpions (69). Guo et al. discovered two linear α-helical peptides, TsAP-1 and TsAP-2, in the venom of the Brazilian yellow scorpion, Tityus serrulatus. These peptides possess antibacterial properties. The peptides were tested and found to have inhibitory effects on the growth of human lung cancer cells, namely a squamous carcinoma cell line (NCI-H157) and a lung adenocarcinoma cell line (NCI-H838). In addition, TsAP-2 exhibits threefold more activity compared to TsAP-1 when tested against an androgen-independent prostate cancer cell line (PC-3), MCF-7 cells, and a human glioblastoma cell line (U251) (70). Ali et al. have discovered a novel chlorotoxin-like peptide (Bs-Tx7) from the venom of the Buthus sindicus scorpion. The activity of the chlorotoxin (ClTx) and CFTR channels (GaTx1) is reduced by 66% and 82% respectively, when inhibited by Bs-Tx7. An investigation of the amino acid sequence of Bs-Tx7 has shown a scissile peptide bond (Gly-Ile) that is targeted by human MMP2, an enzyme whose activity is elevated in malignant tumors. This discovery implies that Bs-Tx7 hinders the growth of tumors by reducing the activity of MMP2 (71). Chlorotoxin (Cltx), a peptide derived from the venom of the scorpion Leiurus quinquestriatus, consists of 36 amino acid residues and contains 4 disulfide linkages and has been discovered to effectively block the entry of chloride ions into glioma cells (72–74). Cltx selectively attaches to glioma cells, blocking chloride channels and decreasing MMP-2 production, while having little impact on healthy cells (75–77) The peptides Scolopendrasin I, II, V, and VII derived from S. subspinipes mutilans have antibacterial and anticancer effects. Specifically, Scolopendrasin V exhibit antimicrobial characteristics by attaching to the surfaces of microbial cell membranes (23–25, 27). Centruroides margaritatus venom, namely MgTX, has been discovered to possess a highly effective and specific inhibitor of the peptidyl K^+ channel. MgTX, consisting of 39 amino acids, effectively suppress the binding of radiolabeled charybdotoxin to voltage-activated channels in synaptic plasma membranes and greatly hinder the development of A549 cells. Furthermore, it has been discovered that MgTX exhibit a reduction in tumor size when tested on a nude mice xenograft model following exposure to malignant tissue (78). Bengalin, a peptide with anticancer properties derived from the venom of Heterometrus bengalensis Koch, has shown the ability to inhibit cell proliferation in K562 and U937 cells with IC50 values of 4.1 and 3.7 $mg{\cdot}mL^{-1}$, respectively. Importantly, this effect was specific to cancer cells and did not impact normal human lymphocytes. The mechanism of action of Bengalin involves inducing apoptosis (79). Gonearrestide, a peptide with 18 amino acids and a molecular weight of 2192 Da, was discovered in a library of scorpion venom. This peptide has shown potential as an anticancer agent and was derived from the scorpion species Androctonus mauritanicus. Following *in vitro* screenings and bioinformatics analysis, it was proven to be efficacious against several human cancer cells, while exhibiting negligible cytotoxicity towards erythrocytes and epithelial cells. Validation tests and experiments conducted *in vivo*, ex vivo, and *in vitro* showed that it effectively impeded the proliferation of primary colon cancer cells and solid tumors by arresting the cell cycle in the G1 phase (80).

2.3.2 Spider venom

Spider venom has a diverse array of proteins and peptides, including as enzymes, neurotoxins, and cytolytic peptides, that have an impact on ion channels (81). Latarcin 2a (Ltc2a), a peptide derived from spider venom, exhibits cytotoxic effects on human erythroleukemia K562 cells. It induces plasma membrane instability, leading to blebbing, swelling, and ultimately cell death (82). The peptide lycosin-1, produced from spider venom, successfully hinders the growth of cancer cells in a laboratory setting and reduces tumor growth in living organisms by disrupting cell signaling pathways through the reduction of crucial protein functions (83).

Snake venom. Pereira et al. conducted experiments to assess the toxicity of the peptide on cancer cells both in a laboratory setting (*in vitro*) and in living organisms (*in vivo*). They discovered that a concentration of 5 μg/ml of the peptide was deadly to B16-F10 cells (a type of melanoma cells found in mice), Mia PaCa-2 cells (a type of pancreatic carcinoma cells found in humans), and SK-Mel-28 cells (a type of melanoma cells found in humans) (84, 85). BF-30, an antimicrobial peptide derived from the venom of Bungarus fasciatus, is composed of 30 amino acids. It effectively hinders the growth of B16F10 cells in a dose and time-dependent manner when tested in a laboratory setting. Moreover, it significantly suppresses the development of melanoma in mice carrying B16F10 tumors, without inducing any weight loss (86).

2.3.3 Bee and wasp venom

Melittin (MEL) is a well-studied and widely recognized peptide generated from the venom of the honeybee Apis mellifera. It consists of 26 amino acid residues and is classified as an amphiphilic peptide (87). MEL demonstrates inhibitory effects on a range of cancer cell types in laboratory settings, including leukemia, ovarian, lung tumor, carcinoma, glioma, squamous carcinoma, hepatocellular carcinoma, osteosarcoma, prostate cancer, and renal cancer cells (88–92). However, it is important to note that MEL is toxic to normal cells, underscoring the need for precise delivery methods to achieve optimal outcomes (93, 94). Mastoparan, a peptide consisting of 14 amino acids derived from the venom of Vespula lewisii, refers to a group of amphiphilic cationic polypeptides that exhibit anticancer effects when tested in a laboratory setting (95, 96). However, it is crucial to ensure accurate administration in order to prevent any adverse reactions and make necessary alterations for *in vivo* application (96). Various structural alterations can enhance the pharmacodynamic effects of the *in vivo* parameters of the chimeric Mastoparan (95, 97). Upon targeted delivery to the tumor cells, the Mastoparan selectively triggers mitochondrial permeability transition, resulting in the elimination of cancer cells while sparing normal cells. Additionally, Mastoparans derived from other species of wasps have demonstrated anticancer properties. Both V. crabro and V. analis Mastoparans demonstrate antitumor properties against ovarian cancer cells. A concentration of 100 μM of V. crabro Mastoparan resulted in a significant reduction (about 80%) in the relative survival fold of SK-OV-3 cells. Similarly, treatment with 100 μM of V. analis Mastoparan led to a remarkably low survival fold (30%) of SK-OV-3 cells (98). MP1, a peptide similar to Mastoparan, has

been found to selectively eliminate cancer cells, including prostate cancer cell line PC-3 (with an IC50 value of 64.68 μM), bladder tumor cells Biu87 (IC50 = 52.16 μM) and EJ (IC50 = 75.51 μM) (99), as well as multidrug-resistant leukemic cells K562/ADM (IC50 = 26.55 μM) (100). Overall, Mastoparan-related peptides produced from wasps have the potential to be considered as primary compounds for the development of innovative anticancer medications (101).

Despite the promising therapeutic benefits of Mastoparan-related peptides produced from wasps on cancer, their implementation in cancer treatment is hindered by various difficulties. Further enhancement is required to improve the instability towards proteases and anticancer activity of MP1 (102). Hence, chemical alterations and substitutions are necessary to enhance the pharmacological characteristics of anticancer peptides. Following the substitution of the thioamide link, MPI-1 exhibited enhanced anticancer activity (IC50 = 20.3 μM for PC-3, IC50 = 21.6 μM for EJ) and reduced adverse effects in both *in vitro* and *in vivo* settings (103). The synthetic derivatives of Decoralin, which is a naturally occurring antimicrobial peptide (AMP) found in wasps. Oreumenes demonstrates significant anticancer effects on MCF-7 breast cancer cells, with an IC50 value of 12.5 μM (104). Both the restriction of conformation and the precise delivery system enhance the therapeutic impact and decrease the toxicity to cells (105–107). This further emphasizes the significance of modifying the conformation and implementing an effective drug delivery system.

3 Immunomodulatory activity of bioactive peptides

3.1 Peptides with immunomodulatory function

Peptides and proteins are crucial macronutrients that provide the necessary building blocks for protein synthesis and are recognized as a significant energy source (108). Moreover, proteins and peptides present in food can exhibit diverse biological functionalities. Bioactive peptides are obtained from animal and plant proteins through diverse techniques such as proteolysis within the intestinal tract, enzymatic or chemical hydrolysis, or microbial fermentation (19, 109). Immunomodulatory peptides are a type of bioactive peptides that encompass constituents responsible for the regulation of immune cell activity, cytokine generation, and antibody production (110). The immunomodulatory and anticancer properties of these substances are contingent upon their amino acid composition, sequence, and length, as stated in reference (19). These peptides exhibit varying effects on the cell proliferation, inflammation, and cellular protection or destruction, depending on the specific level of action (111–113). Therefore, due to their unpredictable effects on both innate and adaptive immune cells, immunomodulatory peptides are currently a topic of investigation. Depending on whether they stimulate or repress immunological responses, they can operate as either immunostimulants or immunosuppressants. As a result, they hold potential for therapeutic applications in disease treatment (15, 114). The determination of the mechanisms of immunomodulatory peptides functions supplies new opportunities for cancer treatment through improving the immune system. So, this part provides a brief overview of several bioactive peptides from plant and animal sources have been used to modify the immune responses.

3.2 Immunomodulatory action BAPs from plant source

Plants are an excellent source of valuable bioactive peptides with various functions. Previous researchers have investigated the immunomodulatory effects of some peptides from plants that are widely used in the human diet like rice, wheat, and legume. Table 2 indicates several of these bioactive peptides. Macrophages, as innate immune cells, can phagocyte cancer cells and pathogens. In addition, they can interact with other constituents of the innate and adaptive immune system to augment their activities, like secretion of cytokines and cytotoxicity (128). Therefore, regulation of macrophage's function by immunomodulators would ameliorate the ability of host immune response against cancer. Wu et al. conducted an evaluation of the immunomodulatory effects of the peptide [Glu-Cys-Phe-Ser-Thr-Ala (ECFSTA)] derived from wheat germ globulin on macrophage RAW 264.7 cells (129). The findings of this study indicated that the peptide ECFSTA could enhance cell phagocytosis function and the secretion of nitric oxide (NO), interleukin 6 (IL-6), tumor necrosis factor α (TNF-α), IL-1β, and reactive oxygen species (ROS) generation by RAW 264.7 cells through activation of toll-like receptor 4 (TLR4) and TLR2 (115). In another investigation, Defatted Wheat Germ Globulin was hydrolyzed with different enzymes, including Alcalase, Neutrase, Papain, Pepsin, and Trypsin. Alcalase-prepared peptides were found to exhibit the greatest immunomodulatory activity in relation to lymphocyte proliferation, phagocytosis, and pro-inflammatory cytokine production in RAW 264.7 cells, as mentioned in a previous study (116). In addition to macrophages, it was reported that wheat peptide can modify NK cells and T cells activities. For example, N. Horiguchi et al. demonstrated an augmentation in NK cell function after further administration of one gram of wheat gluten hydrolysate after each meal for six days in healthy people (117). NK cells play important roles in elimination or control of viral infections and cancer cells. NK cells act against tumor cells with cytotoxic role and also secretion of cytokines, mainly interferon-γ (IFN-γ), to regulate adaptive immune responses (130). Treatment of cell culture supernatants from PHA-stimulated human PBMCs with Alcalase wheat gluten protein hydrolysates (WGPHs) resulted in reduction of Th1 and Th17 cytokines secretion (IFN-γ and IL-17, respectively). Although IL-4 levels were not changed but the ratios of IL-4/IFN-γ, IL-4/IL-17 and IL-10/IFN-γ were significantly increased (118). It was shown that rice protein hydrolysates (RPHs) through trypsin digestion may potentially serve as a source of immunostimulatory peptides on RAW 264.7 cells. The study conducted by Xu Z et al. revealed that the YGIYPR

TABLE 2 Immunomodulatory effects of bioactive peptides from plant source.

Product	Enzyme	Peptide	Immunomodulation	Reference
wheat germ globulin	Alcalase	ECFSTA	Stimulated phagocytosis function and secretion of NO, IL-6, TNF-α and ROS in RAW 264.7 cells.	(115)
Defatted wheat germ globulin	alcalase, neutrase, papain, pepsin or trypsin	-	The highest immunomodulation activity in proliferation of lymphocyte, phagocytosis and production of pro-inflammatory cytokines in RAW 264.7 cells was reported with alcalase prepared peptides.	(116)
wheat gluten hydrolysate	-	Glutamine peptide GP-1	Enhancement of NK cell activity.	(117)
Wheat gluten protein	Alcalase	WGPHs	Decreased Th1 and Th17 pro-inflammatory cytokines in PBMCs.	(118)
Rice protein	Trypsin	YGIYPR	Enhanced the proliferation of RAW 264.7 cells.	(119)
Rice protein	Trypsin	NSVFRALPVDVVANAYR, GIAASPFLQSAAFQLR, LLPPFHQASSLLR TPMGGFLGALSSLSATK	Reduced the secretion of NO, IL-6, TNF-α and IL-1β in LPS-induced RAW264.7 cells.	(120)
Mung bean and soybean	fermented and non-fermented	-	Stimulated splenocyte proliferation and release of serum IL-2 and IFN- γ.	(121)
Lunasin-enriched soybean extract (LES)	-	–	Increasing phagocytic activity and production of NO, IL-6, IL-1β, and IL-10 and EL4 lymphocyte activation.	(122)
Soybean protein	Peptidase R	Fraction	Enhanced the count of mouse spleen IL-12$^+$ CD11b$^+$, IFN-γ $^+$ CD49b$^+$, and IFN-γ $^+$ CD4$^+$ cells.	(123)
***Pseudostellaria heterophylla* protein**	-	RGPPP	Increased TNF-α secretion NO, ROS and TLR2 expression in RAW264.7 cells.	(124)
Chlorella vulgarian	Ethanol and pancreatic at pH values of 7.5-8.0	Three main peptides of molecular masses between 2 and 5 kDa	Stimulated activation of monocyte and macrophage, humoral and cell mediated immune responses.	(125)
Salvia. *hispanica* L. seeds	Pepsin and Pancreatin	Peptide fractions (<1, 1-3, 3-5, 5-10, and >10 kDa)	Decreased of NO, TNF-a, IL-1β and IL-6 on BALB/c peritoneal macrophages.	(126)
Sunflower protein	Flavourzyme	YFVP, SGRDP, MVWGP and TGSYTEGWS)	inhibited NFκB and enhanced the CD14 expression and the differentiation of monocytes a dendritic cell phenotype.	(127)

peptide derived from rice protein hydrolysates which stands for Tyr-Gly-Ile-Tyr-Pro-Arg has the potential to enhance the proliferation of RAW 264.7 cells (119). While another study investigated anti-inflammatory effect of rice peptides on RAW264.7 cells. They employed both immuno-prediction and in silico simulation techniques to scrutinize rice peptides with potential immunomodulatory properties. Out of 3630 sequences, it was observed that the amino acid sequences GBP1 (NSVFRALPVDVVANAYR), PEP1 (GIAASPFLQSAAFQLR), LR13 (LLPPFHQASSLLR), and TK17 (TPMGGFLGALSSLSATK) exhibited the greatest affinity towards MHC-II. The immunomodulatory properties of four peptides were verified in LPS-induced RAW264.7 cells and they were found to decrease the secretion NO, IL-6, TNF-α, and IL-1β (120, 131). Various legume proteins contain valuable bioactive peptides (132, 133). Several biological effects of them have been reported, including antihypertensive, antimicrobial, antioxidant, anti-inflammatory, and anticancer properties (134–136). Mung bean and soybean are widely utilized legumes that are rich in polyphenols and antioxidants. The study conducted by Ali, NM et al. aimed to evaluate the immunomodulatory, cytotoxic, and antioxidant properties of both fermented and non-fermented mung bean and soybean. The findings of the study indicated that both fermented soybean and mung bean have the ability to induce splenocyte proliferation and promote the release of serum IL-2 and IFN-γ (121). IL-2 is a pro-inflammatory cytokine that plays a crucial role in enhancing T cell proliferation and promoting the release of interferon-gamma (IFN-γ). IFN-γ is primarily produced by Th1 cells, CD8+ T cells, and NK cells, playing a significant role in stimulating cellular immunity. Consequently, it contributes to the elimination of tumor cells (137). According to Kong et al. hydrolyzed soy protein with different proteases generate peptides with various molecular weight and charge. It was found that alcalase soy protein peptides possess higher positive charge and lower molecular weight. These peptides have the most immune-stimulating property by boosting the phagocytic function of

macrophages and manipulation of murine spleen lymphocytes (138). In another study, peptide derived from soybean fraction that underwent peptidase R hydrolysis exhibited mitogenic activity and demonstrated a noteworthy increase in the number of IL-12+ CD11b+, IFN-γ + CD49b+ (NK cell), and IFN-γ + CD4+ (Th1) cells in mouse spleens, as well as the activation of cytotoxic activity in spleen cells against the human erythroleukemia cell line (K562). Furthermore, the analysis of DNA microarray revealed the upregulation of genes associated with innate immune response in Peyer's patch cells of mice administered with peptides (123). Lunasin is a 43 amino acids peptide derived from soy, which possesses anti-cancer and hypocholesterolemic properties (29). In context of immunomodulation displayed that Lunasin-enriched soybean extract (LES) has the intriguing capability to induce both pro-inflammatory and anti-inflammatory activities within the immune system. This observation comes from a study conducted by Paterson and colleagues. Specifically, when macrophages were exposed to LES, they exhibited increased phagocytic activity and elevated production of NO, IL-6, IL-1β, and IL-10. Furthermore, the study found that Lunasin and LES peptides also stimulated EL4 lymphocytes and prompted the secretion of IL-4, IL-5, and IL-10 cytokines. This suggests that soybean peptides, such as Lunasin and LES, have the remarkable ability to modulate or regulate both the innate and adaptive arms of the immune system. In essence, they possess the potential to modulate immune responses in different conditions (122).

There are some reports from peptide of other less common plants. For example, the utilization of proteins extracted from Pseudostellaria heterophylla can serve as a dietary supplement for enhancing immune system function. The digestion of P. heterophylla protein has yielded a novel peptide induced the TLR2/NF-κB pathway. This peptide has been observed to induce a significant increase in TNF-α production, pinocytosis, and TLR2 expression in macrophages (124). The peptides derived from enzymatic hydrolysate of Coix glutelin, exhibit immunomodulatory properties by inducing proliferation of splenocytes in mice and stimulating the production of NO from Raw264.7 cells in a dose-dependent manner as demonstrated by Ling-Ling. Additionally, it has the potential to inhibit excessive activation of cells triggered by LPS (139). According to a study conducted by Velliquette et al., the anti-inflammatory and immune-modulating properties of peptides derived from sunflower protein with Flavourzyme enzyme has been revealed. These peptides attenuate the activation of NF-κB while enhance the expression of surface markers like CD14 and CD86, which are linked to a dendritic cell (DC) phenotype (127). The activation of monocyte and macrophage, humoral and cell-mediated immune responses, as well as hemopoietin, were observed to be stimulated by peptides derived from Chlorella vulgarian 87/1 (125). In addition, Chan-Zapata et al. have extracted bioactive peptides from the seeds of Salvia hispanica L. that exhibit anti-inflammatory properties. These peptides have been found to significantly reduce the levels of NO, TNF-α, IL-1β, and IL-6, while do not affect the viability of BALB/c peritoneal macrophages (126). Overall bioactive peptides derived from plants can influence immune responses to a variety of situations, potentially promoting both inflammatory and anti-inflammatory actions in diverse contexts as needed. Further research may provide the potential applications of plants bioactive peptides in modulating of immune function in cancer, alleviating autoimmune diseases, and mitigating tissue damage in inflammatory conditions.

3.3 Immunomodulatory action BAPs from animal source

Previous *in vivo* and *in vitro* studies have reported that bioactive peptides derived from animal sources have the ability of regulating the immune responses, as evidenced in Table 3. Among dietary proteins, fish, milk, egg, and chicken proteins are likely valuable source of bioactive peptides in nutritional perspective. The immunomodulatory activity of peptides found in certain fish families has been observed to potentially result in heightened lymphocyte proliferation and macrophage activity, as well as improved natural killer (NK) cell function and cytokine production (140, 155). The lymphocyte proliferation, NK cell activity, $CD4^+$ T helper cell count in the spleen, and the production of Th1 (IL-2, IFN-γ) and Th2 (IL-5, IL-6) cytokines in mice were enhanced by marine oligopeptides (MOP), which are low-molecular-weight peptide compounds derived from Chum Salmon (140). These findings suggest that MOP may help the inhibition of tumor growth or metastasis through the activation T cells and NK cells as main mediators against cancer cells. Wang YK and colleagues showed that oyster hydrolysates effectively inhibited the growth of transplantable sarcoma-S180 in BALB/c mice. Additionally, these hydrolysates were observed to enhance the proliferation of lymphocytes in the spleen, as well as the activity of NK cells and the phagocytic activity of macrophages in mice. Thus, it is possible to utilize oyster hydrolysates as a nutritional supplement for the purpose of tumor therapy, as suggested by previous research (141). In addition, the immunomodulatory activities of peptides derived from Labeo rohita egg - were assessed on both innate and adaptive responses in BALB/c mice by Chalamaiah et al. Trypsin hydrolysates peptides have been found to have a significant impact on splenic $CD4^+$and $CD8^+$ T cells while pepsin hydrolysate enhanced the production of mucosal IgA, macrophage phagocytose capacity as well as NK cell cytotoxicity. As a result, divers rohu egg protein hydrolysates have the potential to stimulate different immune cells (143). Milk proteins, comprising of approximately 80% casein and 20% whey proteins such as α-lactalbumin, β-lactoglobulin, are considered a significant source of bioactive peptides that possess various health-promoting properties such as anti-microbial, anti-hypertensive, anti-oxidative, and anti-diabetic activities (44, 156). The presence of multiple immunomodulatory peptides that can either suppress or stimulate an immune response has been demonstrated (157, 158). According to Chen et al. the administration of milk-derived peptides at a dose of 200 mg kg^{-1} in mice resulted in the most effective regulation of LPS-induced inflammation. This was achieved through the enhancement of immune activity in the spleen and the regulation of immunoglobulin and cytokine secretion (149). The peptide LFP-20, which consists of 20 amino acids and is derived from porcine lactoferrin, can balance Th1 and Th2 response by regulating the expression of Th1 cytokines (IL-12p70, IFN-γ, TNF-α) and Th2

10.3389/fimmu.2024.1310443

TABLE 3 Immunomodulatory effects of bioactive peptides from animal source.

Product	Enzyme	Peptide	Immunomodulation	References
Chum Salmon	Complex protease	Marine oligopeptide	Increased the lymphocyte proliferation, NK cell action, number of CD4+ T helper cells in spleen and the secretion of Th1 and Th2 cytokines in mice.	(140)
Oyster (*Crassostrea gigas*) hydrolysates	protease	Fraction	Increased the spleen proliferation of lymphocytes, the activity of NK cells, and the phagocytic activity of macrophages in mice.	(141)
Salmon pectoral fin	Pepsin	PAY	Reduce the production of NO, PEG2 TNF-a, IL-1b and IL-6 in RAW264.7 cells.	(142)
Labeo rohita egg	Trypsin, pepsin and alcalase	Fraction	Enhanced the percentage of splenic CD4+ and CD8+ and NK cell cytotoxicity in BALB/c mice.	(143)
Milk protein (Whey b-lactoglobulin)	Trypsin	Fractions	Stimulated TNF-a secretion by monocytes and enhanced IFN-γ.	(144)
α-lactalbumin		Residues 51-53	Enhanced the phagocytic function of macrophages in murine and humans	
Milk protein (casein phosphopeptides preparation (CPP-III)	Trypsin	αs2-casein (1-32) and β-casein (1-28)	Augmented production of IgA, IL-5, and IL-6 in spleen cells.	(145)
Milk protein (casein-derived peptide)	Fermentation by Lactic acid bacteria	–	Stimulated IL-10 secretion in human THP-1 monocytes	(146)
Porcine lactoferrin-derived peptide (LFP-20)	-	KCRQWQSKIRRTNPIFCIRR	Balanced the production of both Th1 (IL-12p70, IFN-γ, TNF-α) and Th2(IL-4, IL-5 and IL-6)cytokines.	(147)
Egg white peptides (EWP)			Enhanced macrophage activation and secretion of NO, IL-6, IL-10 and TNF-α in RAW264.7 cells also, incremented the production of IL-2, IL-6, IL-10 and TNF-α in splenocytes of mice.	(148)
Selenium-enriched egg white peptides (Se-EWP	Alkaline–neutral protease	SeCys-Trp-Leu-Glu, Trp-Ser-SeCys, SeMet-Ala-Pro, and SeMet-Leu	The treated Se-EWP mice had higher white blood cells count and serum levels of IL-6, IL-2, and TNF-α.	(149)
Hydrolysates of ovalbumin, lysozyme and whole egg	Alcalase	–	Decreased lymphocyte proliferation and generation of IL-10, IL-13 and TNF-a inhibited IgG1-class switching induced by LPS.	(150)
Chicken collagen peptides	-	-	Reduced secretion of IL-6, TNF-α, treated with the chicken collagen hydrolysate.	(151)
The hydrolysis chicken cartilage	Trypsin	Filtration into CCH-I (molecular weight (MW) > 10 kDa) and CCH-II (MW <10 kDa)	Alleviated osteoarthritis by declining the IL-1β, IL-10, IL-8 and TNF-α levels in papain-induced model rats	(152)
Silkworm pupa protein	Alcalase	PNPNTN	ameliorated the splenocyte proliferation	(153)
Hysterocrates gigas	–	SNX-482	Triggerd M0-macrophages, increasing costimulatory molecules (CD40, CD68, CD80, CD83, CD86)	(154)

cytokines (IL-4, IL-5, and IL-6), as well as $CD3^+CD8^+$ T cells and B cells, in cases of immune disorder induced by LPS. Although LPS induced remarkable enhancement in production of TNF-α, IL-6, IFN-γ, IL-12p70, IL-4 and IL-5, treatment with LFP-20 declined LPS-induced cytokine secretion (147). Moreover, research has represented that peptides derived from whey and casein proteins play a significant role in regulating the immune system (159). For example, in a study conducted by Rodrıguez-Carrio et al., it was observed that whey β-lactoglobulin fractions, comprising of short peptides, induced the secretion of TNF-α by monocytes. On the other hand, fractions containing large peptides were found to enhance the Th1 cytokine IFN-γ (144). Certain peptide derived from casein generated by strains of Lactic acid bacteria during the process of fermentation have demonstrated the ability to modulate the immune system. The findings of the study revealed that specific peptide fractions derived from fermented milk were capable of inducing the secretion of the anti-inflammatory cytokine IL-10 in human THP-1 monocytes (146). Another peptide from bovine αS1-casein (residues 142-149) significantly increased IFN-γ secretion from CD8+ T cells (160). Therefore, milk peptides may be beneficial

in cancer treatment by modifying host immune responses. The egg white has been shown to contain bioactive peptides that play a crucial role in maintaining the viability of the yolk's embryo (161). The immunoregulatory impact of egg white peptides (EWP) on RAW264.7 macrophage cells and an immunosuppressive BALB/c mice model was evaluated by Zhang, F. et al. The findings obtained from the *in vitro* experiments indicated that the administration of 100 μg/mL EWP resulted in a significant increase in macrophage activation and the secretion of NO, IL-6, IL-10, and TNF-α in RAW264.7 cells. Additionally, an increase in the production of cytokines such as IL-2, IL-6, IL-10, and TNF-α by splenocytes and peripheral blood leukocytes was observed in mice administered with a dose of 150 mg/kg/day of EWP (148). Another study was conducted to investigate the immunomodulatory impact of peptides derived from Selenium-enriched EWP (Se-EWP) on mice that had been immunosuppressed due to cyclophosphamide administration. The group of mice that received the Se-EWP exhibited elevated levels of white blood cells and serum concentrations of IL-6, IL-2, and TNF-α when compared to the EWP groups like pervious research (162). Hence, it is plausible that EWP could potentially serve as a significant factor in mitigating immune-mediated damages and ameliorating the effects of an immunocompromised condition. The hydrolysates of ovalbumin, lysozyme, and whole egg were found to have an inhibitory effect on lymphocyte proliferation and the generation of IL-10 and IL-13. Additionally, these hydrolysates were observed to reduce the TNF-α production from Th1 cells. Furthermore, they were found to inhibit IgG1-class switching induced by LPS and neutralize the release of ROS (150). Thus, the substance in question possesses the ability to serve various functions, including but not limited to acting as an immunostimulant or immunosuppressant and as a mediator for shifting between Th1 and Th2 responses. Chicken is another common nutrient with bioactive peptides. The immunomodulatory function of chicken collagen peptides is attributed to their ability to regulate the secretion of cytokines that promote inflammation. Zhang et al. reported a decrease in the secretion of IL-6, TNF-α, and soluble intercellular adhesion molecule-1 in mice that had received chicken collagen hydrolysate (151). The pathogenesis of osteoarthritis involves the activation of the inflammatory cascade through the stimulation of various cytokines such as TNF-α, IL-10, IL-8, and IL-1β. The study found that the hydrolysis of trypsin in chicken cartilage resulted in a reduction of these cytokine in papain-induced model rats, leading to an alleviation of osteoarthritis symptoms (152). The silkworm pupa (*Bombyx mori*) protein is rich in valuable peptides. It has been used as food and medicine in East Asian Countries (163). Enzymatic hydrolysates of silkworm have demonstrated antioxidant, antitumor and anti-bacterial effects (164, 165). Assessment of immunomodulatory peptides derived from silkworm pupa indicated the administration of 100 μg/ml of identified hexapeptide (PNPNTN) obtained from the alcalase hydrolysate resulted in a significant improvement of Con A- or LPS-induced splenocyte proliferation. The physicochemical properties of this hexapeptide like length, positive charge and hydrophobicity affect its proliferative role. Therefore, novel immunomodulatory peptides are potential therapeutic agent for enhancing immune cell function in the context of food ingredients (153).

The venoms of spiders represent a valuable source of bioactive peptides. Munhoz J et al. conducted an analysis on the effectiveness of SNX-482, a peptide obtained from the venom of African tarantula Hysterocrates gigas, on bone marrow macrophages. The administration of SNX-482 resulted in the activation of M0-macrophages, leading to an increase in the expression of costimulatory molecules such as CD40, CD68, CD80, CD83, and CD86. Additionally, the expression of checkpoint molecules including PD-L1, CTLA-4, and FAS-L was also upregulated, regardless of the administered dosage. Furthermore, it was observed that there was an augmentation in the anticancer response as a result of the upregulation of CCR4, IFN-γ, GZMB, and PDCD1 genes, as well as the secretion of IL-23 (154). So, peptides extracted from venom are likely to be used as adjuvants for improving immunotherapies of cancers. Finally, since previous studies highlight the immunomodulatory applications of different bioactive peptides from animals, they have the potential to serve as immunostimulatory or immunosuppressive agents for the treatment of various diseases like cancers, either independently or in conjunction with other therapies.

4 Bioactive peptides with the modulatory function of cell migration

Cell migration is a fundamental physiological process for developing and maintaining multicellular organisms. It has a crucial role in cancer development. Secondary tumors can be prevented by inhibiting the invasion of cancer cells into healthy tissues. Bioactive peptides are gaining increasing attention for their remarkable potential in regulating cell migration, a critical process in various physiological and pathological contexts. For instance, the tripeptide Arg-Gly-Asp (RGD) has been extensively studied for its role in cell adhesion and migration, particularly in the context of cancer metastasis. RGD sequences are known to interact with integrin receptors on the cell surface, influencing cell behavior and migration patterns. Additionally, the bioactive peptide known as substance P has been shown to play a role in neuroinflammation by modulating immune cell migration. These examples highlight the diverse applications of bioactive peptides in regulating cell migration and underscore their significance in understanding and potentially controlling various biological processes (16, 166). This section aims to provide a concise overview of the bioactive peptides implicated in the regulation of cancer cell migration for readers with an interest in this subject matter.

4.1 Bioactive peptides from animal sources

These peptides have been derived from various sources, including elastin-derived peptides (EDPs), venoms, and

neuropeptide Y (NPY). EDPs released in the extracellular microenvironment during tumoral remodeling of the stroma stimulate cancer cell migration by interacting with their membrane receptor, ribosomal protein SA (RPSA) (167). In pancreatic ductal adenocarcinoma (PDAC), EDPs have been shown to promote cell migration by stimulating the transient receptor potential melastatin-related 7 (TRPM7) channel in human pancreatic cancer cells (167). Bioactive peptides from animal venoms have also been found to affect cancer cell features such as cell proliferation, invasion, migration, and immune response modulation. These peptides selectively target cancer cells without harming normal cells and have been proposed as potential therapeutics for aggressive and deadly brain tumors like glioblastoma (GB) (168). However, these peptides, sometimes, have negative effects and support tumor progression. For example, Bombesin is a bioactive peptide, originally isolated from the skin of the European fire-bellied toad (Bombina bombina) (169) that plays a role in modulating cell migration, particularly in the context of cancer progression. It is a neuropeptide that is highly expressed and secreted by neuroendocrine cells in prostate carcinoma tissues and is believed to be related to the progression of this neoplastic disease (170). In a study on 3T3 and lung fibroblasts, bombesin was found to stimulate cell migration in a time and concentration-dependent manner (171). These results indicate that bombesin may play a role in the cellular processes that are crucial for the advancement of cancer, specifically spread and migration. Overall, bioactive peptides from animal sources may have undesired effects on cancer cell migration and other cancer-related processes.

4.2 Bioactive peptides from plant sources

A study showed that hemp peptides, generated by controlled hydrolysis of hemp proteins, exhibited anticancer properties in Hep3B human liver cancer cells. The treatment with hemp peptides increased apoptosis, reduced cell viability, and reduced cell migration in Hep3B cells without affecting normal liver cells. Increased cellular ROS levels, overexpression of cleaved caspase 3 and Bad, and downregulation of antiapoptotic Bcl-2 were all linked to the anticancer effects of hemp peptides. The study also suggested that the Akt/GSK-3β/β-catenin signaling pathway played a critical role in the anticancer properties of hemp peptides (172). Cyclotides are a family of plant-derived cyclic peptides that exhibit a diverse range of bioactivities, such as antimicrobial, anticancer, and anti-HIV properties. They are known for their unique structure and stability, and there exists a considerable potential for the utilization of this substance in the field of pharmaceuticals. Cyclotides have been shown to target cell membranes, which play a crucial role in their mechanism of action (173). In the context of cancer, cyclotides have demonstrated cytotoxicity against various cancer cell lines. Their high stability, small size, oral bioavailability, and tolerance to amino acid substitution make them an ideal platform for designing peptide-based drugs for cancer treatment (17). Some cyclotides are toxic to cancer cells whereas others can be designed to bind and inhibit particular cancer targets. The toxicity of cyclotides is associated with their ability to target and disrupt lipid bilayers containing phosphatidylethanolamine phospholipids (174).

Further research is needed to better understand the specific mechanisms by which cyclotides modulate cell migration and their potential applications in cancer therapy. However, their unique properties and ability to target cell membranes make them promising candidates for the development of peptide-based drugs for cancer treatment.

Flavokawain is a bioactive compound found in the kava-kava plant (Piper methysticum) and has been shown to possess anti-cancer properties (175). Although there is limited information on the direct role of Flavokawain as a bioactive peptide in the modulation of cell migration, some studies have demonstrated its potential in affecting cell migration and invasion in cancer cells. For instance, Flavokawain A (FKA) has been shown to induce apoptosis in breast cancer cell lines MCF-7 and MDA-MB231 and inhibit the metastatic process *in vitro*. FKA selectively promotes cell cycle arrest in these cell lines and induces apoptosis in a dose-responsive way through the internal mitochondrial route, indicating that FKA's anti-cancer effect is reliant on the presence of p53 (175). Another study looked at FKA's ability to protect endothelial cells from the oxidative stress that ochratoxin A (OTA) causes in *in vitro* models. FKA was found to reduce inflammation via NFκB inhibition and enhance the phosphorylation of PI3K and AKT, which could stimulate antioxidant activity and antiapoptotic signaling. in human umbilical vein endothelial cells (HUVECs). Depending on the dose under the oxidative stress induced by OTA, FKA also increased the phosphorylation of Nrf2 and the expression of antioxidant genes, such as HO-1, NQO-1, and GCLC (176). Further research is needed to better understand the specific mechanisms by which Flavokawain modulates cell migration and its potential applications in cancer therapy.

Lunasin is found in soy, legumes, and some cereal grains, known for its potential anti-inflammatory, antitumor, and antimetastatic properties (45). Although there is limited information on its role in modulating cell migration, some studies have explored its effects on cancer cells. In breast cancer, Lunasin has been shown to suppress the migration and invasion of breast cancer cells by inhibiting matrix metalloproteinase-2/-9 (MMP-2/-9) via the FAK/Akt/ERK and NF-κB signaling pathways (45). This implies that Lunasin may compete with integrins in order to bind with the extracellular matrix (ECM), consequently suppressing the integrin-mediated signaling pathway. In colon cancer, Lunasin has been found to inhibit metastasis by interacting with α5β1 integrin, inhibiting FAK/ERK/NF-B signaling, and enhancing the ability of oxaliplatin to stop metastases from spreading (177). The objective of this study was to examine the impact of peptides derived from soybean protein β-conglycinin on the motility of peripheral polymorphonuclear leukocytes in humans. The findings of the study demonstrated that the peptides MITLAIPVNKPGR and MIT elicited the migration of polymorphonuclear leukocytes via a mechanism that is dependent on FPR1. The migration process was impeded by the presence of tert-butoxycarbonyl (Boc)-MLP, which is an inhibitor of FPR. Additionally, prior treatment with pertussis toxin (PTX) also hindered the migration. The research findings indicated the identification of chemotactic peptides for human

polymorphonuclear leukocytes, which were derived from endogenous enzyme digests of soybean protein (173).

Numerous bioactive cationic peptides (BCPs) have demonstrated the ability to impede cellular migration in breast cancer cells. As an example, the administration of PR39 exhibited notable suppression of invasion and migration in 4T1 cells, potentially working in conjunction with Stat3 siRNA to effectively hinder cellular proliferation and migration. The P44/42 MAP kinase protein, which is essential for the migration of breast cancer cells, was found to be negatively regulated by the peptides FR8P and FR11P Furthermore, it was observed that the compound MAP-04-03 displayed significant inhibitory properties on cellular migration when administered at a concentration of 5 µM. Specifically, it was able to inhibit approximately 40% of cell migration, as determined by an IC50 value of 61.5 Mm (17, 174).

In summary, the intricate interplay between bioactive peptides and cell migration offers an interesting area of study with potential implications for advancing our understanding of cancer progression and treatment.

5 Bioactive Peptides from Complementarity-Determining Regions (CDRs) in Immunoglobulins and their Revolutionary Impact on Cancer Immunotherapy

In historical perspectives, constant regions of immunoglobulins were ascribed primarily supportive roles devoid of direct anti-infective or antitumor attributes. Recent investigations, as exemplified by Polonelli et al., underscore the substantial therapeutic potential residing within immunoglobulins, particularly within the complementarity-determining regions (CDRs) (178). CDRs of antibodies have evolved as pivotal domains yielding bioactive peptides with profound therapeutic implications. The work of L. Polonelli and collaborators highlights the prevalence of bioactive peptides originating from CDRs, indicating that immunoglobulin molecules serve as reservoirs for an extensive array of sequences with potential activities against diverse targets (179). Polonelli et al., employing Cotia's and Kabat's rules, systematically scrutinized CDRs and identified a cytotoxic killer peptide (KP) derived from VLCDR1 and the framework sequence, demonstrating efficacy against various microorganisms (180). Subsequent engineering of KP, featuring an N-terminal substitution (A1E), not only augmented its effectiveness but also expanded its cytotoxic spectrum against fungi, protozoa, bacteria, and viruses (181–185). The recognition that peptides from the framework sequences adjacent to hypervariable CDRs exhibited cytotoxicity against Candida albicans broadened the scope of potential therapeutic candidates (180). Furthermore, synthetic peptides mirroring fragments of the constant region (Fc region) in IgG, IgM, and IgA classes exhibited cytotoxicity against diverse microorganisms (186). Extending the exploration to monoclonal antibodies (mAbs), Dobroff et al. investigated the antimicrobial, antiviral, and antitumor activities of synthetic CDR-related peptides, demonstrating inhibitory effects in both *in vitro* and *in vivo* settings (187, 188). A4, a monoclonal antibody raised against B16F10 cells, induced apoptosis in melanoma cell lines and afforded complete protection against tumor growth in murine models (188). This investigation encompassed synthetic peptides derived from A4, particularly the VH CDR3 peptide, exhibiting inhibitory effects on melanoma cells and inducing DNA degradation (188). Additionally, the *in vivo* administration of the IgM antibody A4M manifested anti-angiogenic effects through bioactive peptides derived from its CDRs (188). Travassos and collaborators identified the peptide C7H2, inducing tumor apoptosis and reducing melanoma growth through interaction with β-actin (179). Subsequent research by Arruda et al. validated the apoptotic effect of C7H2 across various human tumor cell lines, unraveling molecular mechanisms involving G-actin polymerization, F-actin stabilization, caspase activation, and chromatin condensation (189).

Travassos' team has pioneered a paradigm shift in cancer immunotherapy by leveraging the potential of complementarity determining regions (CDRs) from immunoglobulins (Ig) to develop innovative antitumor peptides. The seminal study conducted by Figueiredo et al. (190) represents a noteworthy milestone, aiming to identify CDR-derived peptide sequences with potent antitumor activities and immunostimulatory properties. The investigated peptides, including the C36L1 peptide derived from the light-chain CDR1 sequence, exhibited cytotoxic effects against murine melanoma and human tumor cell lines *in vitro*. C36L1 demonstrated both immunostimulatory and direct antitumor activities by inducing microtubule depolymerization, apoptosis, and modulating the PI3K/Akt signaling axis (191). Figueiredo et al. underscored the immune-dependent nature of C36L1's antitumorigenic responses, elucidating its capacity to restore immunogenic functions in dendritic cells (DCs) by binding CD74 and disrupting interactions with tumor-derived macrophage inhibitory factor (MIF) (192). This groundbreaking discovery laid the groundwork for the development of peptide-based immunotherapies targeting the MIF-CD74 signaling pathway to restore antitumor immune responses in metastatic melanoma. Azevedo et al. extended this work by combining immune checkpoint therapies with MIF inhibitors, demonstrating enhanced responses to anti-CTLA-4 treatment in resistant melanoma. This combined therapy augmented CD8+ T-cell infiltration, facilitated macrophage M1 conversion, and reprogrammed the metabolic pathway of melanoma cells, offering a strategic approach to enhance immune checkpoint blockade therapy responses (193). The research led by Prof Travassos and collaborators has not only revolutionized cancer immunotherapy but has also paved the way for innovative therapeutic development, underscoring the potential of CDR-derived peptides to transcend the conventional scope of antibodies and provide targeted treatment (190–193).

6 Conclusion

Bioactive peptides have emerged as a promising frontier in medicine, poised to transform fields like cancer therapy, immunomodulation, and cell migration. These peptides, sourced diversely, offer versatile solutions to complex health challenges. In cancer treatment, bioactive peptides present a compelling alternative to conventional therapies. They display selective effects on cancer cells, modulate migration, and induce apoptosis, promising enhanced efficacy with fewer side effects. Their immunomodulatory properties offer potential in managing autoimmune disorders and bolstering immunity against diseases, including cancer. These peptides can finely tune both innate and adaptive immune responses, paving the way for innovative therapies. Bioactive peptides also play a role in controlling cell migration, aiding in combating diseases' spread. Both animal and plant-derived peptides exhibit various mechanisms influencing cell migration, shaping disease progression.

While further research and clinical trials are needed to unlock their full potential and address challenges like stability and delivery, bioactive peptides hold immense promise in advancing medicine. They offer more precise, effective, and personalized treatments, heralding a brighter future in healthcare.

Author contributions

NG: Writing – original draft. SS: Writing – original draft. MJ: Writing – original draft. ÖT: Writing – original draft. AP: Writing – original draft. ZL: Writing – review & editing. MTA: Writing – original draft. MG-H: Conceptualization, Writing – review & editing.

Funding

The author(s) declare financial support was received for the research, authorship, and/or publication of this article. This study was supported by grants from the National Natural Science Foundation of China (No.32000802), Science and Technology Planning Project of Guangzhou, China(No. 202102020181), Research Grant of Key Laboratory of Regenerative Medicine, Ministry of Education, Jinan University, China (No. ZSYXM202203) and Russian Science Foundation (No. 21-75-30020).

Acknowledgments

Project ratification number 32000802, 202102020181.

Conflict of interest

The authors declare that the research was conducted in the absence of any commercial or financial relationships that could be construed as a potential conflict of interest.

Publisher's note

References

1. Siegel RL, Miller KD, Goding Sauer A, Fedewa SA, Butterly LF, Anderson JC, et al. Colorectal cancer statistics, 2020. *CA: Cancer J Clin* (2020) 70:145–64. doi: 10.3322/caac.21601

2. Azar MT, Saglam N, Turk M. Anti wnt-1 monoclonal antibody's conjugated with gold nanoparticles, induced apoptosis on MCF-7 breast cancer cell lines. *J Nano Res-Sw* (2019) 58:1–9. doi: 10.4028/www.scientific.net/JNanoR.58.1

3. Dagenais GR, Leong DP, Rangarajan S, Lanas F, Lopez-Jaramillo P, Gupta R, et al. Variations in common diseases, hospital admissions, and deaths in middle-aged adults in 21 countries from five continents (PURE): A prospective cohort study. *Lancet* (2020) 395:785–94. doi: 10.1016/S0140-6736(19)32007-0

4. Marqus S, Pirogova E, Piva TJ. Evaluation of the use of therapeutic peptides for cancer treatment. *J Biomed Sci* (2017) 24:1–15. doi: 10.1186/s12929-017-0328-x

5. Cevenini A, Celia C, Orru S, Sarnataro D, Raia M, Mollo V, et al. Liposome-embedding silicon microparticle for oxaliplatin delivery in tumor chemotherapy. *Pharmaceutics* (2020) 12(6):559. doi: 10.3390/pharmaceutics12060559

6. Parodi A, Rudzinska M, Leporatti S, Anissimov Y, Zamyatnin AA Jr. Smart nanotheranostics responsive to pathological stimuli. *Front Bioeng Biotechnol* (2020) 8:503. doi: 10.3389/fbioe.2020.00503

7. Sánchez A, Vázquez A. Bioactive peptides: A review. *Food Qual Saf* (2017) 1:29–46. doi: 10.1093/fqs/fyx006

8. Faraji N, Arab SS, Doustmohammadi A, Daly NL, Khosroushahi AY. ApInAPDB: a database of apoptosis-inducing anticancer peptides. *Sci Rep* (2022) 12:21341. doi: 10.1038/s41598-022-25530-6

9. Zhang X-X, Eden HS, Chen X. Peptides in cancer nanomedicine: drug carriers, targeting ligands and protease substrates. *J Controlled release* (2012) 159:2–13. doi: 10.1016/j.jconrel.2011.10.023

10. Tyagi A, Tuknait A, Anand P, Gupta S, Sharma M, Mathur D, et al. CancerPPD: A database of anticancer peptides and proteins. *Nucleic Acids Res* (2015) 43:D837–43. doi: 10.1093/nar/gku892

11. Karami Fath M, Babakhaniyan K, Zokaei M, Yaghoubian A, Akbari S, Khorsandi M, et al. Anti-cancer peptide-based therapeutic strategies in solid tumors. *Cell Mol Biol Lett* (2022) 27:33. doi: 10.1186/s11658-022-00332-w

12. Wang L, Wang N, Zhang W, Cheng X, Yan Z, Shao G, et al. Therapeutic peptides: Current applications and future directions. *Signal Transduction Targeted Ther* (2022) 7:48. doi: 10.1038/s41392-022-00904-4

13. Blanco-Míguez A, Gutiérrez-Jácome A, Pérez-Pérez M, Pérez-Rodríguez G, Catalán-García S, Fdez-Riverola F, et al. From amino acid sequence to bioactivity: The biomedical potential of antitumor peptides. *Protein Sci* (2016) 25:1084–95. doi: 10.1002/pro.2927

14. Prasad S, Phromnoi K, Yadav VR, Chaturvedi MM, Aggarwal BB. Targeting inflammatory pathways by flavonoids for prevention and treatment of cancer. *Planta Med* (2010) 76:1044–63. doi: 10.1055/s-0030-1250111

15. Pavlicevic M, Marmiroli N, Maestri E. Immunomodulatory peptides—A promising source for novel functional food production and drug discovery. *Peptides* (2022) 148:170696. doi: 10.1016/j.peptides.2021.170696

16. Gattringer J, Gruber CW, Hellinger R. Peptide modulators of cell migration: Overview, applications and future development. *Drug Discovery Today* (2023) 28:103554. doi: 10.1016/j.drudis.2023.103554

17. Mehta L, Dhankhar R, Gulati P, Kapoor RK, Mohanty A, Kumar S. Natural and grafted cyclotides in cancer therapy: an insight. *J Pept Sci* (2020) 26:e3246. doi: 10.1002/psc.3246

18. Romagnani S. Regulation of the T cell response. *Clin Exp Allergy* (2006) 36:1357–66. doi: 10.1111/j.1365-2222.2006.02606.x

19. Zaky AA, Simal-Gandara J, Eun JB, Shim JH, Abd El-Aty AM. Bioactivities, applications, safety, and health benefits of bioactive peptides from food and by-products: A review. *Front Nutr* (2022) 8. doi: 10.3389/fnut.2021.815640

20. Pan X, Zhao Y-Q, Hu F-Y, Chi C-F, Wang B. Anticancer activity of a hexapeptide from skate (Raja porosa) cartilage protein hydrolysate in HeLa cells. *Mar Drugs* (2016) 14:153. doi: 10.3390/md14080153

21. Vital DAL, De Mejía EG, Dia VP, Loarca-Piña G. Peptides in common bean fractions inhibit human colorectal cancer cells. *Food Chem* (2014) 157:347–55. doi: 10.1016/j.foodchem.2014.02.050

22. Hori K, Sato Y, Ito K, Fujiwara Y, Iwamoto Y, Makino H, et al. Strict specificity for high-mannose type N-glycans and primary structure of a red alga Eucheuma serra lectin. *Glycobiology* (2007) 17:479–91. doi: 10.1093/glycob/cwm007

23. De Mejía EG, Prisecaru VI. Lectins as bioactive plant proteins: a potential in cancer treatment. *Crit Rev Food Sci Nutr* (2005) 45:425–45. doi: 10.1080/10408390591034445

24. Freitas CS, Vericimo MA, da Silva ML, da Costa GCV, Pereira PR, Paschoalin VMF, et al. Encrypted antimicrobial and antitumoral peptides recovered from a protein-rich soybean (Glycine max) by-product. *J Funct Foods* (2019) 54:187–98. doi: 10.1016/j.jff.2019.01.024

25. Ding J, Hou GG, Nemzer BV, Xiong S, Dubat A, Feng H. Effects of controlled germination on selected physicochemical and functional properties of whole-wheat flour and enhanced γ-aminobutyric acid accumulation by ultrasonication. *Food Chem* (2018) 243:214–21. doi: 10.1016/j.foodchem.2017.09.128

26. Soares RAM, Mendonça S, De Castro LÍA, Menezes ACCCC, Arêas JAG. Major peptides from amaranth (Amaranthus cruentus) protein inhibit HMG-CoA reductase activity. *Int J Mol Sci* (2015) 16:4150–60. doi: 10.3390/ijms16024150

27. Montoya-Rodríguez A, de Mejía EG, Dia VP, Reyes-Moreno C, Milán-Carrillo J. Extrusion improved the anti-inflammatory effect of amaranth (Amaranthus hypochondriacus) hydrolysates in LPS-induced human THP-1 macrophage-like and mouse RAW 264.7 macrophages by preventing activation of NF-κB signaling. *Mol Nutr Food Res* (2014) 58:1028–41. doi: 10.1002/mnfr.201300764

28. Theansungnoen T, Maijaroen S, Jangpromma N, Yaraksa N, Daduang S, Temsiripong T, et al. Cationic antimicrobial peptides derived from crocodylus siamensis leukocyte extract, revealing anticancer activity and apoptotic induction on human cervical cancer cells. *Protein J* (2016) 35:202–11. doi: 10.1007/s10930-016-9662-1

29. Luna-Vital DA, De Mejía EG, Mendoza S, Loarca-Piña G. Peptides present in the non-digestible fraction of common beans (Phaseolus vulgaris L.) inhibit the angiotensin-I converting enzyme by interacting with its catalytic cavity independent of their antioxidant capacity. *Food Funct* (2015) 6:1470–9. doi: 10.1039/C5FO00190K

30. Bhandari D, Rafiq S, Gat Y, Gat P, Waghmare R, Kumar V. A review on bioactive peptides: Physiological functions, bioavailability and safety. *Int J Pept Res Ther* (2020) 26:139–50. doi: 10.1007/s10989-019-09823-5

31. Su L-Y, Shi Y-X, Yan M-R, Xi Y, Su X-L. Anticancer bioactive peptides suppress human colorectal tumor cell growth and induce apoptosis via modulating the PARP-p53-Mcl-1 signaling pathway. *Acta Pharmacologica Sin* (2015) 36:1514–9. doi: 10.1038/aps.2015.80

32. Chi CF, Hu FY, Wang B, Li T, Ding GF. Antioxidant and anticancer peptides from the protein hydrolysate of blood clam (Tegillarca granosa) muscle. *J Funct Foods* (2015) 15:301–13. doi: 10.1016/j.jff.2015.03.045

33. Chen G, Chen Y, Hou Y, Huo Y, Gao A, Li S, et al. Preparation, characterization and the *in vitro* bile salts binding capacity of celery seed protein hydrolysates via the fermentation using B. subtilis. *LWT* (2020) 117:108571. doi: 10.1016/j.lwt.2019.108571

34. Stemmer SM, Benjaminov O, Silverman MH, Sandler U, Purim O, Sender N, et al. A phase I clinical trial of dTCApFs, a derivative of a novel human hormone peptide, for the treatment of advanced/metastatic solid tumors. *Mol Clin Oncol* (2018) 8:22–9. doi: 10.3892/mco.2017.1505

35. Chalamaiah M, Yu W, Wu J. Immunomodulatory and anticancer protein hydrolysates (peptides) from food proteins: A review. *Food Chem* (2018) 245:205–22. doi: 10.1016/j.foodchem.2017.10.087

36. Kannan A, Hettiarachchy NS, Lay JO, Liyanage R. Human cancer cell proliferation inhibition by a pentapeptide isolated and characterized from rice bran. *Peptides* (2010) 31:1629–34. doi: 10.1016/j.peptides.2010.05.018

37. Xue Z, Wen H, Zhai L, Yu Y, Li Y, Yu W, et al. Antioxidant activity and anti-proliferative effect of a bioactive peptide from chickpea (Cicer arietinum L.). *Food Res Int* (2015) 77:75–81. doi: 10.1016/j.foodres.2015.09.027

38. Karami Z, Peighambardoust SH, Hesari J, Akbari-Adergani B, Andreu D. Antioxidant, anticancer and ACE-inhibitory activities of bioactive peptides from wheat germ protein hydrolysates. *Food Bioscience* (2019) 32:100450. doi: 10.1016/j.fbio.2019.100450

39. Li M, Zhang Y, Xia S, Ding X. Finding and isolation of novel peptides with anti-proliferation ability of hepatocellular carcinoma cells from mung bean protein hydrolysates. *J Funct Foods* (2019) 62:103557. doi: 10.1016/j.jff.2019.103557

40. Hwang JS, Yoo HJ, Song HJ, Kim KK, Chun YJ, Matsui T, et al. Inflammation-related signaling pathways implicating TGFβ are revealed in the expression profiling of MCF7 cell treated with fermented soybean, chungkookjang. *Nutr Cancer* (2011) 63:645–52. doi: 10.1080/01635581.2011.551987

41. Chen Z, Wang J, Liu W, Chen H. Physicochemical characterization, antioxidant and anticancer activities of proteins from four legume species. *J Food Sci Technol* (2017) 54:964–72. doi: 10.1007/s13197-016-2390-x

42. Zheng Q, Qiu D, Liu X, Zhang L, Cai S, Zhang X. Antiproliferative effect of Dendrobium catenatum Lindley polypeptides against human liver, gastric and breast cancer cell lines. *Food Funct* (2015) 6:1489–95. doi: 10.1039/C5FO00060B

43. Wang J, Hu J, Cui J, Bai X, Du Y, Miyaguchi Y, et al. Purification and identification of a ACE inhibitory peptide from oyster proteins hydrolysate and the antihypertensive effect of hydrolysate in spontaneously hypertensive rats. *Food Chem* (2008) 111:302–8. doi: 10.1016/j.foodchem.2008.03.059

44. Cicero AF, Fogacci F, Colletti A. Potential role of bioactive peptides in prevention and treatment of chronic diseases: A narrative review. *Br J Pharmacol* (2017) 174:1378–94. doi: 10.1111/bph.13608

45. Jiang Q, Pan Y, Cheng Y, Li H, Liu D, Li H. Lunasin suppresses the migration and invasion of breast cancer cells by inhibiting matrix metalloproteinase-2/-9 via the FAK/Akt/ERK and NF-κB signaling pathways. *Oncol Rep* (2016) 36:253–62. doi: 10.3892/or.2016.4798

46. Fernández-Tomé S, Xu F, Han Y, Hernández-Ledesma B, Xiao H. Inhibitory effects of peptide lunasin in colorectal cancer HCT-116 cells and their tumorsphere-derived subpopulation. *Int J Mol Sci* (2020) 21:537. doi: 10.3390/ijms21020537

47. Hsieh C-C, Wang C-H, Huang Y-S. Lunasin attenuates obesity-associated metastasis of 4T1 breast cancer cell through anti-inflammatory property. *Int J Mol Sci* (2016) 17:2109. doi: 10.3390/ijms17122109

48. Ren G, Hao Y, Zhu Y, Shi Z, Zhao G. Expression of bioactive lunasin peptide in transgenic rice grains for the application in functional food. *Molecules* (2018) 23:2373. doi: 10.3390/molecules23092373

49. Mushtaq M, Gani A, Masoodi FA. Himalayan cheese (Kalari/Kradi) fermented with different probiotic strains: *In vitro* investigation of nutraceutical properties. *LWT* (2019) 104:53–60. doi: 10.1016/j.lwt.2019.01.024

50. Ayyash M, Al-Dhaheri AS, Al Mahadin S, Kizhakkayil J, Abushelaibi A. *In vitro* investigation of anticancer, antihypertensive, antidiabetic, and antioxidant activities of camel milk fermented with camel milk probiotic: A comparative study with fermented bovine milk. *J Dairy Sci* (2018) 101:900–11. doi: 10.3168/jds.2017-13400

51. Yang JI, Tang JY, Liu YS, Wang HR, Lee SY, Yen CY, et al. Roe protein hydrolysates of giant grouper (Epinephelus lanceolatus) inhibit cell proliferation of oral cancer cells involving apoptosis and oxidative stress. *BioMed Res Int* (2016) 2016:8305073. doi: 10.1155/2016/8305073

52. Bai R, Roach MC, Jayaram SK, Barkoczy J, Pettit GR, Ludueña RF, et al. Differential effects of active isomers, segments, and analogs of dolastatin 10 on ligand interactions with tubulin. *Correlation cytotoxicity. Biochem Pharmacol* (1993) 45:1503–15. doi: 10.1016/0006-2952(93)90051-W

53. Gentilucci L, Tolomelli A, Squassabia F. Peptides and peptidomimetics in medicine, surgery and biotechnology. *Curr Med Chem* (2006) 13:2449–66. doi: 10.2174/092986706777935041

54. Simmons TL, Andrianasolo E, McPhail K, Flatt P, Gerwick WH. Marine natural products as anticancer drugs. *Mol Cancer Ther* (2005) 4:333–42. doi: 10.1158/1535-7163.333.4.2

55. Donia M, Hamann MT. Marine natural products and their potential applications as anti-infective agents. *Lancet Infect Dis* (2003) 3:338–48. doi: 10.1016/S1473-3099(03)00655-8

56. Su L, Xu G, Shen J, Tuo Y, Zhang X, Jia S, et al. Anticancer bioactive peptide suppresses human gastric cancer growth through modulation of apoptosis and the cell cycle. *Oncol Rep* (2010) 23:3–9. doi: 10.3892/or_00000599

57. Yu L, Yang L, An W, Su X. Anticancer bioactive peptide-3 inhibits human gastric cancer growth by suppressing gastric cancer stem cells. *J Cell Biochem* (2014) 115:697–711. doi: 10.1002/jcb.24711

58. Su X, Dong C, Zhang J, Su L, Wang X, Cui H, et al. Combination therapy of anti-cancer bioactive peptide with Cisplatin decreases chemotherapy dosing and toxicity to improve the quality of life in xenograft nude mice bearing human gastric cancer. *Cell Bioscience* (2014) 4:1–13. doi: 10.1186/2045-3701-4-7

59. Guha P, Kaptan E, Bandyopadhyaya G, Kaczanowska S, Davila E, Thompson K, et al. Cod glycopeptide with picomolar affinity to galectin-3 suppresses T-cell apoptosis and prostate cancer metastasis. *Proc Natl Acad Sci* (2013) 110:5052–7. doi: 10.1073/pnas.1202653110

60. de Oliveira AN, Soares AM, da Silva SL. Peptides from animal venom and poisons. *Int J Pept Res Ther* (2023) 29:83. doi: 10.1007/s10989-023-10557-8

61. Heinen TE, da Veiga AB. Arthropod venoms and cancer. *Toxicon* (2011) 57:497–511. doi: 10.1016/j.toxicon.2011.01.002

62. Ortiz E, Gurrola GB, Schwartz EF, Possani LD. Scorpion venom components as potential candidates for drug development. *Toxicon* (2015) 93:125–35. doi: 10.1016/j.toxicon.2014.11.233

63. Cociancich S, Goyffon M, Bontems F, Bulet P, Bouet F, Menez A, et al. Purification and characterization of a scorpion defensin, a 4kDa antibacterial peptide presenting structural similarities with insect defensins and scorpion toxins. *Biochem Biophys Res Commun* (1993) 194:17–22. doi: 10.1006/bbrc.1993.1778

64. Dai C, Ma Y, Zhao Z, Zhao R, Wang Q, Wu Y, et al. Mucroporin, the first cationic host defense peptide from the venom of Lychas mucronatus. *Antimicrobial Agents chemotherapy* (2008) 52:3967–72. doi: 10.1128/AAC.00542-08

65. Du Q, Hou X, Wang L, Zhang Y, Xi X, Wang H, et al. AaeAP1 and AaeAP2: novel antimicrobial peptides from the venom of the scorpion, Androctonus aeneas: structural characterisation, molecular cloning of biosynthetic precursor-encoding cDNAs and engineering of analogues with enhanced antimicrobial and anticancer activities. *Toxins (Basel)* (2015) 7:219–37. doi: 10.3390/toxins7020219

66. Primon-Barros M, José Macedo A. Animal venom peptides: Potential for new antimicrobial agents. *Curr topics medicinal Chem* (2017) 17:1119–56. doi: 10.2174/1568026616666160930151242

67. Chippaux JP, Goyffon M. Epidemiology of scorpionism: a global appraisal. *Acta Trop* (2008) 107:71–9. doi: 10.1016/j.actatropica.2008.05.021

68. Goudet C, Chi CW, Tytgat J. An overview of toxins and genes from the venom of the Asian scorpion Buthus martensi Karsch. *Toxicon* (2002) 40:1239–58. doi: 10.1016/S0041-0101(02)00142-3

69. Srinivasan KN, Gopalakrishnakone P, Tan PT, Chew KC, Cheng B, Kini RM, et al. SCORPION, a molecular database of scorpion toxins. *Toxicon* (2002) 40:23–31. doi: 10.1016/S0041-0101(01)00182-9

70. Guo X, Ma C, Du Q, Wei R, Wang L, Zhou M, et al. Two peptides, TsAP-1 and TsAP-2, from the venom of the Brazilian yellow scorpion, Tityus serrulatus: evaluation of their antimicrobial and anticancer activities. *Biochimie* (2013) 95:1784–94. doi: 10.1016/j.biochi.2013.06.003

71. Ali SA, Alam M, Abbasi A, Undheim EA, Fry BG, Kalbacher H, et al. Structure-activity relationship of chlorotoxin-like peptides. *Toxins (Basel)* (2016) 8:36. doi: 10.3390/toxins8020036

72. DeBin JA, Maggio JE, Strichartz GR. Purification and characterization of chlorotoxin, a chloride channel ligand from the venom of the scorpion. *Am J Physiol* (1993) 264:C361–9. doi: 10.1152/ajpcell.1993.264.2.C361

73. DeBin JA, Strichartz GR. Chloride channel inhibition by the venom of the scorpion Leiurus quinquestriatus. *Toxicon* (1991) 29:1403–8. doi: 10.1016/0041-0101(91)90128-E

74. Soroceanu L, Manning TJJr., Sontheimer H. Modulation of glioma cell migration and invasion using Cl(-) and K(+) ion channel blockers. *J Neurosci* (1999) 19:5942–54. doi: 10.1523/JNEUROSCI.19-14-05942.1999

75. Deshane J, Garner CC, Sontheimer H. Chlorotoxin inhibits glioma cell invasion via matrix metalloproteinase-2. *J Biol Chem* (2003) 278:4135–44. doi: 10.1074/jbc.M205662200

76. Veiseh M, Gabikian P, Bahrami SB, Veiseh O, Zhang M, Hackman RC, et al. Tumor paint: A chlorotoxin:Cy5.5 bioconjugate for intraoperative visualization of cancer foci. *Cancer Res* (2007) 67:6882–8. doi: 10.1158/0008-5472.CAN-06-3948

77. McFerrin MB, Sontheimer H. A role for ion channels in glioma cell invasion. *Neuron Glia Biol* (2006) 2:39–49. doi: 10.1017/S1740925X06000044

78. Jang SH, Choi SY, Ryu PD, Lee SY. Anti-proliferative effect of Kv1.3 blockers in A549 human lung adenocarcinoma *in vitro* and *in vivo*. *Eur J Pharmacol* (2011) 651:26–32. doi: 10.1016/j.ejphar.2010.10.066

79. Gupta SD, Gomes A, Debnath A, Saha A, Gomes A. Apoptosis induction in human leukemic cells by a novel protein Bengalin, isolated from Indian black scorpion venom: Through mitochondrial pathway and inhibition of heat shock proteins. *Chem Biol Interact* (2010) 183:293–303. doi: 10.1016/j.cbi.2009.11.006

80. Li B, Lyu P, Xi X, Ge L, Mahadevappa R, Shaw C, et al. Triggering of cancer cell cycle arrest by a novel scorpion venom-derived peptide-Gonearrestide. *J Cell Mol Med* (2018) 22:4460–73. doi: 10.1111/jcmm.13745

81. Kuhn-Nentwig L. Antimicrobial and cytolytic peptides of venomous arthropods. *Cell Mol Life Sci* (2003) 60:2651–68. doi: 10.1007/s00018-003-3106-8

82. Vorontsova OV, Egorova NS, Arseniev AS, Feofanov AV. Haemolytic and cytotoxic action of latarcin Ltc2a. *Biochimie* (2011) 93:227–41. doi: 10.1016/j.biochi.2010.09.016

83. Liu Z, Deng M, Xiang J, Ma H, Hu W, Zhao Y, et al. A novel spider peptide toxin suppresses tumor growth through dual signaling pathways. *Curr Mol Med* (2012) 12:1350–60. doi: 10.2174/156652412803833643

84. Pereira A, Kerkis A, Hayashi MA, Pereira AS, Silva FS, Oliveira EB, et al. Crotamine toxicity and efficacy in mouse models of melanoma. *Expert Opin Investig Drugs* (2011) 20:1189–200. doi: 10.1517/13543784.2011.602064

85. León G, Sánchez L, Hernández A, Villalta M, Herrera M, Segura A, et al. Immune response towards snake venoms. *Inflammation Allergy Drug Targets* (2011) 10:381–98. doi: 10.2174/187152811797200605

86. Tian Y, Wang H, Li B, Ke M, Wang J, Dou J, et al. The cathelicidin-BF Lys16 mutant Cbf-K16 selectively inhibits non-small cell lung cancer proliferation *in vitro*. *Oncol Rep* (2013) 30:2502–10. doi: 10.3892/or.2013.2693

87. Havas LJ. Effect of bee venom on colchicine-induced tumours. *Nature* (1950) 166:567–8. doi: 10.1038/166567a0

88. Jo M, Park MH, Kollipara PS, An BJ, Song HS, Han SB, et al. Anti-cancer effect of bee venom toxin and melittin in ovarian cancer cells through induction of death receptors and inhibition of JAK2/STAT3 pathway. *Toxicol Appl Pharmacol* (2012) 258:72–81. doi: 10.1016/j.taap.2011.10.009

89. Wang C, Chen T, Zhang N, Yang M, Li B, Lü X, et al. Melittin, a major component of bee venom, sensitizes human hepatocellular carcinoma cells to tumor necrosis factor-related apoptosis-inducing ligand (TRAIL)-induced apoptosis by activating caMKII-TAK1-JNK/p38 and inhibiting IκBα Kinase-NFκB*. *J Biol Chem* (2009) 284:3804–13. doi: 10.1074/jbc.M807191200

90. Park MH, Choi MS, Kwak DH, Oh KW, Yoon DY, Han SB, et al. Anti-cancer effect of bee venom in prostate cancer cells through activation of caspase pathway via inactivation of NF-κB. *Prostate* (2011) 71:801–12. doi: 10.1002/pros.21296

91. Park JH, Jeong YJ, Park KK, Cho HJ, Chung IK, Min KS, et al. Melittin suppresses PMA-induced tumor cell invasion by inhibiting NF-kappaB and AP-1-dependent MMP-9 expression. *Mol Cells* (2010) 29:209–15. doi: 10.1007/s10059-010-0028-9

92. Gajski G, Garaj-Vrhovac V. Melittin: a lytic peptide with anticancer properties. *Environ Toxicol Pharmacol* (2013) 36:697–705. doi: 10.1016/j.etap.2013.06.009

93. Pan H, Soman NR, Schlesinger PH, Lanza GM, Wickline SA. Cytolytic peptide nanoparticles ('NanoBees') for cancer therapy. *Wiley Interdiscip Rev Nanomed Nanobiotechnol* (2011) 3:318–27. doi: 10.1002/wnan.126

94. Soman NR, Baldwin SL, Hu G, Marsh JN, Lanza GM, Heuser JE, et al. Molecularly targeted nanocarriers deliver the cytolytic peptide melittin specifically to tumor cells in mice, reducing tumor growth. *J Clin Invest* (2009) 119:2830–42. doi: 10.1172/JCI38842

95. Moreno M, Giralt E. Three valuable peptides from bee and wasp venoms for therapeutic and biotechnological use: melittin, apamin and mastoparan. *Toxins (Basel)* (2015) 7:1126–50. doi: 10.3390/toxins7041126

96. Yamada Y, Shinohara Y, Kakudo T, Chaki S, Futaki S, Kamiya H, et al. Mitochondrial delivery of mastoparan with transferrin liposomes equipped with a pH-sensitive fusogenic peptide for selective cancer therapy. *Int J Pharm* (2005) 303:1–7. doi: 10.1016/j.ijpharm.2005.06.009

97. de Azevedo RA, Figueiredo CR, Ferreira AK, Matsuo AL, Massaoka MH, Girola N, et al. Mastoparan induces apoptosis in B16F10-Nex2 melanoma cells via the intrinsic mitochondrial pathway and displays antitumor activity *in vivo*. *Peptides* (2015) 68:113–9. doi: 10.1016/j.peptides.2014.09.024

98. Yoon KA, Kim K, Nguyen P, Seo JB, Park YH, Kim K-G, et al. Comparative bioactivities of mastoparans from social hornets Vespa crabro and Vespa analis. *J Asia-Pacific Entomology* (2015) 18:825–9. doi: 10.1016/j.aspen.2015.10.006

99. Wang KR, Zhang BZ, Zhang W, Yan JX, Li J, Wang R. Antitumor effects, cell selectivity and structure-activity relationship of a novel antimicrobial peptide polybia-MPI. *Peptides* (2008) 29:963–8. doi: 10.1016/j.peptides.2008.01.015

100. Wang KR, Yan JX, Zhang BZ, Song JJ, Jia PF, Wang R. Novel mode of action of polybia-MPI, a novel antimicrobial peptide, in multi-drug resistant leukemic cells. *Cancer Lett* (2009) 278:65–72. doi: 10.1016/j.canlet.2008.12.027

101. Leite NB, Aufderhorst-Roberts A, Palma MS, Connell SD, Ruggiero Neto J, Beales PA. PE and PS lipids synergistically enhance membrane poration by a peptide with anticancer properties. *Biophys J* (2015) 109:936–47. doi: 10.1016/j.bpj.2015.07.033

102. Xuan HL, Duc TD, Thuy AM, Chau PM, Tung TT. Chemical approaches in the development of natural nontoxic peptide Polybia-MP1 as a potential dual antimicrobial and antitumor agent. *Amino Acids* (2021) 53:843–52. doi: 10.1007/s00726-021-02995-9

103. Zhang W, Li J, Liu LW, Wang KR, Song JJ, Yan JX, et al. A novel analog of antimicrobial peptide Polybia-MPI, with thioamide bond substitution, exhibits increased therapeutic efficacy against cancer and diminished toxicity in mice. *Peptides* (2010) 31:1832–8. doi: 10.1016/j.peptides.2010.06.019

104. Torres MDT, Andrade GP, Sato RH, Pedron CN, Manieri TM, Cerchiaro G, et al. Natural and redesigned wasp venom peptides with selective antitumoral activity. *Beilstein J Org Chem* (2018) 14:1693–703. doi: 10.3762/bjoc.14.144

105. He PP, Li XD, Wang L, Wang H. Bispyrene-based self-assembled nanomaterials: *In vivo* self-assembly, transformation, and biomedical effects. *Acc Chem Res* (2019) 52:367–78. doi: 10.1021/acs.accounts.8b00398

106. Carvajal LA, Neriah DB, Senecal A, Benard L, Thiruthuvanathan V, Yatsenko T, et al. Dual inhibition of MDMX and MDM2 as a therapeutic strategy in leukemia. *Sci Transl Med* (2018) 10(436):eaao3003. doi: 10.1126/scitranslmed.aao3003

107. Ng SY, Yoshida N, Christie AL, Ghandi M, Dharia NV, Dempster J, et al. Targetable vulnerabilities in T- and NK-cell lymphomas identified through preclinical models. *Nat Commun* (2018) 9:2024. doi: 10.1038/s41467-018-04356-9

108. Walther B, Sieber R. Bioactive proteins and peptides in foods. *Int J Vitamin Nutr Res* (2011) 81:181. doi: 10.1024/0300-9831/a000054

109. Stadnik J, Kęska P. Meat and fermented meat products as a source of bioactive peptides. *Acta Scientiarum Polonorum Technologia Alimentaria* (2015) 14:181–90. doi: 10.17306/J.AFS.2015.3.19

110. Udenigwe CC, Aluko RE. Food protein-derived bioactive peptides: production, processing, and potential health benefits. *J Food Sci* (2012) 77:R11–24. doi: 10.1111/j.1750-3841.2011.02455.x

111. Nwachukwu ID, Aluko RE. Anticancer and antiproliferative properties of food-derived protein hydrolysates and peptides. *J Food Bioactives* (2019) 7:18-26. doi: 10.31665/JFB.2019.7194

112. Vesely MD, Kershaw MH, Schreiber RD, Smyth MJ. Natural innate and adaptive immunity to cancer. *Annu Rev Immunol* (2011) 29:235–71. doi: 10.1146/annurev-immunol-031210-101324

113. Dadar M, Shahali Y, Chakraborty S, Prasad M, Tahoori F, Tiwari R, et al. Antiinflammatory peptides: current knowledge and promising prospects. *Inflammation Res* (2019) 68:125–45. doi: 10.1007/s00011-018-1208-x

114. Thell K, Hellinger R, Schabbauer G, Gruber CW. Immunosuppressive peptides and their therapeutic applications. *Drug Discovery Today* (2014) 19:645–53. doi: 10.1016/j.drudis.2013.12.002

115. Wu W, Zhang M, Ren Y, Cai X, Yin Z, Zhang X, et al. Characterization and immunomodulatory activity of a novel peptide, ECFSTA, from wheat germ globulin. *J Agric Food Chem* (2017) 65:5561–9. doi: 10.1021/acs.jafc.7b01360

116. Wu W, Zhang M, Sun C, Brennan M, Li H, Wang G, et al. Enzymatic preparation of immunomodulatory hydrolysates from defatted wheat germ (Triticum Vulgare) globulin. *Int J Food Sci Technol* (2016) 51:2556–66. doi: 10.1111/ijfs.13238

117. Horiguchi N, Horiguchi H, Suzuki Y. Effect of wheat gluten hydrolysate on the immune system in healthy human subjects. *Bioscience biotechnology Biochem* (2005) 69:2445–9. doi: 10.1271/bbb.69.2445

118. Cruz-Chamorro I, Álvarez-Sánchez N, Santos-Sánchez G, Pedroche J, Fernández-Pachón M-S, Millán F, et al. Immunomodulatory and antioxidant properties of wheat gluten protein hydrolysates in human peripheral blood mononuclear cells. *Nutrients* (2020) 12:1673. doi: 10.3390/nu12061673

119. Xu Z, Mao T-M, Huang L, Yu Z-C, Yin B, Chen M-L, et al. Purification and identification immunomodulatory peptide from rice protein hydrolysates. *Food Agric Immunol* (2019) 30:150–62. doi: 10.1080/09540105.2018.1553938

120. Wen L, Huang L, Li Y, Feng Y, Zhang Z, Xu Z, et al. New peptides with immunomodulatory activity identified from rice proteins through peptidomic and in silico analysis. *Food Chem* (2021) 364:130357. doi: 10.1016/j.foodchem.2021.130357

121. Ali NM, Yeap SK, Yusof HM, Beh BK, Ho WY, Koh SP, et al. Comparison of free amino acids, antioxidants, soluble phenolic acids, cytotoxicity and immunomodulation of fermented mung bean and soybean. *J Sci Food Agric* (2016) 96:1648–58. doi: 10.1002/jsfa.7267

122. Paterson S, Fernández-Tomé S, Galvez A, Hernández-Ledesma B. Evaluation of the multifunctionality of soybean proteins and peptides in immune cell models. *Nutrients* (2023) 15:1220. doi: 10.3390/nu15051220

123. Egusa S, Otani H. Soybean protein fraction digested with neutral protease preparation,"Peptidase R", produced by Rhizopus oryzae, stimulates innate cellular immune system in mouse. *Int Immunopharmacol* (2009) 9:931–6. doi: 10.1016/j.intimp.2009.03.020

124. Yang Q, Cai X, Huang M, Wang S. A specific peptide with immunomodulatory activity from Pseudostellaria heterophylla and the action mechanism. *J Funct Foods* (2020) 68:103887. doi: 10.1016/j.jff.2020.103887

125. Morris HJ, Carrillo OV, Almarales Á, Bermúdez RC, Alonso ME, Borges L, et al. Protein hydrolysates from the alga Chlorella vulgaris 87/1 with potentialities in immunonutrition. *Biotecnología Aplicada* (2009) 26:162–5.

126. Chan-Zapata I, Arana-Argáez VE, Torres-Romero JC, Segura-Campos MR. Anti-inflammatory effects of the protein hydrolysate and peptide fractions isolated from Salvia hispanica L. seeds. *Food Agric Immunol* (2019) 30:786–803. doi: 10.1080/09540105.2019.1632804

127. Velliquette RA, Fast DJ, Maly ER, Alashi AM, Aluko RE. Enzymatically derived sunflower protein hydrolysate and peptides inhibit NFκB and promote monocyte differentiation to a dendritic cell phenotype. *Food Chem* (2020) 319:126563. doi: 10.1016/j.foodchem.2020.126563

128. Mantovani A, Allavena P, Marchesi F, Garlanda C. Macrophages as tools and targets in cancer therapy. *Nat Rev Drug Discovery* (2022) 21:799–820. doi: 10.1038/s41573-022-00520-5

129. Weng Z, Chen Y, Liang T, Lin Y, Cao H, Song H, et al. A review on processing methods and functions of wheat germ-derived bioactive peptides. *Crit Rev Food Sci Nutr* (2021) 63(22):5577-93. doi: 10.1080/10408398.2021.2021139

130. Wu S-Y, Fu T, Jiang Y-Z, Shao Z-M. Natural killer cells in cancer biology and therapy. *Mol Cancer* (2020) 19:1–26. doi: 10.1186/s12943-020-01238-x

131. Ross SH, Cantrell DA. Signaling and function of interleukin-2 in T lymphocytes. *Annu Rev Immunol* (2018) 36:411–33. doi: 10.1146/annurev-immunol-042617-053352

132. Barbana C, Boye JI. Angiotensin I-converting enzyme inhibitory activity of chickpea and pea protein hydrolysates. *Food Res Int* (2010) 43:1642–9. doi: 10.1016/j.foodres.2010.05.003

133. Kamran F, Reddy N. Bioactive peptides from legumes: Functional and nutraceutical potential. *Recent Adv Food Sci* (2018) 1:134–49.

134. Sitohy M, Osman A. Antimicrobial activity of native and esterified legume proteins against Gram-negative and Gram-positive bacteria. *Food Chem* (2010) 120:66–73. doi: 10.1016/j.foodchem.2009.09.071

135. Li Y, Jiang B, Zhang T, Mu W, Liu J. Antioxidant and free radical-scavenging activities of chickpea protein hydrolysate (CPH). *Food Chem* (2008) 106:444–50. doi: 10.1016/j.foodchem.2007.04.067

136. Tsuruki T, Kishi K, Takahashi M, Tanaka M, Matsukawa T, Yoshikawa M. Soymetide, an immunostimulating peptide derived from soybean β-conglycinin, is an fMLP agonist. *FEBS Lett* (2003) 540:206–10. doi: 10.1016/S0014-5793(03)00265-5

137. Jorgovanovic D, Song M, Wang L, Zhang Y. Roles of IFN-γ in tumor progression and regression: a review. *biomark Res* (2020) 8:1–16. doi: 10.1186/s40364-020-00228-x

138. Kong X, Guo M, Hua Y, Cao D, Zhang C. Enzymatic preparation of immunomodulating hydrolysates from soy proteins. *Bioresource Technol* (2008) 99:8873–9. doi: 10.1016/j.biortech.2008.04.056

139. Li L-L, Li B, Ji H-F, Ma Q, Wang L-Z. Immunomodulatory activity of small molecular (≤ 3 kDa) Coix glutelin enzymatic hydrolysate. *CyTA-Journal Food* (2017) 15:41–8. doi: 10.1080/19476337.2016.1201147

140. Yang R, Zhang Z, Pei X, Han X, Wang J, Wang L, et al. Immunomodulatory effects of marine oligopeptide preparation from Chum Salmon (Oncorhynchus keta) in mice. *Food Chem* (2009) 113:464–70. doi: 10.1016/j.foodchem.2008.07.086

141. Wang Y-K, He H-L, Wang G-F, Wu H, Zhou B-C, Chen X-L, et al. Oyster (Crassostrea gigas) hydrolysates produced on a plant scale have antitumor activity and immunostimulating effects in BALB/c mice. *Mar Drugs* (2010) 8:255–68. doi: 10.3390/md8020255

142. Ahn C-B, Cho Y-S, Je J-Y. Purification and anti-inflammatory action of tripeptide from salmon pectoral fin byproduct protein hydrolysate. *Food Chem* (2015) 168:151–6. doi: 10.1016/j.foodchem.2014.05.112

143. Chalamaiah M, Hemalatha R, Jyothirmayi T, Diwan PV, Kumar PU, Nimgulkar C, et al. Immunomodulatory effects of protein hydrolysates from rohu (Labeo rohita) egg (roe) in BALB/c mice. *Food Res Int* (2014) 62:1054–61. doi: 10.1016/j.foodres.2014.05.050

144. Rodríguez-Carrio J, Fernández A, Riera FA, Suárez A. Immunomodulatory activities of whey β-lactoglobulin tryptic-digested fractions. *Int Dairy J* (2014) 34:65–73. doi: 10.1016/j.idairyj.2013.07.004

145. Otani H, Nakano K, Kawahara T. Stimulatory effect of a dietary casein phosphopeptide preparation on the mucosal IgA response of mice to orally ingested lipopolysaccharide from Salmonella typhimurium. *Bioscience biotechnology Biochem* (2003) 67:729–35. doi: 10.1271/bbb.67.729

146. Adams C, Sawh F, Green-Johnson J, Taggart HJ, Strap J. Characterization of casein-derived peptide bioactivity: Differential effects on angiotensin-converting enzyme inhibition and cytokine and nitric oxide production. *J dairy Sci* (2020) 103:5805–15. doi: 10.3168/jds.2019-17976

147. Zong X, Cao X, Wang H, Zhao J, Lu Z, Wang F, et al. Porcine lactoferrin-derived peptide LFP-20 modulates immune homoeostasis to defend lipopolysaccharide-triggered intestinal inflammation in mice. *Br J Nutr* (2019) 121:1255–63. doi: 10.1017/S0007114519000485

148. Zhang F, Li J, Chang C, Gu L, Su Y, Yang Y. Immunomodulatory function of egg white peptides in RAW264. 7 macrophage cells and immunosuppressive mice induced by cyclophosphamide. *Int J Pept Res Ther* (2022) 29:9. doi: 10.1007/s10989-022-10481-3

149. Chen M, Zhang F, Su Y, Chang C, Li J, Gu L, et al. Identification and immunomodulatory effect on immunosuppressed mice of selenium-enriched peptides of egg white. *J Agric Food Chem* (2022) 70:12663–71. doi: 10.1021/acs.jafc.2c04659

150. Lozano-Ojalvo D, Molina E, López-Fandiño R. Hydrolysates of egg white proteins modulate T-and B-cell responses in mitogen-stimulated murine cells. *Food Funct* (2016) 7:1048–56. doi: 10.1039/C5FO00614G

151. Zhang Y, Kouguchi T, Shimizu K, Sato M, Takahata Y, Morimatsu F. Chicken collagen hydrolysate reduces proinflammatory cytokine production in C57BL/6. KOR-ApoEshl mice. *J Nutr Sci vitaminology* (2010) 56:208–10. doi: 10.3177/jnsv.56.208

152. Yang J, Sun-Waterhouse D, Xiao Y, He W, Zhao M, Su G. Osteoarthritis-alleviating effects in papain-induced model rats of chicken cartilage hydrolysate and its peptide fractions. *Int J Food Sci Technol* (2019) 54:2711–7. doi: 10.1111/ijfs.14182

153. Li Z, Zhao S, Xin X, Zhang B, Thomas A, Charles A, et al. Purification and characterization of a novel immunomodulatory hexapeptide from alcalase hydrolysate of ultramicro-pretreated silkworm (Bombyx mori) pupa protein. *J Asia-Pacific Entomology* (2019) 22:633–7. doi: 10.1016/j.aspen.2019.04.005

154. Munhoz J, Thomé R, Rostami A, Ishikawa LLW, Verinaud L, Rapôso C. The SNX-482 peptide from Hysterocrates gigas spider acts as an immunomodulatory molecule activating macrophages. *Peptides* (2021) 146:170648. doi: 10.1016/j.peptides.2021.170648

155. Cheung RCF, Ng TB, Wong JH. Marine peptides: Bioactivities and applications. *Mar Drugs* (2015) 13:4006–43. doi: 10.3390/md13074006

156. Minshawi F, Lanvermann S, McKenzie E, Jeffery R, Couper K, Papoutsopoulou S, et al. The generation of an engineered interleukin-10 protein with improved stability and biological function. *Front Immunol* (2020) 11:1794. doi: 10.3389/fimmu.2020.01794

157. Gauthier SF, Pouliot Y, Saint-Sauveur D. Immunomodulatory peptides obtained by the enzymatic hydrolysis of whey proteins. *Int dairy J* (2006) 16:1315–23. doi: 10.1016/j.idairyj.2006.06.014

158. Pihlanto-Leppälä A. Bioactive peptides. In: Roginski H, Fuquay JW, Fox PF, editors. *Encyclopedia of dairy sciences*. Elsevier: The University of Melbourne, Institute of Land and Food Resources. (2002).

159. Reyes-Díaz A, González-Córdova AF, Hernández-Mendoza A, Reyes-Díaz R, Vallejo-Cordoba B. Immunomodulation by hydrolysates and peptides derived from milk proteins. *Int J Dairy Technol* (2018) 71:1–9. doi: 10.1111/1471-0307.12421

160. Totsuka M, Kakehi M, Kohyama M, Hachimura S, Hisatsune T, Kaminogawa S. Enhancement of antigen-specific IFN-γ production from CD8+ T cells by a single amino acid-substituted peptide derived from bovine αs1-casein. *Clin Immunol immunopathology* (1998) 88:277–86. doi: 10.1006/clin.1998.4585

161. Zheng J, Bu T, Liu L, He G, Li S, Wu J. Naturally occurring low molecular peptides identified in egg white show antioxidant activity. *Food Res Int* (2020) 138:109766. doi: 10.1016/j.foodres.2020.109766

162. Chen Y, Zhang H, Liu R, Mats L, Zhu H, Pauls KP, et al. Antioxidant and anti-inflammatory polyphenols and peptides of common bean (Phaseolus vulga L.) milk and yogurt in Caco-2 and HT-29 cell models. *J Funct Foods* (2019) 53:125–35. doi: 10.1016/j.jff.2018.12.013

163. Zhou J, Han D. Safety evaluation of protein of silkworm (Antheraea pernyi) pupae. *Food Chem Toxicol* (2006) 44:1123–30. doi: 10.1016/j.fct.2006.01.009

164. Yang R, Zhao X, Kuang Z, Ye M, Luo G, Xiao G, et al. Optimization of antioxidant peptide production in the hydrolysis of silkworm (Bombyx mori L.) pupa protein using response surface methodology. *J Food Agric Environ* (2013) 11:952–6.

165. Hu D, Liu Q, Cui H, Wang H, Han D, Xu H. Effects of amino acids from selenium-rich silkworm pupas on human hepatoma cells. *Life Sci* (2005) 77:2098–110. doi: 10.1016/j.lfs.2005.02.017

166. O'Connor TM, O'Connell J, O'Brien DI, Goode T, Bredin CP, Shanahan F. The role of substance P in inflammatory disease. *J Cell Physiol* (2004) 201:167–80. doi: 10.1002/jcp.20061

167. Lefebvre T, Rybarczyk P, Bretaudeau C, Vanlaeys A, Cousin R, Brassart-Pasco S, et al. TRPM7/RPSA complex regulates pancreatic cancer cell migration. *Front Cell Dev Biol* (2020) 8:549. doi: 10.3389/fcell.2020.00549

168. Majc B, Novak M, Lah TT, Križaj I. Bioactive peptides from venoms against glioma progression. *Front Oncol* (2022) 12:965882. doi: 10.3389/fonc.2022.965882

169. Anastasi A, Erspamer V, Bucci M. Isolation and structure of bombesin and alytesin, two analogous active peptides from the skin of the European amphibians Bombina and Alytes. *Experientia* (1971) 27:166–7. doi: 10.1007/BF02145873

170. Saurin J-C, Fallavier M, Sordat B, Gevrey J-C, Chayvialle J-A, Abello J. Bombesin stimulates invasion and migration of Isreco1 colon carcinoma cells in a Rho-dependent manner. *Cancer Res* (2002) 62:4829–35.

171. Yule KA, White SR. Migration of 3T3 and lung fibroblasts in response to calcitonin gene-related peptide and bombesin. *Exp Lung Res* (1999) 25:261–73. doi: 10.1080/019021499270303

172. Wei LH, Dong Y, Sun YF, Mei XS, Ma XS, Shi J, et al. Anticancer property of Hemp Bioactive Peptides in Hep3B liver cancer cells through Akt/GSK3β/β-catenin signaling pathway. *Food Sci Nutr* (2021) 9:1833–41. doi: 10.1002/fsn3.1976

173. Henriques ST, Craik DJ. Importance of the cell membrane on the mechanism of action of cyclotides. *ACS Chem Biol* (2012) 7:626–36. doi: 10.1021/cb200395f

174. Troeira Henriques S, Huang YH, Chaousis S, Wang CK, Craik DJ. Anticancer and toxic properties of cyclotides are dependent on phosphatidylethanolamine phospholipid targeting. *ChemBioChem* (2014) 15:1956–65. doi: 10.1002/cbic.201402144

175. Abu N, Akhtar MN, Yeap SK, Lim KL, Ho WY, Zulfadli AJ, et al. Flavokawain A induces apoptosis in MCF-7 and MDA-MB231 and inhibits the metastatic process *in vitro*. *PloS One* (2014) 9:e105244. doi: 10.1371/journal.pone.0105244

176. Rajendran P, Alzahrani AM, Priya Veeraraghavan V, Ahmed EA. Anti-apoptotic effect of flavokawain A on ochratoxin-A-induced endothelial cell injury by attenuation of oxidative stress via PI3K/AKT-Mediated Nrf2 signaling cascade. *Toxins* (2021) 13:745. doi: 10.3390/toxins13110745

177. Kareva I, Waxman DJ, Klement GL. Metronomic chemotherapy: An attractive alternative to maximum tolerated dose therapy that can activate anti-tumor immunity and minimize therapeutic resistance. *Cancer Lett* (2015) 358:100–6. doi: 10.1016/j.canlet.2014.12.039

178. Koskela SA, Figueiredo CR. From antimicrobial to anticancer: The pioneering works of Prof. Luiz Rodolpho Travassos on bioactive peptides. *Braz J Microbiol* (2023) 54:2561–70. doi: 10.1007/s42770-023-01118-8

179. Polonelli L, Pontón J, Elguezabal N, Moragues MD, Casoli C, Pilotti E, et al. Antibody complementarity-determining regions (CDRs) can display differential antimicrobial, antiviral and antitumor activities. *PloS One* (2008) 3:e2371. doi: 10.1371/journal.pone.0002371

180. Moragues MD, Omaetxebarria MJ, Elguezabal N, Sevilla MJ, Conti S, Polonelli L, et al. A monoclonal antibody directed against a Candida albicans cell wall mannoprotein exerts three anti-C. albicans activities. *Infection Immun* (2003) 71:5273–9. doi: 10.1128/IAI.71.9.5273-5279.2003

181. de Santana CJC, Pires Júnior OR, Fontes W, Palma MS, Castro MS. Mastoparans: A group of multifunctional α-helical peptides with promising therapeutic properties. *Front Mol Biosci* (2022) 9:824989. doi: 10.3389/fmolb.2022.824989

182. Cenci E, Bistoni F, Mencacci A, Perito S, Magliani W, Conti S, et al. A synthetic peptide as a novel anticryptococcal agent. *Cell Microbiol* (2004) 6:953–61. doi: 10.1111/j.1462-5822.2004.00413.x

183. Travassos LR, Silva LS, Rodrigues EG, Conti S, Salati A, Magliani W, et al. Therapeutic activity of a killer peptide against experimental paracoccidioidomycosis. *J Antimicrobial Chemotherapy* (2004) 54:956–8. doi: 10.1093/jac/dkh430

184. Savoia D, Scutera S, Raimondo S, Conti S, Magliani W, Polonelli L. Activity of an engineered synthetic killer peptide on Leishmania major and Leishmania infantum promastigotes. *Exp Parasitol* (2006) 113:186–92. doi: 10.1016/j.exppara.2006.01.002

185. Casoli C, Pilotti E, Perno CF, Balestra E, Polverini E, Cassone A, et al. A killer mimotope with therapeutic activity against AIDS-related opportunistic micro-organisms inhibits *ex-vivo* HIV-1 replication. *Aids* (2006) 20:975–80. doi: 10.1097/01.aids.0000222068.14878.0d

186. Polonelli L, Ciociola T, Magliani W, Zanello PP, D'Adda T, Galati S, et al. Peptides of the constant region of antibodies display fungicidal activity. *PloS One* (2012) 7:e34105. doi: 10.1371/journal.pone.0034105

187. Dobroff A, Rodrigues E, Moraes J, Travassos L. Protective, anti-tumor monoclonal antibody recognizes a conformational epitope similar to melibiose at the surface of invasive murine melanoma cells. *Hybridoma hybridomics* (2002) 21:321–31. doi: 10.1089/153685902761022661

188. Dobroff AS, Rodrigues EG, Juliano MA, Friaça DM, Nakayasu ES, Almeida IC, et al. Differential antitumor effects of IgG and IgM monoclonal antibodies and their synthetic complementarity-determining regions directed to new targets of B16F10-Nex2 melanoma cells. *Trans Oncol* (2010) 3:204–17. doi: 10.1593/tlo.09316

189. Arruda DC, Santos LC, Melo FM, Pereira FV, Figueiredo CR, Matsuo AL, et al. β-Actin-binding complementarity-determining region 2 of variable heavy chain from monoclonal antibody C7 induces apoptosis in several human tumor cells and is protective against metastatic melanoma. *J Biol Chem* (2012) 287:14912–22. doi: 10.1074/jbc.M111.322362

190. Figueiredo CR, Matsuo AL, Massaoka MH, Polonelli L, Travassos LR. Anti-tumor activities of peptides corresponding to conserved complementary determining regions from different immunoglobulins. *Peptides* (2014) 59:14–9. doi: 10.1016/j.peptides.2014.06.007

191. Figueiredo CR, Matsuo AL, Azevedo RA, Massaoka MH, Girola N, Polonelli L, et al. A novel microtubule de-stabilizing complementarity-determining region C36L1 peptide displays antitumor activity against melanoma *in vitro* and *in vivo*. *Sci Rep* (2015) 5:14310. doi: 10.1038/srep14310

192. Figueiredo CR, Azevedo RA, Mousdell S, Resende-Lara PT, Ireland L, Santos A, et al. Blockade of MIF–CD74 signalling on macrophages and dendritic cells restores the antitumour immune response against metastatic melanoma. *Front Immunol* (2018) 9:1132. doi: 10.3389/fimmu.2018.01132

193. de Azevedo RA, Shoshan E, Whang S, Markel G, Jaiswal AR, Liu A, et al. MIF inhibition as a strategy for overcoming resistance to immune checkpoint blockade therapy in melanoma. *Oncoimmunology* (2020) 9:1846915. doi: 10.1080/2162402X.2020.1846915

frontiers | Frontiers in Oncology

TYPE Original Research
PUBLISHED 15 February 2024
DOI 10.3389/fonc.2024.1357801

OPEN ACCESS

EDITED BY
Mazdak Ganjalikhani Hakemi,
Isfahan University of Medical Sciences, Iran

REVIEWED BY
Vitaly Pozdeev,
University of Luxembourg, Luxembourg
Dmitry Aleksandrovich Zinovkin,
Gomel State Medical University, Belarus

*CORRESPONDENCE
Jamshid Hadjati
hajatij@tums.ac.ir
Hamid Reza Mirzaei
h-mirzaei@tums.ac.ir

RECEIVED 18 December 2023
ACCEPTED 30 January 2024
PUBLISHED 15 February 2024

CITATION
Panahi Meymandi AR, Akbari B, Soltantoyeh T, Shahosseini Z, Hosseini M, Hadjati J and Mirzaei HR (2024) PX-478, an HIF-1α inhibitor, impairs mesoCAR T cell antitumor function in cervical cancer.
Front. Oncol. 14:1357801.
doi: 10.3389/fonc.2024.1357801

PX-478, an HIF-1α inhibitor, impairs mesoCAR T cell antitumor function in cervical cancer

Ahmad Reza Panahi Meymandi[1], Behnia Akbari[1], Tahereh Soltantoyeh[1], Zahra Shahosseini[2,3], Mina Hosseini[4], Jamshid Hadjati[1*] and Hamid Reza Mirzaei[1*]

[1]Department of Medical Immunology, School of Medicine, Tehran University of Medical Sciences, Tehran, Iran, [2]Department of Medical Biotechnology, School of Allied Medical Sciences, Iran University of Medical Sciences, Tehran, Iran, [3]Virology Department, Pasteur Institute of Iran, Tehran, Iran, [4]Department of Pharmaceutical Biotechnology, School of Pharmacy, Tehran University of Medical Sciences, Tehran, Iran

Introduction: Chimeric Antigen Receptor (CAR) T cell therapy has demonstrated remarkable success in treating hematological malignancies. However, its efficacy against solid tumors, including cervical cancer, remains a challenge. Hypoxia, a common feature of the tumor microenvironment, profoundly impacts CAR T cell function, emphasizing the need to explore strategies targeting hypoxia-inducible factor-1α (HIF-1α).

Methods: In this study, we evaluated the effects of the HIF-1α inhibitor PX-478 on mesoCAR T cell function through in-silico and *in vitro* experiments. We conducted comprehensive analyses of HIF-1α expression in cervical cancer patients and examined the impact of PX-478 on T cell proliferation, cytokine production, cytotoxicity, and exhaustion markers.

Results: Our in-silico analyses revealed high expression of HIF-1α in cervical cancer patients, correlating with poor prognosis. PX-478 effectively reduced HIF-1α levels in T and HeLa cells. While PX-478 exhibited dose-dependent inhibition of antigen-nonspecific T and mesoCAR T cell proliferation, it had minimal impact on antigen-specific mesoCAR T cell proliferation. Notably, PX-478 significantly impaired the cytotoxic function of mesoCAR T cells and induced terminally exhausted T cells.

Discussion: Our results underscore the significant potential and physiological relevance of the HIF-1α pathway in determining the fate and function of both T and CAR T cells. However, we recognize the imperative for further molecular investigations aimed at unraveling the intricate downstream targets associated with HIF-1α and its influence on antitumor immunity, particularly within the context of hypoxic tumors. These insights serve as a foundation for the careful

development of combination therapies tailored to counter immunosuppressive pathways within hypoxic environments and fine-tune CAR T cell performance in the intricate tumor microenvironment.

KEYWORDS

CAR T cell therapy, pharmacological targeting, HIF-1α, PX-478, cervical cancer, T cell exhaustion

1 Introduction

Cervical cancer (CC) ranks as the fourth most prevalent cancer among women (1). Despite the existence of various preventive and treatment modalities for CC, such as HPV screening, prophylactic vaccines, surgical interventions, radiotherapy, and chemotherapy, the global burden of the disease remains substantial (2). Therefore, there is an urgent need for new treatment strategies to improve the prognosis of patients with CC.

In recent years, the development of chimeric antigen receptor (CAR) T cell therapies for treating solid tumors has garnered significant interest (3). Currently, numerous clinical trials are underway to assess the effectiveness of CAR-T cell therapy in cervical cancer patients (NCT01583686) (NCT04556669) (NCT03356795). Mesothelin (MSLN) stands out as a crucial target antigen in the pursuit of novel immunotherapies for solid tumors (4). Clinical trials involving anti-MSLN CAR T cells have demonstrated commendable safety profiles but limited efficacy (5). The tumor microenvironment (TME) is widely recognized as a major obstacle, as it impedes T cell survival, proliferation, and cytotoxicity, thereby limiting the application of CAR T cell therapies in the clinical management of solid tumors (6). A common feature of the TME is hypoxia, characterized by inadequate oxygen supply (less than 2% O2) due to heightened metabolic demands and inefficient vasculature, in stark contrast to healthy tissues with oxygen levels of 5%–10% (7). Hypoxia is clinically associated with a poor prognosis and resistance to chemotherapy and radiotherapy (8–10) and it significantly compromises the fitness and efficacy of CAR T cells (11).

At the heart of the cellular response to hypoxia is hypoxia-inducible factor-1 (HIF-1), a master transcription factor that orchestrates the regulation of numerous downstream targets (12). HIF-1 exists as a heterodimeric transcription factor composed of the oxygen-sensitive HIF-1α subunit and the constitutively expressed HIF-1β (ARNT) subunit (13). Under normal oxygen conditions (normoxia), HIF-1α is rapidly degraded through ubiquitin-mediated pathways, primarily governed by proline hydroxylation (14). However, during hypoxia, the inhibition of HIF-1α hydroxylases interferes with VHL-HIF binding, leading to the stabilization of HIF-1α protein and enabling HIF-1 dimerization, which, in turn, activates its transcriptional function (14).

Numerous studies have unveiled the connection between HIF-1α overexpression and poorer prognosis in cervical cancer patients (15–18). Currently, several HIF-1α inhibitors are in development for various cancer types, exhibiting promising antitumor efficacy and manageable toxicity profiles (19–21). Nonetheless, it remains uncertain whether agents that inhibit HIF-1α can enhance the response to CAR-T cell therapy. To elucidate these questions, we explore the impact of the selective HIF-1α inhibitor PX-478 on the antitumoral function of second-generation mesoCAR T cells.

2 Material and methods

2.1 Bioinformatics analysis

Gene expression analysis was conducted using the GEPIA2 database (http://gepia2.cancer-pku.cn), which utilizes data from the TCGA and GTEx databases (22). To compare HIF-1α gene expression levels between squamous cell carcinoma of the cervix (SESC) and corresponding normal tissues, the "box plot" function for expression analysis was employed. The following statistical parameters were utilized: a Log2FC (Logarithm to the base 2-fold change) cutoff value of 1, and a p-value cutoff value of 0.01. Additionally, GEPIA2 was employed to assess the overall survival of SESC patients using the "Survival Analysis" module, with the Group Cutoff set to the Quartile. Hazard ratios (HRs) with 95% confidence intervals (CIs) and log-rank P-values were computed to ascertain survival outcomes. The representative immunohistochemistry image of HIF-1α expression was obtained from the Human Protein Atlas (HPA) database (23).

2.2 Cell lines

HEK293T, Jurkat, Hela, and PANC-1 cell lines were acquired from the Iranian Biological Resource Center (IBRC). HEK293T, Hela, and PANC-1 cells were maintained in D10 media, comprising DMEM (Gibco, Life Technologies), 10% fetal bovine serum (FBS), and 1% penicillin/streptomycin (Gibco, Life Technologies). Jurkat cells were cultured in R10 media, containing RPMI-1640 (Gibco,

Abbreviations: CAR T cells, Chimeric antigen receptors; HIF-1α, Hypoxia-inducible factor-1α; IFN-γ, Interferon-gamma; IL-2, Interleukin 2; mesoCAR T, Fully human anti-mesothelin CAR T cells; TME, Tumor microenvironment; CC, Cervical cancer.

Life Technologies) supplemented with 10% FBS, 25 mM HEPES (Sigma Aldrich), 2 mM glutamine (Gibco), and 1% penicillin/streptomycin. Flow cytometry was used to validate mesothelin expression in the relevant cell lines prior to experiments. Regular mycoplasma contamination checks were conducted on all cell lines.

2.3 Primary human cells

Peripheral blood mononuclear cells (PBMCs) were isolated from fresh blood using standard methods with Histopaque®-1077 (Sigma Aldrich). Primary human T cells were negatively selected with immunomagnetic beads (Pan T Cell Isolation Kit, Miltenyi Biotec) and stored at -80°C. T cells were cultured in TM10 media, composed of TexMACS™ Medium (Miltenyi Biotec), supplemented with 10% human serum and 100 IU/mL premium-grade rhIL-2 (Miltenyi Biotec). Blood samples were obtained from healthy volunteers under approval from the Research Ethics Committees of the School of Medicine, Tehran University of Medical Sciences [IR.TUMS.BLC.1402.015].

2.4 Lentiviral vector production

Lentiviral vectors were produced following previously established protocols (24). HEK293T cells were transfected with lentiviral CAR and packaging plasmids using the calcium phosphate method. Lentiviral supernatants were collected at 48- and 72-hour time points post-transfection and then concentrated through high-speed centrifugation. The concentrated lentivirus batches were resuspended in cold RPMI-1640 media and stored at -80°C. Titration of lentiviral vectors was performed using Jurkat cells.

2.5 Lentiviral transduction

mesoCAR T cells were generated as per previous descriptions (25). Briefly, 1×10^6 T cells were seeded in each well of 12-well tissue culture plates and activated using Dynabeads™ Human T-Expander CD3/CD28 (Gibco, Life Technologies, 11161D) at a 1:1 ratio in TM10 media. Activated T cells were infected with lentiviral vectors supplemented with 8 mg/mL Polybrene (Santacruz) 24 hours after activation. Centrifugation at 850g for 1 hour at 32°C was employed to enhance transduction efficiency. Two hours later, 2 mL/well of TM10 media was added to the transduced T cells. At day 4 post-transduction, Dynabeads™ were removed from transduced T cells using a DynaMag™ magnet, and GFP expression, indicative of mesoCAR expression, was assessed via flow cytometry.

2.6 PX-478 dose-response

PX-478 (MedChemExpress, USA) was dissolved in Dimethyl sulfoxide (DMSO). To assess the impact of PX-478 on T cell proliferation, 2×10^5 CFSE-labeled T cells were seeded in 96-well tissue culture plates and exposed to varying concentrations of PX-478. Human T Cell-Expander Dynabeads™ CD3/CD28 (Gibco, Life Technologies, 11161D) were used at a 1:1 ratio in TM10 medium to activate T cells. After three days, T cells were harvested, and their proliferation was evaluated via flow cytometry.

2.7 Protein extraction and western blotting

Adherent cells were washed twice with PBS, scraped, and transferred to 1.5 ml tubes. T cells were also harvested and washed twice with PBS. After centrifugation, cells were lysed using RIPA buffer containing 1mM PMSF at a ratio of 60 µl per 10^6 cells. Proteins were separated by 10% SDS-PAGE under reducing conditions and subsequently transferred to PVDF membrane. The membrane was then blocked for 1 hour using a 5% BSA blocking reagent in Tris-Buffered Saline (pH=7.5) containing 0.05% Tween-20 (v/v) (TBST) and incubated with Rabbit anti-HIF-1α antibody diluted at 1:2,000 (Novus Biologicals NB100-449, Centennial, Colorado, USA) or Rabbit anti-β-actin antibody (Sigma-Aldrich) diluted at 1:2,000, overnight at 4°C. The blots were further incubated with anti-Rabbit horseradish peroxidase-conjugated antibodies for 1 hour. Protein bands were detected using ECL method and X-ray film was used for visualization. Quantification was conducted using image J (imagej.org).

2.8 Hypoxia assay

Culture plates were incubated either under normoxic conditions (37°C in humidified air, 5% CO2) or under hypoxic conditions (1% O2, 5% CO2, 94% N2). Hypoxia was induced using a hypoxia incubator chamber (StemCell Technologies, Inc.) purged at 25L/min for 4 minutes with a gas mixture containing 1% O2, 5% CO2, and 94% nitrogen as a balance before sealing the chamber.

2.9 *In vitro* cytotoxicity assay

For *in vitro* cytotoxicity assays, $1x10^4$ target cells were seeded in 96-well U-bottomed tissue culture plates and pretreated with 25µM PX-478 for 24 hours under both hypoxic and normoxic conditions. Transduced or non-transduced T cells were then added to the wells at effector-to-target ratios of 1:1, 10:1, and 20:1 for 4 hours in TM10 media, with a final volume of 200 ml/well. To distinguish between effector and target cells, effector cells were stained with CFSE. Prior to flow cytometry analysis, 7-AAD (Miltenyi Biotec) was added to stain dead cells. Flow cytometry analysis utilized CFSE and 7-AAD staining to differentiate T cells from dead tumor cells. The frequency of lysed target cells (CFSE-/7-AAD+ cells) was calculated by subtracting the percentage of spontaneous lysis of target cells from the percentage of lysis of target cells in coculture with mesoCAR T cells. Normalized lysis of target cells (Specific lysis) was reported based on mesothelin expression on target cells.

2.10 *In vitro* proliferation and cytokine production assays

Target cells were treated with 50 mg/ml of mitomycin C (Sigma Aldrich) for 30 minutes at 37°C and subsequently washed. $2x10^5$ target cells were seeded in 48-well tissue culture plates and pretreated with 25μM PX-478 for 24 hours under both hypoxic and normoxic conditions before removal of the media. For cell proliferation analysis, mesoCAR T cells and untransduced T cells were stained with 5 mM CFSE at room temperature for 8 minutes. An equal amount of FBS was added to halt the reaction. After washing three times with complete RPMI 1640 medium, CFSE-labeled cells (0.2×10^6/well) were cocultured with either target cells or media, in the absence of exogenous IL-2, in 48-well plates, with a final volume of 800 μl/well. After 24 hours, 200 μl of the supernatants were harvested and stored at −80°C. The subsequent cytokine analysis was carried out by enzyme-linked immunosorbent assay (ELISA) to quantify IFN-γ and IL-2. After 72 hours, cells were stained with PerCP-conjugated anti-human CD3 antibody (Clone: HIT3a, BioLegend), and CFSE dilution of CD3+ cells was determined by flow cytometry, as an indicator of proliferation.

2.11 Flow cytometric analysis

The purity of isolated T cells was confirmed using APC-conjugated anti-human CD3 (Clone: UCHT1, BioLegend). PE-conjugated anti-human mesothelin (Clone: #420411, R&D Systems) was used to detect mesothelin expression. FITC-conjugated anti-human CD3 (Clone: HIT3a, BioLegend), PE-conjugated anti-human CD279 (PD-1) (Clone: EH12.2H7, BioLegend), and APC-conjugated anti-human CD366 (Tim-3) (Clone: F38-2E2, BioLegend) antibodies were used to measure the expression of exhaustion markers. For proliferation assays, cells were loaded with CellTrace™ CFSE (Life Technologies, #C34554) according to manufacturer's instructions, and T cells were detected using PerCP-conjugated anti-human CD3 antibody (Clone: HIT3a, BioLegend). Data were collected using a BD FACSCalibur (BD Biosciences) and analyzed with FlowJo software (v10.6). All assays were performed in duplicate and repeated two to three times.

2.12 Statistical analysis

Normality tests and one-way/two-way analysis of variance (ANOVA) were performed using GraphPad Prism software (v9) to identify differences among various treatment groups. p-values below 0.05 were considered statistically significant.

3 Results

3.1 Association of HIF-1α overexpression with adverse prognosis in cervical cancer patients

To assess the significance of HIF-1α expression in cervical cancer, we utilized the GEPIA2 database to visualize the mRNA expression levels of HIF-1α in cervical cancer. The analysis involved 13 normal tissue samples and 306 samples from cervical cancer

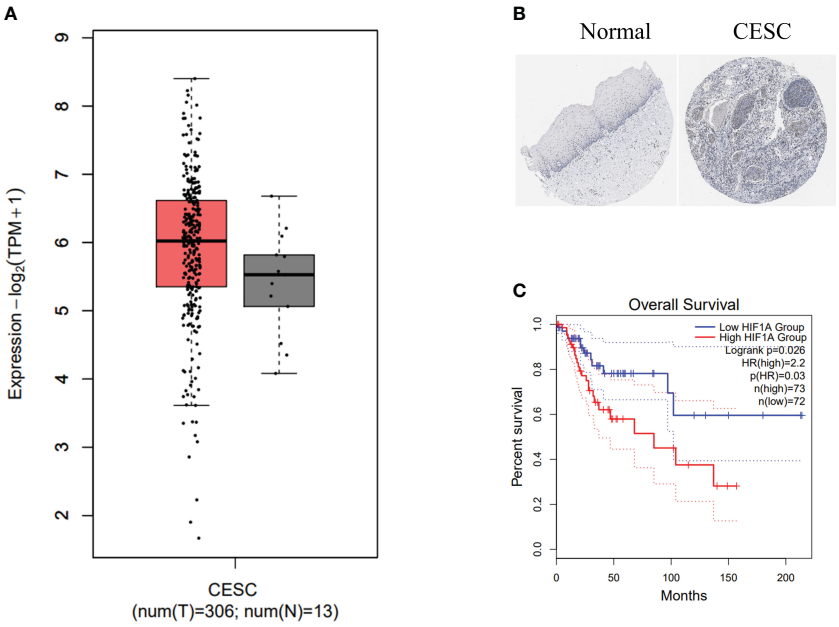

FIGURE 1
HIF-1α overexpression is associated with poor prognosis in cervical cancer patients. **(A)** HIF1A expression levels in biopsies from cervical cancer (CC) patients (highlighted in red) and corresponding normal tissue samples (depicted in grey) were analyzed using data from the TCGA dataset. The data was log2 transformed (TPM+1). **(B)** Representative images from the Human Protein Atlas database illustrate HIF-1α expression in normal (left) and CC (right) tissue samples. **(C)** Kaplan-Meier survival curves present the overall survival time of CC patients categorized into high and low HIF-1α expression groups. Dotted lines indicate a 95% confidence interval.

patients. Our data unequivocally demonstrate an upregulation of HIF-1α in cervical cancer patients (Figure 1A). Complementing this, the immunohistochemistry image of HIF-1α protein levels in tissue samples from the Human Protein Atlas (HPA) dataset confirmed similar findings (Figure 1B).

We further conducted a Kaplan-Meier survival analysis using GEPIA2 to investigate the prognostic value of HIF-1α. Our results reveal a statistically significant association between high expression of the *HIF1A* gene and shorter overall survival in cervical cancer patients (Figure 1C).

3.2 PX-478 reduces HIF-1α protein levels under hypoxic conditions

PX-478, previously identified as a compound that decreases cellular HIF-1α levels, was evaluated in our study. To validate the increase of HIF-1α under hypoxic conditions and assess the inhibitory effect of PX-478, HeLa and T cells were cultured under normoxic and hypoxic (1% O2) conditions while exposed to varying doses of PX-478 for 24 hours. Western blot analysis confirmed the efficient stabilization of HIF1α in hypoxic conditions and demonstrated that PX-478 inhibits the hypoxia-induced increase in HIF-1α protein levels in a dose-dependent manner (Figures 2A-D).

3.3 Effective antitumor activity of mesoCAR T cells against cervical cancer cells

We generated and characterized second-generation mesoCAR T cells, as described previously (25). Briefly, human CD3+ T cells were efficiently infected with lentiviral particles encoding the second-generation mesoCAR transgene (Figure 3A). We subsequently assessed the *in vitro* antitumor capacity of these cells. We used PANC-1 and HeLa cells, which represent mesothelin-negative and positive tumor cells respectively (Figures 3B, C). T cells expressing the mesoCAR transgene exhibited specific cytotoxicity against mesothelin-positive HeLa cells, while no cytotoxicity was observed against mesothelin-negative PANC-1 cells (Figure 3D). To test the effectiveness of mesoCAR T cells against HeLa cells, we investigated their proliferation and their capacity to produce IL-2 and IFN-γ cytokines *in vitro*. mesoCAR T cells demonstrated a high mesothelin-specific proliferation rate comparable to untransduced T cells after being stimulated with Hela and PANC-1 cells (Figure 3E). After CAR T cell stimulation with HeLa, mesoCAR T cells showed high mesothelin-specific proliferation rates and produced large amounts of IFN-γ and IL-2, comparable to untransduced T cells (Figures 3E-G). No IL-2 and IFN-γ secretion was detected in cultures of T cells alone, tumor cells alone, or when irrelevant target cells like PANC-1 were involved (Figures 3F, G).

3.4 Impact of PX-478 on mesoCAR T cell proliferation

The efficacy of CAR T cell immunotherapies against solid tumors hinges on T cell proliferation, persistence, and accumulation (26). To investigate the influence of PX-478 on mesoCAR T cell proliferation, we performed a series of experiments. Initially, T cells activated with anti-CD3/CD28-coated beads were exposed to varying concentrations of orally available PX-478, revealing that PX-478 can dose-dependently reduce antigen-nonspecific T cell proliferation (Figure 4A), while concurrently maintaining T cell viability unchanged (Figure 4B).

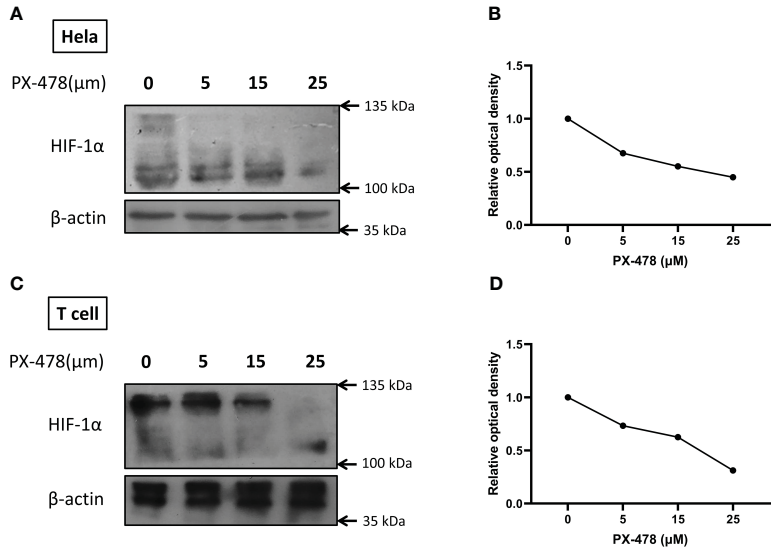

FIGURE 2
PX-478 decreases HIF-1α protein levels in a dose-dependent manner. **(A, C)** Hela and T cells were exposed to varying concentrations of PX-478 for 24 hours under hypoxic conditions, and the levels of HIF-1α protein were assessed through Western blot analysis. **(B, D)** PX-478 demonstrates a dose-dependent inhibition of HIF-1α protein expression. Densitometric quantification of the blots was performed relative to β-actin as a reference protein. Each experiment was repeated two to three times.

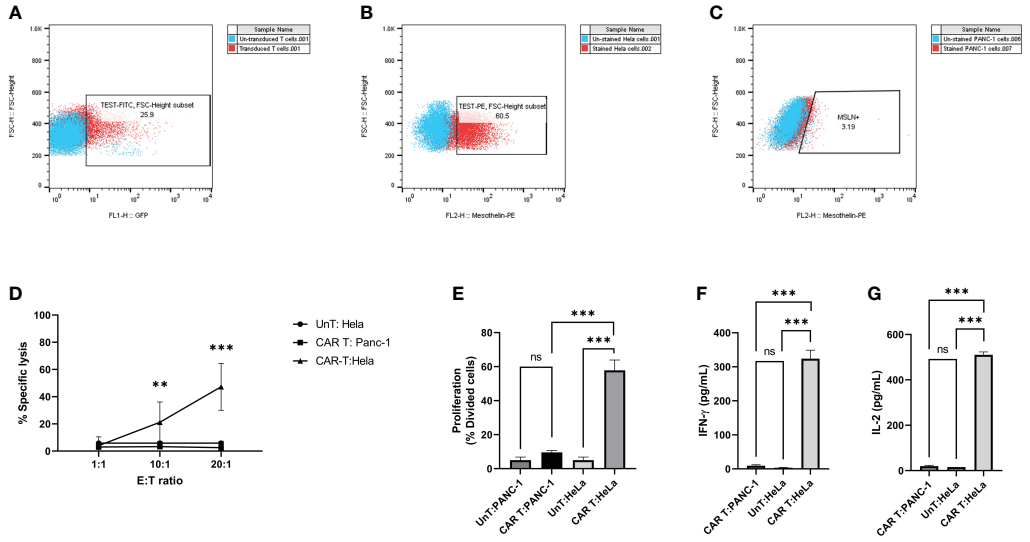

FIGURE 3
Antigen specificity of mesoCAR T cells against HeLa cells. **(A)** Assessment of chimeric antigen receptor (CAR) expression on mesoCAR T cells. **(B, C)** Representative dot plots illustrating mesothelin expression on HeLa and PANC-1 cells, respectively. **(D)** MesoCAR T cells demonstrate specific cytotoxicity against target cells at varying effector-to-target ratios. **(E)** Proliferation of mesoCAR T cells in response to target cells. **(F, G)** Production of IFN-γ and IL-2 by mesoCAR T cells in coculture with target cells. Statistical analysis was conducted using ordinary one-way ANOVA **(E–G)** and two-way ANOVA **(D)**, followed by Tukey's multiple comparison test. Significance denoted by ***($P < 0.001$). Data are presented as mean ± SD. ns, non significant

Consistent with the data obtained from T cells, we observed that the antigen-nonspecific proliferation of mesoCAR T cells in an IL-2-containing medium was also impeded by PX-478 (Figure 4C). Given the observed direct inhibitory effect of PX-478 on T and mesoCAR T cell proliferation, we conducted experiments in which tumor target cells were pretreated with PX-478 for 24 hours under both hypoxia and normoxia conditions. After supernatant removal, mesoCAR T cells were introduced. Interestingly, pretreatment of tumor cells with PX-478 did not significantly impact mesoCAR cell proliferation (Figure 4D). This result was supported by the analysis

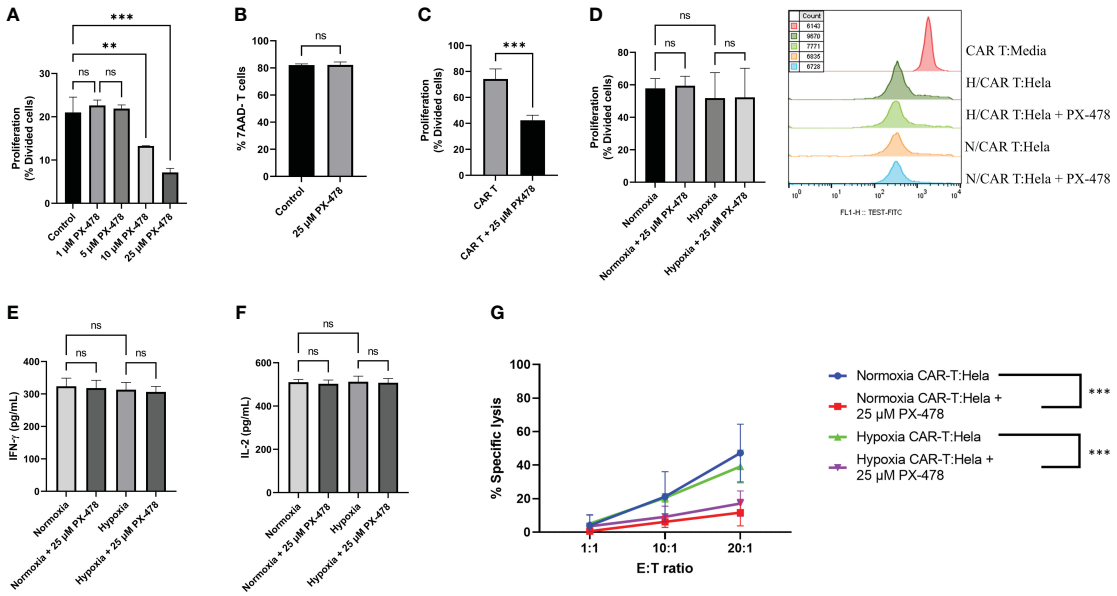

FIGURE 4
The effects of HIF-1α inhibitor PX-478 on the antitumor function of mesoCAR T cells. **(A)** PX-478 significantly inhibits antigen-nonspecific proliferation of T cells. **(B)** Viability of T cells remained unchanged in response to PX-478. **(C)** PX-478 significantly inhibits the IL-2-induced antigen-nonspecific proliferation of mesoCAR T cells. **(D)** Antigen-specific proliferative capacity and representative cell count of mesoCAR T cells over a three-day coculture with pre-treated Hela cells. **(E, F)** Production of IFN-γ and IL-2 by mesoCAR T cells in coculture with pre-treated Hela cells. **(G)** Overlaid plot demonstrating mesoCAR T cell cytotoxicity against Hela cells in the presence of PX-478. Statistical analysis was performed using ordinary one-way ANOVA **(A, C-F)**, Student's t-test **(B)**, two-way ANOVA **(G)**, and Tukey multiple comparison test. **$P < 0.01$; ***$P < 0.001$. Data are presented as mean ± SD. ns, non significant

of cytokine production, where no significant changes in the levels of IL-2 and IFN-γ were observed (Figures 4E, F). Collectively, our findings indicate that PX-478 directly inhibits antigen-nonspecific T and mesoCAR T cell proliferation, while pretreatment of tumor cells with PX-478 has no influence on mesoCAR T cell proliferation and cytokine production.

3.5 PX-478 impairs mesoCAR T cell cytotoxic function

Having established the effect of PX-478 on mesoCAR T cell proliferation, we sought to examine its impact on the cytotoxicity of these cells against tumor target cells. HeLa cervical cancer cells were cultured, pre-exposed to 25μM PX-478 for 24 hours, and then co-incubated with mesoCAR T cells under normoxic and hypoxic (1% O2) conditions. mesoCAR T cells demonstrated effective killing of HeLa cells under both hypoxic and normoxic conditions (Figure 4G). However, PX-478 significantly reduced the cytotoxicity of mesoCAR T cells under both hypoxic and normoxic conditions (Figure 4G).

In an effort to understand the underlying reason for the impairment of mesoCAR T cell cytotoxic function, we considered the possibility that these cells become exhausted in the presence of PX-478. Exhausted T cells can be categorized into progenitor-exhausted T cells (T_{pex}) and terminally exhausted T cells (T_{tex}) based on their function and phenotype (24, 27, 28). T_{pex} cells express PD-1 but not TIM3, retain stem-like characteristics, and remain polyfunctional. In contrast, T_{tex} cells express both PD-1 and TIM3 at high levels, have a limited lifespan, and cannot effectively suppress tumor growth (29). Immune checkpoint blockade can rejuvenate T_{pex} but not T_{tex} cells (30). To explore this, cells from our cocultures were analyzed via flow cytometry for the expression of PD-1 and TIM3. Our results revealed that pretreatment of tumor cells with PX-478 did not significantly alter the expression of PD-1 but led to an increased expression of TIM3 (Supplementary Figure S1A, B). Furthermore, the abundance of T_{tex} cells (PD-1+TIM3+) increased, while the abundance of T_{pex} cells (PD-1+TIM3-) decreased under both normoxic and hypoxic conditions (Supplementary Figure S1C).

4 Discussion

In this study, we delved into the impact of the HIF-1α inhibitor PX-478 on the antitumoral function of mesoCAR T cells. Our in-silico analysis compellingly indicated that the overexpression of HIF-1α in CC patients is strongly associated with an unfavorable prognosis. It is well-established that HIF-1α becomes stabilized within the hypoxic core of rapidly growing, poorly vascularized solid tumors (31). This stabilization of HIFs plays a pivotal role in promoting tumor survival and metastasis by orchestrating changes in glycolysis, nutrient uptake, waste disposal, angiogenesis, apoptosis, and cell migration (32–35).

To target HIF-1α, we employed PX-478, an orally available small molecule known to interfere with HIF-1α transcription and translation, thus leading to reduced deubiquitination of HIF-1α (36). Our Western blot analyses provided clear evidence that PX-478 effectively inhibited HIF-1α in a dose-dependent manner in both T and HeLa cells. Our investigation into the effects of PX-478 on T cell proliferation revealed a dose-dependent suppression. Notably, previous studies have shown that T cell receptor activation stabilizes HIF-1α in T lymphocytes (37), thereby facilitating a metabolic shift towards glycolysis to support T cell proliferation and effector functions (38, 39). Furthermore, PI3K/mTOR activity downstream of TCR and CD28 signaling induces HIF-1α expression by promoting transcription of two HIF-1α mRNA splice isoforms and driving increased protein translation in human and mouse T cells (37, 40). Additionally, PX-478 can prevent the G2/M transition by affecting proteins related to the G2 phase of the cell cycle, such as cyclin B1, thereby inhibiting cell proliferation (41).

Considering the inhibitory effects of PX-478 on T cell proliferation, we explored the potential of pre-treatment with PX-478 prior to CAR-T cell therapy. We pre-treated tumor cells with PX-478 and meticulously evaluated its influence on the proliferation and cytokine production of mesoCAR T cells. Proliferation analyses provided no significant differences in mesoCAR T cell proliferation between hypoxic and normoxic conditions, as well as PX-478-treated and untreated groups. Likewise, our analysis of IFN-γ and IL-2 cytokine production showed no significant differences, thereby confirming the results on proliferation. We further assessed how PX-478 affected the cytotoxicity of mesoCAR T cells. Consistent with previous research, no significant difference was observed in the cytotoxicity of mesoCAR T cells under hypoxic and normoxic conditions (11, 42). However, PX-478 significantly impeded the cytotoxic function of mesoCAR T cells. Earlier studies have indicated that HIF-1α is vital for the cytotoxic function of CAR T cells. For instance, Palazon et al. demonstrated that the deletion of HIF-1α resulted in reduced expression of several proteins critical for tumor rejection by cytotoxic T lymphocytes (43). The genetic ablation of HIF-1α led to decreased production of effector cytokines such as IFN-γ and TNF-α, along with cytolytic molecules like granzyme B (43). HIF-1α hydroxylation at proline residues in normoxia leads to VHL-mediated proteasomal degradation (44). It has been demonstrated that VHL-deficient TILs accumulate and survive in tumors in an HIF-dependent manner, retaining polyfunctionality and cytolytic capacity (45), highlighting the essential role of HIF-1α in T cells' antitumor function.

HIFs have also been found to play a pivotal role in regulating T cell exhaustion in the context of infections and malignancies (43, 45–47). Consequently, we investigated the impact of PX-478 pre-treatment of tumor cells on the expression pattern of exhaustion markers on mesoCAR T cells. Our findings indicated an increase in the percentage of TIM3+ T cells and T_{tex} cells under hypoxia conditions and in PX-478 treated groups. This aligns with previous studies that have shown that the expression of TIM-3, a marker of terminally exhausted T cells, is substantially up-regulated under hypoxic conditions (43, 48, 49). The decrease in cytotoxicity of mesoCAR T cells in the presence of PX-478 may be explained by the increase in T_{tex} cells, which have limited antitumor activity.

Nevertheless, it is essential to acknowledge the limitations of our study. PX-478 may not be entirely specific for reducing HIF-1α

levels; prior research suggests that it may affect other intracellular factors as well (50). In order to exclude off-target effects of PX-478, more specific approaches targeting HIF-1α, such as genetic knockdown or using alternative pharmacological inhibitors, would provide clearer evidence for the role of HIF-1α signaling in regulating antitumor function of mesoCAR T cells. Additionally, selectively rescuing HIF-1α protein levels in the presence of PX-478 using stabilizing agents that do not broadly impact other cell mediators would further elucidate the specific contribution of HIF-1α to the observed phenotypes. Additionally, HIF-1α is physiologically activated by hypoxia and plays a critical role in regulating the expression of several genes, including GLUT1, LDHA, and VEGF (12). Consequently, some downstream genes may exert either a positive or negative influence on the antitumoral function of CAR T cells. Further investigations may uncover specific downstream targets of HIF-1α that modulate the antitumor function of CAR T cells in the tumor microenvironment. Considering previous studies demonstrating HIF-1α can directly regulate expression of T cell activation-related genes such as CD69 in tumor-infiltrating lymphocytes (51), it would be informative to examine how PX-478 impacts levels of canonical activation markers on mesoCAR T cells.

PX-478 has previously demonstrated antitumor efficacy across several human tumor models (41, 52). However, our present investigation exclusively focuses on the *in vitro* evaluation of the potential combination therapy involving PX-478 and mesoCAR T cells. Our data demonstrate PX-478 partially impairs mesoCAR T cell function, but do not reflect the compound's direct effects on cervical tumor cells or overall therapeutic potential *in vivo*. As we only assessed a subset of responses using an isolated cell system, our results should not be interpreted as evidence for negative impacts of HIF-1α inhibitors in cervical cancer more broadly. It is worth noting that our study was limited to *in vitro* assessments using cell lines and CAR T cell cocultures, while prior research has suggested that PX-478 may inhibit tumor angiogenesis, resulting in antitumor effects *in vivo*. Therefore, future *in vivo* studies are essential to provide a more comprehensive understanding of the function of PX-478 in a natural tumor microenvironment.

5 Conclusions

In summary, our study demonstrates the significant impact of HIF-1α inhibition using the PX-478 inhibitor on mesoCAR T cell function within the cervical cancer microenvironment. The inhibition of HIF-1α markedly impairs the cytotoxicity of mesoCAR T cells while minimally affecting their proliferation and cytokine production. Our findings underscore the clinical relevance of HIF-1α overexpression in cervical cancer patients and highlight the potential challenges in targeting HIF-1α for enhancing CAR T cell therapy efficacy. Despite limitations in specificity and the need for further *in vivo* validation, our study provides crucial insights into the interplay between HIF-1α signaling and CAR T cell function, serving as a foundational framework for the development of combination therapies aimed at optimizing CAR T cell performance in solid tumors like cervical cancer.

Data availability statement

The original contributions presented in the study are included in the article/Supplementary Material. Further inquiries can be directed to the corresponding authors.

Ethics statement

This study involves human cell lines and was approved by Research Ethics Committees of Biosafety & Laboratory, Tehran University of Medical Sciences [IR.TUMS.BLC.1402.015]. Informed consent was obtained from all individual participants included in the study.

Author contributions

AP: Conceptualization, Data curation, Formal Analysis, Investigation, Visualization, Writing – original draft. BA: Conceptualization, Methodology, Project administration, Writing – original draft, Writing – review & editing. TS: Methodology, Writing – original draft. ZS: Investigation, Writing – original draft. MH: Investigation, Writing – original draft. JH: Supervision, Writing – review & editing. HM: Conceptualization, Funding acquisition, Supervision, Writing – review & editing.

Funding

The author(s) declare financial support was received for the research, authorship, and/or publication of this article. Research reported in this publication was supported by grants from Tehran University of Medical Sciences (grants nos. 50756 and 50760, awarded to HM), and the National Institute for Medical Research Development (NIMAD) of Iran (grant no. 942554, awarded to JH).

Conflict of interest

The authors declare that the research was conducted in the absence of any commercial or financial relationships that could be construed as a potential conflict of interest.

The author(s) declared that they were an editorial board member of Frontiers, at the time of submission. This had no impact on the peer review process and the final decision.

Publisher's note

Supplementary material

The Supplementary Material for this article can be found online at: https://www.frontiersin.org/articles/10.3389/fonc.2024.1357801/full#supplementary-material

SUPPLEMENTARY FIGURE 1
The effects of HIF-1α inhibitor PX-478 on the expression pattern of exhaustion markers. **(A)** The percentage of PD1+ T cells. **(B)** The frequency of T_{pex} and T_{tex} cells. **(C)** The percentage of TIM3+ T cells. Statistical analysis was performed using ordinary one-way ANOVA **(A-C)**, and Tukey multiple comparison test. *P < 0.05; **P < 0.01; ***P < 0.001. Data are presented as mean ± SD.

References

1. Sung H, Ferlay J, Siegel RL, Laversanne M, Soerjomataram I, Jemal A, et al. Global cancer statistics 2020: globocan estimates of incidence and mortality worldwide for 36 cancers in 185 countries. *CA Cancer J Clin*. (2021) 71:209–49. doi: 10.3322/caac.21660

2. Tang Y, Zhang AX, Chen G, Wu Y, Gu W. Prognostic and therapeutic tils of cervical cancer—Current advances and future perspectives. *Mol Therapy-Oncolytics*. (2021) 22:410–30. doi: 10.1016/j.omto.2021.07.006

3. Johnson LA, June CH. Driving gene-engineered T cell immunotherapy of cancer. *Cell Res*. (2017) 27:38–58. doi: 10.1038/cr.2016.154

4. Lamberts LE, de Groot DJ, Bense RD, de Vries EG, Fehrmann RS. Functional genomic mrna profiling of a large cancer data base demonstrates mesothelin overexpression in a broad range of tumor types. *Oncotarget*. (2015) 6:28164–72. doi: 10.18632/oncotarget.4461

5. Zhai X, Mao L, Wu M, Liu J, Yu S. Challenges of anti-mesothelin car-T-cell therapy. *Cancers (Basel)*. (2023) 15. doi: 10.3390/cancers15051357

6. Martinez M, Moon EK. Car T cells for solid tumors: new strategies for finding, infiltrating, and surviving in the tumor microenvironment. *Front Immunol*. (2019) 10:128. doi: 10.3389/fimmu.2019.00128

7. Muz B, de la Puente P, Azab F, Azab AK. The role of hypoxia in cancer progression, angiogenesis, metastasis, and resistance to therapy. *Hypoxia (Auckl)*. (2015) 3:83–92. doi: 10.2147/hp.S93413

8. Nordsmark M, Bentzen SM, Rudat V, Brizel D, Lartigau E, Stadler P, et al. Prognostic value of tumor oxygenation in 397 head and neck tumors after primary radiation therapy. An international multi-center study. *Radiother Oncol*. (2005) 77:18–24. doi: 10.1016/j.radonc.2005.06.038

9. Guo Q, Lu L, Liao Y, Wang X, Zhang Y, Liu Y, et al. Influence of C-src on hypoxic resistance to paclitaxel in human ovarian cancer cells and reversal of fv-429. *Cell Death Dis*. (2018) 8:e3178. doi: 10.1038/cddis.2017.367

10. Overgaard J. Hypoxic modification of radiotherapy in squamous cell carcinoma of the head and neck–a systematic review and meta-analysis. *Radiother Oncol*. (2011) 100:22–32. doi: 10.1016/j.radonc.2011.03.004

11. Berahovich R, Liu X, Zhou H, Tsadik E, Xu S, Golubovskaya V, et al. Hypoxia selectively impairs car-T cells in vitro. *Cancers (Basel)*. (2019) 11(5). doi: 10.3390/cancers11050602

12. Semenza GL. Targeting hif-1 for cancer therapy. *Nat Rev Cancer*. (2003) 3:721–32. doi: 10.1038/nrc1187

13. Lee JW, Bae SH, Jeong JW, Kim SH, Kim KW. Hypoxia-inducible factor (Hif-1) Alpha: its protein stability and biological functions. *Exp Mol Med*. (2004) 36:1–12. doi: 10.1038/emm.2004.1

14. Masoud GN, Li W. Hif-1α Pathway: role, regulation and intervention for cancer therapy. *Acta Pharm Sin B*. (2015) 5:378–89. doi: 10.1016/j.apsb.2015.05.007

15. Lu ZH, Wright JD, Belt B, Cardiff RD, Arbeit JM. Hypoxia-inducible factor-1 facilitates cervical cancer progression in human papillomavirus type 16 transgenic mice. *Am J Pathol*. (2007) 171:667–81. doi: 10.2353/ajpath.2007.061138

16. Abudoukerimu A, Hasimu A, Abudoukerimu A, Tuerxuntuoheti G, Huang Y, Wei J, et al. Hif-1α Regulates the progression of cervical cancer by targeting Yap/Taz. *J Oncol*. (2022) 2022:3814809. doi: 10.1155/2022/3814809

17. Yan B, Ma QF, Tan WF, Cai HN, Li YL, Zhou ZG, et al. Expression of Hif-1α Is a predictive marker of the efficacy of neoadjuvant chemotherapy for locally advanced cervical cancer. *Oncol Lett*. (2020) 20:841–9. doi: 10.3892/ol.2020.11596

18. Bachtiary B, Schindl M, Pötter R, Dreier B, Knocke TH, Hainfellner JA, et al. Overexpression of hypoxia-inducible factor 1alpha indicates diminished response to radiotherapy and unfavorable prognosis in patients receiving radical radiotherapy for cervical cancer. *Clin Cancer Res*. (2003) 9:2234–40.

19. Koh MY, Spivak-Kroizman T, Venturini S, Welsh S, Williams RR, Kirkpatrick DL, et al. Molecular mechanisms for the activity of Px-478, an antitumor inhibitor of the hypoxia-inducible factor-1α. *Mol Cancer Ther*. (2008) 7:90–100. doi: 10.1158/1535-7163.MCT-07-0463

20. Fallah J, Rini BI. Hif inhibitors: status of current clinical development. *Curr Oncol Rep*. (2019) 21:1–10. doi: 10.1007/s11912-019-0752-z

21. Jordan BF, Runquist M, Raghunand N, Baker A, Williams R, Kirkpatrick L, et al. Dynamic contrast-enhanced and diffusion Mri show rapid and dramatic changes in tumor microenvironment in response to inhibition of Hif-1α Using Px-478. *Neoplasia*. (2005) 7:475–85. doi: 10.1593/neo.04628

22. Tang Z, Kang B, Li C, Chen T, Zhang Z. Gepia2: an enhanced web server for large-scale expression profiling and interactive analysis. *Nucleic Acids Res*. (2019) 47:W556–w60. doi: 10.1093/nar/gkz430

23. Thul PJ, Åkesson L, Wiking M, Mahdessian D, Geladaki A, Ait Blal H, et al. A subcellular map of the human proteome. *Science*. (2017) 356:eaal3321. doi: 10.1126/science.aal3321

24. Akbari B, Soltantoyeh T, Shahosseini Z, Yarandi F, Hadjati J, Mirzaei HR. The inhibitory receptors pd1, tim3, and A2ar are highly expressed during mesocar T cell manufacturing in advanced human epithelial ovarian cancer. *Cancer Cell Int*. (2023) 23:104. doi: 10.1186/s12935-023-02948-0

25. Akbari B, Soltantoyeh T, Shahosseini Z, Jadidi-Niaragh F, Hadjati J, Brown CE, et al. Pge2-ep2/ep4 signaling elicits mesocar T cell immunosuppression in pancreatic cancer. *Front Immunol*. (2023) 14:1209572. doi: 10.3389/fimmu.2023.1209572

26. Ueda T, Shiina S, Iriguchi S, Terakura S, Kawai Y, Kabai R, et al. Optimization of the proliferation and persistency of car T cells derived from human induced pluripotent stem cells. *Nat Biomed Eng*. (2023) 7:24–37. doi: 10.1038/s41551-022-00969-0

27. Miller BC, Sen DR, Al Abosy R, Bi K, Virkud YV, LaFleur MW, et al. Subsets of exhausted cd8(+) T cells differentially mediate tumor control and respond to checkpoint blockade. *Nat Immunol*. (2019) 20:326–36. doi: 10.1038/s41590-019-0312-6

28. Beltra JC, Manne S, Abdel-Hakeem MS, Kurachi M, Giles JR, Chen Z, et al. Developmental relationships of four exhausted cd8(+) T cell subsets reveals underlying transcriptional and epigenetic landscape control mechanisms. *Immunity*. (2020) 52:825–41.e8. doi: 10.1016/j.immuni.2020.04.014

29. Chakravarti M, Dhar S, Bera S, Sinha A, Roy K, Sarkar A, et al. Terminally exhausted Cd8+ T cells resistant to pd-1 blockade promote generation and maintenance of aggressive cancer stem cells. *Cancer Res*. (2023) 83:1815–33. doi: 10.1158/0008-5472.Can-22-3864

30. Kallies A, Zehn D, Utzschneider DT. Precursor exhausted T cells: key to successful immunotherapy? *Nat Rev Immunol*. (2020) 20:128–36. doi: 10.1038/s41577-019-0223-7

31. Jun JC, Rathore A, Younas H, Gilkes D, Polotsky VY. Hypoxia-inducible factors and cancer. *Curr Sleep Med Rep*. (2017) 3:1–10. doi: 10.1007/s40675-017-0062-7

32. Luo D, Wang Z, Wu J, Jiang C, Wu J. The role of hypoxia inducible factor-1 in hepatocellular carcinoma. *BioMed Res Int*. (2014) 2014:409272. doi: 10.1155/2014/409272

33. Xie J, Xiao Y, Zhu XY, Ning ZY, Xu HF, Wu HM. Hypoxia regulates stemness of breast cancer Mda-Mb-231 cells. *Med Oncol*. (2016) 33:42. doi: 10.1007/s12032-016-0755-7

34. Nagaraju GP, Bramhachari PV, Raghu G, El-Rayes BF. Hypoxia inducible factor-1α: its role in colorectal carcinogenesis and metastasis. *Cancer Lett*. (2015) 366:11–8. doi: 10.1016/j.canlet.2015.06.005

35. Parks SK, Cormerais Y, Marchiq I, Pouyssegur J. Hypoxia optimises tumour growth by controlling nutrient import and acidic metabolite export. *Mol Aspects Med*. (2016) 47-48:3–14. doi: 10.1016/j.mam.2015.12.001

36. Palayoor ST, Mitchell JB, Cerna D, Degraff W, John-Aryankalayil M, Coleman CN. Px-478, an inhibitor of hypoxia-inducible factor-1alpha, enhances radiosensitivity of prostate carcinoma cells. *Int J Cancer*. (2008) 123:2430–7. doi: 10.1002/ijc.23807

37. Nakamura H, Makino Y, Okamoto K, Poellinger L, Ohnuma K, Morimoto C, et al. Tcr engagement increases hypoxia-inducible factor-1 alpha protein synthesis via rapamycin-sensitive pathway under hypoxic conditions in human peripheral T cells. *J Immunol*. (2005) 174:7592–9. doi: 10.4049/jimmunol.174.12.7592

38. Buck MD, O'Sullivan D, Pearce EL. T cell metabolism drives immunity. *J Exp Med*. (2015) 212:1345–60. doi: 10.1084/jem.20151159

39. Pearce EL, Poffenberger MC, Chang CH, Jones RG. Fueling immunity: insights into metabolism and lymphocyte function. *Science*. (2013) 342:1242454. doi: 10.1126/science.1242454

40. Lukashev D, Caldwell C, Ohta A, Chen P, Sitkovsky M. Differential regulation of two alternatively spliced isoforms of hypoxia-inducible factor-1 alpha in activated T lymphocytes. *J Biol Chem*. (2001) 276:48754–63. doi: 10.1074/jbc.M104782200

41. Zhu Y, Zang Y, Zhao F, Li Z, Zhang J, Fang L, et al. Inhibition of hif-1α by px-478 suppresses tumor growth of esophageal squamous cell cancer in vitro and in vivo. *Am J Cancer Res*. (2017) 7:1198–212.

42. Kosti P, Opzoomer JW, Larios-Martinez KI, Henley-Smith R, Scudamore CL, Okesola M, et al. Hypoxia-sensing car T cells provide safety and efficacy in treating solid tumors. *Cell Rep Med*. (2021) 2:100227. doi: 10.1016/j.xcrm.2021.100227

43. Palazon A, Tyrakis PA, Macias D, Veliça P, Rundqvist H, Fitzpatrick S, et al. An hif-1α/vegf-a axis in cytotoxic T cells regulates tumor progression. *Cancer Cell*. (2017) 32:669–83.e5. doi: 10.1016/j.ccell.2017.10.003

44. Palazon A, Goldrath AW, Nizet V, Johnson RS. Hif transcription factors, inflammation, and immunity. *Immunity*. (2014) 41:518–28. doi: 10.1016/j.immuni.2014.09.008

45. Liikanen I, Lauhan C, Quon S, Omilusik K, Phan AT, Bartrolí LB, et al. Hypoxia-inducible factor activity promotes antitumor effector function and tissue residency by Cd8+ T cells. *J Clin Invest*. (2021) 131. doi: 10.1172/jci143729

46. Doedens AL, Phan AT, Stradner MH, Fujimoto JK, Nguyen JV, Yang E, et al. Hypoxia-inducible factors enhance the effector responses of Cd8(+) T cells to persistent antigen. *Nat Immunol*. (2013) 14:1173–82. doi: 10.1038/ni.2714

47. Phan AT, Doedens AL, Palazon A, Tyrakis PA, Cheung KP, Johnson RS, et al. Constitutive glycolytic metabolism supports cd8(+) T cell effector memory differentiation during viral infection. *Immunity*. (2016) 45:1024–37. doi: 10.1016/j.immuni.2016.10.017

48. Voron T, Colussi O, Marcheteau E, Pernot S, Nizard M, Pointet AL, et al. Vegf-a modulates expression of inhibitory checkpoints on cd8+ T cells in tumors. *J Exp Med*. (2015) 212:139–48. doi: 10.1084/jem.20140559

49. Bannoud N, Dalotto-Moreno T, Kindgard L, García PA, Blidner AG, Mariño KV, et al. Hypoxia supports differentiation of terminally exhausted cd8 T cells. *Front Immunol*. (2021) 12:660944. doi: 10.3389/fimmu.2021.660944

50. Koh MY, Spivak-Kroizman T, Venturini S, Welsh S, Williams RR, Kirkpatrick DL, et al. Molecular mechanisms for the activity of px-478, an antitumor inhibitor of the hypoxia-inducible factor-1alpha. *Mol Cancer Ther*. (2008) 7:90–100. doi: 10.1158/1535-7163.Mct-07-0463

51. Labiano S, Meléndez-Rodríguez F, Palazón A, Teijeira Á, Garasa S, Etxeberria I, et al. Cd69 is a direct hif-1α Target gene in hypoxia as a mechanism enhancing expression on tumor-infiltrating T lymphocytes. *Oncoimmunology*. (2017) 6:e1283468. doi: 10.1080/2162402x.2017.1283468

52. Welsh S, Williams R, Kirkpatrick L, Paine-Murrieta G, Powis G. Antitumor activity and pharmacodynamic properties of px-478, an inhibitor of hypoxia-inducible factor-1alpha. *Mol Cancer Ther*. (2004) 3:233–44.

frontiers | Frontiers in Immunology

TYPE Clinical Trial
PUBLISHED 29 February 2024
DOI 10.3389/fimmu.2024.1362775

OPEN ACCESS

EDITED BY
Gulderen Yanikkaya Demirel,
Yeditepe University, Türkiye

REVIEWED BY
Qichun Cai,
Clifford Hospital, China
Maryam Sadri,
Iran University of Medical Sciences, Iran

*CORRESPONDENCE
Richard T. Kenney
rkenney@sonnetbio.com

RECEIVED 29 December 2023
ACCEPTED 09 February 2024
PUBLISHED 29 February 2024

CITATION
Kenney RT, Cini JK, Dexter S, DaFonseca M, Bingham J, Kuan I, Chawla SP, Polasek TM, Lickliter J and Ryan PJ (2024) A phase I trial of SON-1010, a tumor-targeted, interleukin-12-linked, albumin-binding cytokine, shows favorable pharmacokinetics, pharmacodynamics, and safety in healthy volunteers.
Front. Immunol. 15:1362775.
doi: 10.3389/fimmu.2024.1362775

A phase I trial of SON-1010, a tumor-targeted, interleukin-12-linked, albumin-binding cytokine, shows favorable pharmacokinetics, pharmacodynamics, and safety in healthy volunteers

Richard T. Kenney[1]*, John K. Cini[1], Susan Dexter[1], Manuel DaFonseca[1], Justus Bingham[2], Isabelle Kuan[2], Sant P. Chawla[3], Thomas M. Polasek[4,5], Jason Lickliter[6] and Philip J. Ryan[6]

[1]Sonnet BioTherapeutics, Inc, Princeton, NJ, United States, [2]Momentum Metrix, LLC, Dublin, CA, United States, [3]Sarcoma Oncology Center, Santa Monica, CA, United States, [4]Centre for Medicine Use and Safety, Monash University, Melbourne, VIC, Australia, [5]InClin, Inc, San Mateo, CA, United States, [6]Nucleus Network Pty Ltd, Melbourne, VIC, Australia

Background: The benefits of recombinant interleukin-12 (rIL-12) as a multifunctional cytokine and potential immunotherapy for cancer have been sought for decades based on its efficacy in multiple mouse models. Unexpected toxicity in the first phase 2 study required careful attention to revised dosing strategies. Despite some signs of efficacy since then, most rIL-12 clinical trials have encountered hurdles such as short terminal elimination half-life ($T_{½}$), limited tumor microenvironment targeting, and substantial systemic toxicity. We developed a strategy to extend the rIL-12 $T_{½}$ that depends on binding albumin *in vivo* to target tumor tissue, using single-chain rIL-12 linked to a fully human albumin binding ($F_{H}AB$) domain (SON-1010). After initiating a dose-escalation trial in patients with cancer (SB101), a randomized, double-blind, placebo-controlled, single-ascending dose (SAD) phase 1 trial in healthy volunteers (SB102) was conducted.

Methods: SB102 (NCT05408572) focused on safety, tolerability, pharmacokinetic (PK), and pharmacodynamic (PD) endpoints. SON-1010 at 50-300 ng/kg or placebo administered subcutaneously on day 1 was studied at a ratio of 6:2, starting with two sentinels; participants were followed through day 29. Safety was reviewed after day 22, before enrolling the next cohort. A non-compartmental analysis of PK was performed and correlations with the PD results were explored, along with a comparison of the SON-1010 PK profile in SB101.

Results: Participants receiving SON-1010 at 100 ng/kg or higher tolerated the injection but generally experienced more treatment-emergent adverse effects (TEAEs) than those receiving the lowest dose. All TEAEs were transient and no other dose relationship was noted. As expected with rIL-12, initial decreases in

neutrophils and lymphocytes returned to baseline by days 9-11. PK analysis showed two-compartment elimination in SB102 with mean $T_{½}$ of 104 h, compared with one-compartment elimination in SB101, which correlated with prolonged but controlled and dose-related increases in interferon-gamma (IFNγ). There was no evidence of cytokine release syndrome based on minimal participant symptoms and responses observed with other cytokines.

Conclusion: SON-1010, a novel presentation for rIL-12, was safe and well-tolerated in healthy volunteers up to 300 ng/kg. Its extended half-life leads to a prolonged but controlled IFNγ response, which may be important for tumor control in patients.

Clinical trial registration: https://clinicaltrials.gov/study/NCT05408572, identifier NCT05408572.

KEYWORDS

SON-1010, recombinant IL-12, albumin, fully human albumin binding (FHAB) domain, healthy volunteers, immunotherapy, advanced solid tumors, ovarian cancer

1 Introduction: Interleukin-12 and SON-1010

First discovered in the late 1980s, Natural Killer Cell Stimulatory Factor, eventually renamed interleukin-12 (IL-12), is a proinflammatory cytokine produced by activated phagocytes and dendritic cells and is a key regulator of cell-mediated immunity (1). Despite the early safety challenges in Phase 2 (2), the clinical development of recombinant human (r)IL-12 and related compounds has been extensive in cancer and immunotherapy indications over the past two decades (3, 4).

As a cytokine, IL-12 has multiple effector functions that bridge the innate and adaptive immune responses in cancer (5) to promote the activation of NK and NKT cells and to polarize $CD4^+$ and $CD8^+$ T cells. IL-12 has been shown to: a) induce the differentiation of naïve T cells into Th1 cells (6), b) increase the activation and cytotoxic capacities of T and NK cells, c) inhibit the differentiation of Treg cells, and d) inhibit or reprogram immunosuppressive cells such as tumor-associated macrophages (TAMs) and myeloid-derived suppressor cells (MDSCs) (7). IL-12 primarily induces the production of large amounts of interferon gamma (IFNγ), which itself is cytostatic/cytotoxic. Tumor necrosis factor-alpha (TNFα) is also produced by T and NK cells, which reduces the IL-4-mediated suppression of IFNγ (8) and upregulates MHC I and II expression in tumor cells for enhanced recognition and lysis (9, 10). There also appears to be a link between IL-2 and the signal transduction of IL-12 in NK cells. IL-12 stimulates the expression of two IL-12 receptors, IL-12Rβ1 and IL-12Rβ2, maintaining the expression of STAT4, a critical protein involved in IL-12 signaling in NK cells. The enhanced functional response is usually demonstrated by IFNγ production and killing of target cells (11).

IL-12 also exhibits anti-angiogenic activity with increased IFNγ production (12–14), which in turn increases the production of a chemokine called inducible protein-10 (IP-10 or CXCL10) (15). IP-10 then mediates this anti-angiogenic effect. Because of its ability to induce immune responses and anti-angiogenic activity, there has been interest in testing rIL-12 as a possible anti-cancer drug, given its effectiveness in murine tumor models. However, it has not been shown to have substantial activity in many human cancer studies, perhaps due to its toxicity and the short half-life of rIL-12 *in vivo* (16). The potential use of rIL-12 in the treatment of psoriasis and inflammatory bowel disease has also been reported (17).

The antitumor and antimetastatic activities of IL-12 have been extensively demonstrated in murine models, including melanomas, mammary carcinomas, colon carcinoma, renal carcinoma, and sarcomas (18). Studies have addressed the issue of local rIL-12 production versus systemic delivery (i.e., intraperitoneal). Production of rIL-12 at the tumor site (by neoplastic cells engineered to release rIL-12 using appropriate expression vectors) induces rejection of neoplastic cells by $CD8^+$ T cells associated with macrophage infiltration, vessel damage, and necrosis (19). Interestingly, the cure rates of mice bearing established tumors were higher after intraperitoneal administration of rIL-12 than after vaccination with tumors releasing rIL-12. Studies using various animal models have expanded our understanding of their potential toxic effects (20). Improved antitumor effects have been observed when rIL-12 is administered along with other cytokines (21) or neoplastic cells expressing costimulatory molecules (22). Analysis of the immune mechanisms activated by IL-12 in these non-clinical models suggested the role of several subsets, including NK cells, $CD4^+$ and $CD8^+$ T cells, and $CD3^+$ $CD56^+$ NKT cells expressing the Va14 invariant T-cell receptor (23, 24).

10.3389/fimmu.2024.1362775

We designed a proprietary fully human albumin binding ($F_HAB^®$) platform technology (Figure 1) that enables the development of innovative targeted biological drugs with enhanced mono- or bi-functional mechanisms (25). SON-1010, the lead drug candidate, is a recombinant, single-chain, unmodified human rIL-12 joined by a flexible ($[Gly_4Ser]_5$) linker to the F_HAB domain. The platform utilizes a single-chain antibody fragment (scFv) that binds to and "hitch-hikes" on mouse, monkey, or human serum albumin (HSA) for transport to target tissues (26). The initial focus is on immunotherapy of solid tumors; however, the technology is suited for drug development across the spectrum of human diseases, as a number of different domain payloads can be linked to the scFv.

The main limiting factor for the clinical application of rIL-12 monotherapy in solid tumors has been its toxicity and the low level of rIL-12 infiltration and retention in the tumor microenvironment (TME). SON-1010 is being developed as an extended pharmacokinetic (PK) and pharmacodynamic (PD) rIL-12 molecule for the treatment of cancer. The F_HAB component was designed to enhance the PK of the payload(s) linked to it, which increases the exposure of the side chains to the TME and lymphatic tissue. SON-1010 is carried into the TME because the F_HAB construct binds to albumin, which then binds to the neonatal fragment crystallizable (Fc) receptor (FcRn) on the surface of endothelial cells, resulting in an increased half-life via cellular recycling of albumin and the F_HAB that is bound to it (27). FcRn and glycoprotein 60 (GP60) are overexpressed in tumor vessels, promoting the delivery of albumin and its bound IL12-F_HAB to that space. SON-1010 retention in the acidic TME is facilitated by the albumin complex binding to the "secreted protein acidic and rich in cysteine" (SPARC) protein, which is often expressed in the TME of solid tumors, providing an improved PK profile overall and a dose-sparing effect that decreases toxicity risk, resulting in a broader therapeutic index in mouse models.

Currently, the first-in-human study of SON-1010 (SB101) is being conducted in patients with advanced solid tumors using a multiple ascending dosing (MAD) design (NCT05352750) (28). A second cancer study (SB221) focuses on patients with platinum-resistant ovarian cancer (PROC), in which dose-escalation of SON-1010 is being studied in combination with the anti-PD-L1 immune checkpoint inhibitor atezolizumab in part 1, which will be compared with the standard-of-care in its second part (NCT05756907). In this paper we present the results of SB102, the complementary phase 1 study in healthy volunteers (29), which used a single-ascending dose (SAD) design (NCT05408572), along with preliminary PK/PD results from SB101 for comparison.

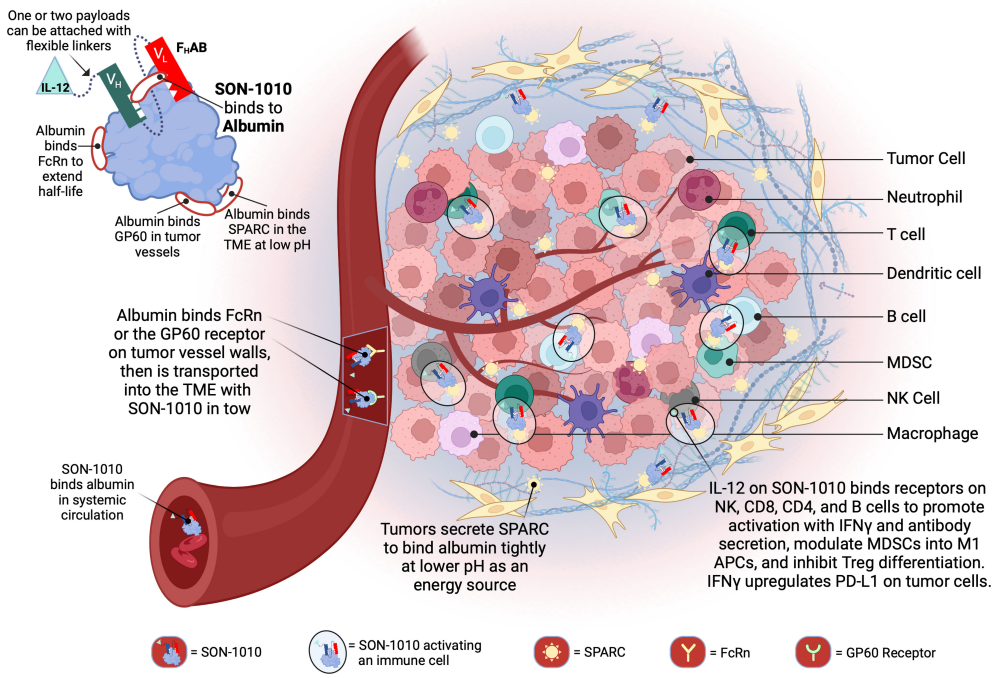

FIGURE 1
Schematic representation of SON-1010 and its mechanism of action. The F_HAB portion on the top left consists of a scFv heavy chain (V_H in green) linked ($[GGGGS]_3$) to a light chain (V_L in red) that comprises an albumin-binding domain. Therapeutic payloads can be fused to each side of the central construct using flexible linkers ($[GGGGS]_5$). SON-1010 includes single-chain human rIL-12 genetically linked to the F_HAB V_H domain, with no payload or linker added to the V_L domain. The scFv binds to a section of albumin at both physiological and acidic pH, without interfering with its binding to FcRn, GP60, or SPARC. Albumin binds systemically to FcRn and SON-1010 can share albumin's extended PK. The entire complex can be carried into the tumor tissue through the bloodstream, where FcRn and GP60 receptors are upregulated, to be transported across the endothelium into the acidic TME. Once there, albumin binds tightly in dynamic equilibrium via its interaction with SPARC, which is overexpressed in the TME. The rIL-12 cytokine domain can activate resident immune cells and recruit more cells, upregulating the expression of IFNγ from NK, $CD4^+$, and $CD8^+$ T cells, which then upregulates PD-L1 expression on tumor cells and antibody production from B cells. Created with BioRender.com. FcRn, neonatal Fc receptor; GP60, albondin/glycoprotein 60; PK, pharmacokinetics; SPARC, secreted protein acidic and rich in cysteine; TME, tumor microenvironment.

2 Materials and Methods

2.1 Study design

The SB102 study was a phase 1, randomized, double-blind, placebo-controlled, dose-escalation study designed to assess the safety, tolerability, PK, and PD of SON-1010 administered as a single subcutaneous (SC) injection in healthy volunteers (Figure 2). A flow diagram for sentinel participants and the rest of each cohort is shown in Supplementary Figure S1. Participants had to be 18-54 years old and healthy based on their medical history, physical examination, and clinical laboratory testing (see the full list of Inclusion/Exclusion Criteria in the Supplementary Material). SB102 was conducted at a single site in Melbourne, Victoria, Australia; blinding included the participants, site staff, clinical research organization (CRO), sponsor, and medical monitors, as well as the Safety Review Committee (SRC). An exploratory objective was to evaluate the relationship between PK and PD in SON-1010 dosing. Safety was carefully tracked, along with the evaluation of acute inflammatory cytokine responses to help with dose escalation decisions. The study was performed in accordance with the Declaration of Helsinki, Council for International Organizations of Medical Sciences International Ethical Guidelines, and Good Clinical Practice, and was approved by the Alfred Human Research Ethics Committee (Alfred Health, Melbourne, VIC) as authorized by the Australian Government through the National Health and Medical Research Council (NHMRC) on 2Aug2022, once the safety of the first two dose levels had been reviewed in SB101.

A SAD approach was used in SB102, including the dosing of sentinel participants before putting larger numbers at risk, with placebo participants in each of five cohorts designated S1 to S5, with eight participants in each dose cohort randomized to receive either SON-1010 (n=6) or a placebo (n=2) (Table 1). Blinding was maintained until the database was closed. One similar trial, a large phase 1 dose escalation study using rIL-12 that was conducted in healthy volunteers as a medical countermeasure for acute radiation syndrome (30), was used as the basis for initial dose selection in the SON-1010 clinical program (31). The first cohort in SB102 received 50 ng/kg SON-1010, which is the molar equivalent of the lowest rIL-12 dose that showed a measurable IFNγ response in that earlier study of healthy volunteers.

2.2 Participant assessment

Participants were followed for 3 days in confinement at the Nucleus Clinical Research Unit and then as outpatients for a total of 28 days after dosing to assess safety, tolerability, and laboratory responses. Safety, including an assessment of adverse events and all available laboratory results, was reviewed at each SRC meeting after all participants in that cohort had completed day 22. If dose-limiting toxicities (DLTs) or a lack of tolerability were observed in at least one participant at a given dose level, the highest previously evaluated dose level without a DLT was defined as the MTD. The cytokine responses are likely to be a better early indicator of an inflammatory response related to SON-1010 than clinical AEs, so, the PD response was followed closely as the dose was escalated with a rapid assessment of 'acute inflammation' labs from day to 1-8 (IFNγ, IL1ß, IL-6, IL-8, IL-10, IL-12, and TNFα by a Luminex assay, Crux Biolabs, Melbourne, Australia). The SRC reviewed these results, then authorized the subsequent dose level for enrollment of the next sentinel participants.

Safety and tolerability were determined by assessing treatment-emergent adverse events (TEAEs), vital signs, laboratory test results (hematology, biochemistry, coagulation, thyroid function tests, and urinalysis), electrocardiograms, and physical examination findings. Adverse events were graded according to the current version of the Common Terminology Criteria for Adverse Events (CTCAE) and were categorized as mild (grade 1), moderate (grade 2), severe (grade 3), life-threatening (grade 4), or death (grade 5), or as serious AEs (SAEs) according to standard definitions. Causal relationships of TEAEs to SON-1010 administration were judged by the investigator as either "unrelated"; or "possibly", "probably", or "definitely" related (treatment-related TEAEs). All TEAEs were coded using the Medical Dictionary of Regulatory Activities (MedRA v24.0).

Serum SON-1010 concentrations were assessed using a validated electrochemiluminescence-based immunoassay (ECLIA)

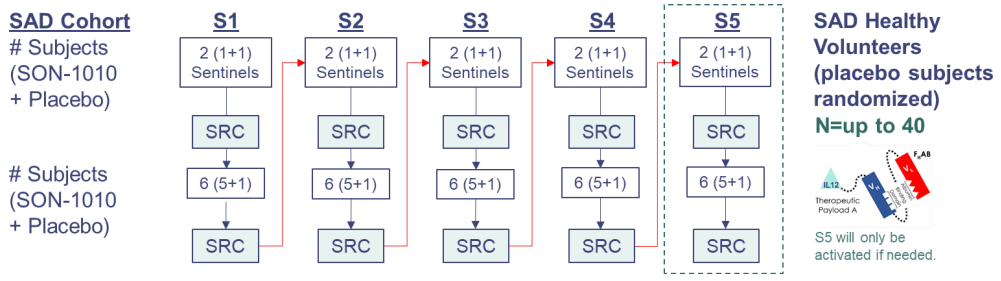

FIGURE 2
SB102 Trial design. Dosing was organized as cohorts that were to receive 50 ng/kg up to 450 ng/kg (the molar equivalent of 33-300 ng/kg rhIL-12). Safety data from the first four days of sentinel dosing were checked by the SRC before proceeding with the rest of the cohort. Data from days 1 to 22 were reviewed at each SRC cohort meeting. S1, SAD cohort 1; S2, SAD cohort 2; S3, SAD cohort 3; S4, SAD cohort 4; S5, SAD cohort 5; SAD, single ascending dose.

10.3389/fimmu.2024.1362775

TABLE 1 SB102 dose escalation schedule.

Cohort	Planned Number (SON-1010 + Placebo)	Planned Dose (μg/kg)[a]	rIL12 ME (μg/kg)[b]	Actual Number of Participants
S1	6 + 2	0.050	0.033	6 + 2
S2	6 + 2	0.100 (= 2 x S1)	0.067	6 + 2
S3	6 + 2	0.150 (= 1.5 x S2)	0.100	6 + 2
S4	6 + 2	0.300 (= 2 x S3)	0.200	5 + 2
S5	6 + 2	0.450 (= 1.5 x S4)	0.300	0

[a]Dose selection was based on all available safety, and real-time pharmacokinetic and pharmacodynamic data. Dosing could change based on prior safety and available PK and PD results.
[b]ME, Molar equivalent dose of rIL12.

for IL-12 (Mesoscale Discovery [MSD] Cat# K151QVD) at Celerion (Omaha, NB, USA). Urine concentrations were evaluated at 360biolabs (Melbourne, Australia) with the same kit after qualification for its use with urine. Primary PK parameters were calculated from concentration versus time data using non-compartmental analysis (NCA), including maximum serum concentration (C_{max}); area under the serum concentration vs. time curve (AUC) from the first dose until 24, 48, or 168 h (AUC_{0-x}); AUC until the last quantifiable concentration (AUC_{0-t}); an estimate of the total AUC (AUC_{inf}); time to peak serum concentration (T_{max}); terminal elimination half-life ($T_{½}$), apparent clearance (CL/F); and apparent volume of distribution (V_z/F). The formal PD parameters included IFNγ, IL-1β, IL-2, IL-4, IL-6, IL-8, IL-10, and TNFα levels, which were determined using a qualified multiplex assay (MSD Cat# K15049G) (Celerion).

2.3 Statistics

The analysis sets for this study included the enrolled set (participants who signed the informed consent form [ICF], met eligibility criteria, and were approved for randomized treatment), the safety set (all participants who received at least one dose of SON-1010 or placebo), and the PD set (participants with sufficient PD samples available). All analysis datasets and outputs were produced by the Biostatistics Department of Resolutum Global using SAS® Version 9.4 (SAS Institute, Cary, North Carolina, USA). The sample size selected (6 active participants per cohort) was based on common practice in phase 1 dose escalation studies. Non-compartmental analysis to estimate PK parameters was performed using R version 4.3.0 (32) and the pkr package version 0.1.3 (R Foundation for Statistical Computing, Vienna, Austria).

3 Results

SON-1010 is composed of a F_HAB domain that is genetically linked to the N-terminus, using a short, non-immunogenic amino acid repeat sequence designed to avoid steric hindrance ($[Gly_4Ser]_5$), to single-chain rIL-12. The molecule binds albumin in the serum after injection to share its extended PK, and the complex is distributed to the tumor tissue after binding to FcRn or GP60 (27). The complex also binds SPARC avidly at a lower pH (26), which is often found in the TME, where the cytokine can then interact with resident immune cells (Figure 1). The SB102 trial evaluated four single-dose cohorts of healthy volunteers given SON-1010 at 50, 100, 150, or 300 ng/kg, or placebo (Table 1), and was designed to support the SB101 MAD study in patients with cancer (29, 33). The planned fifth cohort of SB102 was not enrolled, to avoid potential adverse events at higher doses (Figure 2). The maximal dose in this study will be used as the 'desensitizing first dose' in cancer patients to take advantage of the known rIL-12 tachyphylaxis and controlled increases in IFNγ (2, 4, 34), so a higher MTD can be targeted with subsequent maintenance doses.

The median age of the 31 participants in the study population (23 active, 8 placebo) was 28.0 years (range: 18.0 to 52.0 years). Twenty-one participants (67.7%) were male. Of the 10 female participants, all but one was of child-bearing potential. Most (19/31, 61.3%) participants were Caucasian or Asian (11/31, 35.5%), and none were Hispanic or Latino. The median body mass index (BMI) was 24.10 kg/m^2 (range: 19.4 to 30.7 kg/m^2). This profile was consistent across participants receiving SON-1010 or placebo and across SON-1010 dose cohorts.

The participants were required to be generally healthy to be enrolled in the study. The most frequently reported (≥10%) medical and surgical histories pertained to procedures or infections (12/31, 38.7% each); eye disorders (10/31, 32.3%); injuries and procedural complications (8/31, 25.8%); psychiatric disorders (6/31, 19.4%); and respiratory, mediastinal, and thoracic disorders or skin and subcutaneous tissue disorders (5/31, 16.1% each). The most frequently reported historical conditions were COVID-19 (9/31, 29.0%), myopia (7/31, 22.6%), wisdom tooth removal (5/31, 16.1%), and tonsillectomy, astigmatism, or depression (4/31, 12.9% each).

3.1 Safety and tolerability in healthy volunteers

Blinded dosing in each cohort started with two sentinel participants (one active and one placebo), followed approximately a week later by six participants in the rest of each cohort to assess the safety, tolerability, PK, and PD without the background of prior chemotherapy (29). SON-1010 administration was generally safe and well-tolerated at all doses in this population of healthy volunteers. There were no grade ≥ 3 treatment-emergent adverse events (TEAEs) that were considered related to treatment. There

10.3389/fimmu.2024.1362775

were no serious adverse events (SAEs) and no TEAEs leading to discontinuation of the study.

Participants receiving SON-1010 at doses of 100 ng/kg or higher tolerated the injection but generally experienced more TEAEs than participants receiving SON-1010 at 50 ng/kg (Table 2). However, there was no clear evidence of a dose-related effect among the higher-dosing cohorts. Headache (10/23, 43.4%), myalgia, injection site pain or induration, and pyrexia (3/23, 13.0% each) were reported as related events more frequently among SON-1010 treated participants than among placebo group, who only included one with headache or injection site pain (1/8, 12.5%), with no clear relationship between the SON-1010 dose cohort and frequency. Most TEAEs were mild and were considered possibly, probably, or definitely related to SON-1010. One participant (12.5%) in Cohort S1 developed grade 2 neutropenia on day 5 that returned to normal by day 10. One participant each (12.5%) in Cohorts S2 and S3 reported a recurrent moderate/grade 2 headache requiring acetaminophen for control, and one participant (14.3%) in Cohort 4 reported grade 2 flu-like symptoms requiring acetaminophen for 5 days. One placebo participant (12.5%) reported a grade 2 headache requiring acetaminophen that was considered related as well. During the trial, the most frequently prescribed concomitant medication was acetaminophen (15/31, 48.4%), which was

TABLE 2 SB102 adverse events considered related to SON-1010.

Preferred Term (PT)[a]	50 ng/kg (N=6) n (%)	100 ng/kg (N=6) n (%)	150 ng/kg (N=6) n (%)	300 ng/kg (N=5) n (%)	Placebo (N=8) n (%)
Injection site reaction				2 (40.0%)	
Injection site erythema		1 (16.7%)	1 (16.7%)		
Injection site pain		2 (33.3%)	1 (16.7%)		1 (12.5%)
Injection site induration		1 (16.7%)	2 (33.3%)		
Pyrexia			1 (16.7%)	2 (40.0%)	
Axillary pain			2 (33.3%)		
Fatigue		1 (16.7%)			1 (12.5%)
Chills		1 (16.7%)			
Malaise			1 (16.7%)		
Headache	1 (16.7%)	3 (50.0%)	2 (33.3%)	2 (40.0%)	
Dizziness		1 (16.7%)			
Somnolence	1 (16.7%)				
Myalgia	1 (16.7%)		1 (16.7%)	1 (20.0%)	
Neck pain		1 (16.7%)			
Abdominal pain			1 (16.7%)		1 (12.5%)
Diarrhea		1 (16.7%)			
Nausea					1 (12.5%)
Neutropenia		1 (16.7%)			
Iron deficiency anemia		1 (16.7%)			
Hordeolum					1 (12.5%)
Upper Respiratory Infection		1 (16.7%)			
Night sweats			1 (16.7%)		
Rash			1 (16.7%)		
Transaminases increased				1 (20.0%)	
Blepharospasm	1 (16.7%)				
Hot flush					1 (12.5%)
Influenza like illness (Grade 2)				1 (20.0%)	
Headache (Grade 2)		1 (16.7%)	1 (16.7%)		1 (12.5%)
Neutropenia (Grade 2)	1 (16.7%)				

[a]All TEAEs considered to be possibly, probably, or definitely related to the injection were grade 1, apart from those noted as grade 2. N = number in group; n = number with event.

administered to one placebo vs. five of the six active participants in the SON-1010 100 ng/kg cohort. Other concomitant medications were administered to a single participant, with no apparent patterns across treatments or cohorts.

Dose-related decreases in neutrophils, lymphocytes, and platelets were observed 24-72 hours after the administration of SON-1010 (Figure 3), with resolution by day 7 to 10, which is consistent with other studies that used rIL-12 (30) or rIFNγ (36). Alanine aminotransferase (ALT) levels increased over the first 5 to 10 days then returned to baseline, with lower increases in aspartate aminotransferase (AST) levels or other liver enzymes. All values returned to baseline within a short period of time. A dose-related increase in C-reactive protein concentration was also observed on day 2, which returned to baseline values by day 7. Acute inflammation was assessed in each cohort by Luminex assay, for review by the SRC (Supplementary Figure S2). An increase in IFNγ was observed in all SON-1010 dose cohorts, as well as a much smaller dose-dependent increase in TNFα, IL-8, and IL-10 concentrations. These changes occurred within 24 to 48 h after administration of the study drug. There were minimal transient increases in IL-6 concentrations that were not dose related. All values returned to baseline within a few days. There were no notable changes in vital signs or electrocardiograms. No TEAEs or cytokine responses were observed that might suggest cytokine release syndrome (37).

3.2 Pharmacokinetics

Studying SON-1010 in healthy volunteers in SB102 was an important objective for this non-genotoxic therapeutic oncology drug candidate, as it provided an opportunity to evaluate PK and PD without interference from prior chemotherapy (29, 33). Mean serum concentration versus time profiles following the single SC injection of SON-1010 are presented for the first week (Figure 4). Between the SON-1010 lowest- (50 ng/kg) and highest- (300 ng/kg) dose cohorts (a 6x escalation in dose), the serum C_{max} increased by 4.5x (Momentum Metrix, Dublin, CA), and the time to reach that (T_{max}) was approximately 11 h (Table 3). This was associated with a corresponding 4.5 × increase in the exposure area under the concentration time curve (AUC) from time zero to the time of last observable concentration ($AUC_{0\text{-}t}$), and the shape of the curves indicated typical two-compartment elimination kinetics (Figure 4). The mean $T_{½}$ across all dose cohorts was 104 h, and the serum concentrations for the majority of the participants remained above the lower limit of quantitation (LLOQ) for 336 h. The mean C_{max} value increased in a less than proportional manner between dose cohorts, yielding nonlinear PK. The geometric mean C_{max} values of the low- and high-dose cohorts were 29 pg/mL and 131 pg/mL, respectively. The low dose cohort reported mean $AUC_{0\text{-}t}$ and $AUC_{0\text{-}inf}$ of 1340 (CV % 41.5) h•pg/mL and 1500 (CV% 8.5) h•pg/mL, respectively. The high-dose cohort reported 6030 (CV% 47.1) h•pg/mL and 9850 h•pg/mL, respectively. Urine SON-1010 concentrations were below the level of quantitation at all time points, so that route of elimination was not included in the analysis. The SON-1010 PK parameters C_{max}, $AUC_{0\text{-}24}$, and $AUC_{0\text{-}48}$, are shown graphically in Supplementary Figure S3A. There was relatively large variability in the mean SON-1010 PK parameters with poor linear fits (R^2 adj < 0.8), and nearly all parameters had a geometric mean CV% greater than 30%; therefore, N was too low to calculate accurate summary statistics for other PK parameters, such as CL/F and V_Z/F.

Interim data from repeat dosing in patients with advanced solid tumors in study SB101, including dose escalation up to the same

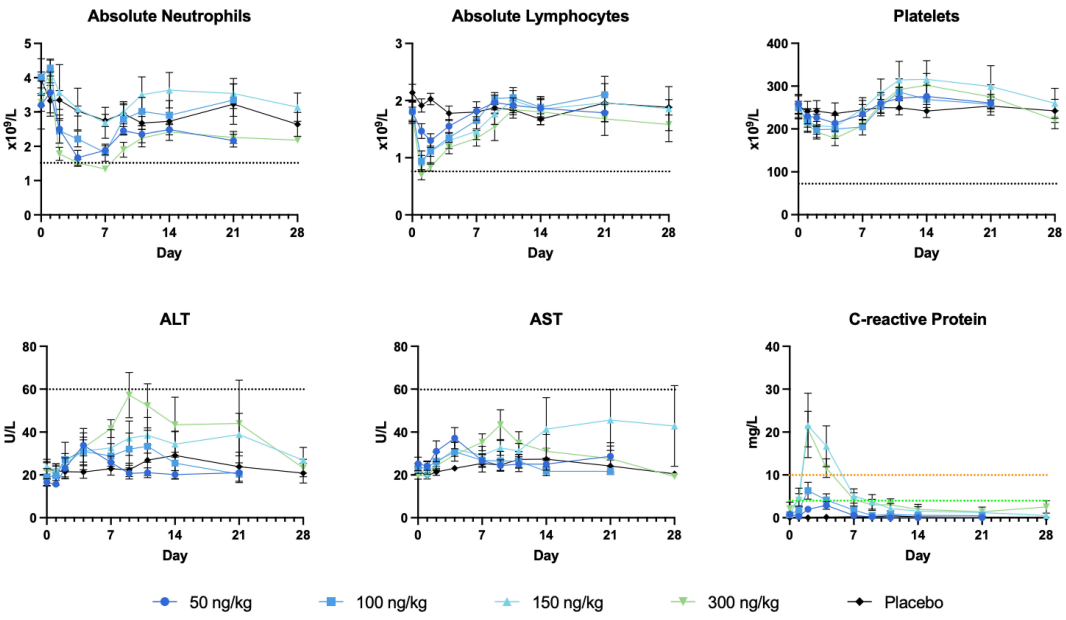

FIGURE 3
Safety laboratory results. The most reactive laboratory results are shown in each panel, along with the grade 1 limit (35) as a black dotted line. C-reactive protein has no defined AE limits: normal < 3 mg/L, minor increase 3-10 mg/L, moderate increase 10-100 mg/L. ALT, alanine aminotransferase, AST, aspartate aminotransferase.

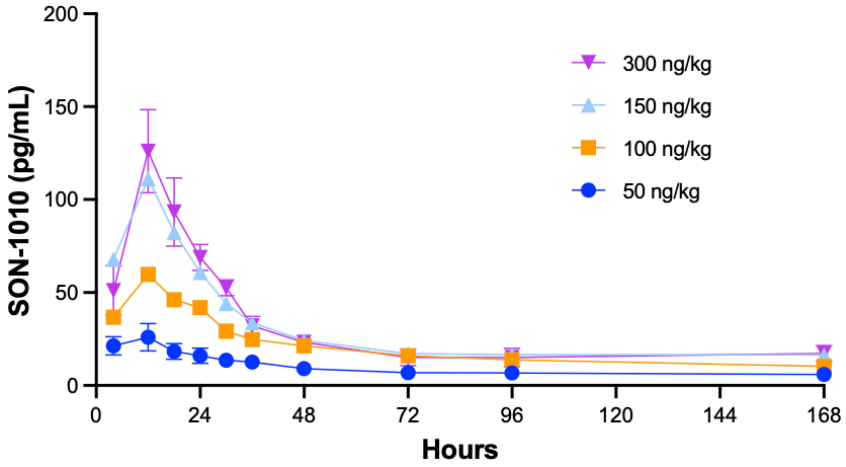

FIGURE 4
SON-1010 Concentration over time by SB102 cohort. Healthy volunteers in study SB102 were given a single dose of SON-1010 SC and followed closely for safety, PK, and PD over the course of 4 weeks. The geometric mean levels of SON-1010 are shown with error bars (geometric mean CV %) for the lowest and highest groups.

maximum dose used in SB102, are now available (Figure 5) (28). Interestingly, the SON-1010 concentration curves, using the same assay in cancer patients, compared with a single dose in healthy volunteers (Figure 4) showed an atypically dissimilar contour. Single-compartment elimination kinetics were noted in patients with cancer, compared to the two-compartment elimination kinetics observed in the healthy volunteers. The C_{max} and AUC PK parameters in SB101 were similar after the second dose compared to the first dose in SB102, while the IFNγ PD parameters of C_{max} and AUC were suppressed in SB101 (Supplementary Figures S3B, S4B), presumably by the induction of SOCS proteins (34).

3.3 Pharmacodynamics

Endogenous biomarkers of interest included IFNγ, IL-1β, IL-2, IL-4, IL-6, IL-8, IL-10 and TNFα. Of these, only IFNγ, TNFα, IL-6, IL-8, and IL-10 met the criteria for analysis, as fewer than 20% of the data were below the limit of quantitation. Mean serum concentration versus time profiles following the single SC injection of SON-1010 are presented for the first 2 weeks (Figure 6). Apart from IL-6, the concentrations remained above the LLOQ for all study participants.

A summary of the NCA parameter values after a single SC dose showed that IFNγ was the most prominent cytokine responding (Table 4). The mean C_{max} value disproportionately increased between the wide range of doses tested, peaking at 977 pg/mL in the highest dose cohort (300 ng/kg). The time taken to achieve maximal IFNγ blood concentrations varied greatly between cohorts and did not correlate with the dose, with the mean time required to peak ranging from 28.8 to 85.0 hours. The AUC_{0-t} also increased disproportionately following the cohort doses and rose to 106,000 h*pg/mL in the highest-dose cohort. However, the partial areas under the concentration-time curve from time zero to 24 h, 48 h, and 168 h increased in a dose-dependent manner. The SON-1010

TABLE 3 Pharmacokinetic summary statistics by dose cohort.

Cohort	Statistic	C_{MAX} (pg/mL)	T_{MAX} (h)	AUC_{0-24h} (h*pg/mL)	AUC_{0-48h} (h*pg/mL)	AUC_{0-t} (h*pg/mL)	AUC_{0-inf} (h*pg/mL)	$T_{1/2}$ (h)
S1: 50 ng/kg (N=6/5M/1F)	GM	29.3	9.80	454	772	1,340	1,500	69.1
	CV%	71.7	34.9	70.7	52.4	41.5	8.5	159.2
S2: 100 ng/kg (N=6/3M/3F)	GM	68.2	11.0	1,110	1,820	3,610	5,370	138
	CV%	104.3	66.2	100.5	72.6	39.6	32.8	50.9
S3: 150 ng/kg (N=6/4M/2F)	GM	125	11.2	1,970	2,930	5,570	10,200	112
	CV%	40.6	31.2	38.8	40.8	58.7	22.2	34.7
S4: 300 ng/kg (N=5/4M/1F)	GM	131	11.1	2,050	3,050	6,030	9,850	110
	CV%	39.4	18.3	36.2	23.7	47.1	NA	NA

AUC, area under the serum concentration vs time curve; AUC_{0-x}, AUC from the first dose until the time indicated or (t) the last quantifiable concentration; C_{max}, maximum observed serum concentration; CV%, geometric mean coefficient of variation; GM, geometric mean; h, hours; NA, not applicable; T_{max}, time to peak serum concentration; $T_{½}$, terminal elimination half-life.

10.3389/fimmu.2024.1362775

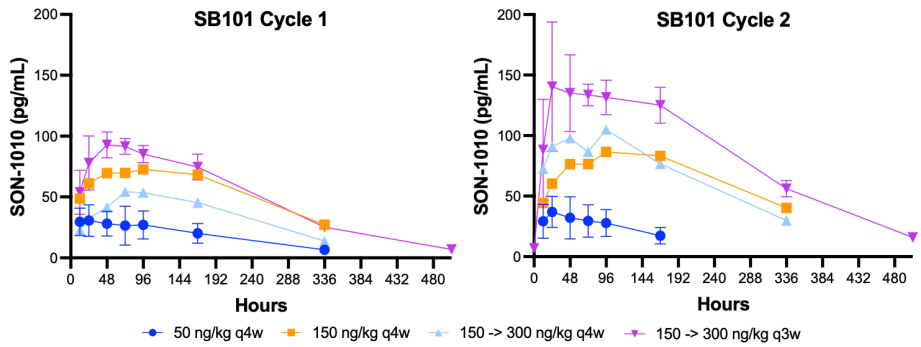

FIGURE 5
SON-1010 concentration over time by SB101 cohort. Patients in study SB101 were administered a fixed dose of SON-1010 (in the first two groups) or a desensitizing first dose followed by a higher maintenance dose (in the last two groups). The dose interval was reduced from every 4 weeks (q4w) to q3w in the last (and subsequent) groups. Error bars (geometric mean CV%) are shown for the lowest and highest groups, respectively.

PD parameters C_{max}, $AUC_{0\text{-}24}$, and $AUC_{0\text{-}48}$, are shown graphically in Supplementary Figure S4A.

Another consideration is to compare SON-1010 PK with the IFNγ PD response after a single dose in healthy volunteers. The greatest linear correlation was observed between C_{max} PK and $AUC_{0\text{-}24h}$ IFNγ PD (Pearson correlation coefficient = 0.77, $p<0.001$) (Supplementary Figure S5). Although it was much less responsive, the C_{max} value for IL-10 increased with each higher SON-1010 dose cohort, peaking at 2.75 pg/mL with the highest dose. The mean time taken to achieve C_{max} ranged from 36.4 to 67.7 h. Although the analyzed IL-10 AUC metrics appeared to suggest dose proportionality, this was less clear for the other cytokines studied. The mean maximum IL-6, IL-8, and TNFα concentrations achieved after a 300 ng/kg dose of SON-1010 were 5.4, 24.6, and 4.6 pg/mL, respectively. The mean times to achieve C_{max} were 27.6, 52.2, and 48.1 h, respectively.

4 Discussion

4.1 Development of rIL-12

Early efforts to advance rIL-12 into the clinic showed in the first phase 1 study that doses up to 500 ng/kg daily could be administered intravenously (IV) with acceptable levels of safety, starting two weeks after a test dose (4). Weekly SC dosing was also well-tolerated at that dose (38). However, in the subsequent phase 2 study of 17 patients who received daily rIL-12 IV, 12 patients were hospitalized and two patients died (2). A thorough scientific investigation to determine the cause of this unexpected toxicity failed to identify any difference in the drug products used or the patient populations enrolled in the two IV studies that could have accounted for the profound difference in toxicity. The schedule-dependent toxicity of rIL-12 and an abrupt increase in IFNγ levels

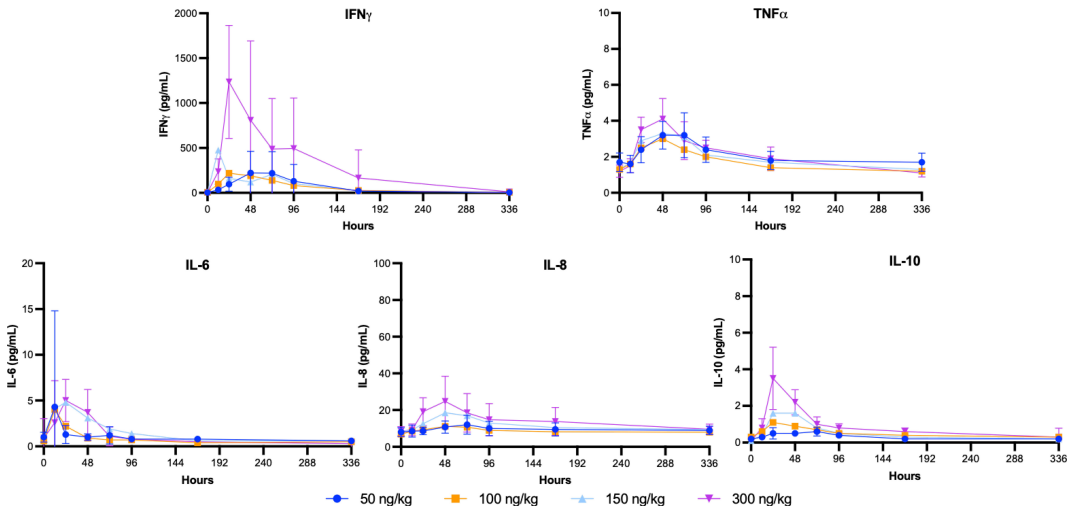

FIGURE 6
SB102 Cytokine concentrations over time. Serum was collected over the course of the study for PD analysis to correlate with the PK findings. The geometric mean levels of each cytokine are shown with error bars (geometric mean CV%) for the lowest and highest groups.

10.3389/fimmu.2024.1362775

TABLE 4 Pharmacodynamic summary statistics by dose cohort.

Cohort	Analyte	Statistic	C_{MAX} (pg/mL)	T_{MAX} (h)	$AUC_{0\text{-}24h}$ (h*pg/mL)	$AUC_{0\text{-}48h}$ (h*pg/mL)	$AUC_{0\text{-}168h}$ (h*pg/mL)	$AUC_{0\text{-}t}$ (h*pg/mL)
S1: 50 ng/kg (N=6/5M/1F)	IFNγ	GM	342	85.0	1,030	5,190	21,100	34,200
		CV%	64.4	137.6	65.9	71.4	92.9	78.0
	IL-10	GM	0.8	67.7	8.3	21.5	78.7	135
		CV%	28.5	187.6	62.7	50.6	40.2	129.4
	IL-6	GM	4.9	16.2	69.4	110	238	740
		CV%	157.6	83.6	168.3	92.3	50.7	88.4
	IL-8	GM	13.0	72.2	205	440	1,700	6,240
		CV%	38.7	48.0	31.0	28.5	33.5	29.1
	TNFα	GM	3.4	54.9	44.0	112	409	1,270
		CV%	26.8	21.1	29.3	26.5	27.8	24.2
S2: 100 ng/kg (N=6/3M/3F)	IFNγ	GM	331	30.3	2,630	8,730	21,800	27,600
		CV%	65.3	61.5	142.6	74.4	28.6	20.9
	IL-10	GM	1.4	38.9	16.1	41.6	113	262
		CV%	63.8	59.2	71.4	62.0	51.1	29.6
	IL-6	GM	4.2	15.2	67.1	107	191	212
		CV%	42.1	36.6	36.2	39.9	23.1	84.7
	IL-8	GM	12.7	54.8	200	449	1,590	5,760
		CV%	33.2	20.7	16.8	20.9	20.8	20.3
	TNFα	GM	3.1	45.7	42.7	109	352	981
		CV%	13.1	36.3	22.3	20.7	12.9	15.7
S3: 150 ng/kg (N=6/4M/2F)	IFNγ	GM	573	28.8	4,070	12,500	32,800	41,800
		CV%	66.3	68.9	160.5	126.5	62.8	68.7
	IL-10	GM	2.1	38.1	15.4	57.3	138	236
		CV%	88.9	36.9	107.2	83.0	65.0	90.2
	IL-6	GM	5.2	24.0	82.4	184	373	587
		CV%	55.0	46.0	67.1	58.2	43.3	47.2
	IL-8	GM	20.3	48.8	238	617	2,280	7,630
		CV%	64.9	41.4	50.4	57.2	47.6	64.2
	TNFα	GM	3.8	43.5	46.2	123	407	1,130
		CV%	35.1	52.4	34.5	32.5	25.0	33.2
S4: 300 ng/kg (N=5/4M/1F)	IFNγ	GM	977	52.3	7,230	26,700	86,000	106,000
		CV%	91.7	55.4	59.2	83.8	97.9	105.4
	IL-10	GM	2.75	36.4	21.6	75.9	195	352
		CV%	51.3	39.4	64.2	52.0	32.3	73.1
	IL-6	GM	5.4	27.6	66.3	150	259	413
		CV%	80.5	63.1	84.9	44.6	32.0	50.5
	IL-8	GM	24.6	52.2	246	718	2,620	7,100
		CV%	53.3	18.6	29.0	42.4	50.8	36.4

(Continued)

TABLE 4 Continued

Cohort	Analyte	Statistic	C_{MAX} (pg/mL)	T_{MAX} (h)	AUC_{0-24h} (h*pg/mL)	AUC_{0-48h} (h*pg/mL)	AUC_{0-168h} (h*pg/mL)	AUC_{0-t} (h*pg/mL)
	TNFα	GM	4.6	48.1	40.3	135	445	993
		CV%	27.8	0.2	19.1	25.2	23.6	19.4

AUC, area under the serum concentration vs time curve; AUC_{0-t}, AUC from the first dose until the last quantifiable concentration; C_{max}, maximum observed serum concentration; CV%, geometric mean coefficient of variation; GM, geometric mean; h, hours; T_{max}, time to peak serum concentration.

were verified in mice and nonhuman primates to be a form of tachyphylaxis; therefore, the dosing level misdirection was thought to have been due to PD effects.

The single test dose injection of rIL-12 administered 2 weeks before consecutive dosing in that first phase 1 study, but not after daily administration in the phase 2 study, apparently had a profound abrogating effect on rIL-12-induced IFNγ production and toxicity with subsequent doses. This was likely a result of the induction of suppressors of cytokine signaling (SOCS) proteins (Figure 7) that normally regulate inflammatory responses (34). Competitive binding of SOCS proteins to the phosphorylated tyrosine residues of cytokine receptors prevents the docking of STAT proteins and the transfer of the signals, thereby reducing toxicity. When the second rIL-12 dose was delayed in phase 1, the subsequent toxic effects may have been suppressed by lingering SOCs proteins. However, in the next study the mean serum IFNγ levels rose to over 25,000 pg/mL after starting with daily injection of rIL-12. This was attributed, at least in part, as the cause of the toxicity, compared to an IFNγ peak of 5,000 pg/mL in phase 1 after the test dose. Interestingly, the phase 2 IFNγ peak was about the same peak level that was measured after intramuscular administration of rIFNγ at its MTD of 5.0 mg/m^2 in patients with cancer in an early phase 1 trial (36), where the most notable toxicity was fatigue. Peak IFNγ levels appeared to correlate with maximum toxicity in that study. Perhaps the more severe toxicity observed in the phase 2 study of rIL-12 was related to the sustained level of IFNγ that was secondarily induced, which had peaked at approximately 10,000 pg/mL after IV administration of 500 ng/kg rIL-12 in phase 1 (4).

Since the initial phase 2 study of rIL-12 (2), numerous trials have been conducted to determine the optimal dosing schedule and potential utility of various forms of rIL-12, both in patients with cancer and in healthy volunteers. In the largest study to date of rIL-12 in healthy volunteers, designed to study its use as a medical countermeasure for humans exposed to lethal radiation, 32 subjects were initially enrolled in a SAD format starting at 2 µg (as a standardized dose) and the MTD was found to be 12 µg when given SC as a standardized dose (30). The maximum serum concentration (C_{max}) values generally increased with increasing dose levels, except for the 20 µg cohort, where only one participant was dosed. Sixty patients were enrolled in a placebo-controlled expansion study at the MTD of 12 µg. In both studies, the most common AEs related to rIL-12 were headache, dizziness, and chills during the first few days of treatment. No immunogenicity was observed. Two-compartment elimination of rIL-12 was noted, suggesting significant distribution into extravascular spaces; the initial $T_{½}$ was 8.7 ± 4.7 hours and the C_{max} was 57.7 ± 49.8 pg/mL. rIL-12 triggered transient reductions in neutrophils, platelets, reticulocytes, lymphocytes, NK cells, and CD34$^+$ hematopoietic progenitor cells by day 2, and correlated with induced increases in IFNγ and CXCL10. The cell subsets returned to above normal by day 7, and all parameters normalized over 1–2 weeks. This suggests that splenic sequestration or margination may account for the cell count changes, rather than destruction, as the return to normal in the standard complete blood count was faster than would be expected from simple replacement.

Multiple studies in patients with various types of cancer have shown similar effects of rIL-12 dosing strategies, ranging from daily

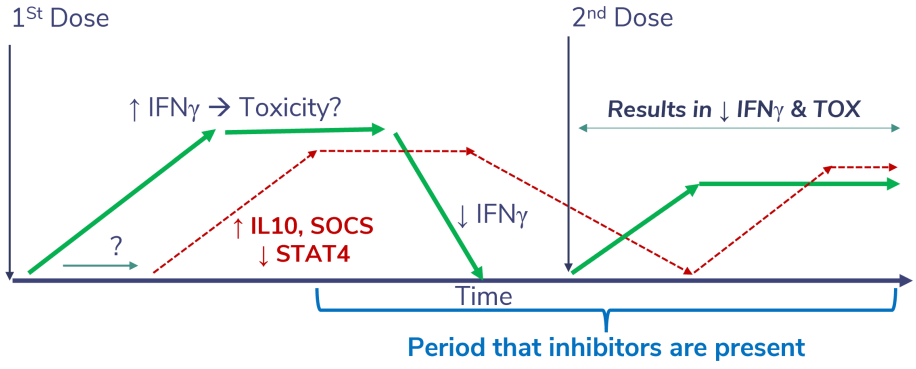

FIGURE 7
Theoretical impact of a desensitizing dose of SON-1010. Injection of rIL-12 leads to a sustained increase in IFNγ levels, which can cause significant toxicity if it reaches much higher levels acutely. This appears to be physiologically limited by SOCS proteins (34). If a second dose of rIL-12 or SON-1010 is given while SOCS is still inhibiting the phosphorylation of STAT4, the resulting toxicity potential should be abrogated, possibly allowing for a higher MTD.

to 2 to 3 times weekly. Most studies reported an MTD of 500–1000 ng/kg after IV or SC administration. Several attempts have been made to extend $T_{½}$ for a superior PK profile; the most advanced is NHS-IL12, an immunocytokine composed of two rIL-12 heterodimers, each fused to the heavy chain of an antibody that binds to DNA (39). The C_{max} of NHS-IL12 was reached at 36 h, and time-dependent elevations of IFNγ and IL-10 were observed after SC NHS-IL12 administration, which returned to normal by day 7. The MTD of NHS-IL12 was determined to be 16.8 µg/kg, which is much higher than the MTD for rIL-12 of 0.5 to 1 µg/kg, suggesting the possibility of steric hindrance of the cytokine portion of NHS-IL12. Note that NHS-IL12 was originally administered every 4 weeks as monotherapy and is currently being developed in combination with a checkpoint inhibitor given every 2 weeks (40).

4.2 Evaluation of SON-1010

The preclinical testing of SON-1010 has been extensive (25, 41). An early proof-of-concept study of F_HAB in the TGFβ$^+$ mouse 4T1 breast tumor model (42) showed the accumulation and prolonged retention of F_HAB in the tumor as well as when anti-TGFβ was linked to the scFv, whereas the anti-TGFβ antibody alone first accumulated in tumor tissue, then rapidly diffused out. In another study, murine (m) rIL-12 linked to F_HAB caused up to a 10-fold increase in serum half-life in mice, compared with the rIL-12 control (41).

Murine rIL-12 (mIL-12) causing a reduction in pulmonary metastases or SC growth of B16F10 melanoma in mice was demonstrated as early as 1993 (23). Dose-dependent increases in anti-tumor activity were also demonstrated with mIL12-F_HAB in that melanoma model, producing a corresponding increase in tumor-infiltrating activated NK and CD8$^+$ T cells (41). Single doses of mIL12-F_HAB were up to 30-fold more effective (by molar equivalence) in reducing B16F10 tumor growth and extending survivability, compared with mIL-12 alone, in a dose-dependent manner in tumor-bearing mice compared to placebo. This resulted in a corresponding increase in the immune response, as reflected by the increased splenic weight and serum IFNγ levels, which was transient and had no effect on mouse body weight. Toxic inflammatory responses were only observed at high levels of mIL12-F_HAB (30 µg/mouse), including moderate increases in IL-6, C-reactive protein, and transaminase levels. Overall, a comparison of the PD and toxicological effects of mIL12-F_HAB in mice suggests that, while the model may be limited to lower doses, B16F10 tumors are well controlled in a dose range that is non-toxic by these measures. Biodistribution studies also suggest delivery to and retention of mIL12-F_HAB in tumor tissue (25).

An *in vitro* evaluation of SON-1010 using cells from Syrian hamsters, Sprague Dawley rats, beagles, cynomolgus macaques, or humans was tested for albumin binding, potency, and binding of the complex to FcRn; only macaque cells responded physiologically (26). Therefore, macaques have been used for single- and multiple-dose toxicological testing of products based on the F_HAB platform *in vivo*. After a single SC dose of SON-1010, drug-related changes in clinical observations, body weight, clinical pathology, cytokines, and immunophenotyping were tolerated up to 250 µg/kg in macaques and were consistent with the anticipated on-target effects of rIL-12 (20). Most parameters recovered to pre-study values by day 22, and SON-1010 displayed improved PK characteristics compared to those reported for rIL-12. In the GLP toxicology study, three SC injections of SON-1010 were tolerated in monkeys at up to 62.5 µg/kg/dose. Hematological changes in red blood cells, reticulocytes, platelets, and neutrophils were suggestive of accelerated maturation, along with transient suppression of monocyte, lymphocyte, eosinophil, and white blood cell counts. Minimal changes occurred in the clinical chemistries. Cytokine data showed SON-1010-related effects on IFNγ, with minimal or no changes in IL-6, IL-8, IL-10, IL-1β, or TNFα. The no adverse effect level (NOAEL) in Cynomolgus macaques following repeated SC administration of SON-1010 was defined as 62.5 µg/kg/dose.

The unusual PK results comparing these two clinical studies suggest the potential for an improved local immune response due to accumulation in the TME in patients, which could make SON-1010 more effective than prior efforts with systemic immunotherapy using rIL-12. The dose relationship also suggests TMDD, perhaps due to the retention of SON-1010 caused by albumin binding to SPARC (27) and its slow release from the tumor tissue. Based on the SON-1010 concentration curves, a dose interval of 3 weeks produces minimal accumulation of SON-1010 before the next dose; therefore, any accumulation of the drug is unlikely to be physiologically significant. The drug product used in SB101 was a liquid formulation manufactured in a fed-batch process, while that used in SB102 was lyophilized and had been produced using a perfusion process, which may have accounted for the distinctive PK profiles. However, both drug products passed GMP release and stability testing with nearly identical results, including potency testing using an IL-12 HEK-Blue bioassay that assesses IFNγ production (43). Although subtle differences in biomolecule manufacturing lots are common and can include minor differences caused by deamidation or glycosylation (44), both lots met manufacturing specifications and were considered to be physically and functionally identical. Thus, variations such as these would not be expected to cause the drug elimination profile differences that were observed. Further testing with subsequent doses is required to substantiate the safety of prolonged dosing, which is planned for the next study (SB221).

Overall, the IFNγ PD response with a single dose in SB102 was dose-related, controlled, and prolonged without the stimulation of a more toxic cytokine response (Figure 6), which may be required to initiate tumor control in humans, as in mice (45). Neutropenia, lymphopenia, and thrombocytopenia have been reported as common AEs with rIL-12. In the large dose-escalation study of rIL-12 in healthy volunteers (30), dose-related neutropenia reached a nadir on day 5 after a single dose and the mean returned to baseline (or above) by 2 weeks. Neutropenia, lymphopenia, and thrombocytopenia were seen in both SB101 and SB102 with similar nadir and recovery times. The SON-1010 C_{max} can also be compared with the IFNγ response using $AUC_{0\text{-}48h}$ in the SB101 cancer patients using a Pearson correlation coefficient (Supplementary Material Figure S5). The Pearson correlation coefficient measures linear correlation between two sets of data

and is the ratio between the covariance of two variables and the product of their standard deviations; thus, it is essentially a normalized measurement of the covariance, such that the result always has a value between -1 and 1. The Pearson coefficient using C_{max} vs AUC_{0-24} in SB102 was also significant. The longer time to C_{max} may reflect retention in the TME in the cancer patients.

Drugs such as SON-1010, which induce IFNγ in the TME, upregulate the expression of PD-L1 on tumor cells and/or immune cells (46). While there is a reasonable chance that SON-1010 inhibits tumor growth at higher doses, owing to its improved targeting of the TME, SON-1010 may have its greatest effect in treating cancer in combination with an immune checkpoint inhibitor (47). The next development step is to determine the SON-1010 MTD when combined with an immune checkpoint inhibitor in patients with a tumor that is high in SPARC, such as platinum-resistant ovarian cancer, which continues to be a high unmet need indication. Proof-of-concept will be assessed in this population in study SB221, using the combination of SON-1010 with atezolizumab, compared with SON-1010 alone or standard-of-care therapy.

Data availability statement

The raw data supporting the conclusions of this article will be made available by the authors, without undue reservation.

Ethics statement

The studies involving humans were approved by Alfred Human Research Ethics Committee and WCG Institutional Review Board. The studies were conducted in accordance with the local legislation and institutional requirements. The participants provided their written informed consent to participate in this study.

Author contributions

RK: Conceptualization, Data curation, Formal analysis, Investigation, Methodology, Project administration, Software, Supervision, Visualization, Writing – original draft, Writing – review & editing. JC: Conceptualization, Methodology, Project administration, Visualization, Writing – review & editing. SD: Conceptualization, Methodology, Project administration, Writing – review & editing. MD: Investigation, Project administration, Supervision, Writing – review & editing. JB: Conceptualization, Data curation, Formal analysis, Methodology, Software, Supervision, Validation, Visualization, Writing – review & editing. IK: Data curation, Formal analysis, Investigation, Validation, Visualization, Writing – review & editing. SC: Conceptualization, Investigation, Methodology, Supervision, Writing – review & editing. TP: Supervision, Writing – review & editing, Investigation, Methodology, Project administration. JL: Investigation, Methodology, Project administration, Supervision, Writing – review & editing. PR: Investigation, Methodology, Project administration, Supervision, Writing – review & editing.

Funding

The author(s) declare that no financial support was received for the research, authorship, and/or publication of this article.

Acknowledgments

The authors would like to thank Swamy Chintapatla, Minh Afaga, Taylor Kilfoil, Chloe Hobbs, and Victoria Chua for their persistence and invaluable help in making the clinical trials successful, as well as the trial participants for volunteering for this novel therapy. We also thank Sarah Peters at Celerion and Jonathan Ferrand at Crux Biolabs for help with sample analysis, Mark Lay at RRD International for help in developing the manuscript, and Grantham Hogeland at Momentum Metrix for assistance with the pharmacometric calculations.

Conflict of interest

RK, JC, SD, and MD were employed by and have stock in Sonnet BioTherapeutics. JB and IK were employed by Momentum Metrix, a Sonnet consultant. SPC was employed by the Sarcoma Center and conducted the SB101 clinical study under contract with Sonnet. TP was employed by InClin, the Contract Research Organization responsible for the study. JL and PR were employed by the Nucleus Network and conducted the SB102 clinical study under contract with Sonnet.

This study received funding from Sonnet BioTherapeutics. The Sonnet team was involved in the design and oversaw the conduct of the trial.

Publisher's note

Supplementary material

The Supplementary Material for this article can be found online at: https://www.frontiersin.org/articles/10.3389/fimmu.2024.1362775/full#supplementary-material

References

1. Aste-Amezaga M, D'Andrea A, Kubin M, Trinchieri G. Cooperation of natural killer cell stimulatory factor/interleukin-12 with other stimuli in the induction of cytokines and cytotoxic cell-associated molecules in human T and NK cells. *Cell Immunol*. (1994) 156:480–92. doi: 10.1006/cimm.1994.1192.

2. Leonard JP, Sherman ML, Fisher GL, Buchanan LJ, Larsen G, Atkins MB, et al. Effects of single-dose interleukin-12 exposure on interleukin-12-associated toxicity and interferon-gamma production. *Blood*. (1997) 90:2541–8. doi: 10.1182/blood.V90.7.2541

3. Mirlekar B, Pylayeva-Gupta Y. IL-12 family cytokines in cancer and immunotherapy. *Cancers*. (2021) 13:1–23. doi: 10.3390/cancers13020167.

4. Atkins MB, Robertson MJ, Gordon M, Lotze MT, DeCoste M, DuBois JS, et al. Phase I evaluation of intravenous recombinant human interleukin 12 in patients with advanced Malignancies. *Clin Cancer Res*. (1997) 3:409–17.

5. Gao W, Pan J, Pan J. Antitumor activities of interleukin-12 in melanoma. *Cancers*. (2022) 14:1–14. doi: 10.3390/cancers14225592.

6. Hsieh CS, Macatonia SE, Tripp CS, Wolf SF, O'Garra A, Murphy KM. Development of TH1 CD4+ T cells through IL-12 produced by Listeria-induced macrophages. *Science*. (1993) 260:547–9. doi: 10.1126/science.8097338.

7. Choi JN, Sun EG, Cho SH. IL-12 enhances immune response by modulation of myeloid derived suppressor cells in tumor microenvironment. *Chonnam Med J*. (2019) 55:31–9. doi: 10.4068/cmj.2019.55.1.31.

8. Zheng H, Ban Y, Wei F, Ma X. Regulation of interleukin-12 production in antigen-presenting cells. *Adv Exp Med Biol*. (2016) 941:117–38. doi: 10.1007/978-94-024-0921-5_6

9. Berraondo P, Etxeberria I, Ponz-Sarvise M, Melero I. Revisiting interleukin-12 as a cancer immunotherapy agent. *Clin Cancer Res*. (2018) 24:2716–8. doi: 10.1158/1078-0432.CCR-18-0381.

10. Nguyen KG, Vrabel MR, Mantooth SM, Hopkins JJ, Wagner ES, Gabaldon TA, et al. Localized interleukin-12 for cancer immunotherapy. *Front Immunol*. (2020) 11:575597. doi: 10.3389/fimmu.2020.575597.

11. Uppendahl LD, Dahl CM, Miller JS, Felices M, Geller MA. Natural killer cell-based immunotherapy in gynecologic Malignancy: A review. *Front Immunol*. (2017) 8:1825. doi: 10.3389/fimmu.2017.01825.

12. Voest EE, Kenyon BM, O'Reilly MS, Truitt G, D'Amato RJ, Folkman J. Inhibition of angiogenesis in *vivo* by interleukin 12. *J Natl Cancer Inst*. (1995) 87:581–6. doi: 10.1093/jnci/87.8.581.

13. Albini A, Brigati C, Ventura A, Lorusso G, Pinter M, Morini M, et al. Angiostatin anti-angiogenesis requires IL-12: the innate immune system as a key target. *J Trans Med*. (2009) 7:5. doi: 10.1186/1479-5876-7-5.

14. Sorensen EW, Gerber SA, Frelinger JG, Lord EM. IL-12 suppresses vascular endothelial growth factor receptor 3 expression on tumor vessels by two distinct IFN-gamma-dependent mechanisms. *J Immunol*. (2010) 184:1858–66. doi: 10.4049/jimmunol.0903210.

15. Waldmann TA. Cytokines in cancer immunotherapy. *Cold Spring Harb Perspect Biol*. (2018) 10:1–25. doi: 10.1101/cshperspect.a028472.

16. Kulig P, Musiol S, Freiberger SN, Schreiner B, Gyulveszi G, Russo G, et al. IL-12 protects from psoriasiform skin inflammation. *Nat Commun*. (2016) 7:13466. doi: 10.1038/ncomms13466.

17. Kashani A, Schwartz D. The expanding role of anti–IL-12 and/or anti–IL-23 antibodies in the treatment of inflammatory bowel disease. *Gastroenterol Hepatol*. (2019) 15:255–65.

18. Colombo MP, Trinchieri G. Interleukin-12 in anti-tumor immunity and immunotherapy. *Cytokine Growth Factor Rev*. (2002) 13:155–68. doi: 10.1016/S1359-6101(01)00032-6.

19. Cavallo F, Signorelli P, Giovarelli M, Musiani P, Modesti A, Brunda MJ, et al. Antitumor efficacy of adenocarcinoma cells engineered to produce interleukin 12 (IL-12) or other cytokines compared with exogenous IL-12. *J Natl Cancer Inst*. (1997) 89:1049–58. doi: 10.1093/jnci/89.14.1049.

20. Car BD, Eng VM, Lipman JM, Anderson TD. The toxicology of interleukin-12: a review. *Toxicol Pathol*. (1999) 27:58–63. doi: 10.1177/019262339902700112.

21. Coughlin CM, Salhany KE, Gee MS, LaTemple DC, Kotenko S, Ma X, et al. Tumor cell responses to IFNgamma affect tumorigenicity and response to IL-12 therapy and antiangiogenesis. *Immunity*. (1998) 9:25–34. doi: 10.1016/S1074-7613(00)80585-3.

22. Zitvogel L, Robbins PD, Storkus WJ, Clarke MR, Maeurer MJ, Campbell RL, et al. Interleukin-12 and B7.1 co-stimulation cooperate in the induction of effective antitumor immunity and therapy of established tumors. *Eur J Immunol*. (1996) 26:1335–41. doi: 10.1002/eji.1830260624.

23. Brunda MJ, Luistro L, Warrier RR, Wright RB, Hubbard BR, Murphy M, et al. Antitumor and antimetastatic activity of interleukin 12 against murine tumors. *J Exp Med*. (1993) 178:1223–30. doi: 10.1084/jem.178.4.1223.

24. Cui J, Shin T, Kawano T, Sato H, Kondo E, Toura I, et al. Requirement for Valpha14 NKT cells in IL-12-mediated rejection of tumors. *Science*. (1997) 278:1623–6. doi: 10.1126/science.278.5343.1623.

25. Cini J, McAndrew S, Evans N, Eraslan RN, Prabagar MG, Dexter S, et al. *An Innovative Human Platform for Targeted Delivery of Bispecific Interleukins to Tumors*. New Orleans: AACR (2022). doi: 10.1158/1538-7445.AM2022-4229.

26. Cini J, Dexter S, Rezac DJ, McAndrew S, Hedou G, Brody R, et al. SON-1210 - A novel bifunctional IL-12 / IL-15 fusion protein that improves cytokine half-life, targets tumors, and enhances therapeutic efficacy. *Front Immunol*. (2023) 14:1326927. doi: 10.3389/fimmu.2023.1326927.

27. Hoogenboezem EN, Duvall CL. Harnessing albumin as a carrier for cancer therapies. *Advanced Drug Deliv Rev*. (2018) 130:73–89. doi: 10.1016/j.addr.2018.07.011.

28. Chawla SP, Chua V, Gordon E, Cini J, Dexter S, DaFonseca M, et al. *Clinical Development of a Novel Form of Interleukin-12 with Extended Pharmacokinetics*. Orlando, FL: AACR (2023). doi: 10.1158/1538-7445.AM2023-CT245.

29. Shen J, Swift B, Mamelok R, Pine S, Sinclair J, Attar M. Design and conduct considerations for first-in-human trials. *Clin Transl Sci*. (2019) 12:6–19. doi: 10.1111/cts.12582.

30. Gokhale MS, Vainstein V, Tom J, Thomas S, Lawrence CE, Gluzman-Poltorak Z, et al. Single low-dose rHuIL-12 safely triggers multilineage hematopoietic and immune-mediated effects. *Exp Hematol Oncol*. (2014) 3:11. doi: 10.1186/2162-3619-3-11.

31. Muller PY, Milton M, Lloyd P, Sims J, Brennan FR. The minimum anticipated biological effect level (MABEL) for selection of first human dose in clinical trials with monoclonal antibodies. *Curr Opin Biotechnol*. (2009) 20:722–9. doi: 10.1016/j.copbio.2009.10.013.

32. R Core Team. *R: A language and environment for statistical computing*. Vienna, Austria: R Foundation for Statistical Computing (2023).

33. Karakunnel JJ, Bui N, Palaniappan L, Schmidt KT, Mahaffey KW, Morrison B, et al. Reviewing the role of healthy volunteer studies in drug development. *J Trans Med*. (2018) 16:336. doi: 10.1186/s12967-018-1710-5.

34. Sobah ML, Liongue C, Ward AC. SOCS proteins in immunity, inflammatory diseases, and immune-related cancer. *Front Med (Lausanne)*. (2021) 8:727987. doi: 10.3389/fmed.2021.727987.

35. NCI. *Common Terminology Criteria for Adverse Events (CTCAE) v5.0*. Bethesda, MD: U.S. Dept. of Health and Human Services, National Institutes of Health, National Cancer Institute (2017). p. 147.

36. Foon KA, Sherwin SA, Abrams PG, Stevenson HC, Holmes P, Maluish AE, et al. A phase I trial of recombinant gamma interferon in patients with cancer. *Cancer Immunol Immunother*. (1985) 20:193–7. doi: 10.1007/BF00205575.

37. Lee DW, Santomasso BD, Locke FL, Ghobadi A, Turtle CJ, Brudno JN, et al. ASTCT consensus grading for cytokine release syndrome and neurologic toxicity associated with immune effector cells. *Biol Blood Marrow Transplant*. (2019) 25:625–38. doi: 10.1016/j.bbmt.2018.12.758.

38. Bajetta E, Del Vecchio M, Mortarini R, Nadeau R, Rakhit A, Rimassa L, et al. Pilot study of subcutaneous recombinant human interleukin 12 in metastatic melanoma. *Clin Cancer Res*. (1998) 4:75–85.

39. Strauss J, Heery CR, Kim JW, Jochems C, Donahue RN, Montgomery AS, et al. First-in-human phase I trial of a tumor-targeted cytokine (NHS-IL12) in subjects with metastatic solid tumors. *Clin Cancer Res*. (2019) 25:99–109. doi: 10.1158/1078-0432.CCR-18-1512.

40. Strauss J, Deville JL, Sznol M, Ravaud A, Maruzzo M, Pachynski RK, et al. First-in-human phase Ib trial of M9241 (NHS-IL12) plus avelumab in patients with advanced solid tumors, including dose expansion in patients with advanced urothelial carcinoma. *J Immunother Cancer*. (2023) 11:1–30. doi: 10.1136/jitc-2022-005813.

41. Huang H, Haenssen K, Bhate A, Sanglikar S, Baradei J, Liu S, et al. *Enhanced Efficacy of Immune Modulators with Albumin Binding Domains (ABD)*. Washington, DC: AACR Annual Meeting 2017 (2017).

42. Pulaski BA, Ostrand-Rosenberg S. Mouse 4T1 breast tumor model. *Curr Protoc Immunol*. (2000) 39:20.2.1–20.2.16. doi: 10.1002/0471142735.im2002s39.

43. Xue D, Moon B, Liao J, Guo J, Zou Z, Han Y, et al. A tumor-specific pro-IL-12 activates preexisting cytotoxic T cells to control established tumors. *Sci Immunol*. (2022) 7:eabi6899. doi: 10.1126/sciimmunol.abi6899.

44. Sosic Z, Houde D, Blum A, Carlage T, Lyubarskaya Y. Application of imaging capillary IEF for characterization and quantitative analysis of recombinant protein charge heterogeneity. *Electrophoresis*. (2008) 29:4368–76. doi: 10.1002/elps.200800157.

45. Tugues S, Burkhard SH, Ohs I, Vrohlings M, Nussbaum K, Vom Berg J, et al. New insights into IL-12-mediated tumor suppression. *Cell Death Differ*. (2015) 22:237–46. doi: 10.1038/cdd.2014.134.

46. Chen S, Crabill GA, Pritchard TS, McMiller TL, Wei P, Pardoll DM, et al. Mechanisms regulating PD-L1 expression on tumor and immune cells. *J Immunother Cancer*. (2019) 7:305. doi: 10.1186/s40425-019-0770-2.

47. Maiorano BA, Maiorano MFP, Lorusso D, Maiello E. Ovarian cancer in the era of immune checkpoint inhibitors: state of the art and future perspectives. *Cancers*. (2021) 13:1–17. doi: 10.20944/preprints202108.0037.v1.

frontiers | Frontiers in Oncology

TYPE Original Research
PUBLISHED 07 March 2024
DOI 10.3389/fonc.2024.1364577

OPEN ACCESS

EDITED BY
Gulderen Yanikkaya Demirel,
Yeditepe University, Türkiye

REVIEWED BY
Dmitry Aleksandrovich Zinovkin,
Gomel State Medical University, Belarus
Avishek Bhuniya,
Wistar Institute, United States

*CORRESPONDENCE
Annette Runge
annette.runge@tirol-kliniken.at

RECEIVED 02 January 2024
ACCEPTED 23 February 2024
PUBLISHED 07 March 2024

CITATION
Greier MdC, Runge A, Dudas J, Hartl R, Santer M, Dejaco D, Steinbichler TB, Federspiel J, Seifarth C, Konschake M, Sprung S, Sopper S, Randhawa A, Mayr M, Hofauer BG and Riechelmann H (2024) Cytotoxic response of tumor-infiltrating lymphocytes of head and neck cancer slice cultures under mitochondrial dysfunction. *Front. Oncol.* 14:1364577. doi: 10.3389/fonc.2024.1364577

Cytotoxic response of tumor-infiltrating lymphocytes of head and neck cancer slice cultures under mitochondrial dysfunction

Maria do Carmo Greier[1], Annette Runge[1]*, Jozsef Dudas[1], Roland Hartl[1], Matthias Santer[1], Daniel Dejaco[1], Teresa Bernadette Steinbichler[1], Julia Federspiel[1], Christof Seifarth[2], Marko Konschake[2], Susanne Sprung[3], Sieghart Sopper[4], Avneet Randhawa[5], Melissa Mayr[6], Benedikt Gabriel Hofauer[1] and Herbert Riechelmann[1]

[1]Department of Otorhinolaryngology, Head and Neck Surgery, Medical University of Innsbruck, Innsbruck, Austria, [2]Institute for Clinical and Functional Anatomy, Medical University Innsbruck (MUI), Innsbruck, Austria, [3]INNPATH GmbH, Institute for Pathology, Innsbruck, Austria, [4]Clinic for Internal Medicine V, Medical University Innsbruck, Innsbruck, Austria, [5]Department of Otolaryngology, Rutgers University Medical School, Newark, NJ, United States, [6]ViraTherapeutics GmbH, Rum, Austria

Background: Head and neck squamous cell carcinomas (HNSCC) are highly heterogeneous tumors. In the harsh tumor microenvironment (TME), metabolic reprogramming and mitochondrial dysfunction may lead to immunosuppressive phenotypes. Aerobic glycolysis is needed for the activation of cytotoxic T-cells and the absence of glucose may hamper the full effector functions of cytotoxic T-cells. To test the effect of mitochondrial dysfunction on cytotoxic T cell function, slice cultures (SC) of HNSCC cancer were cultivated under different metabolic conditions.

Methods: Tumor samples from 21 patients with HNSCC were collected, from which, SC were established and cultivated under six different conditions. These conditions included high glucose, T cell stimulation, and temporarily induced mitochondrial dysfunction (MitoDys) using FCCP and oligomycin A with or without additional T cell stimulation, high glucose and finally, a control medium. Over three days of cultivation, sequential T cell stimulation and MitoDys treatments were performed. Supernatant was collected, and SC were fixed and embedded. Granzyme B was measured in the supernatant and in the SC via immunohistochemistry (IHC). Staining of PD1, CD8/Ki67, and cleavedcaspase3 (CC3) were performed in SC.

Results: Hematoxylin eosin stains showed that overall SC quality remained stable over 3 days of cultivation. T cell stimulation, both alone and combined with MitoDys, led to significantly increased granzyme levels in SC and in supernatant. Apoptosis following T cell stimulation was observed in tumor and stroma. Mitochondrial dysfunction alone increased apoptosis in tumor cell aggregates. High glucose concentration alone had no impact on T cell activity and apoptosis. Apoptosis rates were significantly lower under conditions with high glucose and MitoDys ($p=0.03$).

Conclusion: Stimulation of tumor-infiltrating lymphocytes in SC was feasible, which led to increased apoptosis in tumor cells. Induced mitochondrial dysfunction did not play a significant role in the activation and function of TILs in SC of HNSCC. Moreover, high glucose concentration did not promote cytotoxic T cell activity in HNSCC SC.

KEYWORDS

immune response, cytotoxic T-cells, mitochondrial electron transport chain, head and neck carcinoma, mitochondrial dysfunction

1 Introduction

1.1 HNSCC tumor microenvironment

Head and neck squamous cell carcinomas (HNSCC) are common malignancies with an unfavorable prognosis and severe disease burden. They develop from mucosal epithelial cells, especially in the oral cavity, pharynx, larynx and sinunasal tract. These tumors exhibit great intra- and inter-individual heterogeneity and develop in a complex and hostile tumor microenvironment (TME). Within the microarchitecture of HNSCC, tumor cells often form aggregates of different sizes, sometimes referred to as tumor cell nests. These tumor cell aggregates lie within a tumor stroma of extracellular matrix that harbors a heterogeneous mixture of stromal cells, including endothelial cells, cancer-associated fibroblasts (CAF), and immune cells, of which tumor infiltrating lymphocytes (TILs) are the major type (1–3).

1.2 Immune evasion in HNSCC

In order to survive in the TME, the tumor cells must evade immune surveillance. The microarchitecture of the TME is an important factor in achieving this. In the common immune exclusion phenotype, the immune cells are spatially restricted to the stroma and hardly penetrate the tumor cell aggregates (3, 4). The barrier between tumor cell aggregates and stroma is due to the surrounding thick ECM, the absence of lymphatic vessels, and a disorganized vasculature. Hypoxic conditions, hyperacidity, and substrate deficiency within the tumor cell aggregates also prevent immune cell infiltration (5, 6). Another essential escape mechanism is the immune checkpoint programmed cell death protein 1 (PD-1) (7). PD-1 is mainly expressed on T cells, B cells and natural killer (NK) cells. It inhibits the activity of these cells when activated by its ligand PD-L1, which is frequently expressed on HNSCC tumor cells (8). Interruption of PD-1/PD-L1-mediated immune evasion by monoclonal antibodies is the basis of modern immune checkpoint inhibitors (ICI) and represents a major therapeutic breakthrough, particularly in metastatic and recurrent HNSCC (9). Persistent PD-1 expression has also been recognized as a marker of T cell exhaustion (10, 11), which is another mechanism by which HNSCC tumor cells escape immune surveillance (12). Due to metabolic stress in the microenvironment combined with sustained TCR-mediated stimulation, effector T lymphocytes undergo mitochondrial dysfunction (MitoDys) and, similar to tumor cells, switch from OXPHOS to aerobic glycolysis (13, 14). This leads to competition between T cells and tumor cells for nutrients, especially glucose, and impaired T cell effector functions (15, 16). In HNSCC, MitoDys can be induced experimentally with FCCP (carbonyl cyanide-4-(trifluoromethoxy) phenylhydrazone) and oligomycin A (17).

1.3 HNSCC slice cultures

Although cell cultures are excellent models for mechanistic studies of the metabolism and cellular function of tumor cells and immune cells, they do not adequately reflect the complex three-dimensional relationships in the TME: the different cell populations, the spatial compartmentalization in tumor and stroma, and the high intra- and inter-individual heterogeneity of HNSCC. In recent years, various *in vitro* and ex vivo models have been developed that allow a more realistic investigation of the events in the TME (18). The cultivation of tissue sections from tumor biopsies of patients (slice cultures) reflects the complex relationships in the TME more effectively than cell cultures do (19, 20). However, experimenting with HNSCC slice cultures (SC) requires access to a clinical facility where fresh tumor tissue samples from patients with HNSCC are available. Compared to cell cultures, the possible experimental interventions are limited. Although SC of HNSCC remain viable, maintain their microenvironment, and respond to experimental immunologic interventions (21, 22), they can only do so for a few days. Moreover, they are only available in limited quantities and complex procedures like transgenic interventions are hardly feasible. While cell cultures can be accurately characterized by flow cytometry, the cell separation required for flow cytometry of SC may lead to unreliable results due to possible epitope loss. For this reason, histological evaluation methods are primarily used to analyze SC.

1.4 Image cytometry

Modern image cytometric methods overcome some of the limitations of conventional histopathological analysis. These methods involve the quantitative evaluation of chromogen or fluorescence intensities, based on the segmentation of single cells in tissue sections. This approach yields multiparametric information including size, compactness, and location of cells with chromogenic or fluorescence intensity for each biomarker (23). With the simultaneous use of differently labeled antibodies, multiplex cytometry is possible, allowing a differentiated analysis of the phenotype, spatial distribution, and activation of cells (24) in the TME. Recent imaging cytometric techniques allow automatic differentiation between tumor cell aggregates and tumor stroma in HNSCC (25).

1.5 Study aims

Using SC from patients with HNSCC, we investigated the effects of MitoDys on TME. Specifically, we investigated how MitoDys affects apoptosis in tumor cell aggregates and tumor stroma, how glucose concentration modulates MitoDys-induced apoptosis, and how T cell activation affects apoptosis in tumor and stroma of HNSCC slice cultures. In particular, we were interested in whether MitoDys interferes with the effects of T cell activation. In addition, we examined PD-1 expression under these experimental conditions as a possible indicator of T cell exhaustion.

2 Methods

2.1 Study population and preparation of HNSCC slice cultures

All patients with incident, locally advanced HNSCC treated at the Department of Otorhinolaryngology - Head and Neck Surgery of the Medical University of Innsbruck between January 2022 and September 2022 who agreed to participate were consecutively included. Inclusion criteria were patient age over 18 years, who underwent diagnostic endoscopy under anesthesia (26) with tumor biopsy and had a locally advanced primary tumor (T3-T4). Patients were excluded if there was a contraindication to endoscopy under anesthesia or if the histopathology was not HNSCC. This study was approved by the Ethics Committee of the Medical University of Innsbruck (EC number: 1199/2019). Written informed consent was obtained from all patients. Tumor biopsies from 21 patients with newly diagnosed histologically confirmed HNSCC were obtained. Seventeen primary tumors were located in the oropharynx, three in the oral cavity, and one in the larynx. Six tumors were p16 positive. The patients were between 31 and 87 years old (average 61.4 years), four patients were female. All patients but one had UICC stage III or IV HNSCC by clinical and radiologic evaluation. The tissue samples were taken with biopsy forceps from a non-necrotic tumor area during diagnostic endoscopy under anesthesia and immediately brought to the laboratory for the preparation of slice cultures (SC). Six slices with a thickness of 250 µm were cut from each patient sample using the Compresstome® VF-310-0Z (Precisionary Instruments LLC, MA, USA) and then plated (21).

2.2 Culture conditions

SC were submerged in a 24-well plate (Corning Incorporated-Life Sciences, Durham, USA) under six different conditions (Table 1). One ml of serum-free keratinocyte medium (Keratinocyte SFM; #10724-011, Gibco, Grand Island, NY, USA) was added to all six wells. Keratinocyte SFM is a complete serum-free medium supplemented with human recombinant epidermal growth factor and bovine pituitary extract. It was supplemented with Gibco Antibiotic-Antimycotic (#15240062, Thermo Fischer Scientific, Rochester, NY, USA) diluted 1:100 in the medium, resulting in a final concentration of 100 µg/mL streptomycin, 250 ng/mL amphotericin B and 100 units/mL penicillin.

To experimentally induce MitoDys (Conditions 2, 4 and 6; Table 1), 1µl of a 1mM mixture of FCCP (carbonyl cyanide-4-(trifluoromethoxy) phenylhydrazone, #370-86-5, Sigma Aldrich, Darmstadt, Germany) and oligomycin A (#75351-5MG, Sigma Aldrich, Darmstadt, Germany) was added to the wells after 24 hours for 50 minutes, according to treatment conditions described in the XFp Seahorse Analyzer protocol (17). This procedure was repeated after a further 24 hours (Figure 1). FCCP uncouples the OXPHOS and oligomycin A blocks ATP synthase. Together, they block mitochondrial ATP synthesis.

For T cell stimulation (T Cell stim; conditions 3 and 4; Table 1), 30 µl of a T Cell Activation/Expansion Kit (#130-091-441, Miltenyi Biotec, Gladbach, Germany) was added to the wells. The kit consists

TABLE 1 SC cultivation conditions, glucose concentrations and compounds used for mitochondrial dysfunction and T cell stimulation.

Condition No.	Shortcut	Glucose conc.	Mitochondrial Dysfunction	T Cell stimulation
1	Control	5.8 mmol/l		
2	MitoDys	5.8mmol/l	FFCP/oligomycin	
3	T cell activation	5.8mmol/l		T cell activation kit
4	HighGluc	25 mmol/l		
5	HighGluc+MitoDys	25 mmol/l	FFCP/oligomycin	
6	MitoDys+T cell Stim	5.8mmol/l	FFCP/oligomycin	T cell activation kit

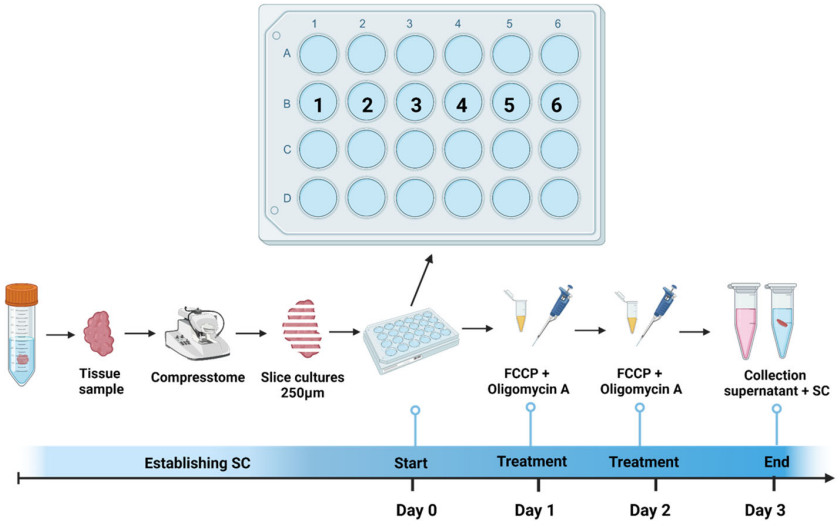

FIGURE 1
Treatment and cultivation procedure. SC were obtained from tumor samples of patients with incident head & neck squamous cell carcinoma during diagnostic endoscopy and sliced using Compresstome. Six SC per patient were plated in a 24-well plate (1=Control; 2=MitoDys; 3= T cell stim; 4= HighGluc; 5=HighGluc+ MitoDys and 6=MitoDys +T cell stim; see Table 1). After one day, three wells (2,5,6) were treated with FCCP + oligomycin A for 50min. After another day, this procedure was repeated, after 3 days in total, SC were fixed, and supernatant was collected.

of anti-biotin-MACSiBead particles and biotinylated antibodies against human CD2, CD3 and CD28. The anti-biotin-MACSiBead particles loaded with the biotinylated antibodies are used to simulate antigen-presenting cells. To achieve T cell expansion beyond T cell activation, the addition of rIL-2 is required on day 5 and 14 of the culture (Miltenyi Biotec, #130-091-441 data sheet), which was not done here.

For high glucose concentrations (HighGluc; conditions 5 and 6; Table 1), Keratinocyte SFM was augmented to 25mM with 45% glucose solution (#25-027-CI, Corning, Arizona, USA).

2.3 Collection of supernatant, ELISA, and dot blot

After 72 hours, the SC were fixed, and the supernatants were collected from each well. (Figure 1) The pH was measured (InoLab ph level 1, Inolab - wtw, Weilheim, Germany). Lactate concentration was detected using the Lactate Assay Kit II (#KA0834, Abnova, Taipei, Taiwan) and measured using an ELISA plate reader (Anthos 2010, Salzburg, Austria). Granzyme B was measured using dot blot analysis. Circles were drawn with a pencil on the Amersham Protran 0.2 µm Nitrocellulose Blotting Membrane (#10600001, GE Healthcare Life Sciences, Amersham, Buckinghamshire, UK) for each supernatant sample. The membranes were briefly treated with methanol and then dried. From each supernatant sample, 20 µl was pipetted into a circle on the membrane. After drying, the membranes were rehydrated in TBS and blocked for one hour at room temperature in Invitrogen TBS Starting Blocking Solution (#37542). The membranes were then incubated with the primary granzyme B antibody IgG2b 1:200 (#3002-MSM4-P1, Invitrogen, Darmstadt, Germany) in Invitrogen TBS Starting Blocking Solution with 0.2% Tween 20 overnight. Anti-mouse IgG IR 800 1:10000 (Azure Biosystem, Houston, TX, USA) was used to detect the antibody reaction. The optical densities of the drawn circles in the membranes were measured with ImageJ 1.46r (1.6.0_20, National Institutes of Health, USA), and the background densities were subtracted.

2.4 SC immunostaining procedures

After cultivation period of 72h, SCs were fixed in 4% paraformaldehyde (#FN-10000-4-1, SAV Liquid Production GMBH, Flintsbach am Inn, Germany) overnight (4° C) and washed with phosphate-buffered saline (PBS; Fresenius Kabi GmbH, Bad Homburg v.d.H, Germany) the next day. Fixed SC were prepared for paraffin embedding with the Histos 5 microwave system (Milestone, Bergamo, Italy) and 5 µm microtome sections were prepared afterwards [2] and dewaxed [35]. Hematoxylin-Eosin (HE) staining followed the manufacturers´ protocol (#1.05174.0500, Merck KGaA, Darmstadt, Germany).

Following the protocol of Fischer et al. (27), cleaved caspase-3 (CC3) staining was performed using the fully automated immunostaining system Ventana Discovery Ultra immunostainer (Ventana Roche Discovery Classic, Tucson, AZ, USA) and the CC3 antibody (1:400x, polyclonal rabbit, #9661, Cell Signaling Technology, Danvers, MA, USA).

For granzyme B detection mouse monoclonal IgG2b antibody 1:200 (#3002-MSM4-P1, Invitrogen, Darmstadt, Germany) was used and for PD1 staining the EH33 antibody 1:100 (mouse monoclonal, Mob573) from Diagnostic Biosystems (Baltimore, MD, USA). For detection of primary mouse and rabbit antibodies, Ventana universal secondary antibody (#05268877) was used. The reaction was fully developed using Ventana DAB Map Detection Kit (#05266360001, Roche Diagnostics, Mannheim,

Germany). Cell nuclei were counterstained using Hematoxylin (#5277965001, Roche Diagnostics). After staining procedure, the slides were dehydrated, mounted with Entellan (MERCK, Darmstadt, Germany) and dried overnight. T-cell proliferation was characterized by immune fluorescence staining with CD8 mouse monoclonal IgG2b 1:50 (#NCL-L-CD8-4B11 Novocastra, Manchester, UK), combined with prediluted mouse monoclonal IgG1 Ki67 antibody (E059, Linaris, Dossenheim, Germany). Mouse IgG1 was detected by Alexa 488 conjugated anti-mouse secondary antibody; mouse IgG2b was detected by Alexa 555 conjugated secondary antibody (Invitrogen, Darmstadt, Germany). Nuclei were counterstained with 4′,6-diamidin-2-phenylindolethen (DAPI, 1:46.000, Thermo Fisher Scientific, Darmstadt, Germany). Autofluorescence was reduced with the Vector TrueVIEW Auto fluorescence Quenching Kit (#VEC-SP-8400, Vector Laboratories, Burlingame, California, USA) [35]. After staining procedures, the slides were mounted with Vectashield Vibrance (Vector Laboratories) [2]. PD1, CD8 and Ki67 clone MIB-1 are diagnostic antibodies which are continuously validated by the provider. Granzyme B was validated in human tonsils as suggested by the provider.

2.5 Image cytometry

For immunofluorescence image acquisition, TissueFAXS PLUS (TissueGnostics GmbH, Vienna, Austria) was used. Images were acquired with Zeiss Axio Imager Z2 Microscope (Jena, Germany) and apochromat 40x, 0.6 air lens. As fluorescence light source Zeiss HBO 100 Mercury Lamp 42301101 (Jena, Germany) was used. For excitation and detection, the following filters were used: Zeiss filter set 44 for Ki67 (AF488), filter set 20 for CD8 (AF555) and filter set 49 for DAPI (24). Colors were arbitrarily chosen for each channel: green for Ki67, red for CD8 and blue for DAPI. For preview and acquisition PCO pixelfly CCD camera (PCO AG, Kelheim, Germany) was used.

TissueFAXS PLUS, containing microscope and lens, as described above, was also used for enzyme immunohistochemistry. For image acquisition, PIXELINK camera (PIXELINK, Ottawa, Canada) was used. Relative staining intensities were determined in whole SC using HistoQuest (TissueGnostics GmbH, Vienna, Austria). Acquired images were imported in HistoQuest. Regions which were not possible to analyze (necrotic, too small) were excluded by the users. Using the possibilities of HistoQuest, the engine single reference shade was used after defining the main colors of Hematoxylin counterstain (blue) and DAB-reaction (brown). The next step was the optimization of cell nuclei recognition, using previous published knowledge (24). The following procedures served the recognition of immunohistochemical staining, considering its localization, membranous or cytoplasmic. Tissue was stratified into macrostructures, to differentiate between stroma and tumor cells. Tumor and stroma cells were identified based on their different hematoxylin equivalent diameter and hematoxylin area (Supplementary Figure 1). Cells were recognized by hematoxylin counterstaining and the immunohistochemical signals were attributed to the identified cell nuclei (Figure 2). Staining intensities were provided by the software based on intensity values for all pixels grouped to cells, which were identified by their cell nuclei (Supplementary Tables 1-6). Mean intensity is a dimensionless number representing the intensity in the color of the IHC reaction products of all pixels grouped into tumor and stroma categories, as described above (28). HistoQuest provides various data including total cell count, specimen area, mean color intensity of IHC reaction products, and mean fluorescence intensities. Pathologist (Su.S.) and histologist (M.K.) supervised morphological procedures.

2.6 Data analysis

The parameters investigated followed a gamma distribution, with the individual test conditions clustered within the patients. Accordingly, a generalized estimating equations model was chosen for the evaluation, based on the gamma distribution with a logarithmic link function including a constant term. The parameters were estimated using the maximum likelihood method and the p-values were calculated according to Wald. The alpha error adjustment was carried out using the least significant difference method. The mean values predicted by the model (estimated marginal means) and their 95% confidence intervals (95% CI) were reported as outcomes. Comparisons of parameters across all experimental conditions were analyzed using the Mann-Whitney U test, with the medians and the 25th and 75th percentiles reported. Calculations were performed with SPPS Statistics Ver. 27 (IBM, Armonk, NY) and graphically presented using GraphPad Prism 9 (GraphPad Software, San Diego, CA, USA).

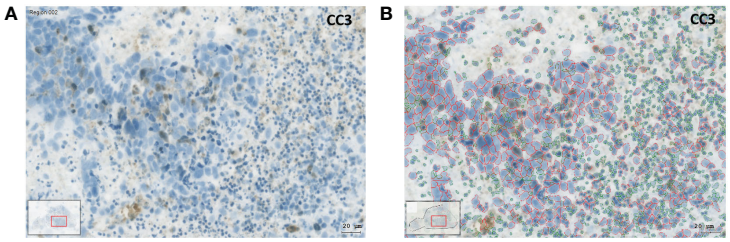

FIGURE 2
Image analysis with the HistoQuest software using the example of an IHC preparation with cleaved caspase 3 (CC3). **(A)** SC after 3 days in culture under control conditions. The brown CC3 reaction products can be recognized. **(B)** Identification of tumor and stromal cells using the HistoQuest software from the same sample. The cells circled in red were identified by the software as tumor cells, the cells circled in green as inflammatory cells (bar corresponds to 20µm).

3 Results

3.1 SC in HE stains at day 0 and 3

After 3 days of cultivation, the SC were fixed, embedded, and sliced. Compared to day 0, HE stains showed preserved tissue architecture with preserved cells. Tumor cell aggregates and tumor stroma could also be differentiated on day 3 (Figure 3). However, across all test conditions, the cell density was lower on day 3 (median 9089; quartiles 4530 to 17478 cells/mm²) than on day 0 (median 14785; quartiles 9350 to 23527 cells/mm²; Wilcoxon p<0.001).

3.2 Cleaved caspase 3 (CC3)

Caspase-3 is a canonical actor of apoptosis. The activation of caspase-3 requires the proteolytic cleavage of its inactive zymogen into activated p17 and p12 fragments. Cleaved Caspase 3 (CC3) forms the core enzyme of apoptotic poly(ADP-ribose) polymerase (PARP) (29). CC3 mean intensity was used as a measure for CC3 expression. Across all experimental conditions, CC3 expression was higher in tumor cell aggregates (median 14.9; quartiles 11.8 to 22.0) than in stroma (10.2; 7.6 to 13.5; p<0.001).

Looking at CC3 expression specifically in the tumor cell aggregates, MitoDys led to higher CC3 expression (21.9; 95% CI 17.6 to 27.2) than control conditions (13.4; 95% CI 11.5 to 15.6; p=0.003; Figure 4A). This effect was substantially mitigated by HighGluc in the medium (15.4; 95% CI 12.1 to 19.6). The difference of MitoDys + HighGluc compared to MitoDys alone was significant (p=0.03). HighGluc alone did not lead to any change in CC3 expression.

Similarly, T-cell activation led to an increase in CC3 expression to 24.6 (95% CI 18.0 to 33.6) when compared with control conditions (13.4; 95% CI 8.0 to 18.1; p=0.005). This effect was maintained with concomitant MitoDys (22.5; 95% CI 16.4 to 30.9; p vs. T-cell activation alone 0.69). In the tumor stroma, the results were essentially equivalent with significantly lower CC3 expression (Figure 4B). However, the difference of CC3 IHC-expression in control (9.3; 95% CI 6.4 to 12.1) and MitoDys (13.1; 95% CI 10.2 to 16.1) was not significant (p=0.065). Overall, T cell activation increased CC3 in both tumor aggregates and stroma. MitoDys however lead to increased CC3 in tumor cell aggregates, but not in stroma.

3.3 Granzyme B and CD8/KI67 co-expression

Together with perforin and granulolysin, the serine protease granzyme B forms the essential components of the cytotoxic pathway of lymphocytes and NK cells (30). Here, granzyme B expression was analyzed by immunohistochemistry and granzyme B release was quantified by dot blots of the supernatants under the 6 experimental conditions. In addition, we investigated the co-expression of CD8 and the proliferation marker KI67 in immunofluorescence using some slice cultures as examples.

Granzyme B concentration in the supernatant increased following T cell stim (p=0.005) and this effect was not counteracted by simultaneous induction of MitoDys (p vs. T cell stim alone =0.54; Figure 5). In detail, T cell activation resulted in a higher relative granzyme B optical density in the dot blots (189.8; 95% CI 148.2 to 243.1) than the control conditions (93.9; 95% CI 62.3 to 141.5; p=0.005), as did T cell activation in combination with MitoDys (214.7; 95% CI 159.5 to 289.1; p<0.001). Similarly, compared to control (10.7; 95% CI 8.7 to 13.1), mean granzyme B intensity increased following T cell stim (15.4; 95% CI 12.1 to 19.4; p=0.015; Figure 6). This effect was not altered by additional induction of MitoDys (15.1; 95% CI 12.5 to 18.1; p vs. T cell stim alone 0.9). Thus, MitoDys did not lead to a dysfunction of the tumor infiltrating lymphocytes of the slice cultures.

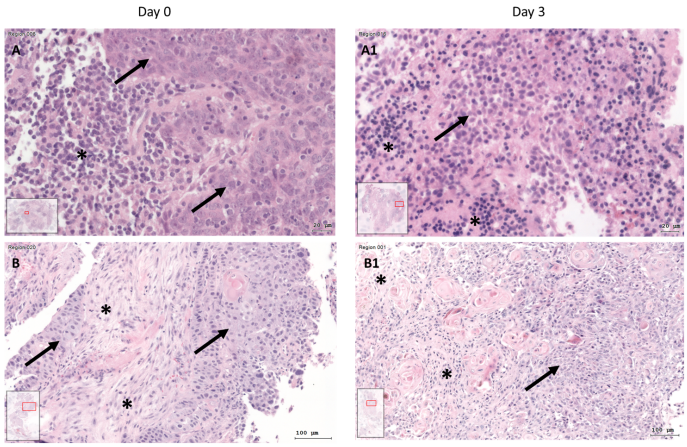

FIGURE 3
HE staining of tissue at day 0 (A+B) and SC after day 3 (A1+B1) of two different patients. **(A)** HNSCC of Oropharynx in a male patient aged 75 years at day 0 (A) and day 3 (A1; Bar: 20µm; arrow: tumor cells; asterisk: inflammatory cells, inlets: position of the image section in the whole slide). At day 0, there are visible tumor cells (arrow) and at day 3 there are tumor cells (arrow) and inflammatory cells (asterisk). B) HE staining of HNSCC of oral cavity (male, 37 years old) at day 0 **(B)** and day 3 (B1; bar: 100µm). Tumor cells (arrows) and tumor stroma (asterisk) are present at day 0 and day 3 of cultivation.

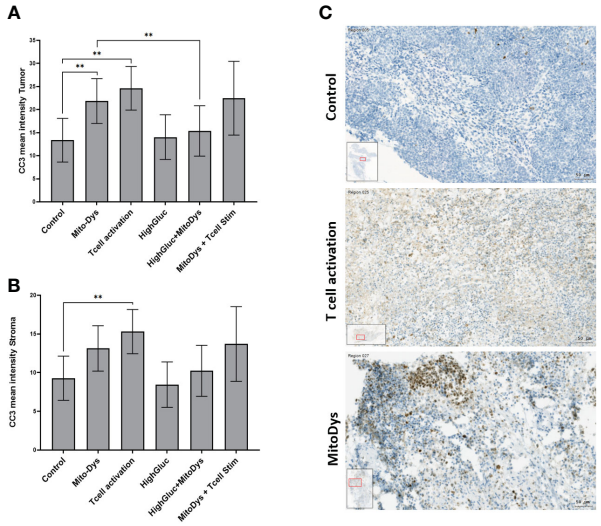

FIGURE 4
Mean intensity of CC3 in tumor **(A)** and stromal cells **(B)** of SC of HNSCC patients and images of CC3 staining of HNSCC SC **(C)**. **(A)** The mean CC3 intensity in tumor cell aggregates increased with MitoDys. CC3 expression was significantly lower with MitoDys+ HighGluc than with MitoDys alone, suggesting an mitigating effect of high glucose on MitoDys-induced CC3 expression. In addition, T cell activation increased CC3 expression in tumor cells, but this was not attenuated by concomitant MitoDys. **(B)** The mean CC3 intensities in the stroma behaved similar to the tumor cell aggregates but at a significantly lower level and the difference between control and MitoDys was not significant. The data is based on an evaluation of the whole slides (** significant < 0.01; error bars represent 95% CI). **(C)** CC3 staining of HNSCC of oral cavity for control condition (male, 37 years old), T cell activation (male, 37 years old) and MitoDys condition (male, 45 years old).CC3 positive cells increased in T cell stimulated SC. In MitoDys treated SC, especially in tumor cells CC3 positivity increased (bar: 50µm).

According to the manufacturer's data sheet, T cell expansion requires repeated stimulation with rIL2 and cultivation for more than seven days, which we did not do in this study. Nevertheless, we used some slice cultures to test whether T cell proliferation can also be observed after activation with the T cell activation and expansion kit. For this purpose, the co-expression of CD8 and KI67 was examined using fluorescence microscopy in some of the SC. Double positivity was investigated in chosen sections and different frequencies of double positive reactions were found, due to unspecific immunofluorescence stainings, regardless of computerized quantitative analysis of double reactivity. Therefore, co-expression could be detected in some, but not all SC (Figure 7).

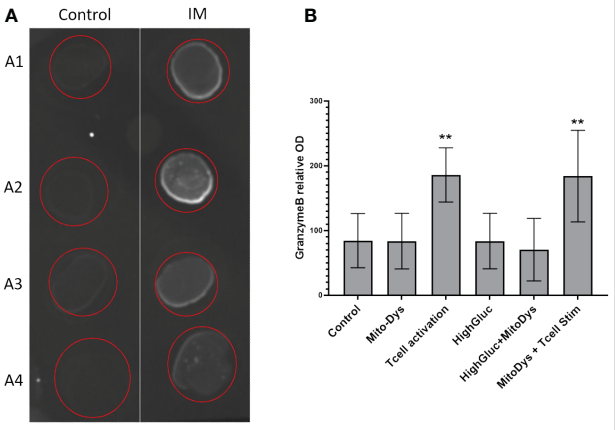

FIGURE 5
Granzyme B in culture supernatants. **(A)** Example of dot blot analysis of 4 different supernatants (A1-A4) for control conditions (Control) and T-cell stimulation (T cell activation); **(B)** Bar chart of mean optical densities (OD) per experimental condition, error bars correspond to 95% CI, **significant <0.01).

3.4 PD-1 expression

The IHC expression of PD-1 was used as an indicator for possible T-cell exhaustion. Compared to control, MitoDys alone did not increase PD-1 expression (p=0.43). A higher mean PD-1 expression compared to the control (7.0; 95% CI 5.2 to 9.5) was only found after T-cell stimulation (12.5; 95% CI 9.3 to 16.9; p=0.004). In particular, there was no increase in PD-1 expression with concomitant induction of MitoDys (p=0.08, Figure 8).

4 Discussion

The current understanding of the pathogenesis, progression, and therapy of HNSCC has reached a high level of complexity. Sequencing of the tumor genome has increasingly improved the identification of multiple mutations in tumor cells (31). Clinically relevant progress has been made in understanding the complex mechanisms of immune evasion of tumor cells (9). However, it is becoming more evident that the complex interactions of tumor and immune cells with other mutually influencing elements of the TME have a significant impact on disease progression (32). Moreover, the hostile metabolic conditions in the TME are becoming a center of interest as they may foster tumor progression and interfere with antitumor immune response (12, 33). Current knowledge on the impact of these conditions on lymphocyte antitumor response is

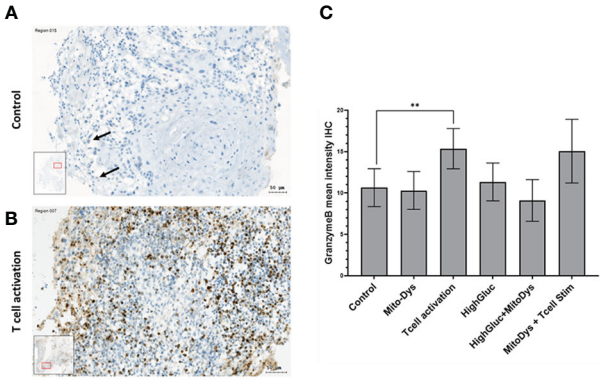

FIGURE 6
(A) Granzyme B-stained SC of an HNSCC of the oral cavity (male, 37 years) on day 3 under control conditions; only few Granzyme B reaction products in smaller inflammatory cells (arrows). **(B)** Under T-cell stimulation: numerous positive cells with granular reaction products of Granzyme (B) **(C)** Mean Granzyme B IHC intensities in SC of HNSCC per experimental condition. The data is based on an evaluation of the whole slide and not just the image section shown (** significant < 0.01; error bars represent 95% CI; inlets: position of the image section in the whole slide).

based on studies in PBMC derived lymphocytes or lymphocyte cell lines (34). Recent studies using these models report that mitochondria play a critical role in T cell metabolism, differentiation, and signaling (11). During activation, T cells undergo metabolic reprogramming, shifting from an OXPHOS-dominated metabolism in naïve CD8+ T cells to a more glycolysis-dominated metabolism in CD8+ effector T cells (35). Lymphocyte cell lines are heterogeneous, particularly in terms of glycolytic or aerobic oxidative activity (36). However, the extent to which these *in vitro* data apply to tumor infiltrating lymphocytes is unknown. The most direct method to study immune activity of tumor-infiltrating lymphocytes (TILs) is to examine them in their control environment. Cultures of patient derived tumor tissue slices provide insights into the complex interactions within their

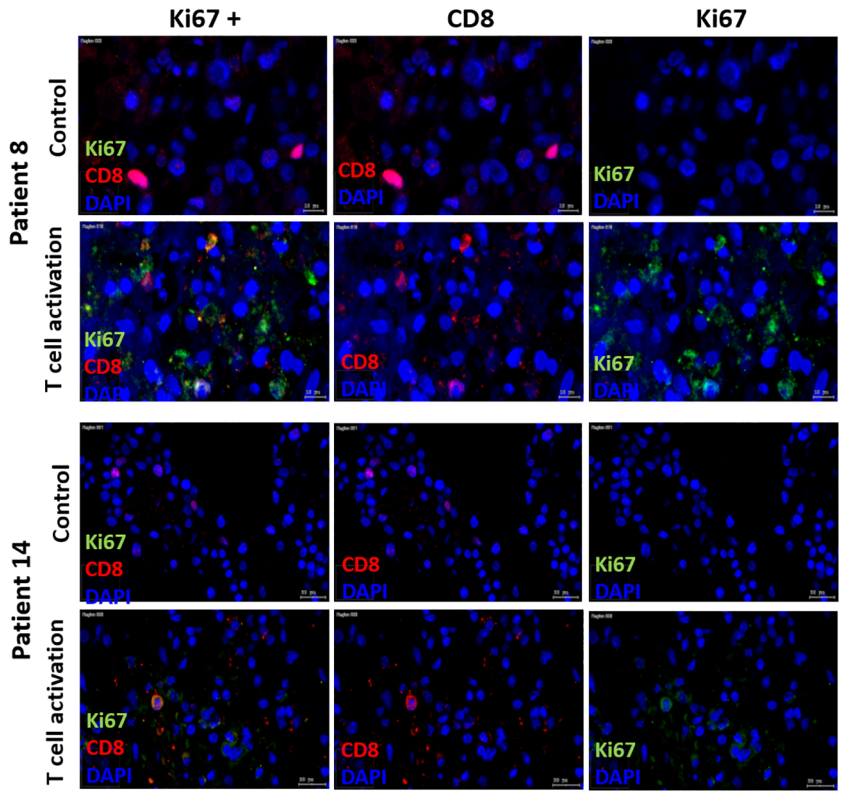

FIGURE 7
Immune fluorescent Ki67/CD8, CD8 and Ki67 staining. Double-staining with Ki67/CD8 of SC after day 3 in two patients (Patient 8 = HNSCC oropharynx, female, 66 years old; Patient 14= HNSCC oral cavity, male, 57 years old) in control and T cell stim conditions. In both patients, Ki67 staining alone in control condition showed no positive Ki67 cells. With T cell stim, amount of Ki67 pos. cells increased.

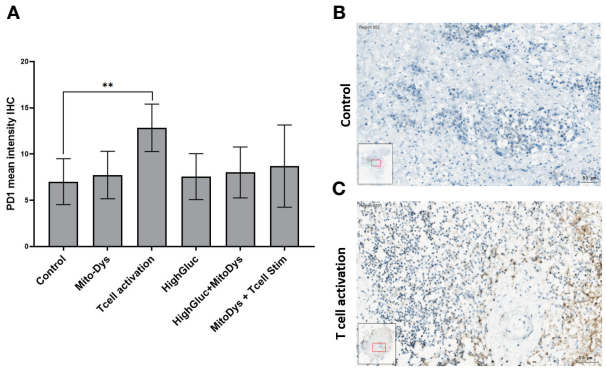

FIGURE 8
Mean PD-1 intensity in IHC of SC from HNSCC patients after 3 days of cultivation under 6 different culture conditions **(A)**. Compared to control, T cell stimulation increased the mean PD-1 intensity (p=0.004; ** significant < 0.01; error bars represent 95% CI). **(B)** PD-1 IHC staining of a SC of an HNSCC of the oral cavity (male, 37 years old) under control conditions. No PD-1 reaction products in the larger tumor cells or the smaller inflammatory cells in the tumor stroma **(C)** PD-1 IHC of the SC under T-cell stimulation. Positive cells show a ring-shaped membrane reaction of PD1.

TME, reflect their high inter- and intra-individual variability and may maintain the metabolic conditions ex vivo (37). The tumor SC of patients with HNSCC remained well preserved over the experimental period of 3 days, and the cell density on day 3, at over 9000 cells/mm², was markedly higher than in a previous study (21). This may be due to the gentle cutting technique of the tumor biopsies with the Compresstome® (38).

4.1 Tumor infiltrating T cells retain their cytotoxic activity in the hostile TME of HNSCC

However, the decrease in cell density compared to post-biopsy and the high proportion of tumor cells expressing the apoptosis marker CC3 (median 44%; quartiles 28% to 71%) under control conditions indicate that the hostile metabolic conditions were preserved within the TME of SC. Despite this, TILs remained responsive to immune stimulation. Stimulation with a commercial T cell activation kit led to increased granzyme B expression in tumor cells, heightened granzyme B release into culture supernatants (Figure 4), and upregulated pro-apoptotic cleaved caspase 3 in tumor cells under control conditions (Figure 3), aligning with previous publications (22). The data sheet of the T cell activation kit indicates that T cell expansion can be expected after 2 additional stimulations with rIL2, 7 days apart. Nevertheless, we observed co-expression of CD8 and the proliferation marker KI67 in some SC after only 3 days. This was not the case in controls (Figure 6), suggesting that the capacity for T cell expansion was also maintained in TILs of HNSCC.

4.2 Tumor infiltrating T cells remain responsive after additional induction of mitochondrial dysfunction

To induce MitoDys in the TME of SC, we added FFCP/oligomycin A to force the cells into glycolysis. A combination of FFCP/oligomycin A inhibits OXPHOS and increases glycolysis in HNSCC tumor cells (17) and lymphocytes (39). Our observations confirmed that FFCP/oligomycin A increased apoptosis makers in HNSCC tumor cells, signifying effective MitoDys induction within the TME of HNSCC slice cultures. This effect was attenuated by high glucose concentration in the medium, indicating that glycolysis was effectively stimulated and that tumor cells used extracellular glucose to evade apoptosis under these glycolytic conditions. While FFCP/oligomycin A induced apoptosis in tumor cells, it had no effect on cytotoxic T cell effector function. The granzyme B response and tumor cell apoptosis under FCCP/oligomycin A conditions was comparable to that with T cell stimulation alone (Figures 3–5).

In Raji cells, a high glucose concentration in lymphocyte cultures under glycolytic conditions increased the cytotoxic T-cell response through mechanisms that are not yet fully understood (34). However, increasing glucose concentrations from 5.8 mmol/l to 25 mmol/l caused neither an increase in the granzyme B response nor an increase in the expression of the apoptosis marker CC3 in tumor cells (Figures 3, 4). *In vivo*, pro-cytotoxic effects of T cells may not increase via high glucose concentration, as it has been demonstrated in studies on mice (40). Furthermore, tumor cell apoptosis may not be affected by high glucose, due to its positive effects on tumor cells (41). The available tumor tissue was not sufficient to investigate the effect of a high glucose concentration on T-cell activation under FCCP/oligomycin A stress.

Using PD-1 expression, we investigated possible effects on T cell exhaustion, which is discussed as a possible cause for the failure of ICI therapy. We assume that PD-1 is only expressed on immune cells and not on HNSCC tumor cells. T cell activation increased PD-1 expression. Assuming that TILs in SC are constantly under metabolic stress, this supports reports that T cell stimulation under metabolic stress promotes T cell exhaustion (42). Interestingly, the upregulation of PD-1 may have been attenuated by FCCP/oligomycin A (Figure 6; p vs. T cell activation alone: 0.078), suggesting that PD-1 upregulation could be an OXPHOS-dependent process (10). There are several examples of persistently OXPHOS-dependent processes in lymphocytes that have largely switched to glycolysis after activation.

4.3 Limitations and perspectives

During the cultivation, staining and cutting of the SC, some samples were lost. Consequently, in some culture conditions, only 94 SC remained for analysis instead of the initially planned 101 SC. Co-expression of PD-1 and TIM-3 would have been a more specific indicator of T cell exhaustion than PD-1 expression alone (43). In this study, FCCP and oligomycin A significantly increased tumor cell apoptosis in HNSCC without affecting cytotoxic T cell function. A clinically suitable substitute for FCCP and oligomycin is IACS-010759 [48], is currently in clinical trials. This inhibitor blocks complex I in the mitochondria and could also have antitumor effects. Furthermore, SC are highly heterogeneous: Even within one individual, slice composition varies greatly.

5 Conclusions

Tumor infiltrating lymphocytes in SC of HNSCC could be activated and led to apoptosis of tumor cells. OXPHOS played a minimal role in the activation of TILs in SC of HNSCC. In contrast to some studies on cultured lymphocytes, a higher glucose concentration did not increase the cytotoxic T cell activity of TILs in HNSCC slice cultures. As in a previous study, slice cultures were found to be a useful model for the investigation of immune processes in the TME of HNSCC.

Data availability statement

The raw data supporting the conclusions of this article will be made available by the authors, without undue reservation.

Ethics statement

The studies involving humans were approved by Ethics Committee of the Medical University of Innsbruck. The studies were conducted in accordance with the local legislation and institutional requirements. The participants provided their written informed consent to participate in this study. Written informed consent was obtained from the individual(s) for the publication of any potentially identifiable images or data included in this article.

Author contributions

MG: Conceptualization, Data curation, Formal Analysis, Investigation, Methodology, Project administration, Writing – original draft, Writing – review & editing, Visualization. AnR: Conceptualization, Data curation, Formal Analysis, Funding acquisition, Investigation, Methodology, Project administration, Writing – original draft, Writing – review & editing. JD: Conceptualization, Data curation, Formal Analysis, Investigation, Methodology, Project administration, Resources, Supervision, Validation, Writing – original draft, Writing – review & editing. RH: Data curation, Formal Analysis, Writing – original draft, Writing – review & editing, Methodology. MS: Data curation, Formal Analysis, Writing – original draft, Writing – review & editing, Methodology. DD: Data curation, Formal Analysis, Writing – original draft, Writing – review & editing. TS: Conceptualization, Data curation, Formal Analysis, Writing – original draft, Writing – review & editing. JF: Conceptualization, Data curation, Formal Analysis, Writing – original draft, Writing – review & editing, Resources. CS: Data curation, Formal Analysis, Methodology, Resources, Writing – original draft, Writing – review & editing. MK: Writing – original draft, Writing – review & editing, Supervision, Conceptualization. SuS: Investigation, Visualization, Writing – original draft, Writing – review & editing, Conceptualization, Methodology. SS: Writing – original draft, Writing – review & editing, Conceptualization. AvR: Writing – original draft, Writing – review & editing, Formal Analysis, Validation. MM: Conceptualization, Formal Analysis, Methodology, Resources, Writing – original draft, Writing – review & editing. BH: Conceptualization, Resources, Supervision, Writing – original draft, Writing – review & editing. HR: Conceptualization, Formal Analysis, Funding acquisition, Methodology, Supervision, Validation, Writing – original draft, Writing – review & editing, Data curation.

Funding

The author(s) declare financial support was received for the research, authorship, and/or publication of this article. This research project was financially funded by ViraTherapeutics GmbH. Acquisition, Production and set up as described in this paper was established in cooperation with ViraTherapeutics GmbH. However, this funder did not influence in the study design, collection, analysis, and interpretation of data, the writing of this article or the decision to submit it for publication.

Conflict of interest

Author MM is employed by ViraTherapeutics GmbH. Author SuS is employed by INNPATH GmbH, Institute for Pathology.

The remaining authors declare that the research was conducted in the absence of any commercial or financial relationships that could be construed as a potential conflict of interest.

Publisher's note

Supplementary material

The Supplementary Material for this article can be found online at: https://www.frontiersin.org/articles/10.3389/fonc.2024.1364577/full#supplementary-material

References

1. Johnson DE, Burtness B, Leemans CR, Lui VWY, Bauman JE, Grandis JR. Head and neck squamous cell carcinoma. *Nat Rev Dis Primers*. (2020) 6:92. doi: 10.1038/s41572-020-00224-3

2. Karpathiou G, Vieville M, Gavid M, Camy F, Dumollard JM, Magné N, et al. Prognostic significance of tumor budding, tumor-stroma ratio, cell nests size, and stroma type in laryngeal and pharyngeal squamous cell carcinomas. *Head Neck*. (2019) 41:1918–27. doi: 10.1002/hed.25629

3. Hendry S, Salgado R, Gevaert T, Russell PA, John T, Thapa B, et al. Assessing tumor-infiltrating lymphocytes in solid tumors: A practical review for pathologists and proposal for a standardized method from the international immunooncology biomarkers working group: part 1: assessing the host immune response, TILs in invasive breast carcinoma and ductal carcinoma *in situ*, metastatic tumor deposits and areas for further research. *Adv Anat Pathol*. (2017) 24:235–51. doi: 10.1097/PAP.0000000000000162

4. Idel C, Ribbat-Idel J, Klapper L, Krupar R, Bruchhage KL, Dreyer E, et al. Spatial distribution of immune cells in head and neck squamous cell carcinomas. *Front Oncol*. (2021) 11:712788. doi: 10.3389/fonc.2021.712788

5. Farlow JL, Brenner JC, Lei YL, Chinn SB. Immune deserts in head and neck squamous cell carcinoma: A review of challenges and opportunities for modulating the tumor immune microenvironment. *Oral Oncol*. (2021) 120:105420. doi: 10.1016/j.oraloncology.2021.105420

6. Desbois M, Wang Y. Cancer-associated fibroblasts: Key players in shaping the tumor immune microenvironment. *Immunol Rev*. (2021) 302:241–58. doi: 10.1111/imr.12982

7. Dong H, Strome SE, Salomao DR, Tamura H, Hirano F, Flies DB, et al. Tumor-associated B7-H1 promotes T-cell apoptosis: a potential mechanism of immune evasion. *Nat Med*. (2002) 8:793–800. doi: 10.1038/nm730

8. Schneider S, Kadletz L, Wiebringhaus R, Kenner L, Selzer E, Füreder T, et al. PD-1 and PD-L1 expression in HNSCC primary cancer and related lymph node metastasis - impact on clinical outcome. *Histopathology*. (2018) 73:573–84. doi: 10.1111/his.13646

9. Burtness B, Harrington KJ, Greil R, Soulieres D, Tahara M, de Castro G Jr., et al. Pembrolizumab alone or with chemotherapy versus cetuximab with chemotherapy for recurrent or metastatic squamous cell carcinoma of the head and neck (KEYNOTE-048): a randomised, open-label, phase 3 study. *Lancet*. (2019) 394:1915–28. doi: 10.1016/S0140-6736(19)32591-7

10. Scharping NE, Rivadeneira DB, Menk AV, Vignali PDA, Ford BR, Rittenhouse NL, et al. Mitochondrial stress induced by continuous stimulation under hypoxia rapidly drives T cell exhaustion. *Nat Immunol*. (2021) 22:205–15. doi: 10.1038/s41590-020-00834-9

11. Liu X, Peng G. Mitochondria orchestrate T cell fate and function. *Nat Immunol*. (2021) 22:276–8. doi: 10.1038/s41590-020-00861-6

12. Chow A, Perica K, Klebanoff CA, Wolchok JD. Clinical implications of T cell exhaustion for cancer immunotherapy. *Nat Rev Clin Oncol*. (2022) 19:775–90. doi: 10.1038/s41571-022-00689-z

13. Vardhana SA, Hwee MA, Berisa M, Wells DK, Yost KE, King B, et al. Impaired mitochondrial oxidative phosphorylation limits the self-renewal of T cells exposed to persistent antigen. *Nat Immunol*. (2020) 21:1022–33. doi: 10.1038/s41590-020-0725-2

14. Yu YR, Imrichova H, Wang H, Chao T, Xiao Z, Gao M, et al. Disturbed mitochondrial dynamics in CD8(+) TILs reinforce T cell exhaustion. *Nat Immunol*. (2020) 21:1540–51. doi: 10.1038/s41590-020-0793-3

15. Cham CM, Driessens G, O'Keefe JP, Gajewski TF. Glucose deprivation inhibits multiple key gene expression events and effector functions in CD8+ T cells. *Eur J Immunol*. (2008) 38:2438–50. doi: 10.1002/eji.200838289

16. Thommen DS, Schumacher TN. T cell dysfunction in cancer. *Cancer Cell*. (2018) 33:547–62. doi: 10.1016/j.ccell.2018.03.012

17. Greier MC, Runge A, Dudas J, Pider V, Skvortsova II, Savic D, et al. Mitochondrial dysfunction and epithelial to mesenchymal transition in head neck cancer cell lines. *Sci Rep*. (2022) 12:13255. doi: 10.1038/s41598-022-16829-5

18. Tinhofer I, Braunholz D, Klinghammer K. Preclinical models of head and neck squamous cell carcinoma for a basic understanding of cancer biology and its translation into efficient therapies. *Cancers Head Neck*. (2020) 5:9. doi: 10.1186/s41199-020-00056-4

19. Jiang X, Seo YD, Sullivan KM, Pillarisetty VG. Establishment of slice cultures as a tool to study the cancer immune microenvironment. *Methods Mol Biol*. (2019) 1884:283–95. doi: 10.1007/978-1-4939-8885-3_20

20. Kenerson HL, Sullivan KM, Seo YD, Stadeli KM, Ussakli C, Yan X, et al. Tumor slice culture as a biologic surrogate of human cancer. *Ann Trans Med*. (2020) 8:114. doi: 10.21037/atm

21. Greier MDC, Runge A, Dudas J, Carpentari L, Schartinger VH, Randhawa A, et al. Optimizing culturing conditions in patient derived 3D primary slice cultures of head and neck cancer. *Front Oncol*. (2023) 13:1145817. doi: 10.3389/fonc.2023.1145817

22. Runge A, Mayr M, Schwaiger T, Sprung S, Chetta P, Gottfried T, et al. Patient-derived head and neck tumor slice cultures: a versatile tool to study oncolytic virus action. *Sci Rep*. (2022) 12:15334. doi: 10.1038/s41598-022-19555-0

23. Ecker RC, Steiner GE. Microscopy-based multicolor tissue cytometry at the single-cell level. *Cytometry A*. (2004) 59:182–90. doi: 10.1002/cyto.a.20052

24. Giotakis AI, Dudas J, Glueckert R, Dejaco D, Ingruber J, Fleischer F, et al. Characterization of epithelial cells, connective tissue cells and immune cells in human upper airway mucosa by immunofluorescence multichannel image cytometry: a pilot study. *Histochem Cell Biol*. (2020) 155:405–21. doi: 10.1007/s00418-020-01945-y

25. Ingruber J, Dudas J, Sprung S, Lungu B, Mungenast F. Interplay between partial EMT and cisplatin resistance as the drivers for recurrence in HNSCC. *Biomedicines*. (2022) 10(10):2482. doi: 10.3390/biomedicines10102482

26. Sharma SJ, Linke JJ, Kroll T, Wuerdemann N, Klussmann JP, Guntinas-Lichius O, et al. Rigid triple endoscopy improves clinical staging of primary head and neck cancer. *Oncol Res Treat*. (2018) 41:35–8. doi: 10.1159/000481173

27. Fischer N, Mathonia NM, Hoellerich G, Veser J, Pinggera L, Dejaco D, et al. Surviving murine experimental sepsis affects the function and morphology of the inner ear. *Biol Open*. (2017) 6:732–40. doi: 10.1242/bio.024588

28. Steinbichler TB, Dudas JA-O, Ingruber J, Glueckert R, Sprung S, Fleischer F, et al. Slug is A surrogate marker of epithelial to mesenchymal transition (EMT) in head and neck cancer. *J Clin Med*. (2020) 9(7):2061. doi: 10.3390/jcm9072061

29. Nicholson DW, Ali A, Thornberry NA, Vaillancourt JP, Ding CK, Gallant M, et al. Identification and inhibition of the ICE/CED-3 protease necessary for mammalian apoptosis. *Nature*. (1995) 376:37–43. doi: 10.1038/376037a0

30. Voskoboinik I, Whisstock JC, Trapani JA. Perforin and granzymes: function, dysfunction and human pathology. *Nat Rev Immunol*. (2015) 15:388–400. doi: 10.1038/nri3839

31. The Cancer Genome Atlas Network. Comprehensive genomic characterization of head and neck squamous cell carcinomas. *Nature*. (2015) 517:576–82. doi: 10.1038/nature14129

32. Verma NK, Wong BHS, Poh ZS, Udayakumar A, Verma R, Goh RKJ, et al. Obstacles for T-lymphocytes in the tumour microenvironment: Therapeutic challenges, advances and opportunities beyond immune checkpoint. *EBioMedicine*. (2022) 83:104216. doi: 10.1016/j.ebiom.2022.104216

33. Chang CH, Qiu J, O'Sullivan D, Buck MD, Noguchi T, Curtis JD, et al. Metabolic competition in the tumor microenvironment is a driver of cancer progression. *Cell*. (2015) 162:1229–41. doi: 10.1016/j.cell.2015.08.016

34. Zhu J, Yang W, Zhou X, Zophel D, Soriano-Baguet L, Dolgener D, et al. High glucose enhances cytotoxic T lymphocyte-mediated cytotoxicity. *Front Immunol*. (2021) 12:689337. doi: 10.3389/fimmu.2021.689337

35. Pearce EL, Pearce EJ. Metabolic pathways in immune cell activation and quiescence. *Immunity*. (2013) 38:633–43. doi: 10.1016/j.immuni.2013.04.005

36. Bondeson K, McCabe M. Apparent heterogeneity between leukemic lymphocyte cell lines. *Adv Exp Med Biol*. (1992) 316:393–8. doi: 10.1007/978-1-4615-3404-4_44

37. Idrisova KF, Simon HU, Gomzikova MO. Role of patient-derived models of cancer in translational oncology. *Cancers (Basel)*. (2022) 15:139. doi: 10.3390/cancers15010139

38. Abdelaal HM, Kim HO, Wagstaff R, Sawahata R, Southern PJ, Skinner PJ. Comparison of Vibratome and Compresstome sectioning of fresh primate lymphoid and genital tissues for in *situ* MHC-tetramer and immunofluorescence staining. *Biol Proced Online*. (2015) 17:2. doi: 10.1186/s12575-014-0012-4

39. van der Windt GJW, Chang CH, Pearce EL. Measuring bioenergetics in T cells using a seahorse extracellular flux analyzer. *Curr Protoc Immunol*. (2016) 113:3.16b.1–3.b.4. doi: 10.1002/0471142735.im0316bs113

40. Recino A, Barkan K, Wong FS, Ladds G, Cooke A, Wallberg M. Hyperglycaemia does not affect antigen-specific activation and cytolytic killing by CD8(+) T cells in *vivo*. *Biosci Rep*. (2017) 37(4):BSR20171079. doi: 10.1042/BSR20171079

41. Li W, Zhang X, Sang H, Zhou Y, Shang C, Wang Y, et al. Effects of hyperglycemia on the progression of tumor diseases. *J Exp Clin Cancer Res*. (2019) 38:327. doi: 10.1186/s13046-019-1309-6

42. Wu H, Zhao X, Hochrein SM, Eckstein M, Gubert GF, Knopper K, et al. Mitochondrial dysfunction promotes the transition of precursor to terminally exhausted T cells through HIF-1alpha-mediated glycolytic reprogramming. *Nat Commun*. (2023) 14:6858. doi: 10.1038/s41467-023-42634-3

43. Jenkins E, Whitehead T, Fellermeyer M, Davis SJ, Sharma S. The current state and future of T-cell exhaustion research. *Oxf Open Immunol*. (2023) 4:iqad006. doi: 10.1093/oxfimm/iqad006

frontiers | Frontiers in Immunology

TYPE Review
PUBLISHED 13 March 2024
DOI 10.3389/fimmu.2024.1344272

OPEN ACCESS

EDITED BY
Mazdak Ganjalikhani Hakemi,
Isfahan University of Medical Sciences, Iran

REVIEWED BY
Muzamil Y. Want,
Children's Hospital of Philadelphia,
United States
Vida Homayouni,
Isfahan University of Medical Sciences, Iran

*CORRESPONDENCE
Guoan Xiang
guoanx_fimmu_edu@163.com
Jin Gong
zaitushuguan@163.com
Zhen Bao
baozhenjnu@126.com

†These authors have contributed equally to this work

RECEIVED 25 November 2023
ACCEPTED 26 February 2024
PUBLISHED 13 March 2024

CITATION
Ouyang P, Wang L, Wu J, Tian Y, Chen C, Li D, Yao Z, Chen R, Xiang G, Gong J and Bao Z (2024) Overcoming cold tumors: a combination strategy of immune checkpoint inhibitors.
Front. Immunol. 15:1344272.
doi: 10.3389/fimmu.2024.1344272

Overcoming cold tumors: a combination strategy of immune checkpoint inhibitors

Peng Ouyang[1†], Lijuan Wang[2†], Jianlong Wu[1†], Yao Tian[1], Caiyun Chen[1], Dengsheng Li[1], Zengxi Yao[1], Ruichang Chen[1], Guoan Xiang[3*], Jin Gong[1*] and Zhen Bao[1*]

[1]Department of General Surgery, The First Affiliated Hospital of Jinan University, Guangzhou, Guangdong, China, [2]Department of Pathophysiology, School of Medicine, Jinan University, Guangzhou, Guangdong, China, [3]Department of General Surgery, Guangdong Second Provincial General Hospital, Guangzhou, Guangdong, China

Immune Checkpoint Inhibitors (ICIs) therapy has advanced significantly in treating malignant tumors, though most 'cold' tumors show no response. This resistance mainly arises from the varied immune evasion mechanisms. Hence, understanding the transformation from 'cold' to 'hot' tumors is essential in developing effective cancer treatments. Furthermore, tumor immune profiling is critical, requiring a range of diagnostic techniques and biomarkers for evaluation. The success of immunotherapy relies on T cells' ability to recognize and eliminate tumor cells. In 'cold' tumors, the absence of T cell infiltration leads to the ineffectiveness of ICI therapy. Addressing these challenges, especially the impairment in T cell activation and homing, is crucial to enhance ICI therapy's efficacy. Concurrently, strategies to convert 'cold' tumors into 'hot' ones, including boosting T cell infiltration and adoptive therapies such as T cell-recruiting bispecific antibodies and Chimeric Antigen Receptor (CAR) T cells, are under extensive exploration. Thus, identifying key factors that impact tumor T cell infiltration is vital for creating effective treatments targeting 'cold' tumors.

KEYWORDS

cold tumors, immune checkpoint inhibitors, tumor-infiltrating T lymphocytes, tumor microenvironment, immunotherapy

1 Introduction

In recent years, Immune Checkpoint Inhibitors (ICIs) have increasingly been incorporated into the treatment of various cancers, becoming a standard part of oncological treatment guidelines. However, a significant proportion of cancer patients still exhibit poor responses to ICI therapy. This trend highlights a need for further research

and development in personalized cancer treatment strategies to improve outcomes for this patient subset (1, 2). In patients with solid tumors, 'hot' tumors ('immune- inflamed') often show a favorable response to ICIs, characterized by extensive lymphocyte infiltration in the tumor parenchyma. In contrast, 'cold' tumors exhibit a poorer response to ICIs. These tumors are marked by an inability of T cells to penetrate the tumor parenchyma, remaining instead in the tumor stroma ('immune-excluded') or by a lack of T cell infiltration in both the tumor parenchyma and stroma ('immune-desert') (3). This distinction underscores the importance of understanding tumor immunology to optimize ICIs therapy efficacy. However, increasing evidence suggests that not all tumors with high T cell infiltration exhibit favorable responses to ICIs. Conversely, some tumors with low T cell infiltration may also demonstrate good responsiveness to ICIs. This observation indicates a more complex relationship between T cell infiltration levels and ICI response, underscoring the need for a deeper understanding of tumor immunobiology to effectively predict and enhance ICIs therapy outcomes (4–6). These findings indicate that T cell infiltration might be necessary, but additional factors may be required for precisely identifying the responsiveness to ICIs. Currently, the treatment of 'cold' tumors remains a significant challenge. In this review, we discuss the definitions of 'cold' and 'hot' tumors, as well as the challenges the immune system may encounter at different stages of the cancer immunity cycle. We also describe therapeutic approaches combining ICIs with other strategies to overcome 'cold' tumors. This integrative approach aims to enhance the understanding and treatment efficacy of tumors with varying immune characteristics.

Abbreviations: CAFs, cancer-associated fibroblasts; CCR5,C-C motif chemokine receptor 5; cDC1, type 1 classical DC; cDC2, type 2 classical DC; CI, confidence interval; CPS, combined positive score; CRC, colorectal cancer; CRT, calreticulin; cSCC, cutaneous squamous cell carcinoma; CSF-1R, colony-stimulating factor 1 receptor; CTLs, cytotoxic T-lymphocytes; CXCR3, CXC-chemokine receptor 3; DCs, dendritic cells; dMMR, defective mismatch repair; DNMT1, DNA methyltransferase 1; ECM, extracellular matrix; EPR, enhanced permeability and retention effect; ETBR, endothelin B receptor; EZH2, enhancer of zeste homologue 2; FasL, Fas ligand; GBM, glioblastoma multiforme; HLA-I LOH, HLA-I loss of heterozygosity; HR, hazard ratio; ICD, immunogenic cell death; ICIs, immune checkpoint inhibitors; mCRPC, metastatic castration-resistant prostate cancer; MDSCs, myeloid-derived suppressor cells; mIF, multiplex immunofluorescence; MIS-H, high microsatellite instability; MMRp, mismatch repair proficient; NK, natural killer; NSCLC, unresectable non-small cell lung cancer; NSSMs, nonsynonymous somatic mutations; ORR, objective response rate; OS, overall survival; OV, oncolytic viruses; PD-1, programmed death-1; PDAC, pancreatic ductal carcinoma; pDCs, plasmacytoid DCs; PFS, progressionfree survival; PRC2, polycomb repressive complex 2; RNS, reactive nitrogen species; scRNA-seq, single-cell RNA sequencing; sGSN, secreted gelsolin; TAAs, tumor-associated antigens; TAMs, tumor-associated macrophages; VCAM-1, vascular cell adhesion protein 1; TCR, T cell receptor; VEGF, vascular endothelial growth factor; TGFβ, transforming growth factor β; Th1, type 1 helper T cells; Th2, type 2 helper T cells; TILs, tumor-infiltrating T lymphocytes; TMB, tumor mutational burden; TME, tumor microenvironment; TNBC, triplenegative breast cancer; Treg, regulatory T cells; TSAs, tumor-specific antigens; TVEC, Talimogene laherparepvec.

2 Definition of "cold" and "hot" tumors

The concept of 'cold' and 'hot' tumors is not new in the field of oncology. It was first described in 2006 by Galon et al. in their publication on the relationship between immune cell types, density, and distribution with the prognosis of colorectal cancer. This seminal work introduced the idea of classifying tumors as 'hot' or 'cold' based on the type, density, and distribution of immune cells within the tumor microenvironment. They posited that this immune-based classification in colorectal cancer could provide a more accurate prognosis assessment than the traditional TNM staging system. This approach underlines the significant role of the immune landscape in understanding and predicting cancer progression (7). In 2007, Galon and colleagues proposed the concept of "immune contexture" based on immunoscore (8). Following this, in 2009, Camus et al. first described three immune coordination profiles (hot, altered, and cold) in primary colorectal cancer (CRC), balancing tumor escape and immune coordination (9). Building on these works, researchers introduced the immunoscore, which assesses the infiltration of lymphocyte populations (CD3 and CD8) in the tumor core and at its margin. The score ranges from immunoscore 0 (I0, low-density CD3 and CD8 stained cells in the tumor center and periphery) to immunoscore 4 (I4, high-density CD3 and CD8 stained cells in these regions) (10, 11). This scoring system classifies cancer based on immune infiltration and introduces the concepts of 'hot' tumors (I4) and 'cold' tumors (I0-I3). As research progressed, the characteristics of hot tumors were expanded to include the presence of tumor-infiltrating lymphocytes (TILs), expression of programmed death-ligand 1 (PD-L1) on tumor-associated immune cells, and a high tumor mutational burden. Conversely, cold tumors, characterized by poor infiltration, also feature low or negligible PD-L1 expression, high proliferation rates, and a low tumor mutational burden (12).

3 Mechanisms of immune escape in "cold" tumors

Immune checkpoints encompass a group of receptors expressed by immune cells, facilitating the dynamic regulation of immune homeostasis. They hold particular relevance for the functioning of T cells. Among these checkpoints, PD-1 and its primary ligand PD-L1 find expression on T cells, tumor cells, and myeloid cells infiltrating tumors. The interaction between PD-1 and PD-L1 leads to $CD8^+$ T cell exhaustion, a potentially irreversible state of dysfunction characterized by diminished or absent effector functions (including cytotoxicity and cytokine production), reduced responsiveness to stimuli, and altered transcriptional and epigenetic profiles (13, 14). Tumor cells exploit this interaction to establish immune tolerance. However, it also serves essential physiological roles, such as limiting autoimmune inflammation, preserving fetal tolerance during pregnancy, and preventing the rejection of transplanted organs (15). Immune checkpoint inhibitors function by blocking immune checkpoints, thus

restoring the anti-tumor activity of CD8+ T cells. Immune checkpoint inhibitors function by blocking immune checkpoints, thus restoring the anti-tumor activity of CD8+ T cells. Any failures during the stages of T cell activation, homing, or infiltration into the tumor bed in the tumor immune process can result in inadequate T cell infiltration into the tumor core (Figure 1). This, in turn, leads to resistance to ICIs therapy.

3.1 Lack of tumor antigens

Tumor antigens can be categorized into two main types: Tumor-specific antigens (TSAs) and Tumor-associated antigens (TAAs) (16). TAAs are antigens that, while not exclusive to tumor cells, are present in normal cells and other tissues but are significantly elevated during cellular transformation into cancer. These antigens exhibit quantitative changes without strict tumor specificity. Although they can also trigger immune responses, the most crucial in activating immune responses are neoantigens, also known as TSAs. TSAs are antigens unique to tumor cells or present only in certain tumor cells and not in normal cells. This includes antigens produced by oncogenic viruses integrated into the genome and those arising from mutant proteins (17). In addition to mutations in DNA coding regions, gene fusions (18), mutations in non-coding regions (19), and alternative splicing (20) can also generate neoantigens. Loss of DNA damage response can lead to gene mutations, including mismatch repair deficiencies (dMMR) and microsatellite instability (MSI) (21). Currently, ICIs treatment has become the preferred therapy for advanced colorectal cancer with high microsatellite instability (22). Therefore, the recognition of TSAs plays a key role in activating T cells and promoting their infiltration into tumor tissues.

Tumor Mutational Burden (TMB) refers to the number of nonsynonymous single nucleotide mutations found in tumor cells. A high TMB implies more mutations, leading to the generation of more TSAs. Research over the past five years has shown that tumors with high TMB respond better to ICIs treatment than those with low TMB (23). McGrail et al. found that in cancers characterized by recurrent mutations, neoantigens are positively correlated with TILs infiltration (24). However, in tumors characterized by recurrent copy number variations, there is no correlation between TILs infiltration and the neoantigen load (24). Spranger et al. found no association between T cell infiltration and nonsynonymous somatic mutations (NSSMs) (25). These studies indicate that the lack of T cell infiltration cannot be solely explained by TMB.

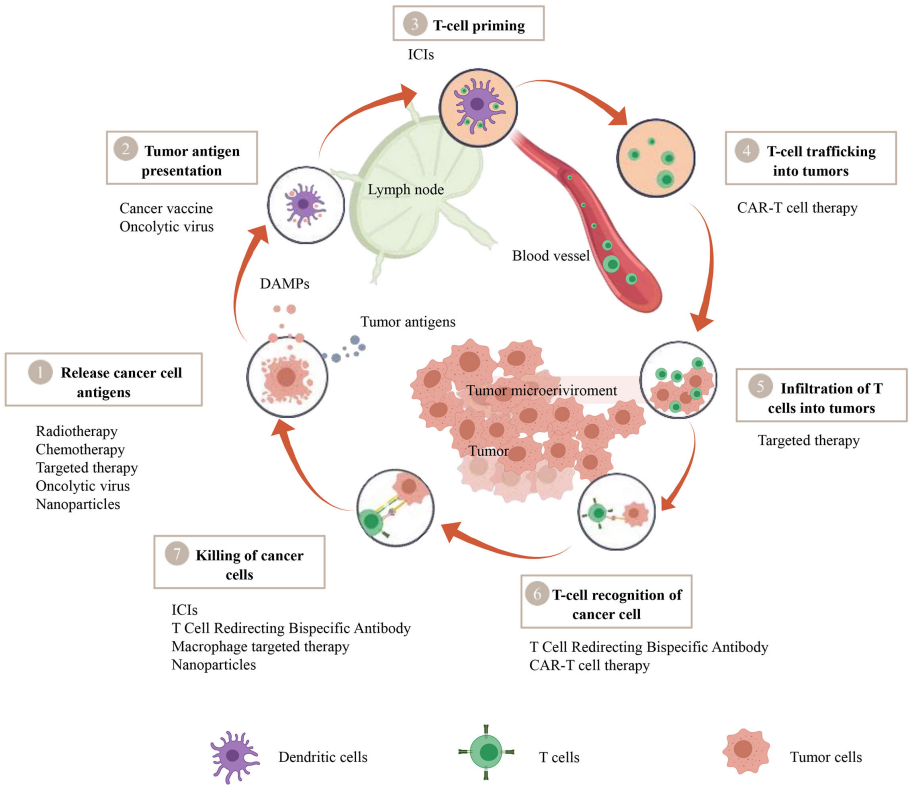

FIGURE 1
A therapeutic strategy to convert cold tumors into hot tumors based on tumor immune cycle. The cancer-immunity cycle encapsulates seven pivotal steps, with each one being integral to the overall mechanism. A malfunction or inefficiency at any juncture can potentially instigate the tumor to evade the immune response. Nevertheless, a wide array of therapeutic approaches such as Chimeric Antigen Receptor T-cell (CAR-T) therapy, T-cell Redirecting Bispecific Antibodies, cancer vaccines, oncolytic viruses, macrophage-targeted therapies, radiotherapy, chemotherapy, targeted therapies, and nanoparticle-assisted treatments manifest their potential to modulate this cycle, thereby amplifying the body's defensive reaction against tumors.

3.2 Defective antigen presentation

Dendritic cells (DCs) are pivotal in the antigen presentation process. They play a critical role in initiating anti-tumor immune responses by capturing and processing tumor antigens, conducting cross-presentation, and activating naive T cells. There are multiple subgroups of DCs, including classical DCs (type 1 cDC1 and type 2 cDC2), plasmacytoid DCs (pDCs), inflammatory DCs, and Langerhans cells. Each subgroup plays a distinct role in immune responses (26). In tumor immunology, DCs are often activated by "danger signals" such as Damage-Associated Molecular Patterns (DAMPs), including ATP, HMGB1, Calreticulin (CRT), and the S100 protein family (27). Among the different DCs subtypes, cDC1s are particularly crucial in tumor immunity. Studies show that Batf3-knockout mice, which lack cDC1s, exhibit reduced TILs and decreased responsiveness to ICIs (28). Research on tumor-bearing mice indicates that cDC1s are essential for reactivating circulating memory anti-tumor T cells and responding to ICIs (29). Tumors can evade detection by DCs through various mechanisms, such as expressing the "don't eat me" signal CD47 (30). Tumor cells also avoid exposing DAMPs, such as CRT, by expressing inflammatory molecules like A20 (31) in CRC, STC1 (32) in certain tumors, and glycosylated B7-H4 (33) in breast cancer. cDC1s cross-present antigens from dying tumor cells, which is fundamental in initiating anti-cancer CD8+ T cell responses. cDC1s express high levels of DNGR-1 (also known as CLEC9A), a receptor that binds to exposed F-actin in dying tumor cells and facilitates antigen cross-presentation. Tumor cells can inhibit this process by secreting extracellular proteins like sGSN, reducing the binding between DNGR-1 and F-actin, thus preventing cDC1s from activating CD8+ T cells (34).

HLA-I Loss of Heterozygosity (HLA-I LOH) is a significant mechanism of immune escape, with approximately 17% of tumors exhibiting HLA-I LOH (35, 36). TRAF3, a factor that inhibits NF-κB activity, negatively regulates the expression of MHC-I. Lower levels of TRAF3 are associated with better responses to ICIs) (37). Notably, MHC-I on the surface of Pancreatic Ductal Adenocarcinoma (PDAC) cells is degraded through autophagy. Inhibiting autophagy can restore MHC-I levels on the surface of PDAC cells. In mouse models of PDAC, combining autophagy inhibitors with dual ICIs enhances the immune response against the tumor (38). Therefore, increasing the expression of HLA-I on tumor cells' surface could be a potential strategy for treating 'cold' tumors.

3.3 T lymphocytes are unable to infiltrate the tumor bed through the blood circulation

3.3.1 Dysregulation of chemokines and cytokines

Chemokines in the TME mediate the recruitment of various immune cells, including T cells, thereby influencing tumor immunity and treatment outcomes. Dysregulation of chemokines within the TME often promotes tumor progression by altering the infiltration of immune cells. For instance, effector CD8+ T cells, Th1 cells, and NK cells can migrate into the tumor in response to chemokines like CXCL9 and CXCL10, facilitated by their shared expression of the CXC chemokine receptor 3 (CXCR3) (39). Enhancer of zeste homologue 2 (EZH2) and DNA methyltransferase 1 (DNMT1) reduce the presence of effector T cells in tumors by inhibiting the production of CXCL9 and CXCL10 by Th1 cells (40). In colorectal cancer, the polycomb repressive complex 2 (PRC2) similarly suppresses the production of these chemokines by Th1 cells, thereby diminishing the entry of effector T cells into the tumor (41). Additionally, the expression of CCL5 is associated with the infiltration of CD8+ T cells, while DNA methylation leads to reduced expression of CCL5, consequently decreasing TILs (42). Reactive nitrogen species (RNS) produced in the TME can also induce nitration of CCL2, impeding T cell infiltration (43).

Cytokines significantly impact tumor cell development and the treatment outcomes of ICIs. For instance, in urothelial cancer, combining Transforming Growth Factor β (TGF-β) blockade with ICIs therapy has been shown to promote T cell infiltration into the tumor core and elicit strong anti-tumor immune responses (44). Similarly, in colorectal cancer, inhibiting TGF-β increases the number of cytotoxic T cells, thereby inhibiting tumor metastasis (45). Additionally, Interferon γ (IFNγ), Interleukin-2 (IL-2), and Interleukin-9 (IL-9) also play crucial roles in the efficacy of ICIs treatment (46).

3.3.2 Immune cell–mediated immunosuppression

Within the tumor microenvironment, tumor cells interact with various immune cells that have immunosuppressive functions, particularly regulatory T cells (Tregs), myeloid-derived suppressor cells (MDSCs), and tumor-associated macrophages (TAMs), playing a crucial role in the regulation of tumor development and progression (47, 48).

Tregs, initially identified as thymus-derived immunosuppressive cells among $CD4^+$ T cells with a high expression of CD25 in mice (49), and later described in humans (50–52), gained recognition in the field of immunology. The discovery of Foxp3, a master regulator of Tregs, firmly established this population as an independent immunosuppressive cell lineage within $CD4^+$ T cells (53–55). In current classification, Tregs are divided into natural/thymic and peripherally induced subsets, based on the sites of their development (56–58). Hence, it becomes imperative to distinguish Tregs from FOXP3-expressing conventional T cells in humans. In human studies, FOXP3-expressing $CD4^+$ T cells are further categorized into three groups, depending on the expression of CD4, CD45RA, CD25, and/or FOXP3: 1) naive/resting Tregs, defined by $CD4^+CD45RA^+CD25^{low}FOXP3^{low}$ T cells; 2) effector/activated Treg (eTreg) cells, characterized by $CD4^+CD45RA^-CD25^{high}FOXP3^{high}$ T cells; and 3) non-Treg cells, identified as $CD4^+CD45RA^-CD25^{low}FOXP3^{low}$ T cells. Naive Tregs, initially displaying weak suppressive activity, have recently exited the thymus but remain quiescent in the periphery (59, 60). Upon TCR stimulation, naive

Tregs exhibit vigorous proliferation and differentiate into highly suppressive eTreg cells. In contrast, non-Treg cells lack immunosuppressive functions and instead produce inflammatory cytokines, including interferon (IFN)-γ and IL-17 (61). Treg cells play a crucial role in dampening antitumor immune responses, particularly those directed towards tumor-specific effector T cells (62). These Treg cells are attracted to the TME, where they undergo local proliferation and differentiation into an activated subset with potent suppressive capabilities (63). Importantly, the presence of a high frequency of Treg cells and an elevated ratio of Treg cells to effector T cells, such as CD8+ T cells, within the TME is consistently associated with an unfavorable prognosis among patients with various cancer types (64, 65). Eliminating Tregs from the tumor environment can thus potentiate the anti-tumor immune response. Moreover, a lower CD8+T/Treg ratio has been identified as a poor prognostic indicator for the effectiveness of anti-PD-1 monoclonal antibody treatments (66). Post-immunotherapy scenarios where there is no appreciable increase in T effector cells coupled with a decrease in Tregs, or a surge in Treg cells within the tumor matrix, are often indicative of resistance to PD-1/PD-L1 monoclonal antibody therapies.

MDSCs, a diverse group of cells, are known to inhibit effector T-cell responses and foster the development of Tregs (67). The efficacy of immunotherapy is often reduced in the presence of the tumor microenvironment (68). These MDSCs are induced in immature myeloid cells by external agents such as tumor-derived factors, and they disrupt the production, proliferation, migration, and activation of MDSCs. MDSCs facilitate tumor invasion and metastasis, predominantly through factors like Indoleamine 2,3-dioxygenase (IDO), Arginase-1 (ARG1), Reactive Oxygen Species (ROS), IL-10, Inducible Nitric Oxide Synthase (iNOS), Cyclooxygenase-2 (COX-2), and Nitric Oxide (NO) (69). Additionally, MDSCs can attract Tregs to the tumor microenvironment to augment immunosuppression. Studies also reveal that inhibiting PI3K can synergize with immunocheckpoint inhibitors. In models where PD-1 monoclonal antibody treatment was ineffective, PI3K inhibition reduced MDSC circulation and recruitment, curtailed the production of immunosuppressive factors like IL-10 and TGF-β, and enhanced the secretion of inflammatory mediators such as Interleukin-12 (IL-12) and Interferon-Gamma (INF-γ), mirroring the combined inhibitory effects on CTLA-4 and PD-1 monoclonal antibodies (70, 71). These findings suggest that PI3K inhibitors could serve as potential adjunctive therapies with PD-1/PD-L1 antibodies, particularly in overcoming single-agent drug resistance. In the metabolic context, MDSCs derive energy from arginine metabolism, primarily through ARG1. Impairment of ARG1 activity can diminish the inhibitory capacity of MDSCs, thereby heightening the sensitivity of tumors to PD-1/PD-L1 antibodies (72).

TAMs, another influential cell type in immunotherapy, consist of M1-like macrophages that bolster anti-tumor immunity and M2-like macrophages that promote cancer. PD-1 expression is more pronounced in M2-like macrophages compared to M1-like macrophages (73, 74), and an increase in PD-1+M2-like macrophages correlates with advanced disease stages, hinting at their progressive accumulation in the tumor microenvironment (75). M2-like macrophages aid in tumor cell immune evasion through PD-1 and are activated by cytokines such as IL-4, IL-10, IL-13, or Colony Stimulating Factor 1 (CSF1), engaging in wound healing, tissue repair, and anti-inflammatory responses through cytokines including IL-10 (76). They also promote tumor invasion and metastasis via angiogenesis and remodeling of the extracellular matrix (77). Clinical studies have correlated high levels of TAMs with poor outcomes in various cancers (78). Targeting the C-C Motif Chemokine Ligand 2 (CCL2) and C-C Motif Chemokine Receptor 2 (CCR2) pathways in a lung adenocarcinoma mouse model led to reduced recruitment of M2 macrophages and inhibited tumor growth (79). Notably, using macrophage Colony Stimulating Factor 1 Receptor (CSF-1R) blockers reduces TAM frequency, increases IFN production, and enhances tumor cell response to drugs in pancreatic cancer models. When combined with PD-1 or CTLA-4 antibodies, and gemcitabine, CSF-1R blockers demonstrated increased efficacy (80).

In conclusion, the heterogeneous nature of inhibitory immune cells within tumors, influenced by chemokines, cytokines, and colony-stimulating factors in the tumor microenvironment, limits the effectiveness of PD-1/PD-L1 blockers when used alone. Resistance to immune checkpoint blockade may be indicated by factors such as the CD8+/Treg ratio, IDO, ARG1, CSF-1R, and the M1/M2 ratio. Addressing these indicators through combined therapeutic strategies could lead to more effective clinical outcomes and prognoses. The concurrent use of drugs targeting immunosuppressive cells, including IDO inhibitors, ARG1 inhibitors, PI3K inhibitors, and ICIs, has shown promise in clinical trials, particularly when used in dual combinations, offering manageable side effects and good clinical compliance. However, the effectiveness of combinations involving three or more such agents remains less explored.

3.3.3 Vascular abnormalities and hypoxia

CD8+ T cells must enter the tumor core through the intratumoral vasculature (16). Their transport into tumor tissue depends on enhanced expression of adhesion molecules and chemokines in the tumor blood vessels, a process known as endothelial cell activation. However, poor activation of tumor blood vessels often leads to impaired transport of CD8+ T cells (81). Studies have shown that the absence of TILs is associated with overexpression of the endothelin B receptor (ETBR) (82). Tumor cells often promote angiogenesis by producing vascular endothelial growth factor (VEGF), which typically reduces the expression of vascular cell adhesion protein 1 (VCAM-1), thereby hindering T cell migration into the TME (83). Additionally, research indicates that Fas ligand (FasL, also known as CD95L) is selectively expressed in the vasculature of human and mouse tumors, whereas it is not expressed in normal vasculature. Expression of FasL enables endothelial cells to kill CD8+ T cells, but not Tregs (84). Tumors with poor vascularization, such as PDAC, due to their abnormal vascular structure and function, reduce the transport of immune cells and often exhibit high resistance to ICIs treatment (85).

Aberrant angiogenesis in tumors frequently precipitates conditions such as hypoxia, acidosis, and necrosis, subsequently impeding anti-tumor immune responses (86). Hypoxia, a defining

characteristic of cancer, arises from a disparity between oxygen consumption and supply within the tumor milieu. This is attributed to the voracious oxygen consumption by rapidly proliferating tumor cells, coupled with inadequate oxygen delivery due to dysfunctional vasculature (87). The impact of hypoxia on TILs is complex and wide-ranging. Notably, hypoxia can stimulate the expression of CCL28 (88), VEGF (86), CD39 (89, 90), and CD73 (89, 90). These molecules are instrumental in angiogenesis and modulate T cell mobilization.

3.3.4 Oncogenic pathway activation

In the field of oncology, the complex interplay between tumor cells and various signaling pathways is pivotal in shaping the tumor microenvironment (TME) and influencing therapy resistance. Tumor cells are known to hijack and modulate numerous pathways, notably including PKC, Notch, and TGF-β signaling. Recently, attention has also been drawn to the cyclic GMP–AMP synthase (cGAS)–stimulator of interferon genes (STING) and Siglec signaling pathways. These pathways play a critical role in sustaining a tumor-friendly microenvironment and fostering resistance to treatment, including multi-drug resistance.

3.3.4.1 Protein kinase C signaling

In oncology, the role of PKC isoforms in the TME is increasingly recognized as critical in determining tumor behavior. PKC, a family of serine/threonine kinases, serves as a signal transducer for various molecules including hormones, growth factors, cytokines, and neurotransmitters. These molecules are key regulators of cell survival, proliferation, differentiation, apoptosis, adhesion, and malignant transformation (91–93). The interaction of ligands with receptors can activate phospholipase C, thereby upregulating activators of PKC signaling like diacylglycerol (DAG) and Ca^{++} (94, 95), subsequently modulating several molecular pathways such as Akt, STAT3, NF-κB, and apoptotic pathways. Interestingly, different PKC isoforms play varying roles in tumorigenesis and metastasis (94). For instance, PKC alpha demonstrates antitumor activity by influencing the polarization of TAMs within the TME (96). Conversely, PKC theta has been shown to suppress tumors by inducing immune suppression through CTLA4-mediated regulatory T-cell function (97–99). However, other isoforms, like PKC beta, are known to facilitate angiogenesis and invasiveness in certain tumors via the VEGF signaling pathway (100–102). The complexity of PKC signaling is further evidenced by its dual role as both a tumor promoter and suppressor, depending on the isoform and the context. This dual role presents both challenges and opportunities for therapeutic interventions.

Recent advancements in cancer treatment strategies have explored the modulation of PKC signaling, utilizing activators like Bryostatins (103) and Epoxytiglianes (104–106), as well as inhibitors such as CGP 41251, to counteract tumor growth and reverse multidrug resistance (107).

3.3.4.2 PI3K-AKT-mTOR signaling pathway

The PI3K/AKT/mTOR signaling pathway, a pivotal regulator of cellular processes such as apoptosis, proliferation, movement, metabolism, and cytokine expression, plays a critical role in tumor development and resistance mechanisms, especially against PD-1/PD-L1 antibodies. Central to this pathway is the lipid phosphatase PTEN, a tumor suppressor that inhibits PI3K activity. PTEN deletion or mutation leads to the activation of PI3K/AKT and resistance to PD-1/PD-L1 in various cancers. PTEN's expression is regulated through diverse mechanisms, including epigenetic silencing, post-transcriptional and post-translational modifications, and protein-protein interactions (108). PTEN's downregulation is key in cancer progression, affecting cell energy metabolism, metabolic reprogramming of cancer cells, and influencing glucose uptake and protein synthesis. PTEN also plays a role in cell migration and senescence, with its loss leading to increased cell viability and promoting EMT and tumor cell migration (109). PTEN loss affects tumor immunotherapy, showing a correlation with resistance to immunotherapy, particularly impacting the tumor microenvironment (110). PTEN deficiency leads to downregulation of SHP-2, a negative regulator of JAK/STAT3 pathway, promoting tumor growth (111, 112). The loss of PTEN in certain cancers is associated with decreased T-cell function, increased VEGF production, and the release of anti-inflammatory cytokines, resulting in non-inflammatory tumors. Moreover, PTEN's role extends to regulating PD-L1 levels, with its absence or constitutive expression of the PI3K/AKT pathway influencing PD-L1 expression (113, 114). This interaction affects PD-1/PD-L1 antibody responses and is subject to modulation by various intracellular signaling pathways, including RAS/RAF/MEK and JAK/STAT, influenced by IFN-γ released by immune cells. Selective inhibition of PI3K has shown to enhance the therapeutic effect of PD-1/PD-L1 and CTLA-4 antibodies in experimental models, indicating potential in reversing resistance to immunocheckpoint inhibitors (115). Further clinical studies are warranted to explore this possibility.

3.3.4.3 TGF-β signaling

Transforming Growth Factor-Beta (TGF-β) plays a multifaceted role in the progression of cancer, affecting a variety of cellular processes including cell proliferation, angiogenesis, epithelial-to-mesenchymal transition, immune infiltration, metastatic dissemination, and drug resistance (116). Interestingly, TGF-β produced by tumor cells can alter the function of tumor-associated plasmacytoid dendritic cells (pDCs), particularly affecting their ability to produce Type I interferon, thereby impacting T cell recruitment (117, 118). This aspect of TGF-β signaling is crucial in understanding its role in excluding T cells from the TME.

Recently, the combined use of TGF-β blocking antibodies with PD-L1 antibodies has been proven effective in enhancing T cell penetration into tumors, boosting anti-tumor immunity, and leading to tumor regression (44). Additionally, TGF-β signaling plays a dual role in cancer progression. Initially, it acts as a tumor suppressor by inhibiting cell proliferation and inducing apoptosis (119). However, as malignancies progress, cancer cells exploit TGF-β signaling to create a favorable TME, activating CAFs, promoting angiogenesis, and suppressing anti-tumor immune responses (120–122). Given its complex role, the side effects of targeting TGF-β signaling in therapeutic interventions are also a concern.

3.3.4.4 cGAS-STING signaling

Recent advancements in cancer research have increasingly focused on the cGAS-STING signaling pathway and its role in tumor progression. Analysis of The Cancer Genome Atlas (TCGA) database, which classifies 18 different types of malignant tumors, has revealed variations in the expression of key genes involved in the cGAS-STING signaling mechanism between normal and cancerous tissues. These include genes encoding cGAS (MB21D1), STING (TMEM-173), TBK-1, and IRF-3. Studies have found that these genes are significantly upregulated in nearly all cancer models, indicating a possible universal activation of cGAS-STING signaling in various cancer types (123, 124). Interestingly, some highly invasive tumors seem to rely on the cGAS-STING pathway to facilitate tumorigenesis, impacting cancer treatment approaches (125, 126). The NF-κB pathway, known for regulating cell proliferation, apoptosis, and survival, also plays a vital role in the inflammatory response. Its activation can contribute to inflammation, tumor development, and immune dysfunction. Chromosomal instability can lead to chronic inflammation by persistently activating the cGAS-STING pathway, which in turn enhances NF-κB function and promotes the progression of metastatic cancer cells (126, 127).

Furthermore, TCGA data analysis has demonstrated a negative correlation between STING expression levels in cancer and the infiltration of immune cells in various tumor models. This suggests that an increase in cGAS-STING signaling may predict poorer outcomes in cancer patients (123). Additionally, certain tumor cells promote brain metastasis by enhancing astrocyte-gap junctions through the expression of PCDH7 (composed of Cx43). These junctions transfer cGAMP from cancer cells to adjacent astrocytes, activating STING and triggering the production of TNF and IFN-α. These paracrine signals further activate NF-κB and STAT-1 pathways in metastatic brain cells, contributing to brain metastasis and resistance to lung and breast cancer therapies (128).

4 Therapeutic strategies for cold tumors

4.1 Dual ICIs

4.1.1 α–CTLA–4 combined with α–PD–1/PD–L1

T cell activation requires two essential signals: the T cell receptor (TCR) and costimulatory pathways (129). Numerous costimulatory receptors have been discovered, which bidirectionally regulate T cell responses (130). Identified as the first molecule to deliver inhibitory signals, CTLA-4 is critical for concluding immune responses (131, 132). It negatively regulates T cell activation by, for instance, competing with CD28 for binding shared ligands B7.1 and B7.2 (133).

In clinical therapeutics, ipilimumab is seldom used in isolation. Physicians typically administer it in combination with nivolumab. While both CTLA-4 and PD-1 serve as immune checkpoints that inhibit T-cell activation via distinct mechanisms, their modulatory effects on immune response are uniquely characterized. Consequently, anti-CTLA-4 monoclonal antibodies may synergize with anti-PD-1/PD-L1 counterparts to potentiate tumor immunity. A growing body of research indicates that dual blockade of PD-1/PD-L1 and CTLA-4 exhibits enhanced antitumor efficacy in certain cancer types (134). Studies from CheckMate-069, CheckMate-067, and CheckMate-142 demonstrate that the combination of ipilimumab and nivolumab significantly improves clinical outcomes compared to monotherapy with either agent alone (135–137). Data from CheckMate-214, CheckMate-227, and CheckMate-743 further reveal superior treatment efficacy of the ipilimumab plus nivolumab regimen over standard targeted or chemotherapy approaches (138–140). To date, the U.S. FDA has approved the use of the ipilimumab and nivolumab combination for the treatment of melanoma, renal cell carcinoma, microsatellite instability-high/mismatch repair-deficient colorectal cancer, hepatocellular carcinoma, PD-L1 positive non-small cell lung cancer, and malignant pleural mesothelioma (134–140).

4.1.2 α–PD–1/PD–L1 combined with ICIs

Emerging dual immune checkpoint blockade strategies, encompassing the combination of α-PD-1/PD-L1 with α-TIM-3, α-LAG-3, α-PVRIG, and α-TIGIT, remain in clinical trials and await regulatory approval. The ligation of TIM-3 to galectin-9 instigates apoptosis in Th1 cells via calcium flux (141). This dual inhibition, when applied to TIM-3 and PD-1/PD-L1 pathways, markedly augments anti-tumor immunity, as shown by slower tumor growth in murine models (142). Data from clinical trials suggest that this combined blockade does not increase adverse effects, although optimization of patient selection is warranted (143–145).

Extending the scope of ICIs, α-LAG-3, α-PVRIG, α-TIGIT, and α-Siglec-10, when used in concert with α-PD-1/PD-L1, enhance TIL functionality and concomitantly inhibit tumor growth (146–149). The RELATIVITY-047 phase 2/3 trial revealed a notable PFS advantage with relatlimab (α-LAG-3) plus nivolumab in late-stage melanoma (10.1 vs. 4.6 months; HR: 0.75), outperforming nivolumab alone (150). Additionally, COM701 (α-PVRIG) with nivolumab exhibited promising antineoplastic activity in phase 1 trial NCT03667716, inclusive of patients with prior ICI treatment (151). In phase 2 trial NCT03563716, tiragolumab (α-TIGIT) plus atezolizumab significantly improved both response rates (OR: 2.57, 95%CI: 1.07–6.14) and PFS (HR: 0.57; 95%CI 0.37–0.90) in PD-L1 positive NSCLC patients, compared with the control group receiving placebo and atezolizumab (152).

4.2 CAR-T cell therapy combined with ICIs

Chimeric Antigen Receptors (CARs) are multifaceted constructs, typically encompassing an extracellular antigen-binding domain, such as a single-chain variable fragment (scFv) targeting CD19, a hinge region to enhance antigen-

receptor and tumor antigen interaction, a transmembrane domain for functional stability, and a T-cell activation domain (CD3 ζ) for primary signaling. Additionally, one or more intracellular co-stimulatory domains, like CD28/4-1BB, are included for secondary T-cell activation signaling (153). CAR T-cell activation is contingent on the presence of TAAs or TSAs. CARs' unique ability to recognize diverse targets, including both protein and non-protein entities, on the cell surface, activates T cells without the necessity for antigen processing and presentation. This capability, bypassing human MHC constraints, positions CAR T-cell therapy as a revolutionary approach in T-cell therapeutic strategies, noted for its distinctive treatment characteristics (154).

CAR-T cell therapy's hallmark is its non-reliance on Major Histocompatibility Complex (MHC) restrictions, coupled with an enhanced tumor-specific immune response, facilitated by the incorporation of co-stimulatory domains such as CD28, OX40, and 4-1BB. This attribute offers the potential to effectively target 'cold tumors', characterized by limited pre-existing T cell infiltration and a paucity of tumor antigens. A multitude of ongoing clinical trials are exploring CAR T-cell therapies against solid tumors, as elaborated in Table 1. Despite the direct tumor cell eradication capabilities of CAR-T cells, they remain susceptible to immunosuppression via immune checkpoints. Consequently, the synergistic approach of integrating ICIs with CAR-T cell therapy emerges as a promising treatment strategy (155, 156).

4.3 CAR-NK cell therapy

A noteworthy attribute of mature NK cells in the field of adoptive cell therapy is their ability to retain functionality when transplanted into new environments with differing MHC expression patterns (157, 158). Unlike T lymphocytes, NK cells predominantly do not trigger graft-versus-host disease but instead exert a regulatory role (159). Advances in genetic modification techniques have shown that NK cells can be customized further, including the introduction of CARs and the knockout of inhibitory genes (160). These advancements enable NK cells from patients with hematologic malignancies to rapidly eliminate autologous tumor cells resistant to unmodified NK cells (161, 162). Preclinical studies on CAR-NK cells in xenograft mouse models have demonstrated *in vivo* activity comparable to CAR-T cells, yet with less cytokine release and improved overall survival rates (163, 164). The inaugural human study of CAR-NK cells has revealed promising anti-tumor responses without significant toxicities such as cytokine release syndrome and graft-versus-host disease (165). These positive outcomes lay the groundwork for further

TABLE 1 Key clinical trials of immunotherapy combined with CAR-T cell/targeted therapy.

Study	Phase	Cancer type	Treatment	status	Start year
NCT04003649	I	GBM, *N*=60	IL13Ra2-CAR T+Ipilimumab	Recruiting	Dec, 2019
NCT03726515	I	GBM, *N*=7	CART-EGFRvIII+Pembrolizumab	Completed	Mar, 2019
NCT02366143	III	NSCLC, *N*=1202	Atezolizumab+bevacizumab +carboplatin + paclitaxel	Completed	Mar, 2015
NCT01984242	II	RCC, *N*=305	Atezolizumab+bevacizumab	Completed	Jan, 2014
NCT02420821	III	RCC, *N*=915	Atezolizumab+bevacizumab	Completed	May, 2015
NCT03434379	III	HCC, *N*=558	Atezolizumab+bevacizumab	Completed	Mar, 2018
NCT02501096	Ib/II	RCC, *N*=357	Lenvatinib+ pembrolizumab	Completed	Jul, 2015
NCT03517449	III	EC, *N*=827	Pembrolizumab+Lenvatinib	Active, not recruiting	Jun, 2018
NCT02853331	III	RCC, *N*=861	Pembrolizumab + axitinib	Active, not recruiting	Sep, 2016
NCT02684006	III	RCC, *N*=888	Avelumab + axitinib	Active, not recruiting	Mar, 2016
NCT03609359	II	GC, *N*=29	Lenvatinib+pembrolizumab (single-arm)	Completed	Oct, 2018
NCT02811861	III	RCC, *N*=1069	lenvatinib + pembrolizumab	Active, not recruiting	Oct, 2016
NCT02967692	III	melanoma, *N*=569	Spartalizumab + dabrafenib + trametinib (single-arm)	Active, not recruiting	Feb, 2017
NCT02752074	III	Melanoma, *N*=706	epacadostat + pembrolizumab	Completed	Jun, 2016
			pembrolizumab		
NCT02908672	III	melanoma, *N*=514	Atezolizumab+vemurafenib + cobimetinib	Active, not recruiting	Jan, 2017
NCT03082534	II	HNSCC, *N*=78	Pembrolizumab + Cetuximab	Active, not recruiting	Mar, 2017
NCT02734004	I/II	BC, *N*=264	Olaparib + durvalumab	Active, not recruiting	Mar, 2016

RCC, Renal Cell Carcinoma; HCC, hepatocellular carcinoma; EC, Endometrial Cancer; HNSCC, neck squamous cell carcinoma; BC, breast cancer; GBM, Glioblastoma.

development of CAR-NK cells as a promising modality for cancer therapy (162).

Currently, CAR-NK cell-mediated immunotherapy is advancing rapidly, offering new therapeutic avenues for patients with malignant tumors. Despite extensive research in the field of cancer immunotherapy, the application of CAR-NK cells remains relatively limited to a variety of tumor models, primarily focusing on hematological malignancies (166). Table 2 summarizes the clinical studies of CAR-NK cells in solid tumors.

4.4 T Cell redirecting bispecific antibody combined with ICIs

T cell-redirecting bispecific antibodies (BsAbs) represent a cutting-edge approach in immunotherapy, merging two monoclonal antibodies into a singular entity. Ingeniously engineered, these antibodies concurrently engage specific receptors on T cells, like CD3, and distinct tumor cell antigens. Central to their dual-specific functionality is the ability to directly steer T cells towards tumor cells, thus enhancing T cell-mediated identification and elimination of tumor cells. A distinctive feature of BsAbs-induced tumor cell lysis is its independence from conventional antigen recognition processes, which typically involve MHC class I or II molecules, antigen-presenting cells, or the necessity of co-stimulatory molecules (167).

Advancements in T cell-redirecting BsAbs for solid tumors lag behind those in hematological malignancies, in part due to a more limited range of available surface targets in solid tumors (167). Despite these challenges, four bispecific antibodies (BsAbs) have currently received FDA approval. These include Catumaxomab (Fresenius/Trion's Removab®), which was withdrawn from the market in 2017, Blinatumomab (Amgen's Blincyto®), Amivantamab-vmjw (Janssen's Rybrevant®), and Tebentafusp-tebn (Immunocore's Kimmtrak®) (168). In addition, there are still many BsAbs in the clinical evaluation stage for cancer treatment (Table 3). These agents signify progress in targeted therapeutic interventions, illustrating the evolving landscape of cancer treatment. However, even with their effectiveness, the T cells activated by these therapies can be rendered inactive by immune checkpoints. Consequently, a synergistic approach of ICIs in conjunction with T cell-redirecting BsAbs presents as a viable and potentially more effective treatment strategy.

4.5 Cancer vaccine

'Cold' tumors, characterized by a dearth of tumor antigens, commonly exhibit immune evasion. Nonetheless, the use of cancer vaccines containing tumor antigens has shown efficacy in eliciting immune responses against such tumors (169). A range of cancer vaccines, designed to bolster the patient's immune system, have received approval, including Tedopi, Ilixadencel, GVAX, and PolyPEPI101884 (170). Notably, Sipuleucel-T is the first FDA-approved cancer vaccine for metastatic castration-resistant prostate cancer (mCRPC), significantly prolonging patient survival (171). However, the therapeutic efficacy of cancer vaccines is often impeded by high PD-1 expression in effector T cells (172, 173). To address this, numerous phase 1 clinical trials have been initiated to investigate the combined use of cancer vaccines and immunoglobulins in cancer treatment, demonstrating their combined potential (174, 175). Ongoing clinical trials in this domain include NCT04300244, NCT03632941, KEYNOTE-603, and NCT03743298.

4.6 Oncolytic virus combined with ICIs therapy

Oncolytic viruses, encompassing both natural and genetically engineered variants, induce tumor cell lysis by selectively infecting and proliferating within tumor cells. Beyond their direct antitumor activity, these viruses also provoke a comprehensive, potent, and enduring anti-tumor immune response. This response is facilitated by the liberation of TAAs and additional DAMPs upon tumor cell demise (176). A significant aspect of oncolytic viral therapy is its

TABLE 2 Clinical trials of CAR-NK cell-based cancer immunotherapy.

Study	Phase	Cancer type	Treatment	status	Start year
NCT03940820	I/II	Solid Tumor, *N*=20	Biological: ROBO1 CAR-NK cells	Recruiting	May, 2019
NCT03415100	I	Solid Tumor, *N*=30	Biological: CAR-NK cells targeting NKG2D ligands	Recruiting	Jan, 2018
NCT03931720	I/II	Malignant Tumor, *N*=20	Biological: BiCAR-NK/T cells (ROBO1 CAR-NK/T cells)	Recruiting	Mar, 2019
NCT03692663	I	Castration-resistant Prostate Cance, *N*=9	Biological: anti-PSMA CAR-NK cell	Recruiting	Dec, 2018
NCT04847466	II	Gastroesophageal Junction Cancers; Advanced HNSCC, *N*=55	Drug: N-803; Drug: Pembrolizumab; Biological: PD-L1 t-haNK	Recruiting	Dec, 2021
NCT03692637	I	Epithelial Ovarian Cancer, *N*=30	Biological: anti-Mesothelin Car-NK cells	Not yet recruiting	Mar, 2019
NCT03941457	I/II	Pancreatic Cancer, *N*=9	Biological: BiCAR-NK cells (ROBO1 CAR-NK cells)	Recruiting	May, 2019

TABLE 3 Bispecific antibody clinical trials ongoing.

Study	Phase	Cancer type	Treatment	status	Start year
NCT04506086	IV	B-precursor Acute Lymphoblastic Leukemia, *N*=45	Blinatumomab	Recruiting	Aug, 2021
NCT03415100	I	B-cell NHL, *N*=116	AZD0486 IV	Recruiting	Mar, 2021
NCT04844073	I/II	Advanced Cancer, *N*=228	MVC-101 (TAK-186)	Recruiting	Mar, 2021
NCT04221542	I	Prostate Cance, *N*=461	AMG 509	Recruiting	Mar, 2020
NCT03564340	I/II	Recurrent Ovarian Cancer, *N*=690	REGN4018	Recruiting	May, 2018
NCT04117958	I	MUC17-positive Solid Tumors, *N*=58	AMG 199	Recruiting	Jan, 2020
NCT04104607	I	Castration-Resistant Prostatic Cancer, *N*=86	CC-1, PSMAxCD3	Recruiting	Nov, 2019

systemic immunomodulatory impact, which extends its effects beyond the injection locus to distant tumor regions (176).

T-VEC, a modified herpes simplex virus, demonstrates augmented anti-tumor efficacy in treating unresectable stage IIIB-IV melanoma when used in conjunction with Ipilimumab, surpassing the results achieved with Ipilimumab alone (177). Furthermore, integrating a PD-1 inhibitor with oncolytic viral therapy significantly boosts its anti-tumor potency in glioma models (178). In the context of triple-negative breast cancer (TNBC), the response to ICIs typically remains suboptimal. Oncolytic viral treatment, however, renders TNBC more responsive to immune checkpoint blockade, successfully averting recurrence in a majority of the treated animal models (179).

4.7 Macrophage targeted therapy combined with ICIs therapy

TAMs, as key immune constituents in the TME, play an integral role in solid tumor development. These cells exhibit dual phenotypes: anti-tumoral (M1) and pro-tumoral (M2), with their behavior governed by their polarization state (180). TAMs significantly modulate immune responses by producing an array of cytokines and effector molecules. They suppress the function of T cells, B cells, NK cells, and dendritic cells, while simultaneously enhancing the roles of Tregs, T helper 17 cells (Th17), γδ T cells, and MDSCs. This multifaceted approach fosters an immunosuppressive milieu within the TME (181). Crucially, TAMs' association with PD-L1 expression suggests that strategies combining ICIs with targeted TAM therapies could offer substantial therapeutic benefits (182, 183).

TAMs are pivotal in cancer treatment strategies. Targeting TAMs typically involves three approaches: 1) eradicating existing TAMs in the TME, 2) curtailing the recruitment of monocytes, and 3) reprogramming TAMs (181). TAMs are pivotal in cancer treatment strategies. Targeting TAMs typically involves three approaches: 1) eradicating existing TAMs in the TME, 2) curtailing the recruitment of monocytes, and 3) reprogramming TAMs (184, 185). In a phase 1b study (NCT02323191), a combination of the CSF-1R inhibitor emactuzumab with atezolizumab exhibited a superior Objective Response Rate (ORR) compared to controls (186). Additionally, in a separate clinical trial, the C-C chemokine receptor type 5 (CCR5) inhibitor maraviroc, used in tandem with pembrolizumab, demonstrated notable efficacy in patients with dMMR CRC (187).

4.8 Radiotherapy combined with ICIs therapy

Radiation therapy, employing ionizing radiation to directly destroy tumor cells, exerts multifaceted impacts on tumor immunity: 1) It can trigger immunogenic cell death (ICD) in tumor cells, culminating in the release of abundant DAMPs. These DAMPs, once phagocytosed by DCs, facilitate DC maturation (188). 2) Mature dendritic cells are capable of cross-presenting tumor antigens to CD8+ T cells, thereby initiating specific immune responses (189). 3) Concurrently, radiation therapy exhibits immunosuppressive properties, encompassing bone marrow suppression, the direct eradication of immune cells, upregulation of immune checkpoints, and the elicitation of immunogenic cytokines and chemokines (190–192). These immunoregulatory effects lay the groundwork for integrating ICIs with radiation therapy.

In certain cases, patients undergoing combined therapies exhibit spontaneous tumor regression beyond the irradiated zones, termed the 'abscopal effect' or radiotherapy's distant impact. This phenomenon is largely attributed to radiotherapy enhancing the antigen presentation of tumor cells, thereby augmenting CD8+ T cell production. These cells then travel via the bloodstream to remote sites, influencing tumors outside the irradiated areas (193, 194). Contemporary research suggests that the abscopal effect can counteract immunosuppression and enhance the efficacy of ICIs (195–198). For instance, preliminary results from a phase III study on stage III unresectable NSCLC patients revealed that post-radiotherapy treatment with durvalumab significantly prolonged progression-free survival (PFS) compared to a placebo (199). Furthermore, another phase III study involving 799 participants demonstrated that, in patients with mCRPC previously treated with docetaxel, a combination of ipilimumab and radiotherapy markedly increased

overall survival (OS) over placebo plus radiotherapy (200). Additional information on clinical trials combining radiotherapy with ICIs is detailed in Table 4.

4.9 Chemotherapy combined with ICIs therapy

Chemotherapy drugs wield a bidirectional impact on the immune system during tumor therapy. Initially, they frequently induce systemic immunosuppression, evident through bone marrow suppression and lymphocyte depletion. Concurrently, these agents can eradicate specific immune cells, contributing to the reconstitution and establishment of a renewed immune system (201). The immunostimulatory actions of chemotherapy are manifested in several ways: 1) Augmenting antigenicity: Agents like cyclophosphamide, gemcitabine, platinum-based drugs, and taxanes boost the antigenicity of tumor cells. 2) Increasing susceptibility to immune assaults: This is primarily achieved by improving the visibility of tumor cells to the immune system. 3) Triggering ICD and antigen-specific responses: Anthracyclines, mitoxantrone, and oxaliplatin accomplish this by interacting with DNA replication and repair mechanisms (202). These pathways illustrate that chemotherapeutic drugs not only directly eradicate tumor cells but also engage in combatting tumors by stimulating and modulating the immune system.

Clinical trials integrating chemotherapy with immunotherapy have demonstrated considerable therapeutic success. In the phase III KEYNOTE-189 trial (NCT02578680), a regimen of pembrolizumab combined with pemetrexed-platinum agents yielded an ORR of 48.3%, markedly surpassing the 19.9% ORR of the placebo plus pemetrexed-platinum cohort. This combination therapy also significantly enhanced OS with a Hazard Ratio (HR) of 0.56 (95% Confidence Interval [CI]: 0.46-0.69) and PFS with an HR of 0.49 (95% CI: 0.41-0.59) (203). The phase III KEYNOTE-355 trial revealed that supplementing standard chemotherapy with pembrolizumab substantially improved PFS in metastatic TNBC patients with a combined positive score (CPS) of 10 or above (204). The KEYNOTE-021 (NCT02039674) trial found that pembrolizumab plus chemotherapy exhibited superior ORR (58% vs 33%) and PFS (median of 24.5 months vs 9.9 months; HR: 0.54; 95% CI: 0.35-0.83) compared to chemotherapy alone (205). Furthermore, in the phase III IMpower133 trial (NCT02763579), the addition of atezolizumab to carboplatin and etoposide significantly prolonged OS and PFS in small-cell lung cancer patients over the placebo with carboplatin and etoposide (206). Other clinical trials of chemotherapy combined with ICIs treatment are detailed in Table 5.

4.10 Targeted therapy combined with ICIs therapy

Targeted cancer therapy is predicated on creating potent inhibitors that specifically target molecular markers of tumor cells, aiming to effectively treat the cancer. The modes of action of this therapy span a range, including suppressing tumor cell proliferation, intervening in the cell cycle, promoting tumor cell differentiation, curbing metastasis, inducing apoptosis, and hampering tumor angiogenesis (207). Despite the considerable successes of many targeted therapies in clinical settings, the emergence of drug resistance in a significant number of patients represents a formidable challenge. Recent research has revealed that these targeted agents can trigger ICD in tumor cells, thereby bolstering the effectiveness of ICIs (207). Consequently, integrating targeted therapy with immunotherapy emerges as a novel and promising approach to surmount drug resistance and enhance therapeutic outcomes.

In the phase III IMspire150 trial (NCT02908672), the combination of vemurafenib, cobimetinib, and atezolizumab was compared against a control regimen of vemurafenib, cobimetinib, and placebo in patients with advanced or metastatic melanoma harboring the BRAF V600 mutation. The study revealed that the addition of atezolizumab significantly extended PFS to 15.1 months, compared to 10.6 months in the control group, with a HR of 0.78 (95% CI: 0.63-0.97, p=0.025) (208). In the phase 1/2 MEDIOLA trial, the efficacy of Olaparib combined with durvalumab was evaluated in patients with metastatic breast cancer with germline BRCA1 or BRCA2 mutations. This trial

TABLE 4 Key clinical trials of immunotherapy combined with radiotherapy.

Study	Phase	Cancer type (population,N)	Interventions and Combination	status	Start year
NCT02855203	I/II	ccRCC, *N*=30	Pembrolizumab+ SABR	Completed	Oct, 2016
NCT02904954	II	NSCLC, *N*=60	Durvalumab+SBRT	Completed	Dec, 2016
NCT02125461	III	NSCLC, *N*=713	Durvalumab + Chemoradiation therapy	Active, not recruiting	May, 2014
NCT02492568	II	NSCLC, *N*=92	Pembrolizumab + SBRT	Completed	Jul, 2015
			Pembrolizumab		
NCT02316002	II	NSCLC, *N*=51	Pembrolizumab + LAT (single-arm)	Active, not recruiting	Jan, 2015
NCT02444741	I/II	NSCLC, *N*=126	Pembrolizumab + SBRT	Active, not recruiting	Sep, 2015

ccRCC, Clear cell renal cell carcinoma; SABR, Stereotactic Ablative Body Radiosurgery; NSCLC, Non-small cell lung cancer; SBRT, Stereotactic body radiotherapy; LAT, Locally ablative therapy.

TABLE 5 Key clinical trials of immunotherapy combined with chemotherapy.

Study	Phase	Cancer type	Treatment	status	Start year
NCT02039674	II	NSCLC, *N*=267	Pembrolizumab + Chemotherapy	Completed	Feb, 2014
NCT02578680	III	NSCLC, *N*=616	Pembrolizumab+pemetrexed+platinum	Completed	Jan, 2016
NCT00324155	III	Melanoma, *N*=681	Ipilimumab+ dacarbazine	Completed	Aug, 2006
NCT00527735	II	NSCLC, *N*=334	Ipilimumab+paclitaxel+Carboplatin	Completed	Feb, 2008
NCT01285609	III	NSCLC, *N*=1289	Ipilimumab + chemotherapy	Completed	Jan, 2011
NCT03036488	III	TNBC, *N*=1174	Pembrolizumab+chemotherapy	Active, not recruiting	Mar, 2017
NCT02425891	III	mTNBC, *N*=902	Atezolizumab+Nab-paclitaxel	Completed	Jun, 2015
NCT02763579	III	ES-SCLC, *N*=503	Atezolizumab+carboplatin+etoposide	Completed	Jun, 2016
NCT02366143	III	NSCLC, *N*=1202	Atezolizumab+bevacizumab +carboplatin + paclitaxel	Completed	Mar, 2015
NCT02775435	III	NSCLC, *N*=559	Pembrolizumab+Chemotherapy	Active, not recruiting	Jun, 2016
NCT03043872	III	ES-SCLC, *N*=987	Durvalumab+tremelimumab +platinum-etoposide	Active, not recruiting	Mar, 2017
NCT02494583	III	GC, *N*=763	Pembrolizumab+chemotherapy	Completed	Jul, 2015
NCT02819518	III	TNBC, *N*=882	Pembrolizumab+chemotherapy	Active, not recruiting	Jul, 2016
NCT03134872	III	NSCLC, *N*=419	Camrelizumab+chemotherapy	Completed	May, 2017
NCT02853305	III	BLCA, *N*=1010	Pembrolizumab+chemotherapy	Completed	Sep, 2016
NCT02872116	III	GC, GEJ, OAC, *N*=2031	Nivolumab+chemotherapy	Active, not recruiting	Oct, 2016

TNBC, Triple-negative breast cancer; mTNBC, Metastatic triple-negative breast cancer; ES-SCLC, Extensive-stage small-cell lung cancer; GC, Gastric cancer; GEJ, Gastro-oesophageal junction cancer; OAC, Oesophageal adenocarcinoma; BLCA, Bladder urothelial carcinoma.

showed positive safety and disease control outcomes in 80% of patients after 12 weeks of treatment. These findings underscore the potential of integrating targeted therapy with immunotherapy in the treatment of certain cancers (209). Detailed information on additional clinical trials combining targeted therapy with ICIs is available in Table 1.

4.11 STING agonist combined with ICIs therapy

The accumulation of cytosolic chromatin fragments and micronuclei, a hallmark of malignant transformation in cancer cells, raises the likelihood of cytosolic DNA escape or DCs engulfing tumor-derived DNA (210). The cGAS-STING pathway, pivotal for cytosolic DNA detection, plays a crucial role in this context. Binding of cytosolic double-stranded DNA (dsDNA) to cGAS triggers the synthesis of cyclic GMP-AMP (cGAMP). This activation leads to the transformation of STING from a monomer to a dimer, facilitating its relocation from the endoplasmic reticulum to perinuclear microsomes. Subsequently, STING engages and phosphorylates TBK1, initiating a cascade that activates IRF3 and boosts IFN-I production (211–213). Additionally, the STING pathway enhances IFN-I through the NF-κB route (214). IFN-I, a multifaceted immune enhancer, significantly augments the functions of DCs, NK cells, and T cells (215). The cGAS-STING pathway's integral role in linking innate and adaptive immunity underscores its potential as a target for cancer immunotherapy.

Initial clinical trials with Dimethyloxoxanthenyl acetic acid (DMXAA), the first STING agonist, were unsuccessful (216). Further research revealed that DMXAA specifically activates the mouse STING pathway, with minimal effects on its human counterpart (217, 218). Consequently, several natural and synthetic cyclic dinucleotides (CDNs), structurally and functionally akin to cGAMP, have emerged as promising STING agonists in cancer immunotherapy (219–221). However, these CDNs typically face challenges like limited transmembrane transport and reliance on intratumoral injection. Recent developments include novel STING agonists like diABZI and MSA-2, which offer systemic administration possibilities (222, 223). Moreover, manganese has been identified as a natural STING agonist, playing a significant role in anti-tumor immunity (224, 225).

In the context of combination therapy, the synergy of STING agonists with α-PD-1/PD-L1 antibodies presents a promising avenue. This approach simultaneously amplifies innate and adaptive immunity, effectively countering immunotherapy resistance. STING agonists enhance immune cell infiltration and amplify the functionality of APCs, NK cells, and T cells (226–228). Concurrently, α-PD-1/PD-L1 antibodies capitalize on the PD-L1 upregulation induced by STING agonists (227). Ongoing clinical trials involving combinations like ADU-S100 with spartalizumab, MK-1454 with pembrolizumab, and manganese with α-PD-1 have shown promising anti-tumor efficacy and tolerable safety profiles (229, 230).

4.12 Nanoparticles combined with ICIs therapy

Rapidly proliferating cancer tissues frequently form enlarged vascular endothelial gaps, with an average size of several hundred nanometers, to draw more nutrients from the body. Such gaps are generally not found in normal tissues. This phenomenon, known as the enhanced permeability and retention effect (EPR), allows nanoparticles of suitable size to infiltrate tumor tissues, while being restricted by the denser structure of normal tissues. This underpins the theoretical foundation for targeting tumor tissues with nanoparticles (231). Nanoparticles can amplify the efficacy of immunotherapy by inducing ICD in tumor cells (232). In melanoma mouse models, pH-sensitive liposomes equipped with a dual delivery system of doxorubicin hydrochloride and deferasirox have shown to enhance antigen presentation and T-cell infiltration, thereby augmenting their anti-tumor action (233). In glioblastoma multiforme (GBM) research, where drug delivery is constrained by the blood-brain barrier, BAMPA-O16B/siRNA liposomes have been able to effectively transport anti-CD47 and PD-L1 siRNA into intracranial GBM tumors in mice (234). Consequently, the strategy of using nanoparticles in combination with ICIs represents a promising avenue of research.

5 Conclusion and perspectives

In the evolving landscape of oncology, ICIs have emerged as a pivotal advancement. However, their efficacy is not uniform across all patient groups, highlighting a need for more nuanced understanding beyond the simplistic 'cold' and 'hot' tumor classifications. Intriguingly, some 'hot' tumors show responsiveness to ICIs despite a scarcity of CD8+ T cells, driven by NK cell-mediated immune responses. Conversely, 'cold' tumors often struggle with T cell activation and infiltration issues. Strategies that combine ICIs with other treatments such as radiotherapy, chemotherapy, CAR-T cell therapy, or targeted therapy are being investigated to transform 'cold' tumors into 'hot' ones, potentially increasing the efficacy of ICIs. Currently, many combination therapies fail to replicate these results in clinical settings. Currently, only a limited number of combinations, including α-PD-1/PD-L1 with chemotherapy, angiogenesis inhibitors, or α-CTLA-4, have received regulatory approval. The efficacy of most combinations remains confined to animal tumor models, underscoring the need for optimal preclinical models, with humanized patient-derived models offering more precise efficacy evaluations. However, combination therapies pose challenges such as increased immune-related adverse events (irAEs) and healthcare costs, and the risk of exposing patients to higher toxicities with inappropriate combinations. Optimizing administration regimens, including dosage, timing, and sequence, is crucial for the development of these therapies. Furthermore, the selection of suitable combination therapies and identification of predictive biomarkers for treatment response are still areas of active investigation. Liquid biopsy, by monitoring the dynamic immune landscape of the tumor microenvironment, offers a promising approach for real-time biomarker identification, guiding precision immunotherapy. Personalized combination therapies based on immune profiling and other predictive biomarkers, and a comprehensive framework integrating genomic, transcriptomic, immune, and microbiome profiles, could enhance patient selection for combination treatments. Particularly for patients with 'cold' tumors, α-PD-1/PD-L1 monotherapy often falls short of clinical benefits, necessitating personalized combinations to overcome drug resistance. In immune-desert scenarios, treatments such as radiotherapy, chemotherapy, and STING agonists can counter low immunogenicity-mediated immune tolerance by inducing immunogenic cell death and promoting antigen-presenting cell function. These combinations with α-PD-1/PD-L1 can simultaneously enhance multiple aspects of the cancer-immunity cycle, reshape the tumor microenvironment, and facilitate the transformation from non-inflamed to inflamed tumors. Additionally, the development of next-generation α-PD-1/PD-L1 drugs, including bifunctional or bispecific antibodies, could extend the indications for α-PD-1/PD-L1 therapies, allowing a broader range of patients to benefit from these advanced treatments.

Author contributions

PO: Visualization, Writing – original draft. LW: Visualization, Writing – original draft. JW: Visualization, Writing – original draft. YT: Writing – original draft. CC: Writing – original draft. DL: Writing – review & editing. ZY: Writing – review & editing. RC: Writing – review & editing. GX: Writing – original draft. JG: Writing – original draft. ZB: Writing – original draft.

Funding

The author(s) declare financial support was received for the research, authorship, and/or publication of this article. This study was supported by the Fundamental Research Funds for the Central Universities (21623305,21623409), Guangdong Medical Science and Technology Research Fund Project(A2023398) and Guangzhou Science and Technology Plan City-School Joint Funding Project (202201020304).

Conflict of interest

The authors declare that the research was conducted in the absence of any commercial or financial relationships that could be construed as a potential conflict of interest.

Publisher's note

References

1. Zhang J, Huang D, Saw PE, Song E. Turning cold tumors hot: from molecular mechanisms to clinical applications. *Trends Immunol*. (2022) 43:523–45. doi: 10.1016/j.it.2022.04.010

2. Rezaei M, Tan J, Zeng C, Li Y, Ganjalikhani-Hakemi M. TIM-3 in leukemia; immune response and beyond. *Front Oncol*. (2021) 11:753677. doi: 10.3389/fonc.2021.753677

3. Chen DS, Mellman I. Elements of cancer immunity and the cancer-immune set point. *Nature*. (2017) 541:321–30. doi: 10.1038/nature21349

4. Dammeijer F, van Gulijk M, Mulder EE, Lukkes M, Klaase L, van den Bosch T, et al. The PD-1/PD-L1-checkpoint restrains T cell immunity in tumor-draining lymph nodes. *Cancer Cell*. (2020) 38:685–700. doi: 10.1016/j.ccell.2020.09.001

5. Hsu J, Hodgins JJ, Marathe M, Nicolai CJ, Bourgeois-Daigneault MC, Trevino TN, et al. Contribution of NK cells to immunotherapy mediated by PD-1/PD-L1 blockade. *J Clin Invest*. (2018) 128:4654–68. doi: 10.1172/JCI99317

6. Dong W, Wu X, Ma S, Wang Y, Nalin AP, Zhu Z, et al. The mechanism of anti-PD-L1 antibody efficacy against PD-L1-negative tumors identifies NK cells expressing PD-L1 as a cytolytic effector. *Cancer Discovery*. (2019) 9:1422–37. doi: 10.1158/2159-8290.CD-18-1259

7. Galon J, Costes A, Sanchez-Cabo F, Kirilovsky A, Mlecnik B, Lagorce-Pages C, et al. Type, density, and location of immune cells within human colorectal tumors predict clinical outcome. *Science*. (2006) 313:1960–64. doi: 10.1126/science.1129139

8. Galon J, Fridman WH, Pages F. The adaptive immunologic microenvironment in colorectal cancer: a novel perspective. *Cancer Res*. (2007) 67:1883–86. doi: 10.1158/0008-5472.CAN-06-4806

9. Camus M, Tosolini M, Trajanoski Z, Herman Fridman W, Galon J, Mlecnik B, et al. Coordination of intratumoral immune reaction and human colorectal cancer recurrence. *Cancer Res (Chicago Ill.)*. (2009) 69:2685–93. doi: 10.1158/0008-5472.CAN-08-2654

10. Galon J, Mlecnik B, Bindea G, Angell HK, Berger A, Lagorce C, et al. Towards the introduction of the 'Immunoscore' in the classification of Malignant tumours. *J Pathol*. (2014) 232:199–209. doi: 10.1002/path.4287

11. Pages F, Mlecnik B, Marliot F, Bindea G, Ou FS, Bifulco C, et al. International validation of the consensus Immunoscore for the classification of colon cancer: a prognostic and accuracy study. *Lancet*. (2018) 391:2128–39. doi: 10.1016/S0140-6736(18)30789-X

12. Galon J, Bruni D. Approaches to treat immune hot, altered and cold tumours with combination immunotherapies. *Nat Rev Drug Discov*. (2019) 18:197–218. doi: 10.1038/s41573-018-0007-y

13. Blank CU, Haining WN, Held W, Hogan PG, Kallies A, Lugli E, et al. Defining 'T cell exhaustion'. *Nat Rev Immunol*. (2019) 19:665–74. doi: 10.1038/s41577-019-0221-9

14. Philip M, Fairchild L, Sun L, Horste EL, Camara S, Shakiba M, et al. Chromatin states define tumour-specific T cell dysfunction and reprogramming. *Nature*. (2017) 545:452–56. doi: 10.1038/nature22367

15. Johnson DB, Nebhan CA, Moslehi JJ, Balko JM. Immune-checkpoint inhibitors: long-term implications of toxicity. *Nat Rev Clin Oncol*. (2022) 19:254–67. doi: 10.1038/s41571-022-00600-w

16. Liu YT, Sun ZJ. Turning cold tumors into hot tumors by improving T-cell infiltration. *Theranostics*. (2021) 11:5365–86. doi: 10.7150/thno.58390

17. Coulie PG, Van den Eynde BJ, van der Bruggen P, Boon T. Tumour antigens recognized by T lymphocytes: at the core of cancer immunotherapy. *Nat Rev Cancer*. (2014) 14:135–46. doi: 10.1038/nrc3670

18. Yang W, Lee KW, Srivastava RM, Kuo F, Krishna C, Chowell D, et al. Immunogenic neoantigens derived from gene fusions stimulate T cell responses. *Nat Med*. (2019) 25:767–75. doi: 10.1038/s41591-019-0434-2

19. Laumont CM, Vincent K, Hesnard L, Audemard É, Bonneil É, Laverdure JP, et al. Noncoding regions are the main source of targetable tumor-specific antigens. *Sci Transl Med*. (2018) 10:767–75. doi: 10.1126/scitranslmed.aau5516

20. Kahles A, Lehmann KV, Toussaint NC, Hüser M, Stark SG, Sachsenberg T, et al. Comprehensive analysis of alternative splicing across tumors from 8,705 patients. *Cancer Cell*. (2018) 34:211–24. doi: 10.1016/j.ccell.2018.07.001

21. Latham A, Srinivasan P, Kemel Y, Shia J, Bandlamudi C, Mandelker D, et al. Microsatellite instability is associated with the presence of lynch syndrome pan-cancer. *J Clin Oncol*. (2019) 37:286–95. doi: 10.1200/JCO.18.00283

22. Fan A, Wang B, Wang X, Nie Y, Fan D, Zhao X, et al. Immunotherapy in colorectal cancer: current achievements and future perspective. *Int J Biol Sci*. (2021) 17:3837–49. doi: 10.7150/ijbs.64077

23. Jardim DL, Goodman A, de Melo GD, Kurzrock R. The challenges of tumor mutational burden as an immunotherapy biomarker. *Cancer Cell*. (2021) 39:154–73. doi: 10.1016/j.ccell.2020.10.001

24. McGrail DJ, Federico L, Li Y, Dai H, Lu Y, Mills GB, et al. Multi-omics analysis reveals neoantigen-independent immune cell infiltration in copy-number driven cancers. *Nat Commun*. (2018) 9:1317. doi: 10.1038/s41467-018-03730-x

25. Spranger S, Luke JJ, Bao R, Zha Y, Hernandez KM, Li Y, et al. Density of immunogenic antigens does not explain the presence or absence of the T-cell-inflamed tumor microenvironment in melanoma. *Proc Natl Acad Sci U.S.A*. (2016) 113:E7759–68. doi: 10.1073/pnas.1609376113

26. Merad M, Sathe P, Helft J, Miller J, Mortha A. The dendritic cell lineage: ontogeny and function of dendritic cells and their subsets in the steady state and the inflamed setting. *Annu Rev Immunol*. (2013) 31:563–604. doi: 10.1146/annurev-immunol-020711-074950

27. de Mingo PÁ, Hänggi K, Celias DP, Gardner A, Li J, Batista-Bittencourt B, et al. The inhibitory receptor TIM-3 limits activation of the cGAS-STING pathway in intra-tumoral dendritic cells by suppressing extracellular DNA uptake. *Immunity*. (2021) 54:1154–67. doi: 10.1016/j.immuni.2021.04.019

28. Hildner K, Edelson BT, Purtha WE, Diamond M, Matsushita H, Kohyama M, et al. Batf3 deficiency reveals a critical role for CD8alpha+ dendritic cells in cytotoxic T cell immunity. *Science*. (2008) 322:1097–100. doi: 10.1126/science.1164206

29. Enamorado M, Iborra S, Priego E, Cueto FJ, Quintana JA, Martínez-Cano S, et al. Enhanced anti-tumour immunity requires the interplay between resident and circulating memory CD8(+) T cells. *Nat Commun*. (2017) 8:16073. doi: 10.1038/ncomms16073

30. Feng M, Jiang W, Kim B, Zhang CC, Fu YX, Weissman IL. Phagocytosis checkpoints as new targets for cancer immunotherapy. *Nat Rev Cancer*. (2019) 19:568–86. doi: 10.1038/s41568-019-0183-z

31. Luo M, Wang X, Wu S, Yang C, Su Q, Huang L, et al. A20 promotes colorectal cancer immune evasion by upregulating STC1 expression to block "eat-me" signal. *Signal Transduct Target Ther*. (2023) 8:312. doi: 10.1038/s41392-023-01545-x

32. Lin H, Kryczek I, Li S, Green MD, Ali A, Hamasha R, et al. Stanniocalcin 1 is a phagocytosis checkpoint driving tumor immune resistance. *Cancer Cell*. (2021) 39:480–93. doi: 10.1016/j.ccell.2020.12.023

33. Song X, Zhou Z, Li H, Xue Y, Lu X, Bahar I, et al. Pharmacologic suppression of B7-H4 glycosylation restores antitumor immunity in immune-cold breast cancers. *Cancer Discovery*. (2020) 10:1872–93. doi: 10.1158/2159-8290.CD-20-0402

34. Giampazolias E, Schulz O, Lim K, Rogers NC, Chakravarty P, Srinivasan N, et al. Secreted gelsolin inhibits DNGR-1-dependent cross-presentation and cancer immunity. *Cell*. (2021) 184:4016–31. doi: 10.1016/j.cell.2021.05.021

35. Montesion M, Murugesan K, Jin DX, Sharaf R, Sanchez N, Guria A, et al. Somatic HLA class I loss is a widespread mechanism of immune evasion which refines the use of tumor mutational burden as a biomarker of checkpoint inhibitor response. *Cancer Discovery*. (2021) 11:282–92. doi: 10.1158/2159-8290.CD-20-0672

36. Chowell D, Morris L, Grigg CM, Weber JK, Samstein RM, Makarov V, et al. Patient HLA class I genotype influences cancer response to checkpoint blockade immunotherapy. *Science*. (2018) 359:582–87. doi: 10.1126/science.aao4572

37. Gu SS, Zhang W, Wang X, Jiang P, Traugh N, Li Z, et al. Therapeutically increasing MHC-I expression potentiates immune checkpoint blockade. *Cancer Discovery*. (2021) 11:1524–41. doi: 10.1158/2159-8290.CD-20-0812

38. Yamamoto K, Venida A, Yano J, Biancur DE, Kakiuchi M, Gupta S, et al. Autophagy promotes immune evasion of pancreatic cancer by degrading MHC-I. *Nature*. (2020) 581:100–05. doi: 10.1038/s41586-020-2229-5

39. Nagarsheth N, Wicha MS, Zou W. Chemokines in the cancer microenvironment and their relevance in cancer immunotherapy. *Nat Rev Immunol*. (2017) 17:559–72. doi: 10.1038/nri.2017.49

40. Peng D, Kryczek I, Nagarsheth N, Zhao L, Wei S, Wang W, et al. Epigenetic silencing of TH1-type chemokines shapes tumour immunity and immunotherapy. *Nature*. (2015) 527:249–53. doi: 10.1038/nature15520

41. Nagarsheth N, Peng D, Kryczek I, Wu K, Li W, Zhao E, et al. PRC2 epigenetically silences th1-type chemokines to suppress effector T-cell trafficking in colon cancer. *Cancer Res*. (2016) 76:275–82. doi: 10.1158/0008-5472.CAN-15-1938

42. Dangaj D, Bruand M, Grimm AJ, Ronet C, Barras D, Duttagupta PA, et al. Cooperation between constitutive and inducible chemokines enables T cell engraftment and immune attack in solid tumors. *Cancer Cell*. (2019) 35:885–900. doi: 10.1016/j.ccell.2019.05.004

43. Molon B, Ugel S, Del PF, Soldani C, Zilio S, Avella D, et al. Chemokine nitration prevents intratumoral infiltration of antigen-specific T cells. *J Exp Med*. (2011) 208:1949–62. doi: 10.1084/jem.20101956

44. Mariathasan S, Turley SJ, Nickles D, Castiglioni A, Yuen K, Wang Y, et al. TGFβ attenuates tumour response to PD-L1 blockade by contributing to exclusion of T cells. *Nature*. (2018) 554:544–48. doi: 10.1038/nature25501

45. Tauriello D, Palomo-Ponce S, Stork D, Berenguer-Llergo A, Badia-Ramentol J, Iglesias M, et al. TGFβ drives immune evasion in genetically reconstituted colon cancer metastasis. *Nature*. (2018) 554:538–43. doi: 10.1038/nature25492

46. Vinokurova D, Apetoh L. The emerging role of IL-9 in the anticancer effects of anti-PD-1 therapy. *Biomolecules*. (2023) 13:5225–37. doi: 10.3390/biom13040670

47. Falcomatà C, Bärthel S, Schneider G, Rad R, Schmidt-Supprian M, Saur D. Context-specific determinants of the immunosuppressive tumor microenvironment in pancreatic cancer. *Cancer Discovery*. (2023) 13:278–97. doi: 10.1158/2159-8290.CD-22-0876

48. Tie Y, Tang F, Wei YQ, Wei XW. Immunosuppressive cells in cancer: mechanisms and potential therapeutic targets. *J Hematol Oncol.* (2022) 15:61. doi: 10.1186/s13045-022-01282-8

49. Sakaguchi S, Sakaguchi N, Asano M, Itoh M, Toda M. Immunologic self-tolerance maintained by activated T cells expressing IL-2 receptor alpha-chains (CD25). Breakdown of a single mechanism of self-tolerance causes various autoimmune diseases. *J Immunol.* (1995) 155:1151–64. doi: 10.4049/jimmunol.155.3.1151

50. Baecher-Allan C, Brown JA, Freeman GJ, Hafler DA. CD4+CD25high regulatory cells in human peripheral blood. *J Immunol.* (2001) 167:1245–53. doi: 10.4049/jimmunol.167.3.1245

51. Jonuleit H, Schmitt E, Stassen M, Tuettenberg A, Knop J, Enk AH. Identification and functional characterization of human CD4(+)CD25(+) T cells with regulatory properties isolated from peripheral blood. *J Exp Med.* (2001) 193:1285–94. doi: 10.1084/jem.193.11.1285

52. Dieckmann D, Plottner H, Berchtold S, Berger T, Schuler G. Ex vivo isolation and characterization of CD4(+)CD25(+) T cells with regulatory properties from human blood. *J Exp Med.* (2001) 193:1303–10. doi: 10.1084/jem.193.11.1303

53. Hori S, Nomura T, Sakaguchi S. Control of regulatory T cell development by the transcription factor Foxp3. *Science.* (2003) 299:1057–61. doi: 10.1126/science.1079490

54. Fontenot JD, Gavin MA, Rudensky AY. Foxp3 programs the development and function of CD4+CD25+ regulatory T cells. *Nat Immunol.* (2003) 4:330–36. doi: 10.1038/ni904

55. Khattri R, Cox T, Yasayko SA, Ramsdell F. An essential role for Scurfin in CD4 +CD25+ T regulatory cells. *Nat Immunol.* (2003) 4:337–42. doi: 10.1038/ni909

56. Lee W, Lee GR. Transcriptional regulation and development of regulatory T cells. *Exp Mol Med.* (2018) 50:e456. doi: 10.1038/emm.2017.313

57. Sharma A, Rudra D. Emerging functions of regulatory T cells in tissue homeostasis. *Front Immunol.* (2018) 9:883. doi: 10.3389/fimmu.2018.00883

58. Togashi Y, Shitara K, Nishikawa H. Regulatory T cells in cancer immunosuppression - implications for anticancer therapy. *Nat Rev Clin Oncol.* (2019) 16:356–71. doi: 10.1038/s41571-019-0175-7

59. Miyara M, Yoshioka Y, Kitoh A, Shima T, Wing K, Niwa A, et al. Functional delineation and differentiation dynamics of human CD4+ T cells expressing the FoxP3 transcription factor. *Immunity.* (2009) 30:899–911. doi: 10.1016/j.immuni.2009.03.019

60. Itahashi K, Irie T, Nishikawa H. Regulatory T-cell development in the tumor microenvironment. *Eur J Immunol.* (2022) 52:1216–27. doi: 10.1002/eji.202149358

61. Ohue Y, Nishikawa H. Regulatory T (Treg) cells in cancer: Can Treg cells be a new therapeutic target? *Cancer Sci.* (2019) 110:2080–89. doi: 10.1111/cas.14069

62. Chen ML, Pittet MJ, Gorelik L, Flavell RA, Weissleder R, von Boehmer H, et al. Regulatory T cells suppress tumor-specific CD8 T cell cytotoxicity through TGF-beta signals in *vivo*. *Proc Natl Acad Sci U.S.A.* (2005) 102:419–24. doi: 10.1073/pnas.0408197102

63. Yano H, Andrews LP, Workman CJ, Vignali D. Intratumoral regulatory T cells: markers, subsets and their impact on anti-tumor immunity. *Immunology.* (2019) 157:232–47. doi: 10.1111/imm.13067

64. Tay C, Tanaka A, Sakaguchi S. Tumor-infiltrating regulatory T cells as targets of cancer immunotherapy. *Cancer Cell.* (2023) 41:450–65. doi: 10.1016/j.ccell.2023.02.014

65. DeLeeuw RJ, Kost SE, Kakal JA, Nelson BH. The prognostic value of FoxP3+ tumor-infiltrating lymphocytes in cancer: a critical review of the literature. *Clin Cancer Res.* (2012) 18:3022–29. doi: 10.1158/1078-0432.CCR-11-3216

66. Ngiow SF, Young A, Jacquelot N, Yamazaki T, Enot D, Zitvogel L, et al. A threshold level of intratumor CD8+ T-cell PD1 expression dictates therapeutic response to anti-PD1. *Cancer Res.* (2015) 75:3800–11. doi: 10.1158/0008-5472.CAN-15-1082

67. Khaled YS, Ammori BJ, Elkord E. Myeloid-derived suppressor cells in cancer: recent progress and prospects. *Immunol Cell Biol.* (2013) 91:493–502. doi: 10.1038/icb.2013.29

68. Meyer C, Cagnon L, Costa-Nunes CM, Baumgaertner P, Montandon N, Leyvraz L, et al. Frequencies of circulating MDSC correlate with clinical outcome of melanoma patients treated with ipilimumab. *Cancer Immunol Immunother.* (2014) 63:247–57. doi: 10.1007/s00262-013-1508-5

69. Groth C, Hu X, Weber R, Fleming V, Altevogt P, Utikal J, et al. Immunosuppression mediated by myeloid-derived suppressor cells (MDSCs) during tumour progression. *Br J Cancer.* (2019) 120:16–25. doi: 10.1038/s41416-018-0333-1

70. Kim K, Skora AD, Li Z, Liu Q, Tam AJ, Blosser RL, et al. Eradication of metastatic mouse cancers resistant to immune checkpoint blockade by suppression of myeloid-derived cells. *Proc Natl Acad Sci U.S.A.* (2014) 111:11774–79. doi: 10.1073/pnas.1410626111

71. De Henau O, Rausch M, Winkler D, Campesato LF, Liu C, Cymerman DH, et al. Overcoming resistance to checkpoint blockade therapy by targeting PI3Kγ in myeloid cells. *Nature.* (2016) 539:443–47. doi: 10.1038/nature20554

72. Condamine T, Ramachandran I, Youn JI, Gabrilovich DI. Regulation of tumor metastasis by myeloid-derived suppressor cells. *Annu Rev Med.* (2015) 66:97–110. doi: 10.1146/annurev-med-051013-052304

73. Chanmee T, Ontong P, Konno K, Itano N. Tumor-associated macrophages as major players in the tumor microenvironment. *Cancers (Basel).* (2014) 6:1670–90. doi: 10.3390/cancers6031670

74. Kumar V, Cheng P, Condamine T, Mony S, Languino LR, McCaffrey JC, et al. CD45 phosphatase inhibits STAT3 transcription factor activity in myeloid cells and promotes tumor-associated macrophage differentiation. *Immunity.* (2016) 44:303–15. doi: 10.1016/j.immuni.2016.01.014

75. Bronte V, Brandau S, Chen SH, Colombo MP, Frey AB, Greten TF, et al. Recommendations for myeloid-derived suppressor cell nomenclature and characterization standards. *Nat Commun.* (2016) 7:12150. doi: 10.1038/ncomms12150

76. Madsen DH, Leonard D, Masedunskas A, Moyer A, Jürgensen HJ, Peters DE, et al. M2-like macrophages are responsible for collagen degradation through a mannose receptor-mediated pathway. *J Cell Biol.* (2013) 202:951–66. doi: 10.1083/jcb.201301081

77. Kawachi A, Yoshida H, Kitano S, Ino Y, Kato T, Hiraoka N. Tumor-associated CD204(+) M2 macrophages are unfavorable prognostic indicators in uterine cervical adenocarcinoma. *Cancer Sci.* (2018) 109:863–70. doi: 10.1111/cas.13476

78. Hu W, Li X, Zhang C, Yang Y, Jiang J, Wu C. Tumor-associated macrophages in cancers. *Clin Transl Oncol.* (2016) 18:251–58. doi: 10.1007/s12094-015-1373-0

79. Fritz JM, Tennis MA, Orlicky DJ, Lin H, Ju C, Redente EF, et al. Depletion of tumor-associated macrophages slows the growth of chemically induced mouse lung adenocarcinomas. *Front Immunol.* (2014) 5:587. doi: 10.3389/fimmu.2014.00587

80. Zhu Y, Knolhoff BL, Meyer MA, Nywening TM, West BL, Luo J, et al. CSF1/CSF1R blockade reprograms tumor-infiltrating macrophages and improves response to T-cell checkpoint immunotherapy in pancreatic cancer models. *Cancer Res.* (2014) 74:5057–69. doi: 10.1158/0008-5472.CAN-13-3723

81. Georganaki M, van Hooren L, Dimberg A. Vascular targeting to increase the efficiency of immune checkpoint blockade in cancer. *Front Immunol.* (2018) 9:3081. doi: 10.3389/fimmu.2018.03081

82. Buckanovich RJ, Facciabene A, Kim S, Benencia F, Sasaroli D, Balint K, et al. Endothelin B receptor mediates the endothelial barrier to T cell homing to tumors and disables immune therapy. *Nat Med.* (2008) 14:28–36. doi: 10.1038/nm1699

83. Apte RS, Chen DS, Ferrara N. VEGF in signaling and disease: beyond discovery and development. *Cell.* (2019) 176:1248–64. doi: 10.1016/j.cell.2019.01.021

84. Motz GT, Santoro SP, Wang LP, Garrabrant T, Lastra RR, Hagemann IS, et al. Tumor endothelium FasL establishes a selective immune barrier promoting tolerance in tumors. *Nat Med.* (2014) 20:607–15. doi: 10.1038/nm.3541

85. Jiang H, Hegde S, Knolhoff BL, Zhu Y, Herndon JM, Meyer MA, et al. Targeting focal adhesion kinase renders pancreatic cancers responsive to checkpoint immunotherapy. *Nat Med.* (2016) 22:851–60. doi: 10.1038/nm.4123

86. Huang Y, Kim B, Chan CK, Hahn SM, Weissman IL, Jiang W. Improving immune-vascular crosstalk for cancer immunotherapy. *Nat Rev Immunol.* (2018) 18:195–203. doi: 10.1038/nri.2017.145

87. McDonald PC, Chafe SC, Dedhar S. Overcoming hypoxia-mediated tumor progression: combinatorial approaches targeting pH regulation, angiogenesis and immune dysfunction. *Front Cell Dev Biol.* (2016) 4:27. doi: 10.3389/fcell.2016.00027

88. Facciabene A, Peng X, Hagemann IS, Balint K, Barchetti A, Wang LP, et al. Tumour hypoxia promotes tolerance and angiogenesis via CCL28 and T(reg) cells. *Nature.* (2011) 475:226–30. doi: 10.1038/nature10169

89. Allard B, Allard D, Buisseret L, Stagg J. The adenosine pathway in immuno-oncology. *Nat Rev Clin Oncol.* (2020) 17:611–29. doi: 10.1038/s41571-020-0382-2

90. Antonioli L, Blandizzi C, Pacher P, Haskó G. Immunity, inflammation and cancer: a leading role for adenosine. *Nat Rev Cancer.* (2013) 13:842–57. doi: 10.1038/nrc3613

91. Garg R, Benedetti LG, Abera MB, Wang H, Abba M, Kazanietz MG. Protein kinase C and cancer: what we know and what we do not. *Oncogene.* (2014) 33:5225–37. doi: 10.1038/onc.2013.524

92. Mochly-Rosen D, Das K, Grimes KV. Protein kinase C, an elusive therapeutic target? *Nat Rev Drug Discovery.* (2012) 11:937–57. doi: 10.1038/nrd3871

93. Kikkawa U, Takai Y, Tanaka Y, Miyake R, Nishizuka Y. Protein kinase C as a possible receptor protein of tumor-promoting phorbol esters. *J Biol Chem.* (1983) 258:11442–45. doi: 10.1016/S0021-9258(17)44245-1

94. Sadeghi MM, Salama MF, Hannun YA. Protein kinase C as a therapeutic target in non-small cell lung cancer. *Int J Mol Sci.* (2021) 22. doi: 10.3390/ijms22115527

95. Black AR, Black JD. Protein kinase C signaling and cell cycle regulation. *Front Immunol.* (2012) 3:423. doi: 10.3389/fimmu.2012.00423

96. Cheng Y, Zhu Y, Xu W, Xu J, Yang M, Chen P, et al. PKCα in colon cancer cells promotes M1 macrophage polarization via MKK3/6-P38 MAPK pathway. *Mol Carcinog.* (2018) 57:1017–29. doi: 10.1002/mc.22822

97. Pfeifhofer C, Kofler K, Gruber T, Tabrizi NG, Lutz C, Maly K, et al. Protein kinase C theta affects Ca2+ mobilization and NFAT cell activation in primary mouse T cells. *J Exp Med.* (2003) 197:1525–35. doi: 10.1084/jem.20020234

98. Kwon MJ, Ma J, Ding Y, Wang R, Sun Z. Protein kinase C-θ promotes Th17 differentiation via upregulation of Stat3. *J Immunol.* (2012) 188:5887–97. doi: 10.4049/jimmunol.1102941

99. He X, Koenen H, Smeets RL, Keijsers R, van Rijssen E, Koerber A, et al. Targeting PKC in human T cells using sotrastaurin (AEB071) preserves regulatory T cells and prevents IL-17 production. *J Invest Dermatol.* (2014) 134:975–83. doi: 10.1038/jid.2013.459

100. Xia P, Aiello LP, Ishii H, Jiang ZY, Park DJ, Robinson GS, et al. Characterization of vascular endothelial growth factor's effect on the activation of protein kinase C, its isoforms, and endothelial cell growth. *J Clin Invest.* (1996) 98:2018–26. doi: 10.1172/JCI119006

101. Suzuma K, Takahara N, Suzuma I, Isshiki K, Ueki K, Leitges M, et al. Characterization of protein kinase C beta isoform's action on retinoblastoma protein phosphorylation, vascular endothelial growth factor-induced endothelial cell proliferation, and retinal neovascularization. *Proc Natl Acad Sci U.S.A.* (2002) 99:721–26. doi: 10.1073/pnas.022644499

102. Goicoechea SM, García-Mata R, Staub J, Valdivia A, Sharek L, McCulloch CG, et al. Palladin promotes invasion of pancreatic cancer cells by enhancing invadopodia formation in cancer-associated fibroblasts. *Oncogene.* (2014) 33:1265–73. doi: 10.1038/onc.2013.68

103. Hennings H, Blumberg PM, Pettit GR, Herald CL, Shores R, Yuspa SH. Bryostatin 1, an activator of protein kinase C, inhibits tumor promotion by phorbol esters in SENCAR mouse skin. *Carcinogenesis.* (1987) 8:1343–46. doi: 10.1093/carcin/8.9.1343

104. Boyle GM, D'Souza MM, Pierce CJ, Adams RA, Cantor AS, Johns JP, et al. Intra-lesional injection of the novel PKC activator EBC-46 rapidly ablates tumors in mouse models. *PloS One.* (2014) 9:e108887. doi: 10.1371/journal.pone.0108887

105. Miller J, Campbell J, Blum A, Reddell P, Gordon V, Schmidt P, et al. Dose characterization of the investigational anticancer drug tigilanol tiglate (EBC-46) in the local treatment of canine mast cell tumors. *Front Vet Sci.* (2019) 6:106. doi: 10.3389/fvets.2019.00106

106. De Ridder TR, Campbell JE, Burke-Schwarz C, Clegg D, Elliot EL, Geller S, et al. Randomized controlled clinical study evaluating the efficacy and safety of intratumoral treatment of canine mast cell tumors with tigilanol tiglate (EBC-46). *J Vet Intern Med.* (2021) 35:415–29. doi: 10.1111/jvim.15806

107. Utz I, Hofer S, Regenass U, Hilbe W, Thaler J, Grunicke H, et al. The protein kinase C inhibitor CGP 41251, a staurosporine derivative with antitumor activity, reverses multidrug resistance. *Int J Cancer.* (1994) 57:104–10. doi: 10.1002/ijc.2910570119

108. Song MS, Salmena L, Pandolfi PP. The functions and regulation of the PTEN tumour suppressor. *Nat Rev Mol Cell Biol.* (2012) 13:283–96. doi: 10.1038/nrm3330

109. Wang Z, Wu X. Study and analysis of antitumor resistance mechanism of PD1/PD-L1 immune checkpoint blocker. *Cancer Med.* (2020) 9:8086–121. doi: 10.1002/cam4.3410

110. Roh W, Chen PL, Reuben A, Spencer CN, Prieto PA, Miller JP, et al. Integrated molecular analysis of tumor biopsies on sequential CTLA-4 and PD-1 blockade reveals markers of response and resistance. *Sci Transl Med.* (2017) 9:104–10. doi: 10.1126/scitranslmed.aah3560

111. Bard-Chapeau EA, Li S, Ding J, Zhang SS, Zhu HH, Princen F, et al. Ptpn11/Shp2 acts as a tumor suppressor in hepatocellular carcinogenesis. *Cancer Cell.* (2011) 19:629–39. doi: 10.1016/j.ccr.2011.03.023

112. Liu JJ, Li Y, Chen WS, Liang Y, Wang G, Zong M, et al. Shp2 deletion in hepatocytes suppresses hepatocarcinogenesis driven by oncogenic β-Catenin, PIK3CA and MET. *J Hepatol.* (2018) 69:79–88. doi: 10.1016/j.jhep.2018.02.014

113. Song M, Chen D, Lu B, Wang C, Zhang J, Huang L, et al. PTEN loss increases PD-L1 protein expression and affects the correlation between PD-L1 expression and clinical parameters in colorectal cancer. *PloS One.* (2013) 8:e65821. doi: 10.1371/journal.pone.0065821

114. Sun C, Mezzadra R, Schumacher TN. Regulation and function of the PD-L1 checkpoint. *Immunity.* (2018) 48:434–52. doi: 10.1016/j.immuni.2018.03.014

115. Peng W, Chen JQ, Liu C, Malu S, Creasy C, Tetzlaff MT, et al. Loss of PTEN promotes resistance to T cell-mediated immunotherapy. *Cancer Discovery.* (2016) 6:202–16. doi: 10.1158/2159-8290.CD-15-0283

116. de Gramont A, Faivre S, Raymond E. Novel TGF-β inhibitors ready for prime time in onco-immunology. *Oncoimmunology.* (2017) 6:e1257453. doi: 10.1080/2162402X.2016.1257453

117. Labidi-Galy SI, Sisirak V, Meeus P, Gobert M, Treilleux I, Bajard A, et al. Quantitative and functional alterations of plasmacytoid dendritic cells contribute to immune tolerance in ovarian cancer. *Cancer Res.* (2011) 71:5423–34. doi: 10.1158/0008-5472.CAN-11-0367

118. Sisirak V, Faget J, Vey N, Blay JY, Ménétrier-Caux C, Caux C, et al. Plasmacytoid dendritic cells deficient in IFNα production promote the amplification of FOXP3(+) regulatory T cells and are associated with poor prognosis in breast cancer patients. *Oncoimmunology.* (2013) 2:e22338. doi: 10.4161/onci.22338

119. Yang L, Moses HL. Transforming growth factor beta: tumor suppressor or promoter? Are host immune cells the answer? *Cancer Res.* (2008) 68:9107–11. doi: 10.1158/0008-5472.CAN-08-2556

120. Batlle E, Massagué J. Transforming growth factor-β Signaling in immunity and cancer. *Immunity.* (2019) 50:924–40. doi: 10.1016/j.immuni.2019.03.024

121. Derynck R, Turley SJ, Akhurst RJ. TGFβ biology in cancer progression and immunotherapy. *Nat Rev Clin Oncol.* (2021) 18:9–34. doi: 10.1038/s41571-020-0403-1

122. Xie F, Ling L, van Dam H, Zhou F, Zhang L. TGF-β signaling in cancer metastasis. *Acta Biochim Biophys Sin (Shanghai).* (2018) 50:121–32. doi: 10.1093/abbs/gmx123

123. An X, Zhu Y, Zheng T, Wang G, Zhang M, Li J, et al. An analysis of the expression and association with immune cell infiltration of the cGAS/STING pathway in pan-cancer. *Mol Ther Nucleic Acids.* (2019) 14:80–9. doi: 10.1016/j.omtn.2018.11.003

124. Bakhoum SF, Ngo B, Laughney AM, Cavallo JA, Murphy CJ, Ly P, et al. Chromosomal instability drives metastasis through a cytosolic DNA response. *Nature.* (2018) 553:467–72. doi: 10.1038/nature25432

125. Woo SR, Fuertes MB, Corrales L, Spranger S, Furdyna MJ, Leung MY, et al. STING-dependent cytosolic DNA sensing mediates innate immune recognition of immunogenic tumors. *Immunity.* (2014) 41:830–42. doi: 10.1016/j.immuni.2014.10.017

126. Decout A, Katz JD, Venkatraman S, Ablasser A. The cGAS-STING pathway as a therapeutic target in inflammatory diseases. *Nat Rev Immunol.* (2021) 21:548–69. doi: 10.1038/s41577-021-00524-z

127. Li J, Duran MA, Dhanota N, Chatila WK, Bettigole SE, Kwon J, et al. Metastasis and immune evasion from extracellular cGAMP hydrolysis. *Cancer Discov.* (2021) 11:1212–27. doi: 10.1158/2159-8290.CD-20-0387

128. Chen Q, Boire A, Jin X, Valiente M, Er EE, Lopez-Soto A, et al. Carcinoma-astrocyte gap junctions promote brain metastasis by cGAMP transfer. *Nature.* (2016) 533:493–98. doi: 10.1038/nature18268

129. Rudd CE, Schneider H. Unifying concepts in CD28, ICOS and CTLA4 co-receptor signalling. *Nat Rev Immunol.* (2003) 3:544–56. doi: 10.1038/nri1131

130. Yokosuka T, Kobayashi W, Takamatsu M, Sakata-Sogawa K, Zeng H, Hashimoto-Tane A, et al. Spatiotemporal basis of CTLA-4 costimulatory molecule-mediated negative regulation of T cell activation. *Immunity.* (2010) 33:326–39. doi: 10.1016/j.immuni.2010.09.006

131. Tivol EA, Borriello F, Schweitzer AN, Lynch WP, Bluestone JA, Sharpe AH. Loss of CTLA-4 leads to massive lymphoproliferation and fatal multiorgan tissue destruction, revealing a critical negative regulatory role of CTLA-4. *Immunity.* (1995) 3:541–47. doi: 10.1016/1074-7613(95)90125-6

132. Waterhouse P, Penninger JM, Timms E, Wakeham A, Shahinian A, Lee KP, et al. Lymphoproliferative disorders with early lethality in mice deficient in Ctla-4. *Science.* (1995) 270:985–88. doi: 10.1126/science.270.5238.985

133. Sharpe AH, Freeman GJ. The B7-CD28 superfamily. *Nat Rev Immunol.* (2002) 2:116–26. doi: 10.1038/nri727

134. Wu K, Yi M, Qin S, Chu Q, Zheng X, Wu K. The efficacy and safety of combination of PD-1 and CTLA-4 inhibitors: a meta-analysis. *Exp Hematol Oncol.* (2019) 8:26. doi: 10.1186/s40164-019-0150-0

135. Hodi FS, Chesney J, Pavlick AC, Robert C, Grossmann KF, McDermott DF, et al. Combined nivolumab and ipilimumab versus ipilimumab alone in patients with advanced melanoma: 2-year overall survival outcomes in a multicentre, randomised, controlled, phase 2 trial. *Lancet Oncol.* (2016) 17:1558–68. doi: 10.1016/S1470-2045(16)30366-7

136. Larkin J, Chiarion-Sileni V, Gonzalez R, Grob JJ, Rutkowski P, Lao CD, et al. Five-year survival with combined nivolumab and ipilimumab in advanced melanoma. *N Engl J Med.* (2019) 381:1535–46. doi: 10.1056/NEJMoa1910836

137. Overman MJ, Lonardi S, Wong K, Lenz HJ, Gelsomino F, Aglietta M, et al. Durable clinical benefit with nivolumab plus ipilimumab in DNA mismatch repair-deficient/microsatellite instability-high metastatic colorectal cancer. *J Clin Oncol.* (2018) 36:773–79. doi: 10.1200/JCO.2017.76.9901

138. Motzer RJ, Rini BI, McDermott DF, Arén FO, Hammers HJ, Carducci MA, et al. Nivolumab plus ipilimumab versus sunitinib in first-line treatment for advanced renal cell carcinoma: extended follow-up of efficacy and safety results from a randomised, controlled, phase 3 trial. *Lancet Oncol.* (2019) 20:1370–85. doi: 10.1016/S1470-2045(19)30413-9

139. Hellmann MD, Paz-Ares L, Bernabe CR, Zurawski B, Kim SW, Carcereny CE, et al. Nivolumab plus ipilimumab in advanced non-small-cell lung cancer. *N Engl J Med.* (2019) 381:2020–31. doi: 10.1056/NEJMoa1910231

140. Baas P, Scherpereel A, Nowak AK, Fujimoto N, Peters S, Tsao AS, et al. First-line nivolumab plus ipilimumab in unresectable Malignant pleural mesothelioma (CheckMate 743): a multicentre, randomised, open-label, phase 3 trial. *Lancet.* (2021) 397:375–86. doi: 10.1016/S0140-6736(20)32714-8

141. Zhu C, Anderson AC, Schubart A, Xiong H, Imitola J, Khoury SJ, et al. The Tim-3 ligand galectin-9 negatively regulates T helper type 1 immunity. *Nat Immunol.* (2005) 6:1245–52. doi: 10.1038/ni1271

142. Sakuishi K, Apetoh L, Sullivan JM, Blazar BR, Kuchroo VK, Anderson AC. Targeting Tim-3 and PD-1 pathways to reverse T cell exhaustion and restore anti-tumor immunity. *J Exp Med.* (2010) 207:2187–94. doi: 10.1084/jem.20100643

143. Harding JJ, Moreno V, Bang YJ, Hong MH, Patnaik A, Trigo J, et al. Blocking TIM-3 in treatment-refractory advanced solid tumors: A phase ia/b study of LY3321367 with or without an anti-PD-L1 antibody. *Clin Cancer Res.* (2021) 27:2168–78. doi: 10.1158/1078-0432.CCR-20-4405

144. Hollebecque A, Chung HC, de Miguel MJ, Italiano A, Machiels JP, Lin CC, et al. Safety and antitumor activity of α-PD-L1 antibody as monotherapy or in combination with α-TIM-3 antibody in patients with microsatellite instability-high/mismatch repair-deficient tumors. *Clin Cancer Res.* (2021) 27:6393–404. doi: 10.1158/1078-0432.CCR-21-0261

145. Curigliano G, Gelderblom H, Mach N, Doi T, Tai D, Forde PM, et al. Phase I/ib clinical trial of sabatolimab, an anti-TIM-3 antibody, alone and in combination with spartalizumab, an anti-PD-1 antibody, in advanced solid tumors. *Clin Cancer Res.* (2021) 27:3620–29. doi: 10.1158/1078-0432.CCR-20-4746

146. Gestermann N, Saugy D, Martignier C, Tillé L, Fuertes MS, Zettl M, et al. LAG-3 and PD-1+LAG-3 inhibition promote anti-tumor immune responses in human autologous melanoma/T cell co-cultures. *Oncoimmunology.* (2020) 9:1736792. doi: 10.1080/2162402X.2020.1736792

147. Li Y, Zhang Y, Cao G, Zheng X, Sun C, Wei H, et al. Blockade of checkpoint receptor PVRIG unleashes anti-tumor immunity of NK cells in murine and human solid tumors. *J Hematol Oncol*. (2021) 14:100. doi: 10.1186/s13045-021-01112-3

148. Mao L, Xiao Y, Yang QC, Yang SC, Yang LL, Sun ZJ. TIGIT/CD155 blockade enhances anti-PD-L1 therapy in head and neck squamous cell carcinoma by targeting myeloid-derived suppressor cells. *Oral Oncol*. (2021) 121:105472. doi: 10.1016/j.oraloncology.2021.105472

149. Xiao N, Zhu X, Li K, Chen Y, Liu X, Xu B, et al. Blocking siglec-10(hi) tumor-associated macrophages improves anti-tumor immunity and enhances immunotherapy for hepatocellular carcinoma. *Exp Hematol Oncol*. (2021) 10:36. doi: 10.1186/s40164-021-00230-5

150. Lipson EJ, Tawbi HA, SChadendorf D, Ascierto PA, Matamala L, Gutiérrez EC, et al. Relatlimab (RELA) plus nivolumab (NIVO) versus NIVO in first-line advanced melanoma: Primary phase III results from RELATIVITY-047 (CA224-047). *J Clin Oncol*. (2021) 39:9503. doi: 10.1200/JCO.2021.39.15_suppl.9503

151. Vaena DA, Fleming GF, Chmielowski B, Sharma M, Hamilton EP, Sullivan RJ, et al. COM701 with or without nivolumab: Results of an ongoing phase 1 study of safety, tolerability and preliminary antitumor activity in patients with advanced solid Malignancies (NCT03667716). *J Clin Oncol*. (2021) 39:2504. doi: 10.1200/JCO.2021.39.15_suppl.2504

152. Rodriguez-Abreu D, Johnson ML, Hussein MA, Cobo M, Patel AJ, Secen NM, et al. Primary analysis of a randomized, double-blind, phase II study of the anti-TIGIT antibody tiragolumab (tira) plus atezolizumab (atezo) versus placebo plus atezo as first-line (1L) treatment in patients with PD-L1-selected NSCLC (CITYSCAPE). *J Clin Oncol*. (2020) 38:9503. doi: 10.1200/JCO.2020.38.15_suppl.9503

153. Daei SA, Mohamed KL, Sarkesh A, Mardi A, Aghebati-Maleki A, Aghebati-Maleki L, et al. The current landscape of CAR T-cell therapy for solid tumors: Mechanisms, research progress, challenges, and counterstrategies. *Front Immunol*. (2023) 14:1113882. doi: 10.3389/fimmu.2023.1113882

154. Mirzaei HR, Rodriguez A, Shepphird J, Brown CE, Badie B. Chimeric antigen receptors T cell therapy in solid tumor: challenges and clinical applications. *Front Immunol*. (2017) 8:1850. doi: 10.3389/fimmu.2017.01850

155. Cherkassky L, Morello A, Villena-Vargas J, Feng Y, Dimitrov DS, Jones DR, et al. Human CAR T cells with cell-intrinsic PD-1 checkpoint blockade resist tumor-mediated inhibition. *J Clin Invest*. (2016) 126:3130–44. doi: 10.1172/JCI83092

156. John LB, Devaud C, Duong CP, Yong CS, Beavis PA, Haynes NM, et al. Anti-PD-1 antibody therapy potently enhances the eradication of established tumors by gene-modified T cells. *Clin Cancer Res*. (2013) 19:5636–46. doi: 10.1158/1078-0432.CCR-13-0458

157. Miller JS, Soignier Y, Panoskaltsis-Mortari A, McNearney SA, Yun GH, Fautsch SK, et al. Successful adoptive transfer and in *vivo* expansion of human haploidentical NK cells in patients with cancer. *Blood*. (2005) 105:3051–57. doi: 10.1182/blood-2004-07-2974

158. Ruggeri L, Capanni M, Urbani E, Perruccio K, Shlomchik WD, Tosti A, et al. Effectiveness of donor natural killer cell alloreactivity in mismatched hematopoietic transplants. *Science*. (2002) 295:2097–100. doi: 10.1126/science.1068440

159. Simonetta F, Alvarez M, Negrin RS. Natural killer cells in graft-versus-host-disease after allogeneic hematopoietic cell transplantation. *Front Immunol*. (2017) 8:465. doi: 10.3389/fimmu.2017.00465

160. Huang RS, Lai MC, Shih HA, Lin S. A robust platform for expansion and genome editing of primary human natural killer cells. *J Exp Med*. (2021) 218:5636–46. doi: 10.1084/jem.20201529

161. Suen WC, Lee WY, Leung KT, Pan XH, Li G. Natural killer cell-based cancer immunotherapy: A review on 10 years completed clinical trials. *Cancer Invest*. (2018) 36:431–57. doi: 10.1080/07357907.2018.1515315

162. Wang W, Jiang J, Wu C. CAR-NK for tumor immunotherapy: Clinical transformation and future prospects. *Cancer Lett*. (2020) 472:175–80. doi: 10.1016/j.canlet.2019.11.033

163. Li Y, Hermanson DL, Moriarity BS, Kaufman DS. Human iPSC-derived natural killer cells engineered with chimeric antigen receptors enhance anti-tumor activity. *Cell Stem Cell*. (2018) 23:181–92. doi: 10.1016/j.stem.2018.06.002

164. Quintarelli C, Sivori S, Caruso S, Carlomagno S, Falco M, Boffa I, et al. Efficacy of third-party chimeric antigen receptor modified peripheral blood natural killer cells for adoptive cell therapy of B-cell precursor acute lymphoblastic leukemia. *Leukemia*. (2020) 34:1102–15. doi: 10.1038/s41375-019-0613-7

165. Liu E, Marin D, Banerjee P, Macapinlac HA, Thompson P, Basar R, et al. Use of CAR-transduced natural killer cells in CD19-positive lymphoid tumors. *N Engl J Med*. (2020) 382:545–53. doi: 10.1056/NEJMoa1910607

166. Zhang L, Meng Y, Feng X, Han Z. CAR-NK cells for cancer immunotherapy: from bench to bedside. *biomark Res*. (2022) 10:12. doi: 10.1186/s40364-022-00364-6

167. van de Donk N, Zweegman S. T-cell-engaging bispecific antibodies in cancer. *Lancet*. (2023) 402:142–58. doi: 10.1016/S0140-6736(23)00521-4

168. Wei J, Yang Y, Wang G, Liu M. Current landscape and future directions of bispecific antibodies in cancer immunotherapy. *Front Immunol*. (2022) 13:6537. doi: 10.3389/fimmu.2022.1035276

169. Rezaei M, Danilova ND, Soltani M, Savvateeva LV, Tarasov VV, Ganjalikhani-Hakemi M, et al. Cancer vaccine in cold tumors: clinical landscape, challenges, and opportunities. *Curr Cancer Drug Targets*. (2022) 22:437–53. doi: 10.2174/1568009622666220214103533

170. Blass E, Ott PA. Advances in the development of personalized neoantigen-based therapeutic cancer vaccines. *Nat Rev Clin Oncol*. (2021) 18:215–29. doi: 10.1038/s41571-020-00460-2

171. Kantoff PW, Higano CS, Shore ND, Berger ER, Small EJ, Penson DF, et al. Sipuleucel-T immunotherapy for castration-resistant prostate cancer. *N Engl J Med*. (2010) 363:411–22. doi: 10.1056/NEJMoa1001294

172. Kinkead HL, Hopkins A, Lutz E, Wu AA, Yarchoan M, Cruz K, et al. Combining STING-based neoantigen-targeted vaccine with checkpoint modulators enhances antitumor immunity in murine pancreatic cancer. *JCI Insight*. (2018) 3:6537. doi: 10.1172/jci.insight.122857

173. Zhu G, Lynn GM, Jacobson O, Chen K, Liu Y, Zhang H, et al. Albumin/vaccine nanocomplexes that assemble in *vivo* for combination cancer immunotherapy. *Nat Commun*. (2017) 8:1954. doi: 10.1038/s41467-017-02191-y

174. Sahin U, Derhovanessian E, Miller M, Kloke BP, Simon P, Löwer M, et al. Personalized RNA mutanome vaccines mobilize poly-specific therapeutic immunity against cancer. *Nature*. (2017) 547:222–26. doi: 10.1038/nature23003

175. Ott PA, Hu-Lieskovan S, Chmielowski B, Govindan R, Naing A, Bhardwaj N, et al. A phase ib trial of personalized neoantigen therapy plus anti-PD-1 in patients with advanced melanoma, non-small cell lung cancer, or bladder cancer. *Cell*. (2020) 183:347–62. doi: 10.1016/j.cell.2020.08.053

176. Innao V, Rizzo V, Allegra AG, Musolino C, Allegra A. Oncolytic viruses and hematological Malignancies: A new class of immunotherapy drugs. *Curr Oncol*. (2020) 28:159–83. doi: 10.3390/curroncol28010019

177. Chesney J, Puzanov I, Collichio F, Singh P, Milhem MM, Glaspy J, et al. Randomized, open-label phase II study evaluating the efficacy and safety of talimogene laherparepvec in combination with ipilimumab versus ipilimumab alone in patients with advanced, unresectable melanoma. *J Clin Oncol*. (2018) 36:1658–67. doi: 10.1200/JCO.2017.73.7379

178. Samson A, Scott KJ, Taggart D, West EJ, Wilson E, Nuovo GJ, et al. Intravenous delivery of oncolytic reovirus to brain tumor patients immunologically primes for subsequent checkpoint blockade. *Sci Transl Med*. (2018) 10:222–6. doi: 10.1126/scitranslmed.aam7577

179. Bourgeois-Daigneault MC, Roy DG, Aitken AS, El SN, Martin NT, Varette O, et al. Neoadjuvant oncolytic virotherapy before surgery sensitizes triple-negative breast cancer to immune checkpoint therapy. *Sci Transl Med*. (2018) 10:362–47. doi: 10.1126/scitranslmed.aao1641

180. Mantovani A, Allavena P, Marchesi F, Garlanda C. Macrophages as tools and targets in cancer therapy. *Nat Rev Drug Discov*. (2022) 21:799–820. doi: 10.1038/s41573-022-00520-5

181. Xiang X, Wang J, Lu D, Xu X. Targeting tumor-associated macrophages to synergize tumor immunotherapy. *Signal Transduct Target Ther*. (2021) 6:75. doi: 10.1038/s41392-021-00484-9

182. Harada K, Dong X, Estrella JS, Correa AM, Xu Y, Hofstetter WL, et al. Tumor-associated macrophage infiltration is highly associated with PD-L1 expression in gastric adenocarcinoma. *Gastric Cancer*. (2018) 21:31–40. doi: 10.1007/s10120-017-0760-3

183. Tsukamoto M, Imai K, Ishimoto T, Komohara Y, Yamashita YI, Nakagawa S, et al. PD-L1 expression enhancement by infiltrating macrophage-derived tumor necrosis factor-α leads to poor pancreatic cancer prognosis. *Cancer Sci*. (2019) 110:310–20. doi: 10.1111/cas.13874

184. Omstead AN, Paskewicz M, Gorbunova A, Zheng P, Salvitti MS, Mansoor R, et al. CSF-1R inhibitor, pexidartinib, sensitizes esophageal adenocarcinoma to PD-1 immune checkpoint blockade in a rat model. *Carcinogenesis*. (2022) 43:842–50. doi: 10.1093/carcin/bgac043

185. Shi G, Yang Q, Zhang Y, Jiang Q, Lin Y, Yang S, et al. Modulating the tumor microenvironment via oncolytic viruses and CSF-1R inhibition synergistically enhances anti-PD-1 immunotherapy. *Mol Ther*. (2019) 27:244–60. doi: 10.1016/j.ymthe.2018.11.010

186. Gomez-Roca C, Cassier P, Zamarin D, Machiels JP, Perez GJ, Stephen HF, et al. Anti-CSF-1R emactuzumab in combination with anti-PD-L1 atezolizumab in advanced solid tumor patients naïve or experienced for immune checkpoint blockade. *J Immunother Cancer*. (2022) 10:799–820. doi: 10.1136/jitc-2021-004076

187. Haag GM, Springfeld C, Grün B, Apostolidis L, Zschäbitz S, Dietrich M, et al. Pembrolizumab and maraviroc in refractory mismatch repair proficient/microsatellite-stable metastatic colorectal cancer - The PICCASSO phase I trial. *Eur J Cancer*. (2022) 167:112–22. doi: 10.1016/j.ejca.2022.03.017

188. Reits EA, Hodge JW, Herberts CA, Groothuis TA, Chakraborty M, Wansley EK, et al. Radiation modulates the peptide repertoire, enhances MHC class I expression, and induces successful antitumor immunotherapy. *J Exp Med*. (2006) 203:1259–71. doi: 10.1084/jem.20052494

189. Tesniere A, Panaretakis T, Kepp O, Apetoh L, Ghiringhelli F, Zitvogel L, et al. Molecular characteristics of immunogenic cancer cell death. *Cell Death Differ*. (2008) 15:3–12. doi: 10.1038/sj.cdd.4402269

190. Deng L, Liang H, Burnette B, Beckett M, Darga T, Weichselbaum RR, et al. Irradiation and anti-PD-L1 treatment synergistically promote antitumor immunity in mice. *J Clin Invest*. (2014) 124:687–95. doi: 10.1172/JCI67313

191. Barker HE, Paget JT, Khan AA, Harrington KJ. The tumour microenvironment after radiotherapy: mechanisms of resistance and recurrence. *Nat Rev Cancer*. (2015) 15:409–25. doi: 10.1038/nrc3958

192. Ngwa W, Irabor OC, Schoenfeld JD, Hesser J, Demaria S, Formenti SC. Using immunotherapy to boost the abscopal effect. *Nat Rev Cancer*. (2018) 18:313–22. doi: 10.1038/nrc.2018.6

193. Postow MA, Callahan MK, Barker CA, Yamada Y, Yuan J, Kitano S, et al. Immunologic correlates of the abscopal effect in a patient with melanoma. *N Engl J Med*. (2012) 366:925–31. doi: 10.1056/NEJMoa1112824

194. Abuodeh Y, Venkat P, Kim S. Systematic review of case reports on the abscopal effect. *Curr Probl Cancer*. (2016) 40:25–37. doi: 10.1016/j.currproblcancer.2015.10.001

195. Park SS, Dong H, Liu X, Harrington SM, Krco CJ, Grams MP, et al. PD-1 restrains radiotherapy-induced abscopal effect. *Cancer Immunol Res*. (2015) 3:610–19. doi: 10.1158/2326-6066.CIR-14-0138

196. Reynders K, Illidge T, Siva S, Chang JY, De Ruysscher D. The abscopal effect of local radiotherapy: using immunotherapy to make a rare event clinically relevant. *Cancer Treat Rev*. (2015) 41:503–10. doi: 10.1016/j.ctrv.2015.03.011

197. Dudzinski SO, Cameron BD, Wang J, Rathmell JC, Giorgio TD, Kirschner AN. Combination immunotherapy and radiotherapy causes an abscopal treatment response in a mouse model of castration resistant prostate cancer. *J Immunother Cancer*. (2019) 7:218. doi: 10.1186/s40425-019-0704-z

198. Ji D, Song C, Li Y, Xia J, Wu Y, Jia J, et al. Combination of radiotherapy and suppression of Tregs enhances abscopal antitumor effect and inhibits metastasis in rectal cancer. *J Immunother Cancer*. (2020) 8:313–22. doi: 10.1136/jitc-2020-000826

199. Antonia SJ, Villegas A, Daniel D, Vicente D, Murakami S, Hui R, et al. Overall survival with durvalumab after chemoradiotherapy in stage III NSCLC. *N Engl J Med*. (2018) 379:2342–50. doi: 10.1056/NEJMoa1809697

200. Fizazi K, Drake CG, Beer TM, Kwon ED, Scher HI, Gerritsen WR, et al. Final analysis of the ipilimumab versus placebo following radiotherapy phase III trial in postdocetaxel metastatic castration-resistant prostate cancer identifies an excess of long-term survivors. *Eur Urol*. (2020) 78:822–30. doi: 10.1016/j.eururo.2020.07.032

201. Zitvogel L, Galluzzi L, Smyth MJ, Kroemer G. Mechanism of action of conventional and targeted anticancer therapies: reinstating immunosurveillance. *Immunity*. (2013) 39:74–88. doi: 10.1016/j.immuni.2013.06.014

202. Wang Q, Ju X, Wang J, Fan Y, Ren M, Zhang H. Immunogenic cell death in anticancer chemotherapy and its impact on clinical studies. *Cancer Lett*. (2018) 438:17–23. doi: 10.1016/j.canlet.2018.08.028

203. Rodríguez-Abreu D, Powell SF, Hochmair MJ, Gadgeel S, Esteban E, Felip E, et al. Pemetrexed plus platinum with or without pembrolizumab in patients with previously untreated metastatic nonsquamous NSCLC: protocol-specified final analysis from KEYNOTE-189. *Ann Oncol*. (2021) 32:881–95. doi: 10.1016/j.annonc.2021.04.008

204. Cortes J, Cescon DW, Rugo HS, Nowecki Z, Im SA, Yusof MM, et al. Pembrolizumab plus chemotherapy versus placebo plus chemotherapy for previously untreated locally recurrent inoperable or metastatic triple-negative breast cancer (KEYNOTE-355): a randomised, placebo-controlled, double-blind, phase 3 clinical trial. *Lancet*. (2020) 396:1817–28. doi: 10.1016/S0140-6736(20)32531-9

205. Awad MM, Gadgeel SM, Borghaei H, Patnaik A, Yang JC, Powell SF, et al. Long-term overall survival from KEYNOTE-021 cohort G: pemetrexed and carboplatin with or without pembrolizumab as first-line therapy for advanced nonsquamous NSCLC. *J Thorac Oncol*. (2021) 16:162–68. doi: 10.1016/j.jtho.2020.09.015

206. Horn L, Mansfield AS, Szczęsna A, Havel L, Krzakowski M, Hochmair MJ, et al. First-line atezolizumab plus chemotherapy in extensive-stage small-cell lung cancer. *N Engl J Med*. (2018) 379:2220–29. doi: 10.1056/NEJMoa1809064

207. Ni JJ, Zhang ZZ, Ge MJ, Chen JY, Zhuo W. Immune-based combination therapy to convert immunologically cold tumors into hot tumors: an update and new insights. *Acta Pharmacol Sin*. (2023) 44:288–307. doi: 10.1038/s41401-022-00953-z

208. Gutzmer R, Stroyakovskiy D, Gogas H, Robert C, Lewis K, Protsenko S, et al. Atezolizumab, vemurafenib, and cobimetinib as first-line treatment for unresectable advanced BRAF(V600) mutation-positive melanoma (IMspire150): primary analysis of the randomised, double-blind, placebo-controlled, phase 3 trial. *Lancet*. (2020) 395:1835–44. doi: 10.1016/S0140-6736(20)30934-X

209. Domchek SM, Postel-Vinay S, Im SA, Park YH, Delord JP, Italiano A, et al. Olaparib and durvalumab in patients with germline BRCA-mutated metastatic breast cancer (MEDIOLA): an open-label, multicentre, phase 1/2, basket study. *Lancet Oncol*. (2020) 21:1155–64. doi: 10.1016/S1470-2045(20)30324-7

210. Khoo LT, Chen LY. Role of the cGAS-STING pathway in cancer development and oncotherapeutic approaches. *EMBO Rep*. (2018) 19:1817–28. doi: 10.15252/embr.201846935

211. Gao P, Ascano M, Wu Y, Barchet W, Gaffney BL, Zillinger T, et al. Cyclic [G(2',5')pA(3',5')p] is the metazoan second messenger produced by DNA-activated cyclic GMP-AMP synthase. *Cell*. (2013) 153:1094–107. doi: 10.1016/j.cell.2013.04.046

212. Ablasser A, Goldeck M, Cavlar T, Deimling T, Witte G, Röhl I, et al. cGAS produces a 2'-5'-linked cyclic dinucleotide second messenger that activates STING. *Nature*. (2013) 498:380–84. doi: 10.1038/nature12306

213. Jiang M, Chen P, Wang L, Li W, Chen B, Liu Y, et al. cGAS-STING, an important pathway in cancer immunotherapy. *J Hematol Oncol*. (2020) 13:81. doi: 10.1186/s13045-020-00916-z

214. Abe T, Barber GN. Cytosolic-DNA-mediated, STING-dependent proinflammatory gene induction necessitates canonical NF-κB activation through TBK1. *J Virol*. (2014) 88:5328–41. doi: 10.1128/JVI.00037-14

215. Fuertes MB, Woo SR, Burnett B, Fu YX, Gajewski TF. Type I interferon response and innate immune sensing of cancer. *Trends Immunol*. (2013) 34:67–73. doi: 10.1016/j.it.2012.10.004

216. Lara PJ, Douillard JY, Nakagawa K, von Pawel J, McKeage MJ, Albert I, et al. Randomized phase III placebo-controlled trial of carboplatin and paclitaxel with or without the vascular disrupting agent vadimezan (ASA404) in advanced non-small-cell lung cancer. *J Clin Oncol*. (2011) 29:2965–71. doi: 10.1200/JCO.2011.35.0660

217. Shih AY, Damm-Ganamet KL, Mirzadegan T. Dynamic structural differences between human and mouse STING lead to differing sensitivity to DMXAA. *Biophys J*. (2018) 114:32–9. doi: 10.1016/j.bpj.2017.10.027

218. Conlon J, Burdette DL, Sharma S, Bhat N, Thompson M, Jiang Z, et al. Mouse, but not human STING, binds and signals in response to the vascular disrupting agent 5,6-dimethylxanthenone-4-acetic acid. *J Immunol*. (2013) 190:5216–25. doi: 10.4049/jimmunol.1300097

219. Burdette DL, Vance RE. STING and the innate immune response to nucleic acids in the cytosol. *Nat Immunol*. (2013) 14:19–26. doi: 10.1038/ni.2491

220. Burdette DL, Monroe KM, Sotelo-Troha K, Iwig JS, Eckert B, Hyodo M, et al. STING is a direct innate immune sensor of cyclic di-GMP. *Nature*. (2011) 478:515–18. doi: 10.1038/nature10429

221. Corrales L, Glickman LH, McWhirter SM, Kanne DB, Sivick KE, Katibah GE, et al. Direct activation of STING in the tumor microenvironment leads to potent and systemic tumor regression and immunity. *Cell Rep*. (2015) 11:1018–30. doi: 10.1016/j.celrep.2015.04.031

222. Ramanjulu JM, Pesiridis GS, Yang J, Concha N, Singhaus R, Zhang SY, et al. Design of amidobenzimidazole STING receptor agonists with systemic activity. *Nature*. (2018) 564:439–43. doi: 10.1038/s41586-018-0705-y

223. Pan BS, Perera SA, Piesvaux JA, Presland JP, Schroeder GK, Cumming JN, et al. An orally available non-nucleotide STING agonist with antitumor activity. *Science*. (2020) 369:32–9. doi: 10.1126/science.aba6098

224. Lv M, Chen M, Zhang R, Zhang W, Wang C, Zhang Y, et al. Manganese is critical for antitumor immune responses via cGAS-STING and improves the efficacy of clinical immunotherapy. *Cell Res*. (2020) 30:966–79. doi: 10.1038/s41422-020-00395-4

225. Wang C, Guan Y, Lv M, Zhang R, Guo Z, Wei X, et al. Manganese Increases the Sensitivity of the cGAS-STING Pathway for Double-Stranded DNA and Is Required for the Host Defense against DNA Viruses. *Immunity*. (2018) 48:675–87. doi: 10.1016/j.immuni.2018.03.017

226. Nakamura T, Sato T, Endo R, Sasaki S, Takahashi N, Sato Y, et al. STING agonist loaded lipid nanoparticles overcome anti-PD-1 resistance in melanoma lung metastasis via NK cell activation. *J Immunother Cancer*. (2021) 9:515–8. doi: 10.1136/jitc-2021-002852

227. Yi M, Niu M, Zhang J, Li S, Zhu S, Yan Y, et al. Combine and conquer: manganese synergizing anti-TGF-β/PD-L1 bispecific antibody YM101 to overcome immunotherapy resistance in non-inflamed cancers. *J Hematol Oncol*. (2021) 14:146. doi: 10.1186/s13045-021-01155-6

228. Song Y, Liu Y, Teo HY, Hanafi ZB, Mei Y, Zhu Y, et al. Manganese enhances the antitumor function of CD8(+) T cells by inducing type I interferon production. *Cell Mol Immunol*. (2021) 18:1571–74. doi: 10.1038/s41423-020-00524-4

229. Meric-Bernstam F, Sandhu SK, Hamid O, Spreafico A, Kasper S, Dummer R, et al. Phase Ib study of MIW815 (ADU-S100) in combination with spartalizumab (PDR001) in patients (pts) with advanced/metastatic solid tumors or lymphomas. *J Clin Oncol*. (2019) 37:2507. doi: 10.1200/JCO.2019.37.15_suppl.2507

230. Harrington KJ, Brody J, Ingham M, Strauss J, Cemerski S, Wang M, et al. Preliminary results of the first-in-human (FIH) study of MK-1454, an agonist of stimulator of interferon genes (STING), as monotherapy or in combination with pembrolizumab (pembro) in patients with advanced solid tumors or lymphomas. *Ann Oncol*. (2018) 29:viii712. doi: 10.1093/annonc/mdy424.015

231. Rodallec A, Sicard G, Fanciullino R, Benzekry S, Lacarelle B, Milano G, et al. Turning cold tumors into hot tumors: harnessing the potential of tumor immunity using nanoparticles. *Expert Opin Drug Metab Toxicol*. (2018) 14:1139–47. doi: 10.1080/17425255.2018.1540588

232. Duan X, Chan C, Lin W. Nanoparticle-mediated immunogenic cell death enables and potentiates cancer immunotherapy. *Angew Chem Int Ed Engl*. (2019) 58:670–80. doi: 10.1002/anie.201804882

233. Song P, Han X, Zheng R, Yan J, Wu X, Wang Y, et al. Upregulation of MHC-I and downregulation of PD-L1 expression by doxorubicin and deferasirox codelivered liposomal nanoparticles for chemoimmunotherapy of melanoma. *Int J Pharm*. (2022) 624:122002. doi: 10.1016/j.ijpharm.2022.122002

234. Liu S, Liu J, Li H, Mao K, Wang H, Meng X, et al. An optimized ionizable cationic lipid for brain tumor-targeted siRNA delivery and glioblastoma immunotherapy. *Biomaterials*. (2022) 287:121645. doi: 10.1016/j.biomaterials.2022.121645

frontiers | Frontiers in Immunology

TYPE Review
PUBLISHED 04 April 2024
DOI 10.3389/fimmu.2024.1379622

OPEN ACCESS

EDITED BY
Simona Kranjc Brezar,
Institute of Oncology Ljubljana, Slovenia

REVIEWED BY
Jozsef Dudas,
Innsbruck Medical University, Austria
Jiqiao Zhu,
Capital Medical University, China

*CORRESPONDENCE
Gülderen Yanıkkaya Demirel
gulderen.ydemirel@yeditepe.edu.tr
Zeynep Akbulut
zeynep.akbulut@maltepe.edu.tr

†These authors have contributed equally to this work and share first authorship

RECEIVED 31 January 2024
ACCEPTED 18 March 2024
PUBLISHED 04 April 2024

CITATION
Akbulut Z, Aru B, Aydın F and Yanıkkaya Demirel G (2024) Immune checkpoint inhibitors in the treatment of hepatocellular carcinoma. *Front. Immunol.* 15:1379622. doi: 10.3389/fimmu.2024.1379622

Immune checkpoint inhibitors in the treatment of hepatocellular carcinoma

Zeynep Akbulut[1,2*†], Başak Aru[3†], Furkan Aydın[3] and Gülderen Yanıkkaya Demirel[3*]

[1]Cancer and Stem Cell Research Center, Maltepe University, Istanbul, Türkiye, [2]Department of Medical Biology and Genetics, Faculty of Medicine, Maltepe University, Istanbul, Türkiye, [3]Department of Immunology, Faculty of Medicine, Yeditepe University, Istanbul, Türkiye

Despite advances in cancer treatment, hepatocellular carcinoma (HCC), the most common form of liver cancer, remains a major public health problem worldwide. The immune microenvironment plays a critical role in regulating tumor progression and resistance to therapy, and in HCC, the tumor microenvironment (TME) is characterized by an abundance of immunosuppressive cells and signals that facilitate immune evasion and metastasis. Recently, anti-cancer immunotherapies, therapeutic interventions designed to modulate the immune system to recognize and eliminate cancer, have become an important cornerstone of cancer therapy. Immunotherapy has demonstrated the ability to improve survival and provide durable cancer control in certain groups of HCC patients, while reducing adverse side effects. These findings represent a significant step toward improving cancer treatment outcomes. As demonstrated in clinical trials, the administration of immune checkpoint inhibitors (ICIs), particularly in combination with anti-angiogenic agents and tyrosine kinase inhibitors, has prolonged survival in a subset of patients with HCC, providing an alternative for patients who progress on first-line therapy. In this review, we aimed to provide an overview of HCC and the role of the immune system in its development, and to summarize the findings of clinical trials involving ICIs, either as monotherapies or in combination with other agents in the treatment of the disease. Challenges and considerations regarding the administration of ICIs in the treatment of HCC are also outlined.

KEYWORDS

hepatocellular carcinoma, immune checkpoint proteins, immune checkpoint inhibition, tumor microenvironment, anticancer immunity

1 Introduction

In 2020, liver cancer emerged as a global health problem with 905,700 new cases, accounting for nearly 5% of all cancer diagnoses, and 830,200 deaths, consolidating its position as the third leading cause of cancer-related deaths worldwide, after lung and colorectal cancer. The mortality/incidence ratio, an indicator of the severity of the disease,

was reported as 0.92, underscoring the significant burden and poor prognosis associated with liver cancer. In particular, hepatocellular carcinoma (HCC), the predominant form of primary liver cancer, accounted for 75% to 85% of all cases within this category. In the United States, the incidence of HCC has tripled since the 1980s, despite efforts to screen individuals with cirrhosis. Projections indicate a concerning increase in this malignancy worldwide, with an expected 55% increase in new cases between 2020 and 2040, resulting in 1.4 million diagnoses by 2040. There is consensus that HCC will remain a significant and challenging global public health problem for years to come (1).

HCC exhibits a notable gender disparity, affecting men at a rate two to three times higher than women, resulting in higher incidence and mortality rates globally. A compelling risk factor for the development of this malignancy is the presence of cirrhosis due to various liver diseases, a condition observed in over 80% of HCC patients (2). Other documented etiologies include metabolic abnormalities such as α1-antitrypsin deficiency, hemochromatosis, and autoimmune disorders (1).

While cirrhosis stemming from diverse etiologies can promote HCC development, chronic viral hepatitis predominates as the causative factor in over 80% of cases on the global scale (3). Hepatitis B virus (HBV) and hepatitis C virus (HCV) infections remain the main etiological factors in many regions, although their prevalence is decreasing in areas implementing specific programs for the elimination of viral hepatitis (4). At the same time, HCC associated with alcohol abuse and non-alcoholic fatty liver disease (NAFLD) has seen an alarming increase in both incidence and mortality, underlining the requirement for public policies targeting these emerging risk factors to facilitate a sustained reduction in HCC incidence (5). Of particular interest, NAFLD has emerged as the leading cause of HCC even in the absence of cirrhosis, with approximately one third of cases occurring in non-cirrhotic individuals. However, further research is needed to delineate which noncirrhotic NAFLD patients warrant HCC surveillance due to sufficient risk. On the other hand, alcohol-associated cirrhosis stands out as a recognized risk factor for HCC, and the combination of alcohol use with other etiologies increases the risk up to five-fold (6). NAFLD, now a significant public health concern, has become the fastest-growing cause of HCC among liver transplant candidates, closely linked to the escalating prevalence of obesity and metabolic syndrome (7, 8).

Several lifestyle factors besides alcohol use increase the risk of HCC (6). Smoking, for example, is associated with a 20-86% increased risk of HCC, with the risk returning to almost baseline after three decades of cessation (9). Obesity is associated with a 1.5-4.5 times higher risk of HCC and contributes to nearly 10% of HCC cases worldwide (10–12). Components of the metabolic syndrome, particularly diabetes, almost double the risk of HCC in the absence of excess weight (13). Physical activity has also been suggested to have beneficial effects in primary HCC prevention and after cancer diagnosis, over and above the confounding effect of weight loss. In addition, dietary exposure to aflatoxin B1 and aristolochic acid serve as recognized cofactors for HCC in patients with HBV infection.

Currently, therapeutic options for HCC include curative resection, liver transplantation, transarterial chemoembolization (TACE), radioembolization, radiofrequency ablation and chemotherapy, but their efficacy is limited, and they benefit only a small subset of patients (14). Among the approaches abovementioned, surgical resection and liver transplantation are considered as the most effective interventions, although their applicability in the treatment of liver disease is limited. For instance, only 5% of HCC patients are suitable for transplantation (15). Thus, other treatment options may be considered including RFA and TACE. TACE is performed by an interventional radiologist who selectively cannulates the artery feeding the tumor and administers high doses of local chemotherapeutic agents such as doxorubicin, cisplatin, or mitomycin C. However, the impact of TACE on clinical outcomes remains controversial, with some studies suggesting no benefit and others reporting a significant improvement in survival (15). On the other hand, RFA holds significant advantages over solo TACE in terms of initial tumor control, though it has comparable OS and recurrence-free survival with TACE in HCC less than 3 cm in size.

In terms of systemic treatment, introduction of the multi tyrosine kinase inhibitor (TKI) sorafenib has revolutionized HCC management (16). In 2018, TKI Lenvatinib was registered as an alternative for sorafenib in the first-line treatment of the disease (17). In the second-line setting, regorafenib and cabozantinib comprise the backbone of the therapy (18). However, these treatments may be ineffective in advanced stages of HCC and may even lead to progression of the underlying liver disease. Despite encouraging results in preclinical and early clinical trials for certain drugs, there remains a significant gap in effective systemic therapies for advanced stages of HCC. This underscores the urgent clinical need for more robust and targeted interventions to address the challenges posed by advanced liver cancer (14).

2 Tumor microenvironment in hepatocellular carcinoma

Immune tolerance in the liver aims to prevent exaggerated responses to harmful stimuli. On the other hand, these tolerance mechanisms also may promote the development and progression of cancer by suppressing immune surveillance. Approximately 80% of HCC cases are associated with persistent inflammation caused by the infiltration of immune cells along with resident cells such as Kupffer cells, hepatic satellite cells (HSCs) and hepatic sinusoidal cells. Prolonged inflammation leads to oxidative stress, creating a microenvironment that induces DNA damage and genetic modifications, paving the way for the initiation and progression of tumor growth (19).

In HCC, the tumor microenvironment (TME) is characterized by an increase in immunosuppressive cells including Kupffer cells, M2-type tumor associated macrophages (TAMs), regulatory T cells (Tregs) and myeloid derived suppressor cells (MDSCs) (Figure 1) (20–29). Kupffer cells are liver-resident macrophages that are responsible for the phagocytic clearance of pathogens under

10.3389/fimmu.2024.1379622

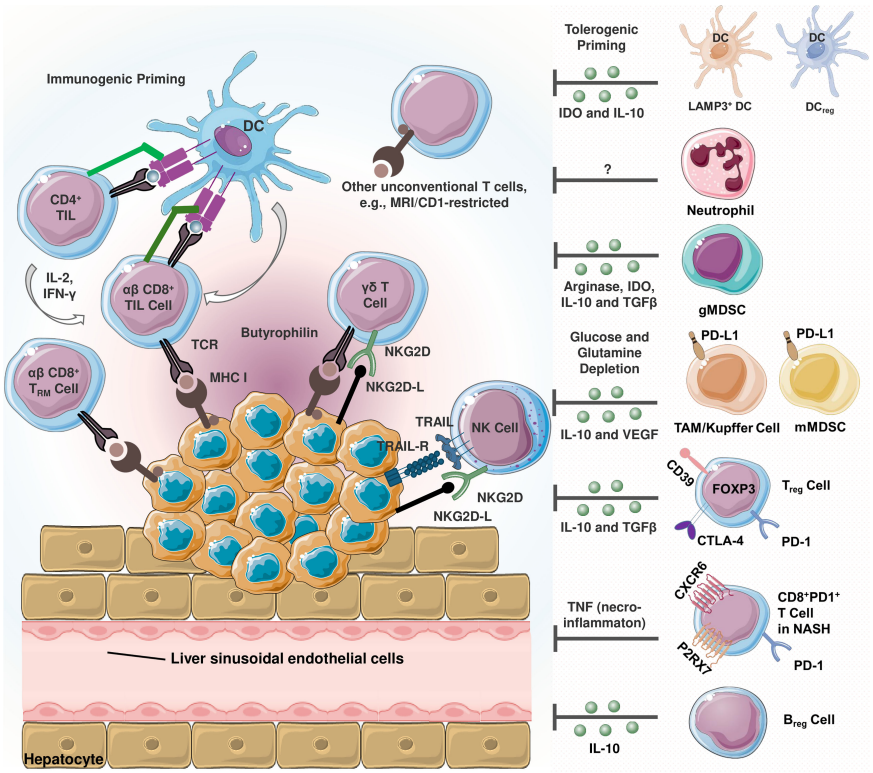

FIGURE 1
Schematization of infiltrating immune cells in hepatocellular carcinoma (HCC) (20). Immunosuppressive and immunostimulatory cells coexist in the tumor microenvironment (TME). HCC cells express TNF-related apoptosis-inducing ligand (TRAIL) receptor (21). TRAIL promotes natural killer (NK) cell infiltration into the TME, and TRAIL-expressing NK cells exert apoptotic effects on HCC cells. The activating cell surface receptor NKG2D is predominantly found on the surface of cytotoxic immune cells, and its ligands can be expressed in virtually all cell types upon induction including oncogenic transformation (22). Tumor-reactive CD8+ T cells recognize cancer cells via peptide- major histocompatibility complex class I (MHC I) complexes. Once recognized, malignant cells are eliminated via perforin- or FAS-dependent mechanisms. MHC I expression is critical since cancer cells lacking MHC I expression can only be eliminated by NK cells (23). In terms of tolerogenic signaling, regulatory dendritic cells (DCreg) are involved in T cell polarization, myeloid-derived suppressor cells (MDSCs) and T regulatory cell (Treg) differentiation and activity (24). Similarly, lysosome-associated membrane glycoprotein 3 (LAMP3)+ dendritic cells (DCs) are positively correlated with the infiltration of exhausted CD8+ T cells and Tregs (25). In TME, MDSCs are reported to promote tumor progression and are correlated with poor prognosis (26). These cells induce immunosuppression by secreting arginase-1, indoleamine 2,3-dioxygenase (IDO), TGF-β and interleukin-10 (IL-10) (27). Being a significant source of the latter, regulatory cells (Breg) also secrete IL-10 (20). Kupffer cells and other tumor associated macrophages (TAMs) are involved in hepatocarcinogenesis and immune evasion in different mechanisms including secreting immunosuppressive mediators, expressing programmed death-ligand 1 (PD-L1), recruiting Tregs as well as IL-17-expressing CD4+ T helper 17 (Th17), and downregulating MHC II expression along with costimulatory molecules (20). In non-alcoholic steatohepatitis (NASH), a subset of activated CD8+ T expressing exhaustion marker PD-1 are elevated (28). These cells exert an auto-aggressive behavior and drive necro-inflammation by secreting tumor necrosis factor alpha (TNF-α).

physiological conditions (30). In case of HCC, these cells can polarize similar to the cancer-promoting TAMs. Kupffer cells and M2-polarized TAMs contribute to immune evasion in HCC through mechanisms such as PD-L1 expression, MHC-II downregulation, secretion of immunosuppressive cytokines, and recruitment of Tregs and CD4+ cells (31). These cells also induce T-cell tolerance by releasing immunosuppressive factors such as interleukin (IL)-10, transforming growth factor (TGF)-β and prostaglandin E2 (PGE-2) (30, 32).

Liver sinusoidal endothelial cells (LSECs) are another resident liver cells, express high levels of PD-L1 and contribute to the induction of Tregs through a TGF-β dependent mechanism (33). These cells are specialized fenestrated endothelial cells that serve as a barrier between parenchymal cells and sinusoidal capillaries, taking part in the removal of blood-borne waste from the systemic circulation and the digestive tract by filtration and endocytosis. Under physiological conditions, fenestrated LSECs contribute to the maintenance of hepatic stem cell quiescence, whereas their capillarized counterparts induce stem cell activation by releasing platelet-derived growth factor (PDGF) and reducing the expression of the protective Kruppel-like factor 2 (KLF2). This process precedes the development of liver fibrosis. Communication between LSECs and other cells in the HCC TME is critical for the progression of liver fibrosis and subsequent HCC development (34).

Characterized as quiescent vitamin A-rich cells, hepatic stellate cells (HSCs) participate in the production of growth factors required for liver development, in addition to amplifying hepatic inflammatory responses (35). In HCC, these cells can acquire a fibrogenic phenotype known as myofibroblastic cells under continuous liver injury and promote fibrosis by altering the ECM (34). They also promote the accumulation of MDSCs and Tregs in the liver, and can induce T-cell apoptosis via PD-1/PD-L1 signaling (36).

In terms of T lymphocytes, these cells are recruited to the tumor site via the chemokine receptor 6 (CCR6) and chemokine ligand 20

(CCL20) axis. A specific subset of MDSCs also induces local differentiation of CD4+ T cells (33, 37). MDSCs contribute to tumor progression through an alternative mechanism involving secretion of vascular endothelial growth factor receptor (VEGFR), which induces vascularization and angiogenesis within the malignant tissue. Other notable players include T helper 17 (Th17) cells, CD4+ T cells expressing CCR4 and CCR6, CD14+ dendritic cells (DCs) expressing CTLA4 and PD1, tumor associated fibroblasts that inhibit NK cell function, and neutrophils that attract macrophages and Tregs (38).

In summary, the TME is composed of various components, including the extracellular matrix, immune cells, helper cells (fibroblasts, HSCs and vascular endothelial cells), cytokines, chemokines and growth factors, which collectively facilitate the immune escape, invasion and metastasis of HCC (39). However, this complexity may also provide potential molecular targets for immunotherapy in the treatment of the disease (39).

3 Immune checkpoints in cancer therapy

Neoplastic cells across a broad spectrum of tumor types express immune checkpoint molecules, a phenomenon that has been recognized for its profound impact on the intrinsic biology of these malignancies, particularly regarding their involvement in epithelial-mesenchymal transition (EMT) and related functions. The term "immune checkpoint proteins" (ICPs) refers to the interplay of ligand-receptor pairs that modulate immune responses. In this context, their cognate receptors expressed on immune cells are referred to as "immune checkpoint receptors", while their counterparts on antigen-presenting cells, tumor cells or other cellular phenotypes are referred to as "immune checkpoint ligands" (40). The vast majority of immune checkpoint molecules characterized to date are expressed predominantly on cells of the adaptive immune system, particularly T cells (Table 1). However, it is noteworthy that cells of the innate immune system also contribute to immune checkpoint expression which underscores the complexity and ubiquitous nature of ICPs (77).

ICPs act as gatekeepers that prevent immune system from overreacting, thereby preventing healthy tissue damage and maintaining immune homeostasis during antimicrobial or antiviral immune responses. Unfortunately, the deceptive mimicry of immune checkpoint ligands by cancer cells poses a significant challenge to immune surveillance. The strategic application of immune checkpoint blockade is emerging as a promising approach to attenuate the expression of these ligands on cancer cells, reverse the exhaustion of effector T cells, and restore their potent antitumor functions (78).

ICPs play a pivotal role in inflammatory responses and can be targeted by ICIs for cancer immunotherapy. A group of ICPs, including but not limited to PD-1/PD-L1, CTLA-4, lymphocyte activation 3 (LAG-3), TIM-3, VISTA, and indoleamine 2,3-

TABLE 1 Immune checkpoint proteins, their receptors and/or ligands and their main functions.

ICPs	Cellular Source	Ligands/ Receptors	Main Functions	References
PD-1	Activated T cells	PD-L1/PD-L2	1. Blocking the interaction between PD-1 and its ligand. 2. Reducing cytokine secretion.	(15, 41, 42)
PD-L1	DCs, MDSCs, Macrophages	PD-1	Inhibiting T cell responses	(43–45)
CTLA-4	Tregs	CD80/86	Inhibiting T cell responses	(15, 46)
PVRIG	DCs, Th1 cells, NK cells	CD112	Inhibiting T cell responses	(47–50)
TIM-3	DCs, NK cells, Th1 cells, Th17 cells, Macrophages	GAL-9, PS	Inhibiting Th responses	(51–54)
GAL-9	Eosinophils, DCs, T cells, Macrophages, Lymphoid cells, Kupffer cells, intestinal epithelial cells, vascular endothelial cells	TIM-3	Regulating immune homeostasis	(55–57)
VISTA	T cells, APCs	NA	Inhibiting T cell responses	(58–60)
LAG3 (CD223)	Plasmacytoid DCs (pDCs), NK T cells, Tregs	MHC-II, GAL-9, FGL1	lnteracting with MHC-II	(61–63)
TIGIT	T cells, NK cells	CD155, CD112	Supressing anti-tumor immunity	(64–66)
CD40	B cells, DCs, hematopoietic progenitor cells	CD154	Activating NF-κB, MAPKs, PI3, JAK3-STAT5 signaling pathways.	(67–69)
CD70	Activated T cells, mature DCs, B cells	CD27	1. Stimulating T cell differentiation. 2. Enhancing cytotoxic T cell activity. 3. Promoting TNF-α production. 4. Activating B cells.	(70–73)
CD47	RBCs, non-hematopoietic cells	SIRPα, TSP-1, Integrins	1. Activating SHP-1 and SHP-2 pathways. 2. Inhibiting macrophage activity.	(74–76)

SHP1/2, Src-homology 2 domain (SH2)-containing protein tyrosine phosphatase.

dioxygenase 1 (IDO1), are shown to be dysregulated in cancer and infectious diseases. These immune checkpoints, along with regulatory cells such as Tregs, MDSCs, M2 macrophages, and cytokines, are upregulated during infection and cancer, effectively altering the immunological milieu. Cancer cells disrupt the immune response and evade immune surveillance by dysregulating immune checkpoint signaling. Blackburn et al. have demonstrated that T-cell function is attenuated with increased expression of immune checkpoints, highlighting the potential of targeted modulation of these ICPs for cancer immunotherapy (79).

ICPs are closely related to and co-evolved with stimulatory immune receptors. These receptors often rely on monotyrosine signaling motifs, specifically the immunoreceptor tyrosine-based inhibitory motif (ITIM) and the immunoreceptor tyrosine-based switch motif (ITSM), to transduce inhibitory signals. As cell-surface molecules, their functional activity is highly susceptible to inhibition by the strategic use of blocking antibodies that interfere with ligand-receptor binding. In the therapeutic field, ICP blockade is emerging as a pioneering approach, demonstrating resilience and longevity that surpasses conventional chemotherapy or targeted therapies. This enhanced durability may reflect the intricate machinery of the immune system's intrinsic memory. Among the broad spectrum of immune checkpoint blockade therapies, the outstanding success story unfolds with anti-PD-1/PD-L1 therapy, a therapeutic approach that has been approved for the treatment of a diverse array of cancers spanning hematologic, cutaneous, pulmonary, hepatic, vesical, and renal malignancies. The remarkable success of this approach underscores its efficacy in treating a broad spectrum of malignancies (80–82).

3.1 Programmed death – 1

PD-1 is expressed on activated T cells and is known to play a key role in immune tolerance. It recognizes two ligands, PD-L1 and PD-L2, which are expressed at low levels in normal tissues but at aberrant levels in certain tumors (15). PD-L1 is ubiquitously expressed on various cells, including B cells, T cells, macrophages, tumor cells and non-immune tissue cells such as vascular endothelial cells (83, 84). The interaction between PD-1 and PD-L1 can induce T-cell dysfunction and anergy, facilitating the escape of PD-L1-expressing tumor cells from cytotoxic T-cell-mediated cell death (41). PD-1 engagement also reduces cytokine secretion, including IL-2, IFN-γ and TNF-α, and inhibits cell proliferation by disrupting the CD28 costimulatory pathway (42). Notably, both tumor and immune cells can express PD-L1, which serves as a valuable biomarker for predicting response to anti-PD-1/PD-L1 axis blockade in various cancers (85). PD-L1, also known as B7-H1 or CD274, contributes to the inhibition of the cancer-immunity cycle by binding to negative regulators of T-cell activation such as PD-1 and B7.1 (CD80) (46).

3.2 Programmed death ligand – 1

PD-L1 has a molecular structure similar to other B7 molecules and conforms to the typical architecture of the immunoglobulin superfamily. PD-L1 is classified as a type I transmembrane glycoprotein with an extracellular domain that has an immunoglobulin structure that includes both an Ig variable (V) distal region and an Ig constant (C) proximal region. The hydrophobic transmembrane sequence anchors PD-L1 to the cell membrane, followed by a short intracytoplasmic region with minimal sequence similarity to other B7 molecules. However, this intracellular region contains three conserved sequences - the RMLDVEKC, DTSSK and QFEET motifs - that are shared among mammalian PD-L1 molecules. Furthermore, accumulating evidence suggests that this region plays a pivotal role in survival signaling, with a particular focus on the functions associated with the RMLDVEKC and DTSSK motifs, as demonstrated in recent studies (43). PD-L1 is continuously expressed at varying levels on cells that belong to the myeloid lineage, including DCs, macrophages, and MDSCs. In addition, PD-L1 is found in other cell types beyond the myeloid lineage, including numerous tumors and cancer cell lines. In cancer, pro-inflammatory stimuli such as interferon gamma (IFN-γ) released by T cells have been shown to stimulate PD-L1 expression. This induction is mediated by activation of the Janus kinase (JAK) signal transducer and activator of transcription (STAT) pathway, which ultimately leads to upregulation of interferon regulatory factor 1 (IRF1). IRF1, in turn, binds to the PD-L1 promoter and contributes to the increased expression of PD-L1 (44). Along with the pro-inflammatory cytokine tumor necrosis factor alpha (TNF-α), IFN-γ leads to the activation of the NF-κB pathway, promoting the transcriptional transactivation of PD-L1. This interaction between these pathways not only provides a sophisticated mechanistic understanding, but also sheds light on the elevated expression levels of PD-L1 in inflamed tissues. This phenomenon is particularly observed in extensively infiltrated "hot" tumors (45). PD-L1 transcription also relies on the cell type and the physiological and pathological situation, for example, in HCC, SOX2 in reported to regulate PD-L1 expression (86).

3.3 Cytotoxic T-lymphocyte-associated protein 4

Cytotoxic T-lymphocyte-associated protein 4 (CTLA-4), a protein receptor predominantly expressed on T cells, was initially recognized as a secondary receptor for the T-cell costimulatory molecule B7, but subsequently revealed its role as a negative regulator of T-cell activity (46). The mechanism of this regulatory action begins with the immediate upregulation of CTLA-4 upon T cell receptor (TCR) engagement, reaching a higher point 2 to 3 days after activation (87). CTLA-4 has two ligands, CD80 and CD86, also known as B7-1 and B7-2 which shares similarities with T cell costimulatory protein CD28. Both CD28 and CTLA-4 bind to as B7-1 and B7-2, and their binding kinetics coupled with differential avidities result in rapid competitive inhibition by CTLA-4. In addition, CTLA-4, encased in intracellular vesicles, makes a rapid journey to the immunological synapse upon T cell activation. Upon interaction, B7 ligand binding stabilizes CTLA-4, allowing it to accumulate and effectively outcompete CD28 (15).

The story of CTLA-4 continues to unravel with the revelation that its inhibition not only enhances a spectrum of helper T cell-dependent immunological responses, but also interacts in a complex manner with Tregs to amplify their suppressive capacity. Constitutively produced by Treg, CTLA-4, a target gene of the forkhead transcription factor FOXP3, orchestrates the Treg responses, though the exact mechanism remains unclear (88). Interestingly, how CTLA-4 drives the immunosuppressive activity of Treg cells remains a mystery. Thus, the dual aspects of enhanced effector CD4+ T cell activity and attenuation of Treg cell-dependent immunosuppression are key elements in the mechanism of CTLA-4 blockade (80).

3.4 Poliovirus receptor-related immunoglobulin domain-containing

Poliovirus Receptor-Related Immunoglobulin Domain-Containing (PVRIG, also called as CD112R), a poliovirus receptor-like protein and has been recognized as a novel co-inhibitory receptor for human T cells as well as NK cells, with a higher affinity for interaction with CD112 compared to CD226 and TIGIT (47). PVRIG has also been shown to be expressed in certain types of cancer, and the highest expression levels in terms of cancer tissues have been reported in kidney, ovary, lung, prostate, and endometrium (48, 89, 90). Moreover, in a study published by Zhu et al., the authors have revealed that it is also expressed on DCs, playing a pivotal role in mediating interactions with DCs and tumor cells through its engagement with PVRIG (90). Disruption of this interaction has been shown to enhance T cell functions, as in TILs, PVRIG expression along with PD-1 and TIGIT has been reported on CD8+ and CD4+ T cells, in correlation with an exhausted phenotype (48). Similarly, PVRIG expression together with CD96, TIGIT, Tim-3 and PD-1 was observed in NK cells (49, 50).

3.5 T cell immunoglobulin and mucin domain-containing protein 3

T cell immunoglobulin and mucin domain-containing protein 3 (TIM-3) is a versatile immune checkpoint receptor that plays a central role in the regulation of immune responses. Being a member of the TIM family, TIM-3 is expressed on various immune cells, including IFN-γ-producing Th1 CD4+ and CD8+ T cells, Th17 cells, Tregs, NK cells, DCs, and macrophages (51–53).

TIM-3 binds to several ligands, in particular galectin-9 (Gal9) and cell surface phosphatidylserine (PS) (54). The interaction between TIM-3 and Gal9 or high-mobility group protein B1 (HMGB1) initiates an inhibitory signal that induces apoptosis of Th1 cells. Notably, prolonged exposure to interleukin-12 induces TIM-3 expression on T cells in the tumor microenvironment, leading to functional impairment and exhaustion. In addition to its role on T cells, TIM-3 on immune cells such as natural killer cells and DCs plays a critical role in immune regulation. For example, TIM-3 regulates the differentiation and immunogenic activities of natural killer cells. In addition, when expressed on DCs, TIM-3 facilitates the phagocytosis of apoptotic cells through PS interaction, thereby enhancing antigen presentation and inducing immune tolerance. At the same time, TIM-3 negatively modulates the innate immune system through pattern recognition. Interestingly, TIM-3 cooperates with Toll-like receptors to induce inflammation by activating the transcription factor nuclear factor kappa B and increasing the secretion of pro-inflammatory mediators, revealing its multifaceted role in immune modulation (54).

3.6 V-domain immunoglobulin suppressor of T cell activation

VISTA, a type I transmembrane protein, has a structural composition comprising a single N-terminal immunoglobulin (Ig) V domain, a connecting stalk of approximately 30 amino acids, a transmembrane domain, and a cytoplasmic tail of 95 amino acids (91). Studies regarding VISTA's IgV domain reveal remarkable homology with PD-L1, highlighting a shared structural similarity. Interestingly, the conserved cytoplasmic tail of VISTA mirrors the features of CD28 and CTLA-4 but lacks the conventional ITIM/ITAM motifs commonly found in other B7 co-receptor molecules. Despite the absence of the abovementioned motifs in its cytoplasmic domain, VISTA exhibits potentially functional elements such as protein kinase C binding sites and a proline-rich motif. These structural features suggest that VISTA may serve as a platform for interaction with various protein complexes. The idea that VISTA acts as a ligand is supported by experimental observations, in particular the inhibitory effects of a VISTA-Ig fusion protein on the proliferation of mouse and human CD4 and CD8 T cells, as well as the production of key cytokines such as IFN-γ and IL-2 upon anti-CD-3 stimulation (58, 59). This dual role underscores VISTA's ability to function as both a ligand and a receptor, underlining its importance in the regulation of immune responses (59).

VISTA has been traditionally recognized for its role in suppressing T cell-associated responses, contributing to immune escape and survival in several human cancers, including prostate cancer, non-small cell lung cancer (NSCLC), colorectal cancer (CRC), acute myeloid leukemia (AML), pancreatic cancer, cutaneous melanoma, metastatic melanoma, hepatocellular carcinoma, ovarian cancer, oral squamous cell carcinoma, and gastric cancer. However, the complex effects of VISTA on cancer immunity go beyond the initially perceived suppressive role. Compelling evidence challenges the simple classification of VISTA as an immunotherapy target, showing that in certain cancers, VISTA assumes stimulatory checkpoint-like functions and actively participates in the activation of anti-cancer immune responses. This complexity underscores the nuanced and controversial nature of VISTA's role in immune regulation (60).

3.7 Lymphocyte activation gene 3

LAG3, also known as CD223, was discovered in 1990 and is a transmembrane molecule expressed on various immune cell types,

including CD4+ and CD8+ T cells, NK T cells, NK cells, plasmacytoid DCs (pDCs), and Tregs (61, 62). It is noteworthy that pDCs and Tregs exhibit continuous expression of LAG3, while in other cell types, LAG3 expression is typically induced upon activation (62). Located on human chromosome 12 (12p13), the LAG3 gene shares a genomic region with the CD4 gene, although their protein-level homology is less than 20% (61, 92). LAG3 protein has a molecular weight of 70 kDa, interacts with major histocompatibility complex II (MHC-II) on antigen-presenting cells (APCs) with a significantly higher affinity than CD4 (61, 63).

The structural composition of LAG3 includes an extracellular region, a transmembrane region, and an intracellular region. The extracellular portion consists of four immunoglobulin superfamily domains, specifically a V region and three C2 regions. The V region is distinct, with an extra ring in the middle and an abnormal in-chain disulfide bridge. Meanwhile, the cytoplasmic region of LAG3 consists of three elements: a serine phosphorylation site, a conserved 'KIEELE' motif, and a glutamate-proline-dipeptide repeat (EP) sequence. The 'KIEELE' motif is highly conserved and exclusive to LAG3, and it takes part in LAG3 related inhibitory signaling (93). In summary, LAG3 is a multifaceted immune regulator with a unique structural profile that expresses dynamic interactions with MHC-II and contributes to intracellular signaling through its distinctive cytoplasmic motifs (93).

3.8 T cell immunoreceptor with Ig and ITIM domains

TIGIT, also known as WUCAM, VSTM3 and VSIG9, is identified in 2009 as a co-inhibitory receptor belonging to the immunoglobulin superfamily which consists of an extracellular domain harboring an immunoglobulin variable region (IgV) linked to a type 1 transmembrane domain, and an intracellular domain containing an immunoreceptor tyrosine-based inhibitory motif (ITIM) and an Ig tail-tyrosine (ITT)-like motif constitute (94). Activated CD4+ and effector CD8+ T cells and NK cells express TIGIT on the cell surface, which interacts with the poliovirus receptor (PVR, also known as CD155) with high affinity and with poliovirus receptor-related 2 (PVRL2, also known as CD112) with lower affinity (64). TIGIT shares these ligands with two other receptors, CD226 (DNAM-1) and CD96 (TACTILE), which transmit co-stimulatory and co-inhibitory signals, respectively (64).

TIGIT expression in humans is a late event in the cancer-immunity cycle, occurring after chronic exposure to tumor antigens (79, 95). TIGIT is found on various immune cells that infiltrate tumors in diseases such as melanoma, NSCLC, CRC, HCC, gastric cancer, glioblastoma and hematologic malignancies. In cases such as follicular lymphoma, increased numbers of TIGIT-expressing CD4+ and CD8+ T cells within tumors are reported to be correlated with worse outcome (65). In AML, high TIGIT expression on peripheral blood CD8+ T cells is associated with treatment resistance (66). In addition, the presence of PD-1+TIGIT+CD8+ T cell populations in the blood is negatively correlated with overall survival and progression-free survival in patients with hepatitis B virus-associated HCC (HBV-HCC) (96). Altogether, these findings suggest that TIGIT plays a suppressive role in anti-tumor immunity in cancer patients.

3.9 Galectin-9

Galectins are a family of β-galactoside-binding proteins that are not only found in animals, but also in bacteria and fungi to varying degrees. Characterized by an evolutionarily conserved carbohydrate recognition domain (CRD), these proteins share a highly conserved core sequence. Initially recognized for their role in identifying endogenous ("self") carbohydrate ligands during embryogenesis and early development, galectins have since been found to play critical roles in tissue repair, adipogenesis, cancer development, and regulation of immune homeostasis. The galectin protein family shares two characteristics: a conserved amino acid sequence with significant similarities and a strong affinity for β-galactoside sugars. To date, 15 galectins have been identified in mammals, 11 of which are expressed in humans (55).

Unlike other members of the galectin family, Galectin-9 (Gal-9) acts as an inhibitor of the immune system. Its function includes promoting the differentiation of Tregs while decreasing Th17 and Th1 cells. This dual action contributes to the suppression of excessive immune responses and inflammation (56, 97). Gal-9 selectively engages its receptor, TIM-3, leading to apoptosis in CD8+ T cells. In addition, this interaction initiates adaptive immune responses by promoting the secretion of IL-12 (56, 57).

In CRC, Gal-9 expression was found to be lower compared to para-cancerous tissues, and a positive correlation between low levels of Gal-9 expression and poor prognosis, including lower histologic grade and the presence of lymph node metastasis, was reported (55, 98). In breast cancer, Gal-9 has been shown to have anti-metastatic potential, most likely by inducing tumor cell aggregation and reduced adhesion of breast cancer cells to the extracellular matrix, thus preventing metastasis and improving patient survival (55, 99).

3.10 CD40

Identified four decades ago, CD40 is a membrane protein found on B lymphocytes, DCs, hematopoietic progenitor cells, epithelial cells, and tumor cells. This 45-50 kDa glycoprotein consists of 277 amino acids and is a member of the tumor necrosis factor receptor (TNFR) superfamily (67, 100). The ligand of CD40 is CD40L (CD154), a 32-39 kDa type II transmembrane protein that belongs to the TNF superfamily and has a distinct extracellular structure with a β-sheet, α-helix loop and another β-sheet. This structure allows CD40L to form trimers, a feature shared with other ligands in the TNF family. CD40L is primarily expressed by activated T cells, B cells and platelets, but is also expressed by monocytes, NK cells, mast cells and basophils under inflammatory conditions. There is also a soluble form of CD40L that participates in similar actions with its membrane-bound counterpart. CD40 signaling relies primarily on adaptor proteins known as TNF receptor-associated factors, which subsequently activate both the

canonical and noncanonical NFκB pathways, as well as the MAP kinase, PI3 kinase, and phospholipase C-γ pathways. When activated, these pathways result in diverse downstream effects, including activation of gene transcription, reorganization of the cytoskeleton, and promotion of cell survival. It has also been reported that CD40 can transmit signals through the JAK3-STAT5 pathway, and when this signaling is absent, DCs promote T cell tolerance. However, further studies are still required to unveil the precise contributions of these pathways, either individually or in combination, to the diverse functional activities of DCs and their differentiation (68).

CD40 binding on the surface of DCs has been shown to promote their cytokine production, induce costimulatory molecules on their surface, and facilitate antigen cross-presentation, eventually "licensing" them to mature, and effectively initiate T cell activation and differentiation. In B cells, CD40 signaling promotes germinal center (GC) formation, immunoglobulin (Ig) isotype switching, somatic hypermutation (SHM) of Ig to increase antigen affinity, and ultimately the generation of long-lived plasma cells and memory B cells. In addition, the CD40 signaling pathway is critical for the survival of several cell types, including GC B cells, DCs, and endothelial cells, both under normal conditions and during inflammation. Dysregulation of CD40 signaling has been observed in autoimmune diseases (69).

In terms of cancer, CD40 expression is observed in 80% of NSCLC cases, 40% of ovarian cancer cases, and 68% of pancreatic adenocarcinoma cases in a recently published study (101). However, it was not found to be prognostic for overall survival for these cancers. On the contrary, cytoplasmic CD40 expression was reported to be positively correlated with higher overall survival, although there was a higher ratio of positive cases in cancer cases in comparison with the normal tissue (102).

3.11 CD70

CD70 is a member of the tumor necrosis factor (TNF) family which is exclusively expressed on activated T cells, B cells, and mature DCs (70). It plays a critical role in the immune response by interacting with its receptor CD27, which is expressed on naive T-cells, memory B-cells, NK-cells, and hematopoietic stem and progenitor cells (71, 72, 103). Being a transmembrane phosphoglycoprotein, CD27 functions as a co-stimulatory immune checkpoint receptor that is consistently present on various T cells (including naive, αβ, γδ, and memory T cells), NK cells, and B cells. Upon CD70 binding, CD27 engages TNF receptor-associated factors (TRAFs) and initiates intracellular signaling that enhances the survival and activation of T, B, and NK cells through TRAF2 and TRAF5 signaling, in addition to activating the NF-κB pathway. The CD70-CD27 pathway not only actively stimulates T cell expansion and differentiation, but also enhances CD8+ T cell cytotoxic activity and promotes T cell TNF-α production (70, 73). In addition, CD27-CD70 signaling has also been shown to induce B-cell activation, their terminal differentiation to plasma cells and in addition to increasing NK-cell activity via IFN-γ and IL-2 (73).

Under physiological conditions, the interaction between CD27-CD70 is tightly controlled to prevent overexpression and subsequent excessive lymphocyte activation (104). In contrast to its restricted expression in normal tissues, CD70 is aberrantly expressed in cancer: in oncology, CD70 is often overexpressed in malignant cells, either independently (solid tumors) or along with CD27 (hematological malignancies) (73, 105). To date, several studies have highlighted the CD70-CD27 signaling axis as a key driver of malignancy in hematological cancers, controlling the regulation of processes such as stemness, proliferation and survival. In addition, the importance of CD70 in solid tumors has become apparent, with aberrations reported in several types of cancer, including renal cell carcinoma, nasopharyngeal carcinoma, glioblastoma, melanoma, lung carcinoma, cervical carcinoma, breast carcinoma, ovarian carcinoma and mesothelioma, all of which are associated with decreased survival (70, 106–109).

3.12 CD47

Identified as a transmembrane protein present on red blood cells (RBCs), CD47 is a 47-50 kDa membrane protein currently known to be expressed by a variety of healthy cells in addition to cancer cells (74–76). Among the various ligands of CD47; SIRPα, TSP-1, and integrins are the most studied (74).

SIRPα belongs to the signal regulatory protein (SIRP) family and is characterized by an intracellular domain containing an immunoreceptor tyrosine-based inhibitor motif (ITIM), a transmembrane spanning region, and three extracellular immunoglobulin superfamily domains. When CD47 binds to SIRPα, the ITIM in the cytoplasmic tail of SIRPα is phosphorylated. This event recruits and activates phosphatases, including Src homology phosphatase (SHP)-1 and SHP-2. Notably, SIRPα is predominantly expressed on myeloid cells such as monocytes, granulocytes, DCs and especially macrophages. The interaction between CD47 and SIRPα serves as a mechanism to distinguish self from non-self. When this binding occurs, it triggers a "don't eat me" signal that inhibits macrophages from phagocytosing the adherent cells. In essence, the CD47-SIRPα interaction acts as a regulatory mechanism to prevent macrophages from engulfing healthy cells (74).

Its role in maintaining immune homeostasis makes CD47 an important target for cancer therapy. In the field of oncology, CD47 was first identified as a tumor antigen in human ovarian cancer and has since been found to be overexpressed in several malignancies, including non-Hodgkin's lymphoma, T-cell lymphoma, AML and myelodysplastic syndrome (MDS). CD47 has the ability to interact with certain extracellular ligands, including SIRPα, thrombospondin-1 (TSP-1), integrins (α2β1, α4β1, α5β1, and α6β1), SIRPγ, CD36, and CD95 (74). The potential of CD47 as an important checkpoint in cancer therapy stems from its critical role in balancing the inhibitory and stimulatory functions of myeloid cells. CD47 engagement induces tumor cell apoptosis

through a caspase-independent mechanism. In addition, blocking CD47 leads to phagocytic uptake of tumor cells by antigen-presenting cells, facilitating subsequent antigen presentation to T cells. In addition, anti-CD47 not only neutralizes the inhibitory effect of TSP-1 on human NK cells, but also enhances NK cell activation and cytotoxicity. Early phase clinical trials have shown promising results for CD47 blockade in various cancers, either as a single agent or in combination with other agents. A preclinical study highlighted that the therapeutic effect of CD47 blockade is based on the STING pathway, which induces a type I/II interferon (IFN) response mediated by DCs and CD8+ T cells. Finally, there is evidence in the literature that the CD47/TSP-1 pathway has diverse effects on the immune system and represents a novel target for potential cancer therapeutics (110).

4 Targeting immune checkpoints for the treatment of hepatocellular carcinoma

HCC is staged and treated according to the Barcelona Clinic Liver Cancer (BCLC) staging system. This classification divides the disease into four stages: (very) early stage (BCLC stage 0/A), which is the only potentially curable stage; intermediate stage (BCLC stage B); advanced stage (BCLC stage C); and end-stage (BCLC stage D). Unfortunately, approximately 75% of patients are diagnosed at a non-curative stage, limiting treatment options to local interventions (BCLC stage B) and systemic treatments (BCLC stage C). This underscores the importance of tailoring therapeutic approaches based on the specific stage of HCC to optimize patient outcomes (111). Over the past thirteen years, there have been significant advances in the systemic treatment of HCC. The landscape was transformed in 2007 with the introduction of sorafenib, a potent multi-TKI, which maintained its prominence in systemic therapy for over a decade. In 2018, lenvatinib, another TKI with similar properties, was approved as an alternative to sorafenib for the first-line treatment of the disease. During this time, an increasing number of patients with HCC were being treated with lenvatinib. In the second line setting, regorafenib, cabozantinib and ramucirumab have emerged as successful additions to the HCC treatment options, contributing to the evolving landscape of therapeutic strategies for the treatment of this disease (Table 2) (111).

Recent advances in immunotherapy and innovative combinations have reshaped the treatment landscape for HCC while ongoing clinical trials continue to illuminate the way forward. Immunotherapy has demonstrated the ability to improve survival and achieve durable cancer control in certain groups of HCC patients, while mitigating adverse side effects. This represents significant progress in tailoring treatments to improve outcomes in the treatment of this cancer (14).

4.1 Nivolumab

Nivolumab is the first anti-PD-1-antibody and demonstrated efficacy as a second-line treatment for patients with HCC in the Phase 1/2, open-label CheckMate040 trial, which enabled its accelerated approval of the drug by the FDA in September 2017. The study enrolled a total of 214 patients, including those with HCV/HBV, in addition to patients who received sorafenib and sorafenib näive (137). In the patient cohort, 20% (42 patients) had an objective response regardless of prior treatment with sorafenib, with three patients achieving a complete response. In addition, 67% (144 patients) had disease that had spread beyond the liver and 29% (63 patients) had major blood vessel involvement. A favorable disease control rate was observed in 64% (138 patients). A total of 48 patients discontinued treatment, with 25% (12 patients) experiencing grade 3/4 treatment-emergent adverse events. These results led to the initiation of the Phase 3 CheckMate459 trial, which was designed to evaluate the efficacy of nivolumab as a first-line treatment to demonstrate superiority over sorafenib (138). A total of 743 patients were enrolled in this study and overall survival was reported to be 16.4 months for nivolumab and 14.7 months for sorafenib. First-line treatment with nivolumab did not show a significant improvement in overall survival compared to sorafenib, although it demonstrated positive clinical activity and a favorable safety profile in patients with advanced HCC. Therefore, nivolumab may be considered as a therapeutic option for patients for whom TKIs and antiangiogenic agents are contraindicated or carry significant risks (112).

4.2 Pembrolizumab

Pembrolizumab, a humanized IgG4 monoclonal antibody, is the second anti-PD-1 antibody to be approved in a range of solid tumors and was evaluated extensively for its potential use in the treatment of HCC (113, 114, 139). In a Phase 2 trial, 29 patients were enrolled where they were treated with 200 mg pembrolizumab in three-week cycles. The primary goal of this study was to assess the drug's efficacy in patients with unresectable HCC. Results of this study revealed that pembrolizumab was effective in the treatment of advanced HCC while its toxicity was generally tolerable and reversible. In addition, analysis of immunological markers in blood plasma, along with PD-L1 staining, suggested that baseline TGF-β levels could serve as a potential predictive biomarker for determining the response to pembrolizumab (139, 140). In KEYNOTE-224, 169 patients were screened and 104 were selected to receive pembrolizumab every three weeks for approximately two years or until disease progression. In KEYNOTE-224, 169 patients were screened and 104 were selected to receive pembrolizumab every three weeks for approximately two years or until disease progression. The overall response rate was reported as 18 out of 104 patients, with one patient achieving a complete response (1%) and 17 patients achieving a partial response (16%) (114). A total of 413 patients were enrolled in KEYNOTE-240 and received pembrolizumab every 3 weeks for approximately 2 years. The primary endpoint of the study was progression-free survival. Although the results of this study were consistent with those of KEYNOTE-224, overall survival and progression-free survival did not reach statistical significance in this study (113). Combinatorial administration of pembrolizumab with levantinib resulted in a

TABLE 2 Clinical trials regarding ICI as monotherapies in HCC treatment.

ICIs	Patients (n)	Disease	mOS	ORR(%)	References
Nivolumab	371	Advanced HCC	16.4	15.4	(112)
Pembrolizumab	278	Advanced HCC	13.9	18.2	(113)
	104	Advanced HCC	12.9	12.9	(114)
Tislelizumab	674	Advanced HCC	15.9	15.9	(115)
Toripalimab	36	Advanced HCC	NR	63.9	(116)
Sintilimab	380	Advanced HCC	10	25	(117)
	36	Advanced HCC	15.9	36.1	(118)
Camrelizumab	217	Advanced HCC	6	14.7	(119)
Spartalizumab	74	HCC	NR	NR	(120)
Cemiplimab	26	Unresectable HCC	3.7	19.2	(121)
	21	Resectable HCC	12.4	15	(122)
Atezolizumab	59	Unresectable HCC	6.6	36	(123)
Atezolizumab and Bevacizumab	336	Advanced HCC	12	67.2	(124)
Durvalumab	24	Advanced HCC	NR	83.3	(125)
	47	Unresectable HCC	NR	21.3	(126)
	389	Unresectable HCC	16.6	17	(127)
Avelumab	30	Advanced HCC	4.4	10	(128)
	22	Advanced HCC	14.1	13.6	(129)
	33	Advanced HCC	17.2	55	(130)
Ipilimumab and Nivolumab	49	HCC	12.8	31	(131)
Tremelimumab	21	HCC	8.2	NR	(132)
	32	HCC	12.3	NR	(133)
	39	HCC	10.9	NR	(134)
Tremelimumab and Durvalumab	40	Unresectable HCC	NR	15	(135)
Cobalimab	42	HCC	NR	46	(136)

ICI, Immune Checkpoint Inhibitors; n, Number; mOS, Median Overall Survival; ORR(%), Overall Response Rate; HCC, Hepatocellular Carcinoma; NR, Not reported.

remarkable overall response rate of 46% where among all patients with unresectable HCC who had not previously undergone systemic treatment, 11% achieved a complete response (CR) and 35% achieved a partial response (113).

4.3 Tislelizumab

Early results indicated that tislelizumab is generally well tolerated and has anti-tumor activity in patients with advanced solid tumors such as esophageal, gastric, hepatocellular and non-small cell lung cancer (141). A total of 674 patients with a minimum follow-up of 33 months were enrolled in a phase Ia/Ib study investigating tislelizumab. The primary endpoint of the study was overall survival, with secondary endpoints including objective response rate, progression-free survival, duration of response and safety. In this study, single agent tislelizumab demonstrated similar overall survival and significantly higher and longer lasting objective responses compared to sorafenib. However, sorafenib demonstrated better disease control rates and median progression-free survival. Tislelizumab demonstrated a favorable safety profile with no new safety concerns compared to sorafenib. Overall, these results suggest that tislelizumab may be a promising first-line treatment option for patients with unresectable HCC (115, 142). Tislelizumab is also currently being investigated in combination with sitravatinib as adjuvant therapy for HCC at high risk of recurrence after curative resection, and alone or in combination with levatinib as neoadjuvant treatment for resectable recurrent HCC (143, 144).

4.4 Toripalimab

Toripalimab is a selective, recombinant, humanized monoclonal antibody targeting PD-1 which is recently been approved for the treatment of metastatic or recurrent, locally advanced nasopharyngeal carcinoma in combination with

cisplatin and gemcitabine (145). In terms of HCC, efficacy and safety of hepatic arterial infusion chemotherapy of oxaliplatin, 5-fluorouracil and leucovorin plus lenvatinib and toripalimab was evaluated. 36 patients were enrolled in this study, and the primary endpoint revealed 80.6% progression free 6 months survival rate. Eight patients were downstaged to resectable disease. Of these, one patient underwent liver transplantation and four underwent curative surgical resection. One patient achieved a pathologic complete response. In addition, all observed adverse events were reported to be manageable and no treatment-related deaths were reported (116).

4.5 Sintilimab

Sintilimab is a fully human IgG4 monoclonal antibody that targets PD-1and firstly has been recognized as treatment for classical Hodgkin's lymphoma in the ORIENT-1 trial (146, 147). The ORIENT-32 study evaluated the safety, tolerability and efficacy of sintilimab in combination with the bevacizumab biosimilar IBI305 as first-line treatment in patients with HCC compared to sorafenib. The results showed that combinatorial treatment with sintilimab and IBI305 significantly increased overall survival and progression-free survival in the first-line setting for unresectable HBV-associated HCC with an acceptable safety profile (117). Efficacy and safety of Sintilimab in combination with levatinib was evaluated for local advanced HCC in a Phase 2 (118). In another Phase 2 trial, combinatorial treatment of donafenib and sintilimab was evaluated in patients with advanced HCC (148).

4.6 Camrelizumab

Camrelizumab is a humanized anti-PD-1 monoclonal antibody that differs from nivolumab and pembrolizumab in terms of its target epitopes. Anticancer activity and safety of camrelizumab was evaluated in pretreated patients with advanced HCC (119). Among a total of 217 patients who received camrelizumab, 32 (14.7%) had an objective response and the overall survival probability at 6 months was reported to be 74.4%. In conclusion, camrelizumab demonstrated efficacy against previously untreated advanced HCC with manageable side effects, suggesting that it may be a promising novel therapeutic option for these patients (119).

4.7 Spartalizumab

Spartalizumab is a humanized IgG4 monoclonal antibody that binds PD-1 (120). A Phase ½ study evaluated the safety and efficacy of spartalizumab in combination with the selective FGFR4 inhibitor FGF401 in patients with FGFR4/KLB expressing tumors, including HCC. The results showed that FGF401 alone or in combination with spartalizumab was safe in patients with FGFR4/KLB-positive tumors (120).

4.8 Cemiplimab

Cemiplimab is a recombinant human IgG4 monoclonal antibody targeting the PD-1 receptor with potent anticancer activity and a safety profile comparable to other anti-PD-1 therapies (149). A Phase 1 study evaluated the safety, tolerability and antitumor activity of cemiplimab in patients with unresectable HCC who had progressed, were intolerant or declined first-line systemic therapy. Of the 26 patients evaluated, 5 (19.2%) showed a partial response, 14 (53.8%) were stable and 6 (23.1%) had progressive disease, while 1 patient was not evaluable. Of note, only 5 patients (19.2%) completed the planned 48 weeks of treatment, while the remaining patients discontinued treatment prematurely, mainly due to disease progression (121). In a Phase 2 study, patients with resectable HCC received neoadjuvant cemiplimab intravenously every 3 weeks, followed by surgical resection. Twenty-one patients were enrolled in the trial, and all received neoadjuvant cemiplimab. Successful tumor resection was achieved in 20 patients. Of these, 4 patients (20%) had significant tumor necrosis. 3 (15%) of the patients who underwent resection had a partial response, while the remaining patients had stable disease. Throughout the neoadjuvant treatment period, 95% of patients experienced treatment-emergent adverse events of various grades (122).

4.9 Atezolizumab

Atezolizumab, the first FDA-approved anti-PD-L1 antibody, is a fully human IgG1 monoclonal antibody used in combination with the VEGF inhibitor bevacizumab in HCC. In a Phase 1b study, patients with unresectable HCC who had not received prior systemic therapy who received a combination of atezolizumab and bevacizumab had longer progression-free survival compared to those who received atezolizumab alone (123). In IMbrave150 trial, efficacy and safety of atezolizumab-bevacizumab combination was compared with sorafenib in participants with locally advanced or metastatic HCC who have received no prior systemic treatment (124). The results revealed that atezolizumab combined with bevacizumab favored overall and progression-free survival outcomes compared to sorafenib in unresectable HCC.

4.10 Durvalumab

Similar to atezolizumab, durvalumab is a human IgG1 monoclonal antibody that targets PD-L1 and has received accelerated approval for the treatment of locally advanced or metastatic urothelial carcinoma (150). The safety and efficacy of durvalumab in combination with radioembolization with yttrium-90 microspheres were evaluated in locally advanced and unresectable HCC. Transarterial radioembolization (TARE) with yttrium-90 microspheres was administered in combination with 1500 mg intravenous (IV) durvalumab every 4 weeks. Of the 24

patients enrolled, seven (29.2%) had a complete response and 13 (54.2%) had a partial response, while none of the participants experienced any treatment-related serious adverse events. These results suggest that this treatment modality has shown promising efficacy and safety in patients with locally advanced unresectable HCC (125).

A Phase 2 trial evaluated durvalumab and the anti-CTLA-4 monoclonal antibody tremelimumab or durvalumab in combination with tremelimumab or bevacizumab for the treatment of patients with unresectable HCC where the results indicated that combinatorial durvalumab and bevacizumab showed promising clinical safety and efficacy (126).

In a Phase 3 study, HIMALAYA trial, durvalumab and tremelimumab combination therapy and durvalumab monotherapy versus sorafenib in the treatment of patients with no prior systemic therapy for unresectable HCC is evaluated. HIMALAYA is unique in that it is the first large Phase 3 trial to enroll a diverse and representative population of patients with unresectable HCC and to include extensive long-term follow-up to evaluate the efficacy of both monotherapy and combination immunotherapy approaches. Outcomes of this study revealed that durvalumab was noninferior to sorafenib with favorable safety; and the combinatorial administration of tremelimumab plus durvalumab may be considered as a first-line standard of care systemic therapy for unresectable HCC (127). Several clinical trials are currently being conducted with durvalumab, either as a monotherapy or in combination, for the treatment of HCC (151, 152).

4.11 Avelumab

Avelumab is a fully human IgG1 monoclonal antibody that is directed against PD-L1 (153). In a Phase 2 study, avelumab was evaluated in patients with advanced HCC following treatment with sorafenib. A total of 30 patients were enrolled and received 10 mg/kg avelumab every 2 weeks until disease progression or unacceptable toxicity. The primary endpoint of the study was objective response rate, and secondary endpoints included time to progression, overall survival, disease control rate and safety. However, no complete responses were observed, while three patients (10.0%) had partial responses. In conclusion, avelumab was well tolerated and showed moderate efficacy in advanced HCC previously treated with sorafenib (128).

A Phase 1b study, VEGF Liver 100, evaluated the safety and efficacy of avelumab plus TKI axitinib in treatment-naive patients with advanced HCC. Of the 22 patients enrolled, 16 patients (72.7%) experienced grade 3 treatment-emergent adverse events and 10 patients (45.5%) experienced immune-related adverse events. There were no treatment-related deaths. The objective response rate was 13.6%. These results suggest that avelumab plus axitinib has anti-tumor activity with a manageable toxicity profile in advanced HCC, which was also consistent with the established safety profiles of avelumab and axitinib when administered alone (129). The activity of TACE and stereotactic body radiotherapy followed by avelumab was evaluated in a Phase 2 study (START-FIT) in advanced unresectable HCC. A total of 33 patients were enrolled in this study; 11 (33%) experienced treatment-emergent adverse events and five (15%) patients experienced grade 3 or higher immune-related adverse events (130).

4.12 Ipilimumab

Ipilimumab is a fully human monoclonal IgG1 antibody targeting CTLA-4 (154). Based on cohort 4 of CheckMate 040 trial, ipilimumab in combination with nivolumab has been approved by the FDA for the treatment of HCC in patients who have received prior treatment with sorafenib (131). An ongoing Phase 2 trial is evaluating the efficacy of ipilimumab in combination with nivolumab in patients with advanced HCC who have progressed after first-line treatment with atezolizumab and bevacizumab (155). In another ongoing Phase 2 study, it is aimed to investigate efficacy of ipilimumab/nivolumab and TACE in patients with HCC who are not eligible for curative intent treatment (156).

4.13 Tremelimumab

Tremelimumab, a fully human monoclonal antibody targeting CTLA-4, was initially evaluated as a checkpoint inhibitor in patients with HCC and chronic HCV infection. The study included 21 patients, of which 3 patients discontinued the study. Among the 17 patients evaluated for tumor response, the overall response rate was 17.6%. Importantly, the treatment was generally well tolerated with only a small number of patients experiencing significant adverse events (132). In a Phase 1/2 study, tremelimumab with chemoembolization or ablation was evaluated for HCC treatment. a total of 61 patients were enrolled in this study, and the results indicated that tremelimumab promotes activation of T cell responses in HCC and in combination with tumor ablation, it can be regarded as a potential novel treatment for patients with advanced HCC (133, 134). Another Phase 1/2 study evaluated the safety and efficacy of tremelimumab in combination with durvalumab; of the 40 patients enrolled, all patients had a partial response and six (15%) had an overall response. No unexpected safety signals with durvalumab and tremelimumab were observed (135).

4.14 Cobolimab

Increased expression of TIM-3 on monocytes in individuals with chronic HBV suggests that patients with HCC have increased expression of TIM-3 on peripheral blood monocytes compared to controls. Furthermore, there appears to be a negative correlation between TIM-3 expression and patient survival, highlighting the potential importance of TIM-3 in HCC prognosis (157). A Phase 2 study is currently evaluating the anti-TIM-3 antibody cobolimab in combination with dostarlimab in advanced HCC, which is expected to be completed in 2025. The study is designed to enroll 42 patients diagnosed with histologically confirmed HCC at BCLC stage B or C.

Participants will receive cobolimab 300 mg and dostarlimab 500 mg on the first day of each 21-day cycle. Interim results indicate that the combined regimen of cobolimab and dostarlimab has an acceptable safety profile with encouraging clinical activity as a first-line treatment in patients with advanced HCC (136).

5 Considerations of immune checkpoint inhibition in hepatocellular carcinoma treatment

The liver is characterized by a distinct immunological milieu, with the presence of immune cells predisposed to promote tolerance and immune suppression. Given the constant exposure of the liver to foreign antigens and bacterial by-products in the portal blood, is advantageous for the maintenance of normal biological function. Unfortunately, this tolerogenic state within the liver creates a conducive environment for the initiation and progression of both primary and metastatic liver tumors. The suppressive nature of intrahepatic immune cells represents a significant barrier to the development of effective anti-tumor immunotherapy strategies. Thus, deeper understanding of liver immune cell biology is essential to pave the way for innovative immunotherapeutic approaches tailored to combat liver tumors (158).

Including HCC, cancers often display a heterogeneous composition of immune cells within the TME, exhibiting variations in type, density, and spatial distribution. The established immunoheterogeneity pattern, which is particularly relevant to the efficacy of ICIs, categorizes tumors into three distinct profiles: hot, excluded, and cold. Hot tumors have an abundance of T cells actively engaged in anticancer activities, making them more likely to respond favorably to ICIs. Conversely, cold tumors lack T cells, indicating a reduced likelihood of a robust response to immunotherapy. In between these extremes, immune-excluded tumors exhibit an intermediate responsiveness to ICIs; here, T cells predominantly accumulate at the tumor periphery and are unable to effectively infiltrate the core. This simplified, yet powerful conceptualization serves as a predictive framework for the therapeutic outcomes of ICIs in various malignancies (159). To overcome resistance to HCC immunotherapy, it may be advantageous to identify targets capable of transforming the TME from immunologically cold to hot in order to enhance their responsiveness to immunotherapy (31). For this purpose, combination therapies may enhance the efficacy of ICI in HCC. An example of this approach may be the combinatorial administration of anti-VEGF antibodies with ICI. Since HCC is a highly vascularized tumor, targeting angiogenesis has emerged as a promising avenue for therapeutic intervention. In addition, VEGF exerts inhibitory effects on the immune response by affecting cytotoxic T cells, DCs, Tregs and MDSCs (160–162). In this context, the combination of atezolizumab and the anti-VEGF antibody bevacizumab is a pioneering systemic therapy which does not only inhibit angiogenesis, but also demonstrates an overall survival benefit that exceeds that of conventional sorafenib, marking a significant advancement in the therapeutic landscape for patients with unresectable HCC (124, 163).

Because liver tumors typically harbor multiple immunosuppressive factors, isolated blockade of a single factor appears insufficient to achieve substantial improvements. Therefore, simultaneous inhibition of non-redundant immunosuppressive pathways is expected to provide superior efficacy compared to singular blockade of one immune checkpoint. Consistent with this, inhibition of the PD-1 and CTLA-4 pathways by administering nivolumab in combination with ipilimumab demonstrated a manageable safety profile and achieved an objective response rate of 32% in patients with advanced HCC previously treated with sorafenib (164). Another study in HCC patients who progressed on prior single-agent ICI therapy showed that dual ICI therapy with ipilimumab in combination with either nivolumab or pembrolizumab resulted in durable anti-tumor responses and encouraging survival outcomes (165).

Currently, TACE, a versatile approach that can be tailored to the specific stage of diagnosis and incorporates techniques such as angiography and computed tomography (CT), is widely accepted as the primary and effective treatment for HCC patients with intermediate stage HCC (166, 167). This method is known for its interdisciplinarity, allowing the combination with various treatments such as radiotherapy, percutaneous ethanol injection and RFA. The release of tumor-associated antigens during all types of locoregional therapy, including TACE, can stimulate immune responses and ideally lead to a synergistic effect of both therapies. Similarly, thermal ablation has been reported to promote inflammation and increase tumor antigens to induce a cancer-immunity cycle and act synergistically with ICI. Both preclinical and clinical research has provided compelling evidence supporting the combination of ICI with thermal ablation as a means to reverse T-cell depletion, however, despite this promising potential, the clinical feasibility of activating immune responses through a combination of ICI monotherapy and thermal ablation appears to be limited as this approach is not widely used in clinical practice (168). In summary, eliminating HCC by ablation may activate the immune system, which can potentially recognize and kill remaining cancer, while ICIs may also enhance this effect (167).

Another area to be explored is biomarkers to predict the ICI treatment efficacy in HCC. In IMbrave150 trial in which the patients were administered atezolizumab plus bevacizumab, pre-existing immunity was characterized by intratumoral CD8+ T cell density, high expression of CD274 encoding PD-L1, and T effector signature were favorably associated with the outcome; whereas a high Treg to effector T cell ratio and high expression of oncofetal genes (GPC3 and AFP) were associated with reduced benefit from the combination therapy (169). In another study aiming to unravel molecular markers that correlate with ICI response in hot tumors, the authors demonstrated that none of the cold or excluded tumors responded to ICI therapy. Interestingly, half of the hot tumors were also reported to be unresponsive. Further analysis revealed an enrichment of terminally exhausted T cells in non-responders, and the presence of intratumoral DC-CD4+ T helper cell niches was reported to promote the efficacy of ICI therapy (170).

Besides TME, the important role of the gut microbiota in regulating systemic immunity and influencing responses to immunotherapy and the immune effect of chemotherapy is widely accepted. Similarly, in ICI therapy, the diversity of the host

microbial flora has been shown to influence clinical outcomes in HCC. In addition, the dynamic changes in gut microbiome characteristics hold the potential for early prediction of immunotherapy outcomes. Understanding the impact of the microbiota on the response to ICI, coupled with evidence from preclinical studies demonstrating HCC prevention through antibiotic-induced modulation of the gut microbiota may form the basis for considering clinical trials exploring the combination of immunotherapies with antibiotics or probiotics (171, 172).

Finally, ICIs may be recognized as non-self by the host immune system and may induce the generation of anti-drug antibodies (ADAs). While ADA formation upon treatment has been studied extensively, data on their clinical significance remains limited, yet it is known that ADAs can reduce drug availability which may result in decreased clinical efficacy (173). In the IMbrave150 study, ADA positivity resulted in decreased treatment efficacy compared to those who did not develop ADAs, most likely due to an increased rate of drug clearance (20). In another study, ADA-positive patients who received atezolizumab plus bevacuzimab for 3 weeks had worse progression-free survival and overall survival compared to placebo (174). In this study, high ADA levels were reported to be positively correlated with impaired CD8+ T cell proliferation and decreased IFN-γ and TNF-α production by CD8+ T cells. All these findings suggest that monitoring ADA formation during treatment regimens that include ICI, not only in HCC but in all malignancies, may improve the safety and efficacy of therapy, in addition to aiding clinicians in determining the ideal combinatorial treatment regimen for their patients (174).

6 Conclusion

In recent years, immunotherapy has brought about a significant and lasting change in the field of systemic therapy for patients with advanced HCC, as the results of numerous phase 2 and 3 trials have shown promising results with the administration of PD-1, PD-L1 and CTLA-4 ICIs. Nevertheless, phase 3 trials evaluating ICI monotherapies versus TKIs as first- or second-line treatment have yielded conflicting results, though they have encouraged further investigation into this therapeutic modality. Moreover, clinical trials of combinatorial administration of ICIs with other targeted therapies in addition to TKIs for the second-line treatment of advanced HCC are ongoing and showing promising results (111, 175). In summary, ICIs hold great promise for becoming the standard of care for HCC treatment in the future. On the other hand, a tumor's response to ICI is strongly influenced by its immune cell composition, so therapeutic interventions aimed at converting "cold" tumors into "hot" tumors may enhance the efficacy of ICI-based therapies. In addition, further studies focused on elucidating biomarkers predictive of ICI treatment response may help to select the optimal patient population that may benefit from ICI. Last but not least, routine monitoring during ICI administration may help clinicians to select the ideal drug combination while increasing the efficacy of the treatment.

Author contributions

ZA: Conceptualization, Data curation, Investigation, Writing – original draft. BA: Conceptualization, Data curation, Investigation, Visualization, Writing – original draft. FA: Visualization, Writing – original draft. GYD: Writing – review & editing.

Funding

The author(s) declare that no financial support was received for the research, authorship, and/or publication of this article.

Conflict of interest

The authors declare that the research was conducted in the absence of any commercial or financial relationships that could be construed as a potential conflict of interest.

Publisher's note

References

1. Ducreux M, Abou-Alfa GK, Bekaii-Saab T, Berlin J, Cervantes A, de Baere T, et al. The management of hepatocellular carcinoma. Current expert opinion and recommendations derived from the 24th ESMO/World Congress on Gastrointestinal Cancer, Barcelona, 2022. *ESMO Open*. (2023) 8:101567. doi: 10.1016/j.esmoop.2023.101567

2. Davis GL, Dempster J, Meler JD, Orr DW, Walberg MW, Brown B, et al. Hepatocellular carcinoma: management of an increasingly common problem. *Baylor Univ Med Cent Proc*. (2008) 21:266–80. doi: 10.1080/08998280.2008.11928410

3. Bosch FX, Ribes J, Díaz M, Cléries R. Primary liver cancer: Worldwide incidence and trends. *Gastroenterology*. (2004) 127:S5–S16. doi: 10.1053/j.gastro.2004.09.011

4. Llovet JM, Kelley RK, Villanueva A, Singal AG, Pikarsky E, Roayaie S, et al. Hepatocellular carcinoma. *Nat Rev Dis Prim*. (2021) 7:6. doi: 10.1038/s41572-020-00240-3

5. Han J, Wang B, Liu W, Wang S, Chen R, Chen M, et al. Declining disease burden of HCC in the United States, 1992–2017: A population-based analysis. *Hepatology*. (2022) 76:576–88. doi: 10.1002/hep.32355

6. Yang JD, Altekruse SF, Nguyen MH, Gores GJ, Roberts LR. Impact of country of birth on age at the time of diagnosis of hepatocellular carcinoma in the United States. *Cancer*. (2017) 123:81–9. doi: 10.1002/cncr.30246

7. Rumgay H, Shield K, Charvat H, Ferrari P, Sornpaisarn B, Obot I, et al. Global burden of cancer in 2020 attributable to alcohol consumption: a population-based study. *Lancet Oncol*. (2021) 22:1071–80. doi: 10.1016/S1470-2045(21)00279-5

8. Ward ZJ, Bleich SN, Cradock AL, Barrett JL, Giles CM, Flax C, et al. Projected U.S. State-level prevalence of adult obesity and severe obesity. *N Engl J Med*. (2019) 381:2440–50. doi: 10.1056/NEJMsa1909301

9. Tan DJH, Ng CH, Lin SY, Pan XH, Tay P, Lim WH, et al. Clinical characteristics, surveillance, treatment allocation, and outcomes of non-alcoholic fatty liver disease-related hepatocellular carcinoma: a systematic review and meta-analysis. *Lancet Oncol.* (2022) 23:521–30. doi: 10.1016/S1470-2045(22)00078-X

10. McGlynn KA, Petrick JL, El-Serag HB. Epidemiology of hepatocellular carcinoma. *Hepatology*. (2021) 73:4–13. doi: 10.1002/hep.31288

11. Saran U, Humar B, Kolly P, Dufour J-F. Hepatocellular carcinoma and lifestyles. *J Hepatol.* (2016) 64:203–14. doi: 10.1016/j.jhep.2015.08.028

12. Petrick JL, Campbell PT, Koshiol J, Thistle JE, Andreotti G, Beane-Freeman LE, et al. Tobacco, alcohol use and risk of hepatocellular carcinoma and intrahepatic cholangiocarcinoma: The Liver Cancer Pooling Project. *Br J Cancer*. (2018) 118:1005–12. doi: 10.1038/s41416-018-0007-z

13. Jinjuvadia R, Patel S, Liangpunsakul S. The association between metabolic syndrome and hepatocellular carcinoma. *J Clin Gastroenterol.* (2014) 48:172–7. doi: 10.1097/MCG.0b013e3182a030c4

14. Mandlik DS, Mandlik SK, Choudhary HB. Immunotherapy for hepatocellular carcinoma: Current status and future perspectives. *World J Gastroenterol.* (2023) 29:1054–75. doi: 10.3748/wjg.v29.i6.1054

15. Guo Z, Zhang R, Yang A-G, Zheng G. Diversity of immune checkpoints in cancer immunotherapy. *Front Immunol*. (2023) 14:1121285. doi: 10.3389/fimmu.2023.1121285

16. Llovet JM, Ricci S, Mazzaferro V, Hilgard P, Gane E, Blanc J-F, et al. Sorafenib in advanced hepatocellular carcinoma. *N Engl J Med.* (2008) 359:378–90. doi: 10.1056/NEJMoa0708857

17. Kudo M, Finn RS, Qin S, Han K-H, Ikeda K, Piscaglia F, et al. Lenvatinib versus sorafenib in first-line treatment of patients with unresectable hepatocellular carcinoma: a randomised phase 3 non-inferiority trial. *Lancet*. (2018) 391:1163–73. doi: 10.1016/S0140-6736(18)30207-1

18. Merle P, Kudo M, Krotneva S, Ozgurdal K, Su Y, Proskorovsky I. Regorafenib versus cabozantinib as a second-line treatment for advanced hepatocellular carcinoma: an anchored matching-adjusted indirect comparison of efficacy and safety. *Liver Cancer*. (2023) 12:145–55. doi: 10.1159/000527403

19. Hanahan D, Weinberg RA. Hallmarks of cancer: the next generation. *Cell*. (2011) 144:646–74. doi: 10.1016/j.cell.2011.02.013

20. Llovet JM, Castet F, Heikenwalder M, Maini MK, Mazzaferro V, Pinato DJ, et al. Immunotherapies for hepatocellular carcinoma. *Nat Rev Clin Oncol*. (2022) 19:151–72. doi: 10.1038/s41571-021-00573-2

21. Sajid M, Liu L, Sun C. The dynamic role of NK cells in liver cancers: role in HCC and HBV associated HCC and its therapeutic implications. *Front Immunol*. (2022) 13:887186. doi: 10.3389/fimmu.2022.887186

22. Wensveen FM, Jelenčić V, Polić B. NKG2D: A master regulator of immune cell responsiveness. *Front Immunol*. (2018) 9:441. doi: 10.3389/fimmu.2018.00441

23. Zhang DY, Friedman SL. Fibrosis-dependent mechanisms of hepatocarcinogenesis. *Hepatology*. (2012) 56:769–75. doi: 10.1002/hep.25670

24. Ma Y, Shurin GV, Gutkin DW, Shurin MR. Tumor associated regulatory dendritic cells. *Semin Cancer Biol.* (2012) 22:298–306. doi: 10.1016/j.semcancer.2012.02.010

25. Zhang Q, He Y, Luo N, Patel SJ, Han Y, Gao R, et al. Landscape and dynamics of single immune cells in hepatocellular carcinoma. *Cell*. (2019) 179:829–845.e20. doi: 10.1016/j.cell.2019.10.003

26. Ma C, Zhang Q, Greten TF. MDSCs in liver cancer: A critical tumor-promoting player and a potential therapeutic target. *Cell Immunol*. (2021) 361:104295. doi: 10.1016/j.cellimm.2021.104295

27. Lu L-C, Chang C-J, Hsu C-H. Targeting myeloid-derived suppressor cells in the treatment of hepatocellular carcinoma: current state and future perspectives. *J Hepatocell Carcinoma*. (2019) 6:71–84. doi: 10.2147/JHC.S159693

28. Adams VR, Collins LB, Williams TI, Holmes J, Hess P, Atkins HM, et al. Myeloid cell MHC I expression drives CD8+ T cell activation in nonalcoholic steatohepatitis. *Front Immunol*. (2024) 14:1302006. doi: 10.3389/fimmu.2023.1302006

29. Ringelhan M, Pfister D, O'Connor T, Pikarsky E, Heikenwalder M. The immunology of hepatocellular carcinoma. *Nat Immunol*. (2018) 19:222–32. doi: 10.1038/s41590-018-0044-z

30. Helmy KY, Katschke KJ, Gorgani NN, Kljavin NM, Elliott JM, Diehl L, et al. CRIg: A macrophage complement receptor required for phagocytosis of circulating pathogens. *Cell*. (2006) 124:915–27. doi: 10.1016/j.cell.2005.12.039

31. Shen W, Chen Y, Lei P, Sheldon M, Sun Y, Yao F, et al. Immunotherapeutic approaches for treating hepatocellular carcinoma. *Cancers (Basel)*. (2022) 14:2. doi: 10.3390/cancers14205013

32. Knolle PA, Gerken G. Local control of the immune response in the liver. *Immunol Rev*. (2000) 174:21–34. doi: 10.1034/j.1600-0528.2002.017408.x

33. Shetty S, Lalor PF, Adams DH. Liver sinusoidal endothelial cells — gatekeepers of hepatic immunity. *Nat Rev Gastroenterol Hepatol.* (2018) 15:555–67. doi: 10.1038/s41575-018-0020-y

34. Sas Z, Cendrowicz E, Weinhäuser I, Rygiel TP. Tumor microenvironment of hepatocellular carcinoma: challenges and opportunities for new treatment options. *Int J Mol Sci*. (2022) 23:3778. doi: 10.3390/ijms23073778

35. Kamm DR, McCommis KS. Hepatic stellate cells in physiology and pathology. *J Physiol.* (2022) 600:1825–37. doi: 10.1113/JP281061

36. Sangro B, Sarobe P, Hervás-Stubbs S, Melero I. Advances in immunotherapy for hepatocellular carcinoma. *Nat Rev Gastroenterol Hepatol.* (2021) 18:525–43. doi: 10.1038/s41575-021-00438-0

37. Gao Q, Qiu S-J, Fan J, Zhou J, Wang X-Y, Xiao Y-S, et al. Intratumoral balance of regulatory and cytotoxic T cells is associated with prognosis of hepatocellular carcinoma after resection. *J Clin Oncol.* (2007) 25:2586–93. doi: 10.1200/JCO.2006.09.4565

38. Zhou S-L, Zhou Z-J, Hu Z-Q, Huang X-W, Wang Z, Chen E-B, et al. Tumor-associated neutrophils recruit macrophages and T-regulatory cells to promote progression of hepatocellular carcinoma and resistance to sorafenib. *Gastroenterology*. (2016) 150:1646–1658.e17. doi: 10.1053/j.gastro.2016.02.040

39. Li Z, Zhang Z, Fang L, Zhao J, Niu Z, Chen H, et al. Tumor microenvironment composition and related therapy in hepatocellular carcinoma. *J Hepatocell Carcinoma*. (2023) 10:2083–99. doi: 10.2147/JHC.S436962

40. Marcucci F, Rumio C, Corti A. Tumor cell-associated immune checkpoint molecules – Drivers of Malignancy and stemness. *Biochim Biophys Acta - Rev Cancer*. (2017) 1868:571–83. doi: 10.1016/j.bbcan.2017.10.006

41. Sharma P, Allison JP. The future of immune checkpoint therapy. *Science (80-).* (2015) 348:56–61. doi: 10.1126/science.aaa8172

42. Han Y, Liu D, Li L. PD-1/PD-L1 pathway: current researches in cancer. *Am J Cancer Res*. (2020) 10:727–42.

43. Escors D, Gato-Cañas M, Zuazo M, Arasanz H, García-Granda MJ, Vera R, et al. The intracellular signalosome of PD-L1 in cancer cells. *Signal Transduct Target Ther*. (2018) 3:26. doi: 10.1038/s41392-018-0022-9

44. Garcia-Diaz A, Shin DS, Moreno BH, Saco J, Escuin-Ordinas H, Rodriguez GA, et al. Interferon receptor signaling pathways regulating PD-L1 and PD-L2 expression. *Cell Rep*. (2017) 19:1189–201. doi: 10.1016/j.celrep.2017.04.031

45. Gowrishankar K, Gunatilake D, Gallagher SJ, Tiffen J, Rizos H, Hersey P. Inducible but not constitutive expression of PD-L1 in human melanoma cells is dependent on activation of NF-κB. *PloS One*. (2015) 10:e0123410. doi: 10.1371/journal.pone.0123410

46. Shiravand Y, Khodadadi F, Kashani SMA, Hosseini-Fard SR, Hosseini S, Sadeghirad H, et al. Immune checkpoint inhibitors in cancer therapy. *Curr Oncol.* (2022) 29:3044–60. doi: 10.3390/curroncol29050247

47. Buckle I, Guillerey C. Inhibitory receptors and immune checkpoints regulating natural killer cell responses to cancer. *Cancers (Basel)*. (2021) 13:4263. doi: 10.3390/cancers13174263

48. Whelan S, Ophir E, Kotturi MF, Levy O, Ganguly S, Leung L, et al. PVRIG and PVRL2 are induced in cancer and inhibit CD8+ T-cell function. *Cancer Immunol Res*. (2019) 7:257–68. doi: 10.1158/2326-6066.CIR-18-0442

49. Li Y, Zhang Y, Cao G, Zheng X, Sun C, Wei H, et al. Blockade of checkpoint receptor PVRIG unleashes anti-tumor immunity of NK cells in murine and human solid tumors. *J Hematol Oncol.* (2021) 14:100. doi: 10.1186/s13045-021-01112-3

50. Sanchez-Correa B, Valhondo I, Hassouneh F, Lopez-Sejas N, Pera A, Bergua JM, et al. DNAM-1 and the TIGIT/PVRIG/TACTILE axis: novel immune checkpoints for natural killer cell-based cancer immunotherapy. *Cancers (Basel)*. (2019) 11:877. doi: 10.3390/cancers11060877

51. Hastings WD, Anderson DE, Kassam N, Koguchi K, Greenfield EA, Kent SC, et al. TIM-3 is expressed on activated human CD4 + T cells and regulates Th1 and Th17 cytokines. *Eur J Immunol*. (2009) 39:2492–501. doi: 10.1002/eji.200939274

52. Das M, Zhu C, Kuchroo VK. Tim-3 and its role in regulating anti-tumor immunity. *Immunol Rev*. (2017) 276:97–111. doi: 10.1111/imr.12520

53. Du W, Yang M, Turner A, Xu C, Ferris R, Huang J, et al. TIM-3 as a target for cancer immunotherapy and mechanisms of action. *Int J Mol Sci*. (2017) 18:645. doi: 10.3390/ijms18030645

54. Jinushi M, Yoneda A. T cell immunoglobulin domain and mucin domain-3 as an emerging target for immunotherapy in cancer management. *ImmunoTargets Ther*. (2013) 2:135. doi: 10.2147/ITT.S38296

55. Lv Y, Ma X, Ma Y, Du Y, Feng J. A new emerging target in cancer immunotherapy: Galectin-9 (LGALS9). *Genes Dis*. (2023) 10:2366–82. doi: 10.1016/j.gendis.2022.05.020

56. Zhu C, Anderson AC, Schubart A, Xiong H, Imitola J, Khoury SJ, et al. The Tim-3 ligand galectin-9 negatively regulates T helper type 1 immunity. *Nat Immunol*. (2005) 6:1245–52. doi: 10.1038/ni1271

57. Labrie M, De Araujo LOF, Communal L, Mes-Masson A-M, St-Pierre Y. Tissue and plasma levels of galectins in patients with high grade serous ovarian carcinoma as new predictive biomarkers. *Sci Rep*. (2017) 7:13244. doi: 10.1038/s41598-017-13802-5

58. Wang L, Rubinstein R, Lines JL, Wasiuk A, Ahonen C, Guo Y, et al. VISTA, a novel mouse Ig superfamily ligand that negatively regulates T cell responses. *J Exp Med*. (2011) 208:577–92. doi: 10.1084/jem.20100619

59. Lines JL, Pantazi E, Mak J, Sempere LF, Wang L, O'Connell S, et al. VISTA is an immune checkpoint molecule for human T cells. *Cancer Res*. (2014) 74:1924–32. doi: 10.1158/0008-5472.CAN-13-1504

60. Huang X, Zhang X, Li E, Zhang G, Wang X, Tang T, et al. VISTA: an immune regulatory protein checking tumor and immune cells in cancer immunotherapy. *J Hematol Oncol.* (2020) 13:83. doi: 10.1186/s13045-020-00917-y

61. Triebel F, Jitsukawa S, Baixeras E, Roman-Roman S, Genevee C, Viegas-Pequignot E, et al. LAG-3, a novel lymphocyte activation gene closely related to CD4. *J Exp Med*. (1990) 171:1393–405. doi: 10.1084/jem.171.5.1393

62. Ruffo E, Wu RC, Bruno TC, Workman CJ, Vignali DAA. Lymphocyte-activation gene 3 (LAG3): The next immune checkpoint receptor. *Semin Immunol*. (2019) 42:101305. doi: 10.1016/j.smim.2019.101305

63. Huard B, Prigent P, Tournier M, Bruniquel D, Triebel F. CD4/major histocompatibility complex class II interaction analyzed with CD4- and lymphocyte activation gene-3 (LAG-3)-Ig fusion proteins. *Eur J Immunol*. (1995) 25:2718–21. doi: 10.1002/eji.1830250949

64. Yu X, Harden K C, Gonzalez L, Francesco M, Chiang E, Irving B, et al. The surface protein TIGIT suppresses T cell activation by promoting the generation of mature immunoregulatory dendritic cells. *Nat Immunol*. (2009) 10:48–57. doi: 10.1038/ni.1674

65. Yang Z-Z, Kim HJ, Wu H, Jalali S, Tang X, Krull JE, et al. TIGIT expression is associated with T-cell suppression and exhaustion and predicts clinical outcome and anti–PD-1 response in follicular lymphoma. *Clin Cancer Res*. (2020) 26:5217–31. doi: 10.1158/1078-0432.CCR-20-0558

66. Kong Y, Zhu L, Schell TD, Zhang J, Claxton DF, Ehmann WC, et al. T-cell immunoglobulin and ITIM domain (TIGIT) associates with CD8+ T-cell exhaustion and poor clinical outcome in AML patients. *Clin Cancer Res*. (2016) 22:3057–66. doi: 10.1158/1078-0432.CCR-15-2626

67. Banchereau J, Bazan F, Blanchard D, Briè F, Galizzi JP, van Kooten C, et al. The CD40 antigen and its ligand. *Annu Rev Immunol*. (1994) 12:881–926. doi: 10.1146/annurev.iy.12.040194.004313

68. Bullock TNJ. CD40 stimulation as a molecular adjuvant for cancer vaccines and other immunotherapies. *Cell Mol Immunol*. (2022) 19:14–22. doi: 10.1038/s41423-021-00734-4

69. Elgueta R, Benson MJ, De Vries VC, Wasiuk A, Guo Y, Noelle RJ. Molecular mechanism and function of CD40/CD40L engagement in the immune system. *Immunol Rev*. (2009) 229:152–72. doi: 10.1111/j.1600-065X.2009.00782.x

70. Inaguma S, Lasota J, Czapiewski P, Langfort R, Rys J, Szpor J, et al. CD70 expression correlates with a worse prognosis in Malignant pleural mesothelioma patients via immune evasion and enhanced invasiveness. *J Pathol*. (2020) 250:205–16. doi: 10.1002/path.5361

71. Lutfi F, Wu L, Sunshine S, Cao X. Targeting the CD27-CD70 pathway to improve outcomes in both checkpoint immunotherapy and allogeneic hematopoietic cell transplantation. *Front Immunol*. (2021) 12:715909. doi: 10.3389/fimmu.2021.715909

72. Denoeud J, Moser M. Role of CD27/CD70 pathway of activation in immunity and tolerance. *J Leukoc Biol*. (2010) 89:195–203. doi: 10.1189/jlb.0610351

73. Jacobs J, Deschoolmeester V, Zwaenepoel K, Rolfo C, Silence K, Rottey S, et al. CD70: An emerging target in cancer immunotherapy. *Pharmacol Ther*. (2015) 155:1–10. doi: 10.1016/j.pharmthera.2015.07.007

74. Yang H, Xun Y, You H. The landscape overview of CD47-based immunotherapy for hematological Malignancies. *biomark Res*. (2023) 11:15. doi: 10.1186/s40364-023-00456-x

75. Huang J, Liu F, Li C, Liang X, Li C, Liu Y, et al. Role of CD47 in tumor immunity: a potential target for combination therapy. *Sci Rep*. (2022) 12:9803. doi: 10.1038/s41598-022-13764-3

76. Wang C, Feng Y, Patel D, Xie H, Lv Y, Zhao H. The role of CD47 in non-neoplastic diseases. *Heliyon*. (2023) 9:e22905. doi: 10.1016/j.heliyon.2023.e22905

77. Pauken KE, Wherry EJ. Overcoming T cell exhaustion in infection and cancer. *Trends Immunol*. (2015) 36:265–76. doi: 10.1016/j.it.2015.02.008

78. Dyck L, Mills KHG. Immune checkpoints and their inhibition in cancer and infectious diseases. *Eur J Immunol*. (2017) 47:765–79. doi: 10.1002/eji.201646875

79. Blackburn SD, Shin H, Haining WN, Zou T, Workman CJ, Polley A, et al. Coregulation of CD8+ T cell exhaustion by multiple inhibitory receptors during chronic viral infection. *Nat Immunol*. (2009) 10:29–37. doi: 10.1038/ni.1679

80. He X, Xu C. Immune checkpoint signaling and cancer immunotherapy. *Cell Res*. (2020) 30:660–9. doi: 10.1038/s41422-020-0343-4

81. Bernard D, Hansen J, Dupasquier L, Lefranc M, Benmansour A, Boudinot P. Costimulatory receptors in jawed vertebrates: Conserved CD28, odd CTLA4 and multiple BTLAs. *Dev Comp Immunol*. (2007) 31:255–71. doi: 10.1016/j.dci.2006.06.003

82. Ribas A, Wolchok JD. Cancer immunotherapy using checkpoint blockade. *Science (80-)*. (2018) 359:1350–5. doi: 10.1126/science.aar4060

83. Ritprajak P, Azuma M. Intrinsic and extrinsic control of expression of the immunoregulatory molecule PD-L1 in epithelial cells and squamous cell carcinoma. *Oral Oncol*. (2015) 51:221–8. doi: 10.1016/j.oraloncology.2014.11.014

84. Dermani FK, Samadi P, Rahmani G, Kohlan AK, Najafi R. PD-1/PD-L1 immune checkpoint: Potential target for cancer therapy. *J Cell Physiol*. (2019) 234:1313–25. doi: 10.1002/jcp.27172

85. Doroshow DB, Bhalla S, Beasley MB, Sholl LM, Kerr KM, Gnjatic S, et al. PD-L1 as a biomarker of response to immune-checkpoint inhibitors. *Nat Rev Clin Oncol*. (2021) 18:345–62. doi: 10.1038/s41571-021-00473-5

86. Zhong F, Cheng X, Sun S, Zhou J. Transcriptional activation of PD-L1 by Sox2 contributes to the proliferation of hepatocellular carcinoma cells. *Oncol Rep*. (2017) 37:3061–7. doi: 10.3892/or.2017.5523

87. Wei SC, Duffy CR, Allison JP. Fundamental mechanisms of immune checkpoint blockade therapy. *Cancer Discovery*. (2018) 8:1069–86. doi: 10.1158/2159-8290.CD-18-0367

88. Chikuma S, Murakami M, Tanaka K, Uede T. Janus kinase 2 is associated with a box 1-like motif and phosphorylates a critical tyrosine residue in the cytoplasmic region of cytotoxic T lymphocyte associated molecule-4. *J Cell Biochem*. (2000) 78:241–50. doi: 10.1002/(SICI)1097-4644(20000801)78:2<241::AID-JCB7>3.0.CO;2-K

89. Turnis ME, Andrews LP, Vignali DAA. Inhibitory receptors as targets for cancer immunotherapy. *Eur J Immunol*. (2015) 45:1892–905. doi: 10.1002/eji.201344413

90. Zhu Y, Paniccia A, Schulick AC, Chen W, Koenig MR, Byers JT, et al. Identification of CD112R as a novel checkpoint for human T cells. *J Exp Med*. (2016) 213:167–76. doi: 10.1084/jem.20150785

91. Flies DB, Wang S, Xu H, Chen L. Cutting edge: A monoclonal antibody specific for the programmed death-1 homolog prevents graft-versus-host disease in mouse models. *J Immunol*. (2011) 187:1537–41. doi: 10.4049/jimmunol.1100660

92. Dijkstra JM, Somamoto T, Moore L, Hordvik I, Ototake M, Fischer U. Identification and characterization of a second CD4-like gene in teleost fish. *Mol Immunol*. (2006) 43:410–9. doi: 10.1016/j.molimm.2005.03.005

93. Shan C, Li X, Zhang J. Progress of immune checkpoint LAG−3 in immunotherapy (Review). *Oncol Lett*. (2020) 20:1–1. doi: 10.3892/ol.2020.12070

94. Tang W, Chen J, Ji T, Cong X. TIGIT, a novel immune checkpoint therapy for melanoma. *Cell Death Dis*. (2023) 14:466. doi: 10.1038/s41419-023-05961-3

95. Zarour HM. Reversing T-cell dysfunction and exhaustion in cancer. *Clin Cancer Res*. (2016) 22:1856–64. doi: 10.1158/1078-0432.CCR-15-1849

96. Liu X, Li M, Wang X, Dang Z, Jiang Y, Wang X, et al. PD-1+ TIGIT+ CD8+ T cells are associated with pathogenesis and progression of patients with hepatitis B virus-related hepatocellular carcinoma. *Cancer Immunol Immunother*. (2019) 68:2041–54. doi: 10.1007/s00262-019-02426-5

97. Seki M, Oomizu S, Sakata K, Sakata A, Arikawa T, Watanabe K, et al. Galectin-9 suppresses the generation of Th17, promotes the induction of regulatory T cells, and regulates experimental autoimmune arthritis. *Clin Immunol*. (2008) 127:78–88. doi: 10.1016/j.clim.2008.01.006

98. Wang Y, Sun J, Ma C, Gao W, Song B, Xue H, et al. Reduced expression of galectin-9 contributes to a poor outcome in colon cancer by inhibiting NK cell chemotaxis partially through the rho/ROCK1 signaling pathway. *PloS One*. (2016) 11:e0152599. doi: 10.1371/journal.pone.0152599

99. Irie A, Yamauchi A, Kontani K, Kihara M, Liu D, Shirato Y, et al. Galectin-9 as a prognostic factor with antimetastatic potential in breast cancer. *Clin Cancer Res*. (2005) 11:2962–8. doi: 10.1158/1078-0432.CCR-04-0861

100. Koho H, Paulie S, Ben-Aissa H, Jónsdóttir I, Hansson Y, Lundblad M-L, et al. Monoclonal antibodies to antigens associated with transitional cell carcinoma of the human urinary bladder. *Cancer Immunol Immunother*. (1984) 17:1. doi: 10.1007/BF00205481

101. Bates KM, Vathiotis I, MacNeil T, Ahmed FS, Aung TN, Katlinskaya Y, et al. Spatial characterization and quantification of CD40 expression across cancer types. *BMC Cancer*. (2023) 23:220. doi: 10.1186/s12885-023-10650-7

102. Slobodova Z, Ehrmann J, Krejci V, Zapletalova J, Melichar B. Analysis of CD40 expression in breast cancer and its relation to clinicopathological characteristics. *Neoplasma*. (2011) 58:189–97. doi: 10.4149/neo_2011_03_189

103. Wiesmann A, Phillips RL, Mojica M, Pierce LJ, Searles AE, Spangrude GJ, et al. Expression of CD27 on murine hematopoietic stem and progenitor cells. *Immunity*. (2000) 12:193–9. doi: 10.1016/S1074-7613(00)80172-7

104. Kuka M, Munitic I, Giardino Torchia ML, Ashwell JD. CD70 is downregulated by interaction with CD27. *J Immunol*. (2013) 191:2282–9. doi: 10.4049/jimmunol.1300868

105. Flieswasser T, Camara-Clayette V, Danu A, Bosq J, Ribrag V, Zabrocki P, et al. Screening a broad range of solid and haematological tumour types for CD70 expression using a uniform IHC methodology as potential patient stratification method. *Cancers (Basel)*. (2019) 11:1611. doi: 10.3390/cancers11101611

106. Liu N, Sheng X, Liu Y, Yu J, Zhang X. Increased CD70 expression is associated with clinical resistance to cisplatin-based chemotherapy and poor survival in advanced ovarian carcinomas. *Onco Targets Ther*. (2013) 6:615. doi: 10.2147/OTT.S44445

107. Jin L, Ge H, Long Y, Yang C, Chang YE, Mu L, et al. CD70, a novel target of CAR T-cell therapy for gliomas. *Neuro Oncol*. (2018) 20:55–65. doi: 10.1093/neuonc/nox116

108. Flieswasser T, Van den Eynde A, Van Audenaerde J, De Waele J, Lardon F, Riether C, et al. The CD70-CD27 axis in oncology: the new kids on the block. *J Exp Clin Cancer Res*. (2022) 41:12. doi: 10.1186/s13046-021-02215-y

109. Jacobs J, Zwaenepoel K, Rolfo C, Van den Bossche J, Deben C, Silence K, et al. Unlocking the potential of CD70 as a novel immunotherapeutic target for non-small cell lung cancer. *Oncotarget*. (2015) 6:13462–75. doi: 10.18632/oncotarget.3880

110. Zhao H, Song S, Ma J, Yan Z, Xie H, Feng Y, et al. CD47 as a promising therapeutic target in oncology. *Front Immunol*. (2022) 13:757480. doi: 10.3389/fimmu.2022.757480

111. van Doorn DJ, Takkenberg RB, Klümpen H-J. Immune checkpoint inhibitors in hepatocellular carcinoma: an overview. *Pharmaceuticals*. (2020) 14:3. doi: 10.3390/ph14010003

112. Yau T, Park J-W, Finn RS, Cheng A-L, Mathurin P, Edeline J, et al. Nivolumab versus sorafenib in advanced hepatocellular carcinoma (CheckMate 459): a randomised, multicentre, open-label, phase 3 trial. *Lancet Oncol*. (2022) 23:77–90. doi: 10.1016/S1470-2045(21)00604-5

113. Finn RS, Ryoo B-Y, Merle P, Kudo M, Bouattour M, Lim HY, et al. Pembrolizumab as second-line therapy in patients with advanced hepatocellular carcinoma in KEYNOTE-240: A randomized, double-blind, phase III trial. *J Clin Oncol*. (2020) 38:193–202. doi: 10.1200/JCO.19.01307

114. Zhu AX, Finn RS, Edeline J, Cattan S, Ogasawara S, Palmer D, et al. Pembrolizumab in patients with advanced hepatocellular carcinoma previously treated with sorafenib (KEYNOTE-224): a non-randomised, open-label phase 2 trial. *Lancet Oncol*. (2018) 19:940–52. doi: 10.1016/S1470-2045(18)30351-6

115. Qin S, Kudo M, Meyer T, Bai Y, Guo Y, Meng Z, et al. Tislelizumab vs sorafenib as first-line treatment for unresectable hepatocellular carcinoma. *JAMA Oncol*. (2023) 9:1651. doi: 10.1001/jamaoncol.2023.4003

116. He M, Ming S, Lai Z, Li Q. A phase II trial of lenvatinib plus toripalimab and hepatic arterial infusion chemotherapy as a first-line treatment for advanced hepatocellular carcinoma (LTHAIC study). *J Clin Oncol*. (2021) 39:4083–3. doi: 10.1200/JCO.2021.39.15_suppl.4083

117. Ren Z, Xu J, Bai Y, Xu A, Cang S, Du C, et al. Sintilimab plus a bevacizumab biosimilar (IBI305) versus sorafenib in unresectable hepatocellular carcinoma (ORIENT-32): a randomised, open-label, phase 2–3 study. *Lancet Oncol*. (2021) 22:977–90. doi: 10.1016/S1470-2045(21)00252-7

118. Wang L, Wang H, Cui Y, Jin K, Liu W, Wang K, et al. Sintilimab plus lenvatinib as conversion therapy in patients with unresectable locally intermediate to advanced hepatocellular carcinoma: A single-arm, single-center, open-label, phase 2 study. *J Clin Oncol*. (2022) 40:449–9. doi: 10.1200/JCO.2022.40.4_suppl.449

119. Qin S, Ren Z, Meng Z, Chen Z, Chai X, Xiong J, et al. Camrelizumab in patients with previously treated advanced hepatocellular carcinoma: a multicentre, open-label, parallel-group, randomised, phase 2 trial. *Lancet Oncol*. (2020) 21:571–80. doi: 10.1016/S1470-2045(20)30011-5

120. Naing A, Gainor JF, Gelderblom H, Forde PM, Butler MO, Lin C-C, et al. A first-in-human phase 1 dose escalation study of spartalizumab (PDR001), an anti–PD-1 antibody, in patients with advanced solid tumors. *J Immunother Cancer*. (2020) 8: e000530. doi: 10.1136/jitc-2020-000530

121. Pishvaian MJ, Weiss GJ, Falchook GS, Yee N, Gil-Martin M, Shahda S, et al. Cemiplimab, a human monoclonal anti-PD-1, in patients (pts) with advanced or metastatic hepatocellular carcinoma (HCC): Data from an expansion cohort in a phase I study. *Ann Oncol*. (2018) 29:viii410. doi: 10.1093/annonc/mdy288.024

122. Marron TU, Fiel MI, Hamon P, Fiaschi N, Kim E, Ward SC, et al. Neoadjuvant cemiplimab for resectable hepatocellular carcinoma: a single-arm, open-label, phase 2 trial. *Lancet Gastroenterol Hepatol*. (2022) 7:219–29. doi: 10.1016/S2468-1253(21)00385-X

123. Lee MS, Ryoo B-Y, Hsu C-H, Numata K, Stein S, Verret W, et al. Atezolizumab with or without bevacizumab in unresectable hepatocellular carcinoma (GO30140): an open-label, multicentre, phase 1b study. *Lancet Oncol*. (2020) 21:808–20. doi: 10.1016/S1470-2045(20)30156-X

124. Finn RS, Qin S, Ikeda M, Galle PR, Ducreux M, Kim T-Y, et al. Atezolizumab plus bevacizumab in unresectable hepatocellular carcinoma. *N Engl J Med*. (2020) 382:1894–905. doi: 10.1056/NEJMoa1915745

125. Lee YB, Nam JY, Cho EJ, Lee J-H, Yu SJ, Kim H-C, et al. A phase I/IIa trial of yttrium-90 radioembolization in combination with durvalumab for locally advanced unresectable hepatocellular carcinoma. *Clin Cancer Res*. (2023) 29:3650–8. doi: 10.1158/1078-0432.CCR-23-0581

126. Lim HY, Heo J, Kim T-Y, Tai WMD, Kang Y-K, Lau G, et al. Safety and efficacy of durvalumab plus bevacizumab in unresectable hepatocellular carcinoma: Results from the phase 2 study 22 (NCT02519348). *J Clin Oncol*. (2022) 40:436–6. doi: 10.1200/JCO.2022.40.4_suppl.436

127. Abou-Alfa GK, Chan SL, Kudo M, Lau G, Kelley RK, Furuse J, et al. Phase 3 randomized, open-label, multicenter study of tremelimumab (T) and durvalumab (D) as first-line therapy in patients (pts) with unresectable hepatocellular carcinoma (uHCC): HIMALAYA. *J Clin Oncol*. (2022) 40:379–9. doi: 10.1200/JCO.2022.40.4_suppl.379

128. Lee D-W, Cho EJ, Lee J-H, Yu SJ, Kim YJ, Yoon J-H, et al. Phase II study of avelumab in patients with advanced hepatocellular carcinoma previously treated with sorafenib. *Clin Cancer Res*. (2021) 27:713–8. doi: 10.1158/1078-0432.CCR-20-3094

129. Kudo M, Motomura K, Wada Y, Inaba Y, Sakamoto Y, Kurosaki M, et al. Avelumab in combination with axitinib as first-line treatment in patients with advanced hepatocellular carcinoma: results from the phase 1b VEGF liver 100 trial. *Liver Cancer*. (2021) 10:249–59. doi: 10.1159/000514420

130. Chiang CL, Chiu KWH, Chan KSK, Lee FAS, Li JCB, Wan CWS, et al. Sequential transarterial chemoembolisation and stereotactic body radiotherapy followed by immunotherapy as conversion therapy for patients with locally advanced, unresectable hepatocellular carcinoma (START-FIT): a single-arm, phase 2 trial. *Lancet Gastroenterol Hepatol*. (2023) 8:169–78. doi: 10.1016/S2468-1253(22)00339-9

131. Saung MT, Pelosof L, Casak S, Donoghue M, Lemery S, Yuan M, et al. FDA approval summary: nivolumab plus ipilimumab for the treatment of patients with hepatocellular carcinoma previously treated with sorafenib. *Oncologist*. (2021) 26:797–806. doi: 10.1002/onco.13819

132. Sangro B, Gomez-Martin C, de la Mata M, Iñarrairaegui M, Garralda E, Barrera P, et al. A clinical trial of CTLA-4 blockade with tremelimumab in patients with hepatocellular carcinoma and chronic hepatitis C. *J Hepatol*. (2013) 59:81–8. doi: 10.1016/j.jhep.2013.02.022

133. Duffy AG, Ulahannan SV, Makorova-Rusher O, Rahma O, Wedemeyer H, Pratt D, et al. Tremelimumab in combination with ablation in patients with advanced hepatocellular carcinoma. *J Hepatol*. (2017) 66:545–51. doi: 10.1016/j.jhep.2016.10.029

134. Agdashian D, ElGindi M, Xie C, Sandhu M, Pratt D, Kleiner DE, et al. The effect of anti-CTLA4 treatment on peripheral and intra-tumoral T cells in patients with hepatocellular carcinoma. *Cancer Immunol Immunother*. (2019) 68:599–608. doi: 10.1007/s00262-019-02299-8

135. Kelley RK, Abou-Alfa GK, Bendell JC, Kim T-Y, Borad MJ, Yong W-P, et al. Phase I/II study of durvalumab and tremelimumab in patients with unresectable hepatocellular carcinoma (HCC): Phase I safety and efficacy analyses. *J Clin Oncol*. (2017) 35:4073–3. doi: 10.1200/JCO.2017.35.15_suppl.4073

136. Acoba JD, Rho Y, Fukaya E. Phase II study of cobolimab in combination with dostarlimab for the treatment of advanced hepatocellular carcinoma. *J Clin Oncol*. (2023) 41:580–0. doi: 10.1200/JCO.2023.41.4_suppl.580

137. El-Khoueiry AB, Sangro B, Yau T, Crocenzi TS, Kudo M, Hsu C, et al. Nivolumab in patients with advanced hepatocellular carcinoma (CheckMate 040): an open-label, non-comparative, phase 1/2 dose escalation and expansion trial. *Lancet*. (2017) 389:2492–502. doi: 10.1016/S0140-6736(17)31046-2

138. Yau T, Park JW, Finn RS, Cheng A-L, Mathurin P, Edeline J, et al. CheckMate 459: A randomized, multi-center phase III study of nivolumab (NIVO) vs sorafenib (SOR) as first-line (1L) treatment in patients (pts) with advanced hepatocellular carcinoma (aHCC). *Ann Oncol*. (2019) 30:v874–5. doi: 10.1093/annonc/mdz394.029

139. Pembrolizumab (Keytruda) in Advanced Hepatocellular Carcinoma. Available online at: https://clinicaltrials.gov/study/NCT02658019 (Accessed January 29, 2024).

140. Feun LG, Li Y, Wu C, Wangpaichitr M, Jones PD, Richman SP, et al. Phase 2 study of pembrolizumab and circulating biomarkers to predict anticancer response in advanced, unresectable hepatocellular carcinoma. *Cancer*. (2019) 125:3603–14. doi: 10.1002/cncr.32339

141. Deva S, Lee J-S, Lin C-C, Yen C-J, Millward M, Chao Y, et al. A phase Ia/Ib trial of tislelizumab, an anti-PD-1 antibody (ab), in patients (pts) with advanced solid tumors. *Ann Oncol*. (2018) 29:x24–5. doi: 10.1093/annonc/mdy487.042

142. Phase 3 Study of Tislelizumab Versus Sorafenib in Participants With Unresectable HCC. Available online at: https://clinicaltrials.gov/study/NCT03412773 (Accessed January 29, 2024).

143. Liu L-X, Peng T, Liu C, Wang J, Zhu G, Zhang X. 39TiP A phase II study of tislelizumab (TIS) plus sitravatinib as adjuvant therapy in patients with hepatocellular carcinoma (HCC) at high risk of recurrence after surgical resection. *Ann Oncol*. (2022) 33:S1444. doi: 10.1016/j.annonc.2022.10.049

144. Chen S, Wang Y, Xie W, Shen S, Peng S, Kuang M. 710P Neoadjuvant tislelizumab for resectable recurrent hepatocellular carcinoma: A non-randomized control, phase II trial (TALENT). *Ann Oncol*. (2022) 33:S867. doi: 10.1016/j.annonc.2022.07.834

145. Zhang L, Hao B, Geng Z, Geng Q. Toripalimab: the first domestic anti-tumor PD-1 antibody in China. *Front Immunol*. (2022) 12:730666. doi: 10.3389/fimmu.2021.730666

146. Hoy SM. Sintilimab: first global approval. *Drugs*. (2019) 79:341–6. doi: 10.1007/s40265-019-1066-z

147. Shi Y, Su H, Song Y, Jiang W, Sun X, Qian W, et al. Safety and activity of sintilimab in patients with relapsed or refractory classical Hodgkin lymphoma (ORIENT-1): a multicentre, single-arm, phase 2 trial. *Lancet Haematol*. (2019) 6: e12–9. doi: 10.1016/S2352-3026(18)30192-3

148. Donafenib Plus Sintilimab for Advanced HCC. Available online at: https://clinicaltrials.gov/ct2/show/NCT05162352 (Accessed January 29, 2024).

149. Yang F, Paccaly AJ, Rippley RK, Davis JD, DiCioccio AT. Population pharmacokinetic characteristics of cemiplimab in patients with advanced Malignancies. *J Pharmacokinet Pharmacodyn*. (2021) 48:479–94. doi: 10.1007/s10928-021-09739-y

150. Syed YY. Durvalumab: first global approval. *Drugs*. (2017) 77:1369–76. doi: 10.1007/s40265-017-0782-5

151. Sangro B, Kudo M, Qin S, Ren Z, Chan S, Joseph E, et al. P-347 A phase 3, randomized, double-blind, placebo-controlled study of transarterial chemoembolization combined with durvalumab or durvalumab plus bevacizumab therapy in patients with locoregional hepatocellular carcinoma: EMERALD-1. *Ann Oncol*. (2020) 31:S202–3. doi: 10.1016/j.annonc.2020.04.429

152. Abou-Alfa GK, Fan J, Heo J, Arai Y, Erinjeri JP, Kuhl CK, et al. 727TiP A randomised phase III study of tremelimumab (T) plus durvalumab (D) with or without lenvatinib combined with concurrent transarterial chemoembolisation (TACE) versus TACE alone in patients (pts) with locoregional hepatocellular carcinoma (HCC): EM. *Ann Oncol*. (2022) 33:S874. doi: 10.1016/j.annonc.2022.07.851

153. Shirley M. Avelumab: A review in metastatic merkel cell carcinoma. *Target Oncol*. (2018) 13:409–16. doi: 10.1007/s11523-018-0571-4

154. Graziani G, Tentori L, Navarra P. Ipilimumab: A novel immunostimulatory monoclonal antibody for the treatment of cancer. *Pharmacol Res*. (2012) 65:9–22. doi: 10.1016/j.phrs.2011.09.002

155. A Phase II Study of Nivolumab + Ipilimumab in Advanced HCC Patients Who Have Progressed on First Line Atezolizumab + Bevacizumab. Available online at: https://clinicaltrials.gov/ct2/show/NCT05199285 (Accessed January 29, 2024).

156. Cabozantinib Combined With Ipilimumab/Nivolumab and TACE in Patients With Hepatocellular Carcinoma. Available online at: https://clinicaltrials.gov/ct2/show/NCT04472767 (Accessed January 29, 2024).

157. Ganjalikhani Hakemi M, Jafarinia M, Azizi M, Rezaeepoor M, Isayev O, Bazhin AV. The role of TIM-3 in hepatocellular carcinoma: A promising target for immunotherapy? *Front Oncol*. (2020) 10:601661. doi: 10.3389/fonc.2020.601661

158. Guha P, Reha J, Katz SC. Immunosuppression in liver tumors: opening the portal to effective immunotherapy. *Cancer Gene Ther*. (2017) 24:114–20. doi: 10.1038/cgt.2016.54

159. Tamai Y, Fujiwara N, Tanaka T, Mizuno S, Nakagawa H. Combination therapy of immune checkpoint inhibitors with locoregional therapy for hepatocellular carcinoma. *Cancers (Basel)*. (2023) 15:5072. doi: 10.3390/cancers15205072

160. Zhang Y, Huang H, Coleman M, Ziemys A, Gopal P, Kazmi SM, et al. VEGFR2 activity on myeloid cells mediates immune suppression in the tumor microenvironment. *JCI Insight*. (2021) 6:9-12. doi: 10.1172/jci.insight.150735

161. Alfaro C, Suarez N, Gonzalez A, Solano S, Erro L, Dubrot J, et al. Influence of bevacizumab, sunitinib and sorafenib as single agents or in combination on the inhibitory effects of VEGF on human dendritic cell differentiation from monocytes. *Br J Cancer*. (2009) 100:1111–9. doi: 10.1038/sj.bjc.6604965

162. Voron T, Colussi O, Marcheteau E, Pernot S, Nizard M, Pointet A-L, et al. VEGF-A modulates expression of inhibitory checkpoints on CD8+ T cells in tumors. *J Exp Med*. (2015) 212:139–48. doi: 10.1084/jem.20140559

163. Cheng A-L, Qin S, Ikeda M, Galle PR, Ducreux M, Kim T-Y, et al. Updated efficacy and safety data from IMbrave150: Atezolizumab plus bevacizumab vs. sorafenib for unresectable hepatocellular carcinoma. *J Hepatol*. (2022) 76:862–73. doi: 10.1016/j.jhep.2021.11.030

164. Yau T, Kang Y-K, Kim T-Y, El-Khoueiry AB, Santoro A, Sangro B, et al. Efficacy and safety of nivolumab plus ipilimumab in patients with advanced hepatocellular carcinoma previously treated with sorafenib. *JAMA Oncol*. (2020) 6:e204564. doi: 10.1001/jamaoncol.2020.4564

165. Wong JSL, Kwok GGW, Tang V, Li BCW, Leung R, Chiu J, et al. Ipilimumab and nivolumab/pembrolizumab in advanced hepatocellular carcinoma refractory to prior immune checkpoint inhibitors. *J Immunother Cancer*. (2021) 9:e001945. doi: 10.1136/jitc-2020-001945

166. Raoul J-L, Forner A, Bolondi L, Cheung TT, Kloeckner R, de Baere T. Updated use of TACE for hepatocellular carcinoma treatment: How and when to use it based on clinical evidence. *Cancer Treat Rev*. (2019) 72:28–36. doi: 10.1016/j.ctrv.2018.11.002

167. Ghanaati H, Mohammadifard M, Mohammadifard M. A review of applying transarterial chemoembolization (TACE) method for management of hepatocellular carcinoma. *J Fam Med Prim Care*. (2021) 10:3553. doi: 10.4103/jfmpc.jfmpc_2347_20

168. Minami Y, Takaki H, Yamakado K, Kudo M. How compatible are immune checkpoint inhibitors and thermal ablation for liver metastases? *Cancers (Basel)*. (2022) 14:2206. doi: 10.3390/cancers14092206

169. Zhu AX, Abbas AR, de Galarreta MR, Guan Y, Lu S, Koeppen H, et al. Molecular correlates of clinical response and resistance to atezolizumab in combination with bevacizumab in advanced hepatocellular carcinoma. *Nat Med*. (2022) 28:1599–611. doi: 10.1038/s41591-022-01868-2

170. Magen A, Hamon P, Fiaschi N, Soong BY, Park MD, Mattiuz R, et al. Intratumoral dendritic cell–CD4+ T helper cell niches enable CD8+ T cell differentiation following PD-1 blockade in hepatocellular carcinoma. *Nat Med*. (2023) 29:1389–99. doi: 10.1038/s41591-023-02345-0

171. Zheng Y, Wang T, Tu X, Huang Y, Zhang H, Tan D, et al. Gut microbiome affects the response to anti-PD-1 immunotherapy in patients with hepatocellular carcinoma. *J Immunother Cancer*. (2019) 7:193. doi: 10.1186/s40425-019-0650-9

172. Dapito DH, Mencin A, Gwak G-Y, Pradere J-P, Jang M-K, Mederacke I, et al. Promotion of hepatocellular carcinoma by the intestinal microbiota and TLR4. *Cancer Cell*. (2012) 21:504–16. doi: 10.1016/j.ccr.2012.02.007

173. Enrico D, Paci A, Chaput N, Karamouza E, Besse B. Antidrug antibodies against immune checkpoint blockers: impairment of drug efficacy or indication of immune activation? *Clin Cancer Res*. (2020) 26:787–92. doi: 10.1158/1078-0432.CCR-19-2337

174. Kim C, Yang H, Kim I, Kang B, Kim H, Kim H, et al. Association of high levels of antidrug antibodies against atezolizumab with clinical outcomes and T-cell responses in patients with hepatocellular carcinoma. *JAMA Oncol*. (2022) 8:1825. doi: 10.1001/jamaoncol.2022.4733

175. Donisi C, Puzzoni M, Ziranu P, Lai E, Mariani S, Saba G, et al. Immune checkpoint inhibitors in the treatment of HCC. *Front Oncol*. (2021) 10:601240. doi: 10.3389/fonc.2020.601240

Frontiers in Immunology

Explores novel approaches and diagnoses to treat immune disorders.

The official journal of the International Union of Immunological Societies (IUIS) and the most cited in its field, leading the way for research across basic, translational and clinical immunology.

Discover the latest Research Topics

See more →

Frontiers

Avenue du Tribunal-Fédéral 34
1005 Lausanne, Switzerland
frontiersin.org

Contact us

+41 (0)21 510 17 00
frontiersin.org/about/contact